BIODIVERSITY AND DISTRIBUTION OF BENTHIC INVERTEBRATES - FROM TAXONOMY TO ECOLOGICAL PATTERNS AND GLOBAL PROCESSES

EDITED BY: Marcos Rubal, Jose Manuel Guerra-García, Juan Moreira Da Rocha, Carlos Navarro Barranco, Macarena Ros and Puri Veiga

PUBLISHED IN: Frontiers in Marine Science

frontiers Research Topics

frontiers

ISSN 1664-8714
ISBN 978-2-88974-722-1
DOI 10.3389/978-2-88974-722-1

About Frontiers

Frontiers is more than just an open-access publisher of scholarly articles: it is a pioneering approach to the world of academia, radically improving the way scholarly research is managed. The grand vision of Frontiers is a world where all people have an equal opportunity to seek, share and generate knowledge. Frontiers provides immediate and permanent online open access to all its publications, but this alone is not enough to realize our grand goals.

Frontiers Journal Series

The Frontiers Journal Series is a multi-tier and interdisciplinary set of open-access, online journals, promising a paradigm shift from the current review, selection and dissemination processes in academic publishing. All Frontiers journals are driven by researchers for researchers; therefore, they constitute a service to the scholarly community. At the same time, the Frontiers Journal Series operates on a revolutionary invention, the tiered publishing system, initially addressing specific communities of scholars, and gradually climbing up to broader public understanding, thus serving the interests of the lay society, too.

Dedication to Quality

Each Frontiers article is a landmark of the highest quality, thanks to genuinely collaborative interactions between authors and review editors, who include some of the world's best academicians. Research must be certified by peers before entering a stream of knowledge that may eventually reach the public - and shape society; therefore, Frontiers only applies the most rigorous and unbiased reviews.
Frontiers revolutionizes research publishing by freely delivering the most outstanding research, evaluated with no bias from both the academic and social point of view. By applying the most advanced information technologies, Frontiers is catapulting scholarly publishing into a new generation.

What are Frontiers Research Topics?

Frontiers Research Topics are very popular trademarks of the Frontiers Journals Series: they are collections of at least ten articles, all centered on a particular subject. With their unique mix of varied contributions from Original Research to Review Articles, Frontiers Research Topics unify the most influential researchers, the latest key findings and historical advances in a hot research area! Find out more on how to host your own Frontiers Research Topic or contribute to one as an author by contacting the Frontiers Editorial Office: frontiersin.org/about/contact

BIODIVERSITY AND DISTRIBUTION OF BENTHIC INVERTEBRATES - FROM TAXONOMY TO ECOLOGICAL PATTERNS AND GLOBAL PROCESSES

Topic Editors:
Marcos Rubal, University of Porto, Portugal
Jose Manuel Guerra-García, Sevilla University, Spain
Juan Moreira Da Rocha, Autonomous University of Madrid, Spain
Carlos Navarro Barranco, Autonomous University of Madrid, Spain
Macarena Ros, Sevilla University, Spain
Puri Veiga, University of Porto, Portugal

Citation: Rubal, M., Guerra-García, J. M., Da Rocha, J. M., Barranco, C. N., Ros, M., Veiga, P., eds. (2022). Biodiversity and Distribution of Benthic Invertebrates - From Taxonomy to Ecological Patterns and Global Processes. Lausanne: Frontiers Media SA. doi: 10.3389/978-2-88974-722-1

Table of Contents

frontiers in Marine Science

EDITORIAL
published: 28 February 2022
doi: 10.3389/fmars.2022.863981

Editorial: Biodiversity and Distribution of Benthic Invertebrates - From Taxonomy to Ecological Patterns and Global Processes

Marcos Rubal[1]*, *José M. Guerra-García*[2], *Juan Moreira*[3], *Carlos Navarro-Barranco*[2], *Macarena Ros*[2] *and Puri Veiga*[1]

[1] *Interdisciplinary Centre of Marine and Environmental Research (CIIMAR), University of Porto, Matosinhos, Portugal,*
[2] *Laboratorio de Biología Marina, Departamento de Zoología, Facultad de Biología, Universidad de Sevilla, Seville, Spain,*
[3] *Departamento de Biología (Unidad de Zoología), Centro de Investigación en Biodiversidad y Cambio Global (CIBC-UAM), Universidad Autónoma de Madrid, Madrid, Spain*

Keywords: macrobenthos, meiobenthos, anthropogenic disturbances, natural variability, environmental drivers

Editorial on the Research Topic

Biodiversity and Distribution of Benthic Invertebrates - From Taxonomy to Ecological Patterns and Global Processes

OPEN ACCESS

Edited and reviewed by:
Daniel Martin,
Spanish National Research Council (CSIC), Spain

***Correspondence:**
Marcos Rubal
marcos.garcia@fc.up.pt

Specialty section:
This article was submitted to Marine Evolutionary Biology, Biogeography and Species Diversity, a section of the journal Frontiers in Marine Science

Received: *27 January 2022*
Accepted: *03 February 2022*
Published: *28 February 2022*

Citation:
Rubal M, Guerra-García JM, Moreira J, Navarro-Barranco C, Ros M and Veiga P (2022) Editorial: Biodiversity and Distribution of Benthic Invertebrates - From Taxonomy to Ecological Patterns and Global Processes. Front. Mar. Sci. 9:863981. doi: 10.3389/fmars.2022.863981

Biodiversity loss due to human activities is increasing worldwide at an alarming rate, and the oceans are not an exception to this pattern (O'Hara et al., 2021). Biodiversity loss weakens the ability of ecosystems to function efficiently and can influence their capacity to provide vital goods and services to humanity (Roe, 2019). We are still far away from a complete inventory of all habitats and lifeforms harbored by Earth's oceans. With the exception of few charismatic (e.g., corals), commercially valuable (e.g., mussels or oysters) or harmful (e.g., jellyfish) invertebrate species, general public and scientific community attention is focused on vertebrates (Troudet et al., 2017). However, invertebrate phyla represent about 75 % of all described animal species both in ocean and land (Eisenhauer and Hines, 2021). The marine benthic realm is one of the largest and probably more diverse habitats on Earth, harboring a huge taxonomical and functional diversity of invertebrates (Snelgrove, 1999, 2016). Unfortunately, knowledge about patterns of biodiversity of benthic invertebrates is still very focused on the most accessible intertidal and shallow subtidal domains; there is also a geographic bias because large areas of the planet remain almost unexplored as well, and because research efforts often focus in well-known biodiversity hotspots (Mugnai et al., 2021).

The main objective of this special topic collection is to improve our knowledge in the above-described gaps on benthic invertebrate biodiversity. We have selected 15 articles by 82 authors encompassing a wide range of phyla and including 12 (ten species, one genus and one family) new invertebrate taxa. Therefore, we are also contributing to the overwhelming but urgent need of discovering and describing as much invertebrate species as possible. Specifically, the new family and five new species belong to deep-sea tanaids (Gellert et al.); three new amphipods and one tanaid came from phytal habitats in an oceanic island (Iwasa-Arai et al.) and the last new species is an harpaticoid copepod described by integrative taxonomy (Yeom et al.). The collection also includes: (1) a comprehensive revision of the poorly studied deep-sea wood-borer bivalves by Romano et al. which resulted in the erection of a new genus while providing important biogeographical information, (2) a revision of the ecology and taxonomy of the amphipod genus *Ampelisca* from the North-East Atlantic (Dauvin et al.), which provided valuable insights on these ecologically relevant

and diverse benthic crustaceans, and (3) two analyses of the role of ecosystem engineers and its conservation in shaping invertebrate biodiversity, focusing on the reef-building annelids of the genus *Sabellaria* (Muller et al.; van der Reijden et al.). Muller et al. together with Srinivas et al. (who studied amphipods in coralline habitats within a Marine Protected Area) also compared functional diversity with taxonomic diversity patterns, and their relevance for biodiversity management.

The collection also incorporates analyses of the effect of human disturbances on natural biodiversity patterns. These include the value of long-term monitoring of intertidal invertebrates in detecting climate change effects (Mieszkowska et al.) and that of soft bottom infauna and epifauna as quality indicators in an industrial harbor (Dreujou et al.) and an estuary (Isabel et al.). We have also selected two articles on economically relevant species: (1) on the role of intraspecific diversity in the fitness and adaptation of different population of *Crassostrea ariakensis* (Li et al.) and (2) on the genetic diversity of different oyster species from a relevant culture area (Liu et al.). The last article provides new evidence on the poorly studied deep-water emergence of many species along the Chilean coasts, changing our traditional view on the relationship between bathymetry and invertebrate distribution (Häussermann et al.).

There are still many unexplored gaps in the knowledge of benthic invertebrate diversity, hindered, for example, by the complex logistics and budgetary constraints of deep-sea exploration or the lack of experts in invertebrate taxa (Boero, 2010). In fact, many gaps identified in the topic description, such as the invertebrate biodiversity in scarcely studied habitats (e.g., marine caves) or among poorly known taxa (e.g., soft bodied meiofaunal gastrotrichs, gnatostomulids, etc.) were not included in this volume due to the lack of submitted manuscripts.

Therefore, we would like to highlight that only by improving our understanding on invertebrate biodiversity, we will be able to improve our ability to manage and preserve marine biodiversity. Having this in mind, we have compiled this volume hoping both to encourage more research in this particular field and to boost benthic diversity knowledge globally.

AUTHOR CONTRIBUTIONS

MR planned and wrote the text. All authors contributed to the discussion and writing. All authors contributed to the article and approved the submitted version.

FUNDING

PV was hired through the Regulamento do Emprego Científico e Tecnológico—RJEC from the Portuguese Foundation for Science and Technology (FCT) Program (CEECIND/03893/2018). This study was partially funded by the FCT, Portugal Strategic Funding UID/Multi/04423/2019.

ACKNOWLEDGMENTS

We are very grateful to all the authors, referees and Frontiers' staff who made this volume possible. Authors are grateful to DM for his valuable suggestions on this manuscript.

REFERENCES

Boero, F. (2010). The study of species in the era of biodiversity: a tale of stupidity. *Diversity* 2, 115–126. doi: 10.3390/d2010115

Eisenhauer, N., and Hines, J. (2021). Invertebrate biodiversity and conservation. *Curr. Biol.* 31, 1214–1278. doi: 10.1016/j.cub.2021.06.058

Mugnai, F., Meglécz, E., Costantini, F., Abbiati, M., Bavestrello, G., Bertasi, F., et al. (2021). Are well-studied marine biodiversity hotspots still blackspots for animal barcoding? *Glob. Ecol. Conserv.* 32, e01909. doi: 10.1016/j.gecco.2021.e01909

O'Hara, C. C., Frazier, M., and Halper, B. S. (2021). At-risk marine biodiversity faces extensive, expanding, and intensifying human impacts. *Science* 372, 84–87. doi: 10.1126/science.abe6731

Roe, D. (2019). Biodiversity loss—more than an environmental emergency. *Lancet Planet Health* 3, e287–e289. doi: 10.1016/S2542-5196(19)30113-5

Snelgrove, P. V. R. (1999). Getting to the bottom of marine biodiversity: sedimentary habitats. *Bioscience* 49, 129–138. doi: 10.2307/1313538

Snelgrove, P. V. R. (2016). An ocean of discovery: biodiversity beyond the census of marine life. *Planta Med.* 82, 790–799. doi: 10.1055/s-0042-103934

Troudet, J., Grandcolas, P., Blin, A., Vignes-Lebbe, R., and Legendre, F. (2017). Taxonomic bias in biodiversity data and societal preferences. *Sci. Rep.* 7, 1–14. doi: 10.1038/s41598-017-09084-6

Conflict of Interest: The authors declare that the research was conducted in the absence of any commercial or financial relationships that could be construed as a potential conflict of interest.

Publisher's Note: All claims expressed in this article are solely those of the authors and do not necessarily represent those of their affiliated organizations, or those of the publisher, the editors and the reviewers. Any product that may be evaluated in this article, or claim that may be made by its manufacturer, is not guaranteed or endorsed by the publisher.

frontiers in Marine Science

ORIGINAL RESEARCH
published: 03 November 2020
doi: 10.3389/fmars.2020.589099

Molecular and Fitness Data Reveal Local Adaptation of Southern and Northern Estuarine Oysters (*Crassostrea ariakensis*)

Ao Li[1,3,4,6†], Chaogang Wang[1,5†], Wei Wang[1,2,3,4], Ziyan Zhang[1,5], Mingkun Liu[1,2,3,4], Zhicai She[7], Zhen Jia[7], Guofan Zhang[1,2,3,4] and Li Li[1,3,4,6]*

[1] CAS Key Laboratory of Experimental Marine Biology, Institute of Oceanology, Chinese Academy of Sciences, Qingdao, China, [2] Laboratory for Marine Biology and Biotechnology, Pilot National Laboratory for Marine Science and Technology, Qingdao, China, [3] Center for Ocean Mega-Science, Chinese Academy of Sciences, Qingdao, China, [4] National and Local Joint Engineering Laboratory of Ecological Mariculture, Institute of Oceanology, Chinese Academy of Sciences, Qingdao, China, [5] University of Chinese Academy of Sciences, Beijing, China, [6] Laboratory for Marine Fisheries Science and Food Production Processes, Pilot National Laboratory for Marine Science and Technology, Qingdao, China, [7] Ocean College, Beibu Gulf University, Qinzhou, China

OPEN ACCESS

Edited by:
Marcos Rubal,
University of Porto, Portugal

Reviewed by:
Zhang Yuehuan,
South China Sea Institute of Oceanology (CAS), China
Cristián E. Hernández,
University of Concepcion, Chile
Yang Zhang,
South China Sea Institute of Oceanology (CAS), China

***Correspondence:**
Li Li
lili@qdio.ac.cn

[†] These authors have contributed equally to this work

Specialty section:
This article was submitted to Marine Evolutionary Biology, Biogeography and Species Diversity, a section of the journal Frontiers in Marine Science

Received: 30 July 2020
Accepted: 15 October 2020
Published: 03 November 2020

Citation:
Li A, Wang C, Wang W, Zhang Z, Liu M, She Z, Jia Z, Zhang G and Li L (2020) Molecular and Fitness Data Reveal Local Adaptation of Southern and Northern Estuarine Oysters (Crassostrea ariakensis). Front. Mar. Sci. 7:589099. doi: 10.3389/fmars.2020.589099

Natural selection and isolation are both important for understanding the geographic distribution of marine species and environmental responses to changing climate. In this study, we revealed distinct genetic variation in *Crassostrea ariakensis* by comparing the *COI* gene segment sequence in northern and southern oysters partitioned by the Yangtze River estuary. Reciprocal hybridization and intrapopulation crosses clarified their taxonomic status as the same species. There was no heterosis in the survival and growth of the hybrids, while the maternal effect was observed in larvae from eggs in the native habitat that showed higher fitness. Both the northern and southern F_1 progenies exhibited positive performance in fitness traits, including survivorship, respiration rate, and growth, in their native habitats compared to that in their non-native habitats, indicating a strong signature of local adaptation. The oysters dwelling in the warm/southern habitats evolved a higher thermotolerance of LT_{50}, while the oysters inhabiting the high-salinity/northern habitats had a 2.43‰ higher LS_{50} than that of their southern counterparts. After strong natural selection in the northern environments, the higher survival of the F_1 progenies from the southern oysters under heat shock indicates an evolved genetic basis for its higher thermal tolerance. Strong environmental gradients, especially for temperature and salinity, and geographic isolation by the interaction between coastal currents and the Yangtze River estuary potentially contribute to shaping the distribution pattern and adaptive divergence of *C. ariakensis* in China.

Keywords: environmental selection, genetic drift, genetic variation, local adaptation, taxonomic analyses, reciprocal hybridization, *Crassostrea ariakensis*

INTRODUCTION

Understanding geographic distribution and the causes that drive the spatiotemporal patterns of species or populations, including selection and isolation, can provide fundamental information on organismal responses and adaptive capacity in the face of rapid global change, as well as further direct implications of marine resources and fisheries management. A growing body of studies

indicates that marine ecosystems are not open with high connectivity, but are accompanied by strong latitudinal, vertical, and mosaic environmental gradients, especially in coastal and estuarine areas, where the temperature, salinity, and other biotic and abiotic factors experience extreme variations at the fine-tuning scale (Bozinovic et al., 2011; Sanford and Kelly, 2011; Somero, 2012). Adaptive differentiation was subsequently reported in many marine species, even in high gene flow animals with high motility, such as fishes (Limborg et al., 2012; Dayan et al., 2015) or those with long-term planktonic stages in their life history, such as sessile mollusks occurring over tens of meters (De Wit and Palumbi, 2013; Burford et al., 2014; Li et al., 2017; Li A. et al., 2018; Li L. et al., 2018; Li et al., 2019; Ghaffari et al., 2019). Geographic or oceanographic isolation or homogenization can also contribute to shaping the spatial distribution and environmental responses of marine species. In China, the Yangtze (Chang Jiang) River has long been rendered as a marine biogeographic boundary causing distinct ecological gradients, especially for temperature and salinity, and shaping adaptive differentiations in warm-tolerant and cold-water populations or species of coastal animals under spatially varying selection. Ni et al. (2017) comprehensively summarized the effects of the Yangtze River as well as its interaction with coastal currents on the genetic diversity of many marine species, such as fishes, crabs, mollusks, etc., Most of the marine species exhibited divergent genetic structures between the northern and southern populations separated by the Yangtze River, while coastal currents facilitate internal gene flows within the northern or southern populations (Xu et al., 2009; Xiao et al., 2016; Li L. et al., 2018). These findings highlight the significant role of stochastic geographic isolation following environmental selection in ecological, evolutionary, and taxonomic studies.

Oysters are marine bivalve mollusks distributed worldwide in intertidal, estuarine, and shallow ocean areas where the environmental conditions are extremely variable, providing a model species for exploring adaptive evolution. Generally, different oyster species inhabit distinct latitudinal or vertical gradients because they have evolved species-specific adaptive capacities in different environments (Wang et al., 2008, 2010; Guo et al., 2018). For sympatric oyster species, however, we need to first classify them before conducting subsequent biological examinations. For example, the congeneric oysters *Crassostrea hongkongensis* sympatrically coexist with *Crassostrea ariakensis* in most estuarine habitats in southern China (Wang et al., 2006) and these two species can unidirectionally hybridize with each other based on molecular, morphological, and fitness assessments (Zhang et al., 2017; Qin et al., 2020). Oyster classification is always difficult because of their high plasticity in shell morphology, which is sensitive to environmental heterogeneity. Genetic markers such as mitochondrial *cytochrome oxidase I* (*COI*) or nuclear 28S ribosomal RNA genes have been developed to identify these oysters in previous studies (Wang et al., 2004; Wang and Guo, 2008; Guo et al., 2018). Moreover, a high-throughput, efficient, and easy to visualize method of high-resolution melting (HRM) curve analysis has been applied to taxonomic studies in the classification of *Crassostrea* oyster species (Wang et al., 2014, 2015), which can be extensively used to rapidly and reliably identify oysters collected from multiple locations in large sampling size.

Crassostrea ariakensis is one of the most common and well-known oysters in China, and is mainly found in rivers and estuaries with salinities of 10–25 ppt (Guo et al., 1999). It is one of the most important economic oyster species and is broadly distributed in China, ranging from the Lizijiang (Oyster River) in the north to the Beihai in the south (Guo et al., 1999; Zhou and Allen, 2003). However, natural resources have dramatically declined in the past decades, especially in the north due to overfishing, decreased runoff, and habitat destruction. Disconnected distribution and significant environmental gradients across inhabited estuaries imply differentiations in genomic components and plasticity among different populations, which requires investigations to assess their adaptive capacity in response to environmental challenges, particularly for elevated temperature and salinity. However, previous studies only revealed sequence variations between northern and southern populations of *C. ariakensis* separated by the Yangtze River estuary using neutral mitochondrial and nuclear gene markers, and speculated the occurrence of reproductive isolation between these two divergent populations (Wang et al., 2004; Zhang et al., 2005; Xiao et al., 2010; Kim et al., 2014). Hybridization experiments need to be carried out after knowing about genetic differentiation, which could provide the most informative findings to verify this hypothesis and further clarify their taxonomic status, e.g., whether they should be considered as two separate species or subspecies (Wang et al., 2004, 2010). Our previous study found divergent transcriptomic responses of eye-spot larvae to salinity gradients between different latitudinal *C. ariakensis* populations and identified several salinity-stress responsive genes (Liu et al., 2019). However, assessments of fitness-related traits, including survival, metabolic rate, and growth, via common garden and reciprocal transplant experiments in different environmental habitats (Sanford and Kelly, 2011) are needed to compare the environmental/stress responses between oysters from northern and southern sampling sites, which could provide direct evidence to reveal whether they are locally adapted to their native habitats as well as examine the primary environmental factors that drove their adaptive divergence if it occurred.

In this study, we collected 278 wild *C. ariakensis* oysters from 11 estuaries in China and found distinct genetic variation between the oysters from northern (seven locations) and southern (four locations) sampling sites using HRM analysis of the *COI* gene segment with *C. hongkongensis* as the outgroup. Reciprocal hybridization experiments were performed to clarify the taxonomic status of the northern and southern oysters. The viability of hybrids from bidirectional crosses classified them as the same species. Long-term common garden and reciprocal transplantation of the northern and southern F_1 oysters between their native habitats were carried out, and fitness-related traits, including survival, metabolic rate, and growth, were measured to explore whether local adaptation occurred. To investigate the potential factors that shape adaptive divergence, we monitored the primary abiotic environmental factors, including temperature and salinity, of the northern and southern habitats, and assessed

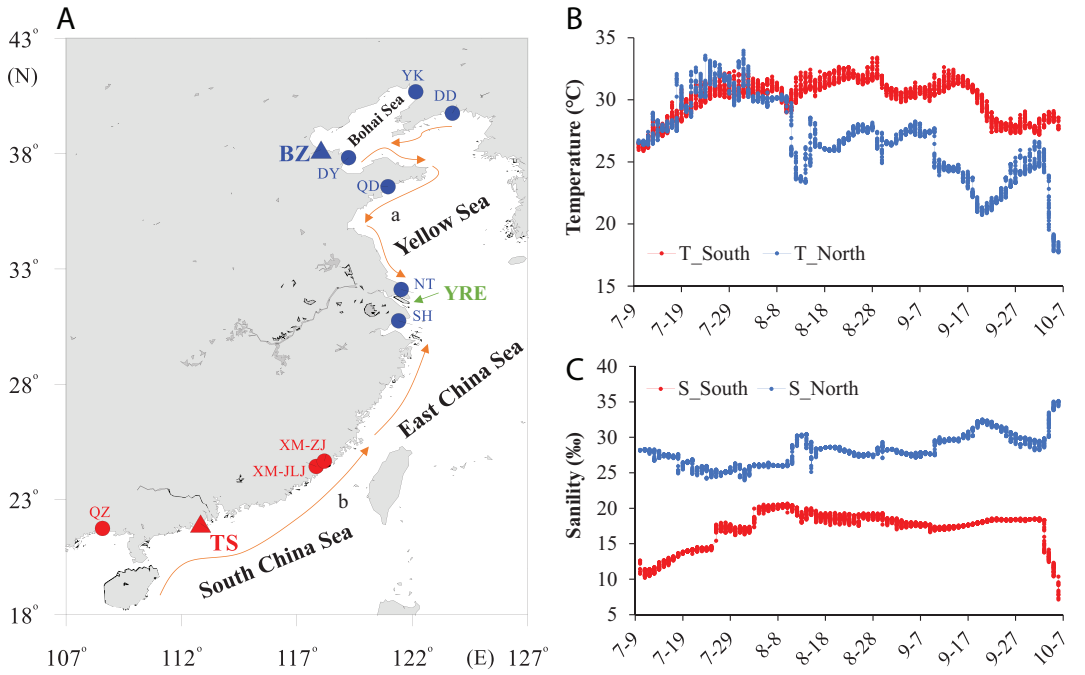

FIGURE 1 | Sampling locations and environmental parameters. **(A)** Sampling map showing the locations of 11 *C. ariakensis* populations dwelling in estuaries along the coasts of China. Two populations derived from the southern (Taishan: TS) and northern (Binzhou: BZ) habitats were selected for the phenotype assessments (triangle). **(A)** China Coastal Current; **(B)** South China Sea Warm Current. **(B)** Seawater temperature and **(C)** salinity of the two selected locations recorded by a conductivity logger with a 1 h interval. T: temperature, S: salinity, YK: Yingkou, DD: Dandong, DY: Dongying, QD: Qingdao, NT: Nantong, SH: Shanghai, XM-ZJ: Xiamen-Zhangjiang, XM-JLJ: Xiamen-Jiulongjiang, QZ: Qinzhou, YRE: Yangtze river estuary. The arrowed curves indicate coastal currents in the summer in China.

the stress tolerance of the northern and southern oysters in response to these two factors. We proposed that strong environmental gradients and the interaction between coastal currents and the Yangtze River estuary potentially contribute to shaping the geographic distribution and adaptive divergence of *C. ariakensis* in China. Identification of genetic diversity among wild *C. ariakensis* populations across most Chinese estuaries and documentation of strong local adaptation between northern and southern populations can provide biological significance for management strategies for the regional mariculture of *C. ariakensis*.

MATERIALS AND METHODS

Sampling Locations and Monitoring of Seawater Temperature and Salinity in the Southern and Northern Habitats

We collected wild oysters of *C. ariakensis* from 11 sampling sites dwelling in northern (seven locations) and southern (four locations) estuary regions to explore the genetic variations in the *COI* gene segment (**Figure 1A**, **Supplementary Table 1**). We selected two locations in the northern (Binzhou, BZ, 38.18°N) and southern (Taishan, TS, 21.95°N) estuaries, which have tremendous environmental differences, especially for temperature and salinity, to monitor these two parameters of the field habitats during summer after larval attachment (July to October) using HOBO Conductivity U24 Data Loggers (ONSET, Adelaide, Australia) with a time interval of 1 h to record the data at the same depth as the cultured oysters.

Taxonomic Analyses of Sequence Variations of the *COI* Gene Segment in Wild Estuarine Oysters

DNA Isolation

Gills of the 278 collected wild oysters from 11 estuaries, as well as those from five *C. hongkongensis* oysters as the outgroup, were sampled for sequence variation detection. DNA of individuals from each oyster population was extracted using a TIANamp Marine Animals DNA Kit (Tiangen, Beijing, China). The quality and quantity of the DNA were determined by agarose gel (1%) electrophoresis and UV spectrometry on a NanoDrop 2000 (Thermo Fisher Scientific, Waltham, MA, United States), respectively.

High-Resolution Melting (HRM) Analysis

An improved small-amplicon HRM analysis (Wang et al., 2015) was adopted to characterize the *COI* gene segment of all sampled individuals. The forward and reverse primer sequences (5′-3′) were the same as those in a previous study (Wang et al., 2014): TACTTAATATTGGGTTTTTAGGGT and CGCGTATCAATATCCATTCC, respectively. The amplicon length was 76 bp, and the melting temperature (Tm) was set at 55°C. The PCR mixture contained 10 ng of template DNA,

5 μL of PCR mix, 0.5 μL (100 pmol/L) each of the forward and reverse primers, and water to 10 μL, which was covered with 15 μL of mineral oil. The *COI* gene fragment was amplified using the following protocol: an initial denaturing at 94°C for 5 min, followed by 55 cycles of denaturing at 95°C for 30 s, annealing at 55°C for 30 s, and extension at 72°C for 30 s, and a final extension at 72°C for 10 min.

Fluorescent melting curves of PCR amplicon duplexes were analyzed using a Light Scanner 96 (Idaho Technology Inc., Salt Lake City, UT, United States). Two unblocked, double-stranded oligonucleotides were used as the high- and low-temperature internal controls in the experiment to calibrate the temperature variation between reactions (Gundry et al., 2008). The duplex controls consisted of the following sequences and their complements: GCGGTCAGTC GGCCTAGCGGTAGCCAGCTGCGGCACTGCGTGACGCTC AG. (high-temperature sequence) and ATCGTGATTTCTATA GTTATCTAAGTAGTTGGCATTAATAATTTCATTTT (low-temperature sequence). Specifically, 1 μL (100 pmol) of the internal controls and 1 μL of LC-green were added to the amplification products, and denaturation was performed at 95°C for 10 min using a thermal cycler prior to HRM analysis. Melting curve data were collected using continuous fluorescence acquisition at 55–98°C at a thermal transition rate of 0.1°C/s. Genotypes were identified by the melting temperatures indicated by peaks on the derived plots using the Light Scanner 96 software.

Sequence Variation Determination

We randomly selected 10 individuals from each of the northern (BZ) and southern (TS) wild oyster populations to sequence the *COI* gene segment using Sanger sequencing based on the observation of their different melting curves (**Figure 2A**).

Cross-Breeding Experiments

We further explored the classification of the southern and northern estuarine oysters by constructing an intrapopulation and their hybrid families of reciprocal crosses in the southern habitat using sperm (♂) and eggs (♀) from the wild northern (N, BZ) and southern (S, TS) parental oysters. The gamete was microscopically examined to filter out hermaphrodites before breeding. Each of the four families was incubated with three replicates in 70 L plastic containers. Larvae and spats were reared using standard practices with temperature and salinity ranges of 22–26°C and 20 ± 1.5‰, respectively. The shell length of the larvae was measured at the D-shaped stage and the density was controlled at 10 ind./mL for each family. At the eye-spot stage (occurrence time of the first family), the shell length and density of the larvae of the four families were further determined to compare their survival and growth rates.

Reciprocal Transplantation Experiments for Fitness Trait Measurements

Two populations derived from the southern (TS) and northern (BZ) environments were selected to reveal the responses of fitness-related traits to each of the natural habitats. To alleviate environmental and maternal effects (Sanford and Kelly, 2011; Somero, 2012; Li L. et al., 2018). Wild oysters from two populations were collected from the estuary and then translocated to identical conditions for a one-month acclimation before breeding. For each population, hermaphrodites were excluded by microscopic examination, and 40 mature male and female oysters were selected to maintain an effective population size. Eggs from the female oysters were mixed and equally divided into 40 beakers. Sperm from the 40 male oysters were individually crossed with each piece of mixed eggs. This breeding protocol warranted each sperm to cross with eggs from different female oysters. The zygotes were individually cultured in 70 L plastic containers until the D-shaped stage, and then larvae were combined into one nursery pond. The culturing conditions for the larvae and spat was the same as those for the cross-breeding experiments described in section "Cross-breeding Experiments."

Reciprocal transplantation was conducted as follows: two-month-old juvenile individuals from each of two populations were outplanted to two source habitats to compare the responses of their fitness-related traits, including survival, respiration rate, and growth parameters (wet weight and shell height, length, and width), after acclimation for three months from July to October. Oysters of each population were cultured with three replicates in cages with the same density at both locations. Live oysters were counted to determine the survival. After cleaning off the attached barnacles, mussels, and other aufwuchs, approximately 100 oysters were used to measure growth parameters, and six oysters were used to measure respiration rate.

Oysters used for the respiration rate measurements were further cleaned by wiping with 50% alcohol on the shell to avoid the influence of epiphytes. Individual oysters were placed in 1.2 L acrylic chambers filled with air-saturated, sand-filtered seawater at ambient temperature controlled by a water bath (20°C). A rotating magnetic stir bar was used to slowly circulate the seawater beneath the experimental chamber. A needle-type fiber-optic oxygen microsensor (oxygen optode) and a temperature probe (PreSens, Regensburg, Germany) were glued into two small holes in the lid. An oxygen transmitter (Microx 4; PreSens) was connected to these two probes and the temperature and oxygen concentration were recorded every 3 s for 1 h. The oxygen microsensors were calibrated to the corresponding temperature and salinity conditions prior to each trial according to the manufacturer's instructions. The slope of the decrease in oxygen concentration was calculated as the respiration rate after correcting the wet weight (% as g^{-1} L^{-1} h^{-1}).

Semi-Lethal Temperature (LT_{50}) and Salinity (LS_{50}) Determination and Stress Responses of the Northern and Southern Oysters

Ten-month-old F_1 progeny of the southern (TS) and northern (BZ) oysters cultured in their native habitat were used to determine LT_{50} after heat shock and LS_{50} after high salinity in the laboratory. Acute short-term exposure to thermal conditions (1 h) and a one-week recovery time were applied in the LT_{50} determination, while long-term exposure under high salinity gradients was applied in the LS_{50} determination. Twenty individuals were used in each treatment gradient. Based on

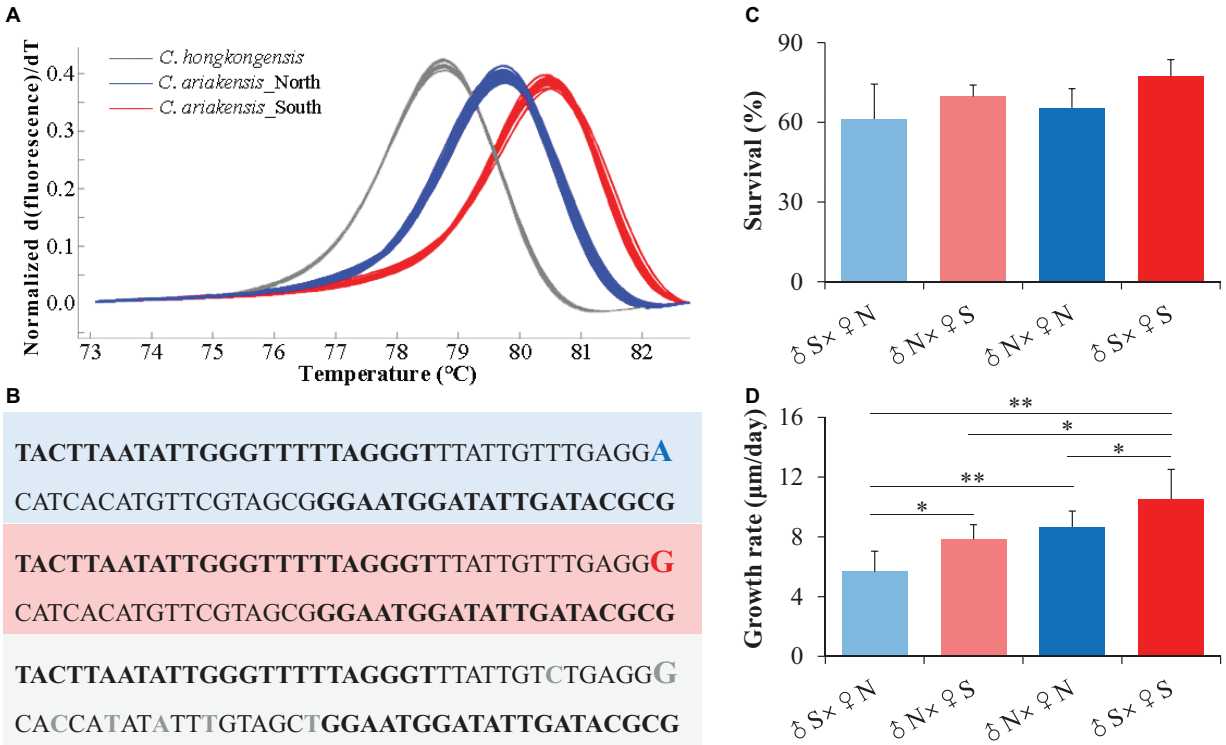

FIGURE 2 | Taxonomic analyses of the northern and southern estuarine *Crassostrea ariakensis* oysters. **(A)** Normalized melting curves of the amplicons from the *COI* gene segment for the northern (blue) and southern (red) *C. ariakensis*, and *Crassostrea hongkongensis* (gray) oysters. **(B)** Sequence variations of the *COI* gene segment among the northern (blue) and southern (red) *C. ariakensis*, and *C. hongkongensis* (gray) oysters. **(C)** Survival and **(D)** growth rates during larvae development from the D-shaped to eye-spot stages of the four full-sib families. $♂_S$: sperm of the southern oysters (TS), $♀_S$: eggs of the southern oysters (TS), $♂_N$: sperm of the northern oysters (BZ), $♀_N$: eggs of the northern oysters (BZ). Asterisks indicate significant differences (*$p < 0.05$ and **$p < 0.01$), and error bars represent sd values.

previous determinations of LT_{50} for northern *Crassostrea gigas* and southern *Crassostrea angulata* (Ghaffari et al., 2019), and a preliminary experiment was performed to narrow the range of treatment gradients; the survival of oysters at 30, 35, 40, and 45°C and 50, 55, 60, and 65‰ were explored. The second part of the experiment with a narrower treatment range was deployed to precisely assess the LT_{50} and LS_{50} of each population. An increase of 1°C from 34°C to 44°C and 2‰ from 50‰ to 64‰ were performed. A trail of oysters that were not stressed was set as a control (temperature [average seawater temperature in the northern habitats during experiment]: 26 ± 1°C; salinity [average seawater salinity in the southern habitats during experiment]: 17 ± 2‰). Stressed oysters were fed with commercial spirulina powder each day, and the seawater was changed every two days. The dead oysters, who could not close the shell after touch, were removed from the tanks.

Ten-month-old southern and northern F_1 progenies cultured in the northern habitat were used to compare stress responses under the LT_{50} of the southern population and the LS_{50} of the northern population in the laboratory, considering that the northern oysters cannot survive in the southern habitat (**Figure 3**). The same stress methods that caused acute heat shock followed recovery and long-term high salinity exposure were applied. Each treatment had three replicates and experimental management was the same as that for LT_{50} and LS_{50} determination.

Statistical Analysis

Shapiro–Wilk and Bartlett tests were used to check the normality and homogeneity of the variances, respectively. Comparisons of the temperature and salinity between two sampling sites were tested with the function *aov* in R software if the data followed a normal distribution and homoscedasticity of variances. Otherwise, a non-parametric Kruskal–Wallis test was performed. Two-way ANOVA was carried out followed by Bonferroni *post hoc* test to determine the differences in survival and growth rates of the larvae from four crosses, growth parameters and metabolic rates of the F_1 progenies among populations cultured in the southern and northern natural habitats, while significant differences in survival at the field for these populations were determined by Pearson's chi-square test. Polynomial (three order) regressions were used to model LT_{50} and LS_{50}. The Kaplan-Meier analysis with log-rank test in the Survival module using SPSS version 19.0 software (IBM SPSS Statistics) was carried out to determine the difference in mortality between the two populations when exposed to LT_{50} and LS_{50}. All data are presented as mean ± standard error of mean (SEM), and a significance level of $\alpha = 0.05$ was applied.

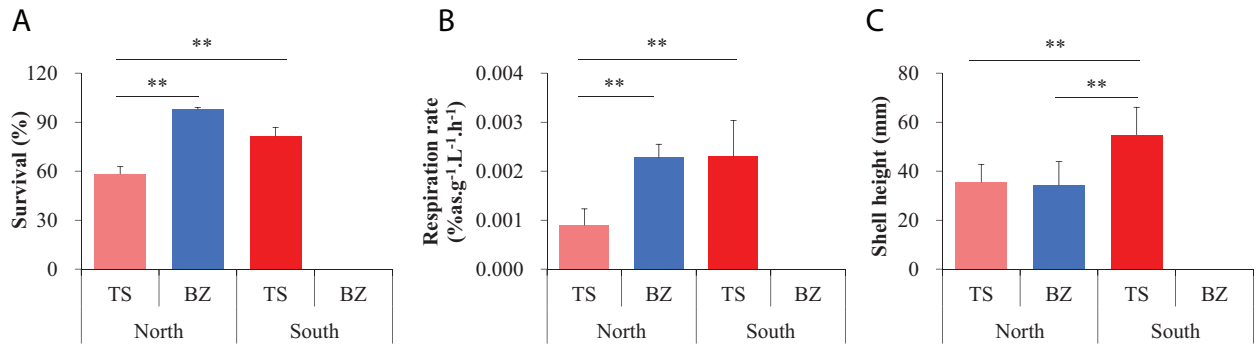

FIGURE 3 | Measurements for fitness-related traits, including **(A)** survival, **(B)** respiration rate, and **(C)** shell height, of the northern and southern estuarine oyster populations in the northern and southern habitats using reciprocal transplant experiments for three months post attachment. Asterisks indicate significant differences (**$p < 0.01$), and error bars represent sd values.

RESULTS

Monitoring Seawater Temperature and Salinity in the Southern and Northern Habitats

We observed tremendous environmental differences in the seawater temperature and salinity between the southern and northern field habitats during summer after larval attachment ($p < 0.01$) (July to October; **Figures 1B,C**). The southern estuary showed a higher seawater temperature, while the northern estuary showed a higher salinity, and the differences in the average seawater temperature (northern: 26.83°C; southern: 30.12°C) and salinity (northern: 28.17%; southern: 17.19%) between the northern and southern habitats were 3.29°C and 10.98%, respectively. In addition, the amplitude of the temperature fluctuation in the northern habitat was 16.25°C, while it was 7.52°C in the southern habitat (**Figure 1B**). Furthermore, the amplitude of the salinity fluctuation in the southern habitat was 2.33 times higher than that in the northern habitat (**Figure 1C**).

Taxonomic Analyses of the Sequence Variation in the *COI* Gene Segments and Cross-Breeding Experiments

The PCR amplicon melting curves could distinguish all of the *C. ariakensis* individuals as well as the *C. hongkongensis* oysters, which showed three independent homozygote peaks, and the peaks of the southern and northern *C. ariakensis* oyster groups were separated according to their different melting temperatures (**Figure 2A**). Two populations inhabiting the northern (NT) and southern (SH) estuaries of the Yangtze River showed the same melting curves that were consistent with the other five northern oyster populations (DD, YK, BZ, DY, and QD), while four southern oyster populations (XM-ZJ, XM-JLJ, TS, and QZ) were clustered together (**Figure 1A** and **Supplementary Figure 1**). We only identified an SNP as A to G between the northern and southern individuals of *C. ariakensis* in this *COI* gene segment using Sanger sequencing. In accordance with the southern *C. ariakensis* oysters, the same G in this locus was detected in *C. hongkongensis*, but was accompanied by six other SNPs in comparison with only one in *C. ariakensis* (**Figure 2B**).

There were no differences in survival during larval development from the D-shaped to eye-spot stages among the four full-sib families derived from BZ (N: northern), TS (S: southern), and their reciprocal cross oysters ($p > 0.05$, two-way ANOVA, **Figure 2C**, **Supplementary Table 2a**). However, the growth rates exhibited significant difference among these four families and interaction between sex and the origin of oysters ($p < 0.05$, **Figure 2D**, **Supplementary Table 2b**), where larvae reproduced from the sperm of the southern oysters and the eggs of the northern oysters ($♂_S \times ♀_N$) showed the lowest growth rate (5.67 μm/day) compared to those of the larvae reproduced from the sperm of the northern oysters and the eggs of the southern oysters ($♂_N \times ♀_S$) (7.83 μm/day, $p = 0.034$, *t*-test), the northern family ($♂_N \times ♀_N$) (8.67 μm/day, $p = 0.012$), and the southern family ($♂_S \times ♀_S$) (10.54 μm/day, $p = 0.010$).

Comparison of Fitness-Related Traits Between the Northern and Southern F_1 Oyster Populations Using Reciprocal Transplant Experiments

Both the northern (BZ) and southern (TS) F_1 oyster populations exhibited significantly greater performance in fitness-related traits in their native environments, including survival, growth, and metabolic rate, and statistically significant interaction between sampling sites and the origin of oysters using reciprocal transplant experiments for three months post-attachment (**Figure 3**, **Supplementary Table 2c,d**). The survival and respiration rates of the northern oysters (97.96%, 0.0024% as g^{-1} L^{-1} h^{-1}) were significantly higher than those of the southern oysters (58.27%, 0.00090% as g^{-1} L^{-1} h^{-1}, $p < 0.01$) in the northern habitats, while the northern oysters could not survive in the southern habitat. Southern oysters showed higher survival and respiration rates in their native environment (81.51%, 0.0023% as g^{-1} L^{-1} h^{-1}) than in the northern habitat ($p < 0.01$) (**Figures 3A,B**). The shell height of the southern oysters in the southern habitats (54.77 mm) was significantly

TABLE 1 | LT_{50}, LS_{50}, and third order regression equations for the northern (BZ) and southern (TS) oysters cultured in their native habitat when exposed to higher temperature and salinity.

Treatment	Population	Third order regression	r^2	*p*-value	LT/S_{50}
Temperature	North	$y = 0.0596x^3 - 8.244x^2 + 357.38x - 4863.9$	0.990	<0.01	40.32
	South	$y = -0.0427x^3 + 3.042x^2 - 54.32x + 108.75$	0.991	<0.01	41.11
Salinity	North	$y = -0.0014x^3 - 0.1022x^2 + 20.414x - 488.35$	0.983	<0.01	62.09
	South	$y = 0.0112x^3 - 2.1946x^2 + 134.44x - 2537.7$	0.984	<0.01	59.66

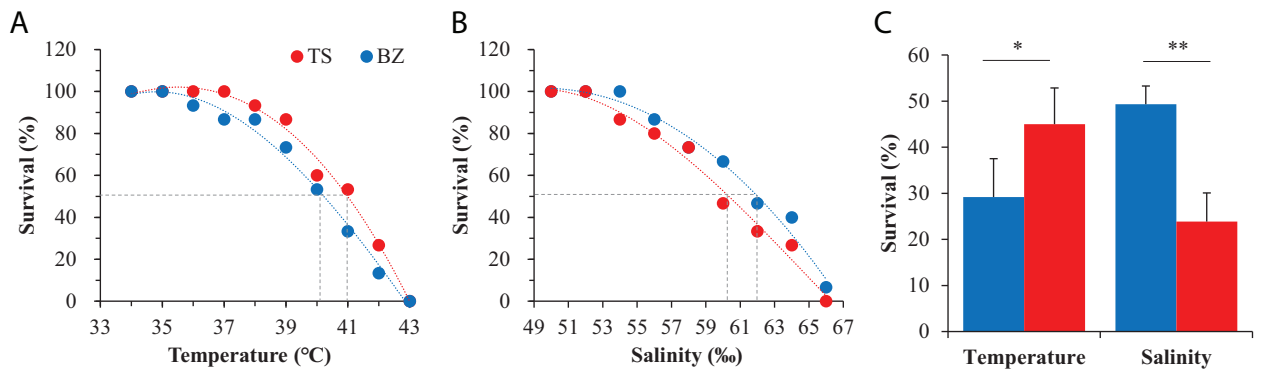

FIGURE 4 | Responses to heat shock and high salinity of the northern (BZ, blue) and southern (TS, red) oysters. **(A)** LT_{50} and **(B)** LS_{50} determinations for the northern and southern F_1 oysters in their native habitats when exposed to high temperature and salinity gradients, respectively. **(C)** Survival of the northern and southern F_1 progeny after exposure to the LT_{50} of the southern population and the LS_{50} of the northern population acclimated to the northern environment.

greater than that of their counterparts (35.52 mm, $p < 0.01$) and the northern oysters (34.42 mm, $p < 0.01$) in the northern habitats, and no difference was detected between the two populations in the northern habitat ($p = 0.32$) (**Figure 3C**). In addition, other growth parameters, including shell length, shell width, and wet weight, exhibited consistent differentiation patterns (**Supplementary Figure 2**).

Responses to High Salinity and Heat Stress in the Northern and Southern F_1 Oyster Populations

Preliminary experiments to evaluate the thermal tolerance limits indicated that 100% survival and mortality occurred at temperatures of 35°C and 45°C, respectively, in both oyster populations, and the tolerance limits of high salinity for 100% survival and mortality occurred at salinities of 50% and 65%, respectively (**Supplementary Figure 3**). Narrower stress ranges were used to determine LT_{50} and LS_{50} values. The survival data were significantly fit to third-order regressions for both oyster populations ($p < 0.01$, **Table 1**). Both oyster populations died at 43°C. There was no mortality at 35°C in the northern population or at 37°C in the southern population. Regression models predicted the LT_{50} to be 40.32°C for the northern oysters and 41.11°C for the southern oysters (**Figure 4A**). Southern oysters showed 100% survival and mortality at a salinity of 52% and 66%, respectively, while no mortality was observed at 54% for northern oysters. Regression models predicted the LS_{50} to be 62.09% for northern oysters and 59.66% for southern oysters (**Figure 4B**). For F_1 progenies of both oyster populations acclimated in the northern habitats, the southern oysters (45.0%) exhibited a significantly higher survival than their northern counterparts (29.2%) when exposed to the temperature of LT_{50} ($p < 0.05$), while the northern oysters (49.3%) exhibited a significantly higher survival than their southern counterparts (23.9%) when exposed to the salinity of LT_{50} ($p < 0.01$) (**Figure 4C**).

DISCUSSION

We collected 11 oyster populations of *C. ariakensis* throughout estuaries in China, ranging from the Bohai Sea and Yellow Sea in the north to the East and South China Seas in the south, which represent their natural distribution in China (Zhou and Allen, 2003; Wang et al., 2004). Phylogenetic analysis using HRM with an SNP of the neutral *COI* marker can clearly reveal genetic variation between northern and southern oyster populations whose melting curves are genetically distinctive. HRM analysis of the specific SNP in the mitochondrial *COI* gene segment can not only identify five common *Crassostrea* oysters in China (Wang et al., 2014), but can also distinguish between northern and southern populations of *C. ariakensis*. Moreover, compared to electrophoresis, this simple, fast, and high-throughput method could be applied to reliably and efficiently identify the existent natural hybrids from the unidirectional cross between *C. hongkongensis* eggs and *C. ariakensis* sperm (Zhang et al., 2017; Qin et al., 2020). This method is easy to visualize and can be extensively applied to studies of genetic diversity in *C. ariakensis*. Our findings were consistent with those of previous molecular taxonomic studies which found that *C. ariakensis* from

northern China, Korea, and Japan were more closely related, but did not share a common haplotype with the southern populations using polymorphic microsatellite markers, mitochondrial *COI* and 16S rRNA sequence variation, and nuclear ITS-1 locus (Wang et al., 2004; Zhang et al., 2005; Xiao et al., 2010; Kim et al., 2014). The molecular data indicate that biogeographic barriers, such as the Yangtze River estuary, exist and isolate the northern and southern *C. ariakensis* populations. The Yangtze River estuary is known to be a notable barrier for the distribution of many marine invertebrates with lower gene flow, such as two oyster congeners of *C. gigas* and *C. angulata* (Xu, 1997; Li et al., 2017), an interpopulation of limpet (*Cellana toreuma*) (Dong et al., 2012) and the bivalve *Cyclina sinensis* (Ni et al., 2012, 2017). Even marine species exhibiting high gene flow with high mobility or a long-term larval stage showed a distinctive genetic structure between the northern and southern coasts of the Yangtze River (Xu et al., 2009; Xiao et al., 2016). In addition, in line with a previous study (Xiao et al., 2010), oysters inhabiting the Yangtze River estuary were clustered with their northern counterparts. We propose that the interaction between coastal currents (Li L. et al., 2018) and the Yangtze River estuary potentially contributes in shaping the distribution of *C. ariakensis* in China.

Hybridization experiments between the northern and southern populations of *C. ariakensis* provide initial evidence to reject the hypothesis of reproductive isolation, and they should not be considered as two species (Wang et al., 2004; Zhang et al., 2005). Whether they should be considered two subspecies requires genomic variations in future studies to classify their taxonomic status by comparing the sequence variation between intra- and inter-specific oysters (Wang et al., 2010). The lower survival and growth rates of larvae bred from reciprocal hybrid crosses between the northern and southern populations than in those from intrapopulation crosses indicate that there is no intraspecific heterosis, which is concordant with interspecific reciprocal crosses between high-salt habit *C. gigas* and low-salt habit *C. ariakensis* in that their hybrids had lower fitness (Yao et al., 2015). For species distributed along similar environmental (salinity) gradients, however, significant interspecific heterosis was detected between *C. ariakensis* and *C. hongkongensis* (Qin et al., 2020). We propose that severe environmental variations (especially for temperature and salinity) and distant geographic distance strongly contribute to genetic incompatibility and subsequently influence the potential heterosis. In addition, environmental and maternal effects (Sanford and Kelly, 2011; Somero, 2012) showed that larvae bred from the eggs of southern oysters had higher fitness of survival and growth, which was also revealed in the hybrids crossed from *C. angulata* eggs and *C. gigas* sperms cultured in southern environments (Tan et al., 2020).

We found a strong signature of local adaptation based on the observations of adaptive differentiations of fitness-related phenotypes between the northern and southern populations. Oysters from the northern estuaries cannot survive in southern environments, and the survival, metabolic rate, and growth for both populations showed greater performance in their native habitats than in their translocated non-native habitats. These findings provide critical evidence for adaptive divergence between the northern and southern *C. ariakensis* in China, which supports previous observations of their differentiation using limited neutral markers (Wang et al., 2004; Zhang et al., 2005; Xiao et al., 2010; Kim et al., 2014). Adaptive divergence in these fitness-related traits as well as in physiological and molecular parameters was also found in two congeneric oyster species, *C. gigas* and *C. angulata*, which are naturally distributed along the northern and southern coasts of the Yangtze River, respectively (Wang et al., 2010; Beck et al., 2011), using the same experimental approaches by combining common garden and reciprocal transplantation (Li et al., 2017, 2018, 2019).

We detected greater climate gradients in both temperature and salinity between the monitored northern and southern locations; the northern locations had lower temperatures but higher salinity. We propose that the tremendous environmental variations resulting from these two fundamental factors have profound effects on adaptive capacity and shape the distribution of northern and southern estuarine oysters (Bozinovic et al., 2011; Sanford and Kelly, 2011; Somero, 2012; Nadeau et al., 2017). Correspondingly, estuarine oysters dwelling in the northern habitat evolved higher tolerance to high salinity (2.43‰), while their southern counterparts evolved higher thermotolerance (0.79°C). The results were in accordance with the general cognition that stress tolerance of organisms is highly related to the conditions of their microhabitats (Sanford and Kelly, 2011; Somero, 2012). Higher thermal tolerance for species/populations inhabiting southern or warmer environments has been pervasively observed in mussels, oysters, corals, and other marine species (Tomanek and Zuzow, 2010; Somero, 2012; Kenkel et al., 2013; Ghaffari et al., 2019). Therefore, we address whether the developmental stage and ambient environmental conditions can severely influence stress tolerance of marine species. The LT_{50} of immature animals of northern *C. gigas* and southern *C. angulata* was 2°C higher than that of mature oysters of northern and southern populations of *C. ariakensis,* respectively (Ghaffari et al., 2019), although the paired latitude and geographic distance and oceanographic conditions were similar. In addition, oysters derived from high-salinity environments evolved higher LS_{50}, which was consistent with our previous findings in eye-spot larvae using transcriptomic analysis (Liu et al., 2019). The higher survival rate of the F_1 progenies from southern oysters under heat shock and from northern oysters under high salinity after strong natural selection in northern environments indicated an evolved genetic basis for their higher stress tolerance. Further research focusing on comparative genomic analysis is needed to reveal the underlying adaptive mechanisms.

Regulation of energy metabolism is one of the critical responses of marine species for survival in challenging environments (Sokolova et al., 2012; Schulte, 2015). We noticed that both the northern and southern oyster populations had lower respiration rates in the translocated habitats than those in their native habitats. This finding indicates the protective role of metabolic repression of estuarine oysters as a physiological mechanism to increase their survivorship in response to non-native challenging environments, which is in agreement with the reduced metabolic index of other marine species suffering from global warming (Deutsch et al., 2015) as well as the calorie

restriction found in other stressed animals (Hebert et al., 2013; Vermeij et al., 2016). However, in contrast with the present results, our previous study found that the northern populations of Pacific oysters increase their metabolic rate to reach optimum fitness levels when translocated to the southern part of the environment (Li L. et al., 2018). We speculate that strong natural selection and intense biogeographic gradients compelled the estuarine oysters to decrease their metabolism in non-native habitats. Furthermore, the estuarine oysters grew slower in non-native habitats, suggesting energy allocation from growth to environmental stress tolerance, which is a pervasive adaptive strategy for adaptation to various changing climates in many marine species by trade-offs among different fitness-related traits (Sokolova et al., 2012; Han et al., 2013; Sussarellu et al., 2016; Li et al., 2017, Li L. et al., 2018). Integrative works focusing on physiological, molecular, and genomic regulations of energy allocation need to be investigated in future studies.

DATA AVAILABILITY STATEMENT

The original contributions presented in the study are included in the article/**Supplementary Materials**, further inquiries can be directed to the corresponding author.

AUTHOR CONTRIBUTIONS

LL and GZ conceived the study. AL carried out the field and laboratory work, participated in the data analysis, and drafted the manuscript. CW contributed to the field work and taxonomic analyses. AL, WW, ZS, ZJ, and LL collected the oyster samples and produced the F_1 progeny. AL, CW, WW, ZZ, ML, ZJ, and ZS contributed to experimental management at the North and South sites. AL, LL, and GZ revised the manuscript. All authors approved the manuscript for publication.

FUNDING

This work was supported by the Strategic Priority Research Program of the Chinese Academy of Sciences (No. XDA23050402 to LL) and National Key R&D Program of China (No. 2018YFD0900304 to LL), China Postdoctoral Science Foundation (No. 2019TQ0324 to AL), Key Deployment Project of Centre for Ocean Mega-Research of Science, Chinese Academy of Sciences (No. COMS2019Q06 to AL and LL), Distinguished Young Scientists Research Fund of the Key Laboratory of Experimental Marine Biology, Chinese Academy of Sciences (No. KLEMB-DYS04 to AL), Technology and Modern Agro-Industry Technology Research System (No. CARS-49 to LL), and Guangxi Key Laboratory of Beibu Gulf Marine Biodiversity Conservation (No. 2020ZB04 to ZJ).

ACKNOWLEDGMENTS

The authors would like to thank Xuegang Wang and Zemin Zhao for their support and assistance in oyster breeding, and Zhen Jia and Yeshao Peng for cultural management and sample collection at the southern site.

SUPPLEMENTARY MATERIAL

The Supplementary Material for this article can be found online at: https://www.frontiersin.org/articles/10.3389/fmars.2020.589099/full#supplementary-material

REFERENCES

Beck, M. W., Brumbaugh, R. D., Airoldi, L., Carranza, A., Coen, L. D., Crawford, C., et al. (2011). Oyster reefs at risk and recommendations for conservation, restoration, and management. *BioScience* 61, 107–116. doi: 10.1525/bio.2011.61.2.5

Bozinovic, F., Calosi, P., and Spicer, J. I. (2011). Physiological correlates of geographic range in animals. *Annu. Rev. Ecol. Evol. Syst.* 42, 155–179. doi: 10.1146/annurev-ecolsys-102710-145055

Burford, M. O., Scarpa, J., Cook, B. J., and Hare, M. P. (2014). Local adaptation of a marine invertebrate with a high dispersal potential: evidence from a reciprocal transplant experiment of the eastern oyster *Crassostrea virginica*. *Mar. Ecol. Prog. Ser.* 505, 161–175. doi: 10.3354/meps10796

Dayan, D. I., Crawford, D. L., and Oleksiak, M. F. (2015). Phenotypic plasticity in gene expression contributes to divergence of locally adapted populations of Fundulus heteroclitus. *Mol. Ecol.* 24, 3345–3359. doi: 10.1111/mec.13188

De Wit, P., and Palumbi, S. R. (2013). Transcriptome-wide polymorphisms of red abalone (Haliotis rufescens) reveal patterns of gene flow and local adaptation. *Mol. Ecol.* 22, 2884–2897. doi: 10.1111/mec.12081

Deutsch, C., Ferrel, A., Seibel, B., Pörtner, H.-O., and Huey, R. B. (2015). Climate change tightens a metabolic constraint on marine habitats. *Science* 348, 1132–1135. doi: 10.1126/science.aaa1605

Dong, Y., Wang, H., Han, G., Ke, C., Zhan, X., Nakano, T., et al. (2012). the impact of yangtze river discharge, ocean currents and historical events on the biogeographic pattern of *Cellana toreuma* along the China Coast. *PLoS One* 7:e36178. doi: 10.1371/journal.pone.0036178.g001

Ghaffari, H., Wang, W., Li, A., Zhang, G., and Li, L. (2019). Thermotolerance divergence revealed by the physiological and molecular responses in two oyster subspecies of *Crassostrea gigas* in China. *Front. Physiol.* 10:1137. doi: 10.3389/fphys.2019.01137

Gundry, C. N., Dobrowolski, S. F., Martin, Y. R., Robbins, T. C., Nay, L. M., Boyd, N., et al. (2008). Base-pair neutral homozygotes can be discriminated by calibrated high-resolution melting of small amplicons. *Nucleic Acids Res.* 36, 3401–3408. doi: 10.1093/nar/gkn204

Guo, X., Li, C., Wang, H., and Xu, Z. (2018). Diversity and evolution of living oysters. *J. Shellfish Res.* 37, 755–771. doi: 10.2983/035.037.0407

Guo, X. M., Ford, S. E., and Zhang, F. S. (1999). Molluscan aquaculture in China. *J. Shellfish Res.* 18, 19–31.

Han, G. D., Zhang, S., Marshall, D. J., Ke, C. H., and Dong, Y. W. (2013). Metabolic energy sensors (AMPK and SIRT1), protein carbonylation and cardiac failure as biomarkers of thermal stress in an intertidal limpet: linking energetic allocation with environmental temperature during aerial emersion. *J. Exp. Biol.* 216(Pt 17), 3273–3282. doi: 10.1242/jeb.084269

Hebert, A. S., Dittenhafer-Reed, K. E., Yu, W., Bailey, D. J., Selen, E. S., Boersma, M. D., et al. (2013). Calorie restriction and SIRT3 trigger global reprogramming of the mitochondrial protein acetylome. *Mol. Cell* 49, 186–199. doi: 10.1016/j.molcel.2012.10.024

Kenkel, C. D., Meyer, E., and Matz, M. V. (2013). Gene expression under chronic heat stress in populations of the mustard hill coral (*Porites astreoides*) from different thermal environments. *Mol. Ecol.* 22, 4322–4334. doi: 10.1111/mec.12390

Kim, W.-J., Dammannagoda, S. T., Jung, H., Baek, I. S., Yoon, H. S., and Choi, S. D. (2014). Mitochondrial DNA sequence analysis from multiple gene fragments reveals genetic heterogeneity of *Crassostrea ariakensis* in East Asia. *Genes Genomics* 36, 611–624. doi: 10.1007/s13258-014-0198-5

Li, A., Li, L., Song, K., Wang, W., and Zhang, G. (2017). Temperature, energy metabolism, and adaptive divergence in two oyster subspecies. *Ecol. Evol.* 7, 6151–6162. doi: 10.1002/ece3.3085

Li, A., Li, L., Wang, W., Song, K., and Zhang, G. (2018). Transcriptomics and fitness data reveal adaptive plasticity of thermal tolerance in oysters inhabiting different tidal zones. *Front. Physiol.* 9:825. doi: 10.3389/fphys.2018.00825

Li, L., Li, A., Song, K., Meng, J., Guo, X., Li, S., et al. (2018). Divergence and plasticity shape adaptive potential of the Pacific oyster. *Nat. Ecol. Evol.* 2, 1751–1760. doi: 10.1038/s41559-018-0668-2

Li, A., Li, L., Wang, W., and Zhang, G. (2019). Evolutionary trade-offs between baseline and plastic gene expression in two congeneric oyster species. *Biol. Lett.* 15:20190202. doi: 10.1098/rsbl.2019.0202

Limborg, M. T., Helyar, S. J., Bruyn, M. D., Martin, I. T., Einar, E. N., Rob, O., et al. (2012). Environmental selection on transcriptome-derived SNPs in a high gene flow marine fish, the Atlantic herring (*Clupea harengus*). *Mol. Ecol.* 21, 3686–3703.

Liu, X., Li, L., Li, A., Li, Y., Wang, W., and Zhang, G. (2019). Transcriptome and gene coexpression network analyses of two wild populations provides insight into the high-salinity adaptation mechanisms of *Crassostrea ariakensis*. *Mar. Biotechnol.* 21, 596–612. doi: 10.1007/s10126-019-09896-9

Nadeau, C. P., Urban, M. C., and Bridle, J. R. (2017). Climates past, present, and yet-to-come shape climate change vulnerabilities. *Trends Ecol. Evol.* 32, 786–800. doi: 10.1016/j.tree.2017.07.012

Ni, G., Kern, E., Dong, Y. W., Li, Q., and Park, J. K. (2017). More than meets the eye: the barrier effect of the Yangtze River outflow. *Mol. Ecol.* 26, 4591–4602. doi: 10.1111/mec.14235

Ni, G., Li, Q., Kong, L., and Zheng, X. D. (2012). Phylogeography of bivalve Cyclina sinensis: testing the historical glaciations and Changjiang River outflow hypotheses in northwestern Pacific. *PLoS One* 7:e49487. doi: 10.1371/journal.pone.0049487.g001

Qin, Y. P., Li, X. Y., Noor, Z., Li, J., Zhou, Z. H., Ma, H. T., et al. (2020). A comparative analysis of the growth, survival and reproduction of Crassostrea hongkongensis. *Crassostrea ariakensis*, and their diploid and triploid hybrids. *Aquaculture* 520:734946.

Sanford, E., and Kelly, M. W. (2011). Local adaptation in marine invertebrates. *Ann. Rev. Mar. Sci.* 3, 509–535. doi: 10.1146/annurev-marine-120709-142756

Schulte, P. M. (2015). The effects of temperature on aerobic metabolism: towards a mechanistic understanding of the responses of ectotherms to a changing environment. *J. Exp. Biol.* 218(Pt 12), 1856–1866. doi: 10.1242/jeb.118851

Sokolova, I. M., Frederich, M., Bagwe, R., Lannig, G., and Sukhotin, A. A. (2012). Energy homeostasis as an integrative tool for assessing limits of environmental stress tolerance in aquatic invertebrates. *Mar. Environ. Res.* 79, 1–15. doi: 10.1016/j.marenvres.2012.04.003

Somero, G. N. (2012). The physiology of global change: linking patterns to mechanisms. *Ann. Rev. Mar. Sci.* 4, 39–61. doi: 10.1146/annurev-marine-120710-100935

Sussarellu, R., Suquet, M., Thomas, Y., Lambert, C., Fabioux, C., Pernet, M. E., et al. (2016). Oyster reproduction is affected by exposure to polystyrene microplastics. *Proc. Natl. Acad. Sci. U.S.A.* 113, 2430–2435. doi: 10.1073/pnas.1519019113

Tan, K., Liu, H., Ye, T., Ma, H., Li, S., and Zheng, H. (2020). Growth, survival and lipid composition of *Crassostrea gigas*, *C. angulata* and their reciprocal hybrids cultured in southern China. *Aquaculture* 516:734524. doi: 10.1016/j.aquaculture.2019.734524

Tomanek, L., and Zuzow, M. J. (2010). The proteomic response of the mussel congeners *Mytilus galloprovincialis* and *M. trossulus* to acute heat stress: implications for thermal tolerance limits and metabolic costs of thermal stress. *J. Exp. Biol.* 213(Pt 20), 3559–3574. doi: 10.1242/jeb.041228

Vermeij, W. P., Dolle, M. E., Reiling, E., Jaarsma, D., Payan-Gomez, C., Bombardieri, C. R., et al. (2016). Restricted diet delays accelerated ageing and genomic stress in DNA-repair-deficient mice. *Nature* 537, 427–431. doi: 10.1038/nature19329

Wang, H., and Guo, X. (2008). Identification of *Crassostrea ariakensis* and related oysters by multiplex species-specific PCR. *J. Shellfish Res.* 27, 481–487.

Wang, H., Guo, X., Zhang, G., and Zhang, F. (2004). Classification of jinjiang oysters Crassostrea rivularis (Gould, 1861) from China, based on morphology and phylogenetic analysis. *Aquaculture* 242, 137–155. doi: 10.1016/j.aquaculture.2004.09.014

Wang, H., Qian, L., Liu, X., Zhang, G., and Guo, X. (2010). Classification of a common cupped oyster from southern China. *J. Shellfish Res.* 29, 857–866. doi: 10.2983/035.029.0420

Wang, H., Qian, L., Zhang, G., Liu, X., Wang, A., Shi, Y., et al. (2006). Distribution of *Crassostrea ariakensis* in China. *J. Shellfish Res.* 25, 789–790.

Wang, H., Zhang, G., Liu, X., and Guo, X. (2008). Classification of Common Oysters from North China. *J. Shellfish Res.* 27, 495–503.

Wang, J., Qi, H., Li, L., Que, H., Wang, D., and Zhang, G. (2015). Discovery and validation of genic single nucleotide polymorphisms in the Pacific oyster *Crassostrea gigas*. *Mol. Ecol. Resour.* 15, 123–135. doi: 10.1111/1755-0998.12278

Wang, J., Xu, F., Li, L., and Zhang, G. (2014). A new identification method for five species of oysters in genus Crassostrea from China based on high-resolution melting analysis. *Chin. J. Oceanol. Limnol.* 32, 419–425. doi: 10.1007/s00343-014-3124-4

Xiao, J., Cordes, J. F., Wang, H., Guo, X., and Reece, K. S. (2010). Population genetics of *Crassostrea ariakensis* in Asia inferred from microsatellite markers. *Mar. Biol.* 157, 1767–1781. doi: 10.1007/s00227-010-1449-x

Xiao, Y., Ma, D., Dai, M., Liu, Q., Xiao, Z., Li, J., et al. (2016). The impact of Yangtze River discharge on the genetic structure of a population of the rock bream,Oplegnathus fasciatus. *Mar. Biol. Res.* 12, 426–434. doi: 10.1080/17451000.2016.1154576

Xu, F. (1997). *Bivalve Mollusca of China Seas*. Beijing: Science Press.

Xu, J., Chan, T. Y., Tsang, L. M., and Chu, K. H. (2009). Phylogeography of the mitten crab Eriocheir sensu stricto in East Asia: pleistocene isolation, population expansion and secondary contact. *Mol. Phylogenet. Evol.* 52, 45–56. doi: 10.1016/j.ympev.2009.02.007

Yao, T., Zhang, Y., Yan, X., Wang, Z., Li, D., Su, J., et al. (2015). Interspecific hybridization between *Crassostrea angulata* and *C. ariakensis*. *J. Ocean Univ. China* 14, 710–716. doi: 10.1007/s11802-015-2546-8

Zhang, Q., Allen, S. K. Jr., and Reece, K. S. (2005). Genetic variation in wild and hatchery stocks of Suminoe Oyster (*Crassostrea ariakensis*) assessed by PCR-RFLP and microsatellite markers. *Mar. Biotechnol.* 7, 588–599. doi: 10.1007/s10126-004-5105-7

Zhang, Y., Zhang, Y., Li, J., and Yu, Z. (2017). Morphological and molecular evidence of hybridization events between two congeneric oysters, *Crassostrea hongkongensis* and *C. ariakensis*, in southern China. *J. Molluscan Stud.* 83, 129–131. doi: 10.1093/mollus/eyw035

Zhou, M. F., and Allen, S. K. (2003). A review of published work on *Crassostrea ariakensis*. *J. Shellfish Res.* 22, 1–20.

Conflict of Interest: The authors declare that the research was conducted in the absence of any commercial or financial relationships that could be construed as a potential conflict of interest.

frontiers in Marine Science

ORIGINAL RESEARCH
published: 12 November 2020
doi: 10.3389/fmars.2020.589195

Diversity and Functional Patterns of Benthic Amphipods in the Coralline Intertidal Zones of a Marine National Park, India

Tatiparthi Srinivas[1], Soniya Sukumaran[1], S. Neetu[2] and K. Ramesh Babu[3]*

[1] CSIR-National Institute of Oceanography, Regional Centre, Mumbai, India, [2] CSIR-National Institute of Oceanography, Panaji, India, [3] Department of Marine Living Resources, College of Science and Technology, Andhra University, Visakhapatnam, India

Coralline intertidal habitats of marine protected areas (MPAs) are important model systems to investigate species diversity and ecological functioning of benthic communities. Spatial variability of amphipod species composition and functional traits were studied over a 3 year period during the summer season at five intertidal transects of the Gulf of Kachchh (GoK) MPAs, India. A total of 22,706 individuals, comprising 71 species belonging to 40 genera and 23 families, were identified. Aoridae, Dexaminidae, Eriopisidae, Lysianassidae, and Maeridae were the best represented families (68.2% of total abundance). Distinct spatial patterns in the amphipod assemblage structure and functional traits were observed along the horizontal and vertical axes. The results demonstrated that the amphipod assemblage functioning was greatly influenced by the vertical gradient, with generally higher functional diversity (FD) in the lower intertidal zones suggesting increased diversity in resource use strategies, whereas the upper zones showed very little FD possibly due to the prevalence of environmental filtering. As higher species and functional diversities promote better resource partitioning and resilience of the ecosystem, these results are important for the management of MPAs facing the dual challenges of global climate change and anthropogenic pressures.

Keywords: intertidal, amphipod, vertical zonation, functional traits, fuzzy coding, Marine National Park

OPEN ACCESS

Edited by:
Puri Veiga,
University of Porto, Portugal

Reviewed by:
Daniel Pech,
The South Border College (ECOSUR), Mexico
Nicolas Sturaro,
University of Mons, Belgium

****Correspondence:***
Soniya Sukumaran
soniya@nio.org

Specialty section:
This article was submitted to Marine Evolutionary Biology, Biogeography and Species Diversity, a section of the journal Frontiers in Marine Science

Received: *30 July 2020*
Accepted: *15 October 2020*
Published: *12 November 2020*

Citation:
Srinivas T, Sukumaran S, Neetu S and Ramesh Babu K (2020) Diversity and Functional Patterns of Benthic Amphipods in the Coralline Intertidal Zones of a Marine National Park, India. Front. Mar. Sci. 7:589195. doi: 10.3389/fmars.2020.589195

INTRODUCTION

Intertidal habitats are dynamic marine environments present at the interface of sea and land and encompass numerous environmental gradients (Underwood, 2000; Pandey and Thiruchitrambalam, 2018). Horizontal variation in floral and faunal composition in intertidal habitats is determined by a combination of biotic interactions, abiotic factors, dispersal processes, and priority effects (i.e., competitive dominance given by early colonization) (Catalán et al., 2020). Apart from the strong spatial horizontal variations, the characteristic feature of regular alternation of high and low tides also causes ubiquitous patterns of species distribution along the vertical axis (i.e., vertical zonation) (Valdivia et al., 2011; Catalán et al., 2020). A strong gradient of environmental conditions such as desiccation, thermal stress, food, and shelter from predators support clear intertidal zonation patterns of diverse intertidal organisms.

Significant works conducted on the diversity and distributional trends of organisms along the vertical axis on intertidal habitats have resulted in the establishment of diverse models on distribution patterns of various benthic communities (Araújo et al., 2005). Critical tidal levels (upper shore, middle shore, and lower shore) are primary determinants in establishing the community zonation patterns of intertidal organisms (Southward, 1958; Lewis, 1964; Newell, 1970).

Intertidal zones are susceptible to the potential effects of climate change as these zones naturally face varying environmental conditions and hydrodynamic forcing (Harley et al., 2006). Hence, the knowledge on the complex patterns presented by its inhabitants is critical toward management of these areas and provides a basis for predicting the impacts of climate change. Quantitative information of distribution patterns of different faunal groups is intrinsic to facilitate adequate and representative conservation of biodiversity (Blanchette et al., 2008), more so in coralline intertidal marine protected areas (MPAs). Despite its ecological importance, the tropical coralline intertidal is a poorly understood ecosystem and hence requires multi-pronged studies investigating its abiotic and biotic components and their interactions for evolving effective management strategies (Sindorf et al., 2015).

While the identity of organisms is important to study the community structure, it is also equally essential to understand their functioning within the ecosystem. Functional characteristics of macrobenthos, being an important link connecting biodiversity and ecosystem functioning, are gaining more credence in ecological studies (Wong and Dowd, 2015). It is often beneficial to combine biological trait analysis (BTA) techniques along with the routine diversity studies to gain a better understanding of the structural and functional dynamics of the macrobenthic communities (Bremner, 2005). Changes in functional diversity (FD) are more relied upon now than before to evaluate the impact of various disturbances on the ecology. Systems with high taxonomical and FD are considered to be balanced and impervious to environmental fluctuations (Bellwood et al., 2003).

Among the ecologically important benthic groups that abound in the coralline intertidal zones, Amphipoda are one of the most diverse and abundant peracarid crustacean groups (Thomas, 1993; Conlan, 1994; de-la-Ossa-Carretero et al., 2012). In addition, they constitute a significant source of food for many higher trophic level organisms (Duffy, 2006; Sanz-Lázaro and Marín, 2011; Legeżyńska et al., 2012) and also act as important contributor of marine benthic productivity (Conradi and Cervera, 1995; Guerra-García et al., 2014). Benthic amphipods are known to play significant role in mineralization of sediment through their bio irrigation and feeding activities (Paz-Ríos and Ardisson, 2018). They are used in many marine monitoring studies as indicators of pollution due to their sensitivity to various environmental disturbances (de-la-Ossa-Carretero et al., 2012, 2016). Due to the lack of a pelagic larval stage and their infaunal behavior, benthic amphipods display low dispersion capabilities causing high levels of endemism and high species diversity in a small geographical area (Paz-Ríos et al., 2019). Intertidal zones are one of the most preferred habitats for many species of benthic amphipods (Surya Rao, 1972) and this group exhibits a variety of lifestyles that display clear habitat preferences (McLachlan, 1983; Wildish, 1988; Brown and McLachlan, 1990; Yu et al., 2002).

Unlike the Polychaeta, the Amphipoda has received scant attention and very little is known on their distribution, ecology, and functioning from the Indian subcontinent (Srinivas et al., 2019). The biodiversity of amphipods in estuaries, intertidal, and shallow coastal areas from east and west coasts of India has been increasingly investigated during the last decade (Guerra-García et al., 2010; Mondal et al., 2010; Rehitha et al., 2019). The documented information available so far is restricted to taxonomical studies including descriptions of new taxa (Myers et al., 2018, 2019), inventory of species (Lyla et al., 1998; Guerra-García et al., 2010), and community structure of amphipods from estuarine and shallow coastal habitats (Nair et al., 1983; Mondal et al., 2010; Raja et al., 2013).

The present study is the first attempt at describing the diversity, distributional, and functional patterns of benthic amphipods in the coralline habitats of the Gulf of Kachchh (GoK), which is a relatively well-conserved coral reef ecosystem in the Indian subcontinent. Since its establishment as a Marine National Park in 1980 and as a Sanctuary in 1982 (MNPS), this reef ecosystem has been subjected to various biodiversity surveys, primarily of corals (Adhavan et al., 2014; Kumar et al., 2014), seagrass (Kamboj, 2014), seaweeds (Roy et al., 2015), reef-dependent ichthyofauna (Parmar et al., 2015), brachyurans (Trivedi et al., 2012), and a brief exploration on macrobenthic communities from shallow coastal environments (Sukumaran et al., 2013). Despite their ecological significance, so far, the amphipods have not been investigated. Species inventories and distribution patterns of major faunal groups are essential for the success of long-term monitoring programs and to develop effective management strategies for sensitive biomes like the tropical coralline zones. Hence, this study was designed to analyze the species distribution and functional patterns of benthic amphipods along the horizontal and vertical gradients of five intertidal transects of the GoK MNPS (**Figure 1**). We hypothesized distinct variations in amphipod diversity along the vertical gradient of the intertidal zones. It was also expected that the vertical variations would be prominent than horizontal patterns. We further investigated whether the amphipod functional patterns mirrored that of taxonomic diversity? To check the consistency of patterns the sampling was repeated for three consecutive years, i.e., 2016, 2017, and 2018.

MATERIALS AND METHODS

Study Site

The GoK is a semi-enclosed sea located in the north-eastern part of the Arabian Sea, occupying a total area of about 7350 km^2 and has one of the four major reef ecosystems of the country on its southern coast. To protect its unique marine ecosystem, an area which extends from Okha (22°30'N, 69°00'E) in the west, to Navlakhi (22°30'N, 70°40'E) in the east, has been designated as MNPS during 1980–1982 under the provisions of the Wildlife (Protection) Act, 1972 of India (Dixit et al., 2010). The MNPS

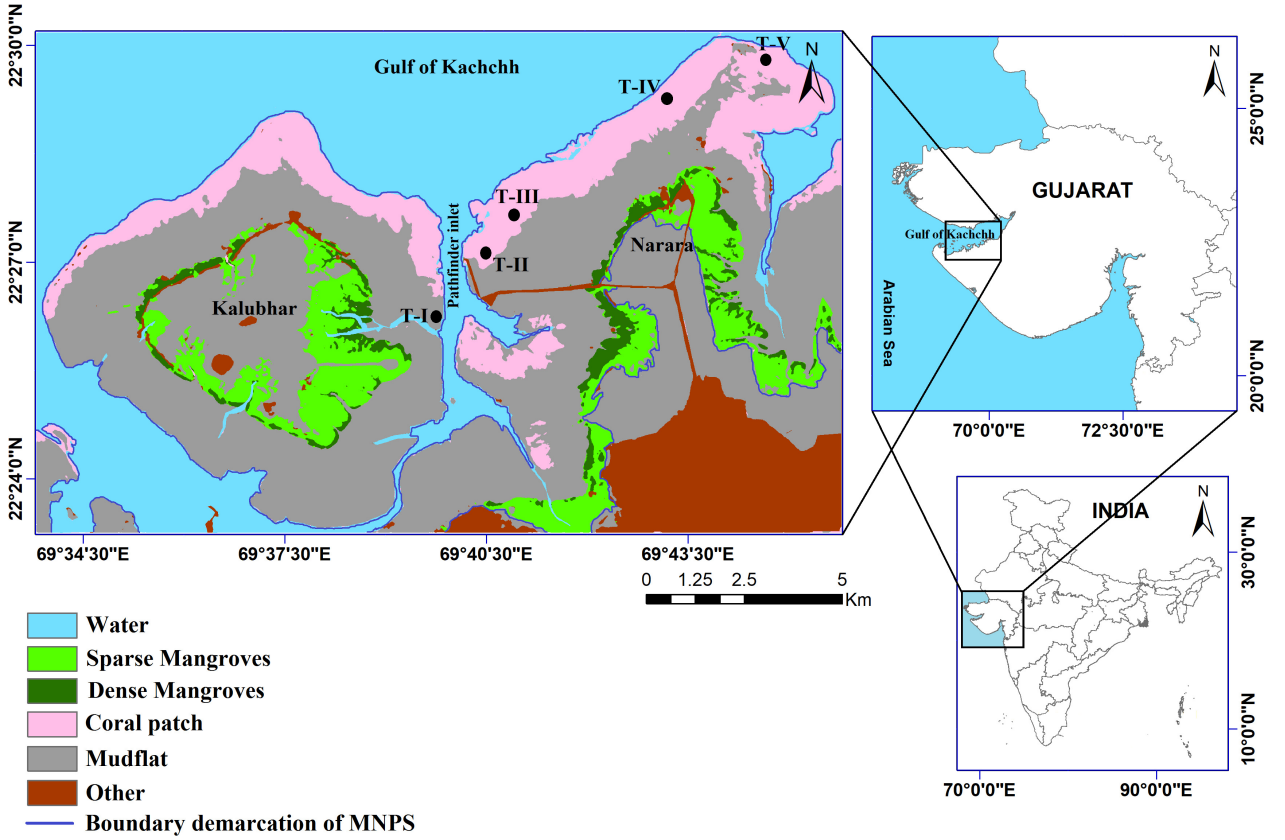

FIGURE 1 | Study area showing the sampling transects along the Gulf of Kachchh Marine National Park and Sanctuary.

supports diverse habitats; including coral reefs, mangrove forests, sandy beaches, mudflats, creeks, rocky coast, sea grass beds, and wide intertidal regions (Satyanarayana and Ramakrishna, 2009). Tides in the GoK are of mixed, predominantly semi-diurnal in nature with a large diurnal inequality (Dixit et al., 2010). Climate of the MNPS is hot and humid and temperature ranges from 7.8°C during winter to 44.8°C during summer (Sukumaran et al., 2013). The characteristics of less rain and more evaporation make the Gulf waters more saline (36 to 44.5). The GoK has one major port, several intermediate and minor ports, fishing harbors, and Single Point Moorings (SPM) associated with oil refineries, in addition to jetties, breakwaters, submarine pipelines, marine intake, and outfall points (National Institute of Oceanography [NIO], 2018).

Five intertidal locations were selected along the Kalubhar (one site on eastern part of the Island; T-I) and Narara islands (four sites; T-II, T-III, T-IV, and T-V) (**Figure 1**). Kalubhar and Narara reefs are integral part of MNPS and consist of dense patches of corals in their subtidal and intertidal zones. Narara Bet (Island) is a tidal wetland, attached to the mainland. The eastern side of the bet is separated from Sikka reef by Gagwa creek whereas the western side of the bet is separated from Kalubhar Island by Pathfinder inlet. The tidal maximum during the spring tide is 4.85 m and during neap tide, it is about 2.65 m. Therefore, during the low tide, the intertidal flat is exposed for about 3–5 km, and has substrata that are mainly sandy, rocky, and small mudflats. Kalubhar is a rectangle type island, bordered by mangrove formations and broad encircled reef areas. The island is separated from the mainland by the Salaya creek in the west, the Pathfinder Inlet in the south and east with Gulf to the north. In order to better understand the habitat structure of the studied intertidal transects, prior to sample collection, an overview of the area was made from high water level to low water level. The intertidal region at T-I is exposed about 1.5 km long. Here, mud is the major benthic component observed from the lower to upper shore. The intertidal expanses of T-II to T-V ranged from 2 to 2.5 km, comprising large number of coral colonies and their associated flora and fauna at their lower shore level. At the middle shore of these transects, rocks and boulders covered with silt were the dominant benthic component. The higher intertidal regions of T-II to T-V had mainly mangrove mud.

Sampling

For this study, the intertidal areas were divided into three zones, i.e., upper shore (henceforth HW), middle shore (henceforth MW), and lower shore (henceforth LW). Sampling was constrained during the summer season (April–May) for three consecutive years (2016, 2017, and 2018) to avoid seasonal influences in species distributional patterns. At all transects with

TABLE 1 | List of functional traits and modalities used in this study along with corresponding codes with indication of the rational for the selection of the traits.

Functional Trait	Trait Modalities	Codes	Rationale for functional traits selection
Mobility (M)			Despite the generally low mobility characteristic of macrobenthic invertebrates (Warwick, 1993), the small-scale mobility of these organisms is essential for the ecology of benthic communities not only regarding the avoidance of physical disturbance (Hinchey et al., 2006) but also in the prey-predatory activities Piló et al., 2016).
	Discretely motile	M.D	
	Motile	M.M	
Habitat (H)	Free living	H.F	Indicates food source availability, influences bioturbation processes and may indicate disturbance. When disturbance increases, only species with specific combinations of traits suitable for survival pass through the environmental filter (Southwood, 1977). For instance, burrow and tube dwellers are expected to increase after disturbance (e.g. anoxic conditions, organic pollution), as opposed to surface dwelling species, as they have some protection from tube or burrow linings and are more likely to have pumping/irrigation features for oxygenation (Reise, 2002, van der Linden et al., 2017).
	Tube building	H.T	
	Burrowing	H.B	
Feeding mode (F)	Detritus feeders	F.DT	Reflects the trophic structure, resources distribution and how organisms adapt to the residential habitat (Bremner, 2008; Webb et al., 2009). Trophic diversity is higher in healthy environment owing to the presence of higher species diversity whereas it decreases in disturbed environment due to the dominance of opportunistic species (Gamito and Furtado, 2009).
	Suspension feeders	F.SU	
	Subsurface deposit feeder	F.SSDE	
	Browsers	F.BR	
	Grazers	F.GR	
	Scavengers	F.SC	
	Predators	F.PR	
Bioturbation (B)	Surface modifiers	B.S	Bioturbation, also known to have an ecosystem engineering function (Kristensen et al., 2012) is strongly linked with an organism's mobility (Pearson, 2001) and mode of feeding that cause movement of sediment particles within the habitat (Dauwe et al., 1998).
	Biodiffusors	B.B	
	Epifauna	B.E	
Size (S)	Very small (<1cm)	S.Vs	Defines and associates with other biological traits, mediates other structuring interactions (Mouillot et al., 2006; Webb et al., 2009). Small-bodied invertebrates may characterise environments with high instability, consequence of abiotic pressures imposed on the organisms (Mouillot et al., 2006). This biometric parameter can be more responsible for the trophic structure than taxonomic identity itself (Jennings et al., 2001).
	Small (1-2cm)	S.S	
	Small-medium (3-10cm)	S.S-M	

the exception of T-I, the samples were collected during spring low tides using a quadrat of 20 × 20 cm (0.04 m^2) at each zone (considered as station). At T-I, due to the difficulty in walking over the vast stretches of soft mud, the sediment samples were collected by boat during spring high tides using a van Veen grab (0.04 m^2). To avoid bias in the results by using different sampling methods between different transects (transect T-I vs other transects), similar area, i.e., 0.04 m^2 was sampled.

During 2016 and 2017, the sediment samples were collected in triplicates at each location, whereas in 2018 the samples were collected in quadruplicates. In quadrat sampling method, all the surface sediment was scraped to a depth of 10 cm and collected in a 500 microns mesh sieve. Similarly in grab sampling method too, upper 10 cm sediment was collected and transferred to a 500 microns mesh sieve. Later the collected sediment samples were sieved and all the organisms retained on sieve were transferred to a plastic bag and preserved with 5% formalin mixed with Rose Bengal solution. In the laboratory, the samples were sieved again and the amphipod crustaceans were separated from the rest of the macrobenthic groups. The separated amphipods were quantified and identified to a lower taxonomic level by using standard identification keys (Barnard, 1979; Lincoln, 1979; Lyla et al., 1998).

Data Analysis

The mean abundance of amphipods collected from the all replicate samples at each shore level was expressed as number of individuals per m^2 (ind m^{-2}). The amphipod abundance data were subjected to univariate diversity measures [e.g., total average abundance—*N*; Margalef's richness index—*d*; Pielou's evenness Index—*J'*; and Shannon–Wiener diversity index—*H'* (log_2)]. Analyses of variance (one-way ANOVA) were performed to test for the differences in the univariate diversity measures using Statistica 7. Prior to ANOVA, data were first examined for normality using Shapiro–Wilk's W test. Data were log transformed when the assumptions of variance were significantly different. For multivariate analyses, the mean amphipod abundance data at each shore level were fourth-root transformed to downweight the influence of numerically dominant species, which were used to construct the similarity index using Bray–Curtis similarity coefficient. The spatial distribution of amphipod assemblages was visualized by using non-metric multidimensional scaling (nMDS).

To test for potential significant differences among different transects, zones, and years in amphipod composition, permutational multivariate analyses of variance (PERMANOVA) was performed. A three-way crossed PERMANOVA was

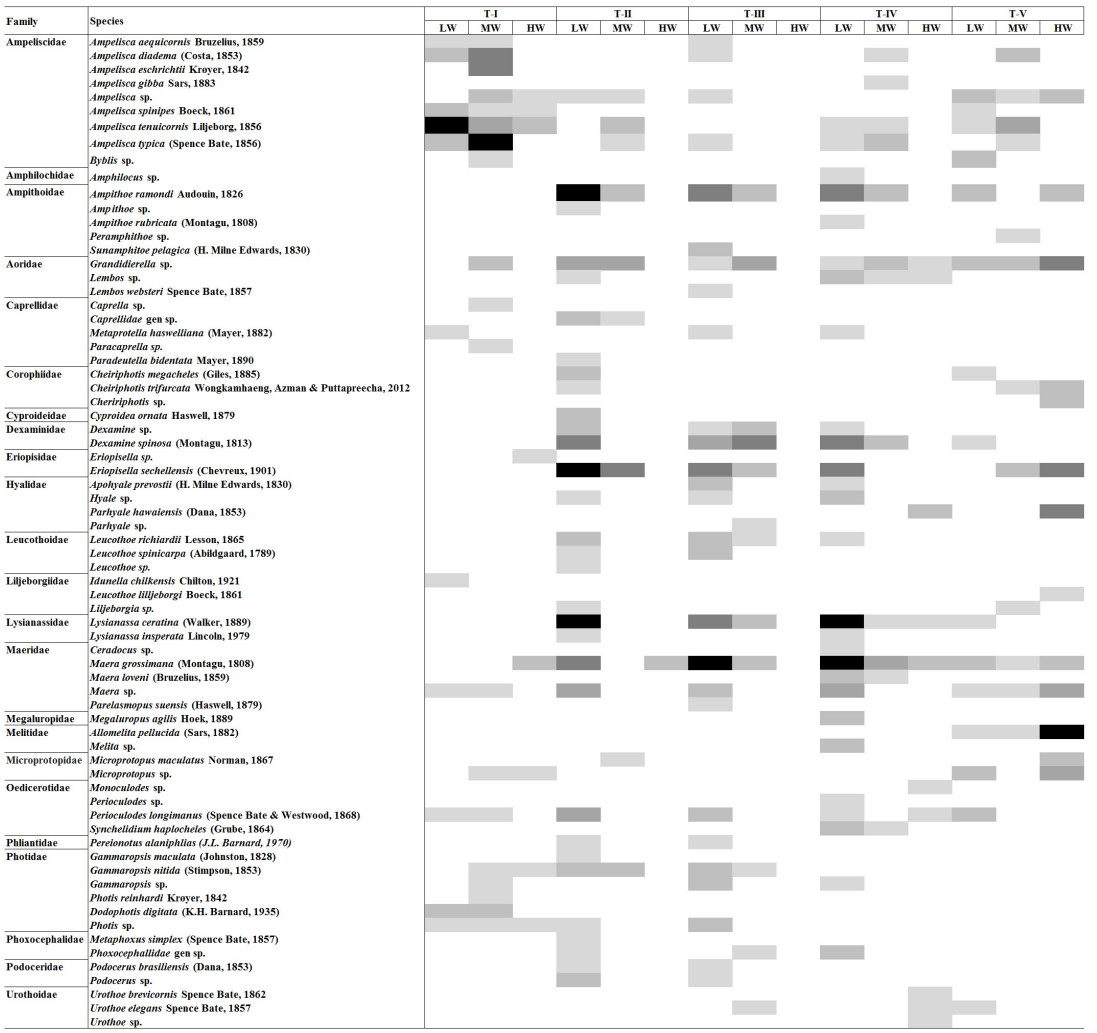

FIGURE 2 | Shade plot illustrating the mean amphipod abundance (ind/m^2) across different transects and shore levels. LW, low shore; MW, mid shore; HW, upper shore.

performed on the Bray–Curtis similarity matrix in order to test the null hypothesis of no significant differences in the multivariate structure and composition of amphipod assemblages between the transects, shore levels, and years. The PERMANOVA design included two fixed factors: "shore levels" with three levels (HW, MW, and LW) and "year" with three levels (2016, 2017, and 2018) and one random factor: "transect" with five levels (T-I, T-II, T-III, T-IV, and T-V). Significant terms were investigated using *a posteriori* pairwise comparisons between transects, shorelines, and years with the PERMANOVA t-statistic and permutations under a reduced model. For the tests, 9999 random permutations were used and a significance level (p) of 0.05 was considered. A similarity percentage analysis (SIMPER) was conducted on fourth root transformed amphipod abundance data to further investigate the amphipod species contributing to the differences between the transects, shorelines, and sampling years. Only species contributing up to 50% to differences were considered in the analysis, thus focusing on the most common species. All the univariate and multivariate analyses were conducted using the PRIMER v.7 software (Clarke and Gorley, 2015) and PERMANOVA analyses were done using the PERMANOVA + PRIMER add-on package (Anderson et al., 2008).

Biological Trait Analysis (BTA)

To analyze the functional characteristics of the amphipod assemblages, five traits (mobility, habitat, feeding mode, bioturbation, and body size) subdivided into 18 categories were selected (**Table 1**). The information of these traits was extracted from a variety of sources, mostly published papers (Macdonald et al., 2010; de-la-Ossa-Carretero et al., 2012; Queirós et al., 2013; Guerra-García et al., 2014) and websites (Biological Traits Information Catalog—BIOTIC, MarLIN, 2006 and Marine Species Traits editorial board, 2019). When information for individual species was not available, data from other species belonging to the same genus were used.

A fuzzy coding approach was employed wherein a score was assigned to each species according to its affinity with the different functional trait categories (Chevenet et al., 1994). In this procedure, a scale was adopted ranging from 0 to 3 for each trait category, where no affinity was coded as 0 and complete affinity was coded as 3. To conduct BTA, three different types of data matrices were required: (a) "taxa by station" (taxa abundance at each zone); (b) "taxa by traits" (biological traits for each taxon); and (c) "traits by station" (biological traits at each zone). To achieve the "traits by station" matrix, trait categories for each taxon present at a zone were multiplied by their abundance at that station, and then summed over all taxa present at each station to obtain a single value for each trait category (Bremner et al., 2006). The resulting "traits by station" data matrix was then subjected to Fuzzy correspondence analysis (FCA) analysis to identify the differences in functional composition between transects and zones which was visualized on an FCA plot. FD of amphipod assemblages was estimated by using Rao's quadratic entropy index (Rao, 1982; Paganelli et al., 2012). FCA was performed with R-3.5.1 open-source software with the packages with "ade4" (Dray and Dufour, 2007) and "vegan" libraries (Oksanen et al., 2016).

RESULTS

Taxonomic Composition

The samples examined yielded 22,706 individuals of amphipods, 71 species belonging to 40 genera under 23 families (**Figure 2** and **Supplementary 1**). The most speciose families in the study area were Ampeliscidae (nine species) and Photidae (six species) (**Figure 2**). Five families, viz., Aoridae, Dexaminidae, Eriopisidae, Lysianassidae, and Maeridae recorded high abundances and together constituted 68.2% of total abundance. Eriopisidae was the most dominant family (18.8%) throughout the study, which was constituted by two species (*Eriopisella* sp. and *Eriopisella sechellensis*) (**Supplementary 1**). The maerid, *Maera grossimana* was a distinct inhabitant at various study sites and accounted for 14% of the total abundance followed by *E. sechellensis* (12.3%), *Lysianassa ceratina* (11.1%), and *Ampithoe ramondi* (9.2%).

Temporal Variation

Significant shifts in amphipod assemblage structure between different sampling years were evidenced (Pseudo-F = 2.45; $p = 0.001$) (**Table 2**). Pair-wise combination of different sampling years indicated that 2016 was significantly dissimilar with 2017 (AvD = 90.70%) and 2018 (AvD = 91.45%). Variations were insignificant between 2017 and 2018 (AvD = 85.34%). The dissimilarities between 2016–2017 and 2017–2018 were due to the relative densities of *M. grossimana*, *Ampelisca tenuicornis*, and *Grandidierella* sp.; whereas, *M. grossimana*, *Grandidierella* sp., and *E. sechellensis* contributed most to the dissimilarities of 2016–2018 (**Supplementary 2A**). Among the three study years investigated, maximum amphipod abundance was observed during 2017 (**Table 3**). No significant variations were observed in univariate diversity indices among different sampling years (**Supplementary 3**).

Horizontal Spatial Distribution

The composition of amphipod assemblages varied significantly between the five intertidal sampling transects (Pseudo-F = 2.65; $p < 0.001$) (**Table 2**). Pair-wise tests indicated that the amphipod assemblages differed significantly between T-I and other transects. Amphipod assemblage structure did not significantly differ between T-II, T-III, T-IV, and T-V. The mean amphipod abundance at different intertidal transects revealed that T-II harbored highest (699 ind m^{-2}) abundances, whereas T-I recorded the lowest (359 ind m^{-2}) average densities (**Figure 3A**). More species were observed at T-II and T-IV (34 species each) whereas T-I recorded the lowest species number (23 species) (**Supplementary 1**). Average Shannon–Weiner diversity (*H'*) index ranged from 1.8 ± 1.6 (T-II, T-III) to 2.6 ± 0.9 (T-IV). Higher mean Margalef's species richness (*d*) was recorded at T-III

TABLE 2 | Results of three-way permutational multivariate analysis of variance (PERMANOVA) based on Bray–Curtis similarities for differences in amphipod assemblages among shorelines (Sh), transects (Tr), and years (Ye) as factors.

Source	*df*	MS	Pseudo-F	*P* (perm)
Sh	2	8405.8	3.38	**0.0021**
Tr	4	5761.1	2.65	**0.0001**
Ye	2	7865.7	2.45	**0.001**
Sh x Tr	7	2534.3	1.16	0.2197
Sh x Ye	4	3936.9	1.81	**0.0051**
Tr x Ye	8	3418	1.57	**0.0079**
Res	11	2175.9		
Total	38			
Pair-wise comparisons				
	shoreline			
		Groups	***t***	***p***
		LW, MW	1.6293	**0.0075**
		LW, HW	1.5994	**0.0022**
		MW, HW	1.2758	0.0813
	transect			
		T-I, T-II,	1.5253	**0.016**
		T-I, T-III	1.938	**0.0013**
		T-I, T-IV	1.8044	**0.001**
		T-I, T-V	1.5463	**0.0128**
		T-II, T-III	0.712	0.8867
		T-II, T-IV	0.83582	0.758
		T-II, T-V	0.85708	0.7046
		T-III, T-IV	0.96906	0.5031
		T-III, T-V	1.3094	0.0727
		T-IV, T-V	1.175	0.1728
	year			
		2016, 2017	1.731	**0.0017**
		2016, 2018	1.7007	**0.0007**
		2017, 2018	0.9731	0.4756

LW, low shore; MW, mid shore; HW, upper shore; T, transect. Significant p-values are shown in bold.

and T-IV (av 1.1 each) (**Figure 3B**). Pielou's evenness *J'* was high at all transects (≥0.6). Univariate diversity indices with the exception of Pielou's evenness *J'* (one-way ANOVA, $F = 4.44$; $p = 0.004$) were not significantly different between different transects (**Figure 3**).

The dominant amphipod species differed between transects (**Figure 4**). The relative densities of the two dominant species, *M. grossimana* and *A. tenuicornis*, were mostly accountable for dissimilarities between the transects (**Supplementary 2B**). The dissimilarity between T-I and T-II (AvD = 93.52%), T-I and T-III (AvD = 96.57%), T-I and T-IV (AvD = 91.84%), and T-I and T-V (AvD = 89.10%) were primarily due to *A. tenuicornis*. The major contributor for distinction between T-II and T-III (AvD = 87.55%), T-II and T-IV (AvD = 85.33%), T-III and T-IV (AvD = 84.85%), T-III and T-V (AvD = 89.05%), and T-IV and T-V (AvD = 82.94%) was *M. grossimana*. *Grandidierella* sp. and *M. grossimana* were the species that majorly distinguished T-II and T-V (AvD = 86.39%).

Vertical Spatial Distribution

Clear spatial vertical patterns in amphipod assemblage structure were evidenced. LW constituted 62.05% of the total amphipod abundance, whereas the MW and HW contributed 22.19 and 15.77% abundances, respectively (**Table 3**). The trend of decreasing amphipod density along the vertical gradient was consistently observed during all 3 years. Evidently, the LW recorded highest average amphipod abundance (939 ind m^{-2}), followed by the MW (336 ind m^{-2}) and the HW (239 ind m^{-2}) (**Figure 5A**). Similarly, the highest species richness, *d* (Margalef index); species evenness, *J'* (Pielou's), and Shannon–Weiner Index, *H'* ($\log^2$) were recorded from the LW (**Figures 5B–D**). All the univariate measures varied significantly among shore levels (**Figure 5**). PERMANOVA analyses showed significant variation among shore levels (Pseudo-F = 3.38; $p = 0.002$) (**Table 2**). Pair-wise test indicated that the amphipod assemblages differed significantly between LW and MW ($t = 1.6293$, $p = 0.007$) and between LW and HW ($t = 1.5994$, $p = 0.002$). However,

TABLE 3 | Species density, species number, and dominant amphipod taxa at different shorelines during various study years.

Year	Lower	Middle	Upper
2016			
Density range	8-650 ind m^{-2}	8-700 ind m^{-2}	8-783 ind m^{-2}
Total density	3956 ind m^{-2}	2447 ind m^{-2}	1432 ind m^{-2}
Species number	25	17	7
Dominant taxa	*Lyssianasa ceratina* (31.8%)	*Ampelisca typica* (31.3%)	*Allomelita pellucida* (54.7%)
	Maera grassimana (14.1%)	*Dexamine spinosa* (17.7%)	*Grandidierella sp.* (38.4%)
	Eriopisella sechellensis (10.7%)	*Ampelisca diadema* (13.9%)	
		Ampelisca eschrichtii (13.6%)	
2017			
Density range	8-1092 ind m^{-2}	8-208 ind m^{-2}	8-233 ind m^{-2}
Total density	6987 ind m^{-2}	1339 ind m^{-2}	1130 ind m^{-2}
Species number	34	16	16
Dominant taxa	*Ampithoe ramondi* (20.3%)	*Ampelisca tenuicornis* (33.5%)	*Maera* sp. (20.6%)
	Maera grassimana (17.5%)	*Grandidierella* sp. (27.3%)	*Microprotopus* sp. (16.2%)
	Eriopisella sechellensis (14.8%)		*Maera grassimana* (14.0%)
	Lyssianasa ceratina (11.2%)		*Ampelisca tenuicornis* (11.0%)
2018			
Density range	6-631 ind m^{-2}	6-338 ind m^{-2}	6-575 ind m^{-2}
Total density	3145 ind m^{-2}	1252 ind m^{-2}	1018 ind m^{-2}
Species number	20	18	6
Dominant taxa	*Maera grassimana* (24.9%)	*Eriopisella sechellensiss* (34.0%)	*Eriopisella sechellensis* (56.4%)
	Ampelisca tenuicornis (15.9%)	*Grandidierella* sp. (25.0%)	*Parhyale hawaiensis* (33.1%)
	Lysianasa ceratina (12.3%)	*Maera grassimana* (19.5%)	
	Dexamine spinosa (11.6%)		
Overall			
Total density	14,088 ind m^{-2}	5,038 ind m^{-2}	3,580 ind m^{-2}
Total species number	56	39	25
Dominant families	Lysianassidae (25.2%)	Dexaminidae (21.7%)	Melitidae (30.3%)
	Eriopisidae (17.4%)	Eriopisidae (21.3%)	Eriopisidae (23.2%)
	Maeridae (15.9%)	Ampeliscidae (20.9%)	Aoridae (11.0%)
Dominant taxa	*Maera grassimana* (18.2%)	*Ampelisca typica* (15.9%)	*Allomelita pellucida* (21.9%)
	Lysianasa ceratina (17.2%)	*Grandidierella* sp. (13.5%)	*Eriopisella sechellensis* (16.0%)
	Ampithoe ramondi (12.9%)	*Ampelisca tenuicornis* (11.2%)	*Grandidierella sp.* (15.3%)
	Eriopisella sechellensis (12.1%)	*Eriopisella sechellensiss* (10.2%)	*Parhyale hawaiensis* (11.0%)

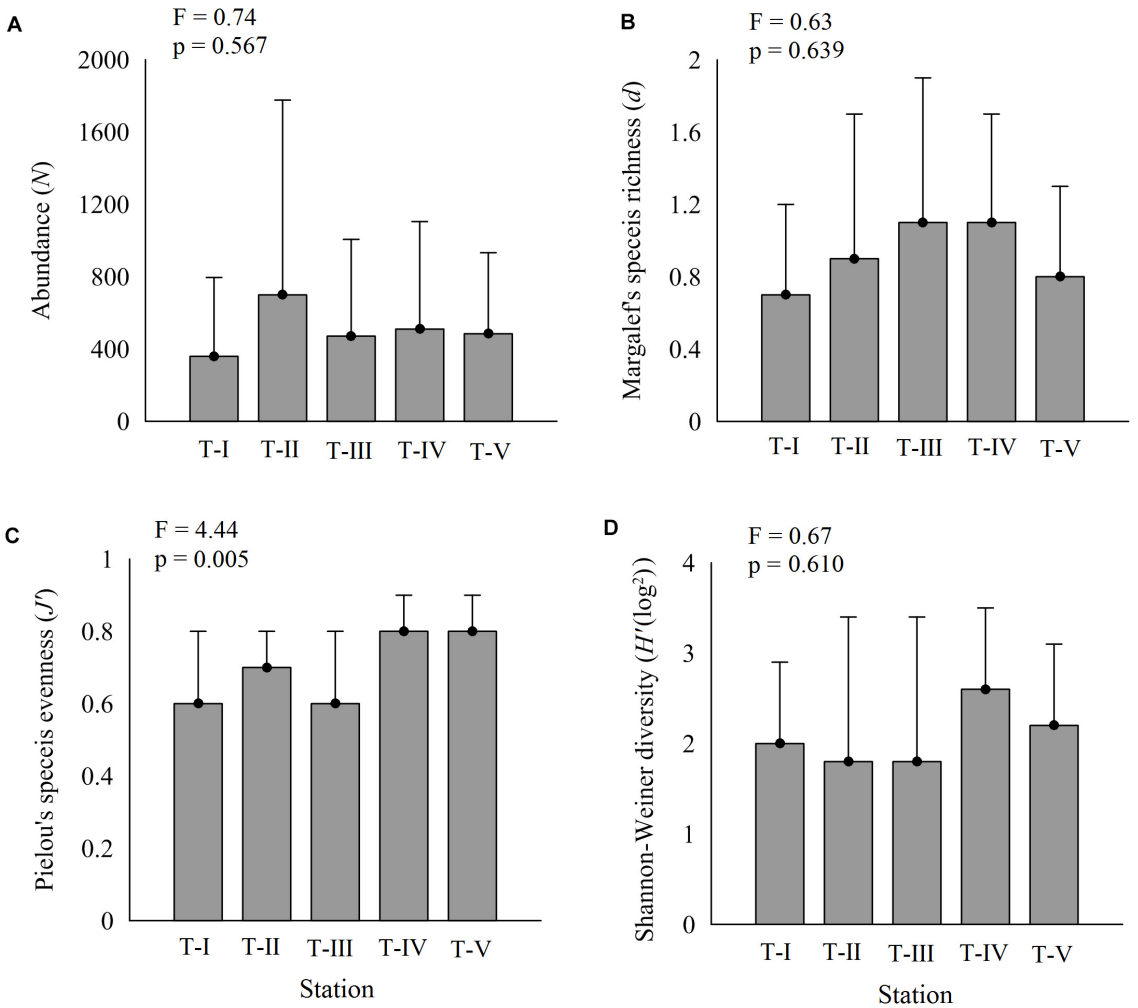

FIGURE 3 | Variations in amphipod diversity indices (avg ± SD) along five transects. **(A)** Amphipod abundance, **(B)** *d*-species richness, **(C)** *J'*—Pielou's evenness, and **(D)** *H'*—Shannon–Wiener index.

this differentiation was not significant between MW and HW (**Table 2**). Ordination of amphipod assemblage structure exposed grouping patterns among different shore levels (**Figure 6**). The LW stations of all transects except T-I were clustered together indicating similarity of amphipod species composition. The LW stations of T-I had a different species composition from that of other four transects. Some HW stations were grouped with MW which confirmed the results of pair wise PERMANOVA analyses. The dissimilarities between different shorelines were mainly due to differences in relative densities of *M. grossimana*, *Dexamine spinosa*, *L. ceratina*, *A. ramondi*, *E. sechellensis* (more abundant in LW), *A. tenuicornis*, *Grandidierella* sp., *Ampelisca typica* (more abundant in MW) (**Supplementary 2C**).

The dominant amphipod species composition varied significantly between shore levels during all 3 years (**Table 3**). The LW displayed consistently high values of *J'* (≥0.6 ± 0.2) and *H'* (≥2.0 ± 0.5). The LW of T-II had the maximum amphipod abundance and that of T-V recorded the lowest. The LW of T-I recorded lower *d*, *J'*, and *H'* values as compared to other transects (**Supplementary 4**). Contrastingly, highest *d* and *H'* values were recorded at T-I in MW. Mostly balanced amphipod assemblages were present at the MW (*J'* = 0.5 ± 0.2 to 0.8 ± 0.2). Among the transects, highest abundance of amphipods was recorded at MW of T-I. The HW of T-V registered maximum *N* and *H'*, whereas the HW of T-IV displayed highest *d* values. At HW, amphipods were close to nil at T-II and completely absent at T-III during all three study periods (**Figure 2** and **Supplementary 4**). At rest of the transects, the HW indicated evenness (*J'*) of ≥0.5.

Biological Trait Analysis

The first two axes of the FCA performed on the "traits-by-station" matrix accounted for 54% of the total variability of which 33% was explained by FC1 and 21% by FC2 (**Figure 7**). The correlation ratios (>10%) indicated that the traits habitat, mobility, and body size were more separated on FC1, whereas the FC2 was associated with the trait bioturbation. Feeding mode was correlated with both axes (**Table 4**).

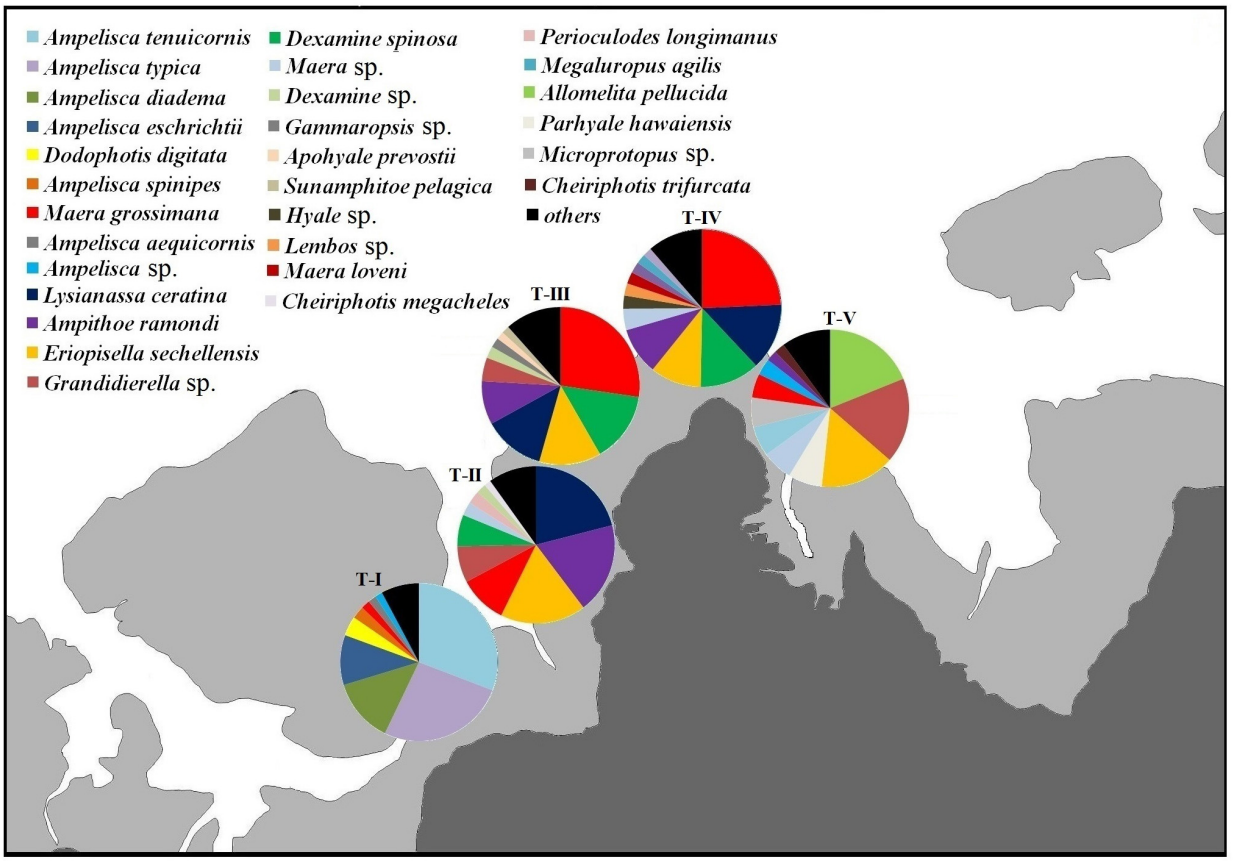

FIGURE 4 | Relative abundances of dominant amphipod species (averaged across different shore levels and years) composition at different transects.

The FCA plot (**Figures 7**, **8**) clearly portrayed the association of the LW stations of T-II, T-III, T-IV, and T-V with small to medium sized amphipod species with the following traits; epifauna, biodiffusers, motile, subsurface deposit feeders, browsers, scavengers, and burrowers. All HW and MW (except T-IV MW) stations and T-I LW were populated by very small sized amphipods with functional traits such as discretely motile, surface modifiers, predators, grazers, detritivores, suspension feeders, tube building, and free living (**Figures 7**, **8**). The highest FD index was recorded at T-IV LW (3.1 ± 0.1), whereas no FD index values were derived at T-II HW and T-III HW due poor representation or absence of amphipods. T-II LW (2.7 ± 0.7), T-III LW (2.7 ± 0.5), and T-V LW (2.5 ± 0.7) had comparable FD values (**Figure 9**). Except at T-I, all LW stations had higher FD than other stations. FD decreased along the spatial vertical gradient from LW to HW.

DISCUSSION

The GoK MNPS harbors some of the most biodiverse and sensitive coralline ecosystems of the Indian subcontinent (Subba Rao and Sastry, 2005). This is the first quantitative study on diversity and functionality of amphipod assemblages in the intertidal habitats of the GoK MNPS, providing valuable baseline for future ecological investigations. An earlier compilation of intertidal amphipods by Surya Rao (1972) recorded 132 species of gammaridean amphipods belonging to 24 families from various intertidal regions along the Indian coast. A total of 17 amphipod species were recorded at Krusadai Islands, an MPA in the Gulf of Mannar (Gravely, 1927; Raj, 1927). Amphipoda contributed to less than 3% of macrobenthic density in the sandy beaches of Lakshadweep, another MPA in the Arabian Sea (Rivonker and Sangodkar, 1997); 117 amphipod species belonging to 33 families were reported from 50 sampling sites of the Alacranes Reef National Park, Gulf of Mexico (Paz-Ríos et al., 2019). A study conducted on temporal distributions of amphipod species from the Mexican Caribbean reef Banco Chinchorro revealed 26 amphipod species represented by 16 families and 24 genera (Oliva-Rivera, 2003). In this study, 71 amphipod species belonging to 23 families were recorded from the five intertidal transects of GoK, signifying the exceptional amphipod diversity of this MPA. These results clearly indicated that the intertidal regions particularly coralline types are favorable habitats for diverse amphipod species (Surya Rao, 1972; Narayanan and Sivadas, 1986).

The amphipod species were well distributed at different transects, though in varying proportions. For example,

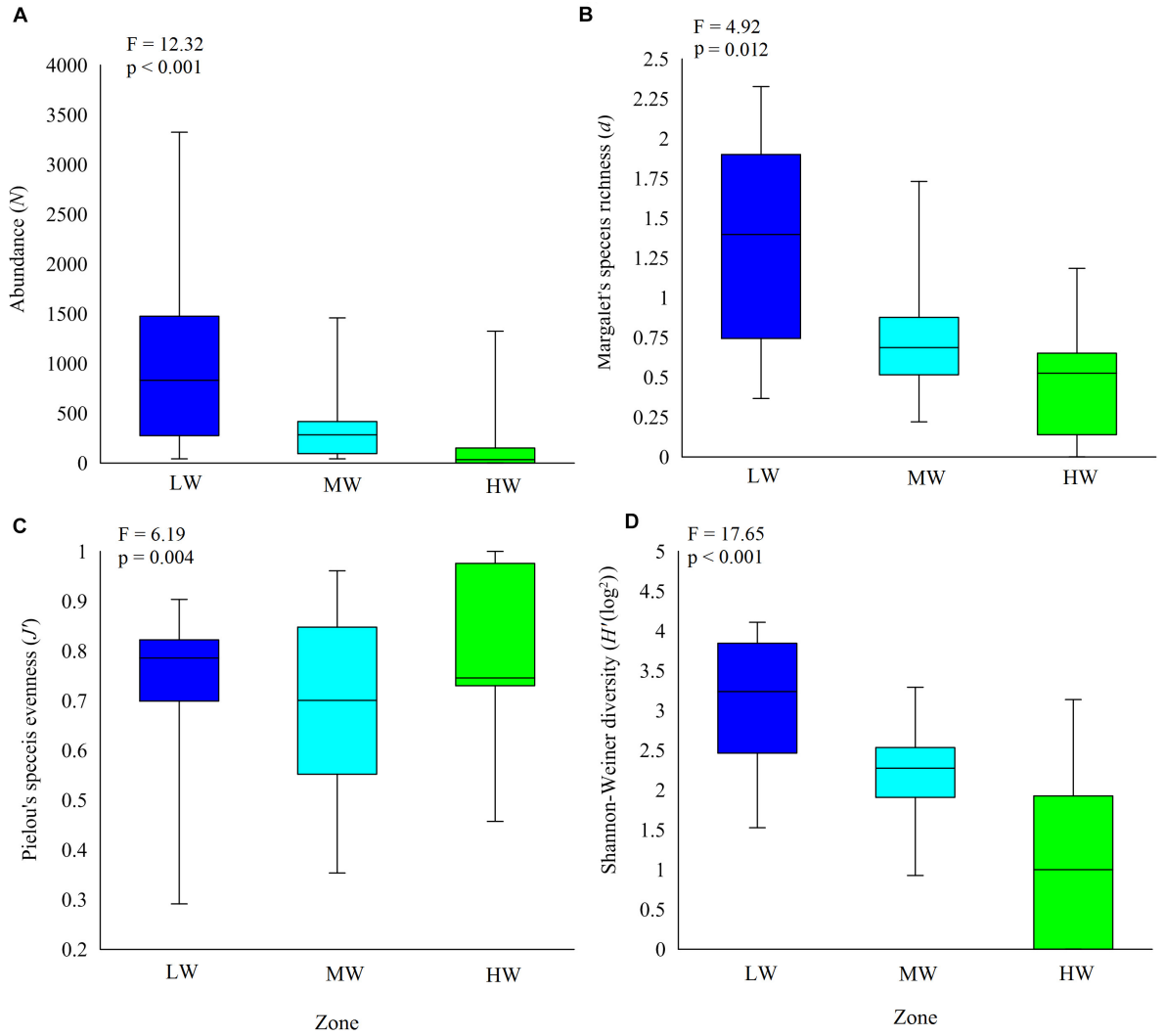

FIGURE 5 | Shore level variation in amphipod species. **(A)** abundance, **(B)** Margalef's species richness, **(C)** Pielou's species evenness, and **(D)** Shanon–Weiner diversity. LW, low shore; MW, mid shore; HW, upper shore. Middle horizontal lines represent the mean.

M. grossimana comprised 27.3% at T-III whereas at other transects the composition of *M. grossimana* varied from 1.8 to 24.3% (**Supplementary 1**). The intertidal zone of T-I was predominantly constituted by fine sediments (Sinha, 1997; National Institute of Oceanography [NIO], 2018) and was populated chiefly by the Ampeliscidae (75.1%). The proportion of ampeliscids were very high at T-I as compared to other transects and was one of the major contributors to the significant spatial differences between the Kalubhar transect and the other four. The ampeliscids are known to have an affinity for finer sediments (Parker, 1984; Marques and Bellan-Santini, 1991). The dominant species at T-I, *A. tenuicornis* and *A. typica* are also reported to be abundant in silty sediments (Mills, 1967; Sheader, 1977; Lourido et al., 2008). While the type of substratum probably influenced the significant difference in amphipod assemblage structure between T-I and others, it was also possible that the different sampling methods employed at this location may have contributed to the variance.

Sharp vertical patterns were apparent in the amphipod assemblage structure in the coralline intertidal areas investigated. The differential abiotic stress known to occur at different shore levels could have influenced the vertical differences observed in the amphipod assemblage structure (Menge and Branch, 2001; Valdivia et al., 2011). Studies have suggested that the vertical gradient of environmental stress occurring along the intertidal habitats influences the intensity of interspecific interactions and governs the variations in community structure (Paine, 1974; Benedetti-Cecchi et al., 1999; Díaz and McQuaid, 2011). Analyses of individual amphipod species distributions along the different transects indicated that the distribution of majority of species was restricted to particular levels on the shore that were best suited for their survival. Thus, the species *Apohyale prevostii*,

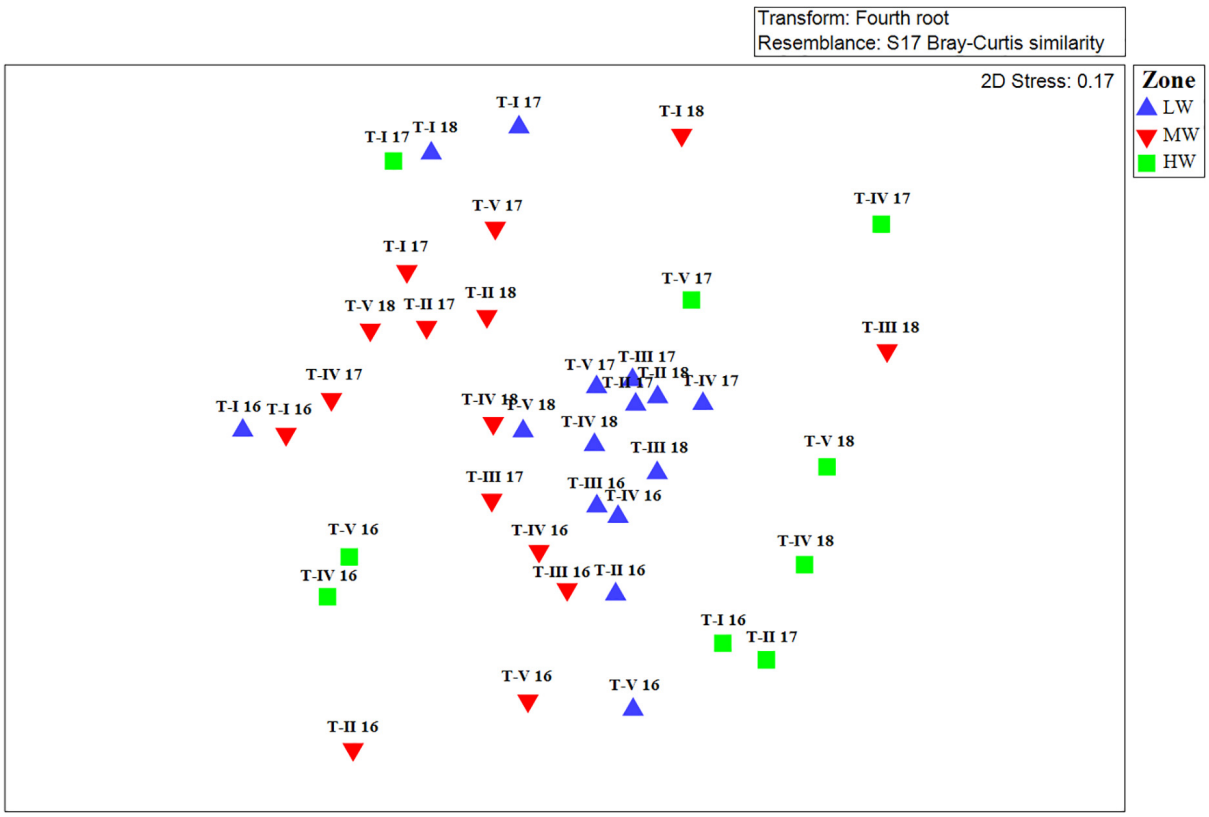

FIGURE 6 | Non-metric Multidimensional scaling (nMDS) ordination of amphipod species abundance data collected at different shore levels. LW, low shore; MW, mid shore; HW, upper shore.

Cyproidea ornata, *Idunella chilkensis*, *Megaluropus agilis*, *Metaphoxus simplex*, *Paradeutella bidentata*, *Parelasmopus suensis*, and *Perionotus alaniphilas* were observed only at LW, *Ampelisca eschrichtii*, *Ampelisca gibba*, *Paracaprella* sp., *Peramphithoe* sp., and *Photis reinhardii* at MW and *Monoculodes* sp., *Parhyale hawaiensis*, and *Urothoe brevicornis* were observed only at HW demonstrating sharp zone specific distributions. Studies have attributed such species distributional patterns at different intertidal zones to diverse physiological requirements in relation to physical stress and various biological relationships (Underwood, 1981; Araújo et al., 2005; Pandey and Thiruchitrambalam, 2018).

The co-existence of a mosaic of amphipod species at low water levels of various transects was also notable. For instance, at T-III and T-IV, the dominant species *M. grossimana* (21–34%) coexisted with another co-dominant species, *L. ceratina* (14–17%) at LW. At T-II LW, high percentages of *L. ceratina* (21%) and *A. ramondi* (20%) were observed. At T-I, the species *A. tenuicornis* (59%) and *A. typica* (15%) together constituted majority of the amphipod population. This kind of mosaic relationship is an important characteristic of intertidal organisms particularly at low shore level (Menge et al., 1993; Araújo et al., 2005). Araújo et al. (2005) observed similar mosaic assemblages from the intertidal rocky shores in the northwest coast of Portugal.

The most diverse amphipod species were observed from the LW areas of all transects of Narara. Most of the peracarid crustaceans especially amphipods prefer areas optimal for their survival such as the low shore areas. These areas are exposed to shorter durations of air exposure and reduced wave action than middle and upper zones (Bueno et al., 2017). In addition, biological factors such as increased food availability and shelter options (host preferences) also make the lower shore a more conducive habitat for the survival of diverse amphipod species (Chavanich and Wilson, 2000). Algae have been identified as a major variable determining the distribution patterns of amphipods in various intertidal habitats (Bueno et al., 2016, 2017, 2019). Hacker and Steneck (1990) suggested that amphipods favored algae with complex morphology to protect them from predators. The common vagile amphipod species such as *M. grossimana*, *L. ceratina*, and *A. ramondi* were present in large numbers at LW, with incrementally reduced densities at MW and HW. These amphipods prefer to reside in algal holdfast and algal tufts mainly to obtain food and using them as hiding places (Penrith and Kensley, 1970; Brawley and Adey, 1981; Duffy and Hay, 2000; Gallmetzer et al., 2005). The lower intertidal shores of Narara reef have been reported to sustain an average algal cover of 89% comprising of 31 species and dominated by Chlorophyta (71.18%) (Roy et al., 2015). The seaweed, *Ulva lactuca* (Family: Chlorophyceae)

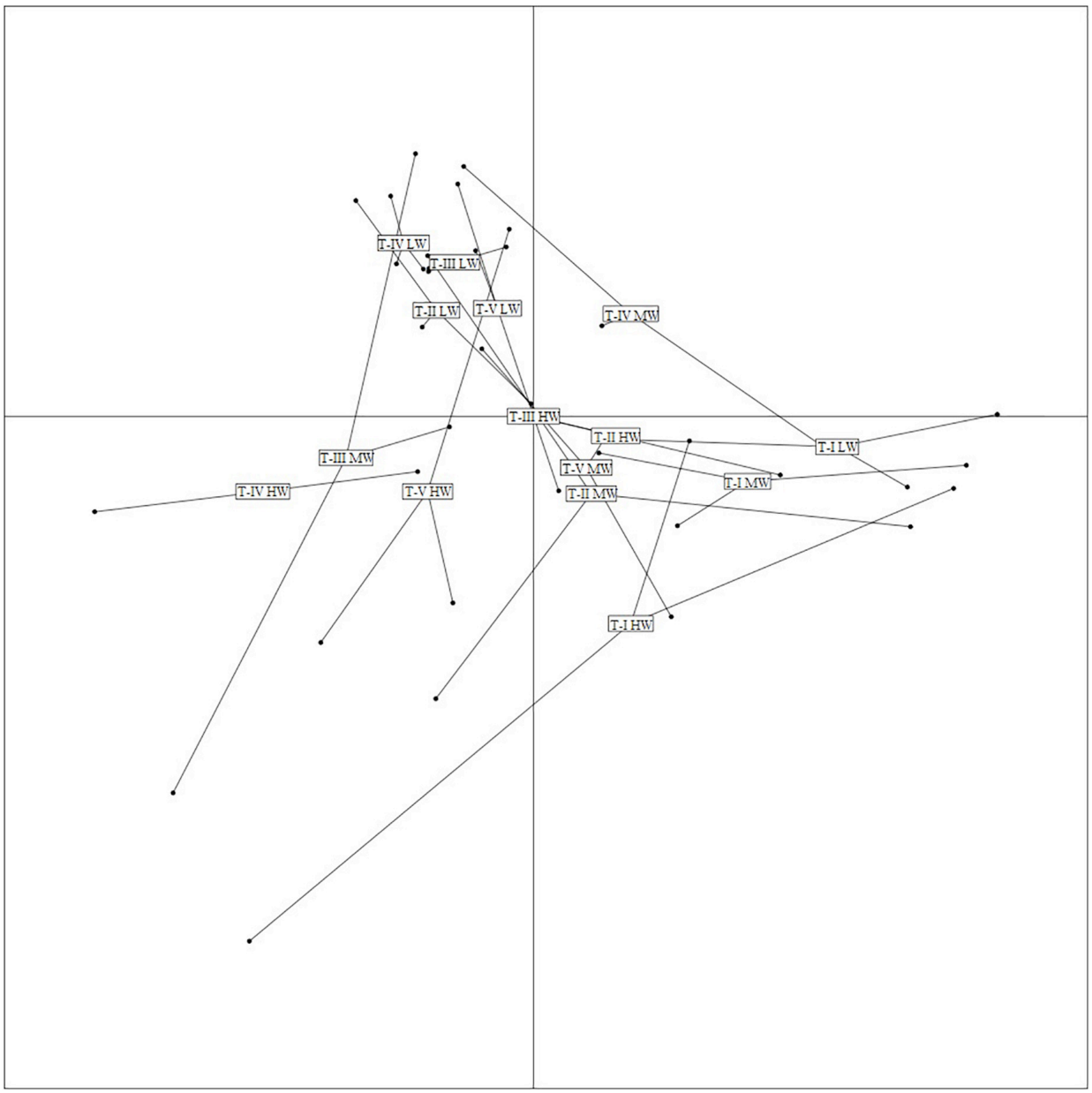

FIGURE 7 | Result of Fuzzy correspondence analysis (FCA) along the first two axes. Ordination of samples based on trait-modalities weighted by amphipod species abundances at various transects during all three study periods. LW, low shore; MW, mid shore; HW, upper shore.

was observed to be the most dominant species in the study area during all the seasons (Adhavan et al., 2015). *Ulva* is known to be a significant food sources for many amphipod species from the different habitats (Sfriso and Marcomini, 1997; Balducci et al., 2001; Zheng et al., 2014). Amphipods are reported to be the major occupants of *Ulva* dominated algal beds (Balducci et al., 2001; Zheng et al., 2014). Therefore, it is surmised that the availability of copious food sources probably helped establish diverse and abundant amphipod assemblages in the low intertidal zones of the study region. In addition to *U. lactuca*, Sargassum *cinereum*, *Sargassum tenerrimum*, *Padina boryana*, *Padina boergesenii* (Phaeophyta), *Caulerpa racemosa*, *Caulerpa taxifolia*, *Ulva fasciata*, *Ulva reticulate* (Chlorophyta), *Acanthophora dendroides*, *Gracilaria corticata*, *Gracilaria verrucosa*, *Scinaia monoliformis* (Rhodophyta) were also found in good numbers at the LW of the Narara transects (Adhavan et al., 2015; Roy et al., 2015). The distinct spatial vertical patterns of amphipod assemblages followed the general model described by Menge and Sutherland (1987). The upper limit of intertidal amphipods was probably set by the inherent physiological ability of species to survive the harsh conditions of prolonged exposure, whereas the lower limit may be determined

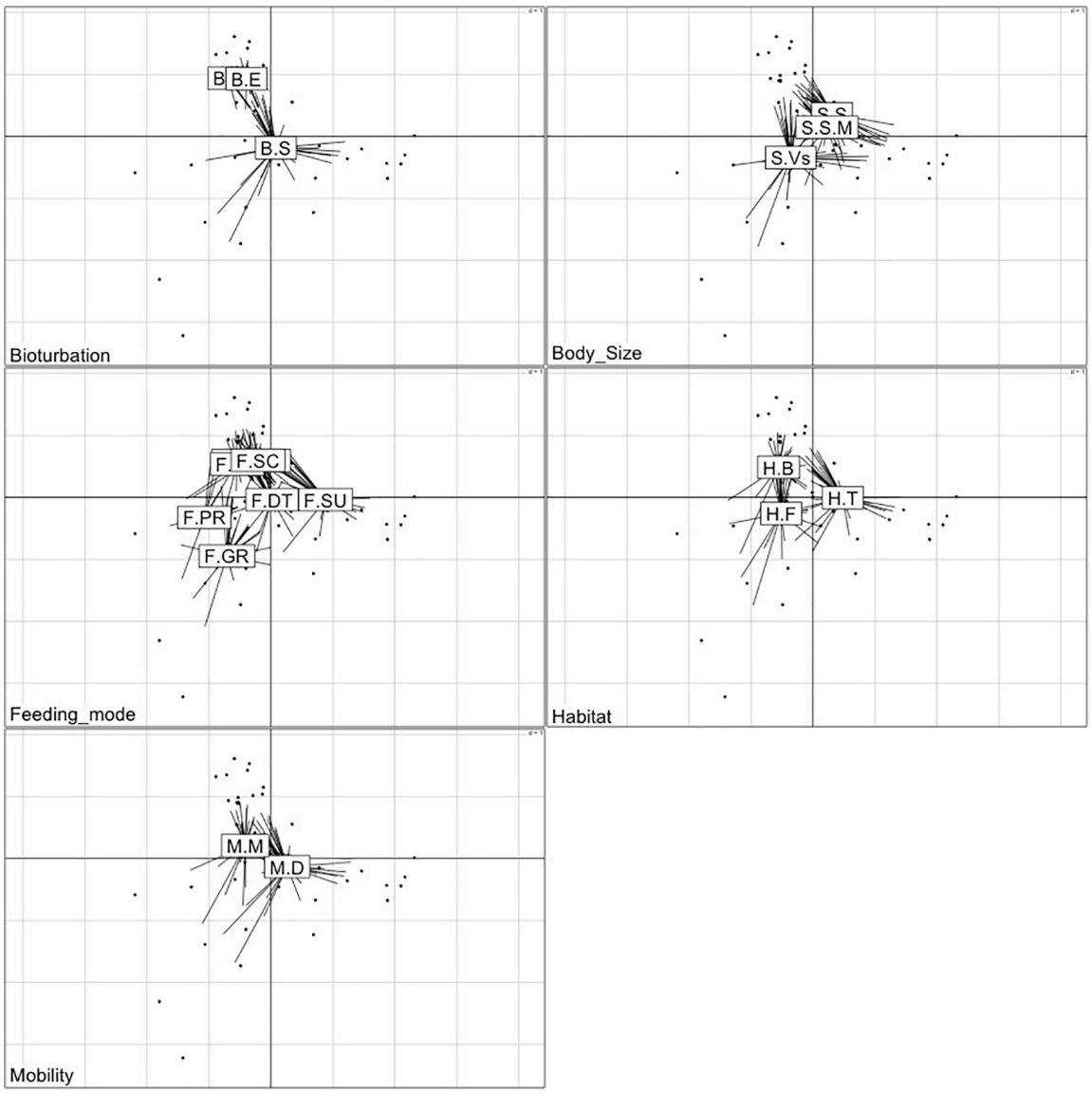

FIGURE 8 | Two-dimensional plots of the functional traits with corresponding modalities based on Fuzzy correspondence analysis (FCA) of the abundance-weighted amphipod assemblage traits. The labels of the modalities within each trait category are provided in **Table 1**.

by the outcome of inter-specific interactions (Chavanich and Wilson, 2000; Bueno et al., 2016).

Previous comparisons between functional and taxonomical composition of natural communities have yielded disparate results, varying from strong to weak congruence between these two dimensions (Cochrane et al., 2012; Frid and Caswell, 2015; Kokarev et al., 2017). This study investigated amphipod FD patterns with reference to the taxonomic diversity patterns in the GoK MNPS. Most amphipod species are mobile in intertidal habitats with relatively high swimming abilities, so they can freely move between the areas rich in food and also to protect them from predation (Jażdżewska and Siciński, 2017). In the current study, mobile epifaunal amphipod abundances were observed to be higher at the LW of the all intertidal transects except T-I. Generally, the increased risk of predation makes more mobile species prevalent at LW (Paine, 1969; Underwood, 2000). Amphipod species roam during night in search of freshly deposited food in the absence of predators, whereas in the presence of predators, the amphipod species find secure places to avoid the predation (Gestoso et al., 2014). In particular, the animals with reduced mobility face increased predation risk at LW zones (Underwood, 2000). Mobility is an important mechanism that reduces competition by allowing co-existence of competing species through avoidance of predators and adverse microclimate conditions (McBane and Croker, 1983).

In the present study, amphipods with burrowing behavior were observed more abundantly at LW. The lysianassid and ampithoid amphipods that occurred in high abundances at

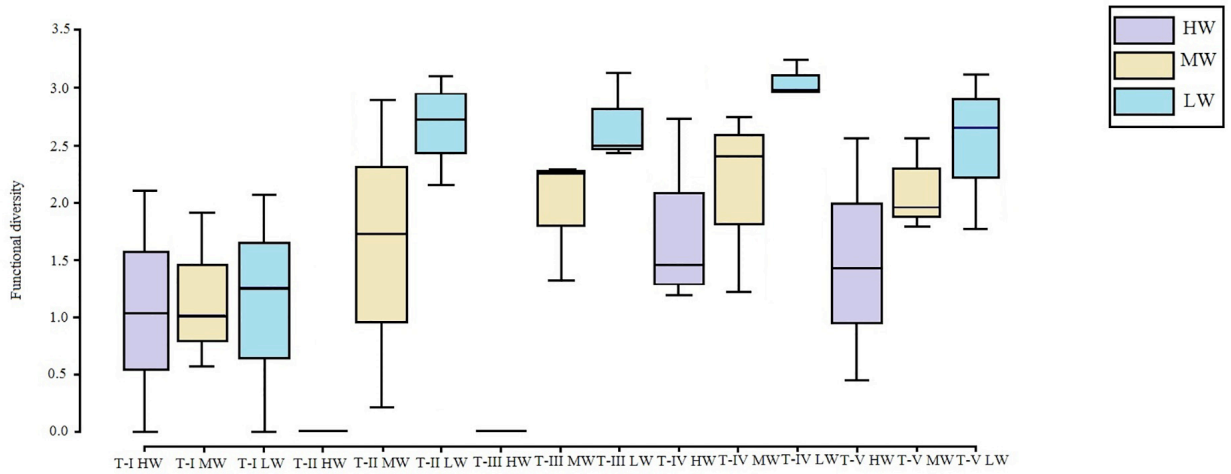

FIGURE 9 | Box plots of functional diversity (FD) (avg ± SD) based on amphipod abundance at all the sampling sites. LW, low shore; MW, mid shore; HW, upper shore.

TABLE 4 | Correlation matrix between the first two axes of the FCA (Fuzzy correspondence analysis) and the functional traits studied.

Functional Traits	FC 1 (33%)	FC 2 (21%)
Feeding mode	**0.38**	**0.23**
Habitat	**0.25**	0.06
Mobility	**0.11**	0.03
Body size	**0.10**	0.09
Bioturbation	0.03	**0.17**

Figures in brackets indicate the variation explained by the corresponding axis. Higher contributions are highlighted in bold.

LW are known to construct burrows in holdfast and stripes of large macroalgae to get aid in reproduction, guaranteed access to food and shelter against predators (Mejaes et al., 2015). Contrary to this, the less mobile and tube dwelling amphipod taxa were present mostly at MW and HW. Tube construction protects the amphipods from strong waves and high temperatures that frequently occur at upper shore (Carter, 1982). During tube construction, amphipods transport particles and fluids which influence the physical and chemical processes in the surface sediments (Rhoads, 1974; Aller, 1988; Kristensen, 1988). Bioturbation is reported to be strongly related to the organism's trophic diversity, mobility, and resident habitats (Dauwe et al., 1998; Pearson, 2001). This was evidenced in our study as surface modifiers were more abundant at the MW and HW and were associated with the tube building and discretely motile traits. Conversely, the epifaunal and bio diffuser functional traits were mostly linked with mobile and burrowing traits at LW (**Figure 8**). Benthic amphipods use diverse food sources within their microhabitats and therefore their trophic diversity is widely used in many ecological studies (Guerra-García et al., 2014). The great variety of feeding mechanisms observed in the amphipods substantiated that the study area provided ample and multiple food sources. More feeding types were observed at the heterogeneous LW, whereas the MW and HW regions sustained lesser trophic diversity. These observations concur with Guerra-García and Tierno de Figueroa (2009) and Vázquez-Luis et al. (2012) who highlighted that the diet of amphipods was more diverse in algal and seagrass habitats than those composed only of bed sediments.

Several hypotheses have been put forward to explain the shore level gradient in body size observed at different intertidal habitats. Olsgard et al. (2008) suggested that the habitats with low stress environmental conditions can sustain large body sized organisms. In the present investigation, bigger amphipods were observed in the low intertidal shore except at T-I. Underwood (2000) opined that the general increase in size gradient of intertidal organisms at low shore levels was due to the lower predation rates of large sized animals. In general, the large animals wandering at low shore will tend to stay there, while the small body sized organisms will continue moving upward. Despite the food available at low shores, the enhanced risk of predation makes the smaller animals move toward upper shore (Paine, 1969; Underwood, 2000). The large body sized organisms survive at low shore due to lower predation rates. Also, the small body size helps to retain more amount of water and the absorbent nature of the amphipod tubes in upper shore helps the organism to tolerate the desiccation from exposure (Carter, 1982). Hacker and Steneck (1990) suggested that amphipod species choose habitats based on body-size scaling in an attempt to avoid predation and desiccation. In the present study, it was evident that the spatial component of habitat architecture was an important criterion in size-dependent habitat selection of benthic amphipods in intertidal regions.

Functional diversity trends also suggested that except at T-I, LW had more functional groups, whereas HW had functionally less diverse amphipod assemblages. At T-I, FD was low at all zones. Moreover, amphipod FD indices mirrored the taxonomic diversity patterns indicating strong inter-correlated changes

along transects and zones. Functional traits can be used to index the ecological functioning of assemblages and one might expect large scale changes in taxonomic composition to result in changes in trait composition and hence ecological functioning (Frid and Caswell, 2015). The relative variance in functional trait composition between zones as observed in this study concurs with the environmental filtering and habitat template concepts, wherein the structure and environmental conditions determine the community assembly through selection of certain species function traits (Pacheco et al., 2011). The strong congruence between the two dimensions of community suggested that the amphipod assemblage structure and functioning in the study area were probably influenced by the same complex of biotic or abiotic parameters.

Present results clearly indicated that vertical variations in amphipod assemblage structure were more distinct than horizontal variations measured at fine spatial scale. These results are consistent with other studies of rocky shores that have indicated large differences in the structure of assemblages from the upper to lower shore (Chavanich and Wilson, 2000; Menge and Branch, 2001; Valdivia et al., 2011). Of late, the horizontal and vertical variations in intertidal communities are being evaluated as a step to classify provenance of dissimilarity. For instance, Valdivia et al. (2011) identified that vertical biological variation in intertidal habitats was higher than horizontal variation measured at local scales, but lower than horizontal variation measured at regional scales. Catalán et al. (2020) reported that horizontal variation in community structure measured from local to regional scales never surpassed vertical variations. Many physical and biological factors are currently invoked to explain these horizontal and vertical zonation patterns of intertidal communities, but their effects are often difficult to evaluate. These studies have offered the observational background for experimental analyses on causal processes, including inter specific competition, predatory effects, physical factors, and the interplay between biological and physical processes (Benedetti-Cecchi, 2001). Although in the present study we have not investigated the causal processes explicitly, the functional trait patterns of amphipod assemblages described here may provide some clues on causes of vertical and horizontal variations of amphipod assemblages in the study region.

CONCLUSION

In this study, the taxonomic and FD patterns of amphipod assemblages in the coralline intertidal zones of GoK MNPS were documented. Pronounced differences were observed in amphipod assemblage structure and functional trait matrices along the horizontal and vertical gradients on the shore. Amphipods showed clear demarcation of spatial vertical zones with higher species diversity and functional trait composition being observed at the low shore levels which sustained structurally complex habitats. Different mosaic of amphipod species assemblages was observed at particular intertidal zones. Vertical variations in amphipod assemblage structure at different shorelines were higher than horizontal variations. Assigning biological traits to amphipod species provided additional insights to those from traditional taxonomic analyses. Patterns of species diversity distribution in the study area were mirrored by the functional traits. Understanding the diversity–function relationships of major faunal groups in sensitive ecosystems such as MPAs is important to understand the multiple ecological services rendered and to predict loss of ecological functions due to potential species loss. Detailed studies focusing on species specific functional characteristics of amphipods and the complex factors influencing the zonation patterns in future will provide a stronger scientific basis for marine ecosystem conservation strategies.

DATA AVAILABILITY STATEMENT

The raw data supporting the conclusions of this article will be made available by the authors, without undue reservation.

AUTHOR CONTRIBUTIONS

TS and SS contributed to the conception, design, and execution of the study and analyzed the data. SN and KR contributed to the software programming and data analysis. TS wrote the first draft of the manuscript. All authors contributed to manuscript revision and read and approved the submitted version.

FUNDING

This research did not receive any specific grant from funding agencies in the public, commercial, or not-for-profit sectors.

ACKNOWLEDGMENTS

The authors express their sincere thanks to Director CSIR-National Institute of Oceanography, India, for extending facilities. The authors express their special thanks to all team members from CSIR-NIO Mumbai Regional Centre, who helped during the field work. The invaluable help of Dr. Rakesh P. S. is gratefully acknowledged.

SUPPLEMENTARY MATERIAL

The Supplementary Material for this article can be found online at: https://www.frontiersin.org/articles/10.3389/fmars.2020.589195/full#supplementary-material

REFERENCES

Adhavan, D., Kamboj, R. D., Chavdaand, D. V., and Bhalodi, M. M. (2014). Status of intertidal biodiversity of Narara Reef Marine National Park, Gulf of Kachchh, Gujarat. *J. Mar. Biol Oceanogr.* 3:2. doi: 10.4172/2324-8661.1000132

Adhavan, D., Marimuthu, N., Tikadar, S., and Sivakumar, K. (2015). Impact of algal bloom on mangrove and coral reef ecosystem in the Marine National Park, Gulf of Kachchh, Gujarat, India. *J. Mar. Biol. Aquacult.* 1, 1–2. doi: 10.15436/2381-0750.15.006

Aller, R. C. (1988). "Benthic fauna and biogeochemical processes in marine sediments: the role of burrow structures," in *Nitrogen Cycling in Coastal Marine Environments (SCOPE)*, eds T. H. Blackburn and J. Sørensen (Chichester: Wiley Press Inc), 301–338.

Anderson, M. J., Gorley, R. N., and Clarke, K. R. (2008). *PERMANOVA for PRIMER: Guide to Software and Statistical Methods*. Plymouth: PRIMER-E.

Araújo, R., Bárbara, I., Sousa-Pinto, I., and Quintino, V. (2005). Spatial variability of intertidal rocky shore assemblages in the northwest coast of Portugal. *Estuar. Coast Shelf Sci.* 64, 658–670. doi: 10.1016/j.ecss.2005.03.020

Balducci, C., Sfriso, A., and Pavoni, B. (2001). Macrofauna impact on Ulva rigida C. *Ag*. production and relationship with environmental variables in the lagoon of Venice. *Mar. Environ. Res.* 52, 27–49. doi: 10.1016/S0141-1136(00)00259-2

Barnard, J. L. (1979). Littoral gammaridean Amphipoda from the Gulf of California and the Galapagos Islands. Smithson. *Contr. Zool.* 271:149.

Bellwood, D. R., Hoey, A. S., and Choat, J. H. (2003). Limited functional redundancy in high diversity systems: resilience and ecosystem function on coral reefs. *Ecol. Lett.* 6, 281–285. doi: 10.1046/j.1461-0248.2003.00432.x

Benedetti-Cecchi, L. (2001). Variability in abundance of algae and invertebrates at different spatial scales on rocky sea shores. *Mar. Ecol. Prog. Ser.* 215, 79–92. doi: 10.3354/meps215079

Benedetti-Cecchi, L., Menconi, M., and Cinelli, F. (1999). Pre-emption of the substratum and the maintenance of spatial pattern on a rocky shore in the northwest Mediterranean. *Mar. Ecol. Prog. Ser.* 181, 13–23. doi: 10.3354/meps181013

Blanchette, C. A., Melissa Miner, C., Raimondi, P. T., Lohse, D., Heady, K. E., and Broitman, B. R. (2008). Biogeographical patterns of rocky intertidal communities along the Pacific coast of North America. *J. Biogeog.* 35, 1593–1607. doi: 10.1111/j.1365-2699.2008.01913.x

Brawley, S. H., and Adey, W. H. (1981). The effect of micrograzers on algal community structure in a coral reef microcosm. *Mar. Biol.* 61, 167–177. doi: 10.1007/BF00386656

Bremner, J. (2005). *Assessing Ecological Functioning in Marine Benthic Communities*. Doctoral dissertation. Newcastle upon Tyne: University of Newcastle upon Tyne.

Bremner, J. (2008). Species' traits and ecological functioning in marine conservation and management. *J. Exp. Mar. Biol. Ecol.* 366, 37–47. doi: 10.1016/j.jembe.2008.07.007

Bremner, J., Rogers, S. I., and Frid, C. L. J. (2006). Matching biological traits to environmental conditions in marine benthic ecosystems. *J. Mar. Syst.* 60, 302–316. doi: 10.1016/j.jmarsys.2006.02.004

Brown, A. C., and McLachlan, A. (1990). *Ecology of Sandy Shores*. Amsterdam: Elsevier Press.

Bueno, M., Dias, G. M., and Leite, F. P. (2017). The importance of shore height and host identity for amphipod assemblages. *Mar. Biol. Res.* 13, 870–877. doi: 10.1080/17451000.2017.1306650

Bueno, M., Flores, A. A. V., and Leite, F. P. P. (2019). Seasonal dynamics of amphipod assemblages in intertidal coralline algal mats on two Brazilian shores. *Bull. Mar. Sci.* 95, 83–99. doi: 10.5343/bms.2018.0028

Bueno, M., Tanaka, M. O., Flores, A. A. V., and Leite, F. P. P. (2016). Vertical differences in species turnover and diversity of amphipod assemblages associated with coralline mats. *Estuar. Coast Shelf Sci.* 181, 153–159. doi: 10.1016/j.ecss.2016.08.037

Carter, J. W. (1982). Natural history observations on the gastropod shell-using amphipod Photis conchicola Alderman, 1936. *J. Crustacean Biol.* 2, 328–341. doi: 10.2307/1548051

Catalán, A. M., Valdivia, N., and Scrosati, R. A. (2020). Interhemispheric comparison of scale-dependent spatial variation in the structure of intertidal rocky-shore communities. *Ecosphere* 11:e03068. doi: 10.1002/ecs2.3068

Chavanich, S., and Wilson, K. A. (2000). Rocky intertidal zonation of gammaridean amphipods in Long Island Sound. Connecticut. *Crustaceana* 73, 835–846. doi: 10.1163/156854000504840

Chevenet, F., Dolédec, S., and Chessel, D. (1994). A fuzzy coding approach for the analysis of long-term ecological data. *Freshw. Biol.* 31, 295–309. doi: 10.1111/j.1365-2427.1994.tb01742.x

Clarke, K. R., and Gorley, R. N. (2015). *PRIMER v7*: *User Manual/Tutorial*, 3rd Edn. Plymouth: Primer-E Ltd.

Cochrane, S. K., Pearson, T. H., Greenacre, M., Costelloe, J., Ellingsen, I. H., Dahle, S., et al. (2012). Benthic fauna and functional traits along a polar front transect in the barents sea–advancing tools for ecosystem-scale assessments. *J. Mar. Syst.* 94, 204–217. doi: 10.1016/j.jmarsys.2011.12.001

Conlan, K. E. (1994). Amphipod crustaceans and environmental disturbance: a review. *J. Nat. His.* 28, 519–554. doi: 10.1080/00222939400770241

Conradi, M., and Cervera, L. (1995). Variability in trophic dominance of amphipods associated with the bryozoan *Bugula neritina* (L., 1758) in Algeciras Bay (Southern Iberian Peninsula). *Pol. Arch. Hydrobiol.* 42, 483–494.

Dauwe, B. P. H. J., Herman, P. M. J., and Heip, C. H. R. (1998). Community structure and bioturbation potential of macrofauna at four North Sea stations with contrasting food supply. *Mar. Ecol. Prog. Ser.* 173, 67–83. doi: 10.3354/meps173067

de-la-Ossa-Carretero, J. A., Del-Pilar-Ruso, Y., Giménez-Casalduero, F., Sánchez-Lizaso, J. L., and Dauvin, J. C. (2012). Sensitivity of amphipods to sewage pollution. *Estuar. Coast Shelf Sci.* 96, 129–138. doi: 10.1016/j.ecss.2011.10.020

de-la-Ossa-Carretero, J. A., Del-Pilar-Ruso, Y., Giménez-Casalduero, F., and Sánchez-Lizaso, J. L. (2016). Amphipoda assemblages in a disturbed area (Alicante, Spain, Western Mediterranean). *Mar. Ecol.* 37, 503–517. doi: 10.1111/maec.12264

Díaz, E. R., and McQuaid, C. D. (2011). A spatially explicit approach to trophic interactions and landscape formation: patchiness in small-scale variability of grazing effects along an intertidal stress gradient. *J. Ecol.* 99, 416–430. doi: 10.1111/j.1365-2745.2010.01779.x

Dixit, A. M., Kumar, P., Kumar, L., Pathak, K. D., and Patel, M. I. (2010). *Economic Valuation of Coral Reef Systems in Gulf of Kachchh. Final Report of World Bank Aided Integrated Coastal Zone Management (ICZM) Project*. Gujarat: Gujarat Ecology Commission, 158.

Dray, S., and Dufour, A. B. (2007). The ade4 package: implementing the duality diagram for ecologists. *J. Stat. Softw.* 22, 1–20.

Duffy, J. E. (2006). Biodiversity and the functioning of seagrass ecosystems. *Mar. Ecol. Prog. Ser.* 311, 233–250. doi: 10.3354/meps311233

Duffy, J. E., and Hay, M. E. (2000). Strong impacts of grazing amphipods on the organization of a benthic community. *Ecol. Monogr.* 70, 237–263. doi: 10.1890/0012-96152000070[0237:SIOGAO]2.0.CO;2

Frid, C. L. J., and Caswell, B. A. (2015). Is long-term ecological functioning stable: the case of the marine benthos? *J. Sea Res.* 98, 15–23. doi: 10.1016/j.seares.2014.08.003

Gallmetzer, I., Pflugfelder, B., Zekely, J., and Ott, J. A. (2005). Macrofauna diversity in *Posidonia oceanica* detritus: distribution and diversity of mobile macrofauna in shallow sublittoral accumulations of *Posidonia oceanica* detritus. *Mar. Biol.* 147, 517–523. doi: 10.1007/s00227-005-1594-9

Gamito, S., and Furtado, R. (2009). Feeding diversity in macroinvertebrate communities: a contribution to estimate the ecological status in shallow waters. *Ecol. Indicat.* 9, 1009–1019. doi: 10.1016/j.ecolind.2008.11.012

Gestoso, I., Olabarria, C., and Troncoso, J. S. (2014). Selection of habitat by a marine amphipod. *Mar. Ecol.* 35, 103–110. doi: 10.1111/maec.12068

Gravely, F. H. (1927). The Littoral Fauna of Krusadai Island in the Gulf of Mannar. Amphipoda Gammaridea. *Bull. Madras Govt. Mus. not. Hist.* 1, 123–124.

Guerra-García, J. M., De Figueroa, J. T., Navarro-Barranco, C., Ros, M., Sánchez-Moyano, J. E., and Moreira, J. (2014). Dietary analysis of the marine Amphipoda (Crustacea: Peracarida) from the Iberian Peninsula. *J. Sea Res.* 85, 508–517. doi: 10.1016/j.seares.2013.08.006

Guerra-García, J. M., Ganesh, T., Jaikumar, M., and Raman, A. V. (2010). Caprellids (Crustacea: Amphipoda) from India. *Helgol. Mar. Res.* 64:297. doi: 10.1007/s10152-009-0183-6

Guerra-García, J. M., and Tierno de Figueroa, J. M. (2009). What do caprellids feed on? *Mar. Biol.* 156, 1881–1890. doi: 10.1007/s00227-009-1220-3

Hacker, S. D., and Steneck, R. S. (1990). Habitat architecture and the abundance and body-size dependent habitat selection of a phytal amphipod. *Ecology* 71, 2269–2285. doi: 10.2307/1938638

Harley, C. D., Randall Hughes, A., Hultgren, K. M., Miner, B. G., Sorte, C. J., Thornber, C. S., et al. (2006). The impacts of climate change in coastal marine systems. *Ecol. Let.* 9, 228–241. doi: 10.1111/j.1461-0248.2005.00871.x

Hinchey, E. K., Schaffner, L. C., Hoar, C. C., Vogt, B. W., and Batte, L. P. (2006). Responses of estuarine benthic invertebrates to sediment burial: the importance of mobility and adaptation. *Hydrobiologia* 556, 85–98. doi: 10.1007/s10750-005-1029-0

Jażdżewska, A. M., and Siciński, J. (2017). Assemblages and habitat preferences of soft bottom Antarctic Amphipoda: admiralty Bay case study. *Polar Biol.* 40, 845–1869. doi: 10.1007/s00300-017-2107-2

Jennings, S., Pinnegar, J. K., Polunin, N. V. C., and Boon, T. W. (2001). Weak cross-species relationships between body size and trophic level belie powerful size-basedtrophic structuring in fish communities. *J. Anim. Ecol.* 70, 934–944. doi: 10.1046/j.0021-8790.2001.00552.x

Kamboj, R. D. (2014). Biology and status of seagrasses in Gulf of Kachchh Marine National Park and Sanctuary India. *Indian Ocean Turt. Newsl.* 19, 9–11.

Kokarev, V. N., Vedenin, A. A., Basin, A. B., and Azovsky, A. I. (2017). Taxonomic and functional patterns of macrobenthic communities on a high-Arctic shelf: a case study from the Laptev. *Sea. J. Sea Res.* 129, 61–69. doi: 10.1016/j.seares.2017.08.011

Kristensen, E. (1988). "Benthic fauna and biogeochemical processes in marine sediments: microbial activities and fluxes," in *Nitrogen Cycling in Coastal Marine Environments*, eds T. H. Blackburn and J. Sørensen (Vijayawada: SCOPE), 275–299.

Kristensen, E., Penha-Lopes, G., Delefosse, M., Valdemarsen, T., Quintana, C. O., and Banta, G. T. (2012). What is bioturbation? The need for a precise definition for fauna in aquatic sciences. *Mar. Ecol. Prog. Ser.* 446, 285–302. doi: 10.3354/meps09506

Kumar, J. Y., Marimuthu, N., Geetha, S., Satyanarayana, C., Venkataraman, K., and Kamboj, R. D. (2014). Longitudinal variations of coral reef features in the Marine National Park, Gulf of Kachchh. *J. Coast Conserv.* 18, 167–175. doi: 10.1007/s11852-014-0303-6

Legeżyńska, J., Kêdra, M., and Walkusz, W. (2012). When season does not matter: summer and winter trophic ecology of Arctic amphipods. *Hydrobiologia* 684, 189–214. doi: 10.1007/s10750-011-0982-z

Lewis, J. R. (1964). *The Ecology of Rocky Shore*. London: English University Press.

Lincoln, R. J. (1979). *British Marine Amphipoda: Gammaridea (No. 818)*. London: British Museum.

Lourido, A., Moreira, J., and Troncoso, J. S. (2008). Assemblages of peracarid crustaceans in subtidal sediments from the Ría de Aldán (Galicia, NW Spain). *Helgol. Mar. Res.* 62, 289–301. doi: 10.1007/s10152-008-0116-9

Lyla, P. S., Velvizhi, S., and Ajmal Khan, S. (1998). *Brackishwater Amphipods of Parangipettai Coast*. Chidambaram: Annamalai University, 1–80.

Macdonald, T. A., Burd, B. J., Macdonald, V. I., and Van Roodselaar, A. (2010). *Taxonomic and Feeding Guild Classification for the Marine Benthic Macroinvertebrates of the Strait of Georgia, British Columbia*. Ottawa, ON: Ocean Sciences Division, Fisheries and Ocean Canada. 63.

Marine Species Traits editorial board (2019). *Marine Species Traits*. Available online at: http://www.marinespecies.org/traits (accessed October 17, 2019).

MarLIN (2006). *BIOTIC - Biological Traits Information Catalogue. Marine Life Information Network*. Plymouth: Marine Biological Association of the United Kingdom.

Marques, J. C., and Bellan-Santini, D. (1991). Gammaridea and Caprellidea (Crustacea - Amphipoda) of the Portuguese south-western continental shelf: taxonomy and distributional ecology. *Bijdr. Dierkd.* 61, 65–87. doi: 10.1163/26660644-06102001

McBane, C. D., and Croker, R. A. (1983). Animal-algal relationships of the amphipod *Hyale nilssoni* (Rathke) in the rocky intertidal. *J. Crust. Biol.* 3, 592–601. doi: 10.1163/193724083X00256

McLachlan, A. (1983). "Sandy beach ecology - a review," in *Sandy Beaches as Ecosystem*, eds A. McLachlan and T. Erasmus (The Hague: Junk Publishers), 321–380. doi: 10.1007/978-94-017-2938-3_25

Mejaes, B. A., Poore, A. G. B., and Thiel, M. (2015). "Crustaceans inhabiting domiciles excavated from macrophytes and stone," in *The Life Styles and Feeding Biology of the Crustacea, Nat. His. Crustacea Ser.*, eds M. Thiel and L. Watling (Oxford: Oxford Univ Press), 2, 118–144.

Menge, B. A., and Branch, G. M. (2001). "Rocky intertidal communities," in *Marine Community Ecology*, eds M. D. Bertness, S. D. Gaines, and M. E. Hay (Sunderland: Sinauer Associates), 221–251.

Menge, B. A., Farrel, T. M., Olson, A. N., Tamelen, P., and Turner, T. (1993). Algal recruitment and the maintenance of a plant mosaic in the low intertidal region of the Oregon coast. *J. Exp. Mar. Biol. Ecol.* 170, 91–116. doi: 10.1016/0022-0981(93)90131-7

Menge, B. A., and Sutherland, J. P. (1987). Community regulation: variation in disturbance, competition, and predation in relation to environmental stress and recruitment. *Am. Nat.* 130, 730–757. doi: 10.1086/284741

Mills, E. L. (1967). A reexamination of some species of Ampelisca (Crustacea: Amphipoda) from the east coast of North America. *Can. J. Zool.* 45, 635–652. doi: 10.1139/z67-080

Mondal, N., Rajkumar, M., Sun, J., Kundu, S., Ajmal, S., and Jean, K. (2010). Biodiversity of brackish water amphipods (crustacean) in two estuaries, southeast coast of India. *Environ. Monit. Asses.* 171, 471–486. doi: 10.1007/s10661-009-1292-z

Mouillot, D., Spatharis, S., Reizopoulou, S., Laugier, T., Sabetta, L., Basset, A., et al. (2006). Alternatives to taxonomic-based approaches to assess changes in transitional water communities. *Aquat. Conserv. Mar. Freshw. Ecosyst.* 16, 469–482. doi: 10.1002/aqc.769

Myers, A. A., Sreepada, R. A., and Sanaye, S. V. (2019). A new species of *Grandidierella* Coutière, 1904, *G. nioensis* sp. nov. (Amphipoda, Aoridae), from the east coast of India. *Zootaxa* 4544, 119–124. doi: 10.11646/zootaxa.4544.1.7

Myers, A. A., Trivedi, J. N., Gosavi, S., and Vachhrajani, K. D. (2018). *Elasmopus sivaprakasami* sp. nov., a new species of amphipod (Senticaudata, Maeridae) from Gujarat State, India. *Zootaxa* 4402, 182–188. doi: 10.11646/zootaxa.4402.1.10

Nair, K. K. C., Gopalakrishnan, T. C., Venugopal, P., Peter, M. G., Jayalakshmi, K. V., and Rao, T. S. S. (1983). Population dynamics of estuarine amphipods in cochin backwaters. *Mar. Ecol. Prog. Ser.* 10, 289–295. doi: 10.3354/meps010289

Narayanan, B., and Sivadas, P. (1986). Studies on the intertidal macrofauna of the sandy beach at Kavaratti Atoll (Lakshadweep). *Mahasagar* 19, 11–22.

National Institute of Oceanography [NIO] (2018). *Comprehensive Monitoring of Marine Ecology off Vadinar (April – 2018)*. Dona Paula: National Institute of Oceanography.

Newell, R. C. (1970). The biology of intertidal animals. Logos Press Ltd, London, 555 PP. of bottom trawling on ecosystem functioning. *J. Exp. Mar. Biol. Ecol.* 366, 123–133. doi: 10.1016/j.jembe.2008.07.036

Oksanen, J., Blanchet, F. G., Friendly, M., Kindt, R., Legendre, P., McGlinn, D., et al. (2016). *Vegan: Community Ecology Package. R Package Version* 2.4- 6. Available online at: https://CRAN.R-project.org/package=vegan (accessed November 10, 2019).

Oliva-Rivera, J. J. (2003). The amphipod fauna of Banco Chinchorro, Quintana Roo, Mexico with ecological notes. *Bull. Mar. Sci.* 73, 77–89.

Olsgard, F., Schaanning, M. T., Widdicombe, S., Kendall, M. A., and Austen, M. C. (2008). Effects of bottom trawling on ecosystem functioning. *J. Exp. Mar. Biol. Ecol.* 366, 123–133.

Pacheco, A. S., González, M. T., Bremner, J., Oliva, M., Heilmayer, O., and Laudien, J. (2011). Functional diversity of marine macrobenthic communities from sublittoral soft-sediment habitats off northern Chile. *Helgol. Mar. Res.* 65:413. doi: 10.1007/s10152-010-0238-8

Paganelli, D., Marchini, A., and Occhipinti-Ambrogi, A. (2012). Functional structure of marine benthic assemblages using biological traits analysis (BTA): a study along the emiliaromagna coastline (Italy, north-west adriatic sea). *Estuar. Coast Shelf Sci.* 96, 245–256. doi: 10.1016/j.ecss.2011.11.014

Paine, R. T. (1969). The Pisaster-Tegula interaction: prey patches, predator food preference, and intertidal community structure. *Ecology* 50, 950–962. doi: 10.2307/1936888

Paine, R. T. (1974). Intertidal community structure. *Oecologia* 15, 93–120. doi: 10.2307/1350837

Pandey, V., and Thiruchitrambalam, G. (2018). Spatial and temporal variability in the vertical distribution of gastropods on the rocky shores along the east coast of South Andaman Island. India. *Mar. Biodiver.* 49, 633–645. doi: 10.1007/s12526-017-0838-5

Parker, J. G. (1984). The distribution of the subtidal Amphipoda in Belfast Lough in relation to sediment types. *Ophelia* 23, 119–140. doi: 10.1080/00785326.1984.10426608

Parmar, H., Barad, D., and Parasharya, D. (2015). Reef dependent ichthyofauna of the Gulf of Kachchh, Gujarat, Western India. *Int. J. Fish. Aquat. Stud.* 2, 33–37.

Paz-Ríos, C. E., and Ardisson, P. L. (2018). Intra-annual variability of a Benthic Amphipod Assemblage (Crustacea: Amphipoda) in a tropical shallow coastal environment. *Thalassas* 34, 289–300. doi: 10.1007/s41208-017-0063-9

Paz-Ríos, C. E., Simões, N., and Pech, D. (2019). Species richness and spatial distribution of benthic amphipods (Crustacea: Peracarida) in the Alacranes Reef National Park, Gulf of Mexico. *Mar. Biodivers.* 49, 673–682. doi: 10.1007/s12526-017-0843-8

Pearson, T. H. (2001). Functional group ecology in soft-sediment marine benthos: the role of bioturbation. *Oceanogr. Mar. Biol. Annu. Rev.* 39, 233–267. doi: 10.1016/0022-0981(92)90177-c

Penrith, M. L., and Kensley, B. F. (1970). The constitution of the intertidal fauna of rocky shores of South West Africa Part. 1. Luderitzbucht. *Cimbebasia* 1, 191–239.

Piló, D., Ben-Hamadou, R., Pereira, F., Carriço, A., Pereira, P., Corzo, A., et al. (2016). How functional traits of estuarine macrobenthic assemblages respond to metal contamination? *Ecol. Indic.* 71, 645–659. doi: 10.1016/j.ecolind.2016.07.019

Queirós, A. M., Birchenough, S. N., Bremner, J., Godbold, J. A., Parker, R. E., Romero-Ramirez, A., et al. (2013). A bioturbation classification of E uropean marine infaunal invertebrates. *Ecol. Evol.* 3, 3958–3985. doi: 10.1002/ece3.769

Raj, B. S. (1927). The Littoral Fauna of the Krusadai Island in the Gulf of Mannar. *Caprellidea. Bull. Madras Govt. Mus. Nat. Hist.* 1, 125–128.

Raja, S., Lyla, P. S., and Khan, S. A. (2013). Diversity of amphipods in the continental shelf sediments of southeast coast of India. *J. Mar. Biol. Assoc. India* 55, 35–41. doi: 10.6024/jmbai.2013.55.1.01742.06

Rao, C. R. (1982). Diversity and dissimilarity coefficients: a unified approach. *Theor. Popul. Biol.* 21, 24–43. doi: 10.1016/0040-5809(82)90004-1

Rehitha, T. V., Madhu, N. V., Vineetha, G., Vipindas, P. V., and Lallu, K. R. (2019). Macrobenthic fauna with special reference to the ecology and population structure of a tubicolous amphipod, *Chelicorophium madrasensis* (Nayar, 1950) in a tropical estuary, southwest coast of India. *Mar. Biodiv.* 49, 1013–1026. doi: 10.1007/s12526-018-0886-5

Reise, K. (2002). Sediment mediated species interactions in coastal waters. *J. Sea Res.* 48, 127–141. doi: 10.1016/S1385-1101(02)00150-8

Rhoads, D. C. (1974). Organism-sediment relations on the muddy sea floor. *Oceanogr. Mar. Bull. A Rev.* 12, 263–300.

Rivonker, C. U., and Sangodkar, U. M. X. (1997). Macrofaunal density along the intertidal region of three atolls of Lakshadweep, Arabian Sea. *Ind. J. Fish* 44, 345–352.

Roy, S., Salvi, H., Brahmbhatt, B., Vaghela, N., Das, L., and Pathak, B. (2015). Diversity and distribution of seaweeds in selected reefs and island in Gulf of Kachchh. *Seaweed Res. Utiln.* 37, 12–19.

Sanz-Lázaro, C., and Marín, A. (2011). Diversity patterns of benthic macrofauna caused by marine fish farming. *Diversity* 3, 176–199. doi: 10.3390/d3020176

Satyanarayana, C. H., and Ramakrishna. (2009). *Handbook on Hard Corals of Gulf of Kachchh*. Kolkata: Zoological Survey of India.

Sfriso, A., and Marcomini, A. (1997). Macrophyte production in a shallow coastal lagoon. Part 1. Coupling with chemico-physical parameters and nutrient concentrations in waters. *Mar. Environ. Res.* 44, 351–375. doi: 10.1016/S0141-1136(97)00012-3

Sheader, M. (1977). Production and population dynamics of *Ampelisca tenuicornis* (Amphipoda) with notes on the biology of its parasite Sphaeronella longipes (Copepoda). *J. Mar. Biol. Ass. U. K.* 57, 955–968. doi: 10.1017/S0025315400026047

Sindorf, V., Cowburn, B., and Sluka, R. D. (2015). Rocky intertidal fish assemblage of the Watamu Marine National Park, Kenya (Western Indian Ocean). *Environ. Biol. Fish.* 98, 1777–1785. doi: 10.1007/s10641-015-0397-1

Sinha, M. P. (1997). *Recent Advances in Ecobiological Research*, Vol. 1. Ladakh: A.P.H. Publication, 630.

Southward, A. J. (1958). The zonation of plants and animals on rocky sea-shores. *Biol. Rev.* 33, 1337–1177. doi: 10.1111/j.1469-185X.1958.tb01305.x

Southwood, T. R. E. (1977). Habitat, the templet for ecological strategies? *J. Anim. Ecol.* 46, 337–365.

Srinivas, T., Sukumaran, S., Mulik, J., and Dias, H. Q. (2019). Community structure of benthic amphipods in four estuaries of northwest India. *Reg. Stud. Mar. Sci.* 27:100532. doi: 10.1016/j.rsma.2019.100532

Subba Rao, N. Y., and Sastry, D. R. K. (2005). Fauna of Marine National Park, Gulf of Kachchh (Gujarat): an overview. *Conserv. Area Ser.* 23, 1–79.

Sukumaran, S., Vijapure, T., Mulik, J., Rokade, M. A., and Gajbhiye, S. N. (2013). Macrobenthos in anthropogenically influenced zones of a coralline marine protected area in the Gulf of Kachchh, India. *J. Sea Res.* 76, 39–49. doi: 10.1016/j.seares.2012.11.001

Surya Rao, K. V. (1972). Intertidal amphipods from the Indian coast. *Proc. Indian Nat. Sci. Acad.* 38, 190–205.

Thomas, J. D. (1993). Biological monitoring and tropical biodiversity in marine environments: a critique with recommendations, and comments on the use of amphipods as bioindicators. *J. Nat. His.* 27, 795–806. doi: 10.1080/00222939300770481

Trivedi, J. N., Gadhavi, M. K., and Vachhrajani, K. D. (2012). Diversity and habitat preference of brachyuran crabs in Gulf of Kutch, Gujarat, India. *Arthropods* 1:13.

Underwood, A. J. (1981). Structure of a rocky intertidal community in New South Wales: patterns of vertical distribution and seasonal changes. *J. Exp. Mar. Biol. Ecol.* 51, 57–85. doi: 10.1016/0022-0981(81)90154-4

Underwood, A. J. (2000). Experimental ecology of rocky intertidal habitats: what are we learning? *J. Exp. Mar. Biol. Ecol.* 250, 51–76. doi: 10.1016/S0022-0981(00)00179-9

Valdivia, N., Scrosati, R. A., Molis, M., and Knox, A. S. (2011). Variation in community structure across vertical intertidal stress gradients: how does it compare with horizontal variation at different scales? *PLoS One* 6:e24062. doi: 10.1371/journal.pone.0024062

van der Linden, P., Marchini, A., Smith, C. J., Dolbeth, M., Simone, L. R. L., Marques, J. C., et al. (2017). Functional changes in polychaete and mollusc communities in two tropical estuaries. *Estuar. Coast Shelf Sci.* 187, 62–73. doi: 10.1016/j.ecss.2016.12.019

Vázquez-Luis, M., Borg, J. A., Sanchez-Jerez, P., and Bayle-Sempere, J. T. (2012). Habitat colonisation by amphipods: comparison between native and alien algae. *J. Exp. Mar. Biol. Ecol.* 432, 162–170. doi: 10.1016/j.jembe.2012.07.016

Warwick, R. M. (1993). Environmental impact studies on marine communities: pragmatical considerations. *Aust. J. Ecol.* 18, 63–80. doi: 10.1111/j.1442-9993.1993.tb00435.x

Webb, T. J., Tyler, E., and Somerfield, P. J. (2009). Life history mediates large-scale population ecology in marine benthic taxa. *Mar. Ecol. Prog. Ser.* 396, 239–306. doi: 10.3354/meps08253

Wildish, D. J. (1988). Ecology and natural history of aquatic Talitroidea. *Can. J. Zool.* 66, 2340–2359. doi: 10.1139/z88-349

Wong, M. C., and Dowd, M. (2015). Patterns in taxonomic and functional diversity of macrobenthic invertebrates across seagrass habitats: a case study in Atlantic Canada. *Estuar. Coast.* 38, 2323–2336. doi: 10.1007/s12237-015-9967-x

Yu, O. H., Soh, H. Y., and Suh, H. L. (2002). Seasonal zonation patterns of benthic amphipods in a sandy shore surf zone of Korea. *J. Crustacean Biol.* 22, 459–466. doi: 10.1163/20021975-99990253

Zheng, X., Huang, L., Wang, Q., and Lin, R. (2014). Amphipods fail to suppress the accumulation of *Ulva lactuca* biomass in eutrophic Yundang Lagoon. *Acta Oceanol. Sin.* 33, 155–162. doi: 10.1007/s13131-014-0532-4

Conflict of Interest: The authors declare that the research was conducted in the absence of any commercial or financial relationships that could be construed as a potential conflict of interest.

frontiers in Marine Science

ORIGINAL RESEARCH
published: 20 November 2020
doi: 10.3389/fmars.2020.579959

Wooden Stepping Stones: Diversity and Biogeography of Deep-Sea Wood Boring Xylophagaidae (Mollusca: Bivalvia) in the North-East Atlantic Ocean, With the Description of a New Genus

Chiara Romano[1†‡], Amandine Nunes-Jorge[2‡], Nadine Le Bris[3†], Greg W. Rouse[4†], Daniel Martin[1†] and Christian Borowski[2*†]*

[1] Centre d'Estudis Avançats de Blanes (CEAB-CSIC), Blanes, Spain, [2] Max Planck Institute for Marine Microbiology, Bremen, Germany, [3] Sorbonne Université, CNRS, Observatoire Océanologique de Banyuls (LECOB), Banyuls-sur-Mer, France, [4] Scripps Institution of Oceanography, University of California, San Diego, La Jolla, CA, United States

Wood boring bivalves of the family Xylophagaidae inhabit sunken wood on the deep-sea floor where they play a key role in the degradation of this organic matter in the ocean. The patchiness of wood-fall habitats is impeding targeted sampling and little is therefore known on xylophagaid biology. We investigated for the first time the diversity and biogeography of Xylophagaidae in the NE-Atlantic and the Mediterranean over a broad geographic range and in various water depths using experimental wood deployments. We combined morphological and molecular analyses for species discrimination. A phylogenetic reconstruction based on 18S and 28S rRNA and COI genes revealed non-monophyly of the type genus, *Xylophaga* Turton (1822), and led us to revise the taxonomy and erect the genus *Xylonora* gen. nov. COI haplotypes of the most abundant species revealed broad Atlanto-Mediterranean genetic connectivity for *Xylophaga dorsalis* and *Xylonora atlantica* new comb., while genetic connectivity appears limited for *Abditoconus brava* across the entrance of the Mediterranean. We provide the first COI barcode data for Xylophagaidae as a solid base for future taxonomic work. Wood deployments in a broad geographic range provided a powerful tool for research on Xylophagaidae allowing for conclusions on ecological requirements of xylophagaid species.

Keywords: genetic connectivity, wood falls, Mediterranean, deep sea, phylogeography

OPEN ACCESS

Edited by:
Marcos Rubal,
University of Porto, Portugal

Reviewed by:
Gonzalo Giribet,
Harvard University, United States
Anna Marie Holmes,
National Museum Wales,
United Kingdom

***Correspondence:**
Chiara Romano
cromano@ceab.csic.es
Christian Borowski
cborowsk@mpi-bremen.de

†ORCID:
Chiara Romano
orcid.org/0000-0001-5078-0082
Nadine Le Bris
orcid.org/0000-0002-0142-4847
Greg W. Rouse
orcid.org/0000-0001-9036-9263
Daniel Martin
orcid.org/0000-0001-6350-7384
Christian Borowski
orcid.org/0000-0001-7921-3022

‡These authors have contributed equally to this work

Specialty section:
This article was submitted to Marine Evolutionary Biology, Biogeography and Species Diversity, a section of the journal Frontiers in Marine Science

Received: *03 July 2020*
Accepted: *29 September 2020*
Published: *20 November 2020*

Citation:
Romano C, Nunes-Jorge A, Le Bris N, Rouse GW, Martin D and Borowski C (2020) Wooden Stepping Stones: Diversity and Biogeography of Deep-Sea Wood Boring Xylophagaidae (Mollusca: Bivalvia) in the North-East Atlantic Ocean, With the Description of a New Genus. Front. Mar. Sci. 7:579959. doi: 10.3389/fmars.2020.579959

INTRODUCTION

The Xylophagaidae Purchon (1941) and the sister family Teredinidae Rafinesque (1815) are among the most abundant wood-degrading organisms in the marine realm (Turner, 1973; Wolff, 1979; Distel, 2003; Distel et al., 2011). Both bivalve families have similar habitats, as they both bore in wood which they use as a shelter and they are both considered obligate wood feeders with limited ability for filter feeding (Purchon, 1941; Saraswathy and Nair, 1971). Nevertheless, their

ecological niches do not overlap. Xylophagaidae live in deep waters where they colonize wood that has sunk to the sea floor. Teredinidae, known also as shipworms, colonize driftwood in surface waters. Shipworms gained a reputation as pests by damaging boats and submerged wooden structures ever since humans started to sail, and their life histories and growth rates are therefore well studied (Haderlie and Mellor, 1973; Culliney, 1975; MacIntosh et al., 2014). Xylophagaidae in contrast, have been recorded mostly below 150 m depth down to hadal environments at 7,000 m depth (Knudsen, 1961; Turner, 2002; Distel, 2003; Voight, 2008) and many aspects of their life histories remain unknown.

Xylophagaids and teredinids ingest wood chips they create by boring with their specialized shells and which then accumulate in a special stomach diverticulum, the caecum (Purchon, 1941; Monari, 2009; Distel et al., 2011). Cellulose, hemicellulose and lignin, the main wood components, are highly refractory polysaccharide polymers that do not hydrolyse easily. Biological degradation uses cellulolytic enzymes that break them down to easily digestible mono- and disaccharides (Klemm et al., 2005). Many bacteria and fungi synthesize cellulolytic enzymes, while most animals do not. Teredinids harbor cellulose-degrading bacteria in their gills (Waterbury et al., 1983; Distel et al., 2002; Distel, 2003) and this symbiosis is considered as the basis for their wood digestion capacity (O'Connor et al., 2014). However, an additional combination of cellulolytic enzymes produced by the molluscs themselves has been recently discovered in the caecum (Sabbadin et al., 2018). Xylophagaidae also host endosymbiotic bacteria in the gills (Distel and Roberts, 1997; Bessette et al., 2014; Fagervold et al., 2014; Voight, 2015), but their role and metabolic pathways remain even less studied.

Wood reaches the open ocean by river transport after storm and flood events (Stockton and DeLaca, 1982; West et al., 2011), and after drifting and becoming saturated with water it eventually sinks down to the seafloor (Wolff, 1979). Sunken wood represents high local carbon inputs to the deep sea which generally lacks primary production and receives extremely limited phototrophic contributions from the surface (Stockton and DeLaca, 1982; Smith et al., 2008). Wood-falls create discrete organic islands on the deep-sea floor harboring distinct and specialized fauna mining the wood, breaking it up and thereby supporting wood polymer degradation by cellulolytic microorganisms (Kalenitchenko et al., 2018b). Consumption of oxygen during this process eventually leads to anoxic and sulfidic environments providing habitats for chemosynthetic microbial communities and invertebrates associated with sulfur-oxidizing symbionts (Gaudron et al., 2010; Bienhold et al., 2013; Fagervold et al., 2013; Yücel et al., 2013; Kalenitchenko et al., 2018a).

Xylophagaids are primarily responsible for the structural degradation of wood in the deep sea (Turner, 1977) building up very dense populations within a few weeks to several months (Romey et al., 1994; Harvey, 1996; Tyler et al., 2007; Romano et al., 2013). Their fast-growing populations become a valuable trophic resource for carnivores, while their fecal materials play a similar role for detritivores. This is certainly a basal shackle of the trophic chain in deep-sea wood-fall ecosystems which makes xylophagaids keystone for the associated assemblages (Turner, 1973; Culliney and Turner, 1976; Distel, 2003).

Deep-sea wood falls are highly fragmented and ephemeral sulfidic habitats comparable to other chemosynthetic ecosystems (e.g., whale falls, hydrothermal vents, hydrocarbon seeps), but they sustain even more rapid ecological cycles (Kalenitchenko et al., 2018b). Organisms living in such patchy habitats often develop long-distance dispersal strategies to colonize areas hundreds of kilometers away (Baco et al., 1999; Tyler and Young, 1999; Van Dover et al., 2002; Breusing et al., 2016). Studies on xylophagaids relied for long on occasionally recovered naturally sunken wood, mainly as by-catch in trawl and dredge hauls. Collections of xylophagaids remained largely untargeted and very little is known on their distribution mechanisms and geographical patterns. A few species have been collected repeatedly at different sites, such as *Xylophaga dorsalis* (Turton, 1819) and *Xylophaga atlantica* Richards, 1942. Both live in wide geographic areas and from littoral to bathyal depths in the northern Atlantic Ocean (Purchon, 1941; Culliney and Turner, 1976; Santhakumaran, 1980; Voight, 2007). Many other species are only known from single records (Knudsen, 1961; Harvey, 1996; Turner, 2002; Voight, 2007, 2008), while some occur in abyssal plains or even in deep-sea trenches, thousands of kilometers away from the nearest land mass, where sunken wood is considered extremely rare (Knudsen, 1961; Voight, 2008; Voight and Segonzac, 2012).

Xylophagaidae currently includes six genera: *Xylophaga* Turton, 1822, *Xylopholas* Turner, 1972, *Xyloredo* Turner, 1972, *Feaya* Voight, 2019, *Abditoconus* Voight, 2019, and *Spiniapex* Voight, 2019 (Voight et al., 2019). *Xylophaga* is the most speciose, containing currently more than 50 species. Historically, the vast majority of taxonomic works on Xylophagaidae have based on morphology, while only two studies also used molecular markers; hence little is currently known about their genetic diversity (Romano et al., 2014; Voight et al., 2019). The main diagnostic morphological characters refer to valves, mesoplax, siphons, and muscle inserts on inner surfaces of the valves (Tyler et al., 2007). These characters and the overall shape of the shells may vary among populations and are affected by environmental conditions such as wood hardness. Even individuals within the same population inhabiting neighboring logs of different wood such as soft pine or hard oak may vary (Turner, 2002). In addition, extraction of the xylophagaids from wood substrates can be challenging and often lead to fragmentation of specimens and damage of their delicate shells. As a result, several species descriptions are based on single or incomplete specimens, lacking information on intraspecific phenotypic variation (Smith, 1903; Knudsen, 1961; Santhakumaran, 1980; Harvey, 1996; Turner, 2002). For these reasons, species determinations relying only on morphological characters can be ambiguous and lead to errors. Molecular tools can circumvent many of these difficulties, and they are particularly useful for increasing rigor of identification, especially in poorly known species.

Recent *in situ* deep-sea experiments used moorings, submersibles or remotely operated vehicles for deploying wood at great depths. These experiments were designed to specifically target wood-fall organisms, including xylophagaids.

Previous studies mainly focused on the eastern Pacific and western Atlantic and very little is currently known on the biogeographic distribution of the European species (Tyler et al., 2007; Voight, 2007, 2008; Reft and Voight, 2009; Voight and Segonzac, 2012). However, several European oceanographic research projects recently deployed wood in the North-East Atlantic and Mediterranean deep sea allowing for comprehensive studies on European Xylophagaidae (Gaudron et al., 2010, 2016; Bienhold et al., 2013; Romano et al., 2013, 2014).

In this study we investigated the diversity and biogeographic distribution of Xylophagaidae in a broad range of boreal to temperate latitudes in North-East Atlantic and Mediterranean waters based on numerous experimental wood deployments. We used molecular methods and analyzed for the first time cytochrome *c* oxidase subunit I (COI) data of Xylophagaidae from a depth range of 130 to 2,300 m to verify morphology-based species identification. The aims of the present study were to (1) assess the diversity and phylogeny of these particular organisms, (2) provide barcode data, (3) reveal genetic connectivity patterns for populations of Xylophagaidae, and (4) draw up conclusions on ecological requirements of xylophagaid species.

MATERIALS AND METHODS

Sampling and Specimens Collection

Wood samples were experimentally deployed on the deep-sea floor and recovered several months later during a number of oceanic research cruises between 2006 and 2013 in various sites in the North-East Atlantic Ocean and the Mediterranean.

Experimental wood deployments in the Atlantic included the Haakon Mosby Mud Volcano (HMMV) in the deep Barents Sea, the Avilés submarine canyon (AC) in the Bay of Biscay, the hydrothermal vent sites Rainbow (Rb) and Menez Gwen (MG) on the Mid-Atlantic Ridge (MAR) and the Meknès and Mercator mud volcanoes in the North Atlantic off Morocco (Morocco mud volcanoes MMV). The Mediterranean sites included three submarine canyons offshore north-eastern Iberian Peninsula and southern France: Blanes (BC), La Fonera (LFC) and Lacaze-Duthiers (LDC) (North Western Mediterranean), and one cold seep site (Central Pockmarks) in the deep Nile Fan (NF) off Egypt (Eastern Mediterranean) (**Figure 1** and **Table 1**). Deployments ranged from 130 to 2,300 m depth. Wood parcels were either placed directly on the deep-sea floor (**Figure 2**) or moored 20 to 30 m above. At hydrothermal vent fields and mud volcanoes, wood was placed away from the influence of active hot fluid emissions or seepage. The experiments used soft (pine and Douglas fir) or hard (oak) wood, either as cubes within colonization devices (Gaudron et al., 2010; Cunha et al., 2013), free logs (Bienhold et al., 2008, 2013) or logs inside net bags (Romano et al., 2013, 2014; Kalenitchenko et al., 2018b). Wood deployment times ranged from 3 to 36 months.

The recovered wood pieces were opened using hammer and chisel or, when degradation had considerably progressed, by hand. The bivalves were carefully extracted and preserved for morphological identification in a 4% paraformaldehyde seawater solution, then transferred to ethanol/sterile filtered seawater solution at v/v 70%. For molecular analyses, they were either directly frozen at −20°C or preserved in 99% ethanol. Before molecular analyses, the specimens were sorted under a dissecting microscope and identified to species or morphotype level, based on the relevant literature (Harvey, 1996; Turner, 2002; Voight, 2007, 2008; Romano et al., 2014).

DNA Extraction, PCR Amplification and Sequencing

We extracted DNA from dissected fragments of siphon or foot tissues from 92 specimens (**Table 2**), following either a modified protocol based on (Zhou et al., 1996) or with a DNeasy Mini Kit (Qiagen)[1]. Nuclear 18S and 28S rRNA genes were amplified by polymerase chain reaction (PCR) using seven primer pairs (Distel et al., 2011; **Supplementary Table S1**) and by using various enzymes and amplification conditions (**Supplementary Table S2**). A fragment of mitochondrial COI was amplified with a combination of the general primer HCO2198 (Folmer et al., 1994) and an unpublished primer developed by Dario Zuccon (National Natural History Museum of Paris, pers.com.), generating a size of ∼300–500 bp (**Supplementary Table S1**). Amplification reactions were conducted with 1 to 2 μl of DNA extract in final volumes of 20 or 50 μl, following the enzyme provider recommendations. PCR products were purified with the QIAquick kit (Qiagen, Hilden, Germany) or ExoSAP product Clean-up.

Bidirectional direct sequencing using the same primers as for PCR (**Supplementary Table S1**) and additional internal primers (**Supplementary Table S1**) was done with the Bigdye v3.1 cycle sequencing kit (Applied Biosystems, Foster City, CA, United States) and the sequencer ABI prism 3130×L (Applied Biosystems, Foster City, UA, United States) or by Macrogen (Korea).

Sequence Analyses and Phylogenetic Reconstructions

The sequences were edited in Geneious 8.1.8 (Kearse et al., 2012) and overlapping fragments merged into consensus sequences. We compared our sequences with the NCBI databases using BLAST (Altschul et al., 1997) to check for sequence contaminations (Vrijenhoek et al., 2009). The NCBI database did not contain COI sequences from Xylophagaidae and the similarity hits targeted COI sequences of unrelated bivalve and gastropod molluscs (max. 70% sequence similarity). COI sequences were translated into amino acid alignment with code 5 for invertebrate mitochondrial genes and checked for stop codons in order to avoid pseudogenes. NCBI comparisons of large and small rRNA subunit sequences revealed highest similarities with species of Xylophagaidae and Teredinidae (max. 98% for 18S rRNA, 84% for 28S rRNA).

We imported our sequences in Mesquite 3.2 (Maddison and Maddison, 2019) and included NCBI sequences of Xylophagaidae, Teredinidae, and Pholadidae

[1]www.qiagen.com

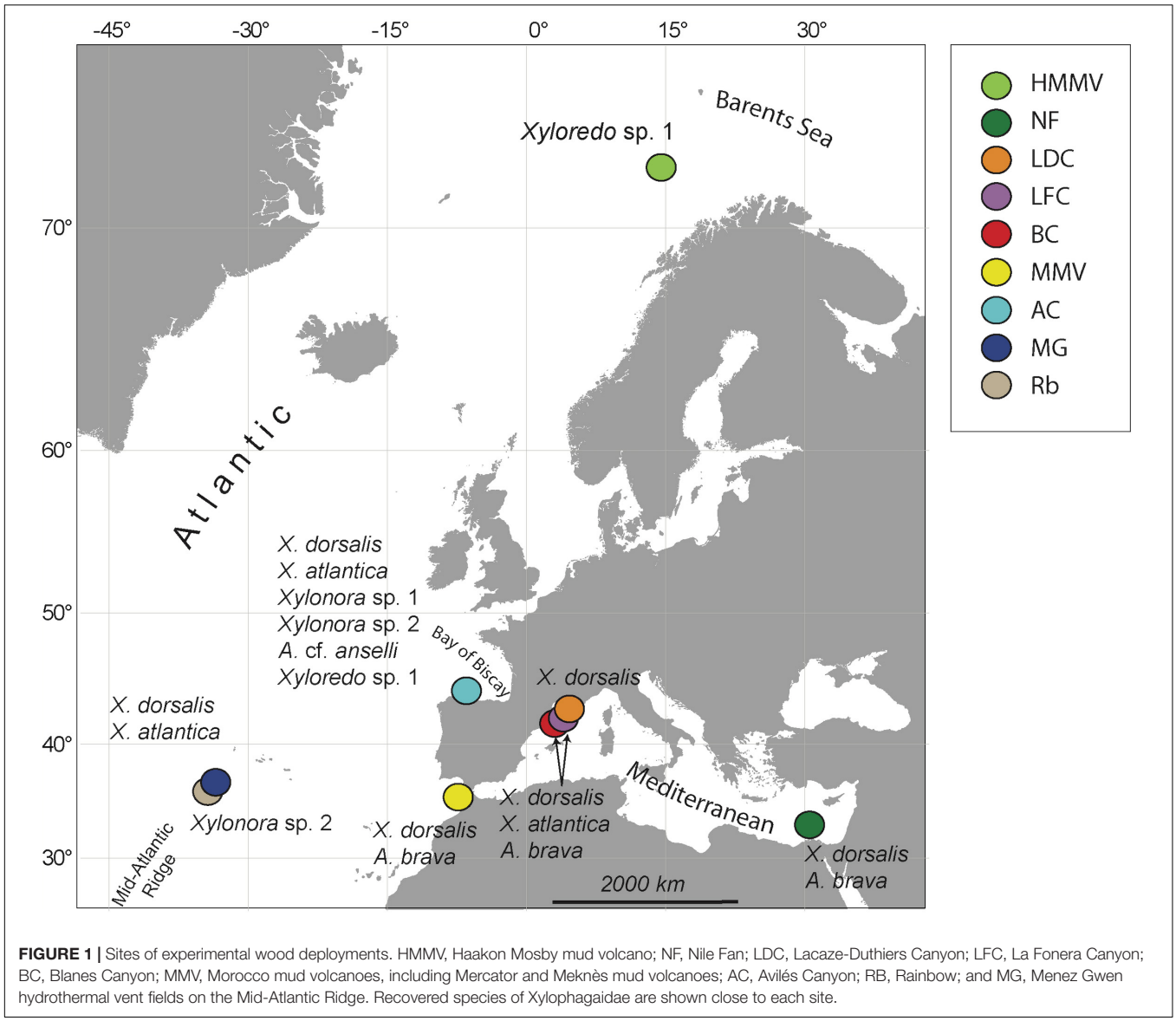

FIGURE 1 | Sites of experimental wood deployments. HMMV, Haakon Mosby mud volcano; NF, Nile Fan; LDC, Lacaze-Duthiers Canyon; LFC, La Fonera Canyon; BC, Blanes Canyon; MMV, Morocco mud volcanoes, including Mercator and Meknès mud volcanoes; AC, Avilés Canyon; RB, Rainbow; and MG, Menez Gwen hydrothermal vent fields on the Mid-Atlantic Ridge. Recovered species of Xylophagaidae are shown close to each site.

(**Supplementary Table S3**). All sequences were aligned using MAFFT and then manually edited, trimmed and cleaned from ambiguous positions. The final alignments included 388 bp (COI), 1353 bp (18S rRNA), and 1104 bp (28S rRNA). All new sequences are deposited on GenBank (**Supplementary Table S3**).

Genetic diversity was evaluated as the number of segregating sites (S), using the MEGA software version 6 (Tamura et al., 2013) and uncorrected pairwise distances with PAUP* v.4.0a161 (Swofford, 2003).

Maximum likelihood (ML) and Bayesian inference (BI) analyses of the molecular data phylogenetic trees were calculated separately for each gene COI, 18S rRNA and 28S rRNA, using RAxML v.8.2.10 (Stamatakis, 2014) and MrBayes v.3.2.6 (Huelsenbeck and Ronquist, 2001), respectively. Analyses of concatenated COI+18S rRNA+28S rRNA, partitioned by gene, were also calculated with RAxML and MrBayes. For the BI analyses, the best-fitting evolutionary model for each gene was estimated with the software package Iq-Tree 1.6.12 (Chernomor et al., 2016) using the Akaike information criterion (AIC). GTR+F+I+G4 was the best fitting nucleotide substitution model for each of the genes. BI analyses were run twice, starting from random trees, with four chains running simultaneously (two cold and two heated). Chains were run for 10^6 generations for 18S rRNA and 28S rRNA and 10^7 generations for COI and the concatenated data, sampled every 1,000 generations and, after verifying that stationarity had been reached, 25% of the generations were discarded as burn-in. The ML analyses were performed using the GTR+G evolutionary model, following the recommendations in the software author. Support values for the ML analyses were generated by 100 bootstrap pseudoreplicates. We used sequences from *Mya arenaria* Linnaeus, 1758, *Mya truncata* Linnaeus, 1758 and *Varicorbula limatula* Conrad, 1846 [here reported as *Varicorbula disparilis* D'Orbigny, 1853 as in NCBI database] and the Teredininae *Lyrodus pedicellatus*

TABLE 1 | Characteristics of deployment sites and colonization experiments.

	Region	Site	Environment	Coordinates	Depth (m)	Temperature (°C)	Deployment /Recovery (Cruise name - Date)	Duration of Deployment (Months)	Research project	References
Atlantic	Barents Sea	Haakon Mosby Mud Volcano	Mud volcano	72°00N, 14°43E	1260	−1	ARKXXII/1b - June 2007 / ARKXXIV/2 - June 2009	24	DiWOOD	Pop Ristova et al., 2017; this study
	Bay of Biscay	Avilés Canyon	Canyon; Slope	44°07'N, 6°14'W	1200; 2000	4; 9	BioCant 2012-2013	7; 13	DosMares	Romano et al., 2014
	Mid-Atlantic Ridge	Menez-Gwen	Hydrothermal vent	37°17'N, 32°15'W	870	9	MenezKart/ POS402 - July 2010/BioBaz July 2013	36	DiWOOD	This study
		Rainbow	Hydrothermal vent	36°13'N, 33°54'W	2300	3.5	MoMARDream-Naut -July 2007/ MoMARDream 08 - Aug.-Sept. 2008	13	CHEMECO	Gaudron et al., 2010
	NW-Atlantic, Morocco	Mercator	Mud volcano	35°17'N, 06°38'W	350	13	JC10 May - 2007 and 64PE284 - March 2008/B09-May 2009	9; 24	CHEMECO/FTC	Cunha et al., 2013
		Meknès	Mud volcano	34°59'N, 07°04'W	700	N.A.		15		Cunha et al., 2013
Mediterranean	Western Mediterranean	Blanes Canyon	Canyon; Slope	41°34'N, 2°50'E	900; 1100; 1200; 1500; 1800	13	Prometeo 2008-2009 Dos Mares 2012-2013	3 & 9 (at 1200 m); 12 (at other depths)	PROMETEO, DosMares	Romano et al., 2013
		La Fonera Canyon	Canyon	41°52"N, 3°16'E	130; 1100	13	DosMares 2012-2013	10 (at 130 m); 7 & 13 (at 1100 m)	Dos Mares	Romano et al., 2014; this study
		Lacaze-Duthiers Canyon	Canyon	42°28'N, 3°28'E	500	13	2011	7	*Extreme Marine Env., Biodiversity and Global Change'*	Kalenitchenko et al., 2015; this study
	Eastern Mediterranean, Nile Fan (NF)	Central Pockmarks	Seep	32°32' N, 30°21' E	1145	14	Bionil M70/2 - Oct./Nov. 2006 /Medeco-2 - Nov. 2007 and Homer MSM13/3 - Oct./Nov. 2009	12; 36	DiWOOD	Bienhold et al., 2013; this study

NA: not available.

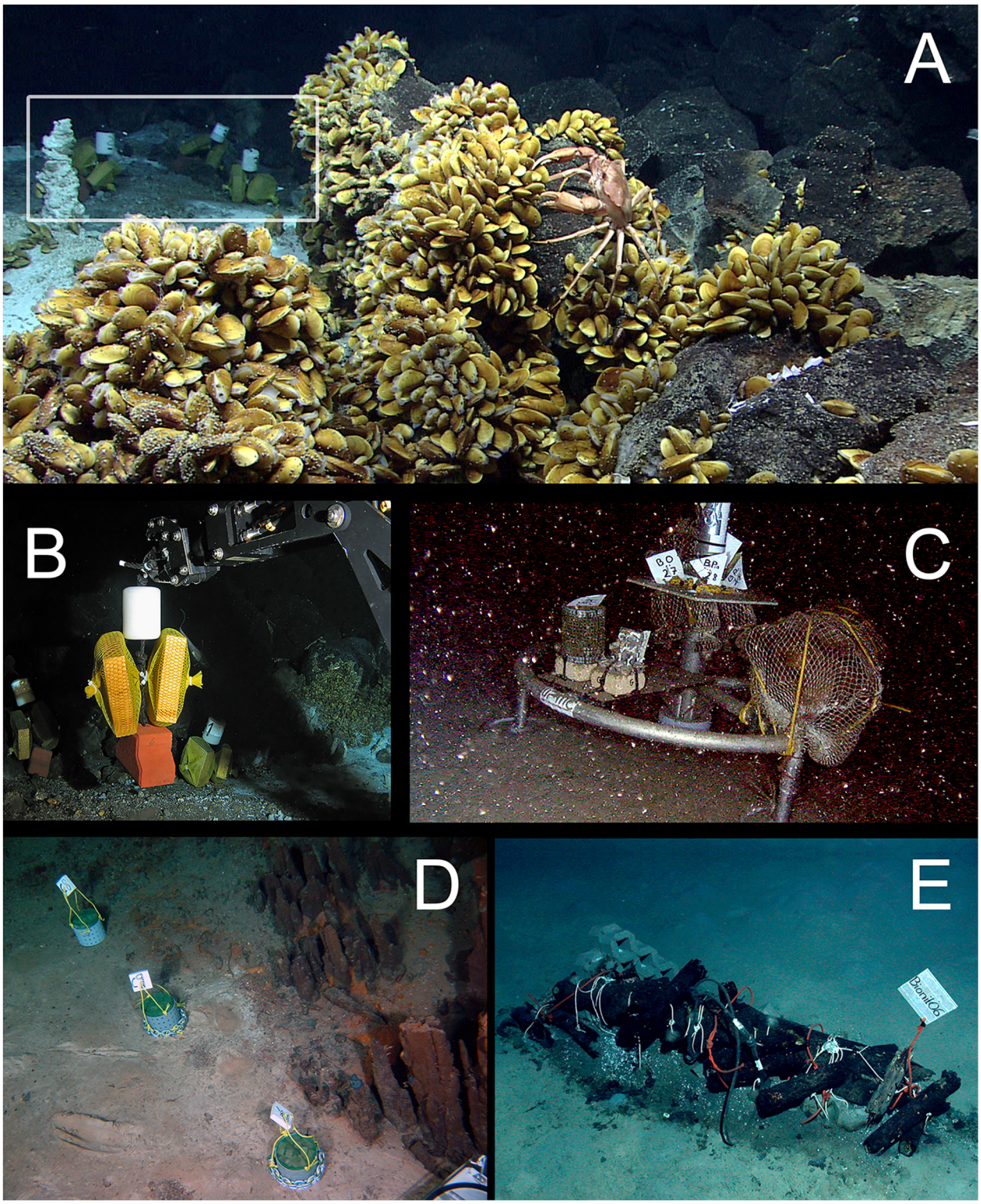

FIGURE 2 | Examples of *in situ* wood deployments. **(A)** Small wood panels (white frame) deposited outside of a diffuse flow area in the Menez Gwen hydrothermal vent field (RV Meteor, cruise M82/3); **(B)** ROV manipulator arm positioning wood panels in panel **(A)** at Menez Gwen (RV Poseidon, cruise POS402); **(C)** Moored lander with net bags containing wood blocks in Lacaze-Duthiers Canyon (LECOB LDC monitoring cruises); **(D)** Chemecoli colonization devices containing small pine wood cubes (2.5 cm³) next to inactive chimneys in the Rainbow hydrothermal vent field (RV Pourquoi Pas?, cruise Momardream); **(E)** Chemecoli colonization devices and large wood logs in the deep Nile Fan (RV Pourquoi Pas?, cruise Medeco). Copy rights: **(A,B,E)** MARUM–Center for Marine Environmental Sciences, University of Bremen; **(C)** Sorbonne Université; **(D)** Ifremer.

TABLE 2 | Number of specimens per species used for each genetic analysis.

	Locations	Sites	Species	18S	28S	18S+28S	COI
Atlantic	Haakon Mosby mud volcano		*Xyloredo* sp. 1	3	3	3	2
	Avilès Canyon		*Xylophaga dorsalis*	3	2	2	2
			Abditconus anselli	2	2	2	1
			Xylonora atlantica	3	3	3	3
			Xylonora sp. 1	1	1	1	1
			Xylonora sp. 2	1	1	1	1
			Xyloredo sp. 1	2	1	1	0
	Mid-Atlantic Ridge	Menez-Gwen	*Xylophaga dorsalis*	5	5	5	5
			Xylonora atlantica	4	5	4	5
		Rainbow	*Xylonora* sp. 2	3	3	3	3
	Morocco Mud Volcanoes	Mercator	*Xylophaga dorsalis*	3	4	3	4
		Meknès	*Abditconus brava*	1	1	1	3
Mediterranean	Western	Blanes Canyon	*Xylophaga dorsalis*	4	5	4	8
			Abditconus brava	7	7	6	5
			Xylonora atlantica	5	5	5	5
		La Fonera Canyon	*Xylophaga dorsalis*	4	4	4	5
			Abditconus brava	3	3	2	3
			Xylonora atlantica	9	9	9	7
		Lacaze Duthiers Canyon	*Xylophaga dorsalis*	8	10	8	5
	Eastern	Nile Fan (NF)	*Xylophaga dorsalis*	5	5	5	5
			Abditconus brava	3	3	3	3
			Total	78	81	74	78

Quatrefages, 1849 and *Bankia carinata* Gray, 1827 as outgroups. Trees were visualized in FigTree v 1.4.2 (Rambaut, 2006). A median-joining haplotype network based on COI sequences was constructed in PopArt (Leigh and Bryant, 2015) for the species that produced a minimum of 15 sequences, i.e., *X. dorsalis*, *Abditoconus brava*, and *X. atlantica*.

Nomenclatural Acts

This article conforms to the requirements of the amended International Code of Zoological Nomenclature (ICZN), and hence the new names contained herein are available under that Code from the electronic edition of this article. This published work including the nomenclatural acts have been registered in the ICZN online registration system ZooBank. The ZooBank Life Science Identifiers (LSID) can be resolved and the associated information viewed through any standard web browser by appending the LSID to the prefix http://zoobank.org/. The LSID for this publication is: urn:lsid:zoobank.org:pub:71C8DF63-5C84-4C6E-B5A2-7902939FEBBD.

RESULTS

Phylogenetic Analyses

The phylogenetic trees obtained with both tree reconstruction methods for the single genes partially resolved the phylogeny. The best resolution was achieved in the combined analysis of all three genes and the BI and ML analyses provided consistent topologies in this respect. We show the BI tree for the three concatenated genes, including the BI posterior probabilities (pp) and the ML bootstrap (bs) on the nodes (**Figure 3**).

Xylophagaidae formed a well-supported clade (1 pp, 100% bs), more closely related to Teredinidae than to Pholadidae (**Figure 3**). Eight "major" clades were recovered within the family, six of them were well supported (**Figure 3**, >0.9 pp, >70% bs) and two of them (clades 1 and 8) had weak support, similar to the result in Voight et al. (2019). Clade 1 was formed by a single lineage originally included in *Xylopholas* (Voight, 2016), but recently moved to *Feaya* (Voight et al., 2019), and this species was sister group to clades 2 and 3, with moderate support. *Xylophaga* was non-monophyletic, with its species distributed over clades 3 and 4. Clade 3 comprised the type species, *X. dorsalis*, *Xylophaga oregona* Voight (2007) and also *Xylophaga washingtona* Bartsch (1921), all three morphologically characterized by truncated excurrent siphons [groups 5 and 6 in (Turner, 2002)]. Their sister-clade relationship to clade 2, which combines recently sequenced specimens of *Xylopholas* (Voight et al., 2019), was well supported. Clade 4 contained other *Xylophaga* species and was well-supported. To resolve the non-monophyly of *Xylophaga*, we propose to assign clade 4 to a new genus, namely *Xylonora* gen. nov., since the type species of *Xylophaga*, *X. dorsalis*, is member of clade 3. The species of *Abditoconus* were united in clade 5, while those of *Spiniapex* were in clade 6, and those of *Xyloredo* in clade 7. A single terminal, supposedly a *Xylopholas* from the Gulf of Mexico, represented by GenBank sequences (Clade 8, 0.9 pp, 58% bp), was isolated from all other *Xylopholas*. This situation is unclear and could possibly result from misidentification of the specimen. Re-collection and examination of the voucher may be needed to solve this in the future.

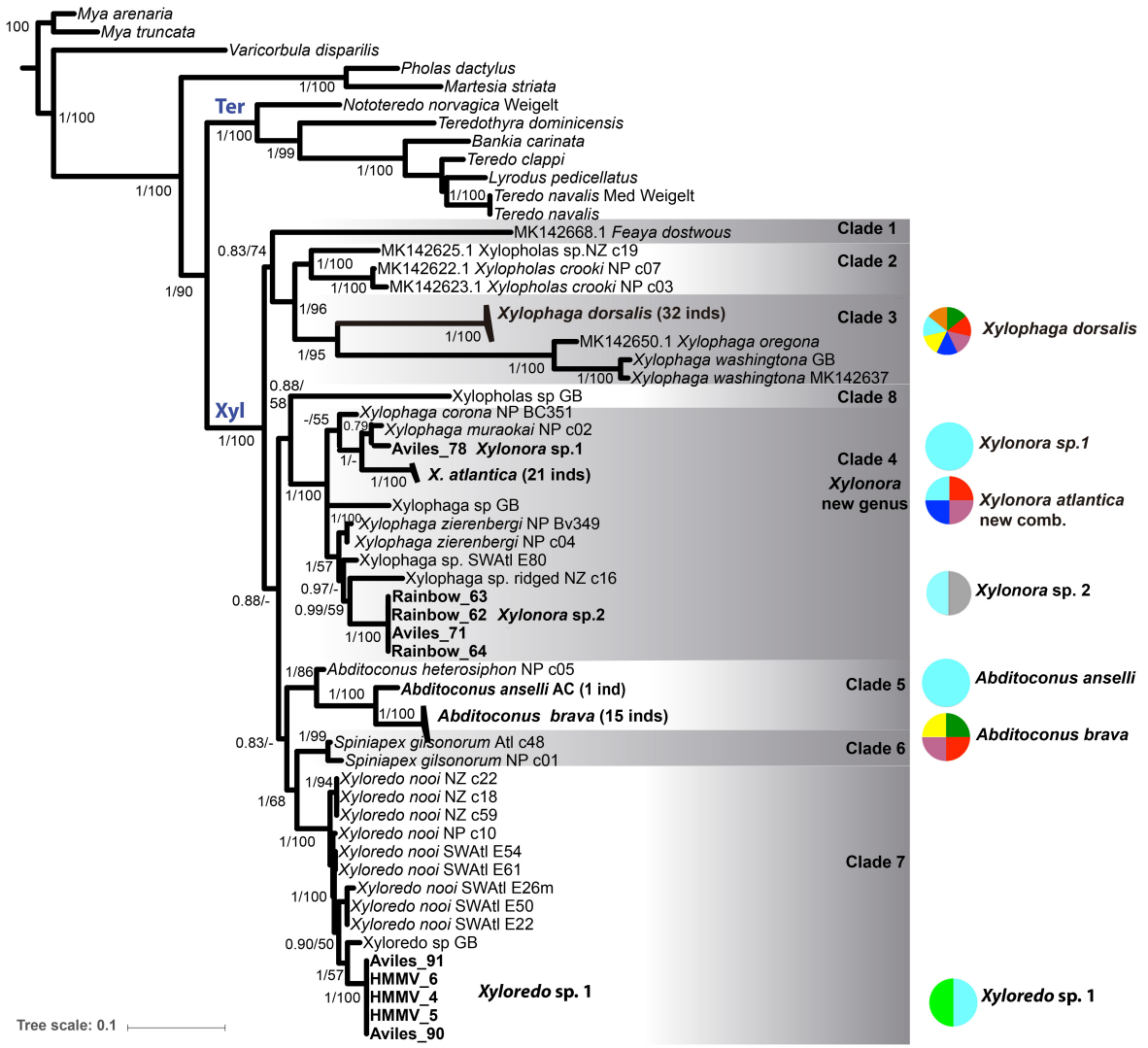

FIGURE 3 | Bayesian inference (BI) and Maximum likelihood (ML) phylogenetic analysis based on the concatenated data set of COI, 18S and 28S rRNA genes (MAFFT aligned). Statistic support is indicated on the nodes (BI/ML, values < 0.5 pp or 50% bs not shown). Bold taxa names: sequences from this study, including locations. Not-bold taxa names: GenBank sequences; inds = number of sequenced individuals. (see **Supplementary Table S3** for accession numbers). Xyl: node of Xylophagaidae; Ter: node of Teredinidae. Colored circles and associated numbers represent the geographic and depth distributions of the species in this study; circle colors as in **Figure 1**.

In summary, the monophyletic and well-supported xylophagaid clades correspond to six genera *Xylonora* gen. nov., *Xylopholas*, *Xylophaga*, *Abditoconus*, *Spiniapex*, and *Xyloredo*, as well as the monotypic *Feaya*.

Taxonomic Account

Xylophaga Turton, 1822 *sensu stricto*

Type species

Xylophaga dorsalis Turton, 1819.

Diagnosis

Mesoplax with two calcareous plates, excurrent siphon truncated, shorter than incurrent siphon, periostracum restricted to basal and lateral siphon, and a furrow on dorsal incurrent siphon distal to excurrent opening.

Species included

Three groups of species are included in the genus at present. The first includes *X. dorsalis*, *X. washingtona*, and *X. oregona* (molecular data of these three species included in this study, **Supplementary Table S3**). For the second group, molecular data are not yet available: *Xylophaga alexisi* Voight and Segonzac, 2012, *Xylophaga aurita* Knudsen, 1961, *Xylophaga bayeri* Turner, 2002, *Xylophaga depalmai* Turner, 2002; *Xylophaga guineensis* Knudsen, 1961, *Xylophaga indica* Smith, 1904, *Xylophaga mexicana* Dall, 1908, *Xylophaga multichela* Voight, 2008, *Xylophaga nidarosiensis* Santhakumaran, 1980,

Xylophaga praestans Smith, 1903, *Xylophaga pacifica* Voight, 2009, *Xylophaga rikuzenica* Taki and Habe, 1945, *Xylophaga turnerae* Knudsen, 1961, *Xylophaga tipperi* Turner, 2002. For the third group, additional morphologic or genetic information are needed: *Xylophaga africana* Knudsen, 1961, *Xylophaga lobata* Knudsen, 1961, *Xylophaga obtusata* Knudsen, 1961, *Xylophaga clenchi* Turner and Culliney, 1971, *Xylophaga noradi* Santhakumaran, 1980, *Xylophaga tubulata* Knudsen, 1961 *Xylophaga whoi* Turner, 2002, *Xylophaga grevei*, *Xylophaga ricei* Harvey, 1996, and *Xylophaga gagei* Harvey, 1996.

Remarks

The morphology of the species of the third group fits better to the diagnosis of the new genus *Xylonora* as their excurrent siphons are equal to subequal with respect to the incurrent siphons rather than truncated as in *Xylophaga*. However, additional morphologic or genetic information is needed before suggesting a transfer to this genus.

Xylonora gen. nov. Romano

LSID: urn:lsid:zoobank.org:act:9D8F449F-8720-4E9C-9814-FCA1292AC0F2.

Type species

Xylonora atlantica (Richards, 1942) new comb.

Diagnosis

Mesoplax with two calcareous plates of variable shape; siphons equal or subequal; excurrent siphon opening dorsally to incurrent one; cirri on both openings present or absent. Small individuals (embryos or dwarf males) may occur attached dorsally on shell, posterior to umbo but seldom to ventral siphon.

Species included

Xylonora atlantica new comb., *Xylonora muraokai* Turner, 2002 new comb., *Xylonora corona* Voight, 2007 new comb. and *Xylonora zierenbergi* Voight, 2007 new comb. (molecular data included in this study, **Supplementary Table S3**).

Etymology

The genus is named in honor of CR's mother Eleonora "Nora" Rivarola, Professor of Chemistry, who always provided inspiration, rigor and motivation as role model for women in science.

Remarks

Our molecular results are consistent with the morphology, showing clade 4 species clearly separated from *Xylophaga sensu stricto* (i.e., clade 3), which have excurrent siphons much shorter than incurrent ones (instead of equal or subequal in *Xylonora* gen. nov.), lateral lobes along the dorsal surface of incurrent siphons (absent in *Xylonora* gen. nov.) and large fecal chimney around the siphon (**Figures 4C,D**) (absent in *Xylonora* gen. nov.). This new genus may include up to 33 nominal species if additional species were to be transferred from *Xylophaga*. This genus would then correspond to species groups 1 to 4 in Turner (2002).

Similar to *Xylopholas scrippsorum* Voight, 2009, in some species of *Xylonora* gen. nov. small individuals or dwarf males attach to the ventral mantle or laterally or ventrally to the adult siphons. The position of the small individuals on the adults is not a distinguishing character for *Xylonora* gen. nov. They have been found dorsally attached on adults in *Xylonora atlantica* new comb., *Xylophaga africana, Xylophaga clenchi, Xylophaga lobata, Xylophaga obtusata, Xylophaga panamensis* Knudsen, 1961, but sometimes attached to ventral siphon like in *Xylophaga concava* Knudsen, 1961, *Xylophaga tubulata* Knudsen, 1961, *Xylophaga wolffi-grevei* Knudsen, 1961, and *X. dorsalis*. However the presence of small individuals attached to adults may have been overlooked in other species or genera.

Species Diversity in European Waters

The COI analysis of the specimens considered in this study identified five sequence groups and two individual sequences (**Supplementary Figure S1**). They were all well separated from each other by uncorrected p-distances of ≥12.3% (COI) and 3.7% (28S rRNA), while distances within groups did not exceed 5.2% (COI) and 0.1% (28S rRNA), respectively (**Table 3A**). This suggested all seven represented separate species. These species groups were congruent with those in phylogenies recovered with concatenated 18S and 28S rRNA gene sequences (data not shown) and also matched morphological specimen determinations.

In the phylogenetic analysis of concatenated COI, 18S and 28S rRNA, all 32 individuals of *X. dorsalis* formed a well-defined sister lineage to *X. oregona*/*X. washingtona* within the major clade 3 (**Figure 3**). *X. atlantica* new comb. (21 individuals) and *Xylonora* sp. 1 (1 individual; clade 4) displayed the closest relationship among all recovered species groups (12.3% uncorrected *p* for COI; **Table 3A**). Their separation was supported by ML/BI analyses of the COI (75% bs, 0.999 pp; **Supplementary Figure S1**), while ML did not reproduce support in the analyses of concatenated genes (**Figure 3**). Because of the genetic distance between these two taxa and consistent grouping by ML and BI with different genes, we consider them as separate species. *Xylonora* sp. 2 was well separated from all other species, revealing a close relationship with *X. atlantica* new comb. (uncorrected p: COI 20.3%, 28S rRNA 5.9%; **Table 3A**) and *Xylonora zierenbergi* new comb. (28S rRNA 3.2%, **Table 3**) which is affiliated with high support to clade 4 (**Figure 3**). *A. brava* and the single sequence of *Abditoconus* cf. *anselli* represented well supported (**Figure 3**) and closely related sister lineages within clade 5 (uncorrected p: COI 14.9%, 28S rRNA 4.5%). *Xyloredo* sp. 1 was well separated from all other species in this study (uncorrected p: COI ≥ 21.1%, 28S rRNA ≥ 7.1%). Its position within *Xyloredo* (clade 7) was well supported by ML and BI analyses and this position was also confirmed by the close relationship to *Xyloredo nooi* from New Zealand (28S rRNA uncorrelated–p distance 1.6; COI sequence not available for *X. nooi*). The 28S rRNA uncorrelated-p distance between *Xyloredo* sp. 1 and *X. nooi* exceeded significantly any value we measured within any other species (max. 0.1). *Xyloredo* sp. 1 and *X. nooi* therefore appear to represent two separate species.

Morphological Observations

Our specimens of *X. dorsalis*, *X. atlantica* new comb. and *A. brava* match the original descriptions and additional observations are highlighting the intraspecific variability of their mesoplax and siphons (Romano et al., 2014). The specimens of *Abditoconus* cf *anselli* from the Avilés Canyon matched to certain degree

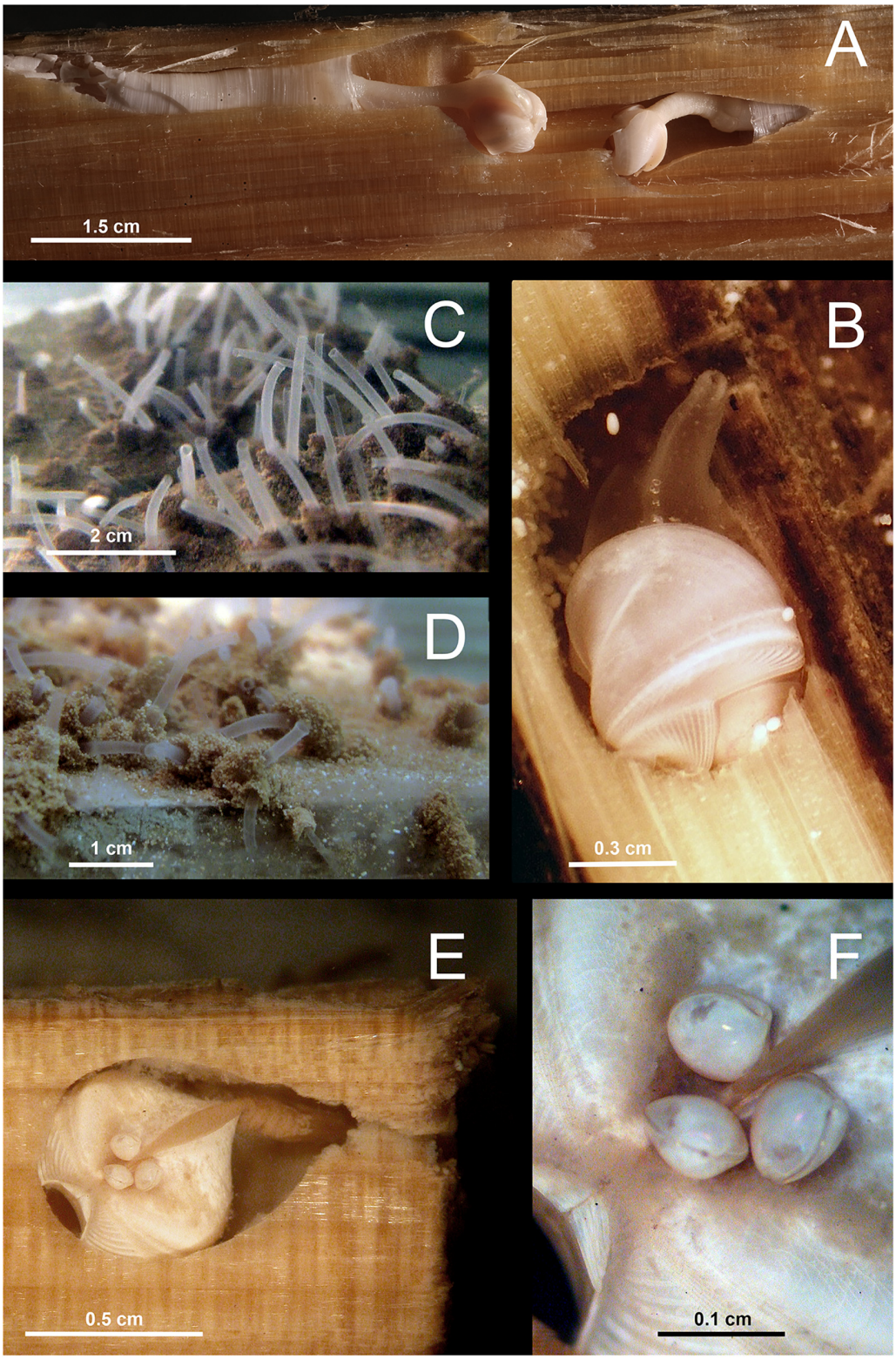

FIGURE 4 | Examples of Xylophagaidae in experimentally deposited wood. **(A)** *Xyloredo* sp. 1 in pine wood from Avilés Canyon, 2,000 m depth. **(B)** *Xylophaga dorsalis* in wood from La Fonera Canyon, 130 m deep. **(C,D)** Living Xylophagaidae from La Fonera Canyon, 1100 m deep, kept in aquarium for several days after recovery. **(C)** Siphons emerging from wood and **(D)** fecal chimneys around the siphons. **(E)** *Xylonora* sp. 2 in a Chemecoli fir wood cube from the Rainbow hydrothermal vent field with small individuals attached on the dorsal shell posterior to umbo. **(F)** Close-up of the small individuals attached to *Xylonora* sp. 2.

TABLE 3 | Pairwise genetic divergence for the species of Xylophagaidae.

(A)	*A. brava* *n* = 12	*A. cf. anselli* *n* = 1	*X. atlantica* *n* = 20	*X. dorsalis* *n* = 34	*Xylonora* sp.1 *n* = 1	*Xylonora* sp.2 *n* = 4	*Xyloredo* sp.1 *n* = 4	Average within species (COI)	Max. within species (COI)
Abditoconus brava	–	**0.149 ± 0.005**	**0.273 ± 0.0047**	**0.264 ± 0.004**	**0.281 ± 0.001**	**0.285 ± 0.004**	**0.286 ± 0.001**	**0.01**	**0.052**
Abditoconus cf. *anselli*	0.045 ± 0.001	–	**0.24 ± 0.003**	**0.241 ± 0.004**	**0.265 ± 0.001**	**0.295 ± 0.001**	**0.284 ± 0.000**	**n.a.**	**n.a.**
Xylonora atlantica	0.096 ± 0.001	0.085 ± 0.002	–	**0.221 ± 0.004**	**0.123 ± 0.0026**	**0.203 ± 0.001**	**0.211 ± 0.005**	**0.014**	**0.036**
Xylophaga dorsalis	0.150 ± 0.001	0.146 ± 0.00	0.15 ± 0.001	–	**0.225 ± 0.0018**	**0.267 ± 0.003**	**0.258 ± 0.004**	**0.005**	**0.021**
Xylonora sp.1	0.085 ± 0.001	0.081 ± 0.00	0.037 ± 0.002	0.146 ± 0.000	–	**0.2250 ± 0.0018**	**0.22 ± 0.002**	**n.a.**	**n.a.**
Xylonora sp.2	0.095 ± 0.000	0.093 ± 0.00	0.059 ± 0.003	0.153 ± 0.000	0.046 ± 0.000	–	**0.211 ± 0.001**	**0.005**	**0.008**
Xyloredo sp.1	0.088 ± 0.000	0.080 ± 0.00	0.082 ± 0.001	0.141 ± 0.000	0.076 ± 0.000	0.071 ± 0.000	–	**0**	**0**
Average within species (28S)	0.0002	n.a.	0.0019	0.0002	n.a	0	0		
Max. within species (28S)	0.001	n.a	0.0096	0.0039	n.a.	0	0		

(B)	*A. brava*	*A. cf. anselli*	*X. atlantica*	*X. dorsalis*	*Xylonora* sp. 1	*Xylonora* sp. 2	*Xyloredo* sp. 1
Xylophaga washingtona	0.141	0.141	0.129	0.136	0.131	0.139	0.134
Xylophaga oregona	0.130	0.129	0.118	0.135	0.118	0.124	0.121
Xylophaga sp. GB	0.099	0.089	0.047	0.143	0.045	0.054	0.085
Feaya dostwous	0.127	0.138	0.147	0.166	0.131	0.13	0.144
Abditoconus heterosiphon	0.055	0.043	0.067	0.124	0.056	0.066	0.052
Xylonora muraokai NP	0.080	0.074	0.038	0.139	0.014	0.048	0.066
Xylonora zierenbergi	0.079	0.074	0.045	0.142	0.034	0.032	0.066
Xyloredo nooi SWAtl	0.102	0.086	0.077	0.136	0.069	0.075	0.029
Xyloredo nooi NZ	0.102	0.086	0.077	0.136	0.069	0.075	0.016
Xylopholas crooki	0.11	0.101	0.095	0.134	0.082	0.088	0.082

(A) *Uncorrected p distances (mean ± standard deviation) are represented above the diagonal for COI (bold) and below for 28S rRNA sequences; average and maximum within-lineage divergences are included;* ***(B)*** *Uncorrected p distances between the 28S rRNA sequences of species analyzed in this study and previously published species (see* ***Supplementary Table S3*** *for accession numbers).*

the description of the type material from the Hebridean Slope (NW Scotland) and they clearly differed from *A. brava* (Romano et al., 2014). However, the original description of *A. anselli* was based on juveniles (<1 mm) and the description was generally poor. Thus the identity of our material cannot be formally confirmed. The specimens of *Xylonora* sp. 2 from Mid-Atlantic Ridge and Avilés Canyon (**Figure 3**) resemble the East Pacific *Xylophaga microchira* Voight, 2007 in shell shape and in having cirri at both siphon openings (Janet Voight, pers. obs.). However, *Xylonora* sp. 2 differs in having a small mesoplax with two plates joining at acute angle and subequal siphons, closely associated, shorter than shell length, the excurrent siphon without long and curved cirri and opening subterminally and dorsally to incurrent siphon. Larger individuals have small individuals attached dorsally (**Figures 4E,F**), but the taxonomic relevance of this character is doubtful. These dissimilarities, combined with the geographical separation, suggest that our specimens represent a different species. Unfortunately, no molecular data are available for the type specimens of *Xylophaga microchira* and further analyses are required to confirm the identity of our material.

The morphology of the single juvenile of *Xylonora* sp. 1 found in Avilés Canyon largely resembled *X. atlantica* new comb., but the separation from that species was supported by the presence of two small elongated and curved mesoplax plates resembling those of *X. gagei* instead of the triangular plates present in *X. atlantica* new comb. However, its small size (0.6 mm) and the fact that siphons were destroyed during sample handling actually prevented a consistent morphological assignation.

Xyloredo sp. 1 (**Figure 4A**) had calcareous tubes lining the burrows and differed in the shapes of shells and posterior adductor muscle scars from the previously known Atlantic species *Xyloredo nooi* and *Xyloredo ingolfia* Turner, 1972. However, its correct identification would require comparison with type material of all known species, which is beyond the scope of this paper.

Geographic Distribution and Intraspecific Genetic Structure of the COI Gene

We recovered seven xylophagaid species. Four of them occurred exclusively in the Atlantic (*Abditoconus* cf. *anselli*, *Xylonora* sp. 1, *Xylonora* sp. 2 and *Xyloredo* sp. 1), while no species was restricted to the Mediterranean.

Xylophaga dorsalis (**Figures 4B, 5**) showed the widest geographic distribution, being present in all locations in the Mediterranean and Atlantic Ocean, except for the northernmost Haakon Mosby Mud Volcano. Its distribution covered a wide bathymetric range from 2,000 m depth to our shallowest sites (Morocco mud volcanoes: 350 m depth; Western Mediterranean canyons: 130–550 m depth; **Figures 1**, **3** and **Table 1**) and a temperature range of 4 to 14°C (**Table 1**).

The COI sequence analysis indicated genetic connectivity across a large geographic range from Mid-Atlantic Ridge, Morocco Mud Volcanoes and throughout the Mediterranean. 29 individuals covering all sampling sites yielded 10 haplotypes (16 segregating sites, maximum within-clade uncorrected p distance: 2.1%). The dominant haplotype was shared by 62.1% of the individuals and it occurred in all sites except for Avilés Canyon. At this site we analyzed a single individual which diverged from the major haplotype by a single substitution (**Figure 6**). Half of all other haplotypes which were all collected in the Mediterranean were similarly closely related.

Xylonora atlantica occurred in the temperate Atlantic Ocean (Mid-Atlantic Ridge and Avilés Canyon) and in the western Mediterranean, while it was not retrieved from Morocco mud volcanoes and the Eastern Mediterranean (**Figures 1**, **5**). Its distribution covered an intermediate bathymetric range (870–2,000 m depth), with temperatures ranging from 4 to 13°C. The COI haplotype analysis of 19 sequences revealed five haplotypes ($S = 16$) displaying intraspecific divergence between the Mediterranean and Atlantic populations (**Figure 6B**). The dominant haplotype (47.4%) was present in Avilés Canyon and in the Western Mediterranean, but not on the Mid-Atlantic Ridge (**Figure 6B**). The second dominant haplotype (31.6%, within-clade divergence $\leq$3.6%) diverged by 13 substitutions from the dominant one and was exclusively recovered from the Atlantic, at Mid-Atlantic Ridge and Avilés Canyon (**Figure 1**). Three satellites of the dominant haplotype (1 substitution) occurred in four individuals from Western Mediterranean (**Figure 6B**).

Abditoconus brava was recovered from Eastern and Western Mediterranean and from the adjacent Morocco mud volcanoes, but not from any other Atlantic location (**Figures 1**, **5**). The depth range was 700–1,700 m (**Figure 3**) and all collection sites shared the same habitat temperature of 13°C. The COI analysis (15 individuals) showed a clear separation between Mediterranean and Atlantic haplotypes, suggesting limited gene flow across the Gibraltar Strait. Among the six haplotypes recovered ($S = 23$), three occurred exclusively in the Mediterranean, while the other three were retrieved from Morocco mud volcanoes (**Figure 6C**). The two haplotype groups were well separated (17–19 substitutions). The largest intraspecific divergence occurred between the two haplotypes from the most distantly separated sites (Morocco mud volcanoes and Eastern Mediterranean, 5.15%). The most dominant haplotype (66.7%) was collected in Western and Eastern Mediterranean suggesting genetic connectivity throughout this oceanic basin.

Two species were recovered from two collection sites. *Xylonora* sp. 2 was found on the Mid-Atlantic Ridge (2,300 m depth, 3.5°C) and in the Avilés Canyon (2,000 m depth, 4–9°C). Three COI haplotypes recovered from four individuals of *Xylonora* sp. 2 were closely related to each other ($S = 3$, $\leq$2 substitutions) and different haplotypes occurred in the two collections sites. *Xyloredo* sp. 1 occurred in the Avilés Canyon in the Bay of Biscay (1200–2000 m depth, 4–9°C) and at the 3,300 km distant Haakon Mosby Mud Volcano (1240 m depth, at −1°C; COI sequences only available from this site). Two other species, *Abditoconus* cf. *anselli* (**Figure 5**) and *Xylonora* sp. 1, were exclusively recovered from the Avilés Canyon (2,000 and 1,200 m deep, respectively, 4–9°C).

DISCUSSION

This study provides the first DNA barcode approach to identifying Xylophagaidae, where we combined molecular data (based on COI, 18S and 28S rRNA sequences) with morphology to discriminate between species and to assess their geographic distributions. Our analyses revealed: (i) a reliable species discrimination based on COI; (ii) a robust sequence divergence supporting the existence of seven species, three of them unidentified (two morphologically similar to *X. atlantica* new comb. and a possible undescribed *Xyloredo*); (iii) wide genetic connectivity throughout the North Atlantic and the Mediterranean for *Xylophaga dorsalis*, the most abundant species in our samples, and for *Xylonora atlantica* new comb.; and (iv) limited genetic connectivity between the Atlantic and Mediterranean populations of *A. brava*.

Phylogeny of Xylophagaidae

Our results (based on 18S rRNA, 28S rRNA and COI genes) agree with those based on 18S and 28S rRNA by Distel et al. (2011) in showing the Teredinidae and Xylophagaidae as sister taxa sharing a xylotrophic common ancestor. Reports considering xylophagaids as a family referred to the names Xylophaginidae, Xylophagidae, and Xylophagaidae (Purchon, 1941; Knudsen, 1961). In order to avoid homonymy with a taxon of Diptera [Xylophagide Fallén (1810), Insecta], the name was amended to Xylophagaidae (International Commission on Zoological Nomenclature, 2018) that has been used most recently (Gaudron et al., 2010; Coan and Valentich-Scott, 2012; Haga and Kase, 2013; Romano et al., 2014; Rosenberg and Gofas, 2015; Voight et al., 2019).

Our phylogenetic reconstruction (**Figure 3**) revealed that *Xylophaga* is polyphyletic, unless the new genus *Xylonora* is erected for the species in clade 4. Our decision to separate it from *Xylophaga* (clade 3) is supported by robust morphological and taxonomic arguments. The rapid evolutionary substitution rate of the mitochondrial COI, compared to the nuclear 18S and 28S rRNA genes, allows for discriminating closely allied species and also different phylogeographic groups within species. For the same reasons, its phylogenetic signal is weak (Hebert et al., 2003; Cunha et al., 2009). However, a number of studies on bivalve phylogenies proved that combining nuclear and COI markers improved the signal (Giribet and Distel, 2003; Bieler et al., 2014; Johnson et al., 2017). Our data support the monophyly of *Xylophaga sensu stricto* and *Xylopholas*. This is in contrast to previous results that were based on 18S and 28S

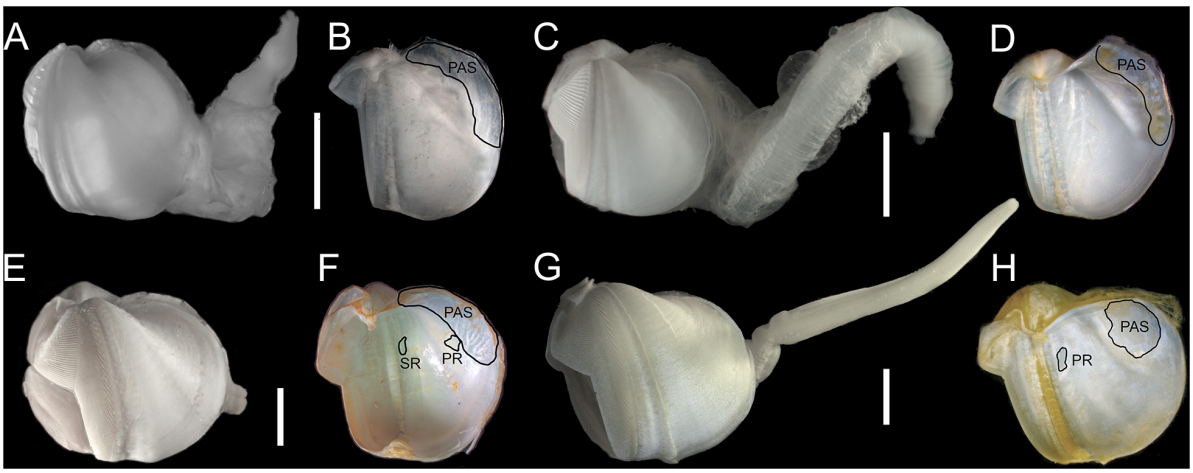

FIGURE 5 | Lateral views of shell with soft parts and inner shells: **(A,B)** *Abditoconus cf. anselli*; **(C,D)** *Abditoconus brava*; **(E,F)** *Xylonora atlantica* new comb.; **(G,H)** *Xylophaga dorsalis.* PAS = posterior adductor scar; PR = pedal retractor scar; SR = siphonal retractor scar. Redrawn from Romano et al. (2014).

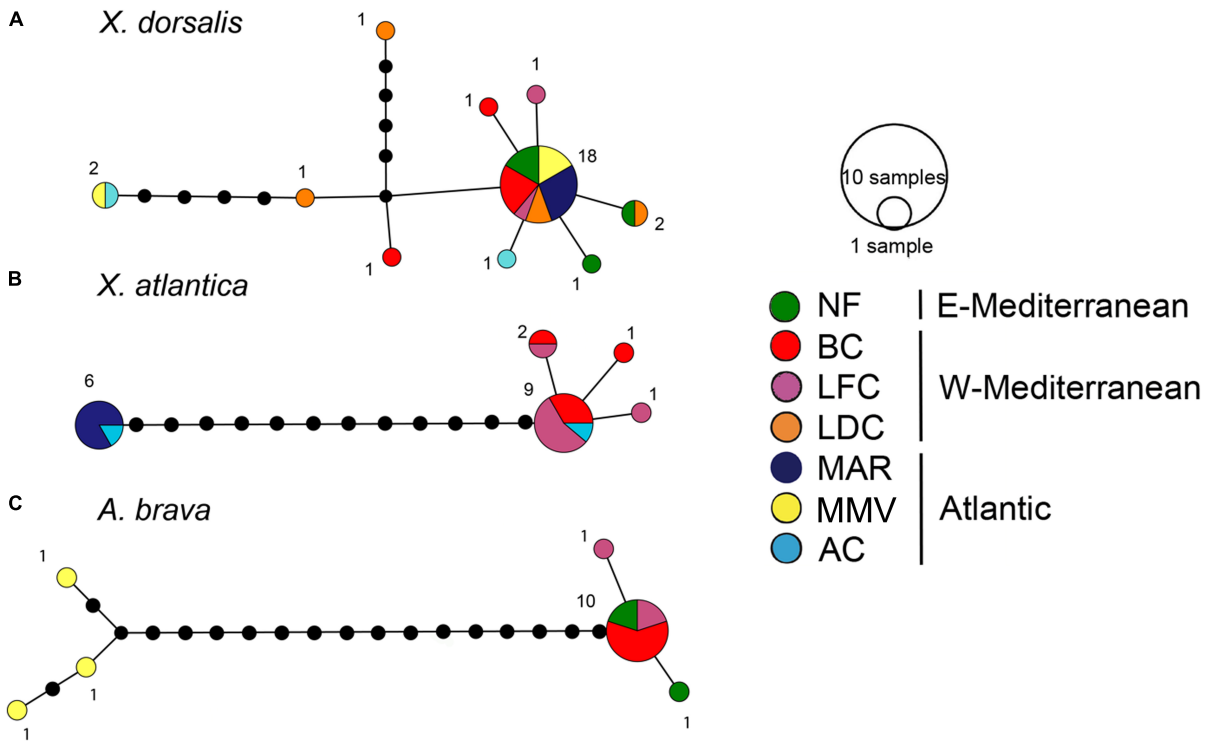

FIGURE 6 | COI haplotype networks. **(A)** *Xylophaga dorsalis* (388 bp, 29 individuals). **(B)** *Xylonora atlantica* new comb. (388 bp, 19 individuals). **(C)** *Abditoconus brava* (389 bp, 15 individuals). Location colors as in **Figure 1**, except for MAR = Menez-Gwen hydrothermal vent filed at Mid-Atlantic Ridge, for location abbreviations see **Figure 1**.

rRNA analyses, but did not include COI (Voight et al., 2019). Additional support for the separation of *Xylonora* new genus and *Xylophaga sensu stricto* may come from recent observations on different trophic ecology of the two genera (Voight et al., 2020). Three members of the *Xylophaga sensu stricto* clade (*X. dorsalis*, *X. washingtona*, and *X. alexisi*) presented higher δ^{15}N signatures than other *Xylonora*-clade species in which δ^{15}N values were consistent with strict xylotrophy. This may suggest that *Xylophaga sensu stricto* can filter feed as an opportunistic alternative to xylotrophy, while members of *Xylonora* are strict xylotrophs (Voight et al., 2020). Our data are furthermore decisive enough to confirm the sister-taxa relationship between representatives of *Xylophaga* in the Atlantic (*X. dorsalis*) and the Pacific (*X. washingtona*/*X. oregona*).

Species Identification Based on Molecular Markers

DNA barcoding allowed us to improve taxonomic resolution to assess the species richness and diversity within xylophagaids. As in shipworms, the high intraspecific phenotypic plasticity of xylophagaids is often not well documented and it makes identifications difficult. Shell morphology often appears to vary in relation to environmental conditions. For instance, shell shape in *X. washingtona* recovered from wood deployments at 2,370 m depth off California varied in relation to different wood substrates (i.e., cedar, pine, ash, maple, oak). The variations included valve size and number of denticulated ridges on the anterior slope in relation to valve length (Turner, 2002). *Xylonora atlantica* new comb. from wood deployments off Cape Cod (MA, United States) revealed different growth rates and a morphology varying during the year as well as with site, substrate, and animals' crowding on wood (Romey et al., 1994). *Xylophaga dorsalis* and *Xylonora atlantica* new comb. recovered from pine and oak in the submarine canyons of Avilés (Bay of Biscay), Blanes and Lacaze-Duthiers (Western Mediterranean) also showed phenotypic variability in a previous study (Romano et al., 2014). Our materials of *X. dorsalis*, *X. atlantica* new comb, and *A. brava* exhibited comparable phenotypic variations among conspecifics collected from pine and oak in an even wider geographic and environmental range in the Atlantic and Mediterranean (**Table 1**). However, ambiguities were well-resolved by the three molecular markers used, which all showed clear and identical clustering (**Figure 3**).

Interspecific disparity can be characterized with thresholds of genetic distance between sequences, which may vary according to the compared taxa and the molecular markers. In COI of birds, an interspecific genetic distance of ten times the average distance within species was suggested (Hebert et al., 2004), while in marine gastropods 4.9–7.8 times revealed to be conservative enough to eliminate false positive species discrimination (Meyer and Paulay, 2005). The wide range of species attributes among these gastropods (e.g., fertilization modes, larval dispersal and feeding strategies) allowed for suggesting that these findings should be applicable to a wide range of marine taxa (Meyer and Paulay, 2005).

The 28S rRNA and COI genetic distances clearly characterized species disparity in our materials based on the "ten times-threshold" criterion. Both markers showed clear barcoding gaps between species without overlapping ranges of intraspecific and interspecific distances (Meyer and Paulay, 2005) and the average distance between two species was as a rule >10 times larger than the average distance within each species (**Table 1**). The only exception occurred in the comparison of the single specimen of *Xylonora* sp. 1 (initially misidentified as *X. atlantica*) and *Xylonora atlantica* new comb., which revealed an interspecific distance of only 8.2× the distance within *X. atlantica* new comb. However, this was well beyond the 4.9–7.8 threshold derived from marine gastropods and we are very confident in that they are two separate species. *Xylonora* sp. 2 and *Xyloredo* sp. 1 are also well separated from the other species within the respective genera. Overall, more individuals of these three morphotypes are needed to allow precise morphological identifications or formal new species descriptions.

Diversity of Xylophagaidae in European Deep Waters and Ecological Considerations

Thirteen xylophagaid species are currently recognized from the North-Eastern Atlantic and adjacent marginal seas. Apart from the seven species covered by this study, there are *Xylophaga praestans, Xylophaga nidarosiensis Xylophaga noradi, Xylophaga ricei, Xylophaga gagei* and *Xyloredo ingolfia*. Xylophagaid diversity in European waters thus exceeds the diversity of teredinids in the same area that consists of nine species (Borges et al., 2014). The higher diversity of Xylophagaidae is remarkable with regard to the, at first glance, very similar habitat requirements and feeding ecologies of the two families and also because abundance and variety of wood are assumed much less in the deep sea than in coastal-near shallow regions. This difference in species diversity cannot be explained by an artifact from sampling bias because xylophagaids from the deep-sea floor are difficult to access and have been investigated far less than shallow water Teredinidae. We hypothesize that factors such as differential adaptation to depth, temperature and salinity and related water mass chemistry are leading to habitat partitioning, which may affect species diversity differently in the two families.

While teredinids are bound to shallow waters, most European xylophagaids cover either very broad bathymetric ranges from the littoral to the abyss (e.g., *X. atlantica* new comb. and *X. dorsalis*) or were exclusively recovered from bathyal or abyssal depths (**Table 4**). Only *Xylophaga nidarosiensis* and *Xylophaga noradi* were solely recovered from shallow waters. However, both species are only known from single records and our view on their bathymetric distributions may change with future collections.

Shallow water species from temperate oceans are generally eurythermic because they must cope with seasonally changing water temperatures. This applies to teredinids and also some xylophagaids. Eurythermic xylophagaids additionally covering broad depth ranges in the north-eastern Atlantic must also tolerate constant low temperatures. Examples are *Xylonora atlantica* new comb. and *Xylophaga dorsalis* which can tolerate 23 and 20°C, respectively (Borges et al., 2014), and they also live in bathyal to abyssal depths where temperatures are constantly low (**Table 4**). Other species may be cold-stenothermic, e.g., *Xyloredo* sp. 1 which we recovered at −1 to +4°C, or *Xyloredo ingolfia*, which occurs only in the deep northern Atlantic. Most other European xylophagaids may be also cold-stenothermic with regard to the depths from which they were retrieved, however, only sporadic or single collections of many xylophagaid species prevent clear interpretations of their temperature tolerances.

North East Atlantic mid- and deep-water fauna is adapted to a salinity range of 34.4–35.3‰ (Bouchet and Taviani, 1992; Emery, 2001). Atlantic xylophagaids living exclusively below 500 m depth may therefore be typical stenohaline deep-sea organisms. Species living in shallower Atlantic waters must tolerate higher salinities of 35.2–36.7‰ (Emery, 2001) and species living in the deep Mediterranean must cope with >38.0‰ (Miller et al., 1970). Xylophagaids covering broad salinity ranges in the Atlantic and occurring also in the Mediterranean such as *Xylonora atlantica* new comb., *Xylophaga dorsalis* and *Abditoconus brava* are therefore considered euryhaline marine species (**Table 4**).

TABLE 4 | Depth distributions (minimum/maximum) of the xylophagaid species recorded in the North East Atlantic and adjacent marginal seas.

Species	Depths in this study		Previously known depths (minimum/maximum)	Geographic distribution	References
	(minimum/maximum)	Locations			
Xylophaga dorsalis	130/2,000 m	NW Mediterranean (LFC)/ Bay of Biscay (AC)	Tidal zone to 2,700 m	Lofoten Islands (Norway) to Canary and Madeira Islands, MMV, W and E Mediterranean	Turner, 1955; Janssen, 1989; Zenetos et al., 2005; this study
Xylophaga praestans			ca. 50–2,173 m	Shallow: eastern England, Norway and W Mediterranean (Tyrrhenian Sea); Deep: E Mediterranean	Smith, 1903; Dons, 1929, 1933; Carrozza, 1975; Janssen, 1989; Turner, 2002; Janssen and Krylova, 2014
Xylophaga nidarosiensis			10 m	Western Norway	Santhakumaran, 1980
Xylophaga noradi			10 m	Western Norway	Santhakumaran, 1980
Xylonora atlantica	870/2000 m	MAR (MG)/Bay of Biscay (AC)	15–2,279 m	W Atlantic (Newfoundland to Virginia), MAR, E Atlantic (Bay of Biscay), W Mediterranean	Turner, 1955, 2002; Romano et al., 2014; Gaudron et al., 2016; this study
Xylonora sp. 1	1200 m	Bay of Biscay (AC)		E Atlantic (Bay of Biscay)	This study
Xylonora sp. 2	2000/2300 m	Bay of Biscay (AC)/MAR (RB)		MAR(RB), E Atlantic (Bay of Biscay)	This study
Xylophaga ricei			5,000 m	Madeira abyssal plane	Harvey, 1996
Xylophaga gagei			1,370 m	Hebridean Slope	Harvey, 1996
Abditoconus brava	700/1800 m	MMV (Mek)/NW Mediterranean (BC)	900–1,800 m	MMV (Mek), W and E Mediterranean	Romano et al., 2014; this study
Abditoconus anselli			1,370 m	Hebridean Slope	Harvey, 1996
Abditoconus cf. *anselli*	1200–2000 m	Bay of Biscay (AC)	1,200 m	E Atlantic (Bay of Biscay)	Romano et al., 2014; this study
Xyloredo ingolfia			1,783–2,906 m	Iceland to Scotland	Turner, 1972; Harvey, 1996; Turner, 2002
Xyloredo sp. 1	1200/2000 m	Bay of Biscay (AC)		E Atlantic (Bay of Biscay), Norwegian Sea (HMMV)	This study

Single depth values indicate single collections. AC, Avilés Canyon; BC, Blanes Canyon; HMMV, Haakon Mosby mud volcano; LFC, La Fonera Canyon; LDC, Lacaze-Duthiers Canyon, MAR, Mid-Atlantic Ridge; MG, Menez Gwen hydrothermal vent field; MMV, Morocco mud volcanoes; Mek, Meknès mud volcano; RB, Rainbow hydrothermal vent field.

Species diversity estimations can be affected by factors that influence seasonal colonization times such as variations of local current regimes or different reproduction and spawning times in different species. Temporal effects became apparent in the eastern Mediterranean because *X. dorsalis* was the only colonizer in 2007 while *A. brava* appeared only in 2009 and became the dominant species. Different colonizers may also be able to select different types of wood. *A. brava* for example was almost exclusively found in pine and not in oak when both types of wood were simultaneously deployed in the Western Mediterranean canyons.

Our study counteracted the risks of ignoring seasonally occurring species by repeated sampling in most sites (**Table 1**). Among them, the highest diversity of six species occurred in Avilés Canyon (**Figure 1**). This site provided various depth and temperature conditions of 1,200 to 2,000 m and 4 and 9°C, respectively, and thus it certainly combined suitable conditions for the generalists *X. atlantica* new comb. and *X. dorsalis* and also for putatively cold-stenothermic/stenohaline deep-water species such as *Abditoconus* cf. *anselli*, *Xylonora* sp. 1, *Xylonora* sp. 2, *Xyloredo* sp. 1. Furthermore, the close vicinity of Avilés Canyon to the coast should support a regular and sufficient reception of wood allowing for continuous maintenance of high species diversity. Our Eastern Mediterranean site showed low diversity of only two species suggesting that only eurythermic and euryhaline species like *X. dorsalis* and *A. brava* were able to tolerate the high salinity and temperature of 13°C at 1200 water depth (Miller et al., 1970).

Dispersal Capabilities

Our results prove that xylophagaids occur in the entire North East Atlantic, from the Barents Sea in the Arctic, along the northern European continental margin and over the temperate Mid-Atlantic Ridge, to the far Eastern Mediterranean. This is a remarkable distribution range if we assume that land-derived

wood is only scarcely available in remote areas such as Arctic deep waters or the Mid-Atlantic Ridge.

Colonization of experimentally deployed wood proves that xylophagaids disperse in the deep ocean and not by colonizing driftwood before it sinks down. The colonization of wood in remote oceanic regions is a strong indication for high dispersal capabilities and for bridging large distances by xylophagaid larvae.

Deep-sea species with long-distance dispersal are usually assumed to have planktotrophic larvae, particularly when they inhabit fragmented and widely separated habitats (Tyler and Young, 1999). Overall knowledge on xylophagaids' larval biology remains scant. Planktotrophic development has been documented at least for the Atlantic *X. atlantica* new comb. and the Western Pacific *Xylophaga supplicata* (Taki and Habe, 1950), both exhibiting typical shell morphologies of long-lived pelagic larvae (Gaudron et al., 2010; Haga and Kase, 2013). Laboratory experiments with reared larvae of *X. atlantica* new comb. showed that metamorphosis can be delayed for up to 6 months (Culliney and Turner, 1976), mirroring the larval trophic strategies, planktonic larval duration and dispersal capacities of other deep-sea bivalves such as the hydrothermal vent and cold seep subfamily Bathymodiolinae. They also live in fragmented habitats, sometimes separated by hundreds of kilometers, and disperse with planktotrophic larvae that can remain up to 13 months in the plankton (Arellano and Young, 2009). We may thus reasonably assume that xylophagaids other than *X. atlantica* new comb. and *X. supplicata* may also have equivalent dispersal strategies.

Biogeography of European Xylophagaidae

All thirteen European xylophagaids occurred in the temperate North East Atlantic, while only four occurred also in the Mediterranean (*Xylophaga dorsalis, Xylophaga praestans, Xylonora atlantica* new comb., *Abditoconus brava*). Compared to the nearby Atlantic, the Mediterranean deep sea generally harbors an impoverished fauna and cold stenothermic species are lacking (Fredj and Laubier, 1985; Breusing et al., 2016). This appears to result from the isolation of the Mediterranean and its desiccation during the Messinian Salinity Crisis in the late Miocene (Cita, 1973; Hsü et al., 1973), followed by its recolonization only after reconnection with the Atlantic (Pérès, 1985; Bouchet and Taviani, 1992). Since then, the Gibraltar Strait and the Siculo-Tunisian sills in combination with the significantly different hydrological conditions supposedly acted as biogeographic barriers controlling the Atlanto–Mediterranean benthic exchanges and preventing establishment of cold-stenothermic and stenohaline deep-sea fauna in the Mediterranean (Bouchet and Taviani, 1992). All xylophagaids occurring in the Mediterranean are considered eurythermic and euryhaline and it is reasonable to assume an Atlantic origin.

Xylophaga dorsalis has a wide distribution range in the East Atlantic, from the Lofoten Islands in the northern Norwegian Sea and the British Isles to the Canary and Madeira Islands and the Western and Eastern Mediterranean (Turner, 1955; Romano et al., 2013, 2014; this study). We recorded this species for the first time on the Mid-Atlantic Ridge. Its bathymetric range covers littoral to abyssal depths (**Table 4**) and it is considered eurybathic, eurythermic and euryhaline. It was also the most common and abundant species in our study sites.

Xylophaga praestans was recorded in shallow northern European waters (British Isles to Norway) and in the Mediterranean down to bathyal depths (**Table 4**). There are doubts on its previous identification and depth range in the deep Eastern Mediterranean (Mienis, 2003). Re-examination of this material is beyond the scope of this study, and we therefore preliminarily consider this species as eurybathic, eurythermal, and euryhaline.

Xylonora atlantica new. comb. is a pan-Atlantic species, well known from the North West Atlantic margin (Turner, 1955; Culliney and Turner, 1976; Romey, 1991; Romey et al., 1994; Voight, 2008; Distel et al., 2011) and only recently recovered from the south European Atlantic margin and the Western Mediterranean (Romano et al., 2014). We found this species also on the Mid-Atlantic Ridge, while it appears to be absent from the Eastern Mediterranean and northern European waters. Its bathymetric distribution ranges from littoral to abyssal depths (**Table 4**) and it is therefore considered eurythermic and euryhaline.

We recovered *Xylonora* sp. 2 from bathyal depths in two locations, the Avilés Canyon and the Mid-Atlantic Ridge and we therefore consider it as a stenothermic and stenohaline deep-sea species.

Abditoconus brava was previously known from the Western Mediterranean (Romano et al., 2014). We recorded it also in the adjacent Atlantic (Morocco mud volcanoes) and in the Eastern Mediterranean. *A. brava* appears to be a bathyal species (**Table 4**) tolerating also the high temperatures and salinities in the deep Eastern Mediterranean.

We found *Xyloredo* sp. 1 in Avilés Canyon and the Haakon Mosby Mud Volcano in the Arctic which represents the northernmost record for a Xylophagaidae. This species occurs in bathyal depths and it is considered cold-stenothermic and stenohaline.

Xyloredo ingolfia is a bathyal species occurring from Iceland to Scotland in the North East Atlantic (Turner, 1972, 2002; Harvey, 1996) and it is therefore considered cold-stenothermic and stenohaline.

All other European xylophagaids were recovered only once, all of them from littoral to abyssal depths at different locations among Norway, the British Isles and Avilés Canyon (**Table 4**).

Inter-Population Connectivity

Our discovery of identical COI haplotypes among the populations of *X. dorsalis*, *X. atlantica* new comb., and *A. brava* sampled in distant locations in the Atlantic and the Mediterranean strongly suggest gene flow over large distances.

The presence of an identical major COI haplotype in *X. dorsalis* across most of our study sites indicated unhindered genetic connectivity between the Mid-Atlantic Ridge and Morocco mud volcanoes, across the Gibraltar Straight and throughout the entire Mediterranean. This is in accordance with the above hypothesized eurybathic, eurythermic and euryhaline

nature of this species which also accounts for tolerance of their larvae toward contrasting environmental conditions in shallow and deep environments of the temperate Atlantic and the warm Mediterranean. The single haplotype retrieved from Avilés Canyon in the Bay of Biscay diverged by only one substitution, and it is likely that more extensive sampling at this site would have revealed the major haplotype as well. We may therefore reasonably assume unimpeded genetic exchange among the populations of *X. dorsalis* in an area exceeding the coverage of our study, within its entire distribution range between northern Europe and the Canary Islands.

Genetic connectivity between the Atlantic and the western Mediterranean was also evidenced for eurybathic and eurythermic *X. atlantica* new comb. Its major haplotype was sampled in Avilés Canyon and in the Western Mediterranean submarine canyons. One divergent haplotype was recovered exclusively in the Atlantic on the Mid-Atlantic Ridge and the Avilés Canyon (**Figure 6**). Future research must reveal if this haplotype is probably representing a typical one for western Atlantic populations and if this may indicate limited connectivity between the Atlantic and the Mediterranean populations.

In *A. brava*, the presence of an identical major haplotype in the Western and Eastern Mediterranean populations suggests unobstructed gene flow throughout the entire Mediterranean. This haplotype and a few closely related ones were limited to the Mediterranean, while a clearly divergent haplotype was recovered exclusively at Morocco mud volcanoes in the adjacent Atlantic. We cannot discard that our limited sampling effort caused a bias and that future research may recover the "Atlantic haplotype group" in the Mediterranean and vice versa. However, the 16-substitution divergence strikingly exceeded what we observed in *Xylonora atlantica* new comb. and *Xylophaga dorsalis* across the Atlantic-Mediterranean transition. *A. brava* was not recovered from shallower than 700 m depth, and it is possibly a strictly bathyal species. The less than 300-m deep Gibraltar Strait at the entrance of the Mediterranean (Gascard and Richez, 1985) could then represent a real biogeographic barrier, significantly limiting gene flow. If so, we may assume a continuing divergence in the Atlantic and Mediterranean populations, which may eventually lead to speciation.

CONCLUSION

Our study integrates morphological and molecular data, including DNA barcoding of deep-sea wood boring bivalves. We thus provide a molecular baseline that is significantly facilitating species discrimination and will greatly enhance taxonomic knowledge in the future. Molecular data confirmed the Xylophagaidae as being composed of seven well-supported major clades corresponding to independent taxa with clear morphological differences. This leads us to erect *Xylonora* as a new genus to resolve the polyphyly of *Xylophaga*.

Repeated recoveries of Xylophagaidae from wood deployed experimentally over wide geographic, bathymetric, temperature and salinity ranges gave insights into the biogeography of European species for the first time, allowing for conclusions on the ecological requirements reaching far beyond what can be drawn from single records. We recovered seven species, some of them occurring regularly (e.g., *Xylophaga dorsalis* and *Xylonora atlantica* new comb.), showing wide Atlanto-Mediterranean distributions, broad bathymetric, temperature and salinity ranges, and genetic connectivity among their widely separated populations. This allowed us to conclude that a broad tolerance toward different hydrographic regimes may be a major clue for their dispersal success.

The biogeographic patterns of other Xylophagaidae may be linked to lower tolerance toward shallow water environments or temperature and salinity variations. *Xyloredo* sp. 1, for example, was exclusively collected in bathyal sites in the temperate North Atlantic, while *A. brava* occurred in bathyal regions throughout the Mediterranean and nearby Atlantic. For this species, the shallow Gibraltar Strait is likely representing a biogeographic barrier limiting gene flow.

The presence of xylophagaids in remote deep-sea locations such as Haakon Mosby Mud Volcano in the Arctic or the Mid-Atlantic Ridge where wood is presumably a scarce habitat suggests that distance alone is not a limiting factor for their dispersal. Rising frequencies of major storms and related flooding of the coasts caused by changing climate conditions may probably enhance the future availability of wood as stepping stones for the dispersal of wood-colonizing benthic organisms on the deep-sea floor. This may also affect the distribution of other wood colonizing deep-sea fauna.

Our results prove that experimentally deployed wood-falls could be used as efficient tools to collect wood specialists, highlighting their potential in future deep-sea studies addressed to improve our knowledge on their population dispersal abilities and connectivity. This may certainly include also macrofaunal taxa not specialized to wood and such research could provide crucial knowledge for planning strategies for a sustainable management of deep-sea species and ecosystems.

DATA AVAILABILITY STATEMENT

All new sequences were deposited in NCBI under Bioproject PRNEB39839; accessions for target genes are COI: LR899288-LR899358, 18S rRNA: LR899359-LR899420, and 28S rRNA: LR899226-LR899286. All accession numbers used in this study can be found in the **Supplementary Material**.

AUTHOR CONTRIBUTIONS

CR, AN-J, DM, NL, and CB conceived and designed the experiments. CR, AN-J, CB, and NL performed the experiments. CR, AN-J, CB, and GR analyzed the data. CR contributed to taxonomic identifications. CR, AN-J, DM, and CB wrote the final manuscript. All authors wrote the draft manuscript.

FUNDING

This work was supported by the Max Planck Society and the French Centre National de la Recherche Scientifique

(CNRS) associating Université de Liège, UPMC, and Museum of Natural History through the GDRE program "Diversity, establishment and function of organisms associated with marine wood falls-DiWOOD"; by project CHEMECO (European Sciences Foundation (ESF)/Eurocores/EURODEEP/0001/2007); by the Chair programme "Extreme Marine Environments, Biodiversity and Global Change" UPMC-Fondation TOTAL; by the EUROFLEET Programme; by the Agencia Española de Investigación (AEI) and the European Funds for Regional Development (FEDER/UE) through the research projects PROMETEO (CTM2007-66316-C02-02/MAR), DOSMARES (CTM2010-21810-C03-03) and PopCOmics (CTM2017-88080); and by Agència de Gestió d'Ajuts Universitaris i de Recerca of the Generalitat of Catalunya through the Consolidated Research Group on Marine Benthic Ecology (2017SGR378). Shiptime during research cruises BioBaz, M70/2-Bionil, MSM13/3-Homer, ARKXXII/1b, ARKXXIV/2, Medeco-2, and POS403-MenezKart received funding from the EU 6th FP HERMES (GOCE-CT-2005-511234), EU 7th FP HERMIONE (grant agreement no. 226354), CNRS, and the DFG. CR was funded by the People Programme (Marie Curie Action IOF to CR) of the European Union's Seventh Framework Programme (FP7/2007-2013) under the "DeepFall" project http://www.deepfall-project.eu; https://twitter.com/DeepFall_Proj (REA grant agreement N. PIOF-GA-2013-628146); AN-J was funded through DiWOOD; CB was funded by the DFG Cluster of Excellence "The Ocean in the Earth System" at MARUM (University of Bremen), a European Research Council Advanced Grant (BathyBiome, Grant 340535) and the Max Planck Society.

ACKNOWLEDGMENTS

We would like to thank the chief scientists, captains and crews and the teams of ROV Victor 6000 (IFREMER, France), ROVs MARUM Quest 4000 and Cherokee (MARUM, Bremen, Germany), ROV Isis (NOC Southampton, United Kingdom), and ROV Genesis (Renard Centre of Marine Geology, Belgium) for their help during the following cruises: DOSMARES (NW Mediterranean canyons) with the Spanish RV Garcia del Cid; BIOCANT (Avilés Canyon) with the Spanish RV Sarmiento de Gamboa; MEDECO (2007, Eastern Mediterranean), MoMARDream-Naut (2007) and MoMARDream-08 (2008, both to Rainbow hydrothermal vent field), (https://doi.org/10.17600/7030060) and BIOBAZ (2013, Menez Gwen hydrothermal vent field) with the French RV Pourquoi Pas? BIONIL/M70-2 (2006, Eastern Mediterranean) with the German RV Meteor; HOMER/MSM13-3 (2009, Eastern Mediterranean) with the German RV MARIA. S. MERIAN; ARKXXII/1b (2007) and ARKXXIV/2 (2009, both to Haakon Mosby mud volcano) with the German RV POLARSTERN; MENEZKART/POS402 (2010, Menez Gwen hydrothermal vent field) with the German RV POSEIDON; JC-10 (2007, Mercator mud volcano, N-Atlantic) with the British RRS James Cook; 64PE284 (2008, Meknès mud volcano, N-Atlantic) with the Dutch RV Pelagia; B09/14 (2009, Mercator and Meknès mud volcanoes) with the Belgian RV Belgica. Wood colonization experiments in the Lacaze-Duthiers Canyon were deployed with the RV Minibex (COMEX). Material from the Morocco mud volcanoes was collected within the Chemeco (Monitoring colonization in chemosynthetic ecosystems) from the European Science Foundation under grant EURODEEP/0001/2007 and FTC (Fundação para a Ciência e a Tecnologia) project; we thank Dr. Marina Cunha, University of Aveiro, Portugal and Sylvie Gaudron, Sorbonne Université, France, for providing specimens. We are grateful to Janet R. Voight from the Field Museum of Natural History, Chicago, IL, United States, and Takuma Haga from JAMSTEC, Kanagawam, Japan, for taxonomic advice. We also thank S. Wetzel, D. Cortese, L. Anducas Comas, G. Carreras for their laboratory help, particularly their perseverance with the PCR and sequencing of such a difficult material.

SUPPLEMENTARY MATERIAL

The Supplementary Material for this article can be found online at: https://www.frontiersin.org/articles/10.3389/fmars.2020.579959/full#supplementary-material

Supplementary Figure 1 | Bayesian Inference analysis (10,000,000 generations, sampling interval 1000×) based on COI sequences (388 bp). Statistical support (BI posterior probabilities >0.85/RAxML 100× bootstraps) is indicated on the nodes. Taxa names include locations (see **Figure 1** for abbreviations) and identity of the specimens (see **Supplementary Table S3** for GenBank accession numbers). Sampling locations are also indicated by color code.

Supplementary Table 1 | List of primers. * = PCR primer pairs; unmarked = internal primers. Annealing temperatures (Ta, °C) modified for amplification steps depending on enzymes (see **Supplementary Table S2**).

Supplementary Table 2 | List of enzyme polymerases and the PCR conditions used in this study.

Supplementary Table 3 | Identity of the specimens used for each genetic analysis, and GenBank sequences and accession numbers. * = outgroup species for tree reconstruction.

REFERENCES

Altschul, S. F., Madden, T. L., Schäffer, A. A., Zhang, J., Zhang, Z., Miller, W., et al. (1997). Gapped BLAST and PSI-BLAST: a new generation of protein database search programs. *Nucl. Acids Res.* 25, 3389–3402. doi: 10.1093/nar/25.17.3389

Arellano, S. M., and Young, C. M. (2009). Spawning, development, and the duration of larval life in a deep-sea cold-seep mussel. *Biol. Bull.* 216, 148-162. doi: 10.1086/BBLv216n2p149

Baco, A. R., Smith, C. R., Peek, A. S., Roderick, G. K., and Vrijenhoek, R. C. (1999). The phylogenetic relationships of whale-fall vesicomyid clams based on mitochondrial COI DNA sequences. *Mar. Ecol. Progr. Ser.* 182, 137–147. doi: 10.3354/meps182137

Bartsch, P. (1921). A new classification of the shipworms and descriptions of some new wood boring mollusks. *Proc. Biol. Soc. Washington* 34, 25–32.

Bessette, S., Fagervold, S., Romano, C., Martin, D., Le Bris, N., and Galand, P. E. (2014). Diversity of bacterial communities on sunken woods in the Mediterranean Sea. *J. Mar. Sci. Technol.* 22, 60–66.

Bieler, R., Mikkelsen, P. M., Collins, T. M., Glover, E. A., Gonzalez, V. L., Graf, D. L., et al. (2014). Investigating the bivalve tree of Life – an exemplar-based

approach combining molecular and novel morphological characters. *Invert. Syst.* 28, 32–115. doi: 10.1071/is13010

Bienhold, C., Pop Ristova, P., Wenzhöfer, F., Dittmar, T., and Boetius, A. (2013). How deep-sea wood falls sustain chemosynthetic life. *PLoS One* 8:e53590. doi: 10.1371/journal.pone.0053590

Bienhold, C., Wenzhöfer, F., Le Bris, N., Ramette, A., and Boetius, A. (2008). Wood colonization experiments in the eastern mediterranean deep sea. *Geophys. Res. Abstr. EGU* 2008:09061.

Borges, L. M. S., Merckelbach, L. M., Sampaio, I., and Cragg, S. M. (2014). Diversity, environmental requirements, and biogeography of bivalve wood-borers (Teredinidae) in European coastal waters. *Front. Zool* 11:13. doi: 10.1186/1742-9994-11-13

Borges, L. M. S., Sivrikaya, H., Le Roux, A., Shipway, J. R., Cragg, S. M., and Costa, F. O. (2012). Investigating the taxonomy and systematics of marine wood borers (Bivalvia : Teredinidae) combining evidence from morphology, DNA barcodes and nuclear locus sequences. *Invert. Syst.* 26, 572–582. doi: 10.1071/IS12028

Bouchet, P., and Taviani, M. (1992). The Mediterranean deep-sea fauna – pseudopopulations of Atlantic species. *Deep Sea Res. Part A Oceanogr. Res. Pap.* 39, 169–184. doi: 10.1016/0198-0149(92)90103-z

Breusing, C., Biastoch, A., Drews, A., Metaxas, A., Jollivet, D., Vrijenhoek, R. C., et al. (2016). Biophysical and population genetic models predict the presence of "phantom" stepping stones connecting Mid-Atlantic Ridge vent ecosystems. *Curr. Biol.* 26, 2257–2267. doi: 10.1016/j.cub.2016.06.062

Carrozza, F. (1975). Microdoride di malacologia mediterranea (Contributo Primo). *Conchiglie* 11, 185–192.

Chernomor, O., Von Haeseler, A., and Minh, B. Q. (2016). Terrace aware data structure for phylogenomic inference from supermatrices. *Syst. Biol.* 65, 997–1008. doi: 10.1093/sysbio/syw037

Cita, M. B. (1973). "Mediterranean evaporite: paleontological arguments for a deep-basin desiccation model," in *Messinian Events in the Mediterranean*, ed. C. W. Drooger (Amsterdam: North-Holland Publishing Co.), 206–228.

Coan, E. V., and Valentich-Scott, P. (2012). *Bivalve Seashells of Tropical West America. Marine Bivalve Mollusks From Baja California to Northern Peru*. Santa Barbara: Santa Barbara Museum of Natural History.

Combosch, D. J., Collins, T. M., Glover, E. A., Graf, D. L., Harper, E. M., Healy, J. M., et al. (2017). A family-level tree of life for bivalves based on a Sanger-sequencing approach. *Mol. Phylogenet. Evol.* 107, 191–208. doi: 10.1016/j.ympev.2016.11.003

Conrad, T. A. (1846). Descriptions of new species of fossil and recent shells and corals. *Proc. Acad. Nat. Sci. Phil.* 3, 19–27.

Culliney, J. L. (1975). Comparative larval development of the shipworms *Bankia gouldi* and *Teredo navalis*. *Mar. Biol.* 29, 245–251. doi: 10.1007/BF00391850

Culliney, J. L., and Turner, R. D. (1976). Larval development of the deep-water wood boring bivalve. Xylophaga atlantica Richards (Mollusca, Bivalvia, Pholadidae). *Ophelia* 15, 149–161. doi: 10.1080/00785326.1976.10425455

Cunha, M. R., Matos, F. L., Génio, L., Hilário, A., Moura, C. J., Ravara, A., et al. (2013). Are organic falls bridging reduced environments in the deep sea? – Results from colonization experiments in the Gulf of Cádiz. *PLoS One* 8:e76688. doi: 10.1371/journal.pone.0076688

Cunha, R. L., Grande, C., and Zardoya, R. (2009). Neogastropod phylogenetic relationships based on entire mitochondrial genomes. *BMC Evol. Biol.* 9:210. doi: 10.1186/1471-2148-9-210

D'Orbigny, A. (1842–1853). "Mollusques," in *Historia Física, Política y Natural de la Isla de Cuba*, Vol. 2, ed. R. De La Sagra (Paris: Librería de Arthus Bertrand).

Distel, D. L. (2000). Phylogenetic relationships among Mytilidae (Bivalvia): 18S rRNA data suggest convergence in mytilid body plans. *Mol. Phylogenet. Evol.* 15, 25–33. doi: 10.1006/mpev.1999.0733

Distel, D. L. (2003). "*The Biology of Marine Wood Boring Bivalves And Their Bacterial Endosymbionts*," *in Wood Deterioration and Preservation*. Wasington: American Chemical Society Publications, 253–271. doi: 10.1021/bk-2003-0845.ch014

Distel, D. L., Amin, M., Burgoyne, A., Linton, E., Mamangkey, G., Morrill, W., et al. (2011). Molecular phylogeny of Pholadoidea Lamarck, 1809 supports a single origin for xylotrophy (wood feeding) and xylotrophic bacterial endosymbiosis in Bivalvia. *Mol. Phylogenet Evol.* 61, 245–254. doi: 10.1016/j.ympev.2011.05.019

Distel, D. L., Beaudoin, D. J., and Morrill, W. (2002). Coexistence of multiple proteobacterial endosymbionts in the gills of the wood-boring bivalve *Lyrodus pedicellatus* (Bivalvia: Teredinidae). *Appl. Envir. Microbiol.* 68, 6292–6299. doi: 10.1128/aem.68.12.6292-6299.2002

Distel, D. L., and Roberts, S. J. (1997). Bacterial endosymbionts in the gills of the deep-sea wood-boring bivalves *Xylophaga atlantica* and *Xylophaga washingtona*. *Biol. Bull.* 192, 253–261. doi: 10.2307/1542719

Dons, C. (1929). Zoologiske Notiser V. *Xylophaga dorsalis I Norge. Det Kongelige. norske Vidensk. Selsk. Forh.* 65, 196–199.

Dons, C. (1933). Zoologiske notiser XX. *Xylophaga praestans, ny for Norges kvartærgeologi. K. norske Vidensk. Selsk. Forh.* 5, 191–193.

Emery, W. (2001). Water types and water masses. *Encyclop. Ocean Sci.* 4, 3179–3187. doi: 10.1006/rwos.2001.0108

Fagervold, S. K., Bessette, S., Romano, C., Martin, D., Plyuscheva, M., Le Bris, N., et al. (2013). Microbial communities associated with the degradation of oak wood in the Blanes submarine canyon and its adjacent open slope (NW Mediterranean). *Prog. Oceanogr.* 118, 137–143.

Fagervold, S. K., Romano, C., Kalenitchenko, D., Borowski, C., Nunes-Jorge, A., Martin, D., et al. (2014). Microbial communities in sunken wood are structured by wood-boring bivalves and location in a submarine canyon. *PLoS One* 9:e96248. doi: 10.1371/journal.pone.0096248

Fallén, C. F. (1810). *Specim. Entomolog. Novam Diptera Disponendi Methodum Exhibens*. Lundae: Berlingianis.

Folmer, O., Black, M., Hoeh, W. W. H., Lutz, R., and Vrijenhoek, R. (1994). DNA primers for amplification of mitochondrial cytochrome *c* oxidase subunit I from diverse metazoan invertebrates. *Mol. Mar. Biol. Biotechnol* 3, 294–299.

Fredj, G., and Laubier, L. (1985). "The deep mediterranean benthos," in *Mediterranean Marine Ecosystems*, eds M. Moraitou-Apostolopoulou and V. Kiortsis (Boston, MA: Springer), 109–145. doi: 10.1007/978-1-4899-2248-9_6

Gascard, J. C., and Richez, C. (1985). Water masses and circulation in the Western Alboran sea and in the Straits of Gibraltar. *Progr. Oceanogra.* 15, 157–216. doi: 10.1016/0079-6611(85)90031-X

Gaudron, S. M., Pradillon, F., Pailleret, M., Duperron, S., Le Bris, N., and Gaill, F. (2010). Colonization of organic substrates deployed in deep-sea reducing habitats by symbiotic species and associated fauna. *Mar. Environ. Res.* 70, 1–12. doi: 10.1016/j.marenvres.2010.02.002

Gaudron, S. M. T. H., Wang, H., Laming, S. R., and Duperron, S. (2016). Plasticity in reproduction and nutrition in wood-boring bivalves (*Xylophaga atlantica*) from the Mid-Atlantic Ridge. *Mar. Biol* 163:213. doi: 10.1007/s00227-016-2988-6

Giribert, G., and Wheeler, W. (2002). On Bivalve phylogeny: a high-level analysis of the Bivalvia (Mollusca) based on combined morphology and DNA sequence data. *Invert. Biol.* 121, 271–324. doi: 10.1111/j.1744-7410.2002.tb00132.x

Giribet, G., and Distel, D. L. (2003). "Bivalve phylogeny and molecular data," in *Molecular Systematics and Phylogeography of Mollusks*, eds C. Lydeard and D. R. Lindberg (Washington, DC: Smithsonian Books), 45–90.

Gray, J. E. (1827). Monograph of the genus *Teredo* of Linne, with descriptive characters of the species in the British Museum. *Phil. Mag.* 2, 409–411. doi: 10.1080/14786442708674441

Haderlie, E. C., and Mellor, J. C. (1973). Settlement growth rates and depth preference of the shipworm *Bankia setacea* in Monterey Bay. *Veliger* 15, 265–286.

Haga, T., and Kase, T. (2013). Progenetic dwarf males in the deep-sea wood-boring genus *Xylophaga* (Bivalvia: Pholadoidea). *J. Moll. Stud.* 79, 90–94. doi: 10.1093/mollus/eys037

Harvey, R. (1996). Deep water Xylophagaidae (Pelecypoda: Pholadacea) from the North Atlantic with descriptions of three new species. *J. Conchiol.* 35, 473–481.

Hebert, P. D. N., Ratnasingham, S., and Dewaard, J. R. (2003). Barcoding animal life: Cytochrome C Oxidase subunit I divergences among closely related species. *Proc. R. Soc. London Ser. B Biol. Sci.* 270, S96–S99. doi: 10.1098/rsbl.2003.0025

Hebert, P. D. N., Stoeckle, M. Y., Zemlak, T. S., and Francis, C. M. (2004). Identification of birds through DNA barcodes. *PLoS Biol.* 2:e312. doi: 10.1371/journal.pbio.0020312

Hsü, K. J., Ryan, W. B. F., and Cita, M. B. (1973). Late Miocene dessication of Mediterranean. *Nature* 242, 240–244. doi: 10.1038/242240a0

Huelsenbeck, J. P., and Ronquist, F. R. (2001). MrBayes: bayesian inference of phylogenetic trees. *Bioinformatics* 17, 754–755. doi: 10.1093/bioinformatics/17.8.754

International Commission on Zoological Nomenclature (2018). Opinion 2429 (Case 3717) – Xylophagidae Purchon, 1941 (Mollusca, Bivalvia): emended to Xylophagaidae to remove homonymy with <Xylophagidae Fallén, 1810

(Insecta, Diptera). *Bull. Zool. Nomencl.* 75, 297–299. doi: 10.21805/bzn.v75.a066

Janssen, R. (1989). Benthos-Mollusken aus dem Tiefenwasser des östliuchen Mittelmeeres, gesammelt während der "METEOR"-Fahrt 5. *Sencken. Mar.* 20, 265–276.

Janssen, R., and Krylova, E. M. (2014). Deep-sea fauna of European seas: An annotated species check-list of benthic invertebrates living deeper than 2000 m in the seas bordering Europe: bivalvia. *Invert. Zool.* 11, 43–82. doi: 10.15298/invertzool.11.1.06

Johnson, S. B., Krylova, E. M., Audzijonyte, A., Sahling, H., and Vrijenhoek, R. C. (2017). Phylogeny and origins of chemosynthetic vesicomyid clams. *Syst. Biodiv.* 15, 346–360. doi: 10.1080/14772000.2016.1252438

Kalenitchenko, D., Fagervold, S. K., Pruski, A. M., Vétion, G., Yücel, M., Le Bris, N., et al. (2015). Temporal and spatial constraints on community assembly during microbial colonization of wood in seawater. *ISME J.* 9, 2657–2670. doi: 10.1038/ismej.2015.61

Kalenitchenko, D., Le Bris, N., Dadaglio, L., Peru, E., Besserer, A., and Galand, P. E. (2018a). Bacteria alone establish the chemical basis of the wood-fall chemosynthetic ecosystem in the deep-sea. *ISME J.* 12, 367–379. doi: 10.1038/ismej.2017.163

Kalenitchenko, D., Peru, E., Pereira, L. C., Petetin, C., Galand, P. E., and Le Bris, N. (2018b). The early conversion of deep-sea wood falls into chemosynthetic hotspots revealed by in situ monitoring. *Sci. Rep* 8:907. doi: 10.1038/s41598-017-17463-2

Kearse, M., Moir, R., Wilson, A., Stones-Havas, S., Cheung, M., Sturrock, S., et al. (2012). Geneious Basic: an integrated and extendable desktop software platform for the organization and analysis of sequence data. *Bioinformatics* 28, 1647–1649. doi: 10.1093/bioinformatics/bts199

Klemm, D., Heublein, B., Fink, H.-P., and Bohn, A. (2005). Cellulose: Fascinating biopolymer and sustainable raw material. *Angew. Chem. Int. Ed.* 44, 3358–3393. doi: 10.1002/anie.200460587

Knudsen, J. (1961). The bathyal and abissal *Xylophaga* (Pholadidae. Bivalvia). *Galathea Rep.* 5, 163–209.

Lane, D. J. (1991). "16S/23S sequencing," in *Nucleic Acid Techniques in Bacterial Systematics*, eds E. Stackebrandt and M. Goodfellow (New York, NY: John Wiley), 115–175.

Leigh, J. W., and Bryant, D. (2015). Popart: Full-feature software for haplotype network construction. *Meth. Ecol. Evol.* 6, 1110–1116. doi: 10.1111/2041-210X.12410

Linnaeus, C. (1758). *Systema Naturae per Regna Tria Naturae, Secundum Classes, Ordines, Genera, Species, cum characteribus, differentiis, synonymis, locis. Tomus I. Editio Decima, Reformata*. Stockholm: Laurentii Salvii. doi: 10.5962/bhl.title.542

MacIntosh, H., De Nys, R., and Whalan, S. (2014). Contrasting life histories in shipworms: Growth, reproductive development and fecundity. *J. Exp. Mar. Biol. Ecol.* 459, 80–86. doi: 10.1016/j.jembe.2014.05.015

Maddison, W. P., and Maddison, D. R. (2019). *Mesquite: A Modular System For Evolutionary Analysis. Version 3.61*. Available online at: http://www.mesquiteproject.org (accessed December, 2019).

Medlin, L., Elwood, H. J., Stickel, S., and Sogin, M. L. (1988). The characterization of enzymatically amplified eukaryotic 16S-like rRNA-coding regions. *Gene* 71, 491–499. doi: 10.1016/0378-1119(88)90066-2

Meyer, C. P., and Paulay, G. (2005). DNA Barcoding: Error rates based on comprehensive sampling. *PLoS Biol.* 3:e422. doi: 10.1371/journal.pbio.0030422

Mienis, H. K. (2003). Woodboring bivalves from shipwrecks in the eastern Mediterranean 2. Xylophaga from the wreck of the submarine "Dakar". *Triton* 8, 5–6.

Miller, A. R., Tchernia, P., Charnock, H., and Mcgill, D. A. (1970). *Mediterranean Sea Atlas of Temperature, Salinity, Oxygen Profiles And Data From The Cruises of R.V. Atlantis and R.V. Chain With Distribution Of Nutrient Chemical Properties*. Woods Hole, MA: Woods Hole Oceanographic Institution.

Monari, S. (2009). Phylogeny and biogeography of pholadid bivalve *Barnea* (*Anchomasa*) with considerations on the phylogeny of Pholadoidea. *Acta Palaeont. Polonica* 54, 315–335. doi: 10.4202/app.2008.0068

O'Connor, R. M., Fung, J. M., Sharp, K. H., Benner, J. S., Mcclung, C., Cushing, S., et al. (2014). Gill bacteria enable a novel digestive strategy in a wood-feeding mollusk. *Proc. Nat. Acad. Sci. U.S.A.* 111, E5096–E5104. doi: 10.1073/pnas.1413110111

Park, J., and O'Foighil, D. (2000). Sphaeriid and corbiculid clams represent separate heterodont bivalve radiations into freshwater environments. *Mol. Phylogenet. Evol.* 14, 75–88. doi: 10.1006/mpev.1999.0691

Pérès, J. M. (1985). "History of the Mediterranean biota and the colonization of the depths," in *Key Environments: Western Mediterranean*, ed. R. Margalef (Oxford: Pergamon Press), 198–232.

Pop Ristova, P., Bienhold, C., Wenzhofer, F., Rossel, P. E., and Boetius, A. (2017). Temporal and spatial variations of bacterial and faunal communities associated with deep-sea wood falls. *PLoS One* 12:e169906. doi: 10.1371/journal.pone.0169906

Purchon, R. D. (1941). On the biology and relationships of the lamellibrach *Xylophaga dorsalis* (Turton). *J. Mar. Biol. Ass. U.K.* 25, 1–39. doi: 10.1017/S0025315400014259

Quatrefages, A. D. (1849). Mémoire sur le genre Taret (*Teredo* Linn.). *Ann. Sci. Nat.* 11, 19–64.

Rafinesque, C. S. (1815). *Analyse de la nature ou Tableau de l'univers et des corps organisés*. Palerme: Aux dépens de l'auteur. doi: 10.5962/bhl.title.106607

Rambaut, A. (2006). *FigTree v1.3.1. Computer Software and Manual*. Available online at: https://tree.bio.ed.ac.uk/software/figtree (accessed July 10, 2017).

Reft, A. J., and Voight, J. R. (2009). Sensory structures on the siphons of wood-boring bivalves (Pholadidae: Xylophagainae: *Xylophaga*). *Nautilus* 123, 43–48.

Richards, H. G. (1942). *Xylophaga atlantica*, new species. *Nautilus* 56:68.

Romano, C., Voight, J. R., Company, J. B., Plyuscheva, M., and Martin, D. (2013). Submarine canyons as the preferred habitat for wood-boring species of *Xylophaga (Mollusca. Bivalvia)*. *Prog. Oceanogr.* 118, 175–187. doi: 10.1016/j.pocean.2013.07.028

Romano, C., Voight, J. R., Pérez-Portela, R., and Martin, D. (2014). Morphological and genetic diversity of the wood-boring *Xylophaga* (Mollusca, Bivalvia): new species and records from deep-sea Iberian canyons. *PLoS One* 9:e102887. doi: 10.1371/journal.pone.0102887

Romey, W. (1991). Recruitment in the deep-sea wood-boring bivalve *Xylophaga atlantica* Richards. *Veliger* 34, 14–20.

Romey, W. L., Bullock, R. C., and Dealteris, J. T. (1994). Rapid growth of a deep-sea wood-boring bivalve. *Cont. Shelf Res.* 14, 1349–1359. doi: 10.1016/0278-4343(94)90052-3
doi: 10.1093/sysbio/sys029

Rosenberg, G., and Gofas, S. (2015). *Xylophagidae: MolluscaBase*. Available online at: http://www.marinespecies.org/aphia.php?p=taxdetails&id=489105 (accessed July, 2019).

Sabbadin, F., Pesante, G., Elias, L., Besser, K., Li, Y., Steele-King, C., et al. (2018). Uncovering the molecular mechanisms of lignocellulose digestion in shipworms. *Biotechnol. Biofuels* 11, 59–69. doi: 10.1186/s13068-018-1058-3

Santhakumaran, L. N. (1980). Two new species of *Xylophaga* from Trondheimsfjorden, western Norway (Mollusca. Pelecypoda). *Sarsia* 65, 269–272. doi: 10.1080/00364827.1980.10431489

Saraswathy, M., and Nair, N. B. (1971). XIV.—Observations on the structure of the shipworms, Nausitora hedleyi, Teredo furcifera and Teredora princesae (Bivalvia: Teredinidae). *Trans. R. Soc. Edinburgh* 68, 507–566. doi: 10.1017/S0080456800014861

Sharma, P. P., Zardus, J. D., Boyle, E. E., González, V. L., Jennings, R. M., Mcintyre, E., et al. (2013). Into the deep: a phylogenetic approach to the bivalve subclass Protobranchia. *Mol. Phylogenet. Evol.* 69, 188–204. doi: 10.1016/j.ympev.2013.05.018

Smith, C. R., De Leo, F. C., Bernardino, A. F., Sweetman, A. K., and Martínez Arbizu, P. (2008). Abyssal food limitation, ecosystem structure and climate change. *Trends Ecol. Evol.* 23, 518–528. doi: 10.1016/j.tree.2008.05.002

Smith, E. A. (1903). *Xylophaga praestans* new sp. *Proc. Malacol. Soc. Lond.* 5, 328–330.

Smith, E. A. (1904). On a collection of marine shells from Port Alfred. Cape Colony. *J. Malacol.* 11, 21–44.

Stamatakis, A. (2014). RAxML version 8: a tool for phylogenetic analysis and post-analysis of large phylogenies. *Bioinformatics* 30, 1312–1313. doi: 10.1093/bioinformatics/btu033

Stockton, W. L., and DeLaca, T. E. (1982). Food falls in the deep sea: occurrence, quality, and significance. *Deep-Sea Res. A Oceanogr. Res. Pap* 29, 157–169. doi: 10.1016/0198-0149(82)90106-6

Swofford, D. L. (2003). *PAUP*. Phylogenetic analysis using parsimony (* and other methods). Version* 4.0. Sunderland: Sinauer Associates.

Taki, I., and Habe, T. (1945). Classification of Japanese Pholadacea. *Jap. J. Malacol.* 14, 108–123.

Taki, I., and Habe, T. (1950). Xylophaginidae in Japan. *Illust. Cat. Jap. Shells.* 7, 45–47. doi: 10.6013/jbrewsocjapan1915.45.3_47

Tamura, K., Stecher, G., Peterson, D., Filipski, A., and Kumar, S. (2013). MEGA6: molecular evolutionary genetics analysis version 6.0. *Mol. Biol. Evol.* 30, 2725–2729. doi: 10.1093/molbev/mst197

Turner, R. D. (1955). The family Pholadidae in the western Atlantic and the eastern Pacific. *Part II – Martesiinae Jouannetiinae Xylopagainae. Johnsonia* 3, 65–160.

Turner, R. D. (1972). *Xyloredo*, a new teredinid-like abyssal wood-borer (Mollusca, Pholadidae, Xylophagainae). *Breviora* 397, 1–19.

Turner, R. D. (1973). Wood-boring bivalves, opportunistic species in the deep sea. *Science* 180, 1377–1379. doi: 10.1126/science.180.4093.1377

Turner, R. D. (1977). Wood, mollusks and deep-sea food chain. *Bull. Am. Malacol. Union* 1976, 13–19.

Turner, R. D. (2002). On the subfamily Xylophagainae (Family Pholadidae. Bivalvia, Mollusca). *Bull. Museum Comp. Zool.* 157, 223–308.

Turner, R. D., and Culliney, J. (1971). Some anatomical and life history studies of wood boring bivalve systematics. *Rep. Am. Malacol. Un. Pacific Div.* 1970, 65–66.

Turton, W. (1819). *A Conchological Dictionary of the British Islands*. London: John Booth. doi: 10.5962/bhl.title.156842

Turton, W. (1822). *Conchylia insularum britannicarum*. London: Nattali and Combe. doi: 10.5962/bhl.title.10443

Tyler, P. A., Young, C. M., and Dove, F. (2007). Settlement, growth and reproduction in the deep-sea wood-boring bivalve mollusc *Xylophaga depalmai*. *Mar. Ecol. Progr. Ser.* 343, 151–159. doi: 10.3354/meps06832

Tyler, P. A., and Young, G. M. (1999). Reproduction and dispersal at vents and cold seeps. *J. Mar. Biol. Ass. U.K.* 79, 193–208. doi: 10.1017/S0025315499000235

Van Dover, C. L., German, C. R., Speer, K. G., Parson, L. M., and Vrijenhoek, R. C. (2002). Evolution and biogeography of deep-sea vent and seep invertebrates. *Science* 295:1253. doi: 10.1126/science.1067361

Voight, J. R. (2007). Experimental deep-sea deployments reveal diverse Northeast Pacific wood-boring bivalves of Xylophagainae (Myoida : Pholadidae). *J. Moll. Stud.* 73, 377–391. doi: 10.1093/mollus/eym034

Voight, J. R. (2008). Deep-sea wood-boring bivalves of *Xylophaga* (Myoida: Pholadidae) on the Continental Shelf: a new species described. *J. Mar. Biol. Ass. U.K.* 88, 1459–1464. doi: 10.1017/S0025315408002117

Voight, J. R. (2009). Diversity and reproduction of near-shore vs offshore wood-boring bivalves (Pholadidae: Xylophagainae) of the deep eastern Pacific ocean, with three new species. *J. Moll. Stud.* 75, 167–174. doi: 10.1093/mollus/eyp012

Voight, J. R. (2015). Xylotrophic bivalves: aspects of their biology and the impacts of humans. *J. Moll. Stud.* 81, 175–186. doi: 10.1093/mollus/eyv008

Voight, J. R. (2016). New insights on *Xylopholas* (Mollusca: Xylophagaidae): diversity, growth and reproduction. *Am. Malacol. Bull.* 34, 138–146. doi: 10.4003/006.034.0210

Voight, J. R., Jacob, C. C., and Raymond, W. L. (2020). Stable isotopic evidence of mixotrophy in xylophagaids, deep-sea wood-boring bivalves. *Front. Mar. Sci* 7:50. doi: 10.3389/fmars.2020.00050

Voight, J. R., Marshall, B. A., Judge, J., Halanych, K. M., Li, Y., Bernardino, A. F., et al. (2019). Life in wood: preliminary phylogeny of deep-sea wood-boring bivalves (Xylophagaidae), with descriptions of three new genera and one new species. *J. Moll. Stud.* 85, 232–243. doi: 10.1093/mollus/eyz003

Voight, J. R., and Segonzac, M. (2012). At the bottom of the deep blue sea: a new wood-boring bivalve (Mollusca. Pholadidae, Xylophaga) from the Cape Verde byssal Plain (subtropical Atlantic). *Zoosystema* 34, 171–180. doi: 10.5252/z2012n1a8

Vrijenhoek, R. C., Johnson, S. B., and Rouse, G. W. (2009). A remarkable diversity of bone-eating worms (*Osedax*; Siboglinidae; Annelida). *BMC Biol.* 7:74. doi: 10.1186/1741-7007-7-74

Waterbury, J. B., Calloway, C. B., and Turner, R. D. (1983). A cellulolytic nitrogen-fixing bacterium cultured from the gland of Deshayes in shipworms (Bivalvia: Teredinidae). *Science* 221, 1401–1403. doi: 10.1126/science.221.4618.1401

Weigelt, R., Lippert, H., Borges, L. M. S., Appelqvist, C., Karsten, U., and Bastrop, R. (2016). First time DNA barcoding of the common shipworm *Teredo navalis* Linnaeus, 1758 (Mollusca: Bivalvia: Teredinidae): molecular-taxonomic investigation and identification of a widespread wood-borer. *J. Exp. Mar. Biol. Ecol.* 475, 154–162. doi: 10.1016/j.jembe.2015.11.008

West, A. J., Lin, C. W., Lin, T. C., Hilton, R. G., Liu, S. H., Chang, C. T., et al. (2011). Mobilization and transport of coarse woody debris to the oceans triggered by an extreme tropical storm. *Limnol. Oceanogr.* 56, 77–85. doi: 10.4319/lo.2011.56.1.0077

Wolff, T. (1979). Macrofaunal utilization of plant remains in the deep-sea. *Sarsia* 64, 117–136. doi: 10.1080/00364827.1979.10411373

Yücel, M., Galand, E., Fagervold, S. A. K., Contreira-Pereira, L., and Le Bris, N. (2013). Sulfide production and consumption in degrading wood in the marine environment. *Chemosphere* 90, 403–409. doi: 10.1016/j.chemosphere.2012.07.036

Zenetos, A., Vardala-Theodoro, E., and Alexandrakis, C. (2005). Update of the marine Bivalvia Mollusca checklist in Greek waters. *J. Mar. Biol. Ass. U.K.* 85, 993–998. doi: 10.1017/S0025315405012014

Zhou, J., Bruns, M. A., and Tiedje, J. M. (1996). DNA recovery from soils of diverse composition. *Appl. Environ. Microbiol* 62, 316–322. doi: 10.1128/AEM.62.2.316-322.1996

Conflict of Interest: The authors declare that the research was conducted in the absence of any commercial or financial relationships that could be construed as a potential conflict of interest.

frontiers in Marine Science

CORRECTION
published: 19 February 2021
doi: 10.3389/fmars.2020.640579

Corrigendum: Wooden Stepping Stones: Diversity and Biogeography of Deep-Sea Wood Boring Xylophagaidae (Mollusca: Bivalvia) in the North-East Atlantic Ocean, With the Description of a New Genus

Chiara Romano[1*†‡], *Amandine Nunes-Jorge*[2‡], *Nadine Le Bris*[3†], *Greg W. Rouse*[4†], *Daniel Martin*[1†] *and Christian Borowski*[2*†]

[1] Centre d'Estudis Avançats de Blanes (CEAB-CSIC), Blanes, Spain, [2] Max Planck Institute for Marine Microbiology, Bremen, Germany, [3] Sorbonne Université, CNRS, Observatoire Océanologique de Banyuls (LECOB), Banyuls-sur-Mer, France, [4] Scripps Institution of Oceanography, University of California, San Diego, La Jolla, CA, United States

Keywords: genetic connectivity, wood falls, Mediterranean, deep sea, phylogeography

OPEN ACCESS

Approved by:
Frontiers Editorial Office, Frontiers Media SA, Switzerland

***Correspondence:**
Chiara Romano
cromano@ceab.csic.es
Christian Borowski
cborowsk@mpi-bremen.de

†ORCID:
Chiara Romano
orcid.org/0000-0001-5078-0082
Nadine Le Bris
orcid.org/0000-0002-0142-4847
Greg W. Rouse
orcid.org/0000-0001-9036-9263
Daniel Martin
orcid.org/0000-0001-6350-7384
Christian Borowski
orcid.org/0000-0001-7921-3022

‡These authors have contributed equally to this work

Specialty section:
This article was submitted to Marine Evolutionary Biology, Biogeography and Species Diversity, a section of the journal Frontiers in Marine Science

Received: *14 December 2020*
Accepted: *23 December 2020*
Published: *19 February 2021*

Citation:
Romano C, Nunes-Jorge A, Le Bris N, Rouse GW, Martin D and Borowski C (2021) Corrigendum: Wooden Stepping Stones: Diversity and Biogeography of Deep-Sea Wood Boring Xylophagaidae (Mollusca: Bivalvia) in the North-East Atlantic Ocean, With the Description of a New Genus. Front. Mar. Sci. 7:640579. doi: 10.3389/fmars.2020.640579

A Corrigendum on

Wooden Stepping Stones: Diversity and Biogeography of Deep-Sea Wood Boring Xylophagaidae (Mollusca: Bivalvia) in the North-East Atlantic Ocean, With the Description of a New Genus

by Romano, C., Nunes-Jorge, A., Le Bris, N., Rouse, G. W., Martin, D., and Borowski, C. (2020). Front. Mar. Sci. 7:579959. doi: 10.3389/fmars.2020.579959

There are errors in the **Funding Statement**. The correct number for project CHEMECO is **(European Sciences Foundation (ESF)/Eurocores/EURODEEP/0001/2007)**. Funding sources for shiptime during cruises BioBaz, M70/2-Bionil, MSM13/3-Homer, ARKXXII/1b, ARKXXIV/2, and Medeco-2 were missing. The links to the DeepFall project page and Twitter were incorrect and have been updated. The corrected **Funding Statement** is as follows:

This work was supported by the Max Planck Society and the French Centre National de la Recherche Scientifique (CNRS) associating Université de Liège, UPMC, and Museum of Natural History through the GDRE program "Diversity, establishment and function of organisms associated with marine wood falls-DiWOOD"; by project CHEMECO (European Sciences Foundation (ESF)/Eurocores/EURODEEP/0001/2007); by the Chair programme "Extreme Marine Environments, Biodiversity and Global Change" UPMC-Fondation TOTAL; by the EUROFLEET Programme; by the Agencia Española de Investigación (AEI) and the European Funds for Regional Development (FEDER/UE) through the research projects PROMETEO (CTM2007-66316-C02-02/MAR), DOSMARES (CTM2010-21810-C03-03) and PopCOmics (CTM2017-88080); and by Agència de Gestió d'Ajuts Universitaris i de Recerca of the Generalitat of Catalunya through the Consolidated Research Group on Marine Benthic Ecology (2017SGR378). Shiptime during research cruises BioBaz, M70/2-Bionil, MSM13/3-Homer, ARKXXII/1b, ARKXXIV/2, Medeco-2, and POS403-MenezKart received funding from the EU 6th FP HERMES (GOCE-CT-2005-511234), EU 7th FP HERMIONE (grant agreement no. 226354), CNRS, and the DFG. CR was funded by the People Programme (Marie Curie Action IOF to CR) of the European Union's Seventh Framework Programme (FP7/2007-2013) under the "DeepFall" project http://www.deepfall-project.eu; https://twitter.com/DeepFall_Proj (REA grant agreement N. PIOF-GA-2013-628146); AN-J was funded through DiWOOD; CB was funded by the DFG Cluster of Excellence "The Ocean in the Earth

TABLE 1 | Characteristics of deployment sites and colonization experiments.

	Region	Site	Environment	Coordinates	Depth (m)	Temperature (°C)	Deployment /Recovery (Cruise name - Date)	Duration of Deployment (Months)	Research project	References
Atlantic	Barents Sea	Haakon Mosby Mud Volcano	Mud volcano	72°00N, 14°43E	1260	−1	ARKXXII/1b - June 2007 / ARKXXIV/2 - June 2009	24	DiWOOD	Pop Ristova et al., 2017; this study
	Bay of Biscay	Avilés Canyon	Canyon; Slope	44°07'N, 6°14'W	1200; 2000	4; 9	BioCant 2012-2013	7; 13	DosMares	Romano et al., 2014
	Mid-Atlantic Ridge	Menez-Gwen	Hydrothermal vent	37°17'N, 32°15'W	870	9	MenezKart/ POS402 - July 2010/BioBaz July 2013	36	DiWOOD	This study
		Rainbow	Hydrothermal vent	36°13'N, 33°54'W	2300	3.5	MoMARDream-Naut -July 2007/ MoMARDream 08 - Aug.-Sept. 2008	13	CHEMECO	Gaudron et al., 2010
	NW-Atlantic, Morocco	Mercator	Mud volcano	35°17'N, 06°38'W	350	13	JC10 May - 2007 and 64PE284 - March 2008/B09-May 2009	9; 24	CHEMECO/FTC	Cunha et al., 2013
		Meknès	Mud volcano	34°59'N, 07°04'W	700	N.A.		15		Cunha et al., 2013
Mediterranean	Western Mediterranean	Blanes Canyon	Canyon; Slope	41°34'N, 2°50'E	900; 1100; 1200; 1500; 1800	13	Prometeo 2008-2009 Dos Mares 2012-2013	3 & 9 (at 1200 m); 12 (at other depths)	PROMETEO, DosMares	Romano et al., 2013
		La Fonera Canyon	Canyon	41°52"N, 3°16'E	130; 1100	13	DosMares 2012-2013	10 (at 130 m); 7 & 13 (at 1100 m)	Dos Mares	Romano et al., 2014; this study
		Lacaze-Duthiers Canyon	Canyon	42°28'N, 3°28'E	500	13	2011	7	*Extreme Marine Env., Biodiversity and Global Change'*	Kalenitchenko et al., 2015; this study
	Eastern Mediterranean, Nile Fan (NF)	Central Pockmarks	Seep	32°32' N, 30°21' E	1145	14	Bionil M70/2 - Oct./Nov. 2006 /Medeco-2 - Nov. 2007 and Homer MSM13/3 - Oct./Nov. 2009	12; 36	DiWOOD	Bienhold et al., 2013; this study

NA: not available.

System" at MARUM (University of Bremen), a European Research Council Advanced Grant (BathyBiome, Grant 340535) and the Max Planck Society.

In the original article, there were mistakes in Table 1 as published. Column "Deployment/Recovery (Cruise name-Date)"/Row 1 should be "ARKXXII/1b - June 2007 / ARKXXIV/2 - June 2009" instead of "ARKXXII/1b - June 2009 / ARKXXIV/2 - June 2009". Column "Deployment/Recovery (Cruise name-Date)"/Row 10 should be "Bionil M70/2 - Oct./Nov. 2006 /Medeco-2 - Nov. 2007 and Homer MSM13/3 - Oct./Nov.2009" instead of "Homer/MSM13/3 - Oct.-Nov. 2009". Column "References"/Row 10 should be "Bienhold et al., 2013; this study" instead of "This study". Column "Research Project"/Row 4 should be "CHEMECO" instead of "DiWOOD". The corrected **Table 1** appears above.

In the original article, there was an error. % units should be ‰.

A correction has been made to ***Discussion, Diversity of Xylophagaidae in European Deep Waters and Ecological Considerations***, ***Paragraph 4***:

North East Atlantic mid- and deep-water fauna is adapted to a salinity range of 34.4–35.3 ‰ (Bouchet and Taviani, 1992; Emery, 2001). Atlantic xylophagaids living exclusively below 500 m depth may therefore be typical stenohaline deep-sea organisms. Species living in shallower Atlantic waters must tolerate higher salinities of 35.2–36.7 ‰ (Emery, 2001) and species living in the deep Mediterranean must cope with >38.0 ‰ (Miller et al., 1970). Xylophagaids covering broad salinity ranges in the Atlantic and occurring also in the Mediterranean such as *Xylonora atlantica* new comb., *Xylophaga dorsalis* and *Abditoconus brava* are therefore considered euryhaline marine species (Table 4).

The authors apologize for these errors and state that this does not change the scientific conclusions of the article in any way. The original article has been updated.

REFERENCES

Bienhold, C., Pop Ristova, P., Wenzhöfer, F., Dittmar, T., and Boetius, A. (2013). How deep-sea wood falls sustain chemosynthetic life. *PLoS One* 8:e53590. doi: 10.1371/journal.pone.0053590

Bouchet, P., and Taviani, M. (1992). The Mediterranean deep-sea fauna – pseudopopulations of Atlantic species. *Deep Sea Res. Part A Oceanogr. Res. Pap.* 39, 169–184. doi: 10.1016/0198-0149(92)90103-z

Cunha, M. R., Matos, F. L., Génio, L., Hilário, A., Moura, C. J., Ravara, A., et al. (2013). Are organic falls bridging reduced environments in the deep sea? – Results from colonization experiments in the Gulf of Cádiz. *PLoS One* 8:e76688. doi: 10.1371/journal.pone.0076688

Emery, W. (2001). Water types and water masses. *Encyclop. Ocean Sci.* 4, 3179–3187. doi: 10.1006/rwos.2001.0108

Gaudron, S. M., Pradillon, F., Pailleret, M., Duperron, S., Le Bris, N., and Gaill, F. (2010). Colonization of organic substrates deployed in deep-sea reducing habitats by symbiotic species and associated fauna. *Mar. Environ. Res.* 70, 1–12. doi: 10.1016/j.marenvres.2010.02.002

Kalenitchenko, D., Fagervold, S. K., Pruski, A. M., Vétion, G., Yücel, M., Le Bris, N., et al. (2015). Temporal and spatial constraints on community assembly during microbial colonization of wood in seawater. *ISME J.* 9, 2657–2670. doi: 10.1038/ismej.2015.61

Miller, A. R., Tchernia, P., Charnock, H., and Mcgill, D. A. (1970). *Mediterranean Sea Atlas of Temperature, Salinity, Oxygen Profiles And Data From The Cruises of R.V. Atlantis and R.V. Chain With Distribution Of Nutrient Chemical Properties.* Woods Hole, MA: Woods Hole Oceanographic Institution.

Pop Ristova, P., Bienhold, C., Wenzhofer, F., Rossel, P. E., and Boetius, A. (2017). Temporal and spatial variations of bacterial and faunal communities associated with deep-sea wood falls. *PLoS One* 12:e169906. doi: 10.1371/journal.pone.0169906

Romano, C., Voight, J. R., Company, J. B., Plyuscheva, M., and Martin, D. (2013). Submarine canyons as the preferred habitat for wood-boring species of *Xylophaga (Mollusca. Bivalvia). Prog. Oceanogr.* 118, 175–187. doi: 10.1016/j.pocean.2013.07.028

Romano, C., Voight, J. R., Pérez-Portela, R., and Martin, D. (2014). Morphological and genetic diversity of the wood-boring *Xylophaga* (Mollusca, Bivalvia): new species and records from deep-sea Iberian canyons. *PLoS One* 9:e102887. doi: 10.1371/journal.pone.0102887

frontiers in Marine Science

SYSTEMATIC REVIEW
published: 15 March 2021
doi: 10.3389/fmars.2021.643078

Taxonomy and Ecology of Sympatric *Ampelisca* Species (Crustacea, Amphipoda) From the Strait of Gibraltar to the Strait of Dover, North-Eastern Atlantic

Jean-Claude Dauvin[1]*, *Leandro Sampaio*[2,3,4], *Ana Maria Rodrigues*[2] and *Victor Quintino*[2]

[1] Normandie Univ., UNICAEN, Université de Caen Normandie, CNRS, Laboratoire Morphodynamique Continentale et Côtière, UMR 6143 M2C, Caen, France, [2] Centre for Environmental and Marine Studies (CESAM), Department of Biology, University of Aveiro, Aveiro, Portugal, [3] CIIMAR Interdisciplinary Centre of Marine and Environmental Research, University of Porto, Matosinhos, Portugal, [4] Department of Biology, Faculty of Sciences, University of Porto, Porto, Portugal

The Ampeliscidae Kröyer, 1842 is amongst the most diverse amphipod families; it comprises four genera, *Ampelisca* being the richest with more than 200 species. The *Ampelisca* genus presents high morphological homogeneity and the identification of the species by ecologists remains difficult. *Ampelisca* are also characterized by a high degree of sympatry, a rare situation in amphipods, and in this study we report up to nine species coexisting at the same site. Recent benthic sampling and publications, namely on the Portuguese continental shelf and the English Channel, permit to revisit the available data on the taxonomy and propose an updated species identification key, as well as the distribution and ecology of the 40-recorded *Ampelisca* species along the North Eastern Atlantic coast, from the Strait of Gibraltar, in the South, to the Strait of Dover, in the North. The data allow discussing on the sympatry and syntopy of such diverse amphipod family with the co-occurrence of several species at various scales of observations, from the wider regional area, to the narrower local habitat. Two *Ampelisca* species were recorded exclusively on hard bottom, while the other tend to inhabit specific types of soft bottom, ranging from deep mud to shallow coarse sand and gravel, with a preference for continental shelf muddy and sandy habitats. A future sea water temperature increase scenario could modify the species geographical distribution and reproductive cycle, in this temperate North-eastern Atlantic province.

Keywords: North-Eastern Atlantic, Ampeliscidae, key of species, distribution, abundance, bio-geographical gradient, co-occurrence

OPEN ACCESS

Edited by:
Juan Moreira Da Rocha, Autonomous University of Madrid, Spain

Reviewed by:
Ignacio Winfield, National Autonomous University of Mexico, Mexico
Xiaoshou Liu, Ocean University of China, China

***Correspondence:**
Jean-Claude Dauvin
jean-claude.dauvin@unicaen.fr

Specialty section:
This article was submitted to Marine Evolutionary Biology, Biogeography and Species Diversity, a section of the journal Frontiers in Marine Science

Received: *17 December 2020*
Accepted: *09 February 2021*
Published: *15 March 2021*

Citation:
Dauvin J-C, Sampaio L, Rodrigues AM and Quintino V (2021) Taxonomy and Ecology of Sympatric Ampelisca Species (Crustacea, Amphipoda) From the Strait of Gibraltar to the Strait of Dover, North-Eastern Atlantic. Front. Mar. Sci. 8:643078. doi: 10.3389/fmars.2021.643078

INTRODUCTION

The Ampeliscidae Kröyer, 1842 is one of the most diverse amphipod families, together with the Gammaridae Leach, 1814 and the Lysianassidae Lana, 1849. Ampeliscidae is composed of four genera comprising more than 300 species, with 9 species of *Byblisoides*, 27 species of *Haploops*, 75 species of *Byblis* and 203 species of *Ampelisca* recorded on the World Register of Marine Species [http://www.marinespecies.org/; accessed on 16th October 2020). The Ampeliscidae family

accounts nowadays for 314 species, representing 3.0% of the described amphipod species, 10,320 in total (Horton et al., 2021)]. New species for this family continue to be annually described. Between 2000 and 2020, 3 *Byblisoides*, 14 *Byblis,* 9 *Haploops*, and 32 *Ampelisca* new to science were described, corresponding to 18% of the known species of this family.

Numerous data and reviews on the Ampeliscidae (see Bellan-Santini, 1982, 1983; Dauvin and Bellan-Santini, 1985, 1986, 1988, 1996, 2000, 2002; Bellan-Santini and Dauvin, 1988a,b, 1989, 1997; Dauvin, 1996) permitted to differentiate the general distribution patterns of the genera, *Byblisoides*, *Byblis* and *Haploops* being mainly deep- and cold-water genera and *Ampelisca* more tropical and sub-tropical and shallow water genus. Nevertheless, dense *Haploops* populations have been reported in South Brittany shallow waters, Northern part of the Bay of Biscay (Rigolet et al., 2012, 2014), while dense *Ampelisca* populations occurred in North Brittany at the entrance of the English Channel (Dauvin, 1988a,b,c,d, 1989).

Given the *Ampelisca* high morphological homogeneity, the taxonomic identification of specimen to the species level remains difficult to ecologists, in spite of the existence of illustrated keys (Dauvin and Bellan-Santini, 1988). As a consequence, most ecological studies tend to report only the presence of *Ampelisca* sp. or *Ampelisca* spp., without detailing the species. This difficulty arises in part from poorly detailed descriptions accompanying the reporting of new *Ampelisca* species, most being known only from the type locality and represented by very few specimens. Other difficulties include the existence of cryptic species, such as *Ampelisca brevicornis* sensu lato and the discovery of several species for this large cosmopolitan species, i.e., *A. cavicoxa* Reid, 1951 and *A. pectenata* Reid, 1951 for the North-Eastern Atlantic (Kaim-Malka, 2000) or more recently the description of *A. troncosoi* Tato et al. (2012) from Galicia, Spain, previously miss-confused with *A. heterodactylta* (Schellenberg, 1925; Tato et al., 2012). Additionally, the high level of taxonomic expertise and the long time required to identify the *Ampelisca* to species level, especially for large sample collections, may not always be compatible with numerous ecological work. Apart from the high diversity of the *Ampelisca*, another particularity of this genus is to present a high degree of sympatry, not only at the regional and local scales, but also at the scale of the grab replicate sample (Dauvin et al., 1993). The *Ampelisca* species tend to inhabit distinct types of substratum. The genus is mostly present on soft bottom, from deep mud to shallow coarse sand and gravel (Bellan-Santini and Dauvin, 1988a,b; Bellan-Santini and Dauvin, 1989) and only very few species are found on hard bottom (i.e., *A. rubella* A. Costa, 1864 or *A. lusitanica* Bellan-Santini and Marques, 1986).

Recent benthic sampling campaigns on the Portuguese continental shelf (Martins et al., 2012, 2013a,b, 2014; Sampaio et al., 2016) and in the English Channel, i.e., in the Rade de Cherbourg (Baux et al., 2017; Andres et al., 2020) and in the Bay of Seine (Alizier, 2011), permit to revisit the available data on the taxonomy, distribution and ecology of the *Ampelisca* species along the North Eastern Atlantic, from the Strait of Gibraltar, in the South to the Strait of Dover, in the North.

MATERIALS AND METHODS

Sampling Sites and Recently Available Data

Portuguese Continental Shelf

A total of 326 sites were visited during sampling campaigns with a 0.1 m² Smith McIntyre grab (one grab per site) conducted on the entire Portuguese continental shelf from Caminha on the Northwest, to Vila Real de Santo António on the Southeast (Martins et al., 2012, 2013a,b, 2014; Sampaio et al., 2016). The shallow and mid depth north-western shelf and areas located close to the major submarine canyons are characterized by coarser sediments with low fines and organic matter content, whereas the south-western and the deep north-western shelf are dominated by fine sands with moderate fines and organic matter content. The western part of the southern shelf is very heterogeneous while muds predominate off the major Portuguese rivers, the Tagus (Lisbon) and the Douro (Porto) on the west and the Guadiana (Vila Real Santo de António), on the south coast (see namely Cardoso et al., 2019).

English Channel

New data was obtained mainly from the Rade the Cherbourg and the Bay of Seine. The Rade de Cherbourg is Europe's largest roadstead, extending over a total area of 15 km², with a maximum depth ∼20 m, and a mean depth of ∼13 m. The macrofauna was sampled with a 0.1 m² Van Veen grab (three replicates per site) for different studies from 2012 to 2018 on the four sediment facies of the Rade and in surrounding bays in the North Cotentin for a total of 61 sites (Baux et al., 2017; Andres et al., 2020). The eastern part of the Bay of Seine (eastern part of the English Channel) and the lower part of the Seine estuary cover an area of ∼ 400 km², with a maximum depth of ∼20 m. Macrofauna was sampled in 2008–2009 (Alizier, 2011) and in 2016–2017 (Baux, 2018) for a total of about 100 sites with a 0.1 m² Van Veen grab (three to five replicates per site).

Geographical Distribution

The coast along the North Eastern Atlantic coast, from the Strait of Gibraltar, in the South, to the Strait of Dover, in the North, was divided in eight zones corresponding to the available data on the *Ampelisca* distribution, i.e., South Spain (Bellan-Santini and Dauvin, 1988b); Portugal (Bellan-Santini and Dauvin, 1988b; Sampaio et al., 2016); Galicia (Bellan-Santini and Dauvin, 1988b); South-Eastern Bay of Biscay (Bachelet et al., 2003); South Brittany (Bellan-Santini and Dauvin, 1988b); Iroise Sea (Dauvin and Toulemont, 1988); Western part of the English Channel (Bellan-Santini and Dauvin, 1988b, 1989; Dauvin, 1999; Le Mao, 2006) and Eastern part of the English Channel North Cotentin (Dauvin, 1999; Alizier, 2011; Baux et al., 2017; Andres et al., 2020).

According to their occurrences, the species were classified in three categories, (1) rare, corresponding to species recorded at up to 10 sites, (2) common, corresponding to species recorded in numerous soft-bottom sites mainly from muddy to sandy sediment, and (3) very common, for species recorded in most of the sampled soft-bottom

TABLE 1 | Latitudinal distribution of *Ampelisca* from the Strait of Gibraltar (south Atlantic coast of Spain) to the Strait of Dover.

Species	South Spain	Portugal	Galicia	SE Bay of Biscay	South Brittany	Iroise Sea	Western EC	Eastern EC
A. aequicornis Bruzelius, 1859				+	+	+		
A. anophthalma Bellan-Santini and Kaim-Malka, 1977	+	+						
A. amblyops Sars, 1895				+				
A. anomala Sars, 1883				+	+			
A. armoricana Bellan-Santini and Dauvin, 1981		+		+	+	+	+	
A. brevicornis Costa, 1853	+	+	+	+	+	+	+	+
A. calypsonis Bellan-Santini and Kaim-Malka, 1977	+	+						
A. cavicoxa Reid, 1951				+				
A. dalmatina Karaman, 1975	+	+						
A. declivitatis Mills, 1967				+				
A. diadema Costa, 1853	+	+	+	+	+	+	+	+
A. eschrichtii Krøyer, 1842					+			
A. gibba Sars, 1883	+	+		+	+	+		
A. heterodactyla Schellenberg, 1925		+		+				
A. latifrons Schellenberg, 1925		+						
A. lusitanica Bellan-Santini and Marques, 1986		+						
A. massiliensis Bellan-Santini and Kaim-Malka, 1977	+	+						
A. multispinosa Bellan-Santini and Kaim-Malka, 1977	+	+						
A.odontoplax G. O. Sars, 1879				+				
A.parabyblisoides Dauvin and Bellan-Santini, 1996				+				
A. pectenata Reid, 1951		+		+	+	+	+	+
A. provincialis Bellan-Santini and Kaim-Malka, 1977	+	+						
A. pseudosarsi Bellan-Santini and Kaim-Malka, 1977	+	+						
A.pseudospinima Bellan-Santini and Kaim-Malka, 1977	+	+						
A. pusilla Sars, 1895				+				
A. remora Bellan-Santini and Dauvin, 1986		+	+					
A. rubella A. Costa, 1864	+	+		+				
A. ruffoi Bellan-Santini and Kaim-Malka, 1977	+	+						
A. sarsi Chevreux, 1888	+	+	+	+	+	+	+	
A. serraticaudata Chevreux, 1888	+	+	+					
A. sorbei Dauvin and Bellan-Santini, 1996				+				
A. spinifer Reid, 1951	+	+	+	+	+	+		
A. spinimana Chevreux, 1900		+	+	+	+	+	+	
A. spinipes Boeck, 1861	+	+	+	+	+	+	+	+
A. tenuicornis Lilljeborg, 1855	+	+	+	+	+	+	+	+
A. troncosoi Tato et al., 2012				+				
A. toulemonti Dauvin and Bellan-Santini, 1982					+	+	+	+
A. typica Bate, 1856	+	+	+	+	+	+	+	+
A. uncinata Chevreux, 1887				+				
A. verga Reid, 1951		+						
Total	19	27	10	24	15	13	10	7

South Spain: Bellan-Santini and Dauvin (1988b); Portugal: Bellan-Santini and Dauvin (1988b); Sampaio et al. (2016); Galicia: Bellan-Santini and Dauvin (1988b); SE Bay of Biscay: Bachelet et al. (2003); South Brittany: Bellan-Santini and Dauvin (1988b); Iroise Sea: Dauvin and Toulemont (1988); Western part of the English Channel: Bellan-Santini and Dauvin (1988b, 1989), Dauvin (1999), Le Mao (2006), and Eastern part of the English Channel: Dauvin (1999), Alizier (2011), Baux et al. (2017) and Andres et al. (2020).

communities from the Strait of Gibraltar to the Dover Strait and at a large range of sediment types, from muddy to gravely sediment.

A Jaccard similarity matrix among the samples was obtained and exploited by cluster analysis using the average clustering algorithm and by ordination analysis, using non-metric multidimensional scaling (nMDS). The Jaccard Similarity Coefficient is most appropriate to analyze our data (presence of species in geographical areas, **Table 1**), because it is precisely devoted to study the similarity between samples solely on the presence-absence of the species. Other presence-absence similarity coefficients could be used, but the Jaccard Coefficient

is a classic choice, possibly one of the most used in Ecology. Moreover, the Jaccard similarity between two samples also has a very straightforward interpretation, representing the proportion of the common species to the two samples. An ordination analysis was also performed using principal components analysis (PCA), following a Hellinger transformation, this analysis allowing the joint plot of the samples (the geographical locations) and the associated species. All multivariate analysis were performed with PRIMER v.6 (Clarke and Gorley, 2006).

RESULTS

Taxonomy

A total of 40 species were recorded along the North-eastern Atlantic coast from the Strait of Gibraltar to the Strait of Dover (Appendix A in **Supplementary Material**). Since the publication of the *Ampelisca* taxonomic key from the north-eastern Atlantic by Dauvin and Bellan-Santini (1988), the number of species known to this area has increased. Two species, *A. declivitatis* and *A. macrocephala,* were added to the list of recorded species in this area (see namely Dauvin and Bellan-Santini, 1996) and four new species were described for science (*Ampelisca cavicoxa, A. parabyblisoides, A. sorbei,* and *A. troncosoi*). The following taxonomic key includes these additions. A1 corresponds to the first pair of antennae, A2 to the second pairs and P7 to the pereiopod 7. The main morphological characters which served to the identification of *Ampelisca* species and used in the following key are indicated in **Figure 1**.

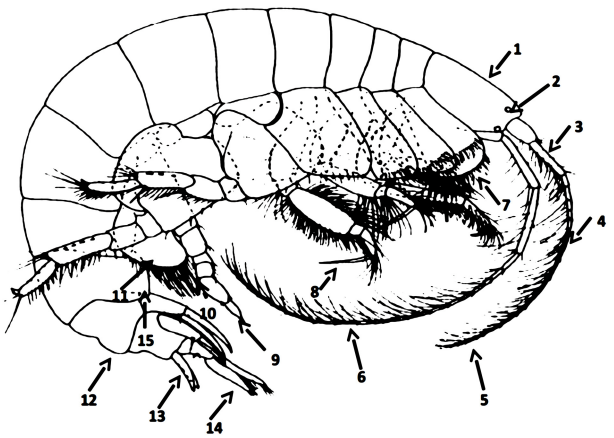

FIGURE 1 | Main morphological characters used in the female *Ampelisca* key. 1. Head shape. 2. Corneal lenses. 3. Length of the peduncle of the first pairs of antennae. 4. Length of the first pairs of antennae vs. length of the peduncle of the second pairs of antennae. 5. Length of the first pair of antennae. 6. Length of the second pairs of antennae. 7. Shape of the coxal plates. 8. Length of the pereiopod 3–4 dactylus. 9. Shape and length of the pereiopod 7 dactylus. 10. Posterior lobe on merus. 11. Shape of the basal of the pereiopod 7 and presence/absence of spines. 12. Form of the carina of the urosome 1. 13. Form of the telson and absence of presence of dorsal spines and setae. 14. Length of the rami of the uropod 3. 15. Postero distal form of the epimeral 2 and 3.

1. Dorsal sucker-like structure on pleon segment 1 ……. *A. remora*

1. Without dorsal sucker-like structure on pleon segment 1……2

2. Without corneal lenses ……3

2. With corneal lenses 11

3. P7, with a large posterior lobe on merus ……..*A uncinata*

3. P7 without large posterior lobe on merus…….. 4

4. Epimera l plate 3 with a tooth…..... 5

4. Epimera l plate 3 without tooth……7

5. Uropod 2 rami with a long subtermina l spine …… *A. odontoplax*

5. Uropod 2 rami without long subterminal spine……6

6. Uropod 2, rami with few short spines, telson dorsal surface with spines *A. amblyops*

7. P7 basis, margin distally excavate *A. heterodactyla*

7. P7 basis, margin rounded..... 8

8. A1 length > head + 3 anterior segments of pereon…….. 9

8. A1 length < head + 3 anterior segments of pereon..... *10*

9. A1, first two articles of peduncle equal in length; first segment of urosome with a slight carina.....*A. declivitatis*

9. Al, article 2 of peduncle > article 1; first segment of urosome virtually without carina.....*A. anophthalma*

10. Al = A2..... ..... *A. pusilla*

10. Al < ped A2..... *A. parabyblisoides*

11. Only one pair of corneal lenses, head with a rostrum, antennae short *A. troncosoi*

11. Two pairs of corneal lenses 12

12. P7, basis outer surface with numerous spines, urosome 1 with a peak-ended keel…… *A. spinifer*

12. P7, basis outer surface without spines, urosome 1 different 13

13. Blots of black pigment behind corneal lenses; P7, ischial to dactylus cylindrical……A. . *rubella*

13. Head without blots of black pigment, P7 different 14

14. P7 merus with a large posterior lobe 15

14. P7 merus without large posterior lobe 18

15. Head with anterior margins not parallel, Urosome seg. 1 with a pronounced angular keel *A. gibba*

15. Head with antero-superior and antero-inferior margins parallel 16

16. Epimeral plate 3, posterior margin bisinuous, postero-distal angle with a large tooth *A. brevicornis*

16. Epimeral plate 3, posterior margin sinuous, posterior distal angle with a small or moderate tooth 17

17. Urosome seg. 1 with a cockscomb dorsal keel. . . . . *A. pectenata*

17. Urosome seg. 1 with a small convex carina *A. cavicoxa*

18. Head, anterior half narrow 19

20. Head different 20

19. A 2 shorter than body length; P3-4, dactylus = carpus + propodus *A. sarsi*

19. A2 more longer than body length; P3-4, dactylus > carpus + propodus *A. pseudosarsi*

20. Head broad, anterior edge truncate 21

20 Head different 22

21. A2< body length; without distinguished *A. latifrons*

21. A2= body length; carina high and rounded *A. provincialis*

22. Uropode 3, inner ramus denticulate or serrulate 23

22. Uropode 3, inner ramus tapered not denticulate or serrulate. 25

23. P7, merus not prolonged anteriorly in peg-shape . . . . . *A. serraticaudata*

23. P7, merus prolonged anteriorly in large peg-shape 24

24 A1 subegal to A2 *A. unidentata*

24. A1 shorter than A2 *A. lusitanica*

25 A2 > body. . . . . *A. sorbei*

25. A2 < body. 26

26. Uropode 2 bearing long spine(s) 27

26. Uropode 2 bearing only short spines 28

27. Uropode 2, outer ramus with long marginal spines increasing in length distally; P7, carpus anterior margin notched *A. eschrichtii*

27. Uropode 2, outer ramus with single long subterminal spine; P7, carpus anterior margin rounded *A. macrocephala*

28. Uropode 2 fringed with numerous small spines 29

28. Uropode 2 with few small spines 35

29. A2 longer than body length 30

29. A2 shorter than body length 32

30. Urosome 1 with high carina dorsally bisinuate. Uropode 2 rami fringed regularly on both sides by rows of small spines *A. multispinosa*

30. Urosome 1 with small rounded carina. Uropode 2 rami not regularly fringed with small spines 31

31. A1 shorter than A2 peduncle *A. ruffoi*

31. A1 slightly longer than A2 peduncle *A. pseudospinimana*

32. A1 shorter than A2 peduncle. Head with antero-distal margin broadly round *A. tenuicornis*

32. A1 longer than A 2 peduncle 33

33. Al slightly longer than A2 peduncle. Epimeral plate 3 rounded *A. diadema*

33. A1 longer than A2 peduncle and equal to half length of A2. Epimeral plate 3 quadrate 34

34. A2 shorter than half length of body. Epimeral 2 postero-distal angle with a small tooth *A. armoricana*

34. A2 longer than half length of body. Epimeral 2 postero-distal angle rounded *A. spinipes*

35. P3-4 dactylus shorter than carpus + propodus 36

35. P3-4 dactylus longer than carpus + propodus 37

36. Epimeral plate 2 postero-distal angle with a distinct tooth *A. verga*

36. Epimeral plate 2 postero-distal angle rounded *A. aequicornis*

37. Gnathopode 1 with large spines on palm *A. spinimana*

37. Gnathopode 1 without spine on palm 38

38. Urosome seg. 1 with prominent carina 39

38. Urosome seg. 1 with moderate carina 41

39. A1 longer than half A2. Telson dorsal surface inermous. Epimera l plate 2 rounded *A. anomala*

39. A1 shorter than half A2. Telson dorsal surface with spines. Epimera l plate 2, posterodistal corner angle a small tooth 40

40. Urosome seg. 1 with pronounced angular carina. A1 shorter than A2 peduncle *A. typica*

40. Urosome seg. 1 with a raiser high dorsal carina, posterior edge overflowing. A1 slightly longer than A2 peduncle *A. toulemonti*

41. A1 equal to A2 length 42

41. A1 shorter than A2, Urosome seg. 1 with a high rounded carina *A. massiliensis*

42. A1 and A2 longer than body length. P7 merus prolonged anteriorly in peg-shape covering a part of carpus *A. calypsonis*

42. A1 and A2 nearly equal to body length. P7 merus without lobe *A. dalmatina.*

DISTRIBUTION

A total of 40 *Ampelisca* species are currently known from the study area, comprehending the North-eastern Atlantic coast between the Strait of Gibraltar, in Southern Spain, to the Strait of Dover, in the Eastern part of the English Channel (**Figure 2**). The presence of these 40 species were reported to eight geographical locations, indicated in **Table 1**, following the studies consulted and mentioned in Appendix A in **Supplementary Material**.

The number of species varied from a maximum of 27 along the Portuguese coast, to a minimum of 7, in the eastern part of the English Channel. The second richest area was the southern part of the Bay of Biscay with 24 species, including eight deep-water species. There was a clear reduction of the number of species from the south to the north and undoubtedly a lack of data for two areas: the southern Atlantic coast of Spain and Galicia.

Five species were present in all areas: *A. brevicornis, A. diadema, A. spinipes, A. tenuicornis,* and *A. typica. A. pectenata* showed also a large distribution but was absent in Galicia and Southern Spain. Twelve species were recorded only in the southern part of the study area; most were Mediterranean and recorded in the Atlantic up to the southern coast of Portugal, in Algarve (Marques and Bellan-Santini, 1991, 1993; Sampaio et al., 2016): *A. anophthalma*, *A. calypsonis, A. dalmatina, A. latifrons,*

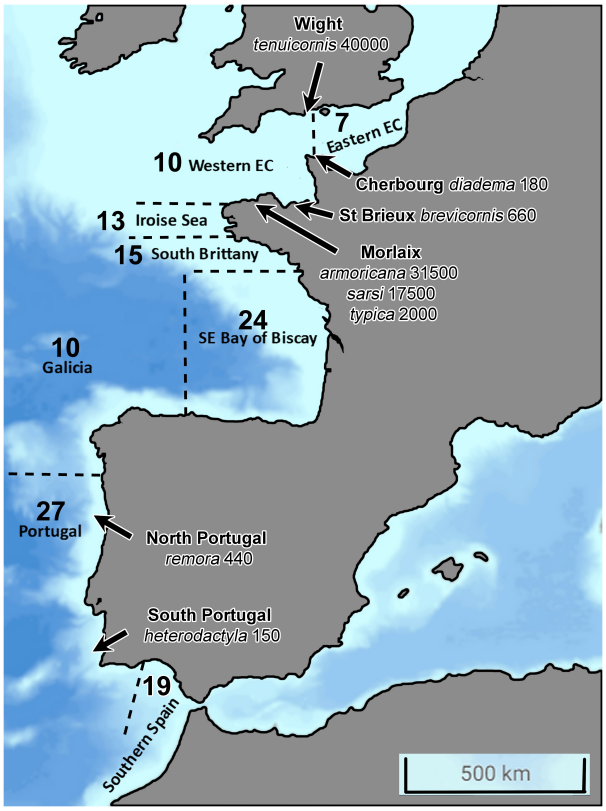

FIGURE 2 | North-eastern Atlantic Coast from the Strait of Gibraltar, South, to the Strait of Dover, North, showing the eight geographical locations under study for the distribution of *Ampelisca* species. The bold number correspond to the number of *Ampelisca* species found in the eight areas; the species name and numbers correspond to the maximal abundances per m^2 in different sites.

A. lusitanica, A. massiliensis, A. multispinosa, A. provincialis, A. pseudosarsi, A; pseudospinima, A. ruffoi and *A. verga*.

Ampelisca aequicornis was present only in the Bay of Biscay.

The Southern species were distributed in the northern areas up to Galicia such as *A. serraticaudata* or the southern part of the Bay of Biscay such as *A. heterodactyla, A. rubella* and *A. serraticaudata. Ampelisca gibba* was absent in the English Channel probably due to the absence of a mud habitat in this megatidal sea due to high hydrodynamics and dominance of coarse sediments. Three species, *A. armoricana, A. sarsi, A. spinimana* were absent in the eastern part of the English Channel. Five species showed a limited spatial distribution, possibly due to lack of data or because they were recently described: *A. caxicoxa, A. remora, A. sorbei, A. troncosoi* and *A. toulemonti.*

Eight deep-water species were only reported in the bathyal part of the Bay of Biscay, possibly because of the deeper sampling solely performed in this study location: *A. amblyops, A. anomala, A; declivitatis, A. eschrichtii, A. parabyblisoides, A. odontoplax, A. pusilla* and *A. uncinata.*

Among the new observations in the study area, *Ampelisca verga,* a West African species originally described as a variety of *A. aequicornis* by Reid (1951, in Dauvin and Bellan-Santini, 1985) off Dakar, Senegal, was recorded in the Algarve coast, southern Portugal, setting a new northern distribution limit for this species (Sampaio et al., 2016). *Ampelisca toulemonti,* described from one female coming from the Iroise Sea (Dauvin and Bellan-Santini, 1982), was recorded in the eastern part of the Rade de Cherbourg in the North Cotentin, setting the eastern most location of this species in the English Channel (Andres et al., 2020).

Among the 40 species (Appendix A in **Supplementary Material**), 17 were found only on the Continental Shelf, 16 were recorded both on the Continental Shelf and the Continental slope at depths up to 510 m. Seven species were strictly bathyal with a maximum sampling depth of 1,097 m.

A data matrix representing **Table 1**, 40 species × 8 locations, was analyzed to study the faunal resemblance among the samples representing the geographical locations.

The dendogram (**Figure 3**) showed high similarity of the fauna between the Iroise Sea and South Brittany, and between Southern Spain and Portugal. This cluster analysis showed two main groups, which were split at a similarity level of 35%, the southern group, including Southern Spain and Portugal, from the northern group, with the other locations. Within this group, at a level of 40% the South Eastern Bay of Biscay was separated, and at 50% Galicia was also separated from the other northern locations.

The nMDS (**Figure 2**) showed the opposition, along the horizontal axis, of the most northern and southern groups. The central locations (Bay of Biscay and Galicia) appeared in a transition position along this axis, between the most southern and northern. The vertical axis isolated the Bay of Biscay. A similar ordination solution was shown by the PCA analysis (**Figure 4**), with the succession along the horizontal axis, from left to right, of the most northern to the most southern locations, with the separation on the positive pole of axis 2 of the samples from Bay of Biscay. This analysis also depicted the species, as vectors. The southern group (South Spain and Portugal) was characterized by 11 species, most of them having a Mediterranean distribution. The Western and the Eastern English Channel, the Iroise Sea and South Brittany areas were characterized by seven species, largely distributed along the south/north gradient and present in the northern areas. The south eastern Bay of Biscay was characterized by 17 species, among which the deep-water *Ampelisca* species.

ECOLOGY

Abundance

The denser populations of *Ampelisca* were registered in the northern part of the study area (**Table 2**). Most of the species occurred rarely and were found in very low numbers of individuals, which, for some species, corresponded only to the specimens used for their description. With the exception of *A. lusitanica* and *A. rubella,* which occurred on hard-bottom, *Ampelisca* were mostly found on soft-bottom sediments, ranging from mud to gravel (Bellan-Santini and Dauvin, 1988b, 1989). Most of the species recorded in the study area inhabited mainly muddy sand and sandy mud habitats and were abundant only in

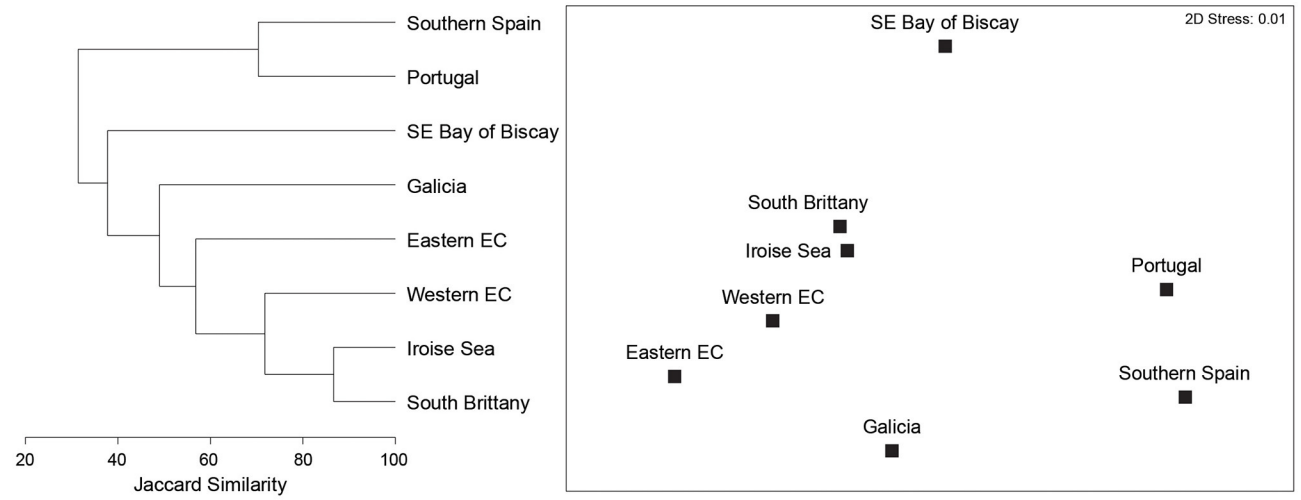

FIGURE 3 | Cluster analysis (dendrogram) and ordination analysis (nMDS) of the Jaccard similarity matrix among the *Ampelisca* samples representing the geographical areas depicted in **Figure 2**.

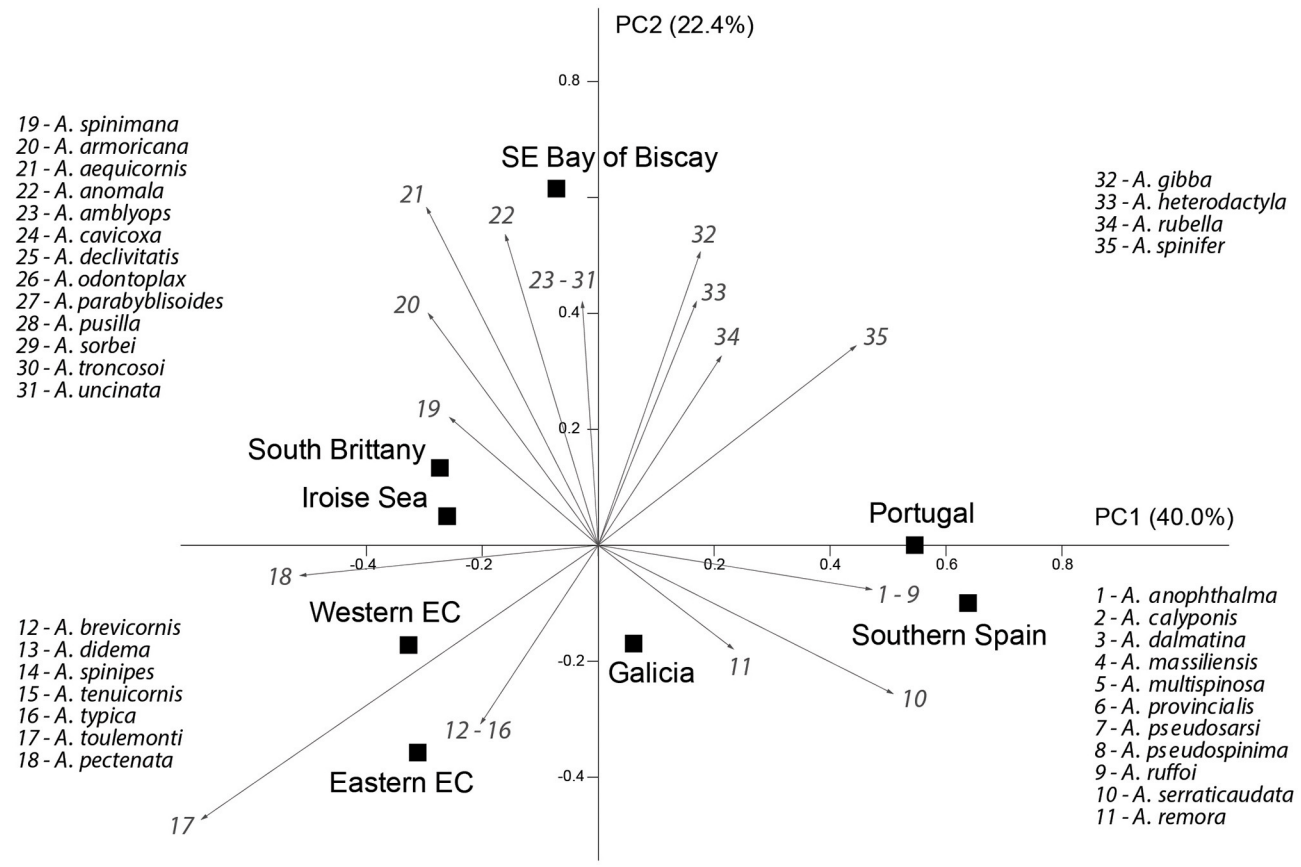

FIGURE 4 | Principal components analysis of the *Ampelisca* data from **Table 1**. The analysis was performed with the full set of species but the figure excluded five species with eigenvectors bellow 0.1 (*A. eschrichtii*, *A. latifrons*, *A. lusitanica*, *A. sarsi* and *A. verga*). The vectors representing the species were amplified (x4) to clarify their position in relation to the samples.

TABLE 2 | *Ampelisca* occurrence of the species classified in three categories: rare, few records; common: numeroux records, and very common species in most of the shallow soft-bottom communities.

Species	Occurrence	Maximum abundance in m^2 or number of know individuals in the area*	Area and depth	References
A. aequicornis	rare	3	SE Bay of Biscay, 125-300 m	Dauvin and Bellan-Santini, 1996
A. anophthalma	rare	57*	Portugal, 500 m	Marques and Bellan-Santini, 1993
A. amblyops	rare	1*	Off Galicia, 512 m	Dauvin and Bellan-Santini, 1986
A. anomala	rare	46*	SE Bay of Biscay, 107-300 m	Dauvin and Bellan-Santini, 1996
A. armoricana	common	31,500	English Channel, Bay of Morlaix, 17 m	Dauvin, 1988d
A. brevicornis	very common	660	English Channel, Bay of Saint Brieux, 10 m	Le Mao, 2006
A. calypsonis	rare	14	Portugal, 49-168 m	Sampaio et al., 2016
A. cavicoxa	rare	21*	SE Bay of Biscay, 14-50 m	Kaim-Malka, 2000
A. dalmatina	rare	17	Portugal, 53-103 m	Sampaio et al., 2016
A. declivitatis	rare	8*	SE Bay of Biscay, 120-300 m	Dauvin and Bellan-Santini, 1996
A. diadema	very common	180	English Channel, North Cotentin, 13 m	Andres et al., 2020
A. eschrichtii	rare	1*	Offshore Brittany, 250 m	Bellan-Santini and Dauvin (1988b)
A. gibba	rare	48*	SE Bay of Biscay, 346-1,024 m	Dauvin and Bellan-Santini, 1996
A. heterodactyla	rare	150	Portugal, 38-58 m	Sampaio et al., 2016
A. latifrons	rare	2	Portugal, 4-508 m	Marques and Bellan-Santini, 1991
A. lusitanica	rare	39*	Portugal, 8-37 m	Bellan-Santini and Marques, 1986
A. massiliensis	rare	1*	Portugal, 110-360 m	Marques and Bellan-Santini, 1991
A. multispinosa	rare	1*	Portugal, 137 m	Marques and Bellan-Santini, 1993
A.odontoplax	rare	1*	Bay of Biscay, 1,000 m	Dauvin and Bellan-Santini, 1986
A.parabyblisoides	rare	3*	SE Bay of Biscay, 300 m	Dauvin and Bellan-Santini, 1996
A. pectenata	common	17	Portugal, 56-182 m	Sampaio et al., 2016
A. provincialis	rare	26	Portugal, 26-53 m	Sampaio et al., 2016
A. pseudosarsi	rare	17	Portugal, 26-140 m	Sampaio et al., 2016
A.pseudospinima	rare	2	Portugal, 16-25 m	Sampaio et al., 2016
A. pusilla	rare	18*	SE Bay of Biscay, 740-1,097 m	Dauvin and Bellan-Santini, 1996
A. remora	rare	440	Portugal, 26-99 m	Sampaio et al., 2016
A. rubella	rare	9*	Portugal, 0-130 m	Marques and Bellan-Santini, 1993
A. ruffoi	rare	21	Portugal, 97-136 m	Sampaio et al., 2016
A. sarsi	common	17,500	English Channel, Bay of Morlaix, 17 m	Dauvin, unpublished data
A. serraticaudata	rare	5*	Portugal, 52 m	Marques and Bellan-Santini, 1991
A. sorbei	rare	1*	SE Bay of Biscay, 120 m	Dauvin and Bellan-Santini, 1996
A. spinifer	common	15	Portugal, 53-147 m	Sampaio et al., 2016
A. spinimana	common	109	English Channel, Bay of Morlaix, 12 m	Dauvin et al., 1993
A. spinipes	very common	270	Portugal, 26-179 m	Sampaio et al., 2016
A. tenuicornis	very common	40,000	English Channel, Wigh Island, 7-9 m	Sheader, 1998
A. troncosoi	rare	114	Galicia, 11 m	Tato et al., 2012
A. toulemonti	rare	63	English Channel, North Cotentin, 11 m	Andres et al., 2020
A. typica	very common	2000	English Channel, Bay of Morlaix, 17 m	Dauvin, 1988c
A.uncinata	rare	28*	SE Bay of Biscay, 680-1,097 m	Dauvin and Bellan-Santini, 1996
A. verga	rare	13	Portugal, 25-94 m	Sampaio et al., 2016

*Maximum abundance in m^2 or number of know individuals, area and depth of records. *Correspond to the number of know individuals in the area.*

shallow muddy fine sand sediment (Bellan-Santini and Dauvin, 1988a, 1989; Sampaio et al., 2016).

The common species formed abundant populations in the English Channel. *Ampelisca brevicornis* reached 500 ind.m^{-2} in October 1982 in the Bay of Morlaix Bay, 403 ind.m^2 in July 1978 and 370 ind.m^2 in October 1979 in the Rance (Dauvin, 1988b). An abundant population was also reported in the subtidal fine sand of the Bay of Saint Brieux with 660 ind.m^{-2} (Le Mao, 2006).

Ampelisca tenuicornis formed very high abundance in the Rance, with 6,020 ind.m^{-2} in summer 1978, 3,870 ind.m^{-2} in summer 1979 and 2,830 ind.m^{-2} in summer 1980 (Dauvin, 1988a), and showed a peak of abundance at the end of September 1996 with 25,000 ind.m^{-2} (Desroy, 1998). In the Bay of

Morlaix, its abundance reached 4,000 ind.m^{-2} in October 1977 (Dauvin, 1988a) and 17,500 ind.m^{-2} in October 1997 (Dauvin, unpublished data). Long-term study at a fine muddy-sand site to the east of the Isle of Wight on the south coast of England (depth 7–9 m) its abundance reached a maximum of about 40,000 ind.m^{-2} in late summer (Sheader, 1998). In the North Cotentin, the population reached 9,000 ind.m^{-2} in the North Cotentin (Andres et al., 2020), while its underpassed 1,000 ind.m^{-2} in the eastern part of the Bay of Seine (Alizier, 2011).

In the Bay of Morlaix, at the Pierre Noire Station located on an *Abra alba* fine sand community, the *Ampelisca* populations showed very high abundances, with 31,500 ind.m^{-2} for *A. armoricana* in October 1977 (Dauvin, 1988d), 17,500 ind.m^{-2} in October 1997 for *A. tenuicornis* in October 1997 (Dauvin, unpublished data), 6,640 ind.m^{-2} in October 1987 (Dauvin, 1989), and 17,500 ind.m^{2} in October 1994 (unpublished data) for *A. sarsi*, and 2,000 ind.m^{2} in October 1987 for *A. typica* (Dauvin, 1988c).

Along the Portugal coast, *Ampelisca armoricana* populations reached 1,050 ind.m^{-2}; while those of *A. brevicornis* showed an abundance of 640 ind.m^{-2} and those of *A. remora* 440 ind.m^{-2} (**Tables 2**, **3**).

Sympatry in *Ampelisca*

Ampelisca populations often occur together, so that their distribution areas overlap or coincide. Several species can occur together in the same habitat and it is possible to identify up to eight species in 1974 in the same station in the Bay of Concarneau, South Brittany (Mesneguen, 1980) and nine species in two stations off the Portugal coast in 2007–2008 (**Table 3**).

In the western English Channel, Bay of Morlaix, nine species were recorded: *A. armoricana*, *A. brevicornis*, *A. diadema*, *A. sarsi*, *A. spinipes*, *A. spinimana*, *A. pectenata*, *A. tenuicornis* and *A. typica* (Dauvin et al., 1993). In 1977, on a subtidal fine sand community of this bay, three species were dominant *A. armoricana*, *A. sarsi* et *A. tenuicornis* (several thousands of individuals per m^{2}) representing 90% of the abundance, 38% of the biomass and 50% of the secondary production of the community (Dauvin et al., 1993). The *Ampelisca* diversity (eight recorded species) and abundance were lower (< 100 ind.m^{-2}, cf. **Table 3**) in a muddy sand community of the Bay of Morlaix at the same period. The *Ampelisca* were shown to be very sensitive to hydrocarbon pollution and as a consequence to the Amoco Cadiz oil spill, which occurred in March 1978 in North Brittany (western English Channel), the species disappeared in the fine sand community (Dauvin, 1988a,b,c,d; Dauvin, 1989). Similar population collapse was also observed following the Aegean oil spill in the North of Galicia, Spain (Gomez Gesteira and Dauvin, 2005). In 1990, 12 years after the Amoco Cadiz oil spill, the abundances of the *Ampelisca* were at the same order of magnitude of those observed before the incident (**Table 3**). *Ampelisca sarsi* dominated the community, replacing *A. armoricana* which became the second most abundant species, while *A. tenuicornis* remained the third most abundant; the three other species showed lower abundances before and after the spill. The long-term survey of the colonization of *Ampelisca* illustrated the high resilience of these holobenthic species, without pelagic larvae, but with high capacity to reconstitute their populations (Dauvin et al., 1993).

In other northern sites, the *Ampelisca* also showed sympatric distribution; nevertheless, the abundances of the populations never surpassed 500 ind.m^{-2} (**Table 3**).

On the 326 stations off the Portuguese continental shelf, *Ampelisca* were found in 221 stations (68% of the sampled stations) for a total of 19 species and the dominance of five species *A. armoricana*, *A. brevicornis, A. spinimana*, *A. spinipes* and *A. tenuicornis*. From two to nine species were found in 60% of the stations, while only one species was recorded in 40% of the stations. Nine stations accounted five species, nine other six species, four seven species, four eight species and finally nine species had been found in two stations (**Table 3**). The total abundances of such sympatric populations were high and included between 1,240 and 1,920 ind. m^{-2} (**Table 3**).

DISCUSSION

Taxonomy and Distribution

The North-eastern Atlantic Coast between the Strait of Gibraltar and the Strait of Dover registers 40 *Ampelisca* species, which is more than the total number of *Ampelisca* recorded for the Mediterranean Sea, 28 species (Bellan-Santini and Ruffo, 2003). The number of species reached was on the same order of magnitude along the Portuguese coast with 27 species where there is a mixture of Mediterranean, Atlantic and African faunas. The second richest area was the southern part of the Bay of Biscay with 24 species, including eight deep-water species, and 16 species habiting the continental shelf, number which remained lower than those of the Portuguese continental shelf. The biodiversity of *Ampelisca* showed a clear decrease from the south to the north in the studied area.

The *Ampelisca* taxonomy is well-established for this North-Atlantic area, and almost 50% of the species (17) had already been described by the end of the nineteenth century, with an extra 19 species during the second part of the twentieth century, while a single species, *Ampelisca troncosoi* Tato et al. (2012) was recently described.

Presently, new species of *Ampelisca* at the scale of the world are mainly described in the tropical zone of the Pacific Ocean and in the Indian Ocean (World Register of Marine Species, consulted on November 1st, 2020). In the early years of the twentieth century, the amphipod fauna of the European part of the North-Atlantic Ocean was amongst the better known worldwide, including the *Ampelisca* mainly due to the large number of new species descriptions by G.O. Sars, and E. Chevreux at the end of the nineteenth and the beginning of the twentieth century. Numerous new species were then described at the end of the twentieth century by D. Bellan-Santini and her co-authors, mainly for the Mediterranean Sea and surrounding areas (North Africa, Portugal and Spain).

Therefore, the discovery of new *Ampelisca* species for science in the study area is improbable. Nevertheless, genetic studies could be used to elucidate the existence of species hidden in "complex" species with a large geographical distribution

TABLE 3 | Abundance of *Ampelisca* species in number of ind. m² in some stations where the species were in sympatry from the English Channel, Bay of Biscay and Portugal coasts.

English Channel	**Bay of Morlaix**				**Bay of Saint-Brieuc**		**North Cotentin**		**Bay of Seine**	
	Pierre Noire		**Rivière de Morlaix**							
	October 1977		**August 1977**		**Spring 2008**		**March 2015**		**September 2008, station 14**	
	A. armoricana	20161	*A. armoricana*	2	*A. armoricana*	40	*A. brevicornis*	15	*A. brevicornis*	126
	A. sarsi	4868	*A. tenuicornis*	15	*A. brevicornis*	28	*A. diadema*	6	*A. diadema*	4
	A. tenuicornis	3962	*A. spinimana*	10	*A. sarsi*	30	*A. tenuicornis*	347	*A. tenuicornis*	108
	A. brevicornis	75	*A. brevicornis*	20	*A. spinimana*	47	*A. typica*	57	*A. typica*	2
	A. typica	32			*A. tenuicornis*	91				
	A. spinipes	10								
	Total	29108	Total	47	Total	236	Total	425	Total	240
	October 1990		**August 1989**				**March 2016**		**September 2008, Station 17**	
	A. armoricana	9612	*A. armoricana*	7			*A. diadema*	23	*A. brevicornis*	66
	A. sarsi	11168	*A. sarsi*	7			*A. spinipes*	17	*A. diadema*	4
	A. tenuicornis	1069	*A. tenuicornis*	1			*A. tenuicornis*	17	*A. tenuicornis*	128
	A. brevicornis	163	*A. brevicornis*	119			*A. toulemonti*	30	*A. typica*	2
	A. typica	136	*A. spinimana*	20			*A. typica*	17		
	A. spinipes	6	*A spinipes*	1						
	Total	22154	Total	155	Total		Total	104	Total	200
Bay of Biscay	**Concarneau, 1974**		**Quiberon, 2018**		**Lorient, 2018**		**Station B54, August 1979**		**Station 300, April 1985**	
	A. armoricana	162	*A. armoricana*	46	*A. armoricana*	35	*A. brevicornis*	19	*A. anomala*	20
	A. brevicornis	79	*A. diadema*	13	*A. brevicornis*	38	*A. spinimana*	180	*A. gibba*	13
	A. diadema	35	*A. sarsi*	173	*A. diadema*	10	*A. spinipes*	15	*A. tenuicornis*	27
	A. sarsi	18	*A. spinimana*	10	*A. sarsi*	20	**Total**	214	**Total**	60
	A. spinimana	50	*A. tenuicornis*	32	*A. spinipes*	10	**Station B54, September 1979**		**Station 300, July 1985**	
	A. spinipes	14	*A. typica*	18	*A. typica*	20	*A. brevicornis*	1	*A. anomala*	2
	A. tenuicornis	52					*A. spinimana*	54	*A. gibba*	10
	A. typica	69					*A. spinipes*	4	*A. tenuicornis*	7
	Total	479	Total	292	Total	133	Total	59	*A. parabyblisoides*	1
									Total	20

(Continued)

TABLE 3 | Continued

English Channel	**Bay of Morlaix**				**Bay of Saint-Brieuc**		**North Cotentin**		**Bay of Seine**	
	Pierre Noire		**Rivière de Morlaix**							
	October 1977		**August 1977**		**Spring 2008**		**March 2015**		**September 2008, station 14**	
	Concarneau, 2018						**Station B54, November 1979**		**Station 300, September 1985**	
	A. armoricana	24					*A. brevicornis*	1	*A. anomala*	22
	A. sarsi	23					*A. spinimana*	13	*A. gibba*	6
	A. spinipes	30					*A. spinipes*	3	*A. tenuicornis*	18
	A. tenuicornis	10							*A. parabyblisoides*	3
	Total	87					Total	17	Total	49
Portugal, 2017-2018	**Station G8**		**Station G18**		**Station G16**		**Station G17**		**Station G26**	
	A. armoricana	500	*A. armoricana*	750	*A. armoricana*	1050	*A. armoricana*	400	*A. armoricana*	680
	A. brevicornis	310	*A. brevicornis*	580	*A. brevicornis*	50	*A. brevicornis*	640	*A. brevicornis*	80
	A. diadema	10	*A. heterodactyla*	150	*A. heterodactyla*	30	*A. diadema*	10	*A. heterodactyla*	10
	A. heterodactyla	100	*A. remora*	140	*A. remora*	430	*A. heterodactyla*	60	*A. provincialis*	10
	A. provincialis	20	*A. ruffoi*	20	*A. ruffoi*	10	*A. remora*	20	*A. remora*	440
	A. remora	130	*A. sarsi*	80	*A. spinimana*	70	*A. sarsi*	50	*A. spinimana*	20
	A. sarsi	40	*A. spinimana*	20	*A. spinipes*	270	*A. spinimana*	40	*A. spinipes*	120
	A. spinimana	60	*A. spinipes*	140	*A. tenuicornis*	10	*A. spinipes*	50	*A. tenuicornis*	10
	A. spinipes	70	*A. tenuicornis*	10						
	Total	1240		1890		1920		1270		1370

such as *Ampelisca brevicornis,* for which sub-species could be morphologically distinguished (Kaim-Malka, 2000).

Changes in the Species Biology and Distribution in Relation to Climatic Changes

Climatic changes with an increase in sea water temperature along the North-eastern Atlantic coasts could affect both the distribution and the biology of the *Ampelisca* species.

Concerning the distribution, species tend to extend north their geographical reach, as observed for *A. armoricana*, *A. sarsi, A. spinimana* and *A. toulemonti* in the eastern part of the English Channel, and *A. aequicornis* and *A. spinifer* in the English Channel. Southern species presently known to occur along the North Atlantic coast of Africa could progress north and reach the south of Spain and the Portuguese coast, such as *A. bidentata, A. ctenopus, A. hupferi, A. monoculata, A. palmata* and *A. senegalensis* (Dauvin and Bellan-Santini, 1988). In both areas, the south of the Iberian Peninsula and the English Channel, encouragement should be given to identify the *Ampelisca* up to species level, in order to fully grasp such geographical changes in target species.

Concerning the biology, two reproductive cycles are known in the *Ampelisca* species (Bellan-Santini and Dauvin, 1988b). Univoltine cycles occurs namely in *A. armoricana* (Dauvin, 1988d) and *A. sarsi* (Dauvin, 1989). Females are ovigerous at the end of spring and release their young in summer, which reproduce only 1 year later, leading to a single generation and class per reproductive year. Other species present a bivoltine cycle such as *A. tenuicornis* (Dauvin, 1988a) and *A. typica* (Dauvin, 1988c). In these, the females are ovigerous at the end of winter-beginning of spring and release their young in spring, which reproduce at the end of summer, beginning of autumn, leading to two generations and one class per reproductive year. Some species are known to show both cycles, depending on the environmental conditions. This is the case of *A. brevicornis,* which showed both reproductive cycles in the English Channel depending on the sea water temperature, with a bivoltine cycle in years with warmer spring (Dauvin, 1988b), while being solely bivoltine in the Mediterranean Sea (Kaim-Malka, 1969). Sea water increase notably in spring could favor a bivoltine reproductive cycle in the future, which will change the secondary production of such amphipods.

Sympatry and Syntopy in *Ampelisca*

Rivas (1964) defined sympatric and syntopic species, which corresponded, respectively to "*the reference to two or more related species which have the same or overlapping geographic distributions, regardless of whether or not they occupy the same macrohabitats (whether or not the species occurred together the same locality*," and "*in reference to two or more related species which occupy the same macrohabitat. These species occur together in the same locality, are observably in close proximity, and could possibly interbreed*." The large geographical and local distributions of *Ampelisca* species illustrate plainly these both concepts. With a high species richness at the scale of a region, such as along the Portuguese coast with the overlapping of 27 species, and the number of species occurring in the same benthic habitat, such as on Brittany and Portuguese soft-bottom habitats, with up to eight species in the same habitat in South Brittany and nine species in two stations from the Portuguese continental shelf (**Table 3**).

Co-occurrence, sympatry and syntopy of amphipods were not very common and mainly described to species living in the intertidal zone or very shallow waters such as the Haustoriidae, where five species cohabited on the New Hampshire intertidal zone (Croker, 1967), the Gammaridae with the case of five species of *Gammarus* coexisting in Danish brackish waters (Kolding and Fenchel, 1979), Pontoporeiidae with two *Pontoporeia* co-occurring in the Swedish Baltic Sea (Hill and Elmgren, 1987), Hyalidae where six phytal amphipod species of the genus *Hyale* occurring on the intertidal rocky shores of Coquirnbo, Chile (Lancelotti and Trucco, 1993), Talidridae with *Talorchestia brito* and of two age classes of *Talitrus saltator* co-existing along the French Atlantic coast (Fallaci et al., 1999) while eight species were collected in some Tunisian lagoons (Jelassi et al., 2015), and Ischyroceridae with three species of the genus *Jassa* co-occurring on a wide range of hard substrates in the Helgoland Island in the south of the North Sea (Jelassi et al., 2015).

In the Bay of Belfast, Parker (1984) examined the distribution of *Ampelisca brevicornis*, *A. tenuicornis* and *A. typica*. He showed that these species could live in the same biotope and had no sedimentary preferences in this region, contrary to Sheader (1977) who showed marked sedimentary preferences for two species *A. brevicornis* and *A. tenuicornis* in the sandy-muddy bottoms of north-eastern England, in the North Sea.

Few studies, such as that of Buhl-Jensen (1986) on the coasts of Norway had showed the coexistence in the same samples of two to four species of *Ampelisca* although one species, *A. gibba* presented high abundances in three of the 21 sampling stations. In the Bay of Concarneau (southern Brittany), Mesneguen (1980) recorded until eight species per station in 1974, but the abundance of the species remained lower than those observed in the Bay of Morlaix in the western entrance of the English Channel in 1977 (**Table 3**). The *Ampelisca* Portuguese continental shelf fauna appeared particularly rich with 19 species recorded in the sampling campaigns in 2007–2008 covered the entire Portugal coast with a more dense number of stations in the North (Sampaio et al., 2016). This was in this location that nine *Ampelisca* species in a single grab (0.1 m^2) were sampled, while between seven to nine species were found in 10 stations. This co-occurrence of *Ampelisca* species in a single grab per station was at our knowledge a record and was incomparable.

Along the North-America Pacific coast from the Baja California to the Bering Sea, large *Ampelisca* populations coexisted but only a single or a couple of species dominate the soft-bottom communities: *A. macrocephala* and *A. eschriichti* in the Bering Sea, *A. agassizi* and A. *careyi* off Vancouver Island (Canada), while in the Baja California only *A. agassizi* was present (Oliver et al., 1983).

Schaffner and Boesch (1982) studied the spatial distribution of *A. agassizi* and *A. vadorum* in the palaeo-dunes of the continental shelf off New Jersey (USA), which reach 6 m high.

The simultaneous sampling of these two species was strongly linked to the exact position of the sample on the dunes: the deep depressions were almost exclusively populated by *A. agassizi*, reaching in this habitat abundances of 10,000 individuals per m^2. The shallower depressions and the sides of the dunes were populated by both species. The authors suggested that *A. agassizi* could be more capable to use nutrient resources.

In the end, if the coexistence of *Ampelisca* species seems to exist most often, the coexistence of large populations such as those observed in Morlaix Bay seems exceptional.

Perspectives

In conclusion, the following research recommendations for the European *Ampelisca* can be put forward:

- *Ampelisca* species with a wide geographical distribution should be further studied using molecular tools in order to elucidate their taxonomy. Such studies could focus in the species *A. brevicornis*, *A. diadema*, *A. tenuicornis*, *A. typica* and *A. spinipes*;
- Encourage ecologists to identify *Ampelisca* to species level in order to increase the overall knowledge on their distribution, including the geographical ranges;
- Study in detail, and possibly experimentally, the reasons behind the important sympatry in *Ampelisca* and how it relates namely to resources competition;
- Verify if trophic guilds, namely suspension feeders and surface deposit feeders, present distinct morphological characteristics, such as length of antennae, presence of setae, and number of setae, and if such adaptations could account for the coexistence of several species without trophic competition;
- Conduct population biology studies at historical sites where the species were previously studied in order to examine the effects of climate change, namely increased temperature in coastal waters, on the life history traits of the *Ampelisca*.

DATA AVAILABILITY STATEMENT

The raw data supporting the conclusions of this article will be made available by the authors, without undue reservation.

AUTHOR CONTRIBUTIONS

J-CD and VQ designed research. J-CD, LS, AR, and VQ performed research and analyzed data. J-CD and VQ wrote the paper. All authors contributed to the article and approved the submitted version.

FUNDING

This study received funding from Normandy Region and the Groupement d'Intérêt Public Seine-Aval for the Bay of Seine sampling, and the Direction Régionale de l'Environnement, de l'Aménagement et du Logement de Normandie for the North-Cotentin sampling. The sampling along the Portuguese coast was supported by the research projects ACOSHELF (POCI/MAR/56441/2004-PPCDT/MAR/56441/2004), MeshAtlantic, with the support of the European Union ERDF-Atlantic Area Program 2009-1/110, and Monitorização Ambiental do Emissário Submarino e da ETAR da Guia do Sistema de Saneamento da Costa do Estoril, funded by SANEST, S.A. The authors declare that this study received funding from SANEST, S.A. The funder was not involved in the study design, collection, analysis, interpretation of data, the writing of this article or the decision to submit it for publication.

ACKNOWLEDGMENTS

Authors acknowledge Normandy Region and the *Groupement d'Intérêt Public Seine-Aval*, the *Direction Régionale de l'Environnement, de l'Aménagement et du Logement de* Normandie and FCT/MCTES for the financial support to CESAM (UIDP/50017/2020+UIDB/50017/2020), through national funds. The authors thank the two reviewers of the first version of the paper for their very useful remarks and suggestions, and Lucie Millet for the **Figures 1**, **2**.

SUPPLEMENTARY MATERIAL

The Supplementary Material for this article can be found online at: https://www.frontiersin.org/articles/10.3389/fmars.2021.643078/full#supplementary-material

REFERENCES

Alizier, S. (2011). *Echelles spatio-temporelles d'observation des relations macrobenthos/sédiments: organisation et changements à long-terme (1988–2009) des communautés benthiques subtidales de la partie orientale de la baie de Seine* (PhD Thesis). France: Université de Lille 1.

Andres, S., Pezy, J. P., Martinez, M., Baux, N., Baffreau, A., Méar, Y., et al. (2020). Soft bottom macrobenthic communities in sandy enclaves from the North Cotentin Peninsula (Central English Channel). *J. Mar. Biol. Oceanogr.* 9:1. doi: 10.4172/2324-8661.1000210

Bachelet, G., Dauvin, J. C., and Sorbe, J. C. (2003). An updated checklist of marine and brackish water amphipoda (crustacea: peracarida) of the southern Bay of Biscay (NE Atlantic). *Cah. Biol. Mar.* 44, 121–151.

Baux, N. (2018). *Dynamique des habitats benthiques sous-contraintes anthropiques: le cas du site de dépôt de dragage d'Octeville* (PhD Thesis). France: Université de Caen Normandie.

Baux, N., Pezy, J. P., Bachelet, Q., Baffreau, A., Méar, Y., Poizot, E., et al. (2017). An exceptional rich soft-bottom macrobenthic habitat in a semi-enclosed bay bordering the english channel: rade de cherbourg. *Reg. Stud. Mar. Sci.* 9, 106–116. doi: 10.1016/j.rsma.2016.11.010

Bellan-Santini, D. (1982). Family ampeliscidae. the amphipoda of the mediteranean. Part 1. gammaridea (acanthonotozomatidae to gammaridea). *Mém. Inst. Océanogr.* 13, 19–69.

Bellan-Santini, D. (1983). *Distribution des Ampelisca (Crustacea, Amphipoda) de Méditerranée. Selected papers on Crustacea. Prof. N. K. Pillai Felicitation Volume.* Trivandrum: The Aquarium. p. 155–161.

Bellan-Santini, D., and Dauvin, J. C. (1981). Description d'une nouvelle espèce d'Ampelisca des côtes françaises (Amphipoda). *Crustaceana* 40, 242–252. doi: 10.1163/156854081X00714

Bellan-Santini, D., and Dauvin, J. C. (1986). *Ampelisca remora* (Amphipoda): nouvelle espèce des côtes de galice (Atlantique Nord-Est). *Crustaceana* 51, 38–48. doi: 10.1163/156854086X00043

Bellan-Santini, D., and Dauvin, J. C. (1988a). *Actualisation des Données sur L'écologie, la Biogéographie et la Phylogénie des Ampeliscidae (Crustacés - Amphipodes) Atlantiques Après la Révision des Collections d'E. Chevreux. Aspects Récents de la Biologie des Crustacés. 10ème Réunion des Carcinologistes de Langue Française, Concarneau, 6-9 juin 1987*. Plouzané: IFREMER. p. 207–215.

Bellan-Santini, D., and Kaim-Malka, R. A. (1977). *Ampelisca* nouvelles de Méditerranée (Crustacea, Amphipoda). *Boll. Mus. Civ. Stor. Nat. Verona* 4, 479–523.

Bellan-Santini, D., and Dauvin, J. C. (1988b). Eléments de synthèse sur les *Ampelisca* du Nord-Est Atlantique. *Crustaceana* 13, 20–60.

Bellan-Santini, D., and Dauvin, J. C. (1989). Distribution verticale et répartition biogéographique de crustacés holobenthiques filtreurs: exemple des amphipodes du genre *Ampelisca*, groupe zoologique à forte spéciation. *Bull. Soc. Géol. France* 3, 561–568.

Bellan-Santini, D., and Dauvin, J. C. (1997). Ampeliscidae (Amphipoda) from Iceland with a description of a new species (Contribution to the BIOICE Research Program. *J. Nat. Hist.* 31, 1157–1173. doi: 10.1080/00222939700770621

Bellan-Santini, D., and Marques, J. C. (1986). Une nouvelle espèce d'*Ampelisca* (Crustacea, Amphipoda) des Côtes du Portugal (Atlantique Nord-Est): *Ampelisca lusitanica* n.sp. *Cah. Biol. Mar.* 27, 153–162.

Bellan-Santini, D., and Ruffo, S. (2003). Biogeography of benthic marine Amphipoda in Mediterranean Sea. *Biogeographia* 24, 273–292. doi: 10.21426/B6110176

Buhl-Jensen, L. (1986). The benthic Amphipod fauna of the west-Norwegian continental shelf compared with the fauna of five adjacent fiords. *Sarsia* 71, 193–208. doi: 10.1080/00364827.1986.10419690

Cardoso, F. G., Dolbeth, M., Sousa, R., Relvas, P., Santos, R., Silva, A., et al. (2019). "The Portuguese coast," in *World Seas: An Environmental Evaluation, Second Edition, Volume I: Europe, The Americas and West Africa*, ed C. Sheppard (London: Academic Press, Elsevier), 189–208. doi: 10.1016/B978-0-12-805068-2.00009-7

Clarke, K. R., and Gorley, R. N. (2006). *PRIMER v6: User Manual/Tutorial*. Plymouth: PRIMER-E, 190 pp.

Croker, R. A. (1967). Niche diversity in five sympatric species of intertidal amphipods (Crustacea: Haustoriidae). *Ecol. Monogr.* 37, 173–200. doi: 10.2307/1948437

Dauvin, J. C. (1988a). Biologie, dynamique et production de populations de Crustacés Amphipodes de la Manche occidentale. 1. *Ampelisca tenuicornis* Liljeborg. *J. Exp. Mar. Biol. Ecol.,* 118, 55–84. doi: 10.1016/0022-0981(88)90122-0

Dauvin, J. C. (1988b). Biologie, dynamique et production de populations de Crustacés Amphipodes de la Manche occidentale. 2. *Ampelisca brevicornis* (Costa). *J. Exp. Mar. Biol. Ecol.,* 119, 213–233. doi: 10.1016/0022-0981(88)90194-3

Dauvin, J. C. (1988c). Biologie, dynamique et production de populations de Crustacés Amphipodes de la Manche occidentale. 3. *Ampelisca typica* (Bate). *J. Exp. Mar. Biol. Ecol.* 121, 1-22. doi: 10.1016/0022-0981(88)90020-2

Dauvin, J. C. (1988d). Life cycle, dynamics and productivity of crustacea-amphipoda from the western part of the English Channel. 4. *Ampelisca armoricana* Bellan-Santini and Dauvin. *J. Exp. Mar. Biol. Ecol.* 123, 235–252. doi: 10.1016/0022-0981(88)90045-7

Dauvin, J. C. (1989). Life cycle, dynamics and productivity of Crustacea-Amphipoda from the western part of the English Channel. 5. *Ampelisca sarsi* Chevreux. *J. Exp. Mar. Biol. Ecol.* 128, 31–56. doi: 10.1016/0022-0981(89)90091-9

Dauvin, J. C. (1996). Ampeliscidae from the Faroe Islands. Contribution to the Biofar programme. *Boll. Mus. Civ. Stor. Nat. Verona* 20, 47–60.

Dauvin, J. C. (1999). Mise à jour de la liste des espèces d'Amphipodes (Crustacea: Peracarida) présents en Manche. *Cah. Biol. Mar.* 40, 165–183.

Dauvin, J. C., and Bellan-Santini, D. (1982). Description de deux nouvelles espèces d'*Ampelisca* des côtes Françaises Atlantiques (Crustacea, Amphipoda): *Ampelisca toulemonti* n.sp. et *Ampelisca spooneri* n.sp. *Cah. Biol. Mar.* 23, 253–268.

Dauvin, J. C., and Bellan-Santini, D. (1985). Collection des Ampeliscides d'Edouard Chevreux du Muséum national d'Histoire naturelle: description d'*Ampelisca melitae* et d'*A. monoculata* n.sp. et *redescription d'A.* verga Reid. *Bull. Mus. Nat. Hist. Nat.* 4, 7A3, 659–675.

Dauvin, J. C., and Bellan-Santini, D. (1986). Révision de la collection des Ampeliscidés (Crustacean, Amphipoda) d'Edouard Chevreux au Muséum national d'Histoire naturelle. *Bull. Mus. Nat. Hist. Nat.* 4, 867–891.

Dauvin, J. C., and Bellan-Santini, D. (1988). Illustrated key to *Ampelisca* species from the North-Eastern Atlantic. *J. Mar. Biol. Assoc.* 68, 659–676. doi: 10.1017/S0025315400028782

Dauvin, J. C., and Bellan-Santini, D. (1996). Ampeliscidae (Amphipoda) from the Bay of Biscay. *J. Crust. Biol.* 16, 149–168. doi: 10.2307/1548938

Dauvin, J. C., and Bellan-Santini, D. (2000). Biodiversity and the biogeographic relationships of the Amphipoda Gammaridea along the French coastline. *J. Mar. Biol. Assoc.* 84, 621–628. doi: 10.1017/S0025315404009658h

Dauvin, J. C., and Bellan-Santini, D. (2002). Les Crustacés Amphipodes Gammaridea benthiques des côtes françaises métropolitaines: bilan des connaissances. *Crustaceana* 75, 299–340. doi: 10.1163/156854002760095408

Dauvin, J. C., Bellan-Santini, D., and Bellan, G. (1993). Les genres *Ophelia* et *Ampelisca* de la région de Roscoff: exemples d'allotopie et de syntopie dans les communautés marines de substrat meuble. *Cah. Biol. Mar.* 34, 1–15.

Dauvin, J. C., and Toulemont, A. (1988). *Données Préliminaires sur les Amphipodes de l'Iroise et de ses Abords, Leurs Affinités Biogéographiques. Aspects Récents de la Biologie des Crustacés. 10ème Réunion des Carcinologistes de Langue Française, CONCARNEAU, 6-9 Juin 1987*. Plouzané: IFREMER. p. 217–222.

Desroy, N. (1998). *Les peuplements benthiques de substrats meubles du bassin maritime de la Rance. Evolution de la biodiversité et effets de l'activité prédatrice de Nephthys hombergii (Annélide polychète) sur le recrutement* (PhD thesis). France: University of Rennes 1. p. 206.

Fallaci, M., Aloia, A., Audoglio, M., Colombini, I., Scapini, F., and Chelazzi, L. (1999). Differences in behavioural strategies between two sympatric talitrids (Amphipoda) inhabiting an exposed sandy beach of the French Atlantic coast. *Estuar. Coast. Shelf Sci.* 48, 469–482. doi: 10.1006/ecss.1998.0437

Gomez Gesteira, J. L., and Dauvin, J. C. (2005). Impact of the Aegean sea oil spill on the Ría of Ares and Betanzos fine sand community (Northwest Spain). *Mar. Envir. Res.* 60, 289–316. doi: 10.1016/j.marenvres.2004.11.001

Hill, C., and Elmgren, R. (1987). Vertical distribution in the sediment in the co-occurring benthic amphipods *Pontoporeia affinis* and *P. femorata*. *Oikos* 49, 221–229. doi: 10.2307/3566029

Horton, T., Lowry, J., De Broyer, C., Bellan-Santini, D., Coleman, C. O., Daneliya, M., et al. (2021). *World Amphipoda Database*. Available online at: http://www.marinespecies.org/amphipoda (accessed January 1, 2021).

Jelassi, R., Khemaissia, H., Zimmer, M., Garbe-Schönberg, D., and Nasri-Ammar, K. (2015). Biodiversity of Talitridae (Crustacea, Amphipoda) in some Tunisian coastal lagoons. *Zool. Studi.* 54:17. doi: 10.1186/s40555-014-0096-1

Kaim-Malka, R. A. (1969). Biologie et écologie de quelques *Ampelisca* de la région de Marseille. *Téthys* 1, 977–1022.

Kaim-Malka, R. A. (2000). Elevation of two eastern Atlantic varieties of *Ampelisca brevicornis* (Costa, 1853) (Crustacea, Amphipoda) to full specific rank with redescription of the species. *J. Nat. Hist.* 34, 1939–1966. doi: 10.1080/00222930050144792

Kolding, S., and Fenchel, T. M. (1979). Coexistence and life cycle characteristics of five species of the amphipod genus *Gammarus*. *Oikos* 33, 323–327. doi: 10.2307/3544009

Lancelotti, D. A., and Trucco, R. G. (1993). Distribution patterns and coexistence of six species of the amphipod genus *Hyale*. *Mar. Ecol. Progr. Ser.* 93, 131–141. doi: 10.3354/meps093131

Le Mao, P. (2006). *Inventaire de la Biodiversité Marine du Golfe Normano-Breton. Les Crustacés Malacostracés*. Amphipodes. Rapport RST/DOP.LER/SM 06–13. Saint-Malo: Ifremer.

Marques, J. C., and Bellan-Santini, D. (1991). Gammaridea and Caprellidea (Crustacea-Amphipoda) of the Portuguese south-western continental shelf: taxonomy and distributional ecology. *Bijdr. Dierk.* 61, 65–87. doi: 10.1163/26660644-06102001

Marques, J. C., and Bellan-Santini, D. (1993). Biodiversity in the ecosystem of the Portuguese continental shelf: distributional ecology and the role of benthic amphipods. *Mar. Biol.* 115, 555–564. doi: 10.1007/BF00349362

Martins, R., Azevedo, M. R., Mamede, R., Sousa, B., Freitas, R., Rocha, F., et al. (2012). Sedimentary and geochemical characterization and provenance of the Portuguese continental shelf soft-bottom sediments. *J. Mar. Syst.* 91, 41–52. doi: 10.1016/j.jmarsys.2011.09.011

Martins, R., Quintino, V., and Rodrigues, A. M. (2013a). Diversity and spatial distribution patterns of the soft-bottom macrofauna communities on the Portuguese continental shelf. *J. Sea Res.* 83, 173–186. doi: 10.1016/j.seares.2013.03.001

Martins, R., Sampaio, L., Quintino, V., and Rodrigues, A. M. (2014). Diversity, distribution and ecology of benthic molluscan communities on the Portuguese continental shelf. *J. Sea Res.* 93, 75–89. doi: 10.1016/j.seares.2013.11.006

Martins, R., Sampaio, L., Rodrigues, A. M., and Quintino, V. (2013b). Soft-bottom Portuguese continental shelf polychaetes: diversity and distribution. *J. Mar. Syst*. 123–124, 41–54. doi: 10.1016/j.jmarsys.2013.04.008

Mesneguen, A. (1980). *La macrofaune benthique de la baie de Concarneau: peuplements, dynamique de populations, prédation exercée par les poissons* (PhD thesis). France: Université de Bretagne Occidentale. 127pp.

Oliver, J. S., Slaitery, P. N., Silberstein, M. A., and O'Connor, E. F. (1983). A comparison of gray whale, *Eschrichtius robustus*, feeding in the Bering Sea and Baja California. *Fish. Bull.* 81, 513–522.

Parker, J. C. (1984). The distribution of the subtidal Amphipoda in Belfast Lough in relation ta sediment types. *Ophelia* 23, 119–140. doi: 10.1080/00785326.1984.10426608

Rigolet, C., Dubois, S. F., Droual, G., Caisey, X., and Thiébaut, E. (2012). Life history and secondary production of the amphipod *Haploops nirae* (Kaim-Malka, 1976) in the Bay of Concarneau (South Brittany). *Estuar. Coast. Shelf Sci.* 113, 259–271. doi: 10.1016/j.ecss.2012.08.014

Rigolet, C., Dufois, S. F., and Thiébaut, E. (2014). Benthic control freaks: effects of the tubiculous amphipod *Haploops nirae* on the specific diversity and functional structure of benthic communities. *J. Sea Res.* 85, 413–427. doi: 10.1016/j.seares.2013.07.013

Rivas, L. R. (1964). A reinterpretation of the concepts "Sympatric" and "Allopatric" with proposal of the additional terms "Syntopic" and "Allotopic". *Syst. Zool.* 13, 42–43. doi: 10.2307/2411436

Sampaio, L., Mamede, R., Ricardo, F., Magalhães, L., Rocha, H., Martins, R., et al. (2016). Soft-sediment crustacean diversity and distribution along the Portuguese continental shelf. *J. Mar. Syst.* 163, 43–60. doi: 10.1016/j.jmarsys.2016.06.011

Schaffner, L. C., and Boesch, D. F. (1982). Spatial and temporal ressource use by dominant benthic Amphipoda (Ampeliscidae and Corophiidae) on the Middle Atlantic Bight outer continental shelf. *Mar. Ecol. Prog. Ser.* 9, 231–243. doi: 10.3354/meps009231

Schellenberg, A. (1925). Crustacea VIII. Amphipoda. In Michaelsen Beitrage zu Kennt. *Meeresfauna West Africas* III, 13–204.

Sheader, M. (1977). Production and population dynamics of *Ampelisca tenuicornis* (Amphipoda) with notes on the biology of its parasite *Sphaeronella longipes* (Copepoda). *J. Mar. Biol. Ass.* 57, 955–968. doi: 10.1017/S0025315400026047

Sheader, M. (1998). Grazing predation on a population of *Ampelisca tenuicornis* (Gammaridae: Amphipoda) off the south coast of England. *Mar. Ecol. Progr. Ser.* 164, 253–262. doi: 10.3354/meps164253

Tato, R., Esquete, P., and Moreira, J. (2012). A new species of *Ampelisca* (Crustacea, Amphipoda) from NW Iberian Peninsula: *Ampelisca troncosoi* sp. *nov. Helgol. Mar. Res.* 66, 319–330. doi: 10.1007/s10152-011-0273-0

Conflict of Interest: The authors declare that the research was conducted in the absence of any commercial or financial relationships that could be construed as a potential conflict of interest.

frontiers in Marine Science

ORIGINAL RESEARCH
published: 31 March 2021
doi: 10.3389/fmars.2021.637546

Determining the Ecological Status of Benthic Coastal Communities: A Case in an Anthropized Sub-Arctic Area

Elliot Dreujou[1,2,3], Nicolas Desroy[4], Julie Carrière[5,6], Lisa Tréau de Coeli[2,3,6], Christopher W. McKindsey[2,7] and Philippe Archambault[2,3,6]*

[1] Institut des Sciences de la Mer, Université du Québec à Rimouski, Rimouski, QC, Canada, [2] Québec-Océan, Université Laval, Québec, QC, Canada, [3] Takuvik Joint Université Laval/Centre National de la Recherche Scientifique Laboratory, Université Laval, Québec, QC, Canada, [4] Laboratoire Environnement Ressources Bretagne Nord, Institut Français pour la Recherche et l'Exploitation de la Mer, Dinard, France, [5] Institut Nordique de Recherche en Environnement et en Santé au Travail, Sept-Îles, QC, Canada, [6] Département de Biologie, Université Laval, Québec, QC, Canada, [7] Maurice Lamontagne Institute, Fisheries and Oceans Canada, Mont-Joli, QC, Canada

OPEN ACCESS

Edited by:
Macarena Ros,
Seville University, Spain

Reviewed by:
Xiaoshou Liu,
Ocean University of China, China
Sarah Samadi,
Muséum National d'Histoire Naturelle, France
Panagiotis D. Dimitriou,
University of Crete, Greece

****Correspondence:***
Elliot Dreujou
elliot.dreujou@uqar.ca

Specialty section:
This article was submitted to Marine Evolutionary Biology, Biogeography and Species Diversity, a section of the journal Frontiers in Marine Science

Received: *03 December 2020*
Accepted: *05 March 2021*
Published: *31 March 2021*

Citation:
Dreujou E, Desroy N, Carrière J, Tréau de Coeli L, McKindsey CW and Archambault P (2021) Determining the Ecological Status of Benthic Coastal Communities: A Case in an Anthropized Sub-Arctic Area. Front. Mar. Sci. 8:637546. doi: 10.3389/fmars.2021.637546

With the widespread influence of human activities on marine ecosystems, evaluation of ecological status provides valuable information for conservation initiatives and sustainable development. To this end, many environmental indicators have been developed worldwide and there is a growing need to evaluate their performance by calculating ecological status in a wide range of ecosystems at multiple spatial and temporal scales. This study calculated and contrasted sixteen indicators of ecological status from three methodological categories: abundance measures, diversity parameters and characteristic species. This selection was applied to coastal benthic ecosystems at Sept-Îles (Québec, Canada), an important industrial harbor area in the Gulf of St. Lawrence, and related to habitat parameters (organic matter, grain size fractions, and heavy metal concentrations). Nearly all indicators highlighted a generally good ecological status in the study area, where communities presented an unperturbed profile with high taxa and functional diversities and without the dominance of opportunistic taxa. Some correlations with habitat parameters were detected, especially with heavy metals, and bootstrap analyses indicated quite robust results. This study provides valuable information on the application of environmental indicators in Canadian coastal ecosystems, along with insights on their use for environmental assessments.

Keywords: environmental indicators, ecological status, coastal benthos, macrofauna, Gulf of St. Lawrence

INTRODUCTION

Anthropogenic influences on marine ecosystems occur globally, with possible perturbation of habitats and communities (Halpern et al., 2007, 2019). Many international organizations have recognized the importance of biologically diverse ecosystems for humanity and have established objectives and targets for their protection and sustainable use (United Nations, 1992;

Secretariat of the CBD, 2010; SDG, 2015). The management of ecosystems requires an understanding of how habitats and communities respond to drivers of change, i.e., forces that affect environmental processes and modify ecosystem state from equilibrium (Boonstra et al., 2015; Beauchesne et al., 2020; Orr et al., 2020). In addition to natural drivers (e.g., temperature anomalies, freshwater inputs, hypoxic events), influences from human activities (e.g., fisheries, chemical pollution, species introductions) are also considered as ecosystem drivers. As natural and anthropogenic drivers may affect ecosystems concomitantly, it is important to understand how both relate to observed effects (Brown et al., 2014). To tackle these questions, environmental assessments rely on the best available knowledge, acquired through ecological groundwork in ecosystems of interest (such as biodiversity surveys, time series monitoring or experimental studies), and on the communication of results to a wide range of stakeholders (Borja et al., 2012; Borja, 2014; Chapman, 2016; Teixeira et al., 2016). Because such assessments are important foundations for decision makers, it is essential to properly account for the inherent complexity and variability of ecological data.

The use of integrative methods, such as indicators, is particularly relevant in this context. An indicator of ecological status is defined as a quantitative measure that synthesizes ecosystem information to infer ecosystem status (Rice, 2003; Rees et al., 2008). Many holistic frameworks, such as ecosystem-based management, marine spatial planning and DPSIR (Driver Pressure State Impact Responses) models, have included indicators in their methodology (Smeets and Weterings, 1999; Niemi and McDonald, 2004; European Commission, 2008; Rees et al., 2008; Levin et al., 2009; Atkins et al., 2011; Borja et al., 2013, 2015, 2016; Santos et al., 2019). However, environmental indicators evaluate specific ecosystem components, perturbations and/or spatiotemporal scales, potentially limiting their applicability in other systems, thus leading to the development of many indicators worldwide (Niemi and McDonald, 2004; Pinto et al., 2009; Teixeira et al., 2016).

One of the ecosystem components most frequently selected for environmental indicators are macrobenthic invertebrates, as they play an important role in the structure and functioning of benthic marine ecosystems (Dauvin and Ruellet, 2007; Pratt et al., 2014). Examples of this include engineering species (e.g., structural features for other species, bioturbation) and interactions with nutrient cycles (e.g., nutrient sequestration in sediments, remineralization, benthic-pelagic coupling) (Largaespada et al., 2012; Link et al., 2013; Belley et al., 2016; Bourque and Demopoulos, 2018). Many macrobenthic species are characterized by a sedentary lifestyle and a relatively long life span, which is particularly interesting when studying human influence as communities will reflect medium-term conditions, resulting in adaptation or local extinction (e.g., Dauer, 1993; Borja et al., 2000; Wei et al., 2020).

As pointed out by Rice (2003) and Salas et al. (2006), environmental indicators may be classed into categories according to their methodological basis, including three main categories used in environmental assessments. Category 1 regroups indicators based on measures of abundance—such as density and biomass of individuals—to infer community status. Relationships between abundance and a community status have frequently been discussed, as species do not have the same tolerance to disturbance (Pearson and Rosenberg, 1978). As such, the use of abundance-biomass curves has been proposed to detect if communities are in a balanced state, where K-selected taxa are dominant, compared to a disturbed state, with a dominance of r-selected taxa (Pearson and Rosenberg, 1978; Gray, 1979; Warwick and Clarke, 1994). Category 2 indicators are biodiversity parameters, i.e., community characteristics such as taxa identity and prevalence, which allow complex information to be aggregated into a unique metric. Finally, indicators in Category 3 are computed based on variations of responses of taxa to disturbance. Pioneer works by Pearson and Rosenberg (1978) proposed a model of benthic community evolution along a gradient of organic enrichment, laying the path toward a set of indicators that relate community structure and ecological status.

Environmental indicators, such as the AZTI Marine Biotic Index or the Infaunal Trophic index, have been applied in a number of North American ecosystems, including Chesapeake Bay, Willapa Bay and the Southern California coast (United States), but efficiency to detect perturbation has been mixed (Word, 1978; Maurer et al., 1999; Ferraro and Cole, 2004; Borja et al., 2008b; Pelletier et al., 2018). Less commonly, studies on the Pacific and Atlantic coasts of Canada have also evaluated the utility of existing indicators, although these studies have most often found poor performance (Sutherland et al., 2007; Burd et al., 2008; Callier et al., 2008; Robert et al., 2013). There is thus a need to test and validate indicators for Canadian ecosystems, in particular by comparing outcomes and efficiency of existing methods, which will greatly benefit to tackle ecosystem management objectives within Canada's Ocean Act and the Oceans Strategy (Government of Canada, 1996; Department of Fisheries and Oceans, 2002).

To this end, we evaluated various indicators of ecological status in a coastal industrial harbor area, where human activities may significantly impact local benthic ecosystems. Industrial harbor areas are regions regrouping significant industrial activities coupled with harbor platforms linking production with commercial shipping routes worldwide. We selected the region of Sept-Îles (Québec, Canada) for this study. Located in the Gulf of St. Lawrence, one of the management areas designated by Fisheries and Oceans Canada and a major strategic region for Québec (Department of Fisheries and Oceans, 2009; Daigle et al., 2017; Schloss et al., 2017; Ferrario and Archambault, in preparation), Sept-Îles is the fourth largest Canadian port in 2019 in terms of total exchanged goods and the second largest in Québec (Statistics Canada, 2011; Binkley, 2020). Industrial activities at Sept-Îles are largely focused on international shipping of iron ore mined in northern Québec and Labrador, the production of aluminum and various fisheries operate in the bay (Department of Fisheries and Oceans, 2019).

The objectives of this study are to (i) compare outcomes of various environmental indicators on benthic ecosystems of the Sept-Îles region and (ii) understand how these indicators relate to habitat parameters for validation and to select appropriate applications.

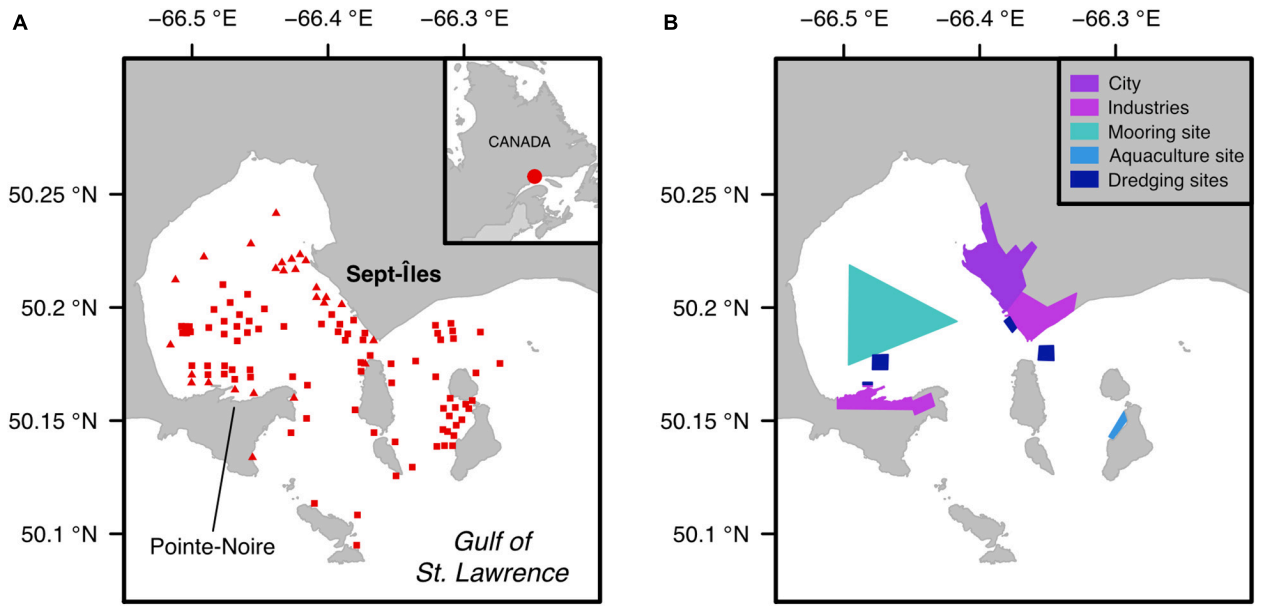

FIGURE 1 | Map of the study area. **(A)** Location of the sampled stations, with light blue triangles and dark blue squares representing shallow (< 15 m) and deep (> 15 m) stations, respectively, **(B)** Location and identity of human activities present in the area.

MATERIALS AND METHODS

Study Area

We targeted ecosystems with a sandy-silty sediment in the industrial harbor area of Sept-Îles (Côte-Nord region of Québec, Canada), which considers ecosystems in the Baie des Sept Îles and the archipelago at its entrance (**Figure 1A**; Dreujou et al., 2018, 2020). Coasts are characterized by sandy beaches, tidal marshes and anthropogenic structures. Mean depth is 35 m in the bay and can reach up to 150 m in the archipelago (Dutil et al., 2012). It is influenced by freshwater inputs from multiple streams and strong tidal currents resulting in a mixed water column and an estuarine circulation (Shaw, 2019). Ecosystems in the Sept-Îles region are considered sub-Arctic due to the formation of ice on the shore in November/December and in the bay in January/February, along with an important freshwater run-off due to snowmelt in April (Demers et al., 2018).

This region hosts several human activities, including industrial, commercial and dredging operations located at the City of Sept-Îles and the Pointe-Noire sector (on the southern section of Baie des Sept Îles), along with an aquaculture site and various fisheries throughout the bay (**Figure 1B**). Many projects have been done in this region to characterize pelagic and benthic communities and habitats in relation to coastal stressors (Canadian Healthy Oceans Network, 2016; Carrière, 2018; Dreujou et al., 2020).

Benthic Ecosystems Sampling

The sampling design and methods used to collect and analyze ecological samples were similar to those presented in Dreujou et al. (2020), with the exception that only one region (Baie des Sept Îles) and one type of community (individuals higher than 0.5 mm) were considered.

A total of 108 stations were selected in the study area, using a randomization algorithm to cover the full extent of the sector, constrained between 0 and 80 m deep, and with increased sampling effort in areas with human activities (**Figure 1A**). Himmelman (1991) showed that benthic communities in the Northern Gulf of St. Lawrence above and below 15–20 m deep differ. Likewise, preliminary fieldwork in the study region detected a thermocline in the water column at ca. 15 m deep. Consequently, we discriminated two groups of stations in order to ensure habitat homogeneity within depth classes: shallow (<15 m, 26 stations) and deep habitats (>15 m, 82 stations). We sampled the benthic ecosystem in July 2017, using a Ponar grab (0.05 m^2) deployed from a boat, with two independent casts at each station.

The first cast collected two subsamples—one for the analyses of organic matter content and another for sediment grain size—stored at -20°C until processing in the laboratory. The percentage of total organic matter (i.e., sum of organic carbon and organic nitrogen) in the sediment was determined using the Loss-on-Ignition method (Davies, 1974). Grain-size analysis was done on a sieving column for the fraction with particles larger than 2 mm and with a Laser Diffraction Particle Size Analyzer for the smaller fractions. Results from both techniques were combined to yield a unified size distribution range from 0.04 µm to 26.5 mm. From this, percentages of gravel, sand, silt and clay were calculated as defined by Wentworth (1922) and Folk (1980).

All sediment obtained from the second cast was sieved on a 0.5 mm mesh size and preserved in a solution of BORAX-buffered formalin (4%) solution for subsequent benthic macrofauna identification (Dreujou et al., 2020). The resulting

samples were sorted using a stereomicroscope and taxa identified to the lowest taxonomic level possible with reference manuals and identification guides; names were validated according to the World Register of Marine Species (WoRMS Editorial Board, 2020). Taxon density and biomass per grab were recorded by counting and weighting (blotted wet mass) individuals in each sample, respectively.

In addition to these parameters, we considered estimates of heavy metal concentrations in the sediment. Concentrations at the sampled stations were calculated based on values obtained in the same area in 2014 and 2016, retrieved from a database hosted by Carrière (2018), using Inverse Distance Weighting interpolation (Dale and Fortin, 2014). We focused on metals for which toxicity criteria have been defined in the Biological Effects Database for Sediments (Environment Canada and Ministère du Développement Durable de l'environnement et des Parcs du Québec, 2007; Centre d'Expertise en Analyse Environnementale du Québec, 2014): arsenic, cadmium, chromium, copper, mercury, lead and zinc; we also included iron and manganese to account for possible contamination from local ore industries.

Environmental Indicator Calculation

Indicators of ecological status were selected from Pinto et al. (2009), DEVOTES (2012), and Teixeira et al. (2016), and grouped into three Categories according to their methodology (**Table 1**). We targeted indicators related to descriptors D1 (biological diversity), D6 (seafloor integrity), and D8 (contaminants) of Good Environmental Status (European Commission, 2008; Borja et al., 2013), choosing those that applied to benthic invertebrates in soft-bottom habitats. We considered each station separately, allowing an assessment of the spatial variability and mean for each indicator, and when possible we pooled all stations together to obtain an estimate for the bay-scale system. We used R v4.0 to perform data manipulations and calculations (R Core Team, 2020).

We included in Category 1 the total density (number of individuals collected per grab), total biomass (wet mass of individuals collected per grab), and the W-Statistic Index, calculated based on abundance-biomass curves for the community (Warwick and Clarke, 1994). Those indicators were computed using benthic taxa abundance sampled at each station.

For Category 2, we considered taxa richness (number of collected taxa) and related metrics to describe the community's structure and the relative prevalence of taxa within it, such as the Shannon index, Margalef index, Simpson index, and Pielou evenness (Legendre and Legendre, 1998; Magurran and McGill, 2011). We also considered taxonomic and functional diversities, based on taxonomic relationships between taxa and information about biological traits, respectively (Warwick and Clarke, 1995; Clarke and Warwick, 1998; Mason et al., 2005; Villéger et al., 2008). Taxa richness, Shannon index, Margalef index, Simpson index, and Pielou evenness were calculated using the benthic community at each station. For taxonomic diversity, we gathered relatedness data for taxa using the WoRMS online database (WoRMS Editorial Board, 2020). To estimate functional diversity, we computed functional richness, functional evenness and functional divergence (Mason et al., 2005; Villéger et al., 2008) by considering five biological traits—body composition, body size, feeding type, mobility and lifestyle—with a total of 26 modalities (**Table 2**). Because taxa can present several modalities for a trait, we assigned a continuous value between 0 (absence of the modality) and 1 (presence of the modality) for each taxon and each trait (the sum of values for every modality within a trait equals 1). Biological trait data was extracted from WoRMS, SealifeBase, the Encyclopedia of Life, and Arctic Traits databases as well as dedicated articles (Degen and Faulwetter, 2019; EoL, 2020; Palomares and Pauly, 2020; WoRMS Editorial Board, 2020). R Packages *vegan* and *FD* were used to calculate indicators in this category (Laliberté and Legendre, 2010; Laliberté et al., 2014; Oksanen et al., 2019).

Finally, indicators in Category 3 included the AZTI Marine Biotic Index (AMBI) and its multivariate version (M-AMBI), which are based on the relative proportion of taxa classified into five ecological groups depending on their tolerance to perturbation (Grall and Glemarec, 1997; Borja et al., 2000; Muxika et al., 2007), BENTIX, where only two ecological groups are considered (Simboura and Zenetos, 2002), and the Benthic Opportunistic Polychaetes Amphipods Index (BOPA), which compares proportions of opportunistic polychaetes and amphipods (Dauvin and Ruellet, 2007). Sampled taxa were assigned to ecological groups, from group I to V, based on the list of Borja et al., version of May 2019 (AZTI, 2019; **Supplementary Table S1**). Because this list was developed for

TABLE 1 | Summary of the evaluated indicators.

Indicator	Unit	Range	References used
Category 1—Abundance measures			
Total density	ind.grab^{-1}	[0; +∞[	–
Total biomass	gWM.grab^{-1}	[0; +∞[	–
W-Statistic index	NA	[–1; 1]	Warwick and Clarke, 1994
Category 2—Diversity measures			
Specific richness	Taxa	[0; +∞[	–
Shannon index	NA	[0; 5]	Magurran and McGill, 2011
Margalef index	NA	[0; +∞[	Magurran and McGill, 2011
Simpson index	NA	[0; 1]	Magurran and McGill, 2011
Pielou evenness	NA	[0; 1]	Magurran and McGill, 2011
Taxonomic diversity	NA	[0; +∞[	Warwick and Clarke, 1995; Clarke and Warwick, 1998
Functional richness	NA	[0; +∞[	Mason et al., 2005; Villéger et al., 2008
Functional evenness	NA	[0; 1]	Mason et al., 2005; Villéger et al., 2008
Functional divergence	NA	[0; 1]	Mason et al., 2005; Villéger et al., 2008
Category 3—Characteristic species			
AZTI Marine Biotic Index (AMBI)	NA	[0; 7]	Borja et al., 2000
Multivariate Marine Biotic Index (M-AMBI)	NA	[0; 1]	Muxika et al., 2007
BENTIX	NA	[0; 6]	Simboura and Zenetos, 2002
Benthic Opportunistic Polychaete Amphipod index (BOPA)	NA	[0; log(2)]	Dauvin and Ruellet, 2007

TABLE 2 | Summary of the functional traits and modalities.

Biological trait	Modality
Body composition	Non-calcified tissue
	Calcareous (not specified)
	Calcareous—calcium carbonate
	Calcareous—amorphous calcium carbonate
	Calcareous—aragonite
	Calcareous—calcite
	Calcareous—high magnesium calcite
	Chitinous
Body length	Small (<3 mm)
	Medium (between 3 and 10 mm)
	Large (>10 mm)
Feeding type	Surface deposit feeder
	Subsurface deposit feeder
	Filter/suspension feeder
	Grazer
	Predator
	Scavenger
	Parasite
Mobility	Sessile
	Limited
	Mobile
Lifestyle	Fixed
	Tubicolous
	Burrower
	Crawler
	Swimmer

European taxa, we assigned groups to unregistered taxa based on species physiology studies and taxonomic relationships (Pelletier et al., 2018). We used this list to further regroup taxa to a "sensitive" (groups I and II) and a "tolerant" (groups III to V) metagroup to compute BENTIX (Simboura and Zenetos, 2002), and to obtain the proportion of opportunistic polychaetes (groups III to V) and sensitive amphipods (group I) to calculate BOPA (Dauvin and Ruellet, 2007; **Supplementary Table S1**). M-AMBI was calculated using the dedicated software AMBI v5.0 (AZTI, 2019), where "bad" and "high" status conditions are required for taxa richness, Shannon index and AMBI (Muxika et al., 2007). Because historical data on benthic invertebrates is scarce in our study area, we used the outcomes of our sampling to establish these values by selecting the 5 and 95 percentiles of the variable distribution (for "bad" and "high" status, respectively, **Supplementary Table S2**) (Buchet, 2010).

Integration and Statistical Analysis

Results for each indicator were reviewed qualitatively and compared to benthic ecosystem data in the Gulf of St. Lawrence, when available. Robustness for indicators in Categories 1 and 2 was calculated as the 95% confidence interval using a resampling routine (bootstrap, 1000 replicates), and the difference between averages of each indicator and the resampling averages (i.e., bootstrap bias).

We computed the Ecological Quality Ratios for Category 3 indicators. This ratio compares the value of an indicator to a reference, such as a targeted state or unperturbed/pristine ecosystem, so that an Ecological Quality Status can be assigned (five categories: "bad," "low," "moderate," "good," and "high" status). The formula to compute the Ecological Quality Ratio is the following (Bund and Solimini, 2007):

$$EQR = \frac{V_{ind} - R_{bad}}{R_{high} - R_{bad}}$$

V_{ind} is the value of an indicator, R_{bad} is the reference value for a "bad" status and R_{high} is the reference value for a "high" status. Limits between each Ecological Quality Status class are specific to the indicator used (Borja et al., 2000; Simboura and Zenetos, 2002; Muxika et al., 2005, 2007; Dauvin and Ruellet, 2007).

Finally, we explored covariation between indicators and habitat parameters (organic matter content, grain size distribution and heavy metal concentrations), using scatterplots for each pair of variables. Correlation was assessed with Spearman's rank coefficients to understand the relevance of each indicator to the computation of ecological status (Quinn and Keough, 2002).

RESULTS

Overview of Benthic Habitats and Communities

Sediment was mostly composed of sand and silt fractions, with concentrations of organic matter rarely surpassing 3% (**Supplementary Table S3**). Heavy metal concentrations did not reach high toxicity levels as defined by Environment Canada (Environment Canada and Ministère du Développement Durable de l'environnement et des Parcs du Québec, 2007; Centre d'Expertise en Analyse Environnementale du Québec, 2014; Dreujou et al., 2020; **Supplementary Table S3**). A total of 132 taxa were identified, belonging to eight phyla, with a dominance of arthropods, mollusks, and annelids (**Supplementary Table S1**). The most abundant taxa were the polychaete *Micronephthys neotena*, the cumacean *Eudorellopsis integra*, the amphipod *Protomedeia grandimana*, Nematoda (adults), and the bivalve *Macoma calcarea* (**Supplementary Table S1**). From this list, no species which can be considered as exotic to this region have been reported (Simard et al., 2013).

Indicator Outcomes

Category 1 Indicators

Indicators in this category presented greater mean values in deep than shallow stations, with the exception of total density (**Table 3**). Shallow stations showed a higher total density than deep stations, but this may be an outlier effect due to a single station close to the City of Sept-Îles (**Supplementary Figures S1A–C**), where density was 899 individuals.grab^{-1} with a dominance of *P. grandimana*. Overall, shallow and deep stations presented low total biomass, except for a couple of stations due to the presence of the echinoderms *Echinarachnius parma*

TABLE 3 | Values of the mean and standard error (SE) for each indicator, the difference between bootstrapped mean and the true mean (bias) and the 95% confidence interval (CI), for shallow and deep stations.

	Shallow stations (*n* = 26)				Deep stations (*n* = 82)			
Indicator	**Bay-scale**	**Mean (SE)**	**Bias**	**95% CI**	**Bay-scale**	**Mean (SE)**	**Bias**	**95% CI**
Category 1								
Total density	3606	138.7 (36.3)	0.38	[136.9; 141.3]	7309	89.13 (7.6)	0.16	[88.81; 89.77]
Total biomass	191.16	7.35 (4.2)	0.057	[7.14; 7.68]	715.06	8.72 (2.3)	0.024	[8.55; 8.84]
W-Statistic index	0.13	0.011 (0.003)	0.016	[0.027; 0.028]	0.11	0.025 (0.002)	0.008	[0.033; 0.033]
Category 2								
Specific richness	65	9.19 (0.9)	0.036	[9.17; 9.29]	117	13.99 (0.5)	0.009	[13.96; 14.03]
Shannon index	2.67	1.353 (0.1)	0.007	[1.354; 1.366]	3.18	1.952 (0.05)	0.0002	[1.949; 1.955]
Margalef index	7.81	1.92 (0.1)	0.014	[1.93; 1.95]	13.04	3.05 (0.1)	0.0001	[3.04; 3.05]
Simpson index	0.88	0.62 (0.04)	0.003	[0.62; 0.63]	0.92	0.77 (0.02)	0.0002	[0.77; 0.77]
Pielou evenness	0.64	0.65 (0.05)	0.004	[0.657; 0.663]	0.67	0.76 (0.02)	0.0003	[0.76; 0.76]
Taxonomic diversity	68.48	51.66 (3.8)	0.357	[51.79; 52.25]	74.8	63.48 (1.3)	0.014	[63.39; 63.55]
Functional richness	–	23.35 (4.6)	3.171	[26.11; 26.93]	–	31.76 (2.5)	7.59	[38.83; 39.88]
Functional evenness	–	0.554 (0.04)	0.002	[0.55; 0.554]	–	0.632 (0.01)	0.002	[0.633; 0.635]
Functional divergence	–	0.77 (0.05)	0.007	[0.77; 0.78]	–	0.83 (0.01)	0.011	[0.82; 0.82]
Category 3								
AMBI	1.57	1.5 (0.1)	–	–	1.53	1.45 (0.05)	–	–
M-AMBI	–	0.68 (0.05)	–	–	–	0.7 (0.03)	–	–
BENTIX	5.15	4.95 (0.2)	–	–	5.25	5.31 (0.09)	–	–
BOPA	0.002	0.003 (0.001)	–	–	0.004	0.007 (0.003)	–	–

AMBI, AZTI Marine Biotic Index; M-AMBI, Multivariate AZTI Marine Biotic Index; BOPA, Benthic Opportunistic Polychaetes Amphipods Index.

and *Strongylocentrotus* sp. (**Supplementary Figures S1A–C**). The W-Statistic Index was positive and close to zero at nearly all shallow and deep stations (**Supplementary Figures S1A–C**) and the abundance-biomass curve presented higher abundance than biomass values when species were ranked (**Figure 2**).

Category 2 Indicators

Category 2 indicators showed similar trends for shallow and deep stations, while being generally higher for the latter (**Table 3**). In particular, there is a close similarity between the spatial distributions of taxa richness, Shannon and Margalef indices and taxonomic diversity (**Supplementary Figures S1D–L**). Variability for shallow stations is quite low, except for a station in front of Pointe-Noire where only one taxon was present, while deep stations tend to display the highest values in the archipelago compared to the center of the bay (**Supplementary Figures S1D–L**). Mean values for the Simpson index and Pielou evenness reached 0.62 (standard error of 0.04) and 0.77 (0.02), respectively, for shallow stations and 0.66 (0.05) and 0.76 (0.02) for deep stations (**Table 3**). The same relationship between shallow and deep stations is observed for these metrics, even though the distribution for both is skewed with some stations closer to coasts presenting very low values (**Supplementary Figures S1D–L**). Concerning functional diversity, deep stations presented higher mean functional richness, functional evenness and functional divergence relative to those at shallow stations (**Table 3**). The most abundant modality for each biological trait was non-calcified tissue for body composition, small individuals for body size, surface deposit-feeders for feeding type, mobile organisms for mobility and burrowers for lifestyle, at both shallow and deep stations.

Category 3 Indicators

Classification of taxa into ecological groups to compute Category 3 indicators yielded 51 taxa in group I (sensitive to disturbance, 38.6% of the taxa), 63 in group II (indifferent to disturbance, 47.7%), 11 in group III (tolerant to disturbance, 8.3%), 1 in each of groups IV and V (second- and first-order opportunists, respectively, 0.8%) and 5 were not assigned due to a too broad taxonomic resolution (**Supplementary Table S1**). This classified 114 taxa in the "sensitive" group and 13 in the "tolerant" group (**Supplementary Table S1**). Concerning polychaetes and amphipods, we observed four opportunistic polychaetes (*Cossura longocirrata*, *Eteone* sp., *Hediste diversicolor*, *Praxillella praetermissa*) and nine sensitive amphipods (*Ameroculodes edwardsi*, *Ampelisca vadorum*, *Byblis gaimardii*, Lysianassidae, *Maera danae*, *Phoxocephalus holbolli*, *Pontoporeia femorata*, *Quasimelita formosa*, *Quasimelita quadrispinosa*).

An AMBI score of 1.57 and 1.53 was obtained for the bay-scale estimate at shallow and deep stations, respectively, which corresponds to a "slight imbalance" site classification (Borja et al., 2000). Overall, low AMBI values were obtained at each station, being 1.5 on average (standard error of 0.13) for shallow stations and 1.45 (0.05) for deep stations, and never exceeding 3, and no particular spatial trend can be observed (**Table 3** and **Supplementary Figures S1M–P**). The bay-scale M-AMBI could not be computed with the percentile method, and at the station level, generally high mean values of 0.68 (0.05) and 0.7 (0.03) were observed for shallow and deep stations, respectively

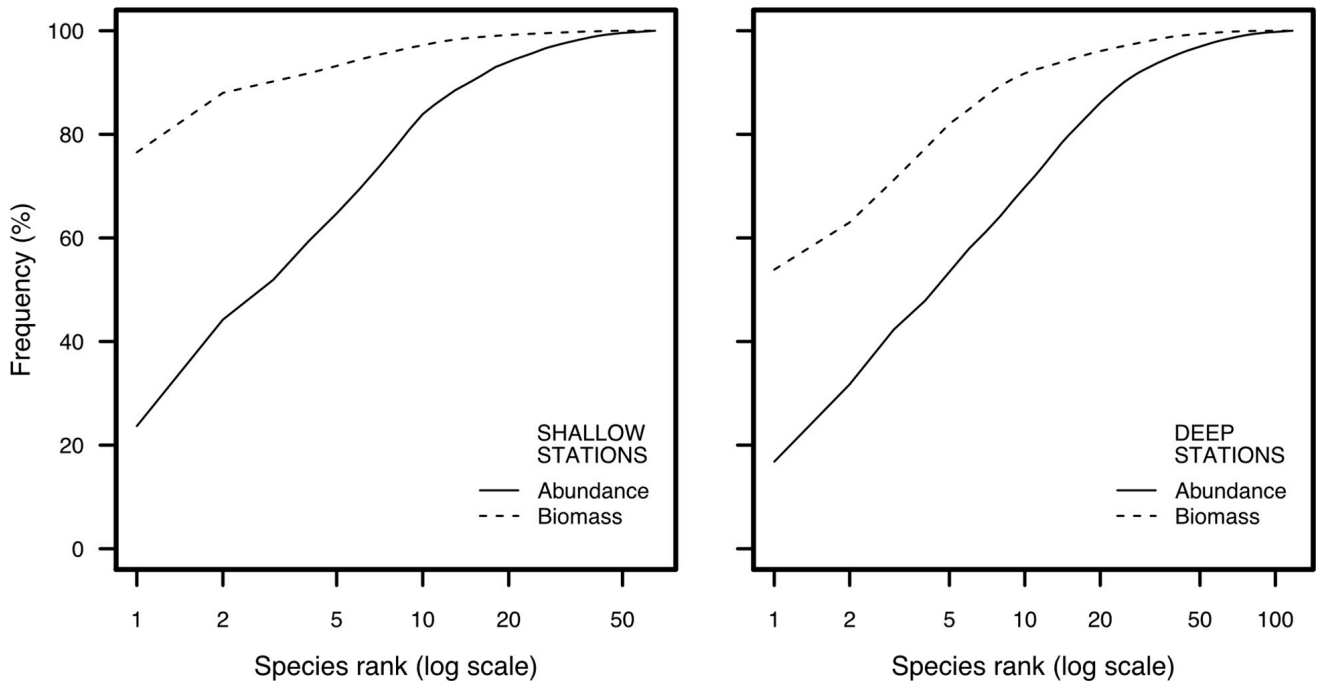

FIGURE 2 | Values of abundance and biomass for ranked species (logarithm scale), for shallow stations and deep stations.

(**Table 3**). Stations outside of the bay tended to be characterized by higher values than those inside it, especially close to the coast and in the northern section of the bay, but this may be related to the spatial distribution of taxa richness and the Shannon index (**Supplementary Figures S1M–P**). The BENTIX bay-scale estimate was 5.15 for shallow stations and 5.25 for deep stations, while at the station-level mean values were 4.95 (0.23) and 5.31 (0.09), respectively (**Table 3**). These values correspond to a "normal/pristine" pollution classification for the majority of the area sampled, except for some stations close to coasts (Simboura and Zenetos, 2002). Finally, BOPA produced low scores of 0.002 and 0.004 for shallow and deep bay-scale estimates, respectively, similar to means of 0.0028 (0.0012) for shallow and 0.0067 (0.003) for deep stations, respectively (**Table 3**), denoting "high status" classifications. Only two stations had a score higher than 0.05, a trend that is not shared with neighboring stations, which may indicate localized low-intensity perturbations (**Supplementary Figures S1M–P**).

Calculation of Ecological Quality Ratios using Category 3 indicators produced similar results for AMBI, BENTIX and BOPA (**Figure 3**). The majority of stations (shallow and deep) presented a "high" or "good" ecological status except for a few stations with a "poor" status (**Figure 3**). In contrast, results for M-AMBI were less uniform, with a high variation among both shallow and deep stations, such that no general trends may be highlighted (**Figure 3**).

Robustness and Covariation

For Category 1 and 2 indicators, bootstrap bias was low at both shallow and deep stations (less than 0.4), except for functional richness where it reached 3.17 and 7.59, respectively (**Table 3**), demonstrating a relatively high robustness of the indicators. The true mean was included in the 95% confidence interval for five indicators at shallow stations (taxa richness, total density, total biomass, functional evenness, functional divergence) and eight at deep stations (taxa richness, total density, total biomass, Shannon index, Margalef index, Simpson index, Pielou evenness, taxonomic diversity) (**Table 3**).

The analysis of covariation between indicators reported moderate to very high Spearman's coefficients ($0.22 < |\rho| < 0.96$) (**Table 4**). Category 2 indicators presented the highest proportion of within-Category significant correlations at both shallow and deep stations (**Table 4**). The vast majority of these correlations were positive, with the strongest correlations between Shannon and Margalef indices, and were represented by linear proportionality between indicators on the scatterplots. Category 2 indicators were also frequently correlated to indicators from Categories 1 and 3, especially for the W-Statistic Index and the M-AMBI (**Table 4**). The latter Categories did not present high within-Category correlations, except between AMBI/BENTIX and M-AMBI/BOPA at shallow stations, and the W-Statistic Index and AMBI at deep stations.

Relationships With Habitat Parameters

Correlations between Category 1 indicators and abiotic parameters detected non-significant relationships with sediment parameters (except between the W-Statistic Index and gravel and sand contents at deep stations), while they were significant and negative between most heavy metals and total density and total biomass at shallow stations, and the W-Statistic

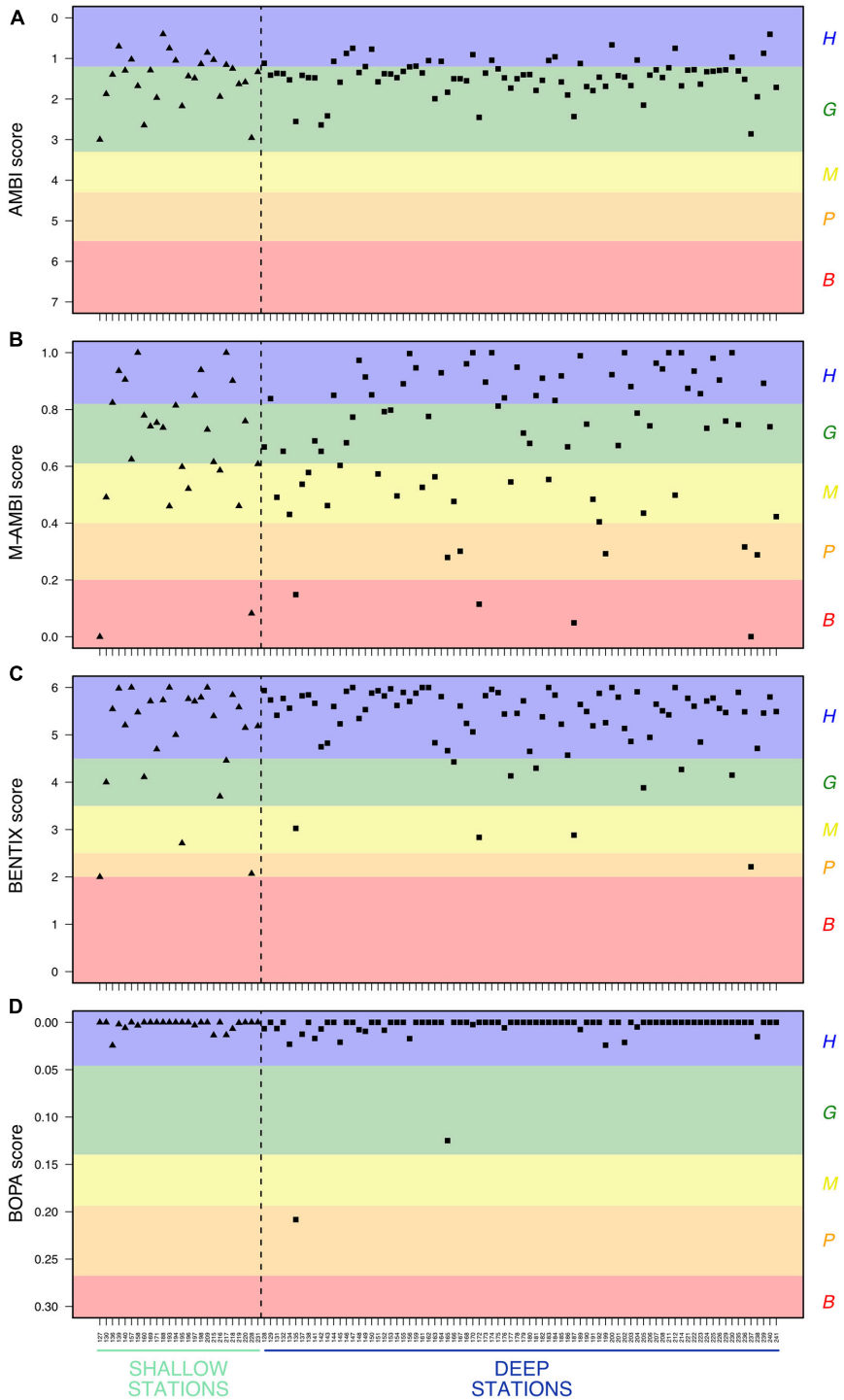

FIGURE 3 | Values of Category 3 indicators ranked according to Ecological Quality Ratios, calculated for shallow and deep stations. **(A)** Calculated with the AZTI Marine Biotic Index (AMBI), **(B)** Calculated with the Multivariate AZTI Marine Biotic Index (M-AMBI), **(C)** Calculated with the BENTIX, **(D)** Calculated with the Benthic Opportunistic Polychaetes Amphipods Index (BOPA). B = "bad" status (red), P = "poor" status (orange), M = "moderate" status (yellow), G = "good" status (green), H = "high" status (blue).

Index at deep stations (**Table 5**). The absolute value of Spearman's rank coefficients was high for total density and total biomass at shallow stations (between −0.4 and −0.61), highlighting relatively strong relationships, while they were less for the W-Statistic Index at deep stations (between −0.22 and −0.29).

TABLE 4 | Spearman rank correlation coefficients between indicators, for shallow and deep stations.

	Category 1			Category 2									Category 3			
Indicator	**TD**	**TB**	**W**	**S**	**H**	**M**	**λ**	**J**	**Δ**	**FR**	**FE**	**FD**	**AMBI**	**M-AMBI**	**BENTIX**	**BOPA**
Shallow stations																
Category 1																
TD																
TB	–															
W	–	–														
Category 2																
S	0.77	0.43	–													
H	–	–	0.62	0.58												
M	–	–	0.53	0.76	0.81											
λ	–	–	0.68	–	0.89	0.61										
J	−0.66	–	0.59	–	0.46	–	0.7									
Δ	−0.44	–	0.71	–	0.59	0.48	0.75	0.86								
FR	0.8	0.5	–	0.87	–	0.58	–	−0.41	–							
FE	–	–	0.67	–	0.58	0.41	0.65	0.54	0.51	–						
FD	–	–	–	0.41	–	–	–	–	–	–	–					
Category 3																
AMBI	–	−0.42	–	–	–	–	–	–	–	–	–	–				
M-AMBI	–	0.48	–	0.8	0.78	0.86	0.5	–	–	0.64	0.4	0.43	–			
BENTIX	–	–	–	–	–	–	–	–	–	–	–	–	−0.78	–		
BOPA	–	–	–	0.45	–	0.41	–	–	–	–	–	–	–	0.53	–	
Deep stations																
Category 1																
TD																
TB	–															
W	−0.31	0.35														
Category 2																
S	0.58	–	0.37													
H	–	–	0.75	0.67												
M	–	–	0.61	0.9	0.86											
λ	−0.23	–	0.75	0.47	0.96	0.7										
J	−0.67	–	0.63	–	0.64	0.29	0.79									
Δ	−0.39	–	0.69	0.28	0.81	0.57	0.89	0.88								
FR	0.35	–	0.32	0.71	0.46	0.67	0.33	–	–							
FE	−0.55	–	0.42	–	–	–	0.31	0.59	0.43	–						
FD	–	–	−0.32	−0.27	−0.39	−0.37	−0.41	−0.39	−0.5	−0.28	–					
Category 3																
AMBI	–	–	−0.29	–	−0.25	−0.23	−0.28	−0.31	−0.3	–	–	0.32				
M-AMBI	–	–	0.64	0.79	0.87	0.89	0.76	0.39	0.6	0.58	–	−0.4	−0.52			
BENTIX	–	–	–	–	–	–	–	–	–	–	–	−0.24	−0.7	–		
BOPA	–	–	–	–	–	–	–	–	−0.22	–	–	–	–	–	–	

Only significant relationships of the triangular matrix are presented. TD, total density, TB, total biomass; W, W-Statistic index; S, taxa richness; H, Shannon index; M, Margalef index; λ, Simpson index; J, Pielou evenness; Δ, taxonomic diversity; FR, functional richness; FE, functional evenness; FD, functional divergence; AMBI, AZTI Marine Biotic Index; M-AMBI, Multivariate AZTI Marine Biotic Index; BOPA, Benthic Opportunistic Polychaetes Amphipods Index.

For Category 2 indicators, correlations with sediment parameters were significant only for some cases involving taxa richness, the Margalef index, taxonomic diversity and functional richness (**Table 5**). Relationships with heavy metals were detected mainly at deep stations, in particular for cadmium, copper, lead and zinc; at shallow stations, functional richness showed significant correlations with all heavy metals except cadmium, while functional divergence and taxa richness presented marginal correlations. The vast majority of these relationships were moderate to high (between −0.22 and −0.45), except at deep stations for gravel and sand contents and between functional divergence and some heavy metals.

Finally, several significant relationships were observed between Category 3 indicators and sediment parameters (organic matter, sand and silt contents), including at shallow stations for AMBI and BENTIX and at deep stations for BENTIX and BOPA

TABLE 5 | Spearman rank correlation coefficients between environmental indicators and habitat parameters, for shallow and deep stations.

	Sediment parameters					Heavy metal concentrations								
Indicator	**OM**	**Gravel**	**Sand**	**Silt**	**Clay**	**As**	**Cd**	**Cr**	**Cu**	**Fe**	**Mn**	**Hg**	**Pb**	**Zn**
Shallow stations														
Category 1														
TD	–	–	–	–	–	−0.46	–	−0.52	−0.55	−0.49	–	−0.52	−0.55	−0.52
TB	–	–	–	–	–	−0.42	−0.42	−0.59	−0.51	−0.39	−0.53	–	−0.5	−0.61
W	–	–	–	–	–	–	−0.4	–	–	–	–	–	–	–
Category 2														
S	–	–	–	–	–	−0.47	–	–	–	–	–	−0.39	–	–
H	–	–	–	–	–	–	–	–	–	–	–	–	–	–
M	–	–	–	–	–	–	–	–	–	–	–	–	–	–
λ	–	–	–	–	–	–	–	–	–	–	–	–	–	–
J	–	–	–	–	–	–	–	–	–	–	–	0.42	–	–
Δ	–	–	–	–	–	–	–	–	–	–	–	–	–	–
FR	–	–	–	–	–	−0.43	–	−0.5	−0.43	−0.47	−0.46	−0.5	−0.42	−0.47
FE	–	–	–	–	–	–	–	–	–	–	–	–	–	–
FD	–	–	–	–	–	−0.6	–	–	–	–	–	–	−0.4	−0.4
Category 3														
AMBI	−0.43	–	0.47	−0.47	–	–	–	–	–	–	–	–	–	–
M-AMBI	–	–	–	–	–	–	–	–	–	–	–	–	–	–
BENTIX	0.45	–	–	–	–	–	–	–	–	–	–	–	–	–
BOPA	–	–	–	–	–	–	–	–	–	–	–	–	–	–
Deep stations														
Category 1														
TD	–	–	–	–	–	–	–	–	–	−0.23	–	–	–	–
TB	–	–	–	–	–	–	–	–	–	–	–	–	–	–
W	–	0.24	−0.22	–	–	−0.29	−0.29	−0.27	−0.24	−0.27	−0.26	–	−0.28	−0.29
Category 2														
S	−0.25	–	–	–	–	−0.27	−0.32	−0.31	−0.32	−0.45	−0.31	–	−0.3	−0.34
H	–	–	–	–	–	−0.29	−0.29	−0.33	−0.29	−0.36	−0.31	−0.25	−0.31	−0.31
M	−0.26	–	–	–	–	−0.32	−0.33	−0.36	−0.37	−0.45	−0.36	−0.28	−0.35	−0.38
λ	–	–	–	–	–	−0.22	−0.23	−0.27	−0.22	−0.28	−0.25	−0.22	−0.26	−0.24
J	–	–	–	–	–	–	–	–	–	–	–	–	–	–
Δ	–	–	0.23	−0.29	–	−0.29	−0.32	−0.35	−0.35	−0.35	−0.34	−0.33	−0.34	−0.35
FR	–	0.25	–	–	–	−0.25	−0.32	−0.29	−0.32	−0.36	−0.29	−0.28	−0.27	−0.33
FE	–	–	–	–	–	–	–	−0.22	−0.25	–	−0.27	−0.27	−0.24	−0.22
FD	–	–	–	–	–	–	0.28	–	0.29	–	–	0.29	0.28	0.34
Category 3														
AMBI	–	–	–	–	–	–	–	–	–	–	–	–	–	–
M-AMBI	–	–	–	–	–	−0.24	−0.3	−0.3	−0.27	−0.38	−0.28	–	−0.28	−0.31
BENTIX	0.27	–	−0.26	0.23	–	0.23	0.23	0.24	0.25	–	–	0.23	–	–
BOPA	–	–	−0.31	0.34	–	0.33	0.28	0.36	0.31	0.33	0.38	0.3	0.33	0.3

Only significant relationships are presented. TD, total density; TB, total biomass; W, W-Statistic index; S, taxa richness; H, Shannon index; M, Margalef index; λ, Simpson index; J, Pielou evenness; Δ, taxonomic diversity; FR, functional richness; FE, functional evenness; FD, functional divergence; AMBI, AZTI Marine Biotic Index; M-AMBI, Multivariate AZTI Marine Biotic Index; BOPA, Benthic Opportunistic Polychaetes Amphipods Index; OM, organic matter; As, arsenic; Cd, cadmium; Cr, chromium; Cu, copper; Fe, iron; Mn, manganese; Hg, mercury; Pb, lead; Zn, zinc.

(**Table 5**). Organic matter was negatively correlated with AMBI values (coefficient of −0.43) at shallow stations and positively with BENTIX values at shallow and deep stations (0.45 and 0.27, respectively); sand and silt contents had the opposite effect at shallow stations for AMBI (0.47 and −0.47, respectively) and at deep stations for BENTIX (−0.26 and 0.23, respectively) and BOPA (−0.31 and 0.34, respectively) values. Many relationships with heavy metals were detected at deep stations for all indicators except AMBI (**Table 5**). In particular, M-AMBI presented negative correlations with heavy metals (between −0.24 and −0.38), whereas correlations with BENTIX and BOPA were positive (between 0.23 and 0.36).

DISCUSSION

Strengths, Limitations, and Ecological Considerations of Indicators

The analysis of benthic communities using Category 1 indicators relies on abundance relationships (either density or biomass

of individuals) without consideration of taxonomic identity. Their calculation requires the least laboratory and analytical time relative to the other calculated indicators. Deep stations present a higher density of benthic organisms than shallow stations, as predicted by patterns of coastal marine biodiversity (Gray and Elliott, 2009; Levinton, 2013; Piacenza et al., 2015). The abundance-biomass curve for shallow and deep stations is characteristic of an unstressed profile (Pearson and Rosenberg, 1978; Warwick and Clarke, 1994), which is further supported by the W-Statistic Index being positive and close to 0 at nearly all stations (Clarke, 1990). Studying communities through abundance relationships thus provides interesting results concerning the status of the ecosystem, but the main assumption behind indicators in this Category is that all species are equivalent and have an identical role in the ecosystem structure and functioning. This, however is not necessarily true, as some species can be considered "key species" in ecosystems due to unique engineering or trophic roles (e.g., Bond, 1994; Lawton and Jones, 1995). Thus, Category 1 indicators should be coupled with ancillary methods focusing on biological characteristics of the species, such as life-history traits and physiological characteristics.

Category 2 indicators focus on community biodiversity, granting additional detail than that provided by Category 1 indicators. The notion of biodiversity can be interpreted along multiple points of view in an ecosystem, such as the diversity of species, genes, habitats or functions (United Nations, 1992; Wilson, 1992; Hooper et al., 2005; Stachowicz et al., 2007). While each targeted component has specific implications for the ecosystem, high richness and high diversity values have generally been interpreted as signs of good ecological status (Covich et al., 2004; Borja et al., 2013). This statement needs to be considered carefully, as it is necessary to discuss results with comparable ecosystems and historical data so that diversity trends are interpreted according to local background patterns (Covich et al., 2004).

Taxa richness indicated a quite diverse community, being nearly twice as great at deep stations, as expected given general trends (Gray and Elliott, 2009; Levinton, 2013; Piacenza et al., 2015). These numbers (132 taxa observed) are comparable to results from available benthic invertebrate surveys done in the study area, such as 27 taxa reported by OBIS (2020) in the Sept-Îles region and 148 taxa by Nozères et al. (2015) in the Gulf of St. Lawrence. Results from diversity indicators (Shannon index, Margalef index, Simpson index, Pielou evenness and taxonomic diversity) showed moderate to high benthic diversity, with no dominance by any taxa (even distribution) and great taxonomic breadth. Few stations differ from this general trend, and those that do are mostly close to coasts where diversity is low and there is no clear evidence of perturbation. Diversity indicators are frequently used in ecological studies to characterize communities and to detect disturbance, which allows discussing their results building on a vast corpus of studies worldwide (Magurran and McGill, 2011). These univariate estimates, however, may mask individual responses arising for example from adaptation or changes in biotic relationships, and they should be coupled with multivariate methods, such as ordination or similarity analysis, so that community-level effects are accurately described (Legendre and Legendre, 1998; Quinn and Keough, 2002; Magurran and McGill, 2011).

Concerning functional diversity, functional richness is generally lower at shallow stations and the two other indicators are in the same range, albeit being slightly greater at deep stations. These results suggest that taxa at shallow stations have more specialized niches, i.e., less diverse functional strategies (Villéger et al., 2008), indicating some redundancy of biological traits. This property is linked to an increased ecosystem stability and resilience, where possible extinctions due to perturbation will not modify the ecosystem structure even if some taxa disappear (Rosenfeld, 2002; Mouillot et al., 2013). However, bootstrap bias was very high for this indicator, making conclusions less robust. Moderate to high functional evenness and divergence denote that values for given biological traits are not evenly distributed and are skewed toward extremes (0 or 1). The consideration of biological traits in addition to species identity allows to study functions of the ecosystem, such as productivity, chemical elements cycling or energy transfers (Somerfield, 2008; Bellwood et al., 2019). This is an important addition to environmental assessments, as biological traits and adaptative responses to disturbance are highly related (Mouillot et al., 2013; Miatta et al., 2021). Indicators of functional diversity thus offer valuable information to characterize communities in complement to other Category 2 indicators, at the expense of increased analytical time to assemble a traits database, for which information may be lacking or difficult to obtain.

For Category 3 indicators, community ecological status is assessed by considering the tolerance of taxa to perturbation. Values for these indicators highlight an overall high status in the study area, where taxa sensitive to perturbation are present without a dominance of opportunists, as illustrated by the number of stations with a "high" Ecological Quality Status. M-AMBI detected greater variability between stations relative to the other indicators, particularly within the bay. A possible interpretation for this result may be the influence of the percentile method used to compute "bad" and "high" status conditions for this indicator, advocating for a careful description of comparison conditions and *a fortiori* references values (Borja et al., 2012). Furthermore, classification into ecological groups may introduce bias, as the list of Borja et al. (2000) were primarily designed for European coastal ecosystems. Inclusion of taxa found on Canadian coasts has been made based on taxonomic similarity with species already included in the list, by reviewing studies on perturbation tolerance and by expert opinion, but these choices need to be ground-truthed by dedicated ecological works. A wide spectrum of indicators may be included within Category 3, as compiled by Pinto et al. (2009) and Teixeira et al. (2016), and their use in environmental assessments is linked to scientific and management objectives. Such indicators have been used with success in a variety of ecosystems (e.g., Borja et al., 2008a; Gillett et al., 2015), but they require a high volume of data to accurately relate taxa and perturbation status, such as field observations, modeling of species distributions (native and non-indigenous), physiological studies and experimental work.

With these results, we can compare strengths and limitations of the calculated indicators. Category 1 indicators gather relevant baseline information on the ecosystem and requires the least time to be computed. The downside is that it is difficult to discriminate between anthropogenic perturbation and natural variability as other community characteristics may be impacted and, most importantly, they cannot be compared to reference conditions of ecological status. Category 2 indicators, such as the commonly used Shannon index or Pielou evenness, are easy to compute from well-built taxa lists, although taxonomic and functional diversity demand more time to gather complementary information about phylogenetic relationships and ecosystem functions. However, the latter indicators provide more information on the community structure and are backed by ecological literature to infer a certain ecological status (Magurran and McGill, 2011). Finally, Category 3 indicators demand the most time to be calculated, in particular with the classification of taxa relative to their response to disturbance, but they have been specifically designed to determine Ecological Quality Ratios and to consider reference conditions. Bias or uncertainty may be introduced during the classification process as extensive experimental groundwork is needed to properly assign taxa to groups, which is not always available. Many of these indicators are region-specific, with possible poor performance in other ecosystems (e.g., Callier et al., 2008; Robert et al., 2013), so that further research is needed to properly assess ecological status in sub-Arctic regions.

Implications for Sept-Îles and Canadian Ecosystems

Sept-Îles is an important industrial harbor area for Québec, with a variety of economic activities taking place in the bay and archipelago. All calculated indicators except M-AMBI pointed toward diverse benthic communities of generally good ecological status and no particular perturbation patterns have been detected in the study area, which is coherent with previous descriptions of benthic ecosystems in this region (Carrière, 2018; Dreujou et al., 2020). When applying Category 3 indicators on the data from these studies, we obtained similar conclusions with ecological status indicated as "good" to "high" for AMBI, BENTIX and BOPA.

No particular trend has been observed for stations identified as potentially impacted by Dreujou et al. (2020) in coastal regions close to the City of Sept-Îles and Pointe-Noire, further suggesting an overall limited effect of perturbations. Compared to the regions where many of the assayed indicators were developed, e.g., in Atlantic and Mediterranean European ecosystems, the magnitude of human activity is considerably lower at Sept-Îles. As such, it is possible the range of variation induced by anthropogenic perturbation is not sufficient to severely impact benthic ecosystems. This is even more relevant when we compare these results to other industrial harbor areas worldwide, where human influence is more pronounced (e.g., Hewitt et al., 2005; Borja et al., 2006; Chan et al., 2016; Birch et al., 2020). Other hypotheses may explain this, such as (i) high community resilience and resistance, (ii) limitation of effective impacts of activities by the dynamic of the ecosystem (e.g., flushing from tidal currents), and (iii) perturbation effects may be more pronounced on other components (such as phytoplankton or pelagic species).

Ecological indicators represent a valuable method to set conservation targets and to guide sustainable environmental projects. In light of initiatives such as the Marine Strategy Framework Directive, where indicators and descriptors have been identified to monitor the ecological status of European marine waters (European Commission, 2008; Borja et al., 2013, 2015, 2016), local stakeholders have the possibility to build on these works to establish ecosystem-based management adapted to Canadian ecosystems. Further research in other industrial coastal areas, including long-term monitoring, is needed to obtained coherent and robust environmental assessments.

Validation and Limitations

Assessing relationships between indicators highlighted correlations, especially among Category 2 indicators. While this does not necessarily imply causality in the interpretations, covariation indicates that information gathered by some indicators is similar. This was expected for indicators relying on specific ecosystem components to be computed, such as M-AMBI and the Shannon index, both of which being a function of taxa richness. With an environmental assessment perspective, these results show that calculation of some indicators will not provide additional information when the objective is to detect trends in a targeted area. Understanding these links will allow refining methodological protocols and to produce more efficient and accurate assessments.

The use of ecological status indicators requires a validation procedure to ensure that outcomes are relevant (Dauvin et al., 2010; Heink et al., 2016; Burgass et al., 2017; Moriarty et al., 2018). Because the region of Sept-Îles is not frequently represented in the scientific literature, it is then difficult to have baseline data to validate ecosystem assessments. The studies of Dreujou et al. (2018, 2020) represent the only campaigns describing benthic habitats and communities in the Baie des Sept Îles, and increased sampling would greatly improve indicator validation, in particular for Category 1 and 2 indicators where references conditions are currently not available. Inference of ecological status based on Category 3 indicators is relying on explicit reference conditions for "bad" and "high" status. Defining values for these conditions based on contemporary ecosystems will most certainly introduce bias, as most are likely to show some level of degradation (which cannot be assessed), and alternatives, such as historical datasets, are rare (Muxika et al., 2007; Borja et al., 2012).

Overall, Category 1 and 2 indicators were relatively robust, with little difference between mean values calculated from the real and bootstrapped datasets (except for functional richness), indicating quite homogeneous results. The vast majority of significant correlations between indicators and environmental factors were found for heavy metal concentrations and most such correlations were negative. This implies that indicators would successfully detect perturbation due to heavy metal content, thus resulting in reduced ecological status, but fail to detect perturbations affecting other habitat parameters. AMBI and BENTIX were correlated to organic matter content,

which was expected as original works of Borja et al. (2000) and Simboura and Zenetos (2002) were based on models predicting community changes in response to an organic enrichment (Pearson and Rosenberg, 1978; Grall and Glemarec, 1997). Concerning grain size variables, only sand and silt contents showed any significant correlations with indicators, mainly at deep stations, which may be due to very low amounts of gravel and clay in the sediments.

It is important to note that indicators summarize complex ecological data into unique values (univariate in a statistical point of view), which may be insufficient to correctly assess perturbation. Category 3 indicators were developed for specific types of disturbance, such as organic matter loading or oil-spill detection (Pearson and Rosenberg, 1978; Borja et al., 2000; Dauvin and Ruellet, 2007), and for specific ecosystems (e.g., European Commission, 2008). Even though we detected significant relationships with heavy metal concentrations, dedicated methods to monitor these types of perturbation would greatly benefit this portrait. Finally, the consideration of cumulative impacts from various sources of disturbance may be a good perspective for environmental assessments (Crain et al., 2008), in order to develop more holistic indicators.

CONCLUSION

This study provides insight on the use of environmental indicators in Canadian coastal ecosystems, in particular by applying and comparing indicators within an important industrial harbor area. An overall good status for benthic ecosystems was detected in our study area, which is a valuable addition to guide stakeholders and ecosystem management at the local scale. We were able to present strengths and caveats for each Categories of indicators, relating them to ecological implications and possible improvements. Finally, we were able to study the robustness of indicators and we highlighted improvements for ground-throughing and validation.

Further environmental assessments in sub-Arctic coastal areas in the Gulf of St. Lawrence and the Canadian Eastern Atlantic coast are needed to obtain a broader portrait of the region with a more diverse range of environmental conditions. Long-term monitoring will also produce reliable time series data to better understand variability of sub-Arctic benthic ecosystems.

DATA AVAILABILITY STATEMENT

The datasets generated for this study can be found in the online repositories. The names of the repository/repositories and accession number(s) can be found below: https://dataverse.scholarsportal.info/dataverse/chone2, doi: 10.5683/SP2/WDDDMI.

AUTHOR CONTRIBUTIONS

ED, JC, CM, and PA contributed to the conception and design of the study. ED gathered the data in the field. ED, ND, and LT organized the database. ED and ND performed the statistical analysis. ED wrote the first draft of the manuscript. All authors contributed to manuscript revision, read and approved the submitted version.

FUNDING

This research was sponsored by the NSERC Canadian Healthy Oceans Network and its partners: Fisheries and Oceans Canada and INREST (representing the Port of Sept-Îles and City of Sept-Îles) to PA (grant number: NETGP 468437-14), by the FRQNT Strategic Network Québec-Océan and by the Joint UL/CNRS Laboratory Takuvik.

ACKNOWLEDGMENTS

We would like to acknowledge and thank all the people that helped during the field campaigns, lab work, and data analysis: Claudy Dechêsne, Serge Gallienne, Dany Lévesque, Aurélie Foveau, Cindy Grant, Laure de Montety, Philippe-Olivier Dumais, and Raphaël Bouchard. This study is a contribution to the research program of FRQNT Strategic Network Québec-Océan, which also provided scientific support.

SUPPLEMENTARY MATERIAL

The Supplementary Material for this article can be found online at: https://www.frontiersin.org/articles/10.3389/fmars.2021.637546/full#supplementary-material

REFERENCES

Atkins, J. P., Gregory, A. J., Burdon, D., and Elliott, M. (2011). Managing the marine environment: Is the DPSIR framework holistic enough? *Syst. Res. Behav. Sci.* 28, 497–508. doi: 10.1002/sres.1111

AZTI (2019). *AZTI Marine Biotic Index Software*. Available online at: https://ambi.azti.es/ (accessed February 26, 2021).

Beauchesne, D., Daigle, R. M., Vissault, S., Gravel, D., Bastien, A., Bélanger, S., et al. (2020). Characterizing exposure to and sharing knowledge of drivers of environmental change in the St. Lawrence system in Canada. *Front. Mar. Sci.* 7:383. doi: 10.3389/fmars.2020.00383

Belley, R., Snelgrove, P. V. R., Archambault, P., and Juniper, S. K. (2016). Environmental drivers of benthic flux variation and ecosystem functioning in Salish Sea and Northeast Pacific Sediments. *PLoS One* 11:e151110. doi: 10.1371/journal.pone.0151110

Bellwood, D. R., Streit, R. P., Brandl, S. J., and Tebbett, S. B. (2019). The meaning of the term 'function' in ecology: a coral reef perspective. *Funct. Ecol.* 33, 948–961. doi: 10.1111/1365-2435.13265

Binkley, A. (2020). Where is the federal port modernization review headed? *Canad. Sail.* 12–16. Available online at: https://www.canadiansailings.ca/documents/weekly_issue/feb_2020/feb_24_2020.pdf (accessed February 26, 2021).

Birch, G. F., Lee, J. H., Tanner, E., Fortune, J., Munksgaard, N., Whitehead, J., et al. (2020). Sediment metal enrichment and ecological risk assessment of ten ports and estuaries in the World Harbours Project. *Mar. Pollut. Bull.* 155:111129. doi: 10.1016/j.marpolbul.2020.111129

Bond, W. J. (1994). "Keystone species," in *Biodiversity and Ecosystem Function*, eds E.-D. Schulze and H. A. Mooney (Berlin: Springer), 237–253. doi: 10.1007/978-3-642-58001-7_11

Boonstra, W. J., Ottosen, K. M., Ferreira, A. S. A., Richter, A., Rogers, L. A., Pedersen, M. W., et al. (2015). What are the major global threats and impacts in marine environments? Investigating the contours of a shared perception among marine scientists from the bottom-up. *Mar. Policy* 60, 197–201. doi: 10.1016/j.marpol.2015.06.007

Borja, Á, Bricker, S. B., Dauer, D. M., Demetriades, N. T., Ferreira, J. G., Forbes, A. T., et al. (2008a). Overview of integrative tools and methods in assessing ecological integrity in estuarine and coastal systems worldwide. *Mar. Pollut. Bull.* 56, 1519–1537. doi: 10.1016/j.marpolbul.2008.07.005

Borja, Á, Dauer, D. M., and Grémare, A. (2012). The importance of setting targets and reference conditions in assessing marine ecosystem quality. *Ecol. Indicat.* 12, 1–7. doi: 10.1016/j.ecolind.2011.06.018

Borja, Á, Muxika, I., and Franco, J. (2006). Long-term recovery of soft-bottom benthos following urban and industrial sewage treatment in the Nervión estuary (southern Bay of Biscay). *Mar. Ecol. Progr. Ser.* 313, 43–55. doi: 10.3354/meps313043

Borja, A. (2014). Grand challenges in marine ecosystems ecology. *Front. Mar. Sci.* 11:1. doi: 10.3389/fmars.2014.00001

Borja, A., Elliott, M., Andersen, J. H., Cardoso, A. C., Carstensen, J., Ferreira, J. G., et al. (2013). Good Environmental Status of marine ecosystems: what is it and how do we know when we have attained it? *Mar. Pollut. Bull.* 76, 16–27. doi: 10.1016/j.marpolbul.2013.08.042

Borja, A., Elliott, M., Andersen, J. H., Cardoso, A., Carstensen, J., Ferreira, J., et al. (2015). *Report on Potential Definition of Good Environmental Status Deliverable 6.2, DEVOTES Project.* 62.

Borja, A., Elliott, M., Snelgrove, P. V. R., Austen, M. C., Berg, T., Cochrane, S., et al. (2016). Bridging the gap between policy and science in assessing the health status of marine ecosystems. *Front. Mar. Sci.* 3:175. doi: 10.3389/fmars.2016.00175

Borja, A., Franco, J., and Pérez, V. (2000). A marine Biotic Index to establish the ecological quality of soft-bottom benthos within European estuarine and coastal environments. *Mar. Pollut. Bull.* 40, 1100–1114. doi: 10.1016/S0025-326X(00)00061-8

Borja, Á., Dauer, D. M., Díaz, R., Llansó, R. J., Muxika, I., Rodríguez, J. G., et al. (2008b). Assessing estuarine benthic quality conditions in Chesapeake Bay: a comparison of three indices. *Ecol. Indicat.* 8, 395–403. doi: 10.1016/j.ecolind.2007.05.003

Bourque, J. R., and Demopoulos, A. W. J. (2018). The influence of different deep-sea coral habitats on sediment macrofaunal community structure and function. *PeerJ* 2018:5276. doi: 10.7717/peerj.5276

Brown, C. J., Saunders, M. I., Possingham, H. P., and Richardson, A. J. (2014). Interactions between global and local stressors of ecosystems determine management effectiveness in cumulative impact mapping. *Divers. Distribut.* 20, 538–546. doi: 10.1111/ddi.12159

Buchet, R. (2010). *Directive Cadre sur l'Eau: Consolidation des Conditions de Référence Pour les L'évaluation des Masses d'eau Biologiques Impliqués Dans Éléments de Qualité Littorales*. Brest: Institut Français pour la Recherche et l'Exploitation de la Mer.

Bund, W. V. D., and Solimini, A. G. (2007). *Ecological Quality Ratios for Ecological Quality Assessment in Inland and Marine Waters*. Luxembourg: European Commission Joint Research Centre, Institute for Environment.

Burd, B. J., Barnes, P. A. G., Wright, C. A., and Thomson, R. E. (2008). A review of subtidal benthic habitats and invertebrate biota of the Strait of Georgia, British Columbia. *Mar. Environ. Res.* 66:4. doi: 10.1016/j.marenvres.2008.09.004

Burgass, M. J., Halpern, B. S., Nicholson, E., and Milner-Gulland, E. J. (2017). Navigating uncertainty in environmental composite indicators. *Ecol. Indicat.* 75, 268–278. doi: 10.1016/j.ecolind.2016.12.034

Callier, M. D., McKindsey, C. W., and Desrosiers, G. (2008). Evaluation of indicators used to detect mussel farm influence on the benthos: two case studies in the Magdalen Islands, Eastern Canada. *Aquaculture* 278, 77–88. doi: 10.1016/j.aquaculture.2008.03.026

Canadian Healthy Oceans Network (2016). *To Evaluate and Model How Natural and Anthropogenic Stressors Interact to Imapct Pelagic and Benthic Communities Along a Sub-Arctic Coastline and Develop Bay-Scale Condition Indicators*. Available online at: https://chone2.ca/find-research/coastal-stressors/ (accessed February 26, 2021).

Carrière, J. (ed.) (2018). *Observatoire de la Baie de Sept Îles*. Sept-Îles, QC: Institut Nordique de Recherche en Environnement et en Santé au Travail.

Centre d'Expertise en Analyse Environnementale du Québec (2014). *Détermination des Métaux : Méthode par Spectrométrie de Masse à Source Ionisante au Plasma D'argon*, Vol. 9. Quebec, QC: Ministère du Développement Durable de l'environnement et de la Lutte contre les Changements Climatiques du Québec.

Chan, A. K. Y., Xu, W. Z., Liu, X. S., Cheung, S. G., and Shin, P. K. S. (2016). Sediment characteristics and benthic ecological status in contrasting marine environments of subtropical Hong Kong. *Mar. Pollut. Bull.* 103, 360–370. doi: 10.1016/j.marpolbul.2015.12.032

Chapman, P. M. (2016). Assessing and managing stressors in a changing marine environment. *Mar. Pollut. Bull.* 124, 587–590. doi: 10.1016/j.marpolbul.2016.10.039

Clarke, K. R. (1990). Comparisons of dominance curves. *J. Exp. Mar. Biol. Ecol.* 138, 143–157. doi: 10.1016/0022-0981(90)90181-B

Clarke, K. R., and Warwick, R. M. (1998). A taxonomic distinctness index and its statistical properties. *J. Appl. Ecol.* 35, 523–531. doi: 10.1046/j.1365-2664.1998.3540523.x

Covich, A. P., Austen, M. C., Bärlocher, F., Chauvet, E., Cardinale, B. J., Biles, C. L., et al. (2004). The role of biodiversity in the functioning of freshwater and marine benthic ecosystems. *BioScience* 54, 767–775.

Crain, C. M., Kroeker, K., and Halpern, B. S. (2008). Interactive and cumulative effects of multiple human stressors in marine systems. *Ecol. Lett.* 11, 1304–1315. doi: 10.1111/j.1461-0248.2008.01253.x

Daigle, R. M., Archambault, P., Halpern, B. S., Lowndes, J. S. S., and Côté, I. M. (2017). Incorporating public priorities in the Ocean Health Index: Canada as a case study. *PLoS One* 12:e0178044. doi: 10.1371/journal.pone.0178044

Dale, M. R. T., and Fortin, M.-J. (2014). *Spatial Analysis: A Guide for Ecologists*, 2nd Edn. Cambridge: Cambridge University Press. doi: 10.1017/CBO9780511978913

Dauer, D. M. (1993). Biological criteria, environmental health and estuarine macrobenthic community structure. *Mar. Pollut. Bull.* 26, 249–257. doi: 10.1016/0025-326X(93)90063-P

Dauvin, J. C., and Ruellet, T. (2007). Polychaete/amphipod ratio revisited. *Mar. Pollut. Bull.* 55, 215–224. doi: 10.1016/j.marpolbul.2006.08.045

Dauvin, J. C., Bellan, G., and Bellan-Santini, D. (2010). Benthic indicators: From subjectivity to objectivity – Where is the line? *Mar. Pollut. Bull.* 60, 947–953. doi: 10.1016/j.marpolbul.2010.03.028

Davies, B. E. (1974). Loss-on-ignition as an estimate of soil organic matter. *Soil Sci. Soc. Am. J.* 38:150. doi: 10.2136/sssaj1974.03615995003800010046x

Degen, R., and Faulwetter, S. (2019). The arctic traits database – a repository of arctic benthic invertebrate traits. *Earth Syst. Sci. Data* 11, 301–322. doi: 10.5194/essd-11-301-2019

Demers, K. A., Le Hénaff, A., and Carrière, J. (2018). "État des glaces," in *Observatoire Environnemental de la Baie de Sept-Îles*, ed. J. Carrière (Sept-Îles, QC: INREST), 593–612.

Department of Fisheries and Oceans (2002). *Canada's Oceans Strategy: Our Oceans, Our Future*. Ottawa, QC: Fisheries and Ocean Canada.

Department of Fisheries and Oceans (2009). *Development of a Framework and Principles for the Biogeographic Classification of Canadian Marine Areas*. Ottawa, QC: Canadian Science Advisory Secretariat.

Department of Fisheries and Oceans (2019). *Update of Stock Status Indicators for Northern Shrimp in the Estuary and Gulf of St. Lawrence. Canadian Science Advisory Secretariat*. Ottawa, ON: Department of Fisheries and Oceans.

DEVOTES (2012). *DEVelopment Of Innovative Tools for Understanding Marine Biodiversity and Assessing Good Environmental Status (DEVOTES)*. Available online at: http://www.devotes-project.eu (accessed February 26, 2021).

Dreujou, E., McKindsey, C. W., Grant, C., Tréau de Coeli, L., St-Louis, R., and Archambault, P. (2020). Biodiversity and habitat assessment of coastal benthic communities in a Sub-Arctic Industrial Harbor Area. *Water* 12:2424. doi: 10.3390/w12092424

Dreujou, E., Paquette, L., Grant, C., Archambault, P., and Carrière, J. (2018). "Caractérisation de la faune benthique," in *Observatoire Environnemental de la Baie de Sept-Îles*, ed. J. Carrière (Sept-Îles, QC: INREST), 377–452.

Dutil, J.-D., Proulx, S., Galbraith, P. S., Chasse, J., Lambert, N., and Laurian, C. (2012). Coastal and epipelagic habitats of the estuary and Gulf of St. Lawrence. *Canad. Tech. Rep. Fisher. Aquat. Sci.* 3009, 1–87.

Environment Canada and Ministère du Développement Durable de l'environnement et des Parcs du Québec (2007). *Criteria for the Assessment of Sediment Quality in Quebec and Application Frameworks: Prevention, Dredging and Remediation. Criteria for the Assessment of Sediment Quality in Quebec and Application Frameworks: Prevention, Dredging and Remediation*. Québec, QC: Environment Canada and Ministère du Développement Durable de l'environnement et des Parcs du Québec.

EoL (2020). *Encyclopedia of Life (EoL)*. Available online at: https://eol.org (accessed February 26, 2021).

European Commission (2008). *Directive 2008/56/EC of the European Parliament and the Council of 17 June 2008 Establishing a Framework for Community Action in the Field of Marine Environmental Policy (Marine Strategy Framework Directive)*. Luxembourg: European Commission.

Ferraro, S. P., and Cole, F. A. (2004). Optimal benthic macrofaunal sampling protocol for detecting differences among four habitats in Willapa Bay, Washington, USA. *Estuaries* 27, 1014–1025. doi: 10.1007/BF02803427

Folk, R. L. (1980). *Petrology of Sedimentary Rocks*, 2 Edn. Austin, TX: Hemphill Publishing Company. doi: 10.1017/cbo9780511626487

Gillett, D. J., Weisberg, S. B., Grayson, T., Hamilton, A., Hansen, V., Leppo, E. W., et al. (2015). Effect of ecological group classification schemes on performance of the AMBI benthic index in US coastal waters. *Ecol. Indicat.* 50, 99–107. doi: 10.1016/j.ecolind.2014.11.005

Government of Canada (1996). *Oceans Act*. Ottawa, ON: Government of Canada.

Grall, J., and Glemarec, M. (1997). Using biotic indices to estimate macrobenthic community perturbations in the Bay of Brest. *Estuar. Coast. Shelf Sci.* 44, 43–53. doi: 10.1016/S0272-7714(97)80006-6

Gray, J. S. (1979). Pollution-induced changes in populations. *Philos. Transact. R. Soc. Lond. Ser. Biol. Sci.* 286, 545–561. doi: 10.1098/rstb.1979.0045

Gray, J. S., and Elliott, M. (2009). *Ecology of Marine Sediments: From Science to Management*. Oxford: Oxford University Press.

Halpern, B. S., Frazier, M., Afflerbach, J., Lowndes, J. S., Micheli, F., O'Hara, C., et al. (2019). Recent pace of change in human impact on the world's ocean. *Sci. Rep.* 9, 1–8. doi: 10.1038/s41598-019-47201-9

Halpern, B. S., Selkoe, K. A., Micheli, F., and Kappel, C. V. (2007). Evaluating and ranking the vulnerability of global marine ecosystems to anthropogenic threats. *Conserv. Biol.* 21, 1301–1315. doi: 10.1111/j.1523-1739.2007.00752.x

Heink, U., Hauck, J., Jax, K., and Sukopp, U. (2016). Requirements for the selection of ecosystem service indicators – the case of MAES indicators. *Ecol. Indicat.* 61, 18–26. doi: 10.1016/j.ecolind.2015.09.031

Hewitt, J. E., Anderson, M. J., and Thrush, S. F. (2005). Assessing and monitoring ecological community health in marine systems. *Ecol. Appl.* 15, 942–953. doi: 10.1890/04-0732

Himmelman, J. H. (1991). "Diving observations of subtidal communities in the Northern Gulf of St. Lawrence," in *The Gulf of St. Lawrence: Small Ocean or Big Estuary?*, (Ottawa, ON: Department of Fisheries and Oceans), 319–332.

Hooper, D. U., Chapin, F. I., Ewel, J., Hector, A., Inchausti, P., Lavorel, S., et al. (2005). Effects of biodiversity on ecosystem functioning: a consensus of current knowledge. *Ecol. Monogr.* 75, 3–35. doi: 10.1890/04-0922

Laliberté, E., and Legendre, P. (2010). A distance-based framework for measuring functional diversity from multiple traits. *Ecology* 91, 299–305. doi: 10.1890/08-2244.1

Laliberté, E., Legendre, P., and Shipley, B. (2014). *FD: Measuring Functional Diversity from Multiple Traits, and Other Tools for Functional Ecology*. R Package Version 1.0-12.

Largaespada, C., Guichard, F., and Archambault, P. (2012). Meta-ecosystem engineering: Nutrient fluxes reveal intraspecific and interspecific feedbacks in fragmented mussel beds. *Ecology* 93, 324–333. doi: 10.1890/10-2359.1

Lawton, J. H., and Jones, C. G. (1995). "Linking species and ecosystems: organisms as ecosystem engineers," in *Linking Species & Ecosystems*, eds C. G. Jones and J. H. Lawton (Boston, MA: Springer), 141–150. doi: 10.1007/978-1-4615-1773-3_14

Legendre, P., and Legendre, L. F. J. (1998). *Numerical Ecology*, 2nd Edn. Amsterdam: Elsevier.

Levin, P. S., Fogarty, M. J., Murawski, S. A., and Fluharty, D. (2009). Integrated ecosystem assessments: developing the scientific basis for ecosystem-based management of the ocean. *PLoS Biol.* 7:14. doi: 10.1371/journal.pbio.1000014

Levinton, J. S. (2013). *Marine Biology: Function, Biodiversity, Ecology*, 4th Edn. Oxford: Oxford University Press.

Link, H., Piepenburg, D., and Archambault, P. (2013). Are hotspots always hotspots? The Relationship between diversity, resource and ecosystem functions in the arctic. *PLoS One* 8:e0074077. doi: 10.1371/journal.pone.0074077

Magurran, A. E., and McGill, B. J. (2011). *Biological Diversity: Frontiers in Measurement and Assessment*. 1st Edn. Oxford: Oxford University Press.

Mason, N. W. H., Mouillot, D., Lee, W. G., and Wilson, J. B. (2005). Functional richness, functional evenness and functional divergence: the primary components of functional diversity. *Oikos* 111, 112–118. doi: 10.1111/j.0030-1299.2005.13886.x

Maurer, D., Nguyen, H., Robertson, G., and Gerlinger, T. (1999). The infaunal trophic index (ITI): its suitability for marine environmental monitoring. *Ecol. Appl.* 9, 699–713.

Miatta, M., Bates, A. E., and Snelgrove, P. V. R. (2021). Incorporating biological traits into conservation strategies. *Annu. Rev. Mar. Sci.* 13, 421–443. doi: 10.1146/annurev-marine-032320-094121

Moriarty, P. E., Hodgson, E. E., Froehlich, H. E., Hennessey, S. M., Marshall, K. N., Oken, K. L., et al. (2018). The need for validation of ecological indices. *Ecol. Indicat.* 84, 546–552. doi: 10.1016/j.ecolind.2017.09.028

Mouillot, D., Graham, N. A. J., Villéger, S., Mason, N. W. H., and Bellwood, D. R. (2013). A functional approach reveals community responses to disturbances. *Trends Ecol. Evol.* 28, 167–177. doi: 10.1016/j.tree.2012.10.004

Muxika, I., Borja, Á, and Bald, J. (2007). Using historical data, expert judgement and multivariate analysis in assessing reference conditions and benthic ecological status, according to the European Water Framework Directive. *Mar. Pollut. Bull.* 55, 16–29. doi: 10.1016/j.marpolbul.2006.05.025

Muxika, I., Borja, Á, and Bonne, W. (2005). The suitability of the marine biotic index (AMBI) to new impact sources along European coasts. *Ecol. Indicat.* 5, 19–31. doi: 10.1016/j.ecolind.2004.08.004

Niemi, G. J., and McDonald, M. E. (2004). Application of ecological indicators. *Annu. Rev. Ecol. Evol. Syst.* 35, 89–111. doi: 10.1146/annurev.ecolsys.35.112202.130132

Nozères, C., Bourassa, M.-N., Gendron, M.-H., Plourde, S., Savenkoff, C., Bourdages, H., et al. (2015). Using annual ecosystemic multispecies surveys to assess biodiversity in the Gulf of St. Lawrence. *Canad. Techn. Rep. Fish. Aquat. Sci.* 3149:126.

OBIS (2020). *Ocean Biodiversity Information System (OBIS)*. Available online at: https://www.obis.org (accessed February 17, 2021).

Oksanen, J., Blanchet, F. G., Friendly, M., Kindt, R., Legendre, P., McGlinn, D., et al. (2019). *vegan: Community Ecology Package*.

Orr, J. A., Vinebrooke, R. D., Jackson, M. C., Kroeker, K. J., Kordas, R. L., Mantyka-pringle, C., et al. (2020). Towards a unified study of multiple stressors: divisions and common goals across research disciplines. *Proc. R. Soc. B Biol. Sci.* 20:20200421. doi: 10.1098/rspb.2020.0421

Palomares, M., and Pauly, D. (2020). *SeaLifeBase*. Available online at: https://sealifebase.ca (accessed February 17, 2021).

Pearson, T. H., and Rosenberg, R. (1978). Macrobenthic succession in relation to organic enrichment and pollution of the marine environment. *Oceanogr. Mar. Biol. Annu. Rev.* 16, 229–311.

Pelletier, M. C., Gillett, D. J., Hamilton, A., Grayson, T., Hansen, V., Leppo, E. W., et al. (2018). Adaptation and application of multivariate AMBI (M-AMBI) in US coastal waters. *Ecol. Indicat.* 89, 818–827. doi: 10.1016/j.ecolind.2017.08.067

Piacenza, S. E., Barner, A. K., Benkwitt, C. E., Boersma, K. S., Cerny-Chipman, E. B., Ingeman, K. E., et al. (2015). Patterns and variation in benthic biodiversity in a large marine ecosystem. *PLoS One* 10:135. doi: 10.1371/journal.pone.0135135

Pinto, R., Patrício, J., Baeta, A., Fath, B. D., Neto, J. M., and Marques, J. C. (2009). Review and evaluation of estuarine biotic indices to assess benthic condition. *Ecol. Indicat.* 9, 1–25. doi: 10.1016/j.ecolind.2008.01.005

Pratt, D. R., Lohrer, A. M., Pilditch, C. A., and Thrush, S. F. (2014). Changes in ecosystem function across sedimentary gradients in estuaries. *Ecosystems* 17, 182–194. doi: 10.1007/s10021-013-9716-6

Quinn, G. P., and Keough, M. J. (2002). *Experimental Design and Data Analysis for Biologists*. Cambridge: Cambridge University Press.

R Core Team (2020). *R: A Language and Environment for Statistical Computing*. Vienna: R Core Team.

Rees, H. L., Hyland, J. L., Hylland, K., Mercer Clarke, C. S. L., Roff, J. C., and Ware, S. (2008). Environmental indicators: Utility in meeting regulatory needs. An overview. *ICES J. Mar. Sci.* 65, 1381–1386. doi: 10.1093/icesjms/fsn153

Rice, J. (2003). Environmental health indicators. *Ocean Coast. Manag.* 46, 235–259. doi: 10.1016/S0964-5691(03)00006-1

Robert, P., McKindsey, C. W., Chaillou, G., and Archambault, P. (2013). Dose-dependent response of a benthic system to biodeposition from suspended blue mussel (Mytilus edulis) culture. *Mar. Pollut. Bull.* 66, 92–104. doi: 10.1016/j.marpolbul.2012.11.003

Rosenfeld, J. S. (2002). Functional redundancy in ecology and conservation. *Oikos* 98, 156–162.

Salas, F., Marcos, C., Neto, J. M., Patrício, J., Pérez-Ruzafa, A., and Marques, J. C. (2006). User-friendly guide for using benthic ecological indicators in coastal and marine quality assessment. *Ocean Coast. Manag.* 49, 308–331. doi: 10.1016/j.ocecoaman.2006.03.001

Santos, C., Ehler, C. N., Agardy, T., Andrade, F., Orbach, M. K., and Crowder, L. B. (2019). "Marine spatial planning," in *World Seas: An Environmental Evaluation*, ed. C. Sheppard (Cambridge, CA: Academic Press), 571–592. doi: 10.1016/B978-0-12-805052-1.00033-4

Schloss, I., Archambault, P., Beauchesne, D., Bourgault, D., Cusson, M., Dumont, D., et al. (2017). "Impacts potentiels cumulés des facteurs de stress liés aux activités humaines sur l'écosystème marin du Saint-Laurent dans Les hydrocarbures dans le golfe du Saint-Laurent — Enjeux sociaux, économiques et environnementaux," in *Les Hydrocarbures Dans le Golfe du Saint-Laurent — Enjeux Sociaux, Économiques et Environnementaux*, eds P. Archambault, I. Schloss, C. Grant, and S. Plante (Rimouski, QC: Notre Golfe), 132–165.

SDG (2015). *Sustainable Development Goals Knowledge Platform (SDG)*. Available online at: http://www.un.org/sustainabledevelopment/news/communications-material/ (accessed February 26, 2021).

Secretariat of the CBD (2010). *Aichi Biodiversity Targets*. Available online at: https://www.cbd.int/sp/targets/ (accessed February 26, 2021).

Shaw, J.-L. (2019). *Hydrodynamique de la Baie de Sept-Îles*. Master's thesis, Université du Québec à Rimouski, Rimouski.

Simard, N., Pereira, S., Estrada, R., and Nadeau, M. (2013). État de la situation des espèces envahissantes marines au Québec. *Rapp. manus. Can. sci. halieut. aquat.* 3020:61.

Simboura, N., and Zenetos, A. (2002). Benthic indicators to use in ecological quality classification of Mediterranean soft bottom marine ecosystems, including a new Biotic Index. *Mediter. Mar. Sci.* 3, 77–111.

Smeets, E., and Weterings, R. (1999). *Environmental Indicators: Typology and Overview*. Copenhagen: European Environment Agency.

Somerfield, P. J. (2008). Identification of the bray-curtis similarity index: comment on Yoshioka (2008). *Mar. Ecol. Prog. Ser.* 372, 303–306. doi: 10.3354/meps07841

Stachowicz, J. J., Bruno, J. F., and Duffy, J. E. (2007). Understanding the effects of marine biodiversity on communities and ecosystems. *Annu. Rev. Ecol. Evol. System.* 38, 739–766. doi: 10.1146/annurev.ecolsys.38.091206.095659

Statistics Canada (2011). *Shipping in Canada: 2011*. Ottawa, ON: Statistics Canada.

Sutherland, T. F., Levings, C. D., Petersen, S. A., Poon, P., and Piercey, B. (2007). The use of meiofauna as an indicator of benthic organic enrichment associated with salmonid aquaculture. *Mar. Pollut. Bull.* 54, 1249–1261. doi: 10.1016/j.marpolbul.2007.03.024

Teixeira, H., Berg, T., Uusitalo, L., Fürhaupter, K., Heiskanen, A. S., Mazik, K., et al. (2016). A catalogue of marine biodiversity indicators. *Front. Mar. Sci.* 3:207. doi: 10.3389/fmars.2016.00207

United Nations (1992). *Convention on Biological Diversity (CBD)*. New York, NY: United Nations. doi: 10.1016/B978-0-12-384719-5.00418-4

Villéger, S., Mason, N. W. H., and Mouillot, D. (2008). New multidimensional functional diversity indices for a multifaceted framework in functional ecology. *Ecology* 89, 2290–2301. doi: 10.1890/07-1206.1

Warwick, R. M., and Clarke, K. R. (1994). Relearning the ABC: taxonomic changes and abundance/biomass relationships in disturbed benthic communities. *Mar. Biol.* 118, 739–744. doi: 10.1007/BF00347523

Warwick, R. M., and Clarke, K. R. (1995). New 'biodiversity' measures reveal a decrease in taxonomic distinctness with increasing stress. *Mar. Ecol. Prog. Ser.* 129, 301–305. doi: 10.3354/meps129301

Wei, C. L., Cusson, M., Archambault, P., Belley, R., Brown, T., Burd, B. J., et al. (2020). Seafloor biodiversity of Canada's three oceans: patterns, hotspots and potential drivers. *Divers. Distribut.* 26, 226–241. doi: 10.1111/ddi.13013

Wentworth, C. K. (1922). A scale of grade and class terms for clastic sediments. *J. Geol.* 30, 377–392. doi: 10.1086/622910

Wilson, E. O. (1992). *The Diversity of Life*. Cambridge, MA: Harvard University Press.

Word, J. (1978). "The infaunal trophic index," in *Southern California Coastal Water Research Project*, ed. W. Bascom (Los Angeles, CA: Wiley), 19–39.

WoRMS Editorial Board (2020). *World Register of Marine Species (WoRMS)*. Available online at: http://marinespecies.org (accessed February 26, 2021).

Conflict of Interest: The authors declare that the research was conducted in the absence of any commercial or financial relationships that could be construed as a potential conflict of interest.

frontiers in Marine Science

ORIGINAL RESEARCH
published: 06 April 2021
doi: 10.3389/fmars.2021.662515

Identification of Main Oyster Species and Comparison of Their Genetic Diversity in Zhejiang Coast, South of Yangtze River Estuary

Sheng Liu[1,2], Qinggang Xue[1,2], Hongqiang Xu[1,2] and Zhihua Lin[1,2]**

[1] Institute of Mariculture Breeding and Seed Industry, Zhejiang Wanli University, Ningbo, China, [2] Zhejiang Key Laboratory of Aquatic Germplasm Resource, Zhejiang Wanli University, Ningbo, China

Oysters are an important aquaculture species distributed worldwide, including in Zhejiang Province, located on the east coast of China. Because of the high diversity and complicated introduction history of oysters and their seedlings, there has been much disagreement regarding the origin of each species, and the dominant and indigenous species remain unclear. We sampled 16 batches of oysters from seven sites in three aquaculture bays and found two main oyster species, *Crassostrea sikamea* and *Crassostrea angulata*. The former occupied the higher intertidal zone and comprised more than 70% of the cultured oysters. Based on the cytochrome oxidase C subunit I (COI) and mitochondrial noncoding region (MNR), *C. sikamea* showed higher genetic diversity than C. *angulata*. The analysis of molecular variance among COI sequences of these species from the Xiangshan Bay populations were comparable to those of other populations and showed that most of the molecular variance was within groups, which was consistent with the low pairwise fixation index F_{ST} values. The neutrality test revealed that *C. sikamea* experienced population expansion events, whereas for *C. angulata*, the significant Fu's *F*s and non-significant Tajima's *D* test results may indicate a possible population expansion event, implying that *C. sikamea* is likely an indigenous species. The method established based on internal transcribed spacer 1 digestion by the HindIII restriction enzyme is useful for identifying *C. sikamea* and *C. angulata* in the local region. The specific primers on the MNR sequence show potential for distinguishing *C. sikamea* from four other important *Crassostrea* oysters. These results highlight the abundance of *C. sikamea* on the Zhejiang coast and lay the foundation for protecting and utilizing the local oyster germplasm resources and for the sustainable development of the oyster industry.

Keywords: oyster distribution, Zhejiang coast, genetic diversity, dominant species, indigenous species, Kumamoto oyster

OPEN ACCESS

Edited by:
Marcos Rubal, University of Porto, Portugal

Reviewed by:
Sylvie Lapegue, Institut Français de Recherche pour l'Exploitation de la Mer (IFREMER), France
Zhang Yuehuan, South China Sea Institute of Oceanology (CAS), China

***Correspondence:**
Qinggang Xue
qxue@zwu.edu.cn
Zhihua Lin
zhihua9988@126.com

Specialty section:
This article was submitted to Marine Evolutionary Biology, Biogeography and Species Diversity, a section of the journal Frontiers in Marine Science

Received: *01 February 2021*
Accepted: *15 March 2021*
Published: *06 April 2021*

Citation:
Liu S, Xue Q, Xu H and Lin Z (2021) Identification of Main Oyster Species and Comparison of Their Genetic Diversity in Zhejiang Coast, South of Yangtze River Estuary. Front. Mar. Sci. 8:662515. doi: 10.3389/fmars.2021.662515

INTRODUCTION

Oysters are important marine aquaculture shellfish that are distributed globally, with an annual production of more than 6 million tons (Botta et al., 2020). There are abundant oyster resources in China, and the dominant species in the northern Liaoning and Shandong Provinces is the Pacific oyster *Crassostrea gigas* (Wang et al., 2008); in Fujian Province, the Portuguese oyster

(*C. angulata*) (Wang et al., 2010); and in Guangdong and Guangxi Provinces, the Hong Kong oyster (*C. hongkongensis*) (Lam and Morton, 2003) and Suminoe oyster (*C. ariakensis*) (Wang et al., 2004). Zhejiang Province is located on the east coast of China, south of the Yangtze River estuary. According to a newly unearthed shell mound, oysters have been utilized for at least 8000 years in the local area (Kaihao, 2020). Important aquaculture bays include Xiangshan Bay, Sanmen Bay, and Yueqing Bay along the coast. The local aquaculture history of the oyster is approximately 800 years old, dating back to the Song dynasty (A.D. 1225). Furthermore, the "Xidian oyster," cultured in the Xidian region, was listed as a tribute to the royal family of the Qing Dynasty and enjoyed a high reputation. As a highly important farmed shellfish in Zhejiang Province, oyster production reached 223,000 tons in 2019 (Bureau of Fisheries, 2020).

Traditionally, Zhejiang's local oysters are obviously different from the above-mentioned dominant species in terms of shell shape, low growth rate, and small body size, and they have been called monk-hat oysters. Previous research found that the most common small oyster in Zhejiang is *C. angulata* (Wang et al., 2010) which is thought to be the main oyster cultured in Zhejiang and Fujian Provinces (Li et al., 2015). Kumamoto oysters (Wang et al., 2013) and Suminoe oysters (Wang et al., 2004) are also distributed in this area, although species abundance has not been reported. In addition, the Pacific oyster *C. gigas* was introduced approximately 20 years ago, in the 1980s, from southern Japan and the spats were thought to have settled, whereas this oyster was gradually abandoned for various reasons (Jin, 2000). Some studies have reported that hybridization occurs naturally between *C. gigas* and *C. angulata* (Huvet et al., 2004). Moreover, for approximately 30 years, local oyster farmers generally purchased seedlings from different locations in Fujian Province, of which the majority are *C. angulata,* and the introduced spat could obviously improve oyster industry yields. These conditions have increased the complexity of oyster species along the coast of Zhejiang. The exchange of seedlings may impact the genetic structure of indigenous populations and reduce genetic diversity (Guo, 2009).

Mitochondrial DNA sequences, such as cytochrome oxidase C subunit I (COI), are preferred genetic markers because they are highly conserved protein-coding genes in the mitochondrial genome of animals (Folmer et al., 1994); thus, they have been widely used for species identification and genetic diversity assessment of mollusks (Hsiao et al., 2016; Sekino et al., 2016; In et al., 2017; Nowland et al., 2019; Özcan Gökçek et al., 2020; Tan et al., 2020; Melo et al., 2021) and other invertebrates (Yue et al., 2020). Moreover, a mitochondrial noncoding region (MNR) lying between the Gly and Val tRNA synthetase regions has the potential to distinguish different oyster populations (Aranishi and Okimoto, 2005) and has recently been used to analyze the population genetics of *C. gigas* and *C. angulata* in Europe and Asia (Moehler et al., 2011; Grade et al., 2016).

Owing to high similarities in the appearance and sympatric distribution of up to four oyster species in many regions (Huvet et al., 2004; Wang and Guo, 2008a; Camara et al., 2009; Xia et al., 2009), distinguishing oyster species based on shell morphology is unreliable and misleading. Several methods have been established for oyster species determination (Wang and Guo, 2008a; Cordes and Reece, 2009; Xia et al., 2009; Wang et al., 2014); however, simpler methods with improved targeting for identifying specific oyster species in the local region need to be established.

In view of the high diversity and complicated introduction history of oysters in Zhejiang Province, efforts are needed to maintain the characteristics and diversity of local oysters. In this study, we aimed to clarify the dominant oyster species on the Zhejiang coast, determine the genetic diversity of different oyster populations based on molecular markers, confirm the indigenous species, and establish specific methods for identifying local oyster species. These results may lay the foundation for the subsequent protection and utilization of local oyster germplasm resources and the sustainable development of the oyster industry.

MATERIALS AND METHODS

Sample Collection

To identify the main oyster species and their distributions, samples from seven sites (**Table 1** and **Figure 1**) were collected from July 2019 to August 2020 in the three major aquaculture bays on the Zhejiang coast. Samples from the upper region of the intertidal zone (muddy intertidal) and longline-cultured samples from intertidal wild spats were collected from all the sampling sites. For one site in Xiangshan Bay (Chunhu), samples from the subtidal region were collected from fish culture cages and longline-cultured samples (spat from Fujian Province) were also collected (**Figure 2**). Thirty oysters of different oyster types were randomly sampled from each location for species identification. To measure growth-related traits, one cultured oyster population from each bay was sampled in August 2020. Shell height, length, and width were measured using vernier calipers (0.01 mm) and total weight was measured using an electronic balance (0.01 g).

TABLE 1 | Oysters sampling sites for species identification.

Location	Abbreviation	Latitude	Longitude	References
Xidian (Xiangshan bay)	XSB	29.474	121.422	This study
Chunhu (Xiangshan bay)		29.492	121.603	
Xianxiang (Xiangshan bay)		29.687	121.776	
Sanmen (Sanmen bay)	SMB	29.042	121.558	
Yishi (Sanmen bay)		29.206	121.486	
Wenling (Yueqing bay)		28.307	121.244	
Yueqing (Yueqing bay)	YQB	28.281	121.129	
Zhangzhou	ZZ	23.99	117.76	
Langqi dao	LQD	26.08	119.59	Li et al., 2015
Fuqing	FQ	25.67	119.47	
Putian	PT	25.42	119.11	
Shantou	ST	23.25	117.04	Grade et al., 2016
Keelung	KL	22.84	120.04	
Nantong	NT	32.11	121.54	Sekino et al., 2012
Ariake sea, Japan	JP	32.88	130.41	

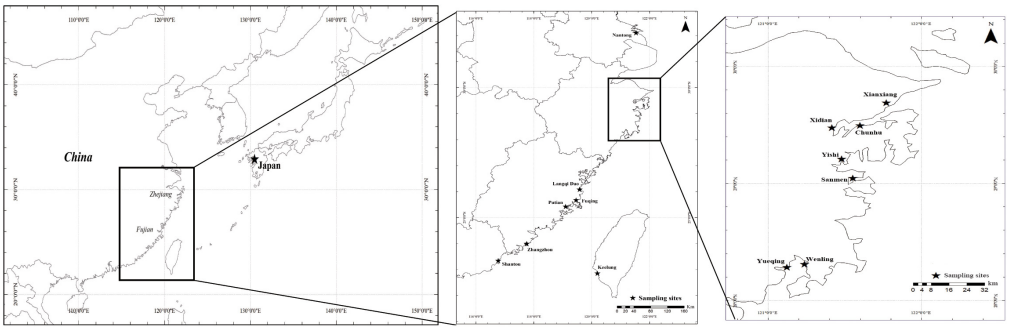

FIGURE 1 | Geographic location in this study, the main aquaculture bay—Xiangshan bay, Sanmen bay and Yueqing bay in the coast of Zhejiang Province as well as other related location including samples in Fujian province and Nantong.

FIGURE 2 | Oyster samples and their habitat. **(A)** Line 1–3 are cultured Kumamoto oyster sampled in Sanmen bay, Xiangshan bay and Yueqing bay, respectively, line 4 are Portuguese oyster sampled in the Xiangshan bay, line 5 are cultured Portuguese oysters originate of artificial breeding spat from Fujian province and line 6 are adult Portuguese oysters from Fujian province. **(B)** Oysters grown in the muddy intertidal zone. **(C)** Oyster seedling collection facilities using the abandoned bicycle tires as attachment in the intertidal zone. **(D)** The longline cultured oyster facilities in the local area hanging the abandoned bicycle tires directly.

After dissection, the mantle edge pigmentation was recorded as yellow or black. The adductor muscle was collected and quickly frozen in liquid nitrogen for subsequent DNA extraction and species identification.

For genetic diversity analysis of *C. angulata*, 88 sequences from Xiangshan Bay (abbreviated as XSB hereafter; $n = 37$) and Zhangzhou (abbreviated as ZZ hereafter; $n = 51$), and some COI haplotypes of Langqi dao (LQD, $n = 39$), Fuqing (FQ, $n = 29$), and Putian (PT, $n = 32$) from the Fujian coast were obtained from the NCBI nucleotide database (KP216768–KP216806), and the abundances of each haplotype in the populations were extracted from a previous study (Li et al., 2015). For MNR, 61 sequences from XSB ($n = 31$) and ZZ ($n = 30$), as well as some sequences (KY217737–KY217796) obtained from Shantou (ST, $n = 27$) and Keelung (KL, $n = 28$) of Guangdong and Taiwan Provinces were used. Haplotype distributions in different populations were included (Grade et al., 2016). For *C. sikamea*, COI sequences from XSB ($n = 63$), Sanmen Bay (SMB, $n = 46$), Yueqing Bay (YQB, $n = 50$), and ZZ ($n = 27$), and data from Nantong, China (CHH in the original paper, AB736731–AB736845), and Ariake Sea, Japan (ARK in the original paper, AB736621–AB736685) (Sekino et al., 2012) were selected for comparison. For MNR, only 147 sequences from XSB ($n = 42$), SMB ($n = 46$), YQB ($n = 34$), and ZZ ($n = 25$) were included; the geographic information of other samples is listed in **Table 1** and **Figure 1**.

Individual *C. gigas* oysters sampled from oyster farms in Qingdao, *C. ariakensis* and *C. hongkongensis* collected in Yangjiang, Guangdong Province, *C. sikamea* and *C. angulata* from XSB, SMB, YQB, and ZZ were selected to verify the method used to distinguish *C. sikamea* from other species.

DNA Extraction and Species Identification

Genomic DNA was isolated from the adductor muscle using a DNA kit (Tiangen, Beijing, China) according to the manufacturer's instructions. The integrity and concentration of DNA were determined using 1.2% agarose gel electrophoresis and spectrophotometry (Allsheng, Hangzhou, China). Oyster species were identified based on the sequences of nuclear internal transcribed spacer 1 (ITS1) and COI markers. The ITS1 fragment was amplified using ITS1-F (5′-GTTTCCGTAGGTGAACCTGC-3′) and ITS1-R (5′-ACACGAGCCGAGTGATCCAC-3′) (Wang and Guo, 2008b). The cycling conditions were as follows: initial denaturation at 94°C for 5 min, followed by 35 cycles of 94°C for 30 s, 50°C for 30 s, and 72°C for 40 s, with a final extension at 72°C for 10 min. Some COI fragments were amplified with universal primer pairs: LCO 1490 (5′-GGTCAACAAATCATAAAGATATTGG-3′) and HCO 2198 (5′-TAAACTTCAGGGTGACCAAAAAATCA-3′) (Folmer et al., 1994). Polymerase chain reactions (PCR) were performed in a final volume of 20 μL containing 7 μL of distilled water and 10 μL of Taq polymerase premix (TaKaRa, Dalian, China). The cycling conditions included initial denaturation at 94°C for 5 min, followed by 35 cycles of 94°C for 30 s, 50°C for 30 s, and 72°C for 50 s, followed by a final extension at 72°C for 10 min. The PCR products were sequenced by Hangzhou Tsingke Company (Hangzhou, China). The sequence was analyzed using BLAST in the NCBI server[1], and oyster species were identified according to the BLAST results of individual COI sequences. Considering that hybrid individuals have difficulty appearing in nature, two individuals were selected for each species and bay to construct a phylogenetic tree using MEGA (Version 6.0) based on the COI and ITS1 sequences of the same individual to eliminate the possible occurrence of hybrid oysters.

Genetic Diversity Analysis of Main Oyster Species

To analyze genetic diversity, COI and MNR were used as the target regions, and the COI sequences were amplified as described in section "DNA Extraction and Species Identification." Primers for MNR-F (5′-TCACAAGTACATTTGTCTTCCA-3′) and MNR-R (5′-AACGTTGTAAGCGTCATGTAAT-3′) were used according to (Aranishi and Okimoto, 2005; Grade et al., 2016). The PCR reaction volume and cycling conditions were the same as those described above.

To analyze the genetic diversity parameters, we calculated the number of polymorphic sites, number of haplotypes, haplotype diversity, average number of nucleotide differences, and nucleotide diversity for COI and MNR using DnaSP software (version 5) (Librado and Rozas, 2009).

Population differentiation was evaluated by computing the global fixation index F_{ST} using the Arlequin software (version 3.5) (Excoffier and Heidi, 2010). To explore the proportion of genetic variation among the populations, we conducted an analysis of molecular variance (AMOVA) in Arlequin. The significance of both the F_{ST} and AMOVA tests was assessed using 1000 permutations. A median joining (MJ) network of haplotypes was constructed using PopART (version 1.7[2]).

To analyze the demographic history of *C. angulata* and *C. sikamea*, Tajima's *D* (Tajima, 1989) and Fu's *F* (Fu, 1997) were calculated, and a mismatch distribution using DnaSP was assessed to test whether they experienced population expansion.

Methods for Identifying *C. sikamea*

ITS1 sequences from NCBI were analyzed (KX345544–KX345547 and KF370432–KF370439 for *C. sikamea* and KU726931–KU726939 and AB735529–AB735533 for *C. angulata*). The HindIII digestion site AGGCCT appeared in the sequence of *C. angulata*, but not in that of *C. sikamea* (**Supplementary Figure 2**). The ITS1 sequence was amplified as described in section "DNA Extraction and Species Identification." The enzyme digestion reaction system contained 3 μL of the PCR product, 1 μL of HindIII (NEB, Ipswich, United Kingdom), 5 μL of the enzyme buffer, and 11 μL of distilled water at a final volume of 20 μL. The reaction was performed in a water bath at 37°C for 60 min.

To design the MNR-specific primers, the complete mitochondrial genome sequences of *C. gigas, C. angulata, C. sikamea, C. ariakensis, C. hongkongensis, C. iredalei,* and *C. nippona* were downloaded and aligned

[1]https://blast.ncbi.nlm.nih.gov/Blast.cgi

[2]http://popart.otago.ac.nz

(**Supplementary Figure 2**). Specific primers were designed for identifying *C. sikamea* based on the mitochondrial non-coding region (MNR-F :5′-TCACAAGTACATTTGTCTTCCA-3′, MNR-S-R: 5′-AGGCTTTCACTCCACTTACT-3′, MNR-R :5′-AACGTTGTAAGCGTCATGTAAT-3′). The PCR reaction volume and cycling conditions were the same as those used for MNR amplification, except that adding three kind of primers instead of two. The product was tested using 1.2% agarose gel electrophoresis for both enzyme digestion and the specific PCR.

RESULTS

Oyster Species Identification in Three Local Bays

Species Distribution and Proportion

There were mainly two oyster species by molecule method in the sampled region: *C. sikamea* and *C. angulata* (**Table 2**). At all seven sites, all oysters sampled in the muddy intertidal area were *C. sikamea*. For longline-cultured oysters from the intertidal wild spat of XSB, 67–70% of the oysters were *C. sikamea,* and the remaining were *C. angulata*. The longline-cultured oysters originating from spats bought from Fujian Province by local farmers were all *C. angulata*. Among the subtidal samples collected from fish culture cages, the Portuguese and Kumamoto oysters comprised 67% and 33% of the samples, respectively. In SMB, for longline-cultured oysters from intertidal wild spat, 87%–97% of the oysters were *C. sikamea*, whereas the rest were *C. angulata*. In YQB, all longline-cultured oysters from intertidal wild spats were *C. sikamea*. ITS1 sequencing and the phylogenetic tree eliminated the possibility of hybrid individuals in the three bays (**Figure 3**).

TABLE 2 | Oyster species distribution and proportion of different sampling sites.

Bays	Sites	Habitat	*C. sikamea* (%)	*C. angulata* (%)
Xiangshan Bay	Xidian	Muddy intertidal	100%	0
		Longline cultured (intertidal wild spat)	70%	30%
	Chunhu	Muddy intertidal	100%	0
		Longline cultured (intertidal wild spat)	70%	30%
		Longline cultured (spat from Fujian province)	0	100%
		Fish culture cage (subtidal)	33%	67%
	Xianxiang	Muddy intertidal	100%	0
		Longline cultured (intertidal wild spat)	67%	33%
Sanmen Bay	Sanmen	Muddy intertidal	100%	0
		Longline cultured (intertidal wild spat)	97%	3%
	Yishi	Muddy intertidal	100%	0
		Longline cultured (intertidal wild spat)	87%	13%
Yueqing Bay	Wenling	Muddy intertidal	100%	0
		Longline cultured (intertidal wild spat)	100%	0
	Yueqing	Muddy intertidal	100%	0
		Longline cultured (intertidal wild spat)	100%	0

Production Performance of the Two Oyster Species

The production performance of 1-year-old oysters is presented in **Table 3**. The shell height, length, and width and total weight of Kumamoto oysters in the three bays ranged from 32.1 ± 4.9 to 35.2 ± 3.3 mm, 22.3 ± 3.3 to 25.8 ± 3.1 mm, 15.1 ± 2.0 to 17.5 ± 1.9 mm, and 6.4 ± 2.2 to 7.5 ± 2.5 g, respectively. Moreover, the corresponding data for Portuguese oysters in XSB were 44.2 ± 4.3 mm, 30.9 ± 2.5 mm, 18.8 ± 1.9 mm, and 14.2 ± 3.3 g, respectively. The growth-related characteristics of Portuguese oysters in XSB were significantly larger than those of the Kumamoto oysters in the three bays. The shell height:length ratio ranged from 1.33 ± 0.19 to 1.46 ± 0.28, which was not significant between the Kumamoto and Portuguese oysters, whereas the shell height:width ratio was much lower for the Kumamoto oyster than for the Portuguese oyster in XSB, although this result was not significance ($p = 0.06$).

Mantle Edge Pigmentation

There were some differences in the mantle edge pigmentation of the Kumamoto and Portuguese oysters. Kumamoto oysters were 77–87% yellow and 13–23% black. In contrast, for Portuguese oysters, the mantle edges were 90% black and 10% yellow (**Table 3**).

Genetic Diversity of the Two Species Based on COI/MNR Sequences

Two mitochondrial sequences (COI and MNR) were amplified for genetic diversity analysis, and a COI fragment of 603 bp was obtained from 188 specimens of the Portuguese oyster. In total, 49 segregating sites and 44 haplotypes were identified. Haplotype diversity and nucleotide diversity were 0.836 ± 0.046 and 0.353 ± 0.039% for XSB and 0.869 ± 0.031 and 0.428 ± 0.036% for ZZ populations, respectively. For Kumamoto oysters, 543 bp sequences from 366 individuals were analyzed, and 105 segregating sites and 145 haplotypes were defined. Haplotype diversity ranged from 0.929 ± 0.027 to 0.983 ± 0.017 for XSB, SMB, YQB, and ZZ populations, and the nucleotide diversity ranged from 0.586 ± 0.053% to 0.727 ± 0.063% (**Table 4**).

For MNR, a 620-bp fragment was obtained from 116 specimens for subsequent analysis of Portuguese oysters, and 25–35 segregating sites and 11–24 haplotypes were found in the four populations, with 81 segregating sites and 67 haplotypes identified in total. The haplotype diversity ranged from 0.832 ± 0.052 (ST) to 0.977 ± 0.020 (ZZ) and nucleotide diversity from 0.59 ± 0.09% (KL) to 0.78 ± 0.07% (XSB). For the Kumamoto oysters, 172 segregating sites and 119 haplotypes were found in 151 individuals. The haplotype diversity and nucleotide diversity were 0.969 ± 0.021 to 1.0 ± 0.011 and 1.02 ± 0.10% to 1.44 ± 0.12%, respectively (**Table 5**). Haplotypes were less common in this sequence, and the haplotype distributions are shown in **Supplementary Table 1**.

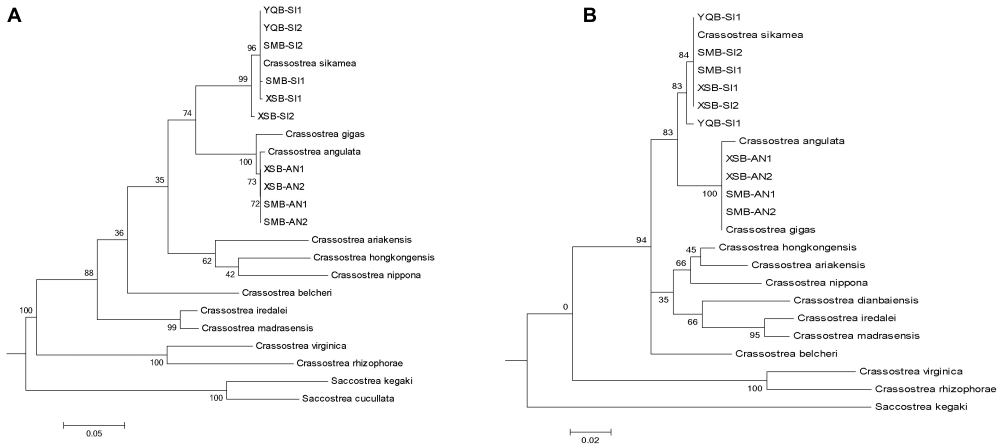

FIGURE 3 | The ITS1 and COI sequences of two identified individuals in each bay are randomly selected and the phylogenetic tree construction of representative oyster species in the database. Accession number of the reference sequences downloaded from NCBI database for **(A)** COI: *Crassostrea_sikamea,*EU007477*; Crassostrea_angulata,*LC383463*; Crassostrea_gigas,* MN862563*; Crassostrea_hongkongensis,*KP734091*; Crassostrea_ariakensis,* KF272859*; Crassostrea_nippona,* FJ743531*; Crassostrea_belcheri,* JF915511*; Crassostrea_iredalei,* JF915503*; Crassostrea_madrasensis,* JF915507*; Crassostrea_virginica,* KU905908*; Crassostrea_rhizophorae, HM003498; Saccostrea_kegaki,* LC110472. **(B)** ITS1: *Crassostrea sikamea,* FJ222345*; Crassostrea hongkongensis,* FJ222331*;Crassostrea gigas,* KM460835*; Crassostrea ariakensis,* EU252081*;Crassostrea angulata,* KU726937*;Crassostrea nippona,* FJ356679*;Crassostrea belcheri,* EU073256*;Crassostrea iredalei,* FJ222362*;Crassostrea madrasensis,* EU073237*;Crassostrea dianbaiensis,* AB972050*;Crassostrea virginica,*EU073344*;Crassostrea rhizophorae,KF370460;Saccostrea kegaki,*LC111294.

TABLE 3 | Production performance and mantle edge pigmentation distribution of one-year-old oysters of Kumamoto oyster and Portuguese oyster.

	Shell height (mm)	Shell length	Shell width	Total weight (g)	SH:SL	SH: SW	Margin-yellow	Margin-black
Cs-XSB	35.2 ± 3.3^{b}	25.1 ± 1.7^{b}	17.5 ± 1.9^{b}	7.3 ± 3.2^{ab}	1.41 ± 0.16^{a}	2.06 ± 0.46^{a}	77%	23%
Cs-SMB	34.2 ± 4.1^{ab}	25.8 ± 3.1^{b}	15.8 ± 4.0^{ab}	7.5 ± 2.5^{b}	1.33 ± 0.19^{a}	2.28 ± 0.58^{a}	87%	13%
Cs-YQB	32.1 ± 4.9^{a}	22.3 ± 3.3^{a}	15.1 ± 2.0^{a}	6.4 ± 2.2^{a}	1.46 ± 0.28^{a}	2.16 ± 0.39^{a}	83%	17%
Ca-XSB	44.2 ± 4.3^{c}	30.9 ± 2.5^{c}	18.8 ± 1.9^{b}	14.2 ± 3.3^{c}	1.43 ± 0.21^{a}	2.44 ± 0.60^{a}	10%	90%

Cs-XSB, Crassostrea sikamea sampled in Xiangshan bay; Cs-SMB, Crassostrea sikamea sampled in Sanmen bay; Cs-YQB, Crassostrea sikamea sampled in Yueqing bay; Ca-XSB, Crassostrea angulata sampled in Xiangshan bay.

Different letters mean that production performances of populations of Kumamoto oyster and Portuguese oyster are significantly different.

Genetic Differentiation and Population Expansion

To conduct the AMOVA among *C. angulata* mitochondrial COI sequences, two groups were defined, one included the XSB population and the other group included LQD, FQ, PT, and ZZ populations. The results showed that the majority of the molecular variance was within groups (99.74%), with −0.62% variance among groups and 0.89% among populations within groups. The variance components of the three origin types were not statistically significant ($p > 0.05$) in the AMOVA analysis. Similar results were obtained for Kumamoto oysters when defining the two groups as XSB with the combination of SMB, YQB, NT, and ZZ, as shown in **Table 6**.

Ten haplotypes were shared among the five *C. angulata* populations based on the COI sequence, and five of the most shared haplotypes (Hap1–2 and 4–6) were found in 71% (134/188) of all individuals. Several major haplotypes located in the center, with a few singletons or low-frequency haplotypes linked by short branches. The MJ haplotype network illustrates evident differences in the population structure between the two species. Furthermore, two haplotypes were shared among all *C. sikamea* populations, and 25 haplotypes were shared among at least two populations and were present in 6.3% and 53% of all individuals (**Supplementary Table 1**). The MJ network showed numerous minor haplotypes with no high proportions, and fewer haplotypes were shared (**Figure 4**).

Population pairwise F_{ST} values were generally low and not significant among the five tested Portuguese oyster populations based on the COI sequence (**Supplementary Table 2**). No significant F_{ST} was observed except for samples from Japan with the other five populations for the Kumamoto oyster (0.283–0.353, **Supplementary Table 2**). A non-significant value was found for both species based on the MNR fragment, except for two significant genetic differentiation populations with low F_{ST} values (**Supplementary Table 2**).

The neutrality test showed that Fu's *F* was significantly different from zero ($p < 0.05$) and Tajima's *D* was not significant ($p > 0.05$) for the Portuguese oyster based on the COI sequences; both parameters were observed to be significantly negative for the MNR fragment. For the four populations of Kumamoto oysters, both Tajima's *D* and Fu's *F*s tests showed

TABLE 4 | Genetic diversity parameters of *Crassostrea angulata* and *Crassostrea sikamea* based on COI sequence.

Species	Pop.	N	S	H	k	Hd	Pi(%)	Tajima's D	Fu'Fs
C. angulata	XSB	37	14	13	2.13	0.836 ± 0.046	0.353 ± 0.039	−1.17	−5.47*
	ZZ	51	17	16	2.59	0.869 ± 0.031	0.428 ± 0.036	−0.99	−6.15*
	LQD	39	21	17	2.35	0.866 ± 0.040	0.390 ± 0.048	−1.75*	−9.94*
	FQ	29	19	13	2.56	0.845 ± 0.059	0.425 ± 0.058	−1.64*	−5.38*
	PT	32	15	14	2.64	0.901 ± 0.032	0.439 ± 0.043	−0.96	−5.91*
	Total	188	49	44	Mean	0.861 ± 0.035	0.409 ± 0.042	−1.30	−6.57
C. sikamea	XSB	63	43	41	3.71	0.957 ± 0.017	0.684 ± 0.047	−1.97*	−26.04*
	SMB	46	31	26	3.18	0.929 ± 0.027	0.586 ± 0.053	−1.86*	−20.40*
	YQB	50	36	33	3.73	0.962 ± 0.018	0.687 ± 0.039	−1.81*	−25.99*
	ZZ	27	24	23	3.95	0.983 ± 0.017	0.727 ± 0.063	−1.32	−21.16*
	JP	65	17	15	1.31	0.695 ± 0.049	0.242 ± 0.039	−1.91*	−9.72*
	NT	115	61	61	3.53	0.953 ± 0.012	0.650 ± 0.037	−2.20*	−26.10*
	Total	366	105	145	Mean	0.959 ± 0.035	0.645 ± 0.039	−1.84*	−21.57*

S, Number of segregating sites; h, Number of haplotypes; Hd, Haplotype diversity; K, Average number of nucleotide differences; Pi (π), Nucleotide diversity. Asterisk means that Tajima's D or Fu'Fs test is different from zero ($p < 0.05$) and corresponding population may experience expansion.

TABLE 5 | Genetic diversity parameters of *Crassostrea angulata* and *Crassostrea sikamea* based on MNR sequence.

Species	Pop.	N	S	h	K	Hd	Pi(%)	Tajima's D	Fu'Fs
C. angulata	XSB	31	35	22	4.76	0.970 ± 0.017	0.78 ± 0.07	−1.66*	−13.21*
	ZZ	30	35	24	4.58	0.977 ± 0.020	0.75 ± 0.07	−1.81*	−18.82*
	ST	27	25	11	3.68	0.832 ± 0.052	0.60 ± 0.09	−1.57	−1.61
	KE	28	33	21	3.61	0.942 ± 0.037	0.59 ± 0.09	−2.11*	−16.45*
	Total	116	81	67	Mean	0.962 ± 0.010	0.73 ± 0.04	−1.77*	−12.56*
C. sikamea	XSB	42	80	40	7.41	0.998 ± 0.006	1.28 ± 0.14	−2.29*	−41.54*
	SMB	46	95	41	7.48	0.994 ± 0.006	1.31 ± 0.13	−2.39*	−38.09*
	YQB	38	62	27	5.99	0.969 ± 0.021	1.02 ± 0.10	−2.27*	−18.37*
	ZZ	25	59	25	8.26	1.0 ± 0.011	1.44 ± 0.12	−1.96*	−19.81*
	Total	151	172	119	Mean	0.993 ± 0.003	1.18 ± 0.06	−2.16*	−22.95*

S, Number of segregating sites; h, Number of haplotypes; Hd, Haplotype diversity; K, Average number of nucleotide differences; Pi (π), Nucleotide diversity. Asterisk means that Tajima's D or Fu'Fs test is different from zero ($p < 0.05$) and corresponding population may experience expansion.

significant results for the two sequences (**Tables 4**, **5**). The mismatch distribution was unimodal for *C. angulata* in XSB and ZZ and for *C. sikamea* populations in the six locations (**Supplementary Figure 1**).

Establishment of Species Identification Method

Considering that there are mainly two oyster species on the Zhejiang coast, the ITS1-RFLP method was established. The ITS1 product was digested with the HindIII restriction enzyme to obtain 200 and 310 bp fragments from *C. angulata*, and the product could not be confused for *C. sikamea*, leaving a 530 bp fragment, as shown in **Figure 5**.

To distinguish *C. sikamea* from additional oyster species, specific primers were designed based on the highly variable MNR. A 660 bp fragment was successfully amplified for *C. sikamea*, with a larger unspecific bands for *C. angulata, C. gigas, C. ariakensis,* or *C. hongkongensis* on the agarose gel (**Figure 5D**). For samples from XSB, SMB, YQB, and ZZ, a specific band was observed for *C. sikamea*, while a larger band was observed for *C. angulata* (**Figure 5C**).

DISCUSSION

Dominant Species and Its Distribution

In this study, oyster species were identified using molecular diagnosis based on the BLAST result of the COI sequence of

TABLE 6 | AMOVA of *C. angulata* and *C. sikamea* based on the COI sequence of XSB with other populations.

Groups	Source of variation	df	Sum of squares	Percentage of variation	*P*-value
C. angulata of XSB with LQD, FQ, PT, and ZZ	Among groups	1	0.261	−0.62	1.0
	Among populations within groups	3	1.202	0.89	0.158
	Within populations	183	79.037	99.74	0.190
C. sikamea of XSB with SMB, YQB, NT, and ZZ	Among groups	1	1.63	−0.37	0.795
	Among populations within groups	3	6.59	0.42	0.182
	Within populations	296	530.496	99.95	0.255

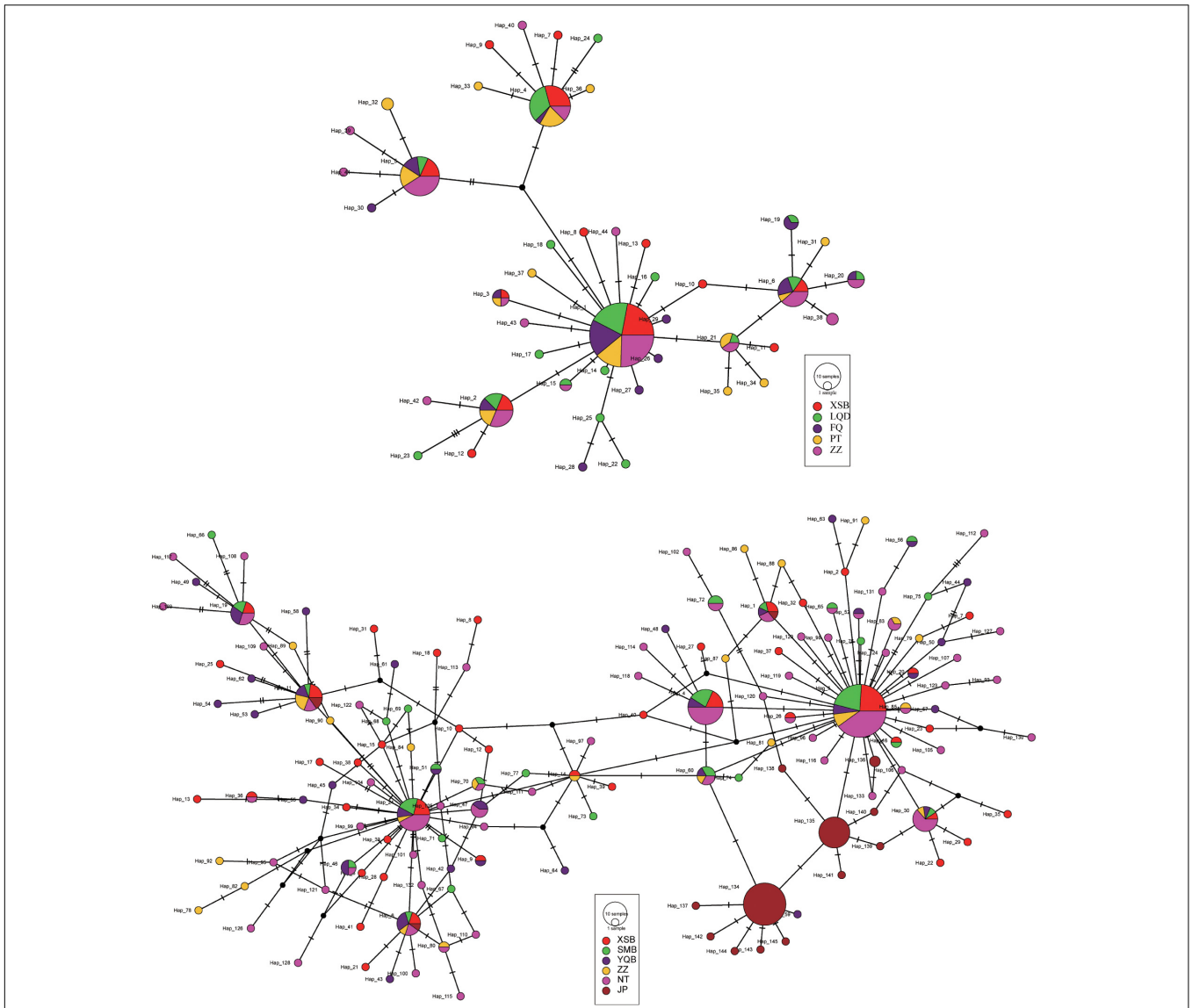

FIGURE 4 | Median joining network for *Crassostrea angulata* (upper) and *C. sikamea* (lower) COI haplotypes. The circles represent haplotypes, geographical population samples are marked by distinctive colors, and size of circles are in proportion to the haplotype frequencies. The number of perpendicular bars on branches represents the number of mutations between haplotypes.

individuals, and we found that *C. sikamea* was widely distributed and cultivated in large numbers on the Zhejiang coast. *C. sikamea* comprised more than 70% of the oyster samples in 14 batches collected from the three bays in this area. Zhejiang Province has an annual oyster production of approximately 223,000 metric tons (Bureau of Fisheries, 2020); thus, we speculate that at least 50,000 metric tons of this yield is *C. sikamea*. Previous studies have mentioned its occurrence in this area, but its abundance has not been reported (Wang et al., 2013). It is the dominant species on the Zhejiang coast, whereas in the Ariake Sea, where it was first found, and in the South Korean peninsula, it coexists with the Pacific oyster and was once thought to be endangered at these locations (Hedgecock et al., 1999). The natural distribution of this species has been reported to include South Korea and southern Japan (Ariake Sea and Seto Inland Sea) (Banks et al., 1994; Hamaguchi et al., 2013), southern China (Wang et al., 2013), and Vietnam (In et al., 2017). The Kumamoto oysters were distributed especially in the warmer estuary and intertidal zones. For instance, in Yueqing, samples were collected in the estuary of the Qingjiang River, and all oysters were *C. sikamea*. This species shows a habitat preference for estuaries with mesohaline environments (Camara et al., 2009). In addition, its more frequent occurrence in the middle and high regions of the intertidal zone in the estuaries of the Ariake Sea has been reported (Camara et al., 2009). Furthermore, the Kumamoto oyster occupies the intertidal zone, and the Suminoe oyster occupies the subtidal zone (Xu et al., 2009). These reports are consistent with our result that oysters

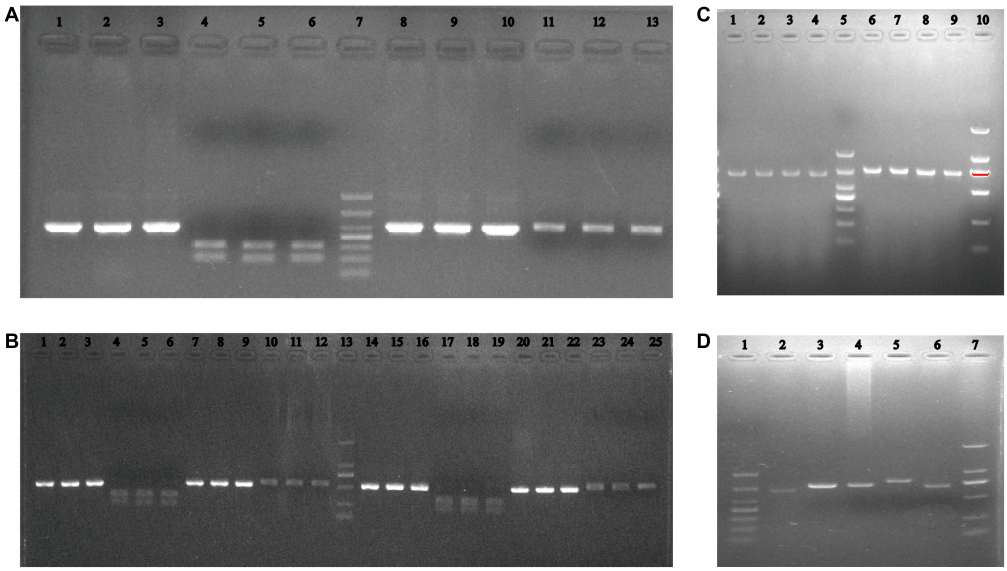

FIGURE 5 | Agarose electrophoresis of PCR-RFLP for ITS1 for oysters. **(A)** Lane 1–3 are PCR product of ITS1 of three individuals and lane 4–6 are corresponding digested product by Hind III restricted enzyme of *Crassostrea angulata* from ZZ and lane 8–13 are PCR product and corresponding digested product for *Crassostrea sikamea* from YQB and lane 7: DL1000 DNA marker. **(B)** Lane 1–6, 7–12: PCR product and corresponding digested product of three *Crassostrea angulata* and three *Crassostrea sikamea* individuals in XSB and lane 14–25 for SMB, lane 13:DL2000 DNA marker. Verification of MNR specific identification primer, agarose electrophoresis of **(C)** oysters samples from different geographic locations, lane 1–4: SMB, YQB, and ZZ, 6–9: *C.angulata* in XSB, SMB, YQB and ZZ; 5&10: DL1000 and DL2000 DNA marker; **(D)** five Crassostrea oysters, lane 2: *Crassostrea sikamea*, 3: *C.angulata*, 4: *C.gigas*,5 *C.ariakensis*,6: *C.hongkongensis* and lane 1&7: DL1000 and DL2000 DNA marker.

collected in the upper region of the intertidal zone were all *C. sikamea*, and of those collected in the subtidal zone, 67% were *C. angulata*.

Studies have found that the most common small-cupped oyster from Zhejiang to Hainan in southern China is *C. angulata*, which is also thought to be the main oyster cultured in Zhejiang and Fujian Provinces (Wang et al., 2010; Li et al., 2015). We found that the Portuguese oysters indeed exist in a narrow region and comprise 30% of the wild spat in XSB, which is a long and narrow bay with an inland distance of 60 km, and the salinity is higher (average salinity around 25) than that of SNB and YQB (You and Jiao, 2011). Portuguese oysters have been reported to be distributed as far as the Okinawa (Ryukyu Archipelago) and Shikoku Islands in southern Japan, although the authors were unsure whether the oysters were indigenous (Sekino and Yamashita, 2012; Sekino et al., 2016). The latitude of Zhejiang Province is similar to that of the above locations, and Portuguese oysters prefer high salinity and high-temperature environments (Shi et al., 2019); therefore, we cannot exclude the natural distribution of Portuguese oysters here.

The Kumamoto oyster is very small compared to the Portuguese oyster, with the former weighing half as much as the latter in this study, and this is the primary reason why local farmers transport oysters from Fujian Province. Kumamoto oysters tend to be deeper cupped than other species (Hedgecock et al., 1999; Camara et al., 2009). Our results seem to support the opinion that the shell height:width ratio for *C. sikamea* is smaller than that of *C. angulata* sampled in XSB. The shell shape seems to be heritable, although some studies have found that it has low heritability (Sang et al., 2019) or is affected mainly by the type of sediment (Mizuta and Wikfors, 2018).

For approximately 30 years, local oyster farmers in XSB have continually transported oyster seeds from Fujian Province, which is the core distribution area of the Portuguese oyster (Wang et al., 2010). As identified by us, artificial spawning seeds purchased from Fujian Province were all *C. angulata*, and they were usually transported in September and successfully spawned in the next summer in the local bay; thus, the origin of the Portuguese oyster is not clear. Moreover, we found that the mantle edge color was light for *C. sikamea* and dark for *C. angulata*. Mantle edge pigmentation has moderate heritability (0.215 ± 0.092) among Pacific oysters (Xing et al., 2017) and successive selective breeding for the golden-shell strains of this species has yielded lighter-margined oysters (Han and Li, 2019). Local farmers usually distinguish oysters by mantle color, as they believe that local oysters have yellow mantle edges, whereas imported ones have black mantle color. Therefore, it is necessary to perform genetic evaluations to analyze the indigenous oysters of the two species.

Genetic Diversity of the Two Species and Identification of Indigenous Species

For Portuguese oysters, the nucleotide and haplotype diversity based on the COI sequence of oysters collected in XSB was lower than that of the sampled populations from ZZ as well as four sites on the Chinese coast (Hsiao et al., 2016), and four populations on the Fujian coast (Li et al., 2015). The significant results of Fu's *Fs* test and non-significant Tajima's *D* test showed that the

Portuguese oysters in XSB may have experienced a population expansion event, and the unimodal distribution of nucleotide mismatch analysis also supported this conclusion. It seems that Portuguese oysters on the coast of southern China form a large group, and gene flow exists (Hsiao et al., 2016).

Taking into account that farmers in XSB have introduced large amounts of artificially spawned Portuguese oyster spats from many geographic locations ranging from the south to the north of Fujian Province for many years, the introduced or invasive species tend to show low genetic diversity. Oysters have great fecundity and high polymorphism in DNA sequences (Li et al., 2018); thus, even if the Portuguese oysters spat that were sampled in this study are not indigenous (the offspring of the introduced individuals), the genetic diversity should not be very low. Therefore, it is difficult to determine whether the oysters were the original or offspring of the introduced populations (Grade et al., 2016; Hsiao et al., 2016). Oyster larvae have a long swimming period of up to 3 or 4 weeks, and there are many islands along the coast of Zhejiang; therefore, it is possible that ocean currents drive larvae to settle (Sekino and Yamashita, 2012; Sekino et al., 2016). Molecular markers at the genome-wide level may be needed to further determine their exact source, such as with Pacific oysters in the Northern Hemisphere, where a clear lineage of different populations has been provided (Sutherland et al., 2020) and oysters in Europe (Vendrami et al., 2018).

For Kumamoto oysters, the nucleotide and haplotype diversity was much higher in our samples than in the Japanese and Korean populations, as well as in the Portuguese oysters based on the COI sequence (Sekino et al., 2012). High diversity was found in three Kumamoto oyster populations in Zhejiang Province when analyzing the population history of this species along the coastal regions of the Northwest Pacific (Hu et al., 2018). Significant Fu's *Fs* and Tajima's *D* test results showed that Kumamoto oysters on the Zhejiang coast experienced a population expansion event. There was no significant genetic differentiation among the XSB population and the other four populations along the coast of China (NT, SMB, YQB, and ZZ). However, populations sampled along the Zhejiang coast were quite distinct from the Japanese populations, and the MJ haplotype network indicated that fewer haplotypes were shared among all populations and that private haplotypes accounted for a larger proportion (Sekino et al., 2012). Kumamoto oyster populations on the Zhejiang coast show high genetic diversity comparable to that of other populations along the coast of China, and large-scale artificial spawning and breeding programs have not been conducted as has been done with the Pacific and Portuguese oysters.

Portuguese oysters are thought to be distributed south of the Yangtze River (Wang et al., 2010) and have not been found to the north (Wang et al., 2008), although sporadic reports exist (Lapègue et al., 2004). The diluted water of Changjiang may be a barrier for marine animal distribution to the north (Ni et al., 2017), whereas the distribution of Kumamoto oysters seems to cross this barrier, as indicated by the non-significant F_{ST}, implying its tolerance to low salinity (Camara et al., 2009). Our results indicate that the Kumamoto oysters have high genetic diversity and are likely an indigenous species along the coast of Zhejiang. Portuguese oysters have relatively low genetic diversity, but their sources require further exploration.

Distinguishing Kumamoto Oysters for Better Utilization of Resources

Conducting species identification to eliminate other oyster species before artificial breeding and exploring simple methods of species discrimination are highly important for protecting and utilizing Kumamoto oyster germplasm resources. Although the shell shape of Kumamoto oysters is somewhat different from that of other species, it remains difficult to classify oyster taxonomy according to morphology (Wang et al., 2004). Our results revealed a sympatric distribution between the Kumamoto and Portuguese oysters and between the Hong Kong and Suminoe oysters on the southern coast of China (Wang and Guo, 2008a; Xia et al., 2009).

The results of ITS1-RFLP showed that after digesting the PCR product of the ITS1 sequence with HindIII, the Kumamoto and Portuguese oysters could be clearly distinguished. The sequence alignment results also supported this finding (**Supplementary Figure 2**), as being an effective method for distinguishing between the Kumamoto and Pacific oysters and their artificial hybrids (Xu et al., 2019). This may reflect the subspecies relationship and sequence similarity of the Pacific and Portuguese oysters. The use of PCR-RFLP analysis of several gene fragments for distinguishing seven *Crassostrea* oysters from the South China Sea showed wider applicability, whereas it was somewhat difficult to utilize two or more restriction enzymes with one to five fragments after digestion (Xia et al., 2009).

The MNR sequence could be used to distinguish the Kumamoto oysters from the five main species of *Crassostrea* oysters, and the results of four populations (XSB, SMB, YQB, and ZZ) also demonstrated the versatility of this method. Previous results based on the MNR sequence have shown its potential in discriminating different populations of the Pacific and Portuguese oysters (Aranishi and Okimoto, 2005; Grade et al., 2016). It is not surprising that there are great differences between species because of the high polymorphism of the sequences. A multiplex PCR method based on COI was powerful and widely used for differentiating five *Crassostrea* species (Wang and Guo, 2008a) and we applied this method at the beginning of the species identification process; however, when distinguishing between Kumamoto and Portuguese oysters in XSB, sometimes the latter species exhibited two specific bands, which muddled the determination. Kumamoto oysters were mistaken as Pacific oysters from the Ariake Sea in Japan and introduced to the United States in the 1940s (Hedgecock et al., 1999). At that time, molecular identification methods were not established; therefore, the American population of Kumamoto oysters has been contaminated by Pacific oysters because of purposeful or unintentional hybridization (Hedgecock et al., 1999; Camara et al., 2009). These newly established species identification methods are more practical locally and it has a certain value for the identification of Kumamoto oysters in other regions.

In this study, we found abundant *C. sikamea* resources distributed along the Zhejiang coast, and these oysters preferred

intertidal and estuarial habitats. It is possible that at least 50,000 tons of the annual oyster production is *C. sikamea*, making this region the world's largest Kumamoto oyster farming area. Our results indicate that Kumamoto oysters have high genetic diversity and should be an indigenous species along the coast of Zhejiang. Portuguese oysters have relatively lower genetic diversity than Kumamoto oysters, but their sources require further exploration. Established species identification methods are of practical significance and are useful for broodstock discrimination. These results have enriched our understanding of the distribution and biological characteristics of Kumamoto oysters, and the genetic diversity assessment is beneficial for better protection and utilization of local oyster germplasm resources and for the development of the oyster industry.

DATA AVAILABILITY STATEMENT

The datasets presented in this study can be found in online repositories. The names of the repository/repositories and accession number(s) can be found below: https://www.ncbi.nlm.nih.gov/, MW675439-MW675650 for MNR, MW663490-MW663763 for cytochrome c oxidase subunit I (COX1) gene and MW481329-MW481338 for ITS1.

AUTHOR CONTRIBUTIONS

QX and ZL conceived and designed the study. SL and HX collected and sampled the oysters. SL performed the statistical analyses. SL and QX wrote and polished the manuscript. All authors read and approved the final manuscript.

FUNDING

This work was financially supported by the Project "Studies on Technologies for Disease Mitigation in Marine Mollusk Aquaculture" of "3315" Innovative Team of Ningbo City, the fundamental research foundation for Provincial University supported by Zhejiang Wanli University, Earmarked Fund for China Agriculture Research System (CARS-49), and the Science and Technology Planning Project of Ningbo City (2019C10046).

ACKNOWLEDGMENTS

We would like to sincerely thank Dr. Lin He for the designing and contacting the sampling site, Yuanyuan Zheng for map preparation, staffs of Fisheries Technical Extension Station of Fenghua, Ninghai, Sanmen, and Yueqing county for their kind support and information for oyster aquaculture, Frederico Batista in Cefas (United Kingdom) for providing the haplotype frequencies of the MNR sequence of Portuguese oysters we used in the manuscript, Jing Ye, Shoushuo Jian, and Loutao Xu for their help of sampling and Mr. Mingkun Liu for data analysis and using the software and Youli Liu for constructive discussion. We would like to thank Editage (www.editage.cn) for English language editing.

SUPPLEMENTARY MATERIAL

The Supplementary Material for this article can be found online at: https://www.frontiersin.org/articles/10.3389/fmars.2021.662515/full#supplementary-material

Supplementary Figure 1 | Nucleotide mismatch distribution analysis of *Crassostrea angulata* from XSB **(A)** and ZZ **(B)** as well as *Crassostrea sikamea* from XSB **(C)**, SMB **(D)**, YQB **(E)**, ZZ **(F)**, NT **(G)**, and JP **(H)**, the ordinate represents frequency of differences in the corresponding populations.

Supplementary Figure 2 | (A) The sequence alignment of the ITS1 of *Crassostrea sikamea* and *Crassostrea angulata*, of which the serial number and accession number in the NCBI database were included, Hind III restriction sites were highlighted. **(B)** The forward primer (MNR-F) and **(C)** reverse primer (MNR-S-R) alignment of the specific MNR of *Crassostrea sikamea* and other six Crassostrea oysters, of which the serial number and accession number in the NCBI database were included, primers sequences were highlighted.

REFERENCES

Aranishi, F., and Okimoto, T. (2005). Sequence polymorphism in a novel noncoding region of Pacific oyster mitochondria DNA. *J. Appl. Genet.* 46, 201–206.

Banks, M., McGoldrick, D., Borgeson, W., and Hedgecock, D. (1994). Gametic incompatibility and genetic divergence of Pacific and Kumamoto oysters, *Crassostrea gigas* and *C. sikamea*. *Mar. Biol.* 121, 127–135. doi: 10.1007/bf00349481

Botta, R., Asche, F., Borsum, J., and Camp, E. (2020). A review of global oyster aquaculture production and consumption. *Mar. Policy* 117:103952. doi: 10.1016/j.marpol.2020.103952

Bureau of Fisheries (2020). *China Fisheries Statistic Yearbook 2019*. Beijing: China Agriculture Press.

Camara, M., Davis, J., Sekino, M., Hedgecock, D., Li, G., Langdon, C., et al. (2009). The kumamoto oyster *Crassostrea sikamea* is neither rare nor threatened by hybridization in the Northern Ariake Sea. Japan. *J. Shellfish Res.* 27, 313–322. doi: 10.2983/0730-8000(2008)27[313:tkocsi]2.0.co;2

Cordes, J., and Reece, K. (2009). Discrimination of nine *Crassostrea* oyster species based upon restriction fragment-length polymorphism analysis of nuclear and mitochondrial DNA markers. *J. Shellfish Res.* 27, 1155–1161. doi: 10.2983/0730-8000-27.5.1155

Excoffier, L., and Heidi, L. (2010). Arlequin (version 3.5.1.2): an integrated software package for population genetics data analysis. *Evol. Bioinform. Online* 1, 47–50.

Folmer, O., Black, M., Wr, H., Lutz, R., and Vrijenhoek, R. (1994). DNA primers for amplification of mitochondrial Cytochrome C oxidase subunit I from diverse metazoan invertebrates. *Mol. Mar. Biol. Biotechnol.* 3, 294–299.

Fu, Y. X. (1997). Statistical tests of neutrality of mutations against population growth, hitchhiking and background selection. *Genetics* 147, 915–925. doi: 10.1093/genetics/147.2.915

Grade, A., Chairi, H., Lallias, D., Power, D., Ruano, F., Leitão, A., et al. (2016). New insights about the introduction of the Portuguese oyster, *Crassostrea angulata*, into the North East Atlantic from Asia based on a highly polymorphic mitochondrial region. *Aquatic. Living Resour.* 29:404. doi: 10.1051/alr/2016035

Guo, X. (2009). Use and exchange of genetic resources in molluscan aquaculture. *Rev. Aquacul.* 1, 251–259. doi: 10.1111/j.1753-5131.2009.01014.x

Hamaguchi, M., Shimabukuro, H., Kawane, M., and Hamaguchi, T. (2013). "A new record of the kumamoto oyster *Crassostrea sikamea* in the Seto Inland Sea, Japan," in *Marine Biodiversity Records*, ed. L. Ann (Cambridge: Cambridge University Press).

Han, Z., and Li, Q. (2019). Mendelian inheritance of orange shell color in the Pacific oyster *Crassostrea gigas*. *Aquaculture* 516:734616. doi: 10.1016/j.aquaculture.2019.734616

Hedgecock, D., Li, G., Banks, M., and Kain, Z. (1999). Occurrence of the kumamoto oyster *Crassostrea sikamea* in the Ariake Sea, Japan. *Mar. Biol.* 133, 65–68. doi: 10.1007/s002270050443

Hsiao, S.-T., Chuang, S.-C., Chen, K.-S., Ho, P.-H., Wu, C.-L., and Chen, C. (2016). DNA barcoding reveals that the common cupped oyster in Taiwan is the Portuguese oyster *Crassostrea angulata* (Ostreoida; Ostreidae), not *C. gigas*. *Sci. Rep.* 6:34057.

Hu, L., Zhang, Z., Wang, H., and Zhang, T. (2018). Molecular phylogeography and population history of *Crassostrea sikamea* (Amemiya, 1928) based on mitochondrial DNA. *J. Exp. Mar. Biol. Ecol.* 503, 23–30. doi: 10.1016/j.jembe.2017.11.004

Huvet, A., Fabioux, C., McCombie, H., Lapègue, S., and Boudry, P. (2004). Natural hybridization between genetically differentiated populations of *Crassostrea gigas* and *C. angulata* highlighted by sequence variation in flanking regions of a microsatellite locus. *Mar. Ecol. Prog. Series* 272, 141–152. doi: 10.3354/meps272141

In, V., O'Connor, W., Sang, V., Van, P., and Knibb, W. (2017). Resolution of the controversial relationship between Pacific and Portuguese oysters internationally and in Vietnam. *Aquaculture* 473, 389–399. doi: 10.1016/j.aquaculture.2017.03.004

Jin, B. (2000). A study on the status and perspective for oyster aquaculture inZhejiang province. *Mod. Fish. Inf.* 15, 6–10.

Kaihao, W. (2020). *A Shell of a Discovery, China Daily*. Available online at: https://www.chinadailyhk.com/article/132991 (accessed June 06, 2020).

Lam, K., and Morton, B. (2003). Mitochondrial DNA and morphological identification of a new species of *Crassostrea* (Bivalvia: Ostreidae) cultured for centuries in the Pearl River Delta, Hong Kong, China. *Aquaculture* 228, 1–13. doi: 10.1016/s0044-8486(03)00215-1

Lapègue, S., Batista, F., Heurtebise, S., Yu, Z., and Boudry, P. (2004). Evidence for the presence of the Portuguese oyster, *Crassostrea angulata*, in northern China. *J. Shellfish Res.* 23, 759–763.

Li, L., Li, A., Song, K., Meng, J., Guo, X. M., Li, S. M., et al. (2018). Divergence and plasticity shape adaptive potential of the Pacific oyster. *Nat. Ecol. Evol.* 2, 1751–1760. doi: 10.1038/s41559-018-0668-2

Li, S., Li, Q., Yu, H., and Kong, L. (2015). Genetic structure and population history of *Crassostrea angulata* from the coast of Zhejiang and Fujian Provinces. *J. Fish. China* 22, 1260–1269.

Librado, P. J. R., and Rozas, J. (2009). DnaSP v5: a software for comprehensive analysis of DNA polymorphism data. *Bioinformatics (Oxf. Engl.)* 25, 1451–1452. doi: 10.1093/bioinformatics/btp187

Melo, C., Divilov, K., Durland, E., Schoolfield, B., Davis, J., Carnegie, R., et al. (2021). Introduction and evaluation on the US West Coast of a new strain (Midori) of Pacific oyster (*Crassostrea gigas*) collected from the Ariake Sea, southern Japan. *Aquaculture* 531:735970. doi: 10.1016/j.aquaculture.2020.735970

Mizuta, D., and Wikfors, G. H. (2018). Seeking the perfect oyster shell: a brief review of the current knowledge. *Rev. Aquacul.* 11, 586–602. doi: 10.1111/raq.12247

Moehler, J., Wegner, M., Reise, K., and Jacobsen, S. (2011). Invasion genetics of Pacific oyster *Crassostrea gigas* shaped by aquaculture stocking practices. *J. Sea Res.* 66, 256–262. doi: 10.1016/j.seares.2011.08.004

Ni, G., Hassell, E., Dong, Y., and Park, J.-K. (2017). More than meets the eye: the barrier effect of the Yangtze River outflow. *Mol. Ecol.* 26, 4591–4602. doi: 10.1111/mec.14235

Nowland, S., Silva, C., Southgate, P., and Strugnell, J. M. (2019). Mitochondrial and nuclear genetic analyses of the tropical black-lip rock oyster (*Saccostrea echinata*) reveals population subdivision and informs sustainable aquaculture development. *BMC Genomics* 20:711. doi: 10.1186/s12864-019-6052-z

Özcan Gökçek, E., Acarli, S., Karahan, B., Vural, P., and Koban, E. (2020). First molecular record of the alien species Pacific oyster (*Crassostrea gigas*, Thunberg 1793) in the Marmara Sea. *Mar. Sci. Technol. Bull.* 9, 23–31. doi: 10.33714/masteb.668529

Sang, V., Knibb, W., Ngoc, N., In, V., O'Connor, W., Dove, M., et al. (2019). First breeding program of the Portuguese oyster *Crassostrea angulata* demonstrated significant selection response in traits of economic importance. *Aquaculture* 518:734664. doi: 10.1016/j.aquaculture.2019.734664

Sekino, M., Ishikawa, H., Fujiwara, A., and Yamashita, H. (2016). Occurrence of the Portuguese oyster *Crassostrea angulata* (Lamarck, 1819) along the coast of Shikoku Island, Japan. *Plankton Benthos Res.* 11, 71–74. doi: 10.3800/pbr.11.71

Sekino, M., Sato, S. i, Hong, J.-S., and Li, Q. (2012). Contrasting pattern of mitochondrial population diversity between an estuarine bivalve, the Kumamoto oyster *Crassostrea sikamea*, and the closely related Pacific oyster *C. gigas*. *Mar. Biol.* 159, 2757–2776. doi: 10.1007/s00227-012-2037-z

Sekino, M., and Yamashita, H. (2012). Mitochondrial DNA barcoding for Okinawan oysters: a cryptic population of the Portuguese oyster *Crassostrea angulata* in Japanese waters. *Fish. Sci.* 79, 61–76. doi: 10.1007/s12562-012-0577-2

Shi, B., Wu, Y., Zhou, L., You, W., and Ke, C.-H. (2019). Influence of gonadal development on metal accumulation in the Portuguese oyster, *Crassostrea angulata*, in subtropical areas. *Aquacul. Res.* 50, 1142–1152.

Sutherland, B. J. G., Rycroft, C., Ferchaud, A. L., Saunders, R., Li, L., Liu, S., et al. (2020). Relative genomic impacts of translocation history, hatchery practices, and farm selection in Pacific oyster *Crassostrea gigas* throughout the Northern Hemisphere. *Evol. Appl.* 13, 1380–1399. doi: 10.1111/eva.12965

Tajima, F. V. (1989). Statistical method for testing the neutral mutation hypothesis by DNA Polymorphism. *Genetics* 123, 585–595. doi: 10.1093/genetics/123.3.585

Tan, Y., Fang, L., Qiu, M., Huo, Z., and Yan, X. (2020). Population genetics of the Manila clam (*Ruditapes philippinarum*) in East Asia. *Sci. Rep.* 10:21890.

Vendrami, D., Houston, R., Gharbi, K., Telesca, L., Gutierrez, A. P., Gurney-Smith, H., et al. (2018). Detailed insights into pan-European population structure and inbreeding in wild and hatchery Pacific oyster (*Crassostrea gigas*) populations revealed by genome-wide SNP data. *Evol. Appl.* 12, 519–534. doi: 10.1111/eva.12736

Wang, H., and Guo, X. (2008a). Identification of *Crassostrea ariakensis* and related oysters by multiplex species-specific PCR. *J. Shellfish Res.* 27, 481–487. doi: 10.2983/0730-8000(2008)27[481:iocaar]2.0.co;2

Wang, H., Guo, X., Zhang, G., and Zhang, F. (2004). Classification of Jinjiang oysters Crassostrea rivularis (Gould, 1861) from China, based on morphology and phylogenetic analysis. *Aquaculture* 242, 137–155. doi: 10.1016/j.aquaculture.2004.09.014

Wang, H., Qian, L., Liu, X., Zhang, G., and Guo, X. (2010). Classification of a common cupped oyster from Southern China. *J. Shellfish Res.* 29, 857–866. doi: 10.2983/035.029.0420

Wang, H., Qian, L., Wang, A., and Guo, X. (2013). Occurrence and distribution of *Crassostrea sikamea* (Amemiya 1928) in China. *J. Shellfish Res.* 32, 439–446. doi: 10.2983/035.032.0224

Wang, H., Zhang, G., Liu, X., and Guo, X. (2008). Classification of common oysters from North China. *J. Shellfish Res.* 27, 495–503. doi: 10.2983/0730-8000(2008)27[495:cocofn]2.0.co;2

Wang, J., Xu, F., Li, L., and Zhang, G. (2014). A new identification method for five species of oysters in genus *Crassostrea* from China based on high-resolution melting analysis. *Chin. J. Oceanol. Limnol.* 32, 419–425. doi: 10.1007/s00343-014-3124-4

Wang, Y., and Guo, X. (2008b). ITS length polymorphism in oysters and its potential use in species identification. *J. Shellfish Res.* 27, 489–493. doi: 10.2983/0730-8000(2008)27[489:ilpioa]2.0.co;2

Xia, J., Yu, Z., and Kong, X. (2009). Identification of seven *Crassostrea* oysters from the South China Sea using PCR-RFLP analysis. *J. Molluscan Stud.* 75, 139–146. doi: 10.1093/mollus/eyp001

Xing, D., Li, Q., Kong, L., and Yu, H. (2017). Heritability estimate for mantle edge pigmentation and correlation with shell pigmentation in the white-shell strain of Pacific oyster. *Crassostrea gigas*. *Aquaculture* 482, 73–77. doi: 10.1016/j.aquaculture.2017.09.026

Xu, F., Zhang, G., Liu, X., Zhang, S., Shi, B., and Guo, X. (2009). Laboratory Hybridization between *Crassostrea ariakensis* and *C. Sikamea*. *J. Shellfish Res.* 28, 453–458.

Xu, H., Kong, L., Yu, H., and Liu, S. (2019). Fertilization, survival and growth of hybrids between *Crassostrea gigas* and *Crassostrea sikamea*. *Fish. Sci.* 85, 821–828.

You, Z., and Jiao, H. (2011). *Research on Ecological Environment Protection and Restoration Technology of Xiangshan Bay*. Beijing: China Ocean Press.

Yue, G. H., Xia, J., Cao, S., and Wang, C. (2020). Inferring the invasion mechanisms of the red swamp crayfish in China using mitochondrial DNA sequences. *Aquacul. Fish.* 6, 35–41.

Conflict of Interest: The authors declare that the research was conducted in the absence of any commercial or financial relationships that could be construed as a potential conflict of interest.

frontiers in Marine Science

ORIGINAL RESEARCH
published: 12 April 2021
doi: 10.3389/fmars.2021.641236

The Unique Amphipoda and Tanaidacea (Crustacea: Peracarida) Associated With the Brown Algae *Dictyota* sp. From the Oceanic Trindade Island, Southwestern Atlantic, With Biogeographic and Phylogenetic Insights

Tammy Iwasa-Arai[1,2], Silvana G. L. Siqueira[1], Juliana L. Segadilha[1,3] and Fosca P. P. Leite[1]*

[1] Departamento de Biologia Animal, Instituto de Biologia, Universidade Estadual de Campinas, Campinas, Brazil, [2] Programa de Pós-Graduação em Biologia Animal, Instituto de Biologia, Universidade Estadual de Campinas, Campinas, Brazil, [3] Laboratório de Carcinologia, Departamento de Invertebrados, National Museum, Federal University of Rio de Janeiro, Rio de Janeiro, Brazil

OPEN ACCESS

Edited by:
Jose Manuel Guerra-García, Seville University, Spain

Reviewed by:
Jesser F. Souza-Filho, Federal University of Pernambuco, Brazil
Charles Oliver Coleman, Museum of Natural History Berlin (MfN), Germany
Andre De Senna, Rio de Janeiro State University, Brazil

***Correspondence:**
Tammy Iwasa-Arai
araitammy@gmail.com

Specialty section:
This article was submitted to Marine Evolutionary Biology, Biogeography and Species Diversity, a section of the journal Frontiers in Marine Science

Received: 13 December 2020
Accepted: 09 March 2021
Published: 12 April 2021

Citation:
Iwasa-Arai T, Siqueira SGL, Segadilha JL and Leite FPP (2021) The Unique Amphipoda and Tanaidacea (Crustacea: Peracarida) Associated With the Brown Algae Dictyota sp. From the Oceanic Trindade Island, Southwestern Atlantic, With Biogeographic and Phylogenetic Insights. Front. Mar. Sci. 8:641236. doi: 10.3389/fmars.2021.641236

Oceanic islands are known by their unique evolutionary histories and high endemicity caused by isolation. This is the first survey on the biodiversity of Peracarida from Trindade Island, a volcanic island located about 1,160 km off the Brazilian coast, with the first reports of Tanaidacea from the island and the description of *Synapseudes isis* sp. nov. and three new species of Amphipoda (*Ampithoe thaix* **sp. nov.**, *Elasmopus gabrieli* **sp. nov.**, and *Eusiroides lucai* **sp. nov.**). The results of the phylogenetic analysis of *Synapseudes* based on morphological characters and its biogeography through the Bayesian Binary MCMC analysis (BBM) suggested an Indo-Pacific origin for the genus. Finally, the biodiversity of Trindade Island is compared to that of the Abrolhos Archipelago, the closest islands from the coast on the continental shelf, suggesting a high endemicity of Peracarida, corresponding to 44% of Amphipoda and 50% of Tanaidacea species in the island of Trindade.

Keywords: dispersal, event-based biogeography, cladistics, morphology, taxonomy

INTRODUCTION

Oceanic islands are of great interest because of their isolation, high endemicity, and evolutionary history (Pinheiro et al., 2017). The Trindade and Martin Vaz Archipelago, located southeastern off Brazil, is a unique place with high endemism rate compared to other Atlantic Ocean localities and the seamounts that connect Trindade and Martin Vaz to the South American continent, known as Vitória-Trindade Seamount Chain (VTC). These areas are considered a biodiversity hotspot for fishes and invertebrates (Pinheiro et al., 2015), with the number of new species described for VTC, and especially to the Trindade Island (TR), still rapidly increasing (Lima et al., 2019; Cunha et al., 2020; Pachelle and Tavares, 2020; Simone and Cavallari, 2020).

Among the environments found in TR, the rocky shores comprise a large amount of the coastal area, with tidepools being found all over the island (Macieira et al., 2015), providing a stressful

and changing habitat based on tide dynamics coupled with environmental characteristics and ecological processes that drive the community (Gibson, 1986). Such intertidal environment can harbor macrophytal beds that allow the increase of biodiversity by providing substrata to epiphytic algae and bryozoans and food resources and shelter to several vertebrates and invertebrates (Duffy and Hay, 1991; Christie et al., 2009). In the island of Trindade, 36 species of macroalgae were previously reported, including nine species of brown algae (Pereira-Filho et al., 2011).

These marine macrophytes form habitat patches to the epifaunal assemblages dominated by crustaceans of the order Peracarida (Tanaka and Leite, 2003), such as amphipods, isopods, and tanaidaceans, that have direct development and consequently low dispersion, favoring the establishment of endemic species (Hurtado et al., 2016; Pinheiro et al., 2017). However, data on Peracarida biodiversity from TR remain scarce, with only two amphipod species reported from the archipelago so far and one endemic to TR (Oliveira, 1951; Barnard, 1965; Andrade and Senna, 2017). Records of isopods from TR are still restricted to terrestrial fauna and ectoparasites (Barth, 1958; Moreira, 1977; Souza et al., 2013), while tanaidaceans are unknown.

Although benthic Peracarida members are considered to present high levels of endemicity, they show good ability to disperse long distances, especially on macroalgae, which provide both high food value and floating potential, once organisms with direct development may reproduce and their offspring recruit within the parental raft (Thiel, 2003). Therefore, according to Błażewicz-Paszkowycz et al. (2012), transport in floating algae (rafting) and vicariance are likely to create new habitats and to provide dispersion as well as to isolate populations, allowing them to diversify and speciate. However, the lack of studies on the events that have driven the current distribution of Peracarida associated with macroalgae hinders a better understanding of the evolutionary biogeographic processes involved.

Therefore, we aim to report on the Peracarida fauna associated with the brown algae of the genus *Dictyota* sp. from TR, with the first report of tanaidaceans and the description of one new species of *Synapseudes* (Tanaidacea: Apseudomorpha) and three new species of Amphipoda. We also comment on the phylogenetic position of the new species *Synapseudes isis* **sp. nov.** based on morphological characters and perform an event-based biogeographic analysis of the genus to further understand the processes underlying the faunal diversity associated with macroalgae worldwide. Finally, we provide a discussion on the biogeographical patterns inferred for Peracarida comparing the taxa from TR with those from the Abrolhos Archipelago, the closest islands from the coast on the continental shelf.

MATERIALS AND METHODS

Study Area

Specimens were collected from the brown algae of the genus *Dictyota* sp. under permission SISBIO 60924-3. Sampling was carried out on Trindade Island in September 2018 and April 2019 at Piscinas do Parcel (20°31′10.812″S, 20°31′10.812″W), Ilha do Sul (20°31′27.5″S, 29°19′25.2″W), and Piscina da Praia do Lixo (20°31′27.624″S, 29°19′22.188″W) (**Figure 1**).

The island of Trindade is located at the eastern limit of the VTC (20°30′S, 29°20′W) together with Martin Vaz, in southeastern Brazil, the easternmost group of islands off Brazil, about 1,160 km from the coast (**Figure 1**). Trindade and Martin Vaz hold the most isolated intertidal habitats within the Brazilian Province and are surrounded by calcareous algal reefs throughout the littoral zone (Gasparini and Floeter, 2001).

Sampling Method

Algal fronds were collected underwater by free diving, from 1 to 10 m, stored in fabric bags (0.2 mm mesh size) within seawater and washed off for fauna separation. The associated fauna was fixed and preserved in ethanol 90% for later identification. Appendages and mouthparts of dissected specimens were mounted on glass slides and sealed with glycerol. Drawings were made with a camera lucida at a Zeiss Axioscope stereomicroscope and digitally drawn with Inkscape. Types are deposited at the Museu de Zoologia da Universidade Estadual de Campinas (ZUEC).

Phylogenetic Analysis

We inferred the phylogenetic position of *Synapseudes isis* **sp. nov.** by analyzing published characters from the revision of Synapseudinae Guțu (1972). A character matrix was developed with 26 terminal taxa and 22 morphological characters, including 13 characters from the cephalothorax (including antennae, mouthparts, and cheliped), three from the pereon (including pereopods and gills), and six from the pleon (**Supplementary Materials 1, 2**). Characters were combined into multistate groupings to avoid overly dependent characters, resulting in nine binary characters, 11 multistate characters, and two continuous characters. Polarization of the characters was conducted through outgroup comparison. *Metapseudes wilsoni* Błażewicz-Paszkowycz and Bamber, 2007, and *Ronabus idios* (Gardiner, 1973) were chosen as out-groups based on Heard et al. (2018).

Data matrix of discrete characters was constructed using MorphoBank 3.0 (O'Leary and Kaufman, 2012), and continuous characters were subsequently added at the data file. We adopted the parsimony criterion and performed phylogenetic reconstructions in TNT version 1.1 (Goloboff et al., 2008). A heuristic analysis was conducted using the traditional search algorithm, with 8,000 replications and 500 trees held per replicate. Polymorphic characters were considered unordered. The branch-swapping algorithm used was "tree bisection and reconnection" (TBR). Branch support was calculated using the relative Bremer support (subtrees up to 10 extra steps; relative fit difference of 0.9; Bremer, 1994) implemented in TNT. Character polarization was conducted *a posteriori* according to Nixon and Carpenter (1993), and character optimization was made with Winclada (Nixon, 2002). For character discussion, the abbreviation used [SX(Y)] means the "state Y of character X" (Iwasa-Arai and Serejo, 2018; Iwasa-Arai et al., 2019). Synapomorphic characters whose secondary homology (sensu De Pinna, 1991) was rejected are herein

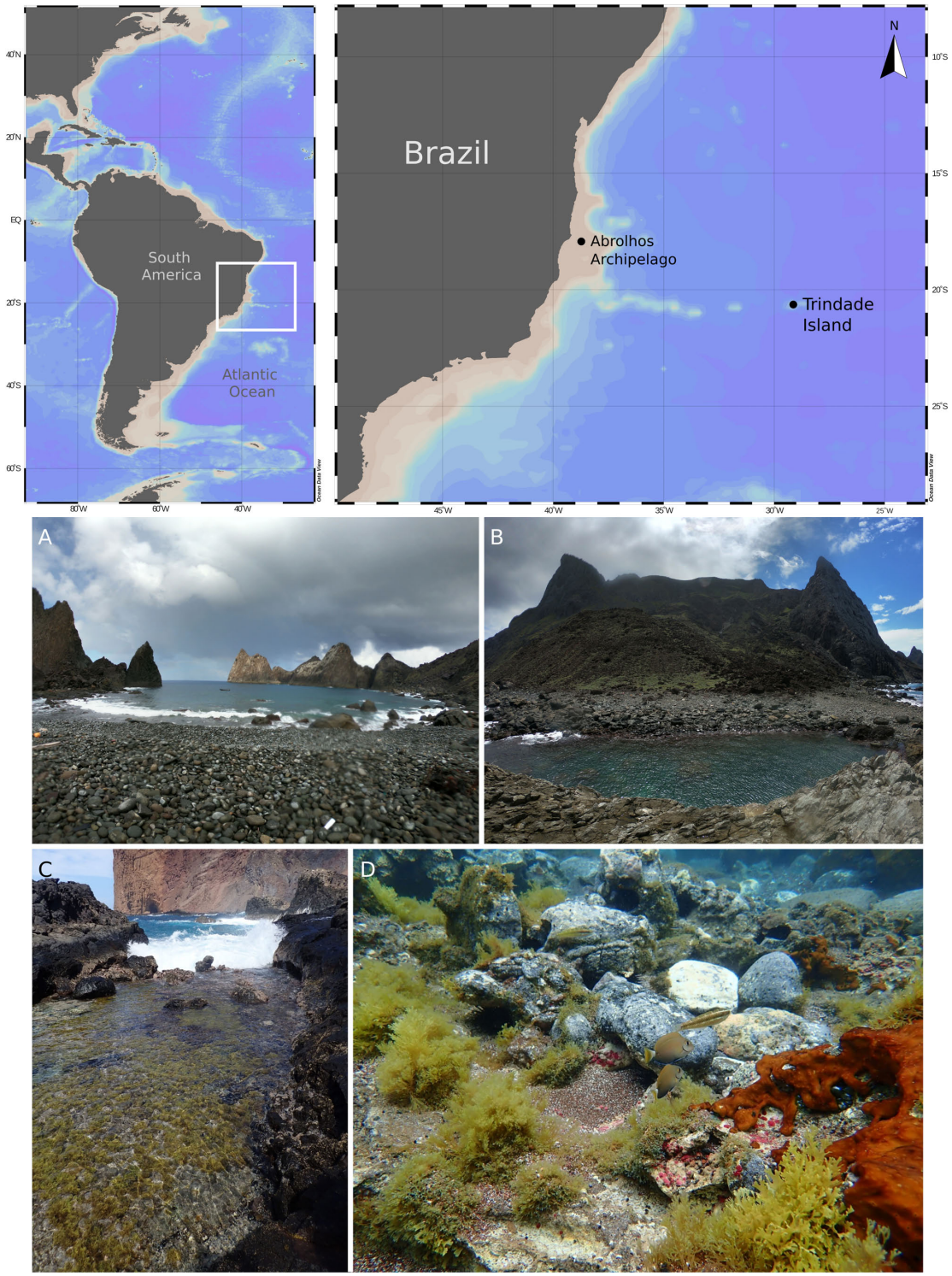

FIGURE 1 | Location of Trindade Island and Abrolhos Archipelago and sampling localities of *Dictyota* sp. at Trindade Island. **(A)** Ilha do Sul. **(B)** Piscina da Praia do Lixo. **(C,D)** Piscina do Parcel.

referred to as "homoplastic synapomorphy" synapomorphies (e.g., Wheeler et al., 1993; Gomes-da-Silva and Souza-Chies, 2017; Iwasa-Arai and Serejo, 2018).

The abbreviations used are as follows: A, antenna; Che, cheliped; CI, consistency index; Ep, pleonal epimera; f, female; Gn, gnathopod; Hd, head; l, left; L, length; LL, lower lip; m, male;

Md, mandible; Mx, maxilla; Mxp, Maxilliped; P, pereopod; Per, pereonite; Pl, pleon; r, right; RI, retention index; S, state; T, telson; and U, uropod; UL, upper lip.

Biogeographical Analysis

The distribution range of *Synapseudes* was divided into 12 areas based on the presence of one or more endemic species according to the marine realms proposed by Costello et al. (2017). These areas are Mediterranean (A), North Pacific (B), Mid-Tropical North Pacific (C), Caribbean and Gulf of Mexico (D), Gulf of California (E), Indo-Pacific and Indian Ocean (F), Coral Sea (G), Offshore Western Pacific (H), Offshore South Atlantic (I), and Rio de la Plata (J).

To examine the possible ancestral ranges of *Synapseudes*, we used the Bayesian Binary MCMC analysis (BBM) implemented in the program Reconstruct Ancestral State in Phylogenies (RASP; Yu et al., 2015) by using the morphological phylogeny described above (see section "*Materials and Methods, Phylogenetic Analysis*") as input topology. BBM was primarily designed for reconstructing the ancestral state of given nodes by calculating the probabilities of ancestral ranges using the probabilities of each area unit generated by MrBayes (Ronquist and Huelsenbeck, 2003), and it was chosen because of the ability to deal with phylogenetic uncertainty. The MCMC chains of BBM analysis were run simultaneously for two million generations, with a sampling frequency of every 100 generations and a 10% burn-in. The maximum number of areas for this analysis was kept at four.

RESULTS

Eleven species of Peracarida are reported herein associated with *Dictyota* sp. from TR. Since records of peracarid crustaceans for this location are scarce, all observations but one are new records for the island. Of the two amphipod species previously reported, *Elasmopus besnardi* Oliveira, 1951, is currently considered a synonym of *Elasmopus brasiliensis* (Dana, 1853; Horton et al., 2020), and *Cymadusa trindadensis* Andrade and Senna, 2017, endemic to TR, was the only previously reported species (**Figure 2**). Herein, we give the first records of Tanaidacea for TR, comprising two species, one new species of Apseudomorpha and one new record of Tanaidomorpha.

Taxonomy

Order Amphipoda Latreille, 1816

Suborder Senticaudata Lowry and Myers, 2013

Family Ampithoidae Boeck, 1871

Genus *Ampithoe* Leach, 1814

***Ampithoe marcuzzii* Ruffo, 1954**

(**Figures 2A,B**)

Ampithoe marcuzzii Ruffo, 1954: 120, figs I–II.—Barnard, 1958: 25.—Ortíz et al., 2007: 484.—Siqueira, 2012: 28, Anexo 1B.—Martín et al., 2013: 1705.—Paz-Ríos et al., 2013b: 9, fig. 9.—Campos et al., 2020: 2, figs. 1–3.

Ampithoe cf. *marcuzzii*—LeCroy, 2002: 245, fig. 262.

Material examined: Three individuals (not sexed), Piscinas do Parcel (20°31′10.812″S, 29°19′25.8″W), from *Dictyota* sp., September 2018, T. P. Macedo col. (ZUEC-CRU-4354); three individuals (not sexed), Ilha do Sul (20°31′27.5″S, 29°19′25.2″W), from *Dictyota* sp., April 2019, I. Batistela col. (ZUEC-CRU-4354).

Remarks: *Ampithoe marcuzzii* was described from Los Roques, Venezuela, and its current distribution ranges the western Atlantic Ocean, from Florida to state of São Paulo (SP), southeastern Brazil (Serejo and Siqueira, 2018; Campos et al., 2020). Specimens from TR are larger (up to 14 mm) than in the original description by Ruffo (1954), as observed by Siqueira (2012) in SP.

***Ampithoe suapensis* Correia et al., 2016**

Ampithoe suapensis Correia et al., 2016: 196, figs 1–4.

Material examined: Five individuals (not sexed), Piscinas do Parcel (20°31′10.812″S, 29°19′25.8″W), from *Dictyota* sp., September 2018, T. P. Macedo col. (ZUEC-CRU-4356).

Remarks: *Ampithoe suapensis* was previously known only from its type locality in Suape Beach, state of Pernambuco, Brazil. The TR specimens agree well with the original description of *A. suapensis*.

***Ampithoe thaix* Siqueira and Iwasa-Arai sp. nov.**

http://zoobank.org/F4432581-ECA0-49EE-90C0-3DE39566F7E1

(**Figures 3–5**)

Material examined: Holotype: male, Piscinas do Parcel (20°31′10.812″S, 29°19′25.8″W), from *Dictyota* sp., September 2018, T. P. Macedo col. (ZUEC-CRU-4357).

Paratype: one female, same as holotype. (ZUEC-CRU-4358).

Diagnosis: A2 heavily setose. Md palp article 2 2 × longer than article 3, with one or two setae on the margin. Mx1, inner plate with one seta. Gn1 slightly shorter than Gn2, Gn1 coxa produced anteriorly; propodus subrectangular and setose, palm transverse. Gn2, coxa oval; carpus with long setae on the anterior margin, propodus subrectangular, palm transverse with one robust seta. P5–7 propodus with 3–5 robust setae posteriorly. U1 with round spur apical margin of the peduncle, inner and outer rami lacking anterior robust setae. T subtriangular.

Etymology: This species is named after the marine biologist Thais Peixoto Macedo.

Description: Male (ZUEC-CRU-4357). Body (**Figure 3**). Length 4.7 mm.

Eyes rounded and well developed. A1 moderately setose; flagellum 13-articulate. A2 heavily setose; flagellum 8-articulate. UL rounded. LL notched, inner and outer lobes setose apically. rMd, incisor and *lacinia mobilis* seven- and four-toothed, respectively, accessory setal row with three serrated setae; palp 3-articulate, article 1 3.2 × shorter than article 2; article 2 2 × longer than article 3; article 3 1.5 × longer than article 1; article 3 with four long plumose setae apically. lMd, molar with one long plumose seta and one short seta; incisor and *lacinia mobilis* four- and five-toothed, respectively, accessory setal row with four serrated setae; palp 3-articulate, article 3 with four long plumose setae apically, similar to right palp. Mx1, inner plate small and rounded, inner margin with one single short seta; outer plate with seven stout serrated setae apically; palp 2-articulate with three stout setae and one long seta. Mx2, inner plate as

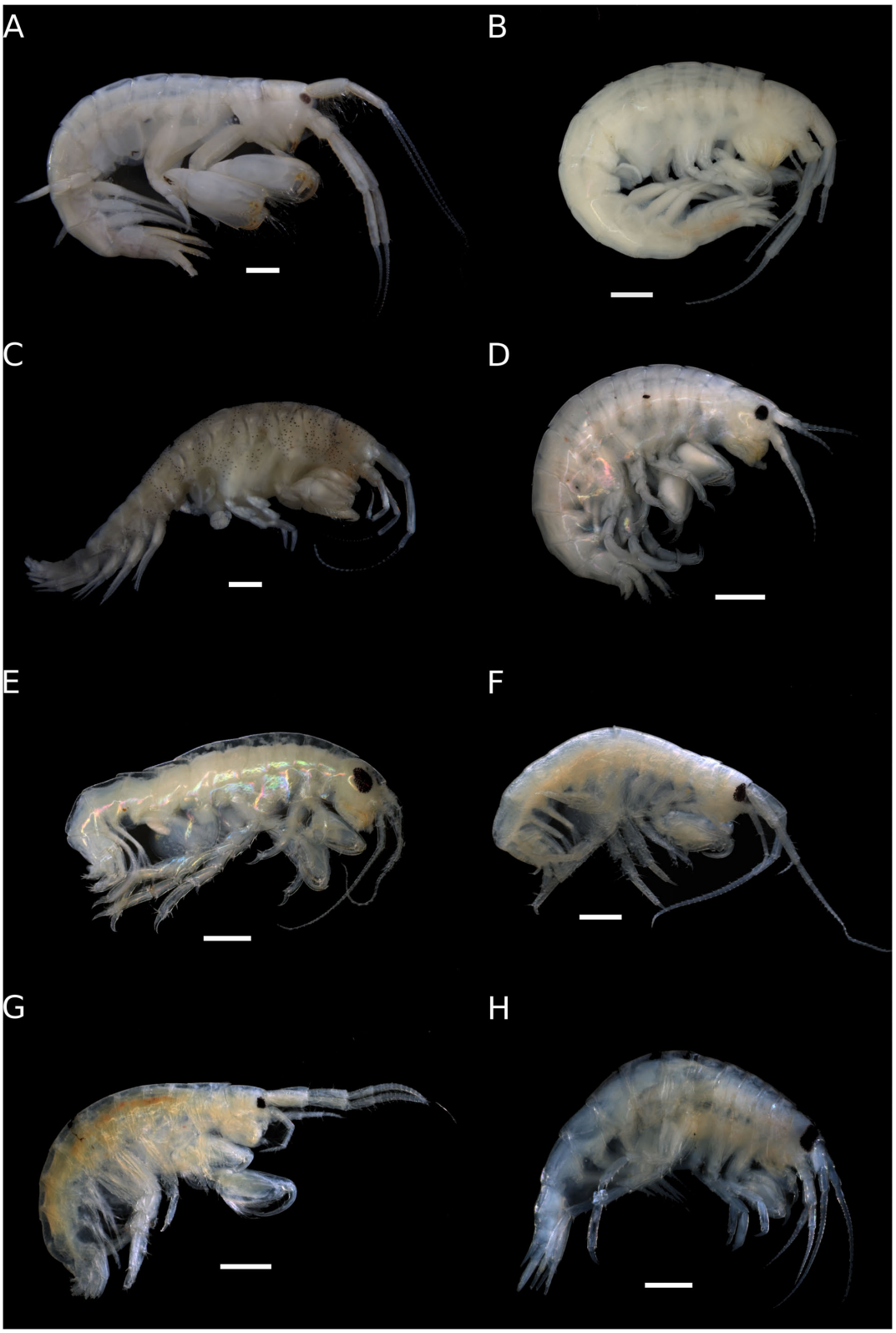

FIGURE 2 | Amphipoda from Trindade Island. **(A)** *Ampithoe marcuzzii* male (ZUEC-CRU-4354). **(B)** *Ampithoe marcuzzii* female (ZUEC-CRU-4355). **(C)** *Cymadusa trindadensis* (ZUEC-CRU-4359). **(D)** *Hyale niger* (ZUEC-CRU-4360). **(E)** *Protohyale macrodactyla* (ZUEC-CRU-4362). **(F)** *Elasmopus gabrieli* **sp. nov.** (ZUEC-CRU-5364) **(G)** *Elasmopus viracochai* (ZUEC-CRU-4367). **(H)** *Eusiroides lucai* **sp. nov.** (ZUEC-CRU-4368). Scale bar: 1 mm.

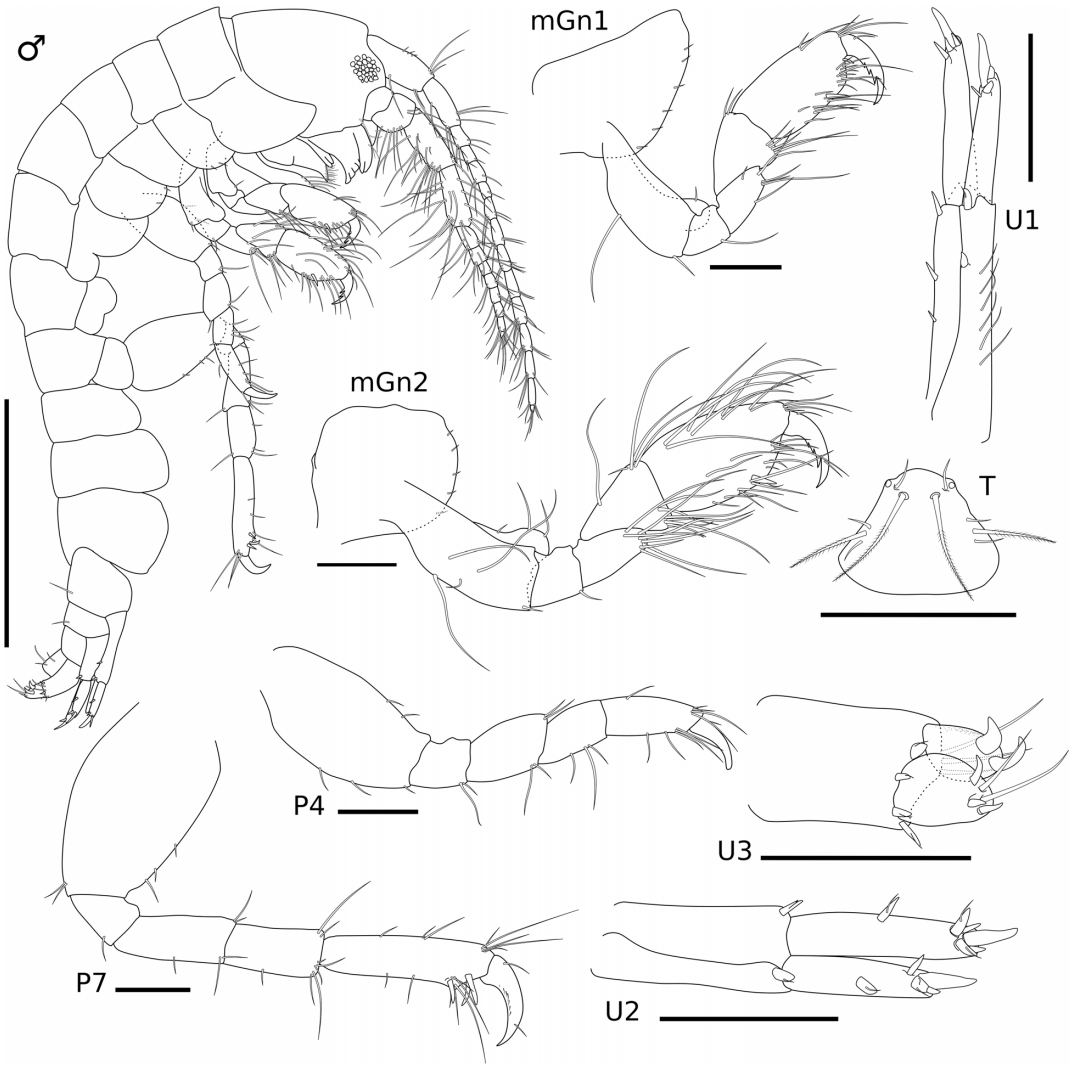

FIGURE 3 | *Ampithoe thaix* Siqueira and Iwasa-Arai **sp. nov.** Male (ZUEC-CRU- 4357). Scale bar: 1 mm. Gnathopods, pereopods, uropods, and telson. Scale bar: 100 μm.

long as outer plate, with marginal row of short setae, seven long plumose setae on the inner margin and six long plumose apical setae; outer plate, row of short setae on the inner and outer margins, long plumose setae on the apical and inner margin. Mxp, inner plate about 3 × longer than wide, inner margin and apex with long setae and plumose long setae, apical margin with two robust setae; outer plate, 1.8 × longer than wide, inner margin with three long plumose setae and five serrate robust setae, outer and apical margins with row of long plumose setae; palp 4-articulate, article 1, subtriangular, outer margin with one long setae, article 2 subrectangular, inner margin with row of long plumose setae, article 3 subrectangular inner margin with six long setae, outer margin with five long setae, article 4 with two long setae and one plumose seta (**Figure 4**).

Gn1, slightly smaller than Gn2; coxa subtriangular, enlarged anteriorly, ventral margin bearing row of short setae; basis 2.3 × longer than wide, anterodistal margin with one short seta, posterior margin with two setae; ischium subrectangular, 1.1 × longer than wide, posterior margin with one long seta; merus 1.5 × longer than wide, posterior margin with five long setae; carpus 1.1 × longer than wide, anterodistal margin with two setae, posterior margin setose; propodus subrectangular, 1.8 × longer than wide, anterior margin with two setae, anterodistal angle with four setae, posterior margin setose, posterodistal margin with one robust seta, palm transverse; dactylus 1.5 × longer than palm, serrated, with two setae. Gn2, coxa oval, ventral margin bearing row of short setae; basis 1.8 × longer than wide, anterior margin with three setae, posterior margin with three setae, inner face with two long setae; ischium small and subquadrate, as long as wide, posterior margin with one short seta; merus, 1.8 × longer than wide, posterior margin setose; carpus, 1.3 × longer than wide, anterior margin with one short and four long setae, posterior margin setose; propodus subrectangular, 1.8 × longer than wide, anterior and

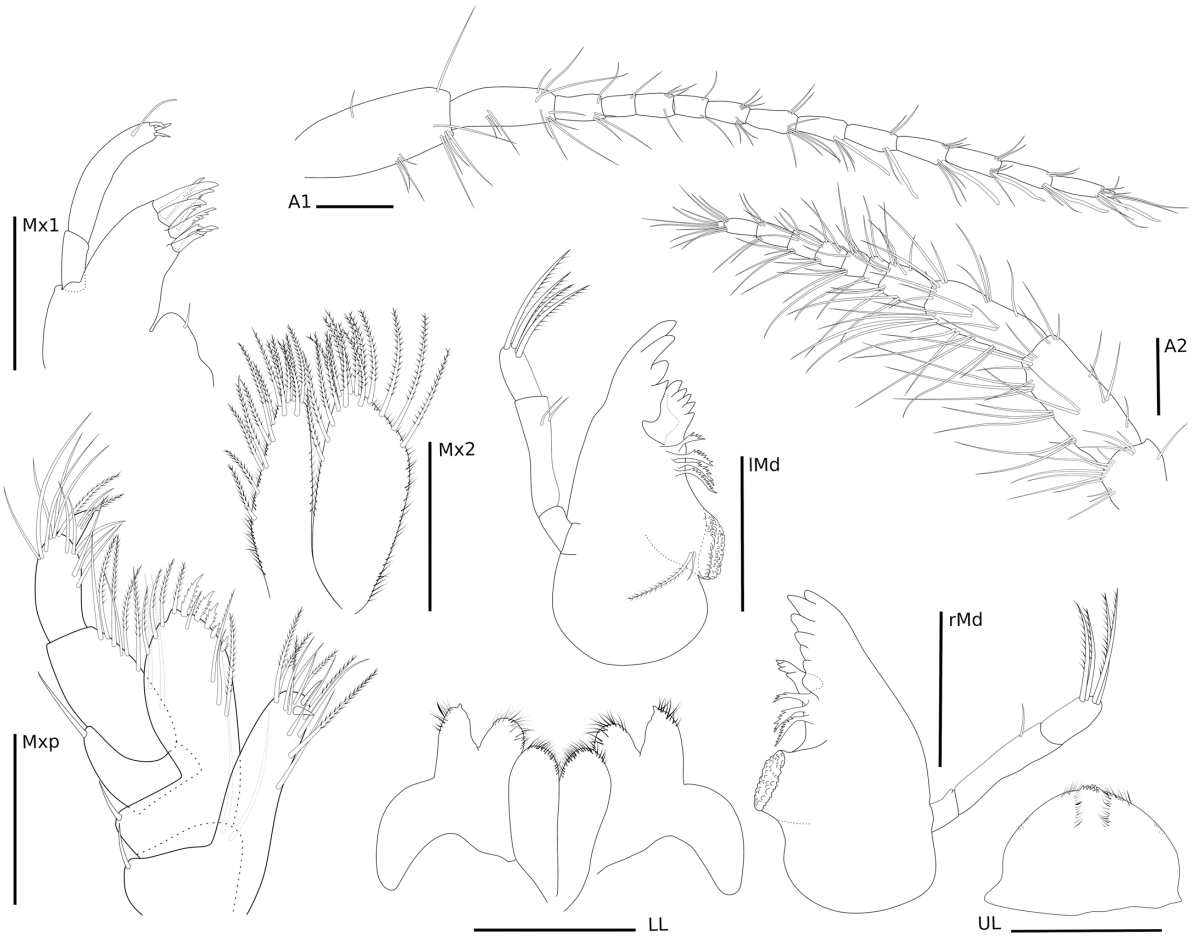

FIGURE 4 | *Ampithoe thaix* Siqueira and Iwasa-Arai **sp. nov.** Antennae and mouth parts. Scale bar: 100 μm.

posterior margins setose; palm transverse, with one robust seta delimiting palm; dactylus 1.5 × longer than palm, with two setae (**Figure 3**).

P3 not recovered (described from female). P4, coxa not recovered, basis subrectangular, 1.8 × longer than wide, anterior margin with two setae, posterior margin with two setae; ischium small and subrectangular, 1.2 × longer than wide, posterior margin with two long setae; merus subrectangular, 1.4 × longer than wide, anterior margin with two setae, posterior margin with two setae; carpus subrectangular, 1.5 × longer than wide, posterior margin with three setae; propodus subrectangular, 2.5 × longer than wide, anterior margin with five setae, posterior margin with five setae; dactylus slightly curved, with one short seta. P5 not recovered (described from female). P6 not recovered (described from female). P7, coxa not recovered, basis 1.5 × longer than wide, anterior margin with three setae, posterior margin with two setae; ischium small and subrectangular, 1.2 × longer than wide, posterior margin with one seta; merus subrectangular, 2.2 × longer than wide, anterior and posterior margins with setae; carpus subrectangular, 2.1 × longer than wide, anterior margin with two setae, posterior margin with six setae; propodus elongate, 3.8 × longer than wide, anterior margin with eight long setae, posterior margin with three robust setae and six setae; dactylus slightly curved, with two short setae (**Figure 3**).

U1, peduncle 3.5 × longer than wide, with distoventral rounded spur, inner margin with three robust setae, outer margin with two robust setae and a row of long setae; inner ramus 1.2 × longer than outer ramus, apical margin with four robust setae; outer ramus, apical margin with four robust setae. U2, peduncle 2.1 × longer than wide, inner and outer margins with one robust setae each; inner ramus 1.2 × longer than outer ramus, inner margin with one robust seta, apical margin with five robust setae; outer ramus, outer margin with one robust seta, apical margin with four robust setae. U3, peduncle slightly elongate, about 1.6 × longer than wide, with three long setae and four robust setae; inner ramus slightly longer than outer ramus, apical margin with two long setae and three robust setae; outer ramus, apical margin with two curved robust setae. T subtriangular, lateral margins with one long plumose and two short setae, distolateral angles with one cusp and one short seta each (**Figure 4**).

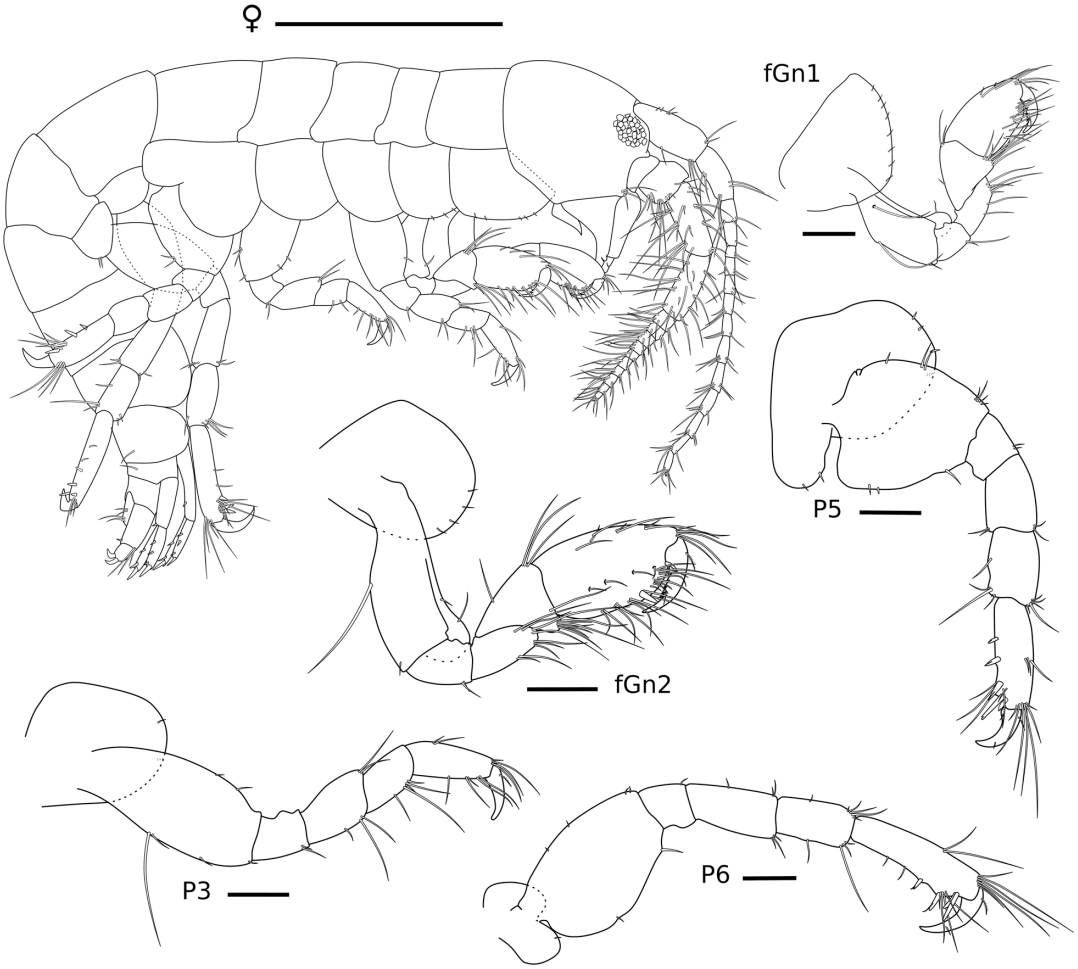

FIGURE 5 | *Ampithoe thaix* Siqueira and Iwasa-Arai **sp. nov.** Female (ZUEC-CRU-4358). Scale bar: 1 mm. Gnathopods and pereopods. Scale bar: 100 μm.

Female (ZUEC-CRU-4758). Body (**Figure 5**). Length 4.8 mm.

Gn1, slightly smaller than Gn2; coxa subtriangular, enlarged anteriorly; basis 2.6 × longer than wide, anterior and posterior margins with one long and one short setae each; ischium small and subrectangular, 1.3 × longer than wide, posterodistal margin with two setae; merus 1.8 × longer than wide, posterior margin setose; carpus 1.8 × longer than wide, anterior margin with three setae, posterior margin setose; propodus subrectangular, 1.6 × longer than wide, anterodistal and posterior margin setose, palm slightly convex, lacking robust seta; dactylus 3 × longer than palm, serrated, with one plumose seta. Gn2, coxa oval, ventral margin with row of short setae; basis 2.4 × longer than wide, anterior margin with two short setae, posterior margin with one short seta; ischium small and subrectangular, 1.4 × longer than wide; merus 1.7 × longer than wide, posterodistal margin setose; carpus triangular, 1.3 × wider than long, anterior margin with few setae, posterior margin setose; propodus 1.7 × longer than wide, anterior and posterior margins setose; palm slightly convex, with one robust seta delimiting palm; dactylus 2.2 × longer than palm, with one plumose seta (**Figure 5**).

P3, coxa oval, with one short seta; basis 2.2 × longer than wide, anterior margin with two setae, posterior margin with one long and three short setae; ischium subrectangular, 1.2 × longer than wide, posterior margin with two setae; merus subrectangular, 1.3 × longer than wide, anterior margin with two setae, posterior margin with three setae; carpus subrectangular, 1.8 × longer than wide, posterior margin with five setae; propodus subrectangular, 1.5 × longer than wide, anterior margin with six setae, posterior margin with five setae; dactylus slightly curved, with one short seta. P5, coxa, ventral margin rounded with three short setae, lobe with two short setae; basis 1.2 × longer than wide, anterior margin with seven setae, posterior margin with three short setae; ischium subrectangular, 1.3 × wider than long, anterior margin with two short setae; merus subrectangular, 1.7 × longer than wide, anterior and posterior margins with two setae each; carpus subrectangular, 1.6 × longer than wide, anterior margin with a tuft of apical setae, posterior margin with four setae; propodus elongate, 3 × longer than wide, anterior margin with three setae and a tuft of apical setae, posterior margin with five robust and five simple setae; dactylus slightly curved, with two short setae. P6, coxa, ventral margin rounded and naked, lobe with one

short setae; basis 1.5 × longer than wide, anterior margin with four short setae, posterior margin with two short setae; ischium subrectangular, as wide as long, anterior margin with one short seta; merus subrectangular, 2 × longer than wide, anterior and posterior margins with three setae each; carpus subrectangular, 1.8 × longer than wide, anterior margin with a tuft of apical setae, posterior margin with four setae; propodus elongate, 3.4 × longer than wide, anterior margin with two long setae and a tuft of apical setae, posterior margin with four robust and seven setae; dactylus slightly curved, with two short setae (**Figure 5**).

Type locality: Trindade Island, Espírito Santo state, Brazil.

Distribution: Currently known only from the type locality.

Remarks: The genus *Ampithoe* is the most speciose among Ampithoidae (Sotka et al., 2017), with 78 species described worldwide (Horton et al., 2020). Six species of *Ampithoe* were previously reported from the Brazilian coast: *Ampithoe divisura* Shoemaker, 1938, *Ampithoe marcuzzii* Ruffo, 1954, *Ampithoe ramondi* Audouin, 1826, *Ampithoe robustimana* Andrade and Senna, 2017, *Ampithoe seticoxae* Serejo and Licínio, 2002, and *Ampithoe suapensis* Correia et al., 2016 (Serejo and Siqueira, 2018). Among these species, *Ampithoe thaix* **sp. nov.** is morphologically closer to *A. divisura* and *A. suapensis* by presenting a round projection on the distal margin of the uropod 1 peduncle. Although the validity of *A. divisura* was previously questioned (LeCroy et al., 2009), *Ampithoe thaix* **sp. nov.** can be easily differentiated from the *A. divisura* specimens from the Brazilian coast identified by Serejo and Licínio (2002) by lacking a digitiform process on gnathopod 2 palm and an anterodistal propodus projection, as well as by presenting robust setae on propodus of pereopods 5–7 (vs. striated in *A. divisura*). *Ampithoe thaix* **sp. nov.** can also be differentiated from *A. suapensis* based on characters from mandible, gnathopods, uropods, and telson. The mandible palp of *Ampithoe thaix* sp. nov. is large and robust, with four plumose setae on article 3, while *A. suapensis* presents a short and slender mandible palp with three setae on the apex. The propodus of gnathopod in *A. thaix* **sp. nov.** is subrectangular and setose on both dorsal and ventral margins, and the palm is defined by a robust seta, while the propodus of gnathopod 1 is oval and setose only on the palmar margin, which is not defined by a robust seta. The uropods of *A. thaix* **sp. nov.** have asymmetric rami without setae on the inner margins, different from *A. suapensis*, where asymmetry is only observed on uropod 2, and both uropods 1 and 2 of *A. suapensis* have setae on the inner margins of the rami. Finally, *A. thaix* sp. nov. and *A. suapensis* can be distinguished by the telson shape, which is subtriangular in *A. thaix* **sp. nov.** and trapezoidal in *A. suapensis*. *Ampithoe thaix* **sp. nov.** is the third *Ampithoe* species reported from Brazilian oceanic islands.

Genus *Cymadusa* Savigny, 1816

***Cymadusa trindadensis* Andrade and Senna, 2017**
(**Figure 2C**)

Cymadusa trindadensis Andrade and Senna, 2017: 378, figs 12–15.

Material examined: Four females, Piscinas do Parcel (20°31′10.812″S, 29°19′25.8″W), from *Dictyota* sp., September 2018, T. P. Macedo col. (ZUEC-CRU-4359).

Remarks: *Cymadusa trindadensis* is so far endemic to TR. Type specimens were collected over 40 years ago and lacked complete antenna. Specimens found herein differ from the original description in the number of articles in the antenna 1 flagellum, which is bi-articulate in *C. trindadensis* types and uni-articulate in the examined specimens. The number of robust and short setae on uropods 1 and 3 also varies, with the present specimens presenting uropod 1 with marginal robust setae on both rami, while in types, it is present only on the inner margin of the outer ramus, and uropod 3 bearing four robust setae and nine long setae on the apical margin of the inner ramus, whereas types have only four setae, as well as one short robust seta on the distolateral margin, which is not present in the original description. The outer margin has four marginal setae instead of one, as described by Andrade and Senna (2017).

Family Hyalidae Bulyčeva, 1957
Genus *Hyale* Rathke, 1836

***Hyale niger* (Haswell, 1879)**
(**Figure 2D**)

Allorchestes niger Haswell, 1879: 319.—1885: 95, pl. 11 figs 1–3.

Hyale nigra.—Stebbing, 1906: 571.—Schellenberg, 1928: 659, fig. 204.—Ledoyer, 1972: 273.—1979: 137, fig. 89.—1986: 1002, fig. 397.—J. L. Barnard, 1974: 66.—Serejo, 1999: 600, figs 5–7.—Leite, 2011: 176, fig. 3.14B.—Leite et al., 2011: 328.

Hyale niger.—Lowry and Stoddart, 2003: 129.

Material examined: Sixteen individuals (not sexed), Piscinas do Parcel (20°31′10.812″S, 29°19′25.8″W), from *Dictyota* sp., September 2018, T. P. Macedo col. (ZUEC-CRU-4360). One individual (not sexed), Ilha do Sul (20°31′27.5″S, 29°19′25.2″W), from *Dictyota* sp., April 2019, I. Batistela col. (ZUEC-CRU-4361).

Remarks: *Hyale niger* is a species with disjunct distribution, described for southeastern Australia and later found in Brazil and Madagascar (Serejo, 1999). Future work encompassing its broad distribution, detailed morphology, and molecular data may elucidate the species status. The specimens from TR agree well with the specimens found in the southeastern Brazilian continental coast, where the species is usually observed especially in *Sargassum* spp. from São Paulo state (Leite, 2011; Leite et al., 2011).

Protohyale Bousfield and Hendrycks, 2002

***Protohyale macrodactyla* Stebbing, 1899**
(**Figure 2E**)

Hyale macrodactylus Stebbing, 1899: 404, pl. 31d.

Hyale macrodactyla.—Stebbing, 1906: 565, fig. 96.—Oliveira, 1953: 339. Ledoyer, 1972: 273, pl. 77A.—1986: 1001, fig. 396.—Serejo, 1999: 592, figs 1, 2.—Leite, 2011.—Leite et al., 2011.

Protohyale (Protohyale) macrodactyla.—Bousfield and Hendrycks, 2002: 79.

Protohyale macrodactyla.—LeCroy et al., 2009: 959.—Paz-Ríos et al., 2013a: 4, fig. 3.

Material examined: Seven individuals (not sexed), Piscinas do Parcel (20°31′10.812″S, 29°19′25.8″W), from *Dictyota* sp., September 2018, T. P. Macedo col. (ZUEC-CRU-4362); 18 individuals (not sexed), Ilha do Sul (20°31′27.5″S,

29°19′25.2″W), from *Dictyota* sp., April 2019, I. Batistela col. (ZUEC-CRU-4363).

Remarks: *Protohyale macrodactyla* is a common species found in the Atlantic Ocean. The species was originally described from the Caribbean and later found along the Brazilian coast (Stebbing, 1899; Serejo, 1999; Leite, 2011; Leite et al., 2011). The TR material agrees well with the specimens found on the Brazilian continental coast.

Family Maeridae Krapp-Schickel, 2008
Genus *Elasmopus* Costa, 1853

***Elasmopus gabrieli* Siqueira and Iwasa-Arai sp. nov.**
http://zoobank.org/9AA8C7EB-56BD-4071-82E3-49045225BF82

(**Figures 2F**, **6**–**8**)

Material examined: Holotype: male, Piscinas do Parcel (20°31′10.812″S, 29°19′25.8″W), from *Dictyota* sp., September 2018, T. P. Macedo col. (ZUEC-CRU-5364).

Paratypes: one male, two females, two juveniles, same as holotype (ZUEC-CRU-5365). Two females, one juvenile, same as holotype (ZUEC-CRU-5366).

Diagnosis: A1 1/2 of body length, with accessory flagellum 3-articulate. A2 short, 1/3 the length of A1. Md palp article 3 falcate, with plumose setae along the margin, margin concave with three long setae on the apex. Mxp palp with 4-articulate with terminal unguis. Gn1 propodus palm serrated. Gn2 propodus oval, with triangular process delimiting palm, with one subquadrate and one subrectangular processes close to the dactylus articulation. Pereopods 3–7 propodus with row of robust setae on the posterior margin and one locking seta distally. Pereopods 5–7 basis slightly serrated and convex. Epimeral plate 3 with the posterior margin slightly serrated with four notches. U3 with several long plumose robust setae. T cleft (approximately 1/2 on its length), lobes apex slightly concave with one long robust plumose seta and one short robust seta.

Etymology: This species is named after the son of SGLS, Gabriel Siqueira.

Description: Male (ZUEC-CRU-5364). Body (**Figure 6**). Length 8.5 mm.

Head with eyes rounded and well developed (**Figure 6**), lateral cephalic lobes rounded, with anteroventral notch. A1 longer than A2, about 0.5 × body length, peduncular article 1 with one robust seta and three setae on the distolateral margin and row of short setae laterally; peduncular articles 2 and 3 with tufts of setae on the lateral and distal margins; accessory flagellum 3-articulate, shorter than the first proximal article of the flagellum, with three long setae on the apex; flagellum 23-articulate and 1.1 × longer than peduncular articles 1–3 combined, with aesthetascs present from articles 3–19. A2 stout, 3 × shorter than A1; peduncular articles setose; flagellum 8-articulate, 2.3 × shorter than peduncular articles 3–5 combined, proximal article longest, setae present in all articles. UL rounded, setose apically. LL notched, inner and outer lobes setose apically, outer lobe with one small projection on the inner margin. rMd, molar with one long plumose seta; incisor with three teeth and medial part of the plate without evident teeth, *lacinia mobilis* seven-toothed; accessory setal row with three serrated setae. lMd, molar with one long plumose seta; incisor and *lacinia mobilis* two- and five-toothed, respectively; accessory setal row with four serrated setae; palp 3-articulate, article 1 short, 1.5 × longer than wide, article 2 elongate, 2 × longer than wide, article 3 falcate, similar in size to article 2, with three long setae apically and a row of plumose setae on the inner margin, with 21 setae in total, 18 of them plumose and three simple setae. Mx1, inner plate small and subtriangular, inner margin with row of thin setae, apex with two long plumose setae; outer plate with seven stout serrated setae apically; palp 2-articulate, article 2 with long setae apically and on the inner margin. Mx2, inner plate as long as the outer plate, with marginal row of short setae on the inner margin, three long plumose setae on the inner margin and several long apical setae; outer plate, row of long setae apically, with two long plumose setae on the inner margin. Mxp, inner plate about 2.4 × longer than wide, inner margin and apex with plumose long setae; outer plate, 1.8 × longer than wide, inner margin with four long plumose setae and seven serrated robust setae; palp 4-articulate, article 1, subtriangular, naked, article 2 subrectangular, inner margin with row of long setae, article 3 subrectangular inner margin with long setae, outer margin with five long setae, thin setae apically, article 4 with three setae, unguis with one short seta, falcate (**Figure 7**).

Gn1 subchelate, smaller than Gn2; coxa subtriangular, enlarged anteriorly, ventral margin bearing row of short and long setae; basis 2.5 × longer than wide, anterior margin with two short setae, posterior margin with two long setae, posterodistal margin with one seta; ischium subtriangular, as long as wide, posterior margin with a tuft of setae; merus subrectangular, about 1.5 × longer than wide, distal margin setose; carpus 1.6 × longer than wide, anterodistal margin with two setae, posterior margin heavily setose; propodus subrectangular, 1.8 × longer than wide, anterior margin with three pairs of short setae and one long seta each, anterodistal angle with a tuft of setae, posterior margin setose with a row of setae, palm transverse, serrated, with long and short setae along its margin and delimited by a robust seta; dactylus falcate, with two short setae. Gn2 subchelate, coxa oval, ventral margin bearing row of short setae and three long setae; basis 2.1 × longer than wide, anterior margin with row of setae, posterior margin with three long and two short setae; ischium small and subquadrate, 1.2 × longer than wide, posterodistal margin with one seta; merus subrectangular, 1.6 × longer than wide, posterodistal margin setose; carpus subtriangular, 1.3 × wider than long, anterodistal margin with one robust and five long setae, posterior margin setose with a row of plumose setae and one long seta distally; propodus elongate, 2.1 × longer than wide, anterior margin with row of short setae, anterodistal angle with a tuft of setae, posterior margin setose, with one triangular process delimiting palm and one distal subquadrate and one proximal subrectangular processes with four robust setae distally, palm slightly concave; dactylus falcate, fitting palm, posterior margin with tiny setae, with one single short seta on the anterior margin, and apically blunt (**Figure 6**).

P3, coxa oval, 1.8 × longer than wide, anterior margin two long setae; basis subrectangular, 3.5 × longer than wide, anterodistal margin with two short setae, posterior margin

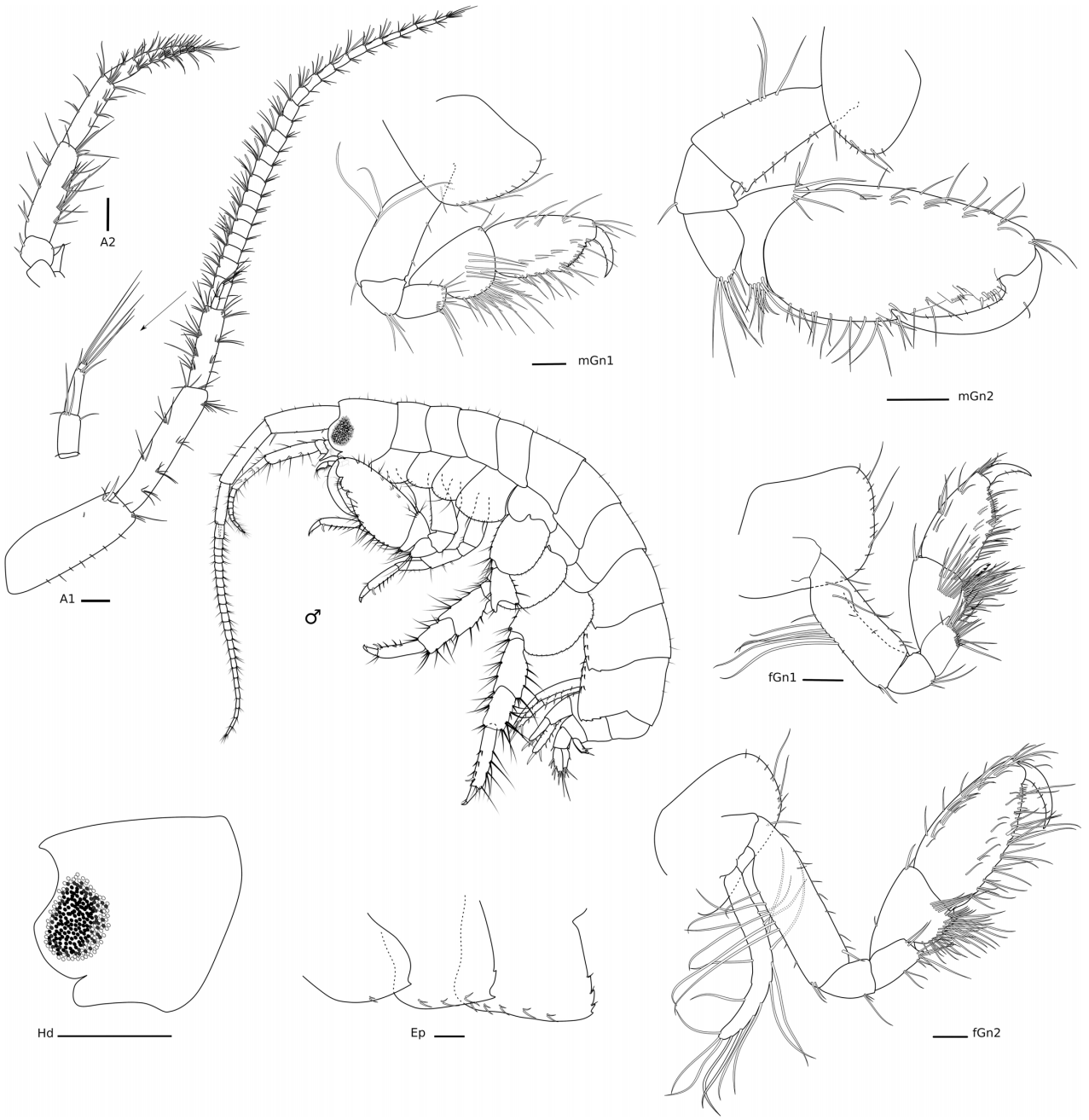

FIGURE 6 | *Elasmopus gabrieli* Siqueira and Iwasa-Arai **sp. nov.** Male (ZUEC-CRU-5364). Head and gnathopods. Scale bar: 0.5 mm. Antennae and epimeral plates. Scale bar: 100 μm.

with three short setae; ischium small and subrectangular, as long as wide, posterior margin with one short seta; merus subrectangular, 2.6 × longer than wide, anterior margin with three setae, posterior margin with five setae; carpus subrectangular, 2.1 × longer than wide, anterior margin with two setae, posterior margin with five setae; propodus subrectangular, 3.4 × longer than wide, anterior margin with one seta, posterior margin with five and one posterodistal locking setae; dactylus stout, with one distal short seta. P4, coxa oval, ventrally produced, 1.3 × longer than wide, anterior margin with row of short setae and one long seta, ventral margin with long seta; basis subrectangular, 3.5 × longer than wide, anterior margin with sparse short setae, anterodistal margin with two short setae, posterior margin with four setae; ischium small and subrectangular, 1.1 × longer than wide, with one short setae posteriorly; merus subrectangular, 2.4 × longer than wide,

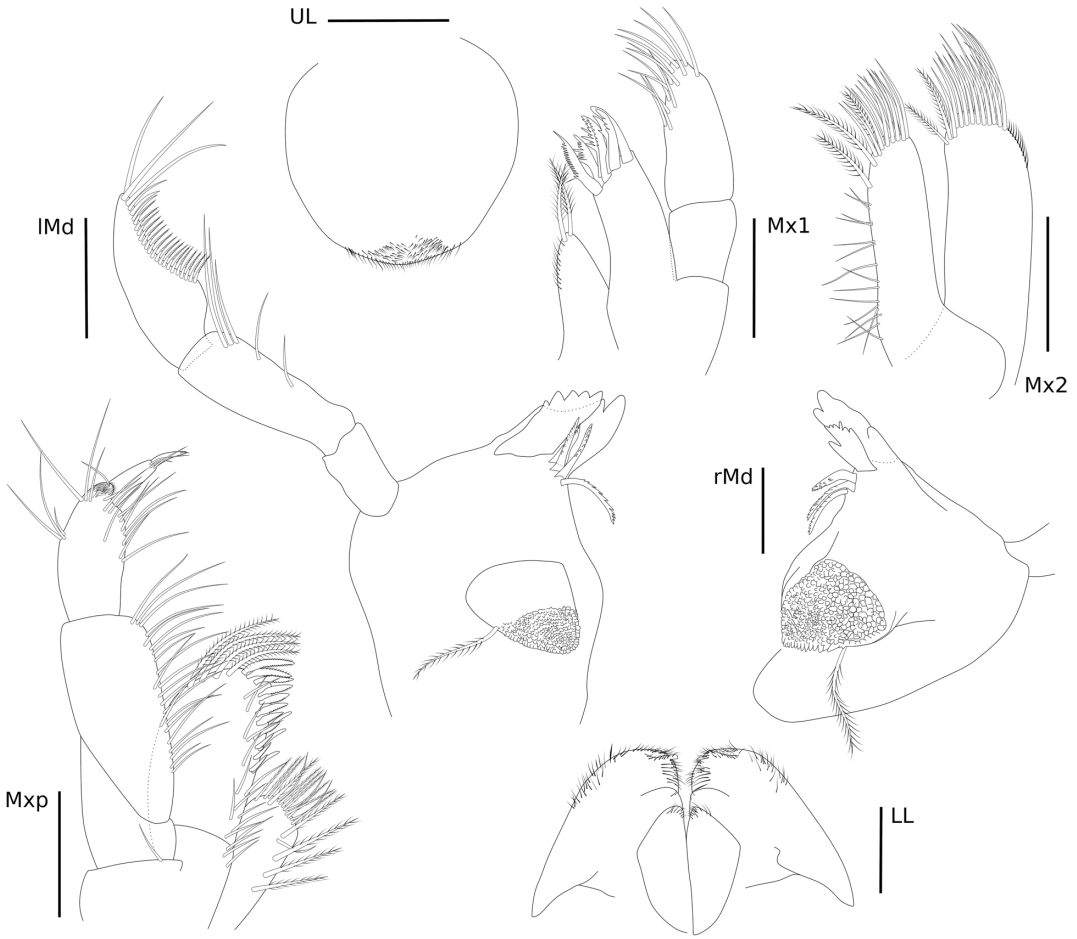

FIGURE 7 | *Elasmopus gabrieli* Siqueira and Iwasa-Arai **sp. nov.** Mouth parts. Scale bar: 100 μm.

anterior margin with five setae, posterior margin with three setae; carpus subrectangular, 2.5 × longer than wide, anterior margin with three setae, posterior margin with six setae; propodus subrectangular, 3.7 × longer than wide, anterior margin with two setae, posterior margin with five and one robust setae, and one posterodistal locking seta; dactylus stout, with two short setae. P5, coxa bilobed, posterior lobe narrower, with three short robust setae; basis oval, 1.3 × longer than wide, anterior margin with a row of short setae, posterior margin convex and slightly serrated; ischium subquadrate, as wide as long, posterodistal margin with tuft of setae; merus subrectangular, 1.3 × longer than wide, anterior margin with five setae and one short robust seta, posterior margin with two tufts of setae, posterodistal margin produced with three setae; carpus subrectangular, 1.5 × longer than wide, anterior margin with long setae, anterodistal margin with one short robust seta, posterior margin with seven setae; propodus subrectangular, 3.5 × longer than wide, anterior margin with two setae, anterodistal margin with three setae and one short robust seta, posterior margin with two single and three paired setae; dactylus stout, with one short seta. P6, coxa bilobed, posterior lobe narrower, with three short robust setae and two short setae; basis oval, 1.3 × longer than wide, anterior and posterior margins with a row of short setae, posterior margin convex and casteloserrated; ischium small and subquadrate, 1.1 × wider than long, anterodistal margin with two setae; merus subtriangular, 1.6 × longer than wide, anterior margin with tufts of setae, anterodistal margin produced, with two setae, posterior margin with two long and two short setae, posterodistal margin with four short setae; carpus subtriangular, 1.9 × longer than wide, anterior and posterior margins with tufts of setae; propodus subrectangular, 4.2 × longer than wide, anterior margin with four setae, posterior margin with four paired robust setae, and one posterodistal locking seta; dactylus stout, with one short seta. P7, coxa naked; basis oval, 1.1 × longer than wide, anterior and posterior margins with a row of short setae, posterior margin convex and slightly casteloserrated; ischium small and subrectangular, 1.1 × longer than wide, posterodistal margin with three long setae; merus subrectangular, 1.7 × longer than wide, anterior margin with pairs of setae, anterodistal margin with tuft of setae, posterior margin with three pairs of setae, posterodistal margin produced; carpus subrectangular, 1.8 × longer than wide, anterior margin with three tufts of three setae each, anterodistal margin with four setae, posterior margin with 10 setae; propodus subrectangular, 3.5 × longer than wide, anterior margin with tufts

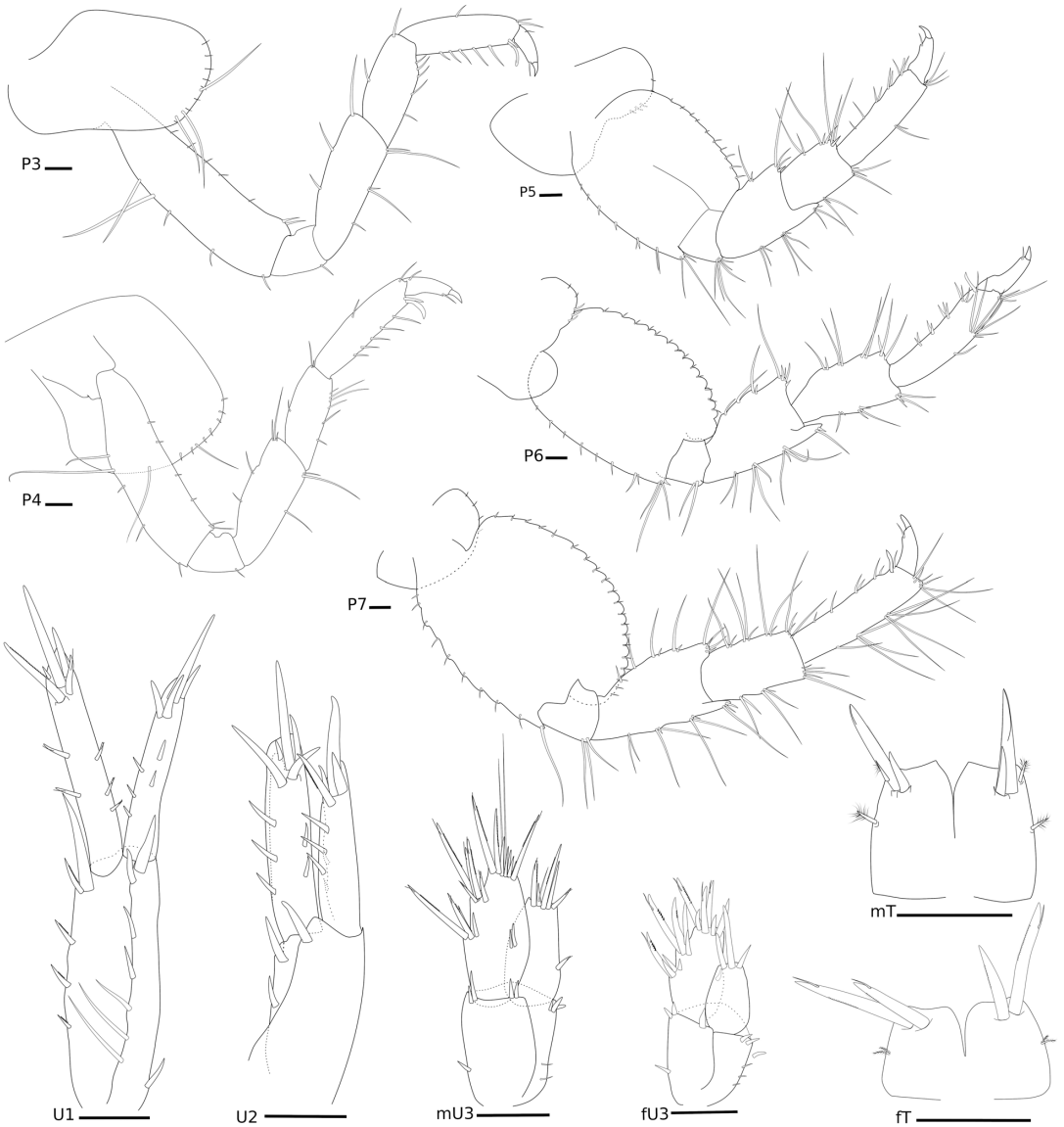

FIGURE 8 | *Elasmopus gabrieli* Siqueira and Iwasa-Arai **sp. nov.** Pereopods, uropods, and telson. Scale bar: 100 μm.

of long setae, posterior margin with seven setae and one locking setae distally; dactylus stout, with one seta (**Figure 8**).

Ep, epimeron 1 with one oblique ledge on surface, with two setae on the ventral margin, with one small posterior projection; epimeron 2 flattened ventrally, with three pairs of setae on the ventral margin, posterior margin with two small projections; epimeron 3 largest, slightly serrated, flattened ventrally, with five pairs of setae on the ventral margin, posterior margin with four projections, three of them with one seta (**Figure 6**).

U1, peduncle 2.7 × longer than wide, inner margin with four short pinnate robust setae and one long robust seta apically, outer margin with four robust setae and three long setae, one robust seta posteriorly; inner ramus 1.4 × longer than outer ramus, inner margin with two robust setae, outer margin with three robust setae, apical margin with five robust setae; outer ramus, inner margin with three robust seta, outer margin with two robust setae, apical margin with four robust setae. U2, peduncle 2 × longer than wide, inner margin with two robust setae, outer margin with one robust seta; inner ramus 1.3 × longer than outer ramus, inner margin with three robust setae, outer margin with two robust setae, apical margin with five robust setae; outer ramus, inner margin with two robust setae, outer margin with three robust setae, apical margin with four robust setae, one of them pinnate. U3, peduncle subrectangular, about 1.5 × longer than wide, inner margin with one robust seta, outer margin with two setae, distal margin with seven robust setae; outer ramus longer than inner ramus, outer margin with nine robust setae, four of them pinnated, inner margin with two robust setae, apical margin with two setae and eight robust setae, three of them pinnated; inner ramus, outer margin with one robust seta, apical

margin with five robust setae, two of them pinnated. T cleft (about 1/2 length), lateral margins with one pappose seta, posterolateral margins with two robust setae (one long and plumose, one short) and one pappose seta (**Figure 8**).

Female (ZUEC-CRU-4365). Length 7.9 mm.

Gn1 similar to male, subchelate, smaller than Gn2. Gn2 subchelate, coxa oval, ventral margin bearing row of short setae and two long setae; basis 3.1 × longer than wide, anterior margin with row of setae, posterior margin with two medium and two short setae; ischium small and subquadrate, 1.4 × longer than wide, posterodistal margin with one long and two short setae; merus subrectangular, 1.4 × longer than wide, posterodistal margin setose; carpus subtriangular, 1.3 × wider than long, anterodistal margin with two setae, posterior margin heavily setose, with a row of plumose and a row of simple long setae; propodus elongate, 2.2 × longer than wide, anterior margin with row of short seta, anterodistal angle with a tuft of setae, posterior margin setose, lacking processes, palm slightly concave, delimited by two robust setae; dactylus falcate, length similar to palm, with four short setae and apically blunt (**Figure 6**).

U3, peduncle subrectangular, about 1.5 × longer than wide, inner margin with one robust seta, outer margin with three setae, distal margin with six robust setae; outer ramus longer than inner ramus, inner margin with eight robust setae, three of them pinnated, outer margin with one robust seta, apical margin with six robust setae, one of them pinnated; inner ramus, margins smooth, apical margin with three robust setae. T cleft (about ½ length), lateral margins with two pappose setae, posterolateral margins with two robust setae (**Figure 8**).

Type locality: Trindade Island, Espírito Santo, Brazil.

Distribution: Currently known only from the type locality.

Remarks: *Elasmopus besnardi* was firstly described from TR based on a female specimen, and it was reported as *nomen dubium* by Ruffo (1959). It is currently considered a synonym of *E. brasiliensis* (Dana, 1853; Horton et al., 2020), with types of the *E. besnardi* being lost (Souza-Filho and Serejo, 2012) and the species never reported after its description. *Elasmopus gabrieli* **sp. nov.** female differs from the former *E. besnardi* in several characters, including accessory flagellum 3-articulate, shorter than first proximal article of flagellum (vs. accessory flagellum 2-articulate, larger than first proximal article of flagellum), articles 2 and 3 of mandibular palp similar in length (vs. article 3 larger than 2), palm of gnathopods delimited by robust setae and length dactylus similar to palm (vs. not delimited palm and length dactylus shorter to palm); inner ramus of uropod 3 without robust setae on the inner margins (vs. inner margins with robust setae) and telson cleft about ½ length (vs. telson totally cleft). Alves et al. (2016) observed that the species of *Elasmopus* have some morphological patterns and therefore suggested the species separation into four groups, in which *E. gabrieli* sp. nov. can be placed in group 3, together with *E. longipropodus* Senna and Souza-Filho, 2011, *E. rapax* Costa, 1853, *E. thalyae* Gouillieux and Sorbe, 2015, *E. thomasi* Ortiz and Lalana, 1994, and *E. yupanquii* Alves et al., 2016, by having three palmar processes on gnathopod 1 of the male. Within the group, *E. gabrieli* **sp. nov.** is more related to *E. longipropodus* from Brazil and *E. thalyae* from France by sharing the following characters: antenna 1 accessory flagellum with three articles, pereopod 5 basis with convex posterior margin, epimeral plate 3 serrated, and uropod 3 inner ramus slightly shorter than the outer ramus. *Elasmopus gabrieli* **sp. nov.** differs from *E. thalyae* by having gnathopod 1 palm serrated (vs. smooth), three processes on gnathopod 2 palm, one proximal triangular, and one subquadrate and one subrectangular processes distally (vs. triangular, triangular and subquadrate, respectively), epimeron 1–3 with short setae on the ventral margin (vs. long and short setae), telson cleft 0.5 × length (vs. 0.84 × length), lobes apical margin slightly concave with undeveloped cusps (vs. lobes apical margins concave with well-developed cusps). *Elasmopus gabrieli* **sp. nov.** also differs from *E. longipropodus* by having an accessory flagellum shorter than the first proximal article of the flagellum of antenna 1 (vs. larger than the first proximal article of the flagellum), mandible palp articles 2 and 3 with the same length (vs. article 2 shorter than article 3), article 3 falcate with plumose setae along its concave margin and with three long setae on the apex (vs. four apical setae), gnathopod 2 propodus 2 × longer than wide (vs. 2.5 × longer than wide), palm defined by a triangular process, palm margin with a subquadrate and a subrectangular process distally (vs. a subacute process and a palmar corner defined by a strong acute triagular process), length dactylus similar to palm (vs. length dactylus shorter to palm), pereopods 3–7 propodus with one locking seta distally (without locking seta), uropod 3 with two setae on the inner margin of the outer ramus (vs. one seta), and telson with undeveloped cusps, with two robust seta, one long and plumose, and one short in each lobe (vs. with apicolateral cusps well developed, with three robust setae).

Krapp-Schikel and Ruffo (1990) grouped the species *Elasmopus canarius* Krapp-Schikel and Ruffo, 1990, *E. pectenicrus* (Bate, 1862), *E. serricatus* J. L. Barnard, 1969, *E. spinibasus* Sivaprakasam, 1970, *E. crenulatus* Berents, 1983, *E. laufolii* Myers, 1986, based on the presence of a very dense fringe of long setae on the posterior margin of gnathopod 2 of the male and by a casteloserrate posterior margin of the basis of pereopods 6 and 7. The herein described species, *E. gabrieli* **sp. nov.**, shares the casteloserrate pattern on the basis of pereopods 6 and 7; however, it lacks a very dense fringe of long setae on gnathopod 2 of the male. Most of these species have an intertropical distribution in the Indo-Pacific region, and future cladistic biogeographic analysis may elucidate the evolution of these characters across the ocean basins.

***Elasmopus viracochai* Alves et al., 2016**
(**Figure 2G**)

Elasmopus viracochai Alves et al., 2016: 21, figs 17–22.

Material examined: One male, Ilha do Sul (20°31′27.5″S, 29°19′25.2″W), from *Dictyota* sp., April 2019, I. Batistela col. (ZUEC-CRU-4367).

Remarks: *Elasmopus viracochai* was so far known only from its type locality, in Ceará state, northeastern Brazil. Only one male specimen was found in TR samples, and it agrees well with the original description.

Family Pontogeneiidae Stebbing, 1906

Genus *Eusiroides* Stebbing, 1888

***Eusiroides lucai* Siqueira and Iwasa-Arai sp. nov.**

http://zoobank.org/B1EE8F0A-A0DB-43DB-846B-66122E836110

(**Figures 2H**, **9**, **10**)

Material examined: Holotype: female, Piscinas do Parcel (20°31′10.812″S, 29°19′25.8″W), from *Dictyota* sp., September 2018, T. P. Macedo col. (ZUEC-CRU-4368).

Diagnosis: Antennae with stout peduncular articles, with calceoli on flagellum; accessory flagellum of A1 uni-articulate, shorter than first proximal article of flagellum. rMd molar without seta, incisor with two teeth, one wide and the other weakly developed, *lacinia mobilis* serrated. lMd incisor with three teeth, *lacinia mobilis* six-toothed; palp article 3 with three long plumose setae apically. Mx1 outer plate with 10 stout serrated setae apically, palp 2-articulate. Mx2, inner plate longer than outer plate. Mxp palp with five articles, article 5 falcate. Gnathopods similar to each other, dactylus falcate, with proximal plumose seta. P3–7 propodus with row of robust setae on the posterior margin and one locking seta distally. Pleonal epimera each with two marginal setae ventrally; epimera 2 and 3 with oblique edge on surface; epimeron 3 with one process posteriorly. U1 peduncle with row of robust setae. U2 shorter than U1, inner ramus 2 × shorter than the outer ramus. U3 inner ramus with a row of plumose setae. T deeply cleft (approximately 1/2 on its length).

Etymology: This species is named after the son of SGLS, Luca Siqueira.

Description: Female (ZUEC-CRU-4368). Body (**Figure 9**). Length 8.3 mm.

Head with eyes reniform and well developed. A1 2.1 × shorter than body length; peduncular article 1 with two plumose setae distolateral margin and one plumose seta laterally, with a few setae on the lateral and distal margins; peduncular articles 2 and 3 with setae on the lateral and distal margins; accessory flagellum uni-articulate, shorter than the first proximal article of the flagellum, with four setae on the apex; flagellum 26-articulate and 2.1 × longer than peduncular articles 1–3 combined, with calceoli present from articles 2 to 10, and aesthetascs present from articles 2 to 25 discontinuously. A2 stout, 1.7 × shorter than A1; peduncular articles setose; flagellum 23-articulate, slightly longer than peduncular articles 3–5 combined, proximal article longest, with calceoli present from articles 1 to 20. UL rounded, setose in medial region. LL notched, inner lobe setose on the outer margin; outer lobes setose apically and on the inner margin. rMd, molar without setae; incisor with two teeth, one wide and the other weakly developed, *lacinia mobilis* serrated; accessory setal row with three serrated setae; palp 3-articulate, article 3 with three long plumose setae apically. lMd, molar with two short setae; incisor and lacinia mobilis three- and six-toothed, respectively, accessory setal row with three serrated setae and one seta; palp 3-articulate, article 3 with three long plumose setae apically. Mx1, inner plate small and rounded, inner margin with two short setae; outer plate with 10 stout serrated setae apically; palp 2-articulate with seven long setae. Mx2, inner plate longer than outer plate; inner plate, marginal row of short setae, robust setae on the inner margin and short setae apically; outer plate, long plumose setae on the apical and inner margin. Mxp, inner plate small, 1.3 × shorter than the outer plate, inner plate, inner margin and apex with four plumose long setae, apical margin with five robust setae; outer plate, 3.2 × longer than wide, inner margin and apex with row of long plumose setae; palp 5-articulate, article 1, subtriangular, apex with two long setae, article 2 subrectangular, inner margin with row of long setae, article 3 subrectangular inner margin with long setae, outer margin with six serrated long setae, three long plumose setae and short seta, article 4 with three short setae; article 5 naked, falcate (**Figure 10**).

Gn1, as long as Gn2; coxa subtriangular, enlarged anteriorly, ventral margin bearing row of short setae; basis 3 × longer than wide, anterior margin with three setae, posterior margin with one long and one short setae, anterodistal margin with a tuft of setae and two robust setae, posterodistal margin with one seta; ischium subquadrate, as long as wide, posterior margin with a tuft of setae; merus subrectangular, about 1.2 × longer than wide, posterior margin heavily setose; carpus 1.1 × wider than long, anterodistal margin with one long seta, posterior margin heavily setose; propodus oval, 1.4 × longer than wide, anterior margin with one short seta, anterodistal angle with a tuft of setae, posterior margin setose with a row of robust setae, palm slightly convex, serrated; dactylus falcate, with a proximal plumose setae and a row of short setae. Gn2, coxa subrectangular, ventral margin bearing row of short setae; basis 3 × longer than wide, anterodistal margin with three setae, posterior margin with one seta; ischium small and subquadrate, as long as wide, posterodistal margin with one long seta; merus, 1.4 × longer than wide, with a setose posterodistal projection, distal margin with a row of setae; carpus, 1.2 × wider than long, anterodistal margin with one short seta, posterior margin setose; propodus oval, 1.6 × longer than wide, anterior margin with one short seta, anterodistal angle with a tuft of setae, posterior margin setose with a row of robust setae, palm slightly convex, serrated; dactylus falcate, with a proximal plumose setae and a row of short setae (**Figure 9**).

P3, coxa subrectangular, 1.7 × longer than wide, anterior margin with a row of short setae; basis subrectangular, 3.6 × longer than wide, with proximal long seta and anterodistal margin with three setae; ischium small and subrectangular, 1.5 × longer than wide, posterior margin with one short seta; merus subrectangular, 2.5 × longer than wide, anterior margin with three setae, posterior margin with three setae; carpus subrectangular, 2.2 × longer than wide, anterior margin with two setae, posterior margin with five setae; propodus subrectangular, 3.8 × longer than wide, anterior margin with four setae, posterior margin with four simple and four robust setae, and one posterodistal locking seta; dactylus falcate, bi-articulated, with one plumose seta and two short setae. P4, coxa acutely produced backward posteriorly, 1.1 × longer than wide, anterior margin with two short setae; basis subrectangular, 3.6 × longer than wide, anterodistal margin with three setae and posterodistal margin with two setae; ischium small and subrectangular, 1.1 × longer than wide, naked; merus subrectangular, 2.3 × longer than wide, anterior margin with four setae, posterior margin with four setae; carpus subrectangular, 2.1 × longer than wide, anterior margin with three setae, posterior margin with four

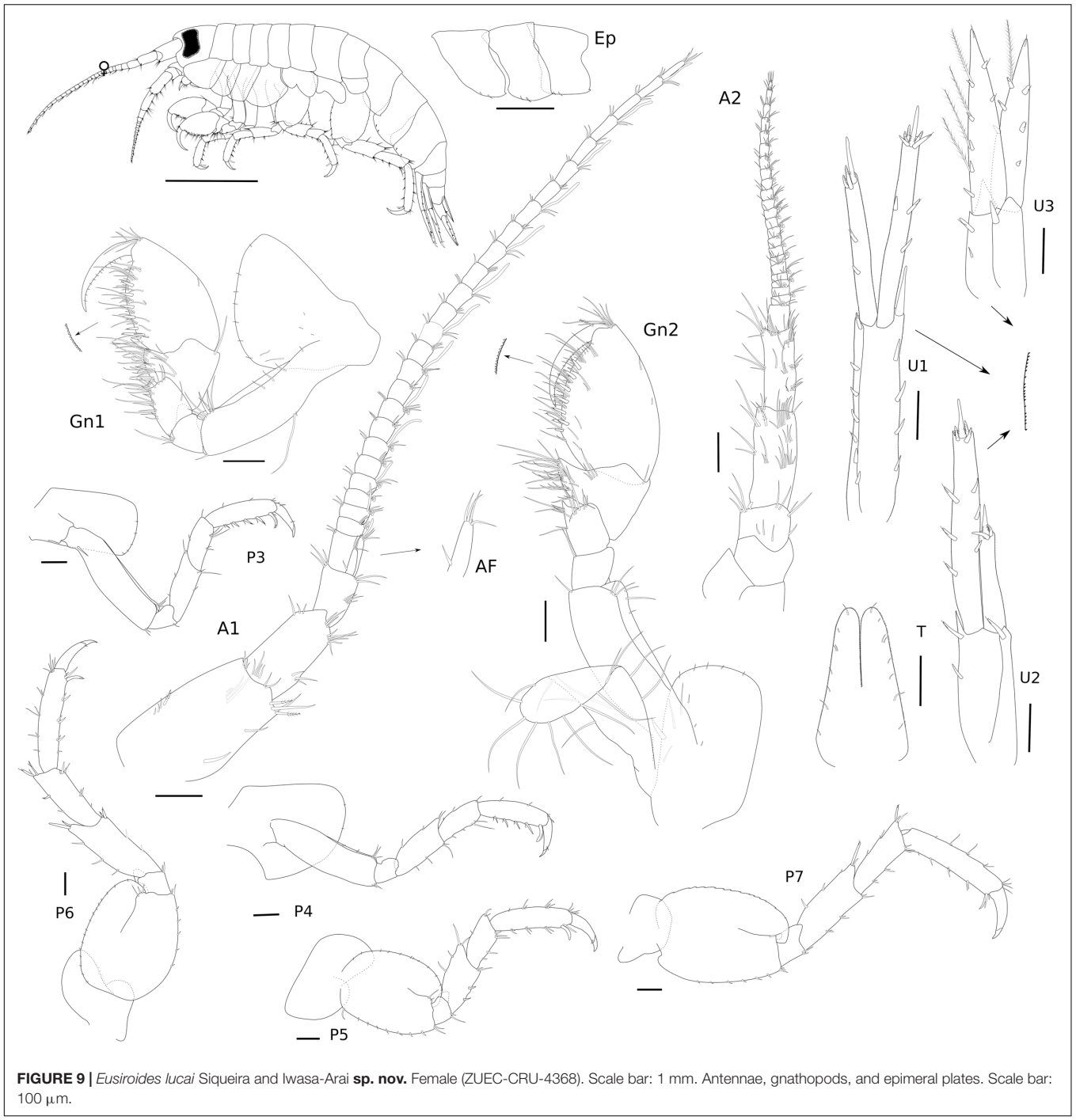

FIGURE 9 | *Eusiroides lucai* Siqueira and Iwasa-Arai **sp. nov.** Female (ZUEC-CRU-4368). Scale bar: 1 mm. Antennae, gnathopods, and epimeral plates. Scale bar: 100 μm.

setae; propodus subrectangular, 3.7 × longer than wide, anterior margin with four setae, posterior margin with four slender and four robust setae, and one posterodistal locking seta; dactylus falcate, bi-articulated, with one plumose seta and one short setae. P5, coxa bilobed, posterior lobe narrower and more ventrally produced than the anterior lobe, naked; basis oval, 1.3 × longer than wide, anterior and posterior margins with a row of short setae; ischium small and subrectangular, 1.3 × wider than long, posterodistal margin with two setae; merus subrectangular, 1.5 × longer than wide, anterior margin with four setae, posterior margin with two robust setae and posterodistal margin with two setae; carpus subrectangular, 1.6 × longer than wide, anterior margin with three setae, posterior margin with five setae; propodus subrectangular, 4 × longer than wide, anterior margin with tufts of setae, posterior margin with three paired setae, and one posterodistal locking seta;

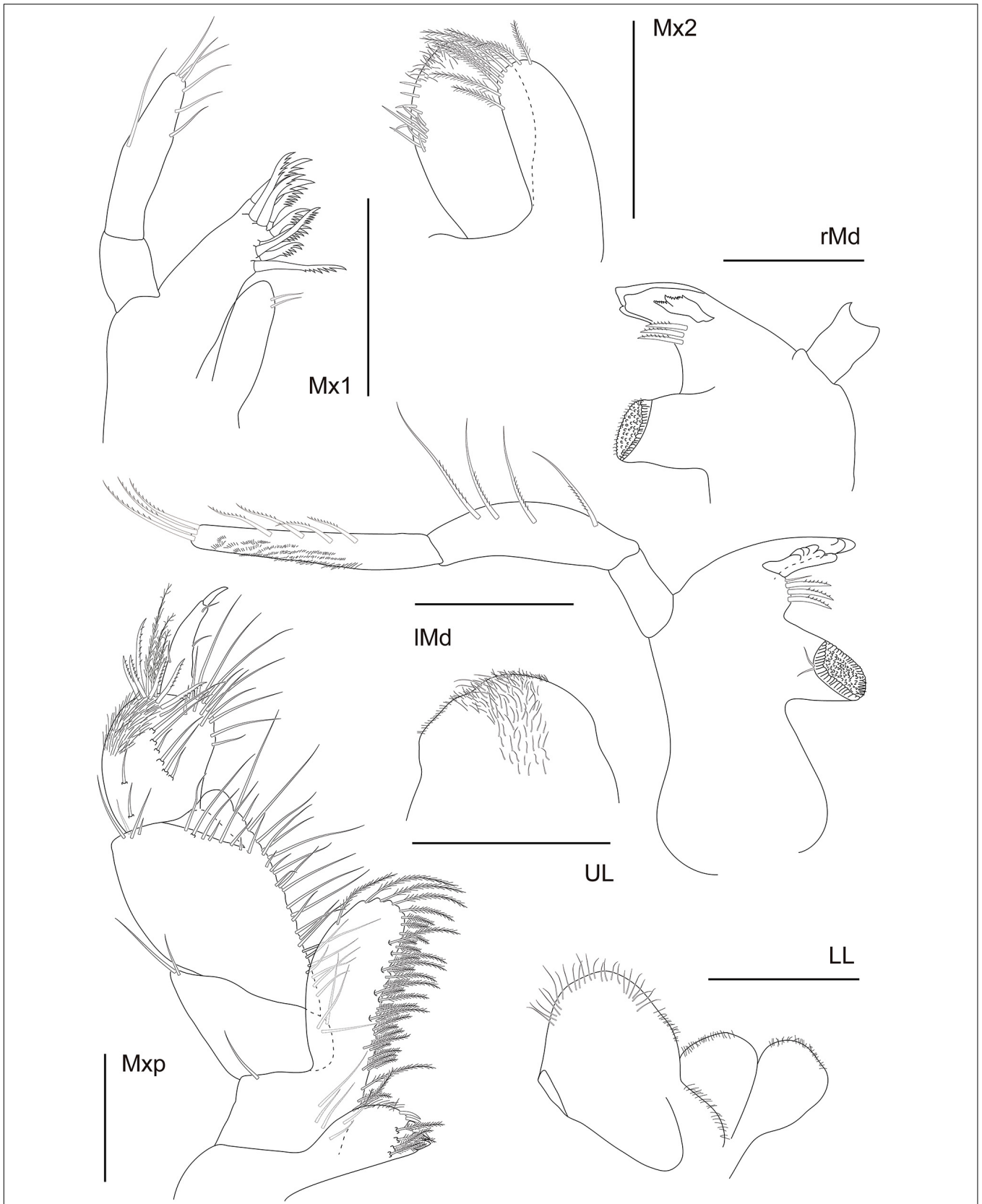

FIGURE 10 | *Eusiroides lucai* Siqueira and Iwasa-Arai **sp. nov.** Mouthparts. Scale bar: 100 μm.

dactylus falcate, bi-articulate, with two short setae (**Figure 9**). P6, coxa bilobed, posterior lobe narrower and more ventrally produced than the anterior lobe, naked; basis oval, 1.2 × longer than wide, anterior and posterior margins with a row of short setae; ischium small and subrectangular, 1.1 × wider than long, posterodistal margin with two setae; merus subrectangular, 2.4 × longer than wide, anterior margin with three setae, anterodistal margin with two robust setae, posterior margin with two setae and posterodistal margin with two robust setae; carpus subrectangular, 2.5 × longer than wide, anterior margin with two setae and three robust setae, posterior margin with seven setae; propodus subrectangular, 4.7 × longer than wide, anterior margin with tufts of setae, posterior margin with three paired robust setae, and one posterodistal locking seta; dactylus falcate, bi-articulate, with one short seta and one plumose seta. P7, coxa oval, naked; basis oval, 1.3 × longer than wide, anterior and posterior margins with a row of short setae; ischium small and subrectangular, 1.1 × wider than long, posterodistal margin with two setae; merus subrectangular, 2.3 × longer than wide, anterior margin with three setae, anterodistal margin with two robust setae, posterior margin with three pairs of setae; carpus subrectangular, 2.5 × longer than wide, anterior margin with three setae and three robust setae, posterior margin with six slender setae and one robust seta; propodus subrectangular, 4.7 × longer than wide, anterior margin with tufts of setae, posterior margin with paired robust setae; dactylus falcate (**Figure 9**).

Ep, epimeron 1 with one oblique ledge on the surface, with two setae on the ventral margin anteriorly; epimeron 2 with two setae on the ventral margin anteriorly; epimeron 3 largest, flattened ventrally, with two setae on the anterior half of the ventral margin, posterior margin with one tooth (**Figure 9**).

U1, margins with tiny setae, peduncle 4.7 × longer than wide, inner margin with six robust setae, outer margin with four robust setae, margins with tiny setae; inner ramus 1.2 × longer than the outer ramus, inner margin with two robust setae, apical margin with three robust setae; outer ramus, inner margin with one robust seta, outer margin with two robust setae, apical margin with six robust setae. U2, peduncle 2.3 × longer than wide, inner margin with two robust setae, outer margin with one robust seta; inner ramus 2 × shorter than the outer ramus, inner and outer margins with three robust setae each, apical margin with four robust setae; outer ramus, apical margin with three robust setae, margins with tiny setae. U3, lanceolate and foliaceous, peduncle subrectangular, about 1.7 × longer than wide, inner margin with two robust setae, outer margin with one robust seta; inner ramus as long as outer ramus, inner margin with five robust setae and four long plumose setae, outer margin with two robust setae, apex with one seta; outer ramus, inner margin with three robust setae and one plumose seta, outer margin with three robust setae, apex with one seta, margins with tiny setae. T cleft (about 1/2 length), lateral margins with row of setae, margins with tiny setae, lobes with round apex (**Figure 9**).

Type locality: Trindade Island, Espírito Santo state, Brazil.

Distribution: Currently known only from the type locality.

Remarks: The genus *Eusiroides* currently has 16 described species (Horton et al., 2020), which are very similar according to the morphology of antennae, eyes, gnathopods, and uropod 3 (Barnard and Karaman, 1991). Species of *Eusiroides* can be distinguished from each other by the presence or absence of teeth and serrated posterior margin of epimeron 3 and by telson shape (cleft, moderate or deeply cleft) (Barnard, 1932; Ledoyer, 1982; Thomas, 1993). Based on these characters, *Eusiroides lucai* **sp. nov.** is more similar to *E. georgiana* K. H. Barnard, 1932, by having a tooth on the posterior margin of epimeron 3; however, *E. lucai* **sp. nov.** can be distinguished from its congeneric by presenting gnathopods 1 and 2 palm serrated, pereopods 3–4 with one distal locking seta on propodus, uropods 1–3 with tiny setae on the margins, inner ramus of uropod 2 2 × shorter than the outer ramus (vs. 1.5), telson ½ cleft (vs. 2/3), lateral margin of lobes with row of setae and apex round with one seta (vs. one seta on the lateral margins and acute apex). Although the species was described based on a single specimen, its isolated geographical distribution and its conspicuous morphological characters suggest *E. lucai* **sp. nov.** to be a new species, and further samplings on TR are likely to report more individuals. This is the third record of Pontogeniidae for Brazil, where *Eusiroides* sp. was reported from Pernambuco state (Santos and Soares, 1999), and *Tethygeneia longleyi* (Shoemaker, 1933) was previously reported from São Paulo and Paraná states (southeastern Brazil).

Order Tanaidacea Dana, 1849
Suborder Apseudomorpha Sieg, 1980
Superfamily Apseudoidea Leach, 1814
Family Metapseudidae Lang, 1970
Subfamily Synapseudinae Guţu, 1972
Genus *Synapseudes* Miller, 1940

***Synapseudes isis* Segadilha, Siqueira and Iwasa-Arai sp. nov.**
http://zoobank.org/733CEA04-27C6-42D5-AE0F-3D048DF66F6E
(**Figures 11**, **12**)

Material examined: Holotype: female, Ilha do Sul (20°31′27.5″S, 29°19′25.2″W), from *Dictyota* sp., April 2019, I. Batistela col. (ZUEC-CRU-4369).

Paratypes: one male, same as holotype (ZUEC-CRU-4370).

Diagnosis: Female. Body 4 × longer than wide. Cephalothorax shorter than Per 1–3 lengths combined. Rostrum appearing undifferentiated, truncated. Pleon with three segments appearing functionally fused; but with two pleonite remnants delineated by sutures, at least dorsally. Antennule article 2 without tubercles or spiniform apophysis. Antenna article 1 with inner margin strongly serrated; flagellum bi-articulate terminating in one long and one short setae. Mxp palp article 1 with distolateral seta strongly developed; palp article 2 distolateral stout seta 1.5 × longer than that on palp article 1. Cheliped merus, carpus, and propodus with plumose setae ventrally; fixed finger with row of 10 setae on the incisive margin. Pereopod 1 propodus with four stout spiniform setae on the ventral margin. P1–3 basis with three, two, and

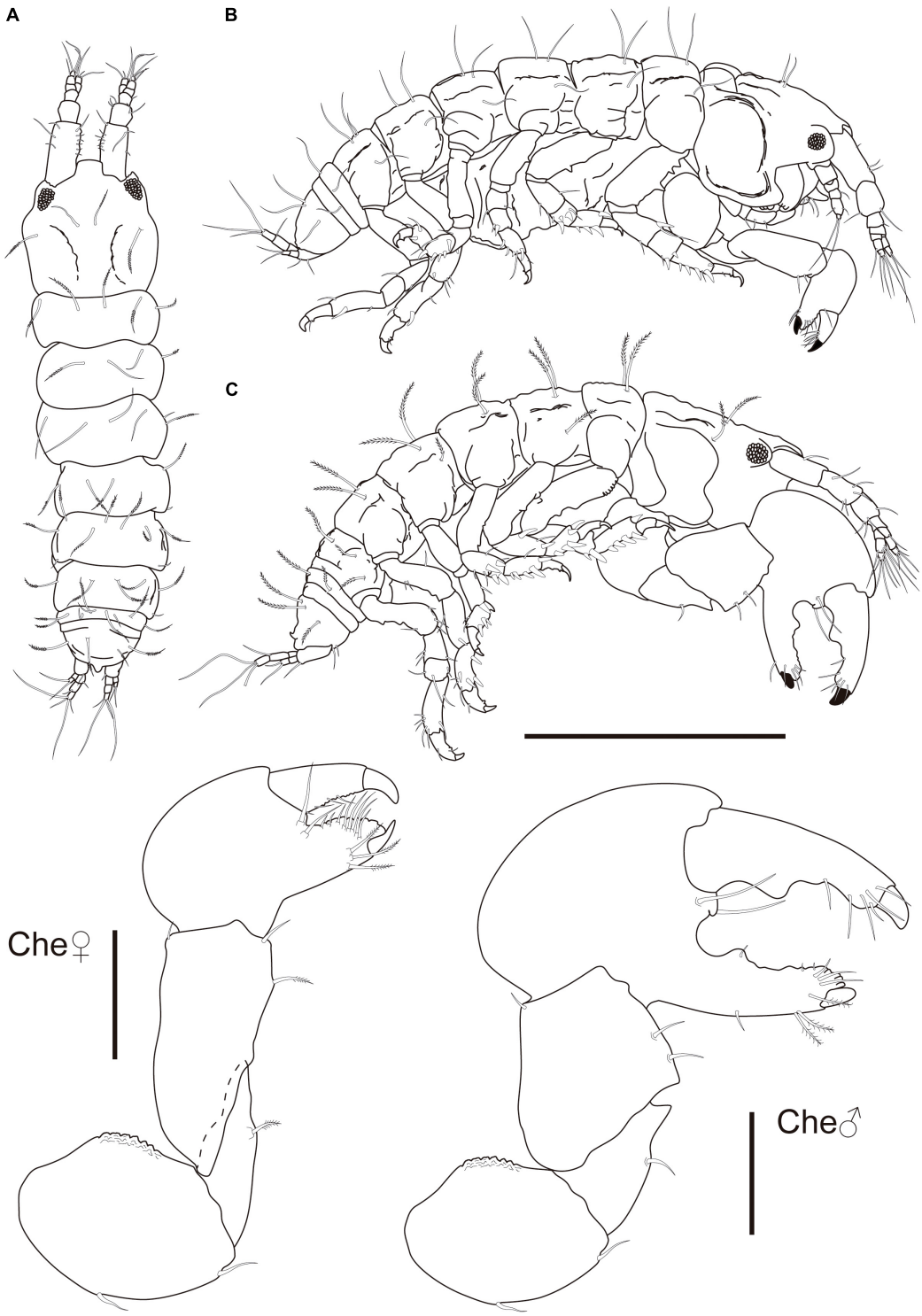

FIGURE 11 | *Synapseudes isis* Segadilha, Siqueira, and Iwasa-Arai **sp. nov.** Female (ZUEC-CRU-4369). **(A)** Ventral view. **(B)** Lateral view. **(C)** Male (ZUEC-CRU-4370) lateral view. Scale bar: 0.5 mm.

one spiniform apophyses on the ventral margin, respectively. Uropod endopod composed of three articles and exopod of two articles.

Male. Cheliped basis dorsal margin with strong crenulation; merus ventral margin with medial seta and large pointed apophyses distally; carpus more trapezoidal shaped than in

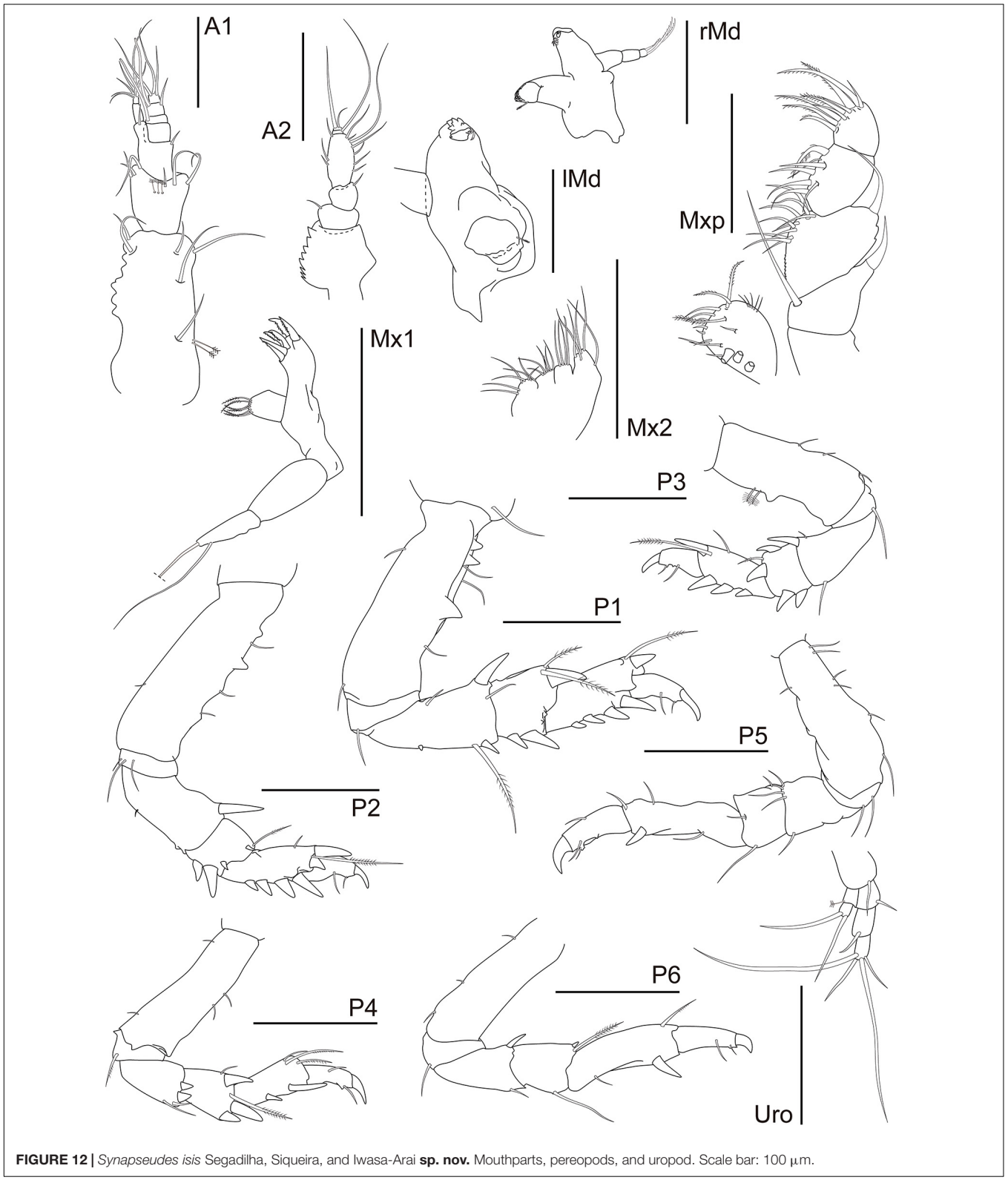

FIGURE 12 | *Synapseudes isis* Segadilha, Siqueira, and Iwasa-Arai **sp. nov.** Mouthparts, pereopods, and uropod. Scale bar: 100 μm.

female, ventral margin with two setae and small acute subdistal apophyses; propodus with two setae near articulation of dactylus; fixed finger with one rounded tubercle, three submarginal and 3 min marginal setae on the outer incisive margin. Dactylus with two rounded tubercles and six setae on the ventral margin.

Etymology: The specific epithet is a noun in apposition after the oceanographer Isis Batistela.

Description: Female (ZUEC-CRU-4369). Body (**Figure 11**). Length 1.1 mm, almost 4 × longer than wide.

Cephalothorax 27% of TBL, shorter than Per 1–3 lengths combined, longer than wide; rostrum truncated with broad base, smooth; eyelobes well defined, pigment and ommatidia present. Carapace with finely plumose setae on the lateral margin and near each ocular lobe (**Figure 11**).

A1 shorter than cephalothorax. Peduncle with four articles. Article 1 robust, 2.2 × longer than wide; inner margin with row of seven irregularly shaped blunt teeth or tubercles and two setae distally; outer margin with two medial penicillate and one and three subdistal setae. Article 2 as long as wide; with six setae distally. Article 3 slightly longer than wide; with distal seta. Article 4 0.7 × longer than wide; with distal seta. Outer flagellum with three articles. Article 1 wider than long, with distal aesthetasc. Article 2 0.8 × longer than wide; with aesthetasc and seta distally. Article 3 short, with three terminal setae. Inner flagellum with two articles. Article 1 twice longer than wide, naked. Article 2 minute, distally with six setae. A2 peduncle with four articles: Article 1 robust with bulge, with serrated inner margin. Article 2 inner margin with seta; squama absent. Article 3 about as long as article 2; outer margin with seta. Article 4 1.8 × longer than wide, inner margin with two medial and one distal setae; with seven setae along the outer margin. Flagellum with two articles. Article 1 with very long seta and article 2 with two terminal setae of different widths. rMd incisor smooth; setiferous lobe with reduced bifurcate *lacinia mobilis* and three serrated setae, *pars molaris* with one acute and two blunt lobes and plumose seta distally. Palp with three articles; article 1 longest, 1.3 × longer than article 2, naked; article 2 1.5 × longer than wide, naked; article 3 with three serrated setae. lMd serrate *pars incisiva*, *lacinia mobilis* smooth; setiferous lobe with three serrated setae, *pars molaris* robust, blunt, with plumose seta distally; mandibular palp broken during dissection. Mx1 outer endite with apparently six terminal strong serrated spines; inner endite bearing six finely plumose setae. Palp bi-articulate with two long subdistal setae. Mx2 with long seta on the outer margin. Movable endite outer lobe with distal margin bearing four long setae; inner lobe of movable endite with four setae. Fixed endite outer lobe with six setae; inner fixed endite with seven setae. Mxp basis naked, narrow. Palp article 1 trapezoidal, with long seta (reaching article 3) on the inner distal margin and robust spine on the outer distal margin; article 2 longest, inner margin finely serrated proximally, with 10 setae, outer margin with two small apophyses and distal long seta; article 3 with six setae along inner margin and one plumose seta distally; article 4 with six plumose inner setae and three subdistal setae. Endite inner margin with three subcylindrical tubercles proximally and five subdistal setae; five setae apically; outer margin with five thin setae (**Figure 12**).

Che basis, 1.2 × longer than wide; ventral margin with medial and distal setae; dorsal margin with strong crenulation. Merus triangular; ventral margin with plumose seta subdistally. Carpus 2.7 × longer than wide, longer than basis, widest distally; ventral margin with medial plumose and distal setae; dorsal margin with minute distodorsal seta. Propodus 1.4 × longer than wide; with two setae near the articulation of the dactylus; fixed finger with three ventral plumose setae, with five submarginal and three marginal setae on the outer incisive margin. Dactylus and unguis slightly longer than fixed finger; with four setae on the ventral margin (**Figure 11**).

Pereon about 60% of TBL, all pereonites wider than long, all with two finely plumose setae on the subdistal dorsal margin and one seta on each anterolateral margin; Per 1–3 wider than others; Per 2–3 longer than Per 1; Per 6 shortest. P1 coxa lacking apophysis, with seta. Basis 2.9 × longer than wide; ventral margin with subproximal and distal setae; three setae and two smaller and one larger triangular apophyses along the dorsal margin. Ischium wider than long, with ventral seta. Merus 1.9 × longer than wide, widest distally; ventral margin with small medial spine and subdistal long plumose seta and spine; dorsal margin with proximal seta and distal seta and large spine. Carpus about as long as wide, widest distally, ventral margin with two subdistal spines; distodorsal margin with two plumose setae (one longer than the other) and one spine. Propodus twice longer than wide, with four spines along the ventral margin; dorsal margin with subdistal long plumose seta and spine. Dactylus together with unguis shorter than the propodus, dactylus longer than the unguis; dactylus with 2 minute ventral setae and small subdistal denticle. Unguis curved. P2 coxa lacking apophysis, naked. Basis 3.1 × longer than wide; ventral margin with minute medial seta; three setae and one rounded and two triangular apophyses along the dorsal margin. Ischium wider than long, with three ventral setae. Merus 1.9 × longer than wide, widest distally; ventral margin with minute medial seta; distodorsal margin with large spine. Carpus 0.8 × longer than wide; ventral margin with subdistal spines and two distal apophyses; distodorsal margin with plumose seta and small spine. Propodus 1.8 × longer than wide; with four spines along the ventral margin; dorsal margin with medial seta, distal long plumose seta, spine, and triangular apophyses. Dactylus together with unguis shorter than the propodus, dactylus longer than the unguis; dactylus with 2 minute ventral setae and small subdistal denticle. Unguis curved. P3 basis 2.7 × longer than wide; ventral margin with two medial and one distal setae; dorsal margin with two penicillate setae and rounded apophysis. Ischium with ventral seta. Merus 1.9 × longer than wide, widest distally; ventral margin subdistal seta; distodorsal margin with seta and spine. Carpus 0.8 × longer than wide; ventral margin with two subdistal spines; distodorsal margin with one plumose seta and two spines. Propodus twice longer than wide; with three spines along the ventral margin; dorsal margin with medial seta, distal long plumose seta and spine. Dactylus together with unguis shorter than the propodus, dactylus longer than the unguis; dactylus with 2 minute ventral setae and small subdistal denticle. Unguis curved. P4 basis 3.4 × longer than wide; ventral margin with proximal and distal setae; dorsal margin with two setae. Ischium wider than long, with ventral

plumose seta. Merus 1.5 × longer than wide; widest distally; distoventral margin with two setae and two spines. Carpus 1.4 × longer than wide; ventral margin with spine; distodorsal margin with two setae (one longer than other) and one spine. Propodus 2.7 × longer than wide; ventral margin with three spines; distodorsal margin with two plumose and one simple setae. Dactylus curved, together with unguis shorter than the propodus, dactylus longer than the unguis, with two (one medial and one subdistal) ventral setae and small subdistal denticle. Unguis curved. P5 basis 3 × longer than wide; with six setae along the ventral margin; dorsal margin subproximal seta. Ischium with two ventral setae. Merus about as long as wide; distoventral margin with seta; distodorsal margin with four setae. Carpus 0.8 × longer than wide; ventral margin with seta; distodorsal margin with seta. Propodus 3.7 × longer than wide; ventral margin with medial seta and subdistal spine; dorsal margin with subdistal and distal setae. Dactylus together with unguis shorter than the propodus, dactylus longer than the unguis, with one middorsal and two subdistal ventral setae and small subdistal denticle ventrally. Unguis curved. P6 basis 3.3 × longer than wide; with three setae along the dorsal margin. Ischium with ventral setae. Merus 1.5 × longer than wide; ventral margin with subdistal seta; distodorsal margin with spine. Carpus 1.2 × longer than wide; ventral margin with subdistal seta; distodorsal margin with seta and spine. Propodus 3.7 × longer than wide; ventral margin with subproximal seta and subdistal spine; dorsal margin with subdistal seta. Dactylus together with unguis shorter than the propodus, dactylus longer than the unguis; dactylus with one subdistal ventral seta. Unguis curved (**Figure 12**).

Pleon about 13% of TBL, shorter than Per 1–2 lengths combined, slightly longer than wide; last three pleonites fused to pleotelson, all indications of pleonites similar in length, without pleopods; pleonite 1 with three pairs of finely plumose dorsal setae and one seta on each lateral margin; pleonite 3 with two finely plumose setae dorsally. Pleotelson length 0.2 × that of all pleonites combined, apex large and rounded tip. Pleopods absent.

U biramous. Basal article longer than wide; inner margin with distal seta. Exopod with two articles, shorter than endopod articles 1–2 combined; article 1 with penicillate seta; article 2 with two distal setae. Endopod with three articles; article 1 with distal seta; article 2 longest, with distal seta; article 3 with two long and two short terminal setae (**Figure 12**).

Male (ZUEC-CRU-4370). Body (**Figure 11**). Length 1.1 mm.

Che, chela symmetrical. Similar but more robust and distinctly larger than those of the female. Basis ventral margin with medial and distal setae; dorsal margin with strong crenulation. Merus triangular, ventral margin with medial seta and large pointed apophyses distally. Carpus broad and short, more trapezoidal shaped than in female, ventral margin with two setae and small acute subdistal apophyses. Propodus with two setae near articulation of dactylus; fixed finger with one medial and three subdistal plumose setae on the ventral margin; with one rounded tubercle, three submarginal and 3 minute marginal setae on the outer incisive margin. Dactylus and unguis slightly longer than the fixed finger; with two rounded tubercles and six setae on the ventral margin.

Type locality: Trindade Island, Espírito Santo state, Brazil.

Distribution: Currently known only from the type locality.

Remarks: *Synapseudes isis* **sp. nov.**, *Synapseudes menziesi* Băcescu, 1976, *S. pinosensis* (Guţu and Ortiz, 2009) and *S. rectifrons* Guţu, 1996, are distinguished from the other 23 members of the genus as follows: bi-articulate antennal flagellum terminating in a long seta, remnants of two pleonites present, and uropod endopod composed of three articles. The new species from Brazil can be separated from *S. pinosensis* by having the ventral margin of pereopod 1 propodus with four stout spiniform setae (three spiniform setae in *S. pinosensis*) and antennule article 2 without distal spiniform apophysis (peduncular article 2 inner distally with a dentiform expansion in *S. pinosensis*). *Synapseudes isis* **sp. nov.** is different from *S. menziesi* by rostrum appearing undifferentiated, truncated (rostrum with irregularly bilobed anterior margin in *S. menziesi*) and Maxilliped palp article 2 distolateral stout seta 1.5 × longer than that on palp article 1 (as long as in *S. menziesi*).

Synapseudes isis **sp. nov.** closely resembles the other Brazilian species *S. rectifrons* but can be distinguished from it by antennule article 2 without tubercles or spines (with a spine on the inner margin and a small tubercle on the outer margin in *S. rectifrons*), antenna article 1 with inner margin strongly serrated (smooth in *S. rectifrons*) and maxilliped palp article 1 with distolateral seta strongly developed (thin and weakly developed in *S. rectifrons*). Also, *S. isis* sp. nov. appears unique by having cheliped merus, carpus, and propodus with plumose setae ventrally, cheliped fixed finger with row of 10 setae on the incisive margin, and pereopod 1–3 with three, two, and one spiniform apophyses on the ventral margin of the basis, respectively.

Suborder Tanaidomorpha Sieg, 1980
Family Leptocheliidae Lang, 1973
Genus *Chondrochelia* Guţu, 2016

***Chondrochelia dubia* (Krøyer, 1842)**

Material examined: Nine females, Piscinas do Parcel (20°31′10.812″S, 29°19′25.8″W), from *Dictyota* sp., September 2018, T. P. Macedo col. (ZUEC-CRU-4371); three females, Ilha do Sul (20°31′27.5″S, 29°19′25.2″W), from *Dictyota* sp., April 2019, I. Batistela col. (ZUEC-CRU-4372).

Remarks: *Chondrochelia* is a shallow water genus with dimorphic males and females, and *C. dubia* was firstly described as *Tanais dubius* from Brazil, and currently shows a worldwide distribution. Differences in morphological characters among *Chondrochelia* species are subtle, and further molecular studies may elucidate species delimitation within the genus. The new record agrees with the overall diagnosis of *C. dubia* and extends its distribution to the island of Trindade.

Phylogenetic Analysis

Heuristic searches resulted in four most parsimonious trees (L = 65 steps; CI = 50 and RI = 61), which were combined into a strict consensus tree, and this topology was used for the following data interpretation (**Figure 13**). Clade letters are represented below branches for the clades discussed ahead.

Clade A encompasses the genus *Synapseudes*, supported by four synapomorphies, including three non-homoplastic

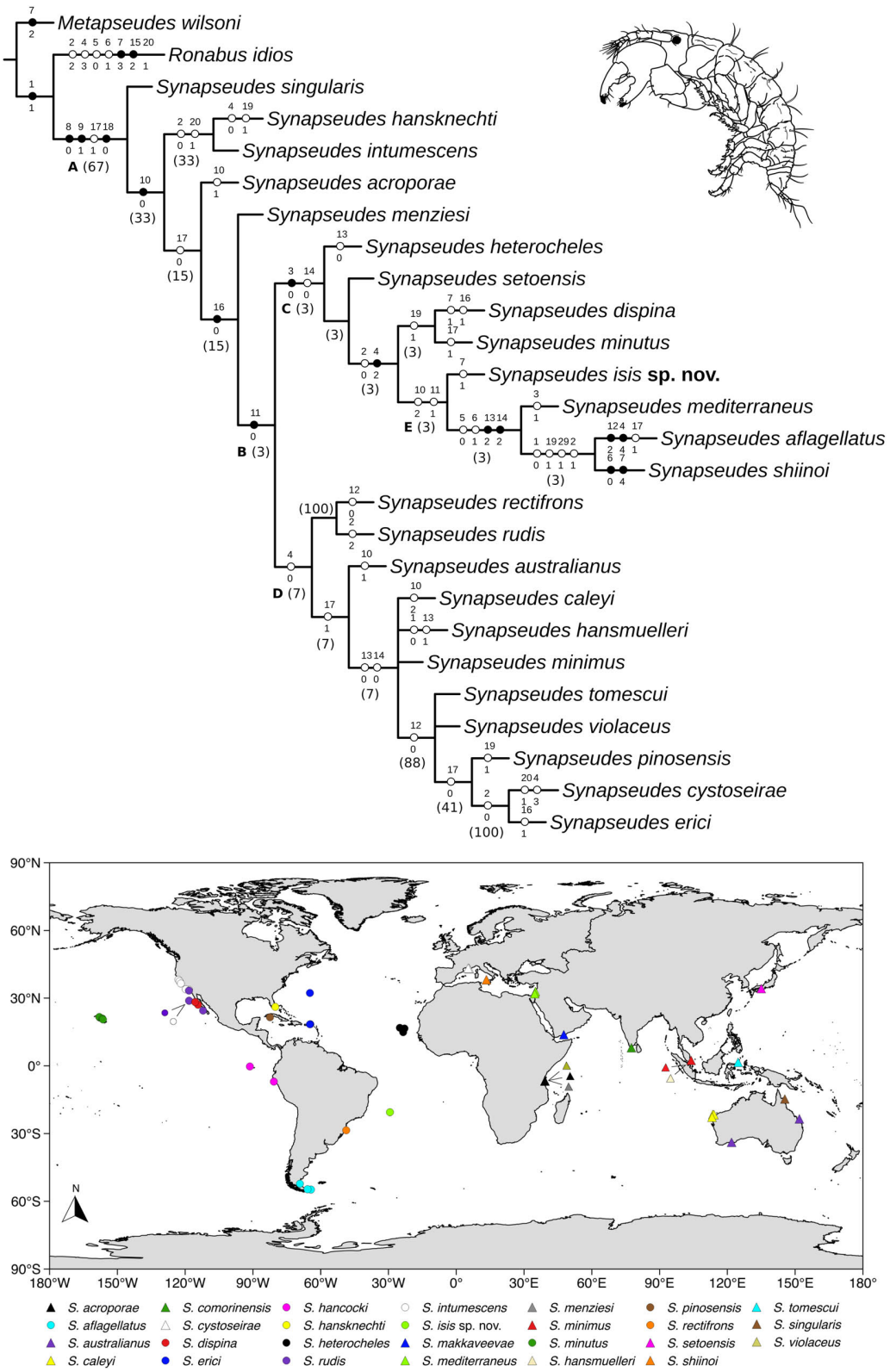

FIGURE 13 | Details of the Synapseudes Miller, 1940 consensus cladogram. Letters below branches represent clades mentioned in the discussion, numbers in parenthesis correspond to Bremmer relative support. Black circles represent non-homoplastic synapomorphies; white circles represent homoplastic synapomorphies. Numbers above branches represent the characters, and states are represented below. Map shows the current distribution of *Synapseudes*.

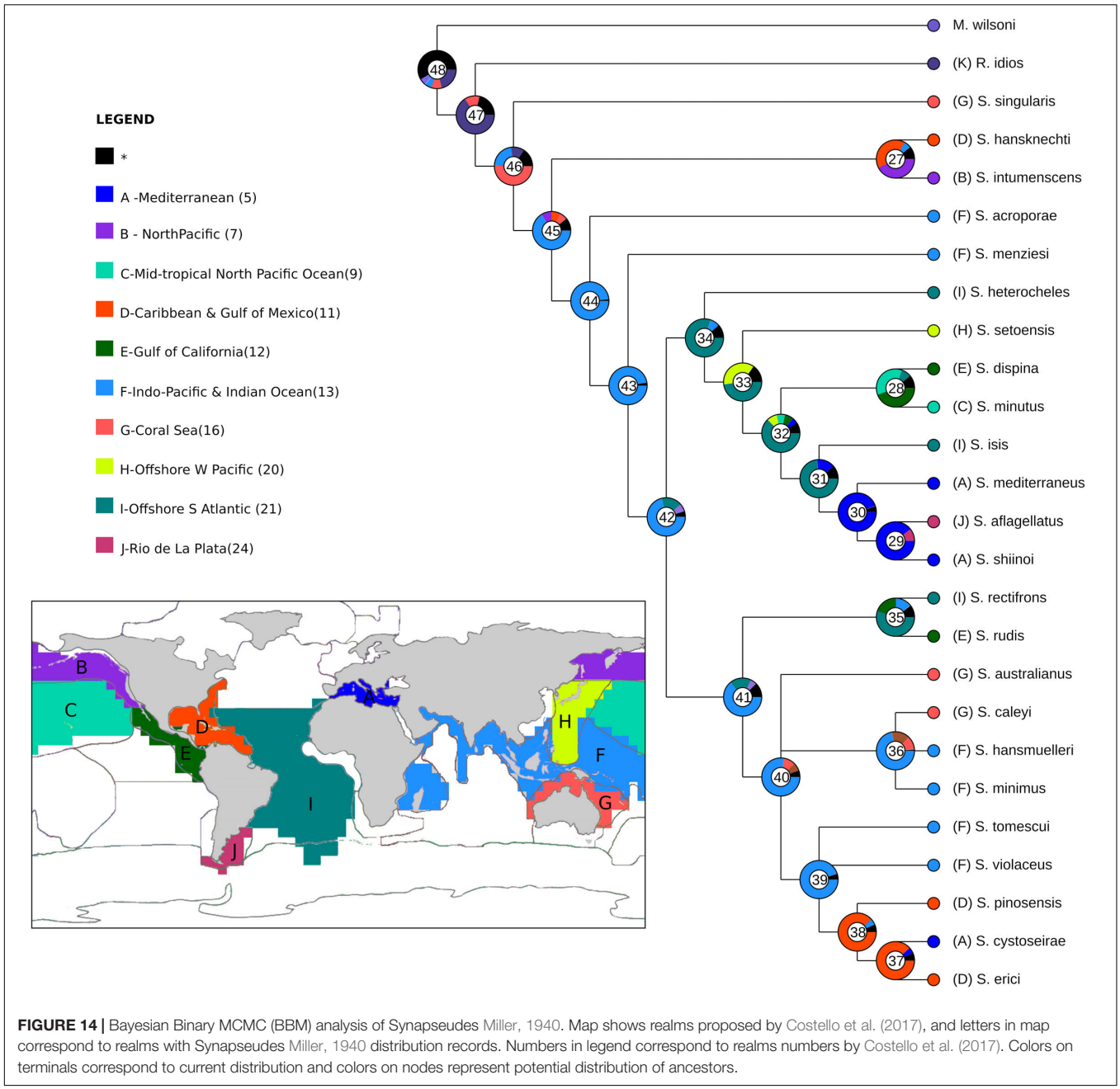

FIGURE 14 | Bayesian Binary MCMC (BBM) analysis of Synapseudes Miller, 1940. Map shows realms proposed by Costello et al. (2017), and letters in map correspond to realms with Synapseudes Miller, 1940 distribution records. Numbers in legend correspond to realms numbers by Costello et al. (2017). Colors on terminals correspond to current distribution and colors on nodes represent potential distribution of ancestors.

synapomorphies: presence of three terminal setae on mandibular palp [S6(0)], presence of setae on palp article 2 of Md [S7(1)], and two coupling hooks (retinacula) on endite of Mxp [S19(0)]; and one homoplastic synapomorphy: four articles on the uropodal endopod [S16(1)].

Clade B includes two clades of *Synapseudes* (clades C and D), and it is supported by two pleonites [S17(0)]. Clade C is composed of *S. heterocheles* (Vanhöffen, 1914), *S. setoensis* Shiino, 1951, *S. dispina* Menzies, 1953, *S. minutus* Miller, 1940, *S. isis* sp. nov., *S. mediterraneus* Băcescu, 1977, *S. aflagellatus* Sieg, 1986, and *S. shiinoi* Riggio, 1973, grouped by one non-homoplastic synapomorphy, the presence of three spiniform setae on the ventral margin of the propodus of pereopod 2 [S10(0)], and one homoplastic synapomorphy, one article on antennal flagellum [S12(0)]. Clade D comprises *S. rectifrons*, *S. rudis* Menzies, 1953, *S. australianus* Băcescu, 1981, *S. caleyi* Heard et al., 2018, *S. hansmuelleri* Guţu, 2006, *S. minimus* Guţu, 2006, *S. tomescui* Guţu, 2006, *S. violaceus* Băcescu, 1976, *S. pinosensis*, *S. cystoseirae* Amar and Cazaubon, 1978, and *S. erici* Błażewicz-Paszkowycz et al., 2011. This clade is clustered by the absence of distal spiniform apophyses on antennular peduncle article 2 [S13(0)].

Finally, clade E comprises *S. isis* sp. nov. as the sister clade of *S. mediterraneus*, *S. aflagellatus*, and *S. shiinoi,* supported by

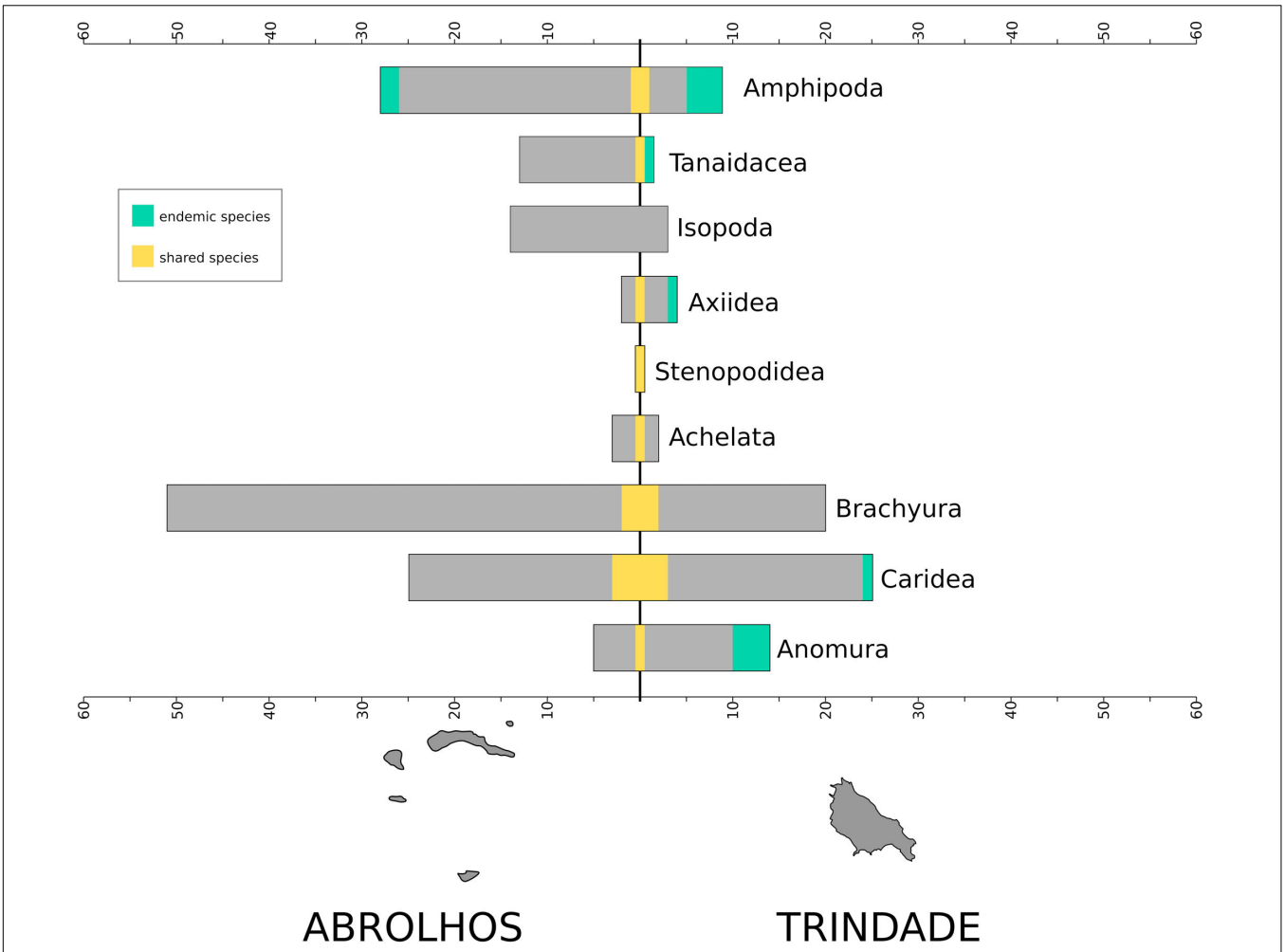

FIGURE 15 | Crustacea species richness reported from Abrolhos Archipelago (left) and Trindade Island (right). Gray bars correspond to species not shared by both islands, yellow bars correspond to shared species, and seafoam green bars correspond to endemic species. References: Amphipoda: Cunha et al. (2013), Andrade and Senna (2017), Serejo and Siqueira (2018); Tanaidacea: Brum (1973); Guţu (1996), Cunha et al. (2013); Isopoda: Barth (1958), Moreira (1977), Cunha et al. (2013), Souza et al. (2013), Campos-Filho et al. (2018); Axiidea: Pachelle and Tavares (2020); Stenopodidea: Soledade et al. (2015), Tavares et al. (2017); Achelata: Faria-Júnior et al. (2014), Tavares et al. (2017); Brachyura: Almeida and Coelho (2008), Tavares et al. (2017); Caridea: Soledade et al. (2017), Tavares et al. (2017), Lima et al. (2019).

the homoplastic synapomorphy of three pleonites [S17(1)] and symmetrical chelipeds in male [S18(2)].

Biogeographical Analysis

The results of the BBM analysis indicated that dispersal played a key role in shaping the current distribution patterns of *Synapseudes* (**Figure 14**), totaling 15 dispersals between areas within the genus. According to the analysis, the neighbor realms (G) Coral Sea and (F) Indo-Pacific and Indian Ocean are the two most likely ancestral areas of *Synapseudes* (node 46), with 50.50 and 22.48% marginal probability, respectively. The analysis suggests an early dispersal to the North Pacific (B) and the Caribbean and Gulf of Mexico (D), followed by sympatric speciation events along the Indo-Pacific and Indian Oceans.

A transoceanic dispersion is proposed for ancestors on node 42, with a single dispersion from the Pacific to the Atlantic Ocean before the separation into two main *Synapseudes* clades. The first main clade (clade C; **Figure 13**) shares a strict evolutionary relationship with the Atlantic followed by a late dispersal to the Mediterranean (A). On the other hand, the second main clade (clade D; **Figure 13**) mostly remains in the Indo-Pacific and Coral Sea realms, with a second dispersal to the Caribbean and Gulf of Mexico.

Concerning the new species from TR, *Synapseudes isis* sp. nov., its ancestor's area of distribution (node 31) suggests the last Atlantic speciation before the dispersal to the Mediterranean, with 73.26 and 15.25% marginal probabilities, respectively.

DISCUSSION

According to the classical Theory of Island Biogeography (IBT) proposed by MacArthur and Wilson (1967), species richness is

positively correlated with island area and negatively correlated with isolation. Additionally, Rosenzweig (1995) also commented on the importance of island age for predicting species richness. The General Dynamic Theory of Oceanic Island Biogeography (GDM; Whittaker et al., 2008) also takes into account island age as an important factor for predicting island species richness on islands, together with island area and isolation, but relies on not only the island birth but also the death processes that lead to erosion and consequent habitat loss (Hachich et al., 2019). Although these factors are known to influence species richness, species richness is highly determined by the taxon studied, as observed for reef fishes, seaweed, and marine gastropods in shallow waters (Hachich et al., 2015). Therefore, the results presented herein aim to contribute to the knowledge of Peracarida biogeography in shallow water habitats from oceanic islands.

The fauna of Peracarida from TR indeed agrees with the isolation of the island, in which only 11 species were sampled associated with *Dictyota* sp., whereas 30 species were found in the same algae at the Abrolhos Bank (Cunha et al., 2013), a 46,000 km^2 projection of the Brazilian continental shelf (Dutra et al., 2005), including two orders (Cumacea and Isopoda) not observed in TR (**Figures 1**, **15**). The Abrolhos Bank harbors the largest and most diverse reef complex of the South Atlantic (Leão, 1982; Dutra et al., 2005) presenting high levels of coral endemism (Leão and Dominguez, 2000); however, benthic invertebrates such as crustaceans and polychaetes showed low levels of endemicity for the area (Paiva, 2005; Young and Serejo, 2005; Cunha et al., 2013).

Regarding its endemicity, Peracarida is one of the most endemic taxa among the marine invertebrate fauna (Costello et al., 2017; Arfianti and Costello, 2020), and TR shows a high endemicity rate of 45%, higher than that observed for other Crustacea taxa previously reported for the island, such as Anomura, Axiidea, and Caridea, with 28, 25, and 4%, respectively (Anker et al., 2016; Tavares et al., 2017; Lima et al., 2019; Pachelle and Tavares, 2020). Other Decapoda taxa such as Achelata, Brachyura, and Stenopodidea lacked any species endemic to TR (Tavares et al., 2017). Nonetheless, we believe that the actual number of Peracarida species from TR is still underestimated, once only Peracarida members associated with *Dictyota* up to 10 m deep were sampled herein. Therefore, considering the broad range of Peracarida lifestyles, from planktonic to benthic and parasitic, further samplings are recommended to better assess TR biodiversity.

The cladistic analysis of *Synapseudes* supported the monophyly of the genus and agreed with the erection of the genus *Ronabus* by Heard et al. (2018). *Ronabus* is separated from *Synapseudes* based on the number of antennal flagella [S2(2)], the number of antennal terminal setae [S4(3)], the number of articles in the inner and outer antennular flagellum [S5(0) and S6(1)], the number of terminal setae on the mandibular palp [S7(3)], number of articles on the uropodal exopod [S15(2)], and telson with bulgae [S20(1)]. The analysis also showed two main clades within *Synapseudes* (clades C and D), which are discussed according to its distribution (**Figure 13**).

The BBM analysis of the genus *Synapseudes* is the first event-based biogeographic attempt to understand the dynamics of fauna associated with macroalgae over long periods of time. Even though it is well known that macroalgae are the best drifter substrata particularly for Peracarida because of lack of larval phase (Thiel, 2003), providing shelter and nutrition even in harsh environments, knowledge on the evolutionary processes that have driven the current distribution is scarce.

We recovered the Indo-Pacific + Coral Sea realms as the ancestral distribution area of *Synapseudes* (**Figure 14**), supporting the proposal of an Indo-Pacific "center of origin," where species originated in the biodiversity center colonize marginal areas and speciate (Bowen et al., 2013). Six species presented the current distribution within the realm of Indo-Pacific and Indian Ocean (realm F), followed by three species distributed in the Mediterranean (realm A), the Caribbean and Gulf of Mexico (realm D), and Offshore South Atlantic (realm I). Therefore, the BBM analysis suggests an Indo-Pacific + Coral Sea origin followed by multiple dispersals to other ocean realms. From the Indo-Pacific + Coral Sea origin, the first dispersal of *Synapseudes* ancestors was to the North Pacific (realm B) and to the Caribbean and Gulf of Mexico (realm D), while consecutive sympatric speciations continued to raise species number in the Indo-Pacific (**Figure 14**).

The separation of *Synapseudes* into two main clades corresponds to the first dispersal to the Offshore South Atlantic (realm I), where most of the ancestors speciated, suggesting a niche suitability for the genus. A possible return to the Pacific Ocean is suggested on node 33, where three dispersals to new realms within the Pacific are observed (nodes 28, 32, and 33), while the ancestors that remained in the Atlantic later dispersed to the neighboring realms of the Mediterranean (realm A) and Rio de La Plata (realm J). The second main clade remained in the Indo-Pacific region, with a second dispersal to the Atlantic, whereas successive sympatric speciations in the Indo-Pacific and Coral Sea continued to happen. Lastly, another dispersal to the Caribbean and Gulf of Mexico (realm D) followed by sympatric speciation were observed for *Synapseudes* (**Figure 14**).

This first attempt to understand the evolution of Peracarida associated with macroalgae suggests multiple dispersions from an Indo-Pacific center of origin, and better understanding of the paleocurrent dynamics, other Peracarida taxa phylogenetics, and molecular data will certainly help unpuzzling the historical biogeography of fauna–macroalgae association.

DATA AVAILABILITY STATEMENT

The datasets presented in this study can be found in online repositories. The names of the repository/repositories and accession number(s) can be found in the article/ **Supplementary Material**.

AUTHOR CONTRIBUTIONS

TI-A and SS: conceptualization. TI-A, SS, and JS: methodology and formal analysis. TI-A: writing–original draft. TI-A, SS, JS, and FL: writing–review and editing. FL: funding acquisition and supervision.

FUNDING

This study was funded by the Fundação de Amparo à Pesquisa do Estado de São Paulo-FAPESP (grant numbers 2018/00488–7 and 2018/10313–0).

ACKNOWLEDGMENTS

We are thankful to Projeto Ecológico de Longa Duração–Ilhas Oceânicas Brasileiras (PELD-ILOC), Thais Peixoto Macedo and Isis Batistela (Universidade Federal de Santa Catarina) for collecting the Dictyota material from the Trindade Island. We thank Francisco Andrade Montenegro for helping with Synapseudes drawings. We are also grateful to Profs. Silvio Nihei, Fabio Laurindo, and Andre Carvalho (Universidade de São Paulo) for reviewing the manuscript and for the helpful comments and suggestions. Finally, we thank FAPESP for TI-A's scholarship (2018/00488-7) and TI-A, SS and FL grant (2018/10313-0).

SUPPLEMENTARY MATERIAL

The Supplementary Material for this article can be found online at: https://www.frontiersin.org/articles/10.3389/fmars.2021.641236/full#supplementary-material

Supplementary Material 1 | Morphological characters used on *Synapseudes* phylogenetic analysis.

Supplementary Material 2 | Taxa and characters matrix.

REFERENCES

Almeida, A. O., and Coelho, P. A. (2008). Estuarine and marine brachyuran crabs (Crustacea: Decapoda) from Bahia, Brazil: checklist and zoogeographical considerations. *Lat. Am. J. Aquat. Res.* 36, 183–222. doi: 10.3856/vol36-issue2-fulltext-4

Alves, J., Johnsson, R., and Senna, A. R. (2016). On the genus *Elasmopus* Costa, 1853 from the Northeastern coast of Brazil with five new species and new records. *Zootaxa* 4184, 1–40. doi: 10.11646/zootaxa.4184.1.1

Amar, R., and Cazaubon, A. (1978). Une nouvelle espèce de *Synapseudes Crustacea*, *Tanaidacea* des côtes méditerrannéennes. *Téthys* 8, 327–333.

Andrade, L. F., and Senna, A. R. (2017). Four new species of *Cymadusa* Savigny, 1816 (*Amphipoda*: *Ampithoidae*) and new records of *C. filosa* Savigny, 1816 from Brazilian coast. *Zootaxa* 4226, 359–389. doi: 10.11646/zootaxa.4226.3.3

Anker, A., Tavares, M., and Mendonça, J. B. (2016). Alpheid shrimps (*Decapoda*: *Caridea*) of the Trindade & Martin Vaz Archipelago, off Brazil, with new records, description of a new species of *Synalpheus* and remarks on zoogeographical patterns in the oceanic islands of the tropical southern Atlantic. *Zootaxa* 4138, 1–58. doi: 10.11646/zootaxa.4138.1.1

Arfianti, T., and Costello, M. J. (2020). Global biogeography of marine amphipod crustaceans: latitude, regionalization, and beta diversity. *Mar. Ecol. Prog. Ser.* 638, 83–94. doi: 10.3354/meps13272

Audouin, V. (1826). Explication sommaire des planches de crustacesde l'Egypte et de la Syrie, publiees par Jules-Cesar Savigny, membre de l'Institut; offrant un expose des caracteres naturels des genres, avec la distinction des especes. *Description de l'Egypte, Histoire Naturelle* 1, 77–98.

Băcescu, M. (1976). Representatives of the family Synapseudidae (*Crustacea*, *Tanaidacea*) from the Tanzanian coral reefs: one new genus (*Curtipleon*) and three new species of *Synapseudes*. *Trav. du Muséum Natl. d'Histoire Nat. 'Grigore Antipa'* 17, 51–63.

Băcescu, M. (1977). *Heterotanais longidactylus* n. sp. and *Synapseudes mediterraneus* n. sp., *Tanaidacea* new for the eastern Mediterranean fauna. *Rev. Roum. Biol. Série Biol. Anim.* 22, 119–125.

Băcescu, M. (1981). Contribution to the knowledge of the Monokonophora (*Crustacea*, *Tanaidacea*) of the eastern Australia coral reefs. *Rev. Roum. Biol. Série Biol. Anim.* 26, 111–120.

Barnard, J. L. (1958). A remarkable new genus of corophiid amphipod from coastal marine bottoms of southern California. *Bull. South Calif. Acad. Sci.* 57, 85–90.

Barnard, J. L. (1965). Marine *Amphipoda* of the family *Ampithoidae* from southern California. *Proc. U. S. Natl. Mus.* 118, 1–46. doi: 10.5479/si.00963801.118-3522.1

Barnard, J. L. (1969). *Gammaridean Amphipoda* of the rocky intertidal of California: Monterey Bay to La Jolla. *Bul. U. S. Natl. Mus.* 258, 1–230. doi: 10.5479/si.03629236.258.1

Barnard, J. L. (1974). *Gammaridean Amphipoda* of Australia, part II. Smithson. *Contr. Zool.* 139, 1–148. doi: 10.5479/si.00810282.139

Barnard, J. L., and Karaman, G. S. (1991). The families and genera of marine *Amphipoda* (except marine Gammaroids). *Rec. Aust. Mus. Suppl.* 13, 1–866. doi: 10.3853/j.0812-7387.13.1991.91

Barnard, K. H. (1932). *Amphipoda*. *Discov. Rep*. 5, 1–326.

Barth, R. (1958). Observações biológicas e meteorológicas feitas na Ilha de Trindade. *Mem. Inst. Oswaldo Cruz* 56, 261–279. doi: 10.1590/s0074-02761958000100013

Bate, C. S. (1862). Catalogue of the specimens of amphipodous *Crustacea* in the collection of the British Museum. *Br. Mus.* 1–399.

Berents, P. B. (1983). The Melitidae of Lizard Island and adjacent reefs, The Great Barrier Reef, Australia (*Crustacea*: *Amphipoda*). *Rec. Aust. Mus.* 35, 101–143. doi: 10.3853/j.0067-1975.35.1983.313

Błażewicz-Paszkowycz, M., Bamber, R., and Anderson, G. (2012). Diversity of *Tanaidacea* (*Crustacea*: *Peracarida*) in the world's oceans–how far have we come? *PLoS One* 7:e33068. doi: 10.1371/journal.pone.0033068

Błażewicz-Paszkowycz, M., and Bamber, R. N. (2007). New apseudomorph tanaidaceans (*Crustacea*: *Peracarida*: *Tanaidacea*) from eastern Australia: apseudidae, whiteleggiidae, metapseudidae and pagurapseudidae. *Mem. Mus. Vic.* 64, 107–148. doi: 10.24199/j.mmv.2007.64.11

Błażewicz-Paszkowycz, M., Heard, R. W., and Bamber, R. N. (2011). A new species of shallow-water metapseudid (*Crustacea*: *Malacostraca*: *Peracarida*: *Tanaidacea*) from Bermuda (Caribbean). *Bull. Peabody Mus. Nat. Hist.* 52, 127–134. doi: 10.3374/014.052.0103

Boeck, A. (1871). *Crustacea Amphipoda* borealia et arctica. *Forhandlinger i Videnskabs- Selskabet i Christiania* 1870, 83–280.

Bousfield, E. L., and Hendrycks, E. A. (2002). The Talitroidean amphipod family Hyalidae revised with emphasis on the North Pacific fauna: systematic and distributional ecology. *Amphipacifica* 3, 17–134.

Bowen, B. W., Rocha, L. A., Toonen, R. J., and Karl, S. A. (2013). The origins of tropical marine biodiversity. *Trends Ecol. Evol.* 28, 359–366. doi: 10.1016/j.tree.2013.01.018

Bremer, K. (1994). Branch support and tree stability. *Cladistics* 10, 295–304. doi: 10.1111/j.1096-0031.1994.tb00179.x

Brum, I. N. (1973) Contribuição ao conhecimento da fauna do Arquipélago de Abrolhos, Bahia, Brasil, N°4. Crustacea–Tanaidacea. Boletim do Museu de História Natural da Universidade Federal de Minas Gerais. *Zoologia* 18, 1–14.

BulyĆeva, A. N. (1957) Beach-fleas of the seas of the USSR and adjacent waters (Amphipoda — Talitroidea). *Akademiia Nauk SSSR, Opredeliteli po Faune SSSR* 65, 1–185.

Campos, J. M. P., Correia, F. R., and Rosa Filho, J. S. (2020). Primeiro registro de *Ampithoe marcuzzii* Ruffo, 1954 (*Crustacea*: *Amphitoidae*) para o Nordeste do Brasil. *Pesquisa e Ensino em Ciências Exatas e da Natureza* 4, 01–07.

Campos-Filho, I. S., Cardoso, G. M., and Aguiar, J. O. (2018). Catalogue of terrestrial isopods (Crustacea, Isopoda, Oniscidea) from Brazil: an update with some considerations. *Nauplius* 26:e2018038. doi: 10.1590/2358-2936e2018038

Christie, H., Norderhaug, K. M., and Fredriksen, S. (2009). Macrophytes as habitat for fauna. *Mar. Ecol. Prog. Ser.* 396, 221–233. doi: 10.3354/meps08351

Correia, F. R., Guedes-Silva, E., and Souza-Filho, J. F. (2016). A new species of *Ampithoe* Leach, 1814 (*Senticaudata*, *Ampithoidae*) from Brazilian coast. *Zootaxa* 4136, 195–200. doi: 10.11646/zootaxa.4136.1.12

Costa, A. (1853). Descrizione di tre nuovi Crostacei del Mediterraneo discoperti dal Rev. G.F. Hope. *Fauna del Regno di Napoli* 83, 1–10.

Costello, M. J., Tsai, P., Wong, P. S., Cheung, A. K. L., Basher, Z., and Chaudhary, C. (2017). Marine biogeographic realms and species endemicity. *Nat. Commun.* 8:1057. doi: 10.1038/s41467-017-01121-2

Cunha, R., Tavares, M., and Mendonça, J. B. J. (2020). Asteroidea (*Echinodermata*) from shallow-waters of the remote oceanic archipelago Trindade and Martin Vaz, southeastern Atlantic, with taxonomic and zoogeographical notes. *Zootaxa* 4742:zootaxa.4742.1.2. doi: 10.11646/zootaxa.4742.1.2

Cunha, T. J., Güth, A. Z., Bromberg, S., and Sumida, P. Y. G. (2013). Macrofauna associated with the brown algae *Dictyota* spp. (*Phaeophyceae*, *Dictyotaceae*) in the Sebastião Gomes Reef and Abrolhos Archipelago, Bahia, Brazil. *Cont. Shelf Res.* 70, 140–149. doi: 10.1016/j.csr.2013.09.001

Dana, J. D. (1849). Conspectus crustaceorum, conspectus of the *Crustacea* of the U.S. exploring expedition. *Am. J. Sci. Arts* 8, 424–428.

Dana, J. D. (1853). *Crustacea*. Part II. United States Exploring Expedition During the Years 1838, 1839, 1840, 1841, 1842; Under the Command of Charles Wilkes 14: 689–1618, 96 pls. doi: 10.5962/bhl.title.23237

De Pinna, M. C. C. (1991). Concepts and tests of homology in the cladistic paradigm. *Cladistics* 7, 367–394. doi: 10.1111/j.1096-0031.1991.tb00045.x

Duffy, J. E., and Hay, M. E. (1991). Food and shelter as determinants of food choice by an herbivorous marine amphipod. *Ecology* 72, 1286–1298. doi: 10.2307/1941102

Dutra, G., Allen, G., Werner, T., and McKenna, S. (2005). *A Rapid Marine Biodiversity Assessment of the Abrolhos Bank, Bahia, Brazil. The RAP Bulletin of Biological Assessment*, 38th Edn. Washington, DC: Conservation International.

Faria-Júnior, E., de Carvalho Gaeta, J., and Freire, A. S. (2014). Una actualización de las especies de langosta (Panulirus White, 1847) en el Parque Nacional de Abrolhos, Norte de Brazil/An update on the lobster species (Panulirus White, 1847) from the Abrolhos Marine National Park, Northern Brazil. *Rev. Investig. Marinas* 33, 37–42.

Gardiner, L. F. (1973). New species of the genera *Synapseudes* and *Cyclopoapseudes* with notes on morphological variation, postmarsupial development, and phylogenetic relationships within the family Metapseudidae (*Crustacea*: *Tanaidacea*). *Zool. J. Linn. Soc.* 53, 25–58. doi: 10.1111/j.1096-3642.1973.tb01410.x

Gasparini, J. L., and Floeter, S. R. (2001). The shore fishes of Trindade Island, western south Atlantic. *J. Nat. Hist.* 35, 1639–1656. doi: 10.1080/00222930131709237 9

Gibson, R. N. (1986). "Intertidal teleosts: life in a fluctuating environment," in *The Behaviour of Teleost Fishes*, ed. T. J. Pitcher (Boston, MA: Springer), 388–408. doi: 10.1007/978-1-4684-8261-4_15

Goloboff, P. A., Farris, J. S., and Nixon, K. C. (2008). TNT, a free program for phylogenetic analysis. *Cladistics* 24, 774–786. doi: 10.1111/j.1096-0031.2008.00217.x

Gomes-da-Silva, J., and Souza-Chies, T. T. (2017). What actually is Vriesea? A total evidence approach in a polyphyletic genus of Tillandsioideae (*Bromeliaceae*, *Poales*). *Cladistics* 34, 181–199. doi: 10.1111/cla.12200

Gouillieux, B., and Sorbe, J. C. (2015). *Elasmopus thalyae* sp. nov.(*Crustacea*: *Amphipoda*: *Maeridae*), a new benthic species from soft and hard bottoms of Arcachon Bay (SE Bay of Biscay). *Zootaxa* 3905, 107–118. doi: 10.11646/zootaxa.3905.1.6

Guţu, M. (1972). Phylogenetic and systematic considerations upon the Monokonophora (Crustacea – Tanaidacea) with the suggestions of a new family and several new subfamilies. *Revue Roumaine de Biologie, Série de Zoologie* 17, 297–305.

Guţu, M. (1996). Tanaidaceans (*Crustacea*, *Peracarida*) from Brazil, with description of new taxa and systematical remarks on some families. *Trav. du Muséum Natl. d'Histoire Nat. 'Grigore Antipa'* 36, 23–133.

Guţu, M. (2006). *New Apseudomorph Taxa (Crustacea, Tanaidacea) of the World Ocean*. Bucharest: Curtea Veche.

Guţu, M. (2016). *Systematic Novelties of the Enigmatic Universe of the Leptocheliids (Crustacea: Tanaidacea)*. Bucharest: ePublishers.

Guţu, M., and Ortiz, M. (2009). A new genus and two new species of the Metapseudids from the Southern waters of Cuba (*Crustacea*: *Tanaidacea*: *Apseudomorpha*). *Trav. du Muséum Natl. d'Histoire Nat. 'Grigore Antipa'* 52, 87–99.

Hachich, N. F., Bonsall, M. B., Arraut, E. M., Barneche, D. R., Lewinsohn, T. M., and Floeter, S. R. (2015). Island biogeography: patterns of marine shallow-water organisms in the Atlantic Ocean. *J. Biogeogr.* 45, 1871–1882. doi: 10.1111/jbi.12560

Hachich, N. F., Ferrari, D. S., Quimbayo, J. P., Pinheiro, H. T., and Floeter, S. R. (2019). "Island biogeography of marine shallow-water organisms," in *Encyclopedia of the World's Biomes*, eds M. Goldstein and D. DellaSala (Amsterdam: Elsevier), 61–75. doi: 10.1016/B978-0-12-409548-9.11947-5

Haswell, W. A. (1879). On australian *amphipoda*. *Proc. Linn. Soc. N. S. W.* 4, 245–279.

Heard, R. W., Stępień, A., Drumm, D. T., Błażewicz, M., and Anderson, G. (2018). Systematic and taxonomic observations on the subfamily Synapseudinae Guţu, 1972 and related metapseudid taxa (*Crustacea*: *Tanaidacea*: *Apseudomorpha*), with the erection of a new genus and descriptions of three new species. *Zootaxa* 4370, 301–344. doi: 10.11646/zootaxa.4370.4.1

Horton, T., Lowry, J., De Broyer, C., Bellan-Santini, D., Coleman, C. O., Corbari, L., et al. (2020). *World Amphipoda Database. Elasmopus besnardi Oliveira, 1951. Accessed through: World Register of Marine Species*. Avaliable at: http://www.marinespecies.org/aphia.php?p=taxdetails&id=531472 (accessed December 3, 2020).

Hurtado, L. A., Mateos, M., Mattos, G., Liu, S., Haye, P. A., and Paiva, P. C. (2016). Multiple transisthmian divergences, extensive cryptic diversity, occasional long-distance dispersal, and biogeographic patterns in a marine coastal isopod with an amphi-American distribution. *Ecol. Evol.* 6, 7794–7808. doi: 10.1002/ece3.2397

Iwasa-Arai, T., and Serejo, C. S. (2018). Phylogenetic analysis of the family Cyamidae (*Crustacea*: *Amphipoda*): a review based on morphological characters. *Zool. J. Linn. Soc., zlx* 101, 1–29.

Iwasa-Arai, T., Siqueira, S. G. L., Machado, G. B. D. O., and Leite, F. P. P. (2019). Phylogenetic reconstruction of the genus *Pseudaeginella* (*Amphipoda*: *Caprellidae*), with the description of a new species from Brazil. *System. Biodivers.* 17, 179–189. doi: 10.1080/14772000.2019.1572668

Krapp-Schikel, G., and Ruffo, S. (1990). Marine amphipods of the Canary Islands with description of a new species of *Elasmopus*. *Misc. Zool.* 14, 53–58.

Krapp-Schickel, T. (2008). What has happened with the Maera-clade (*Crustacea*, *Amphipoda*) during the last decades? *Bolletino del Museo di Storia Naturale di Verona* 32, 3–32.

Krøyer, H. (1842). Nye Arter af Slaegten *Tanais*. *Naturhistorisk Tidsskr. Ser.* 1, 167–188.

Lang, K. (1970). Taxonomische und phylogenetische Untersuchungen über die Tanaidaceen. 4. Aufteilung der Apseudiden in vier Familien nebst Aufstellung von zwei Gattungen und einer Art der neuen Familie Leiopidae. *Ark. för Zool.* 22, 595–626.

Lang, K. (1973). Taxonomische und phylogenetische Untersuchungen über die Tanaidaceen (*Crustacea*). 8. Die Gattungen *Leptochelia* Dana, *Paratanais* Dana, *Heterotanais* G.O. Sars und *Nototanais* Richardson. Dazu einige Bemerkungen über die Monokonophora und ein Nachtrag. *Zool. Scr.* 2, 197–229. doi: 10.1111/j.1463-6409.1974.tb00752.x

Latreille, P. A. (1816). Nouveau Dictionnaire d'histoire naturelle, appliquée aux arts, à l'Agriculture, à l'Economic rurale et domestique, à la Médecine, etc. *Par une Société de Naturalistes et d'Agriculteurs. Nouvelle Édition. Paris.* 1, 467–469.

Leach, W. E. (1814). "Crustaceology," in *The Edinburgh Encyclopedia*, ed. D. Brewster (Edinburgh: William Blackwood), 383–437.

Leão, Z. M. A. N. (1982). *Morphology, Geology and Developmental History of the Southermost Coral Reefs of Western Atlantic. Abrolhos Bank, Brazil*. Doctoral Thesis, University of Miami, Coral Gables, FL.

Leão, Z. M. A. N., and Dominguez, J. M. L. (2000). "Tropical coast of Brazil," in *Seas at the Millennium: An Environmental Evaluation*, Vol. 1, ed. C. R. C. Sheppard (Pergamon: Europe, the Americas and West Africa), 719–729.

LeCroy, S. E., Gasca, R., Winfield, I., Ortiz, M., and Escobar-Briones, E. (2009). "*Amphipoda* (*Crustacea*) of the Gulf of Mexico," in *Gulf of Mexico–Origins, Waters, and Biota*, Vol. 1, eds D. L. Felder and D. K. Camp (College Station, TX: Texas A&M University Press), 941–972.

LeCroy, S. E. (2002). "An illustrated identification guide to the nearshore marine and estuarine *Gammaridean Amphipoda* of Florida," in *Families Ampeliscidae, Amphilochidae, Ampithoidae, Aoride, Argissidae, and Haustoriidae*, Vol. 2, (Tallahassee, FL: Florida Department of Environmental Protection), 213.

Ledoyer, M. (1972). Presence de *Perioculodes aequimanus* (Kossmann) dans les eaux mediterranennes (region de Marseille) et comparaison avec *P. longimanus* (Bate et Westwood) (*Crustacea*, *Amphipoda*). *Bull. Mus. Natl. d'histoire Nat. Zool.* 491, 775–781.

Ledoyer, M. (1982). Crustacés amphipodes gammariens. Familles des Acanthonotozomatidae à Gammaridae. *Faune de Madagascar* 59, 1–598.

Leite, F. P. P. (2011). "*Amphipoda*," in *Biodiversidade e Ecossistemas Bentônicos Marinhos do Litoral Norte de São Paulo Susteste do Brasil*, eds A. C. Z. Amaral and S. A. H. Nallin (Campinas: Unicamp/IB), 327–333.

Leite, F. P. P., Siqueira, S. G. L., Oliveira, D. A., Hoff, C., Requel, A. C., Brumatt, P. N., et al. (2011). "Peracáridos dos substratos biológicos de costões rochosos," in *Biodiversidade e Ecossistemas Bentônicos Marinhos do Litoral Norte de São Paulo Susteste do Brasil*, eds A. C. Z. Amaral and S. A. H. Nallin (Campinas: Unicamp/IB), 327–333.

Lima, D., Tavares, M., and Mendonça, J. B. (2019). Paguroids (*Decapoda*: *Anomura*: *Diogenidae* and *Paguridae*) of the remote oceanic Archipelago Trindade and Martin Vaz, off southeast Brazil, with new records, description of three new species and zoogeographical notes. *Zootaxa* 4694, 1–63. doi: 10.11646/zootaxa.4694.1.1

Lowry, J. K., and Myers, A. A. (2013). A phylogeny and classification of the Senticaudata subord. nov. (*Crustacea*: *Amphipoda*). *Zootaxa* 3610, 1–80. doi: 10.11646/zootaxa.3610.1.1

Lowry, J. K., and Stoddart, H. E. (2003). "*Crustacea*: malacostraca: peracarida: *Amphipoda*, cumacea, mysidacea," in *Zoological Catalogue of Australia*, Vol. 19.2B, eds P. L. Beesley and W. W. K. Houston (Melbourne: CSIRO Publishing), 1–479.

MacArthur, R. H., and Wilson, E. O. (1967). *The theory of Island Biogeography*. Princeton: Princeton University Press.

Macieira, R. M., Simon, T., Pimentel, C. R., and Joyeux, J.-C. (2015). Isolation and speciation of tidepool fishes as a consequence of Quaternary sea-level fluctuations. *Environ. Biol. Fishes* 98, 385–393. doi: 10.1007/s10641-014-0269-0

Martín, A., Díaz, Y., Miloslavich, P., Escobar-Briones, E., Guerra-García, J. M., Ortiz, M., et al. (2013). Regional diversity of *Amphipoda* in the Caribbean Sea. *Rev. Biol. Trop.* 61, 1681–1720. doi: 10.15517/rbt.v61i4.12816

Menzies, R. J. (1953). No. 9- The apseudid Chelifera of the eastern tropical and north temperate Pacific Ocean. *Bull. Mus. Comp. Zool. Harvard Coll.* 107, 443–496.

Miller, M. A. (1940). The Isopod *Crustacea* of the Hawaiian Islands (Chelifera and Valvifera). Bernice Pauahi Bish. *Mus. Occas. Pap.* 15, 295–319.

Moreira, P. S. (1977). Occurrence and ecological notes on *Rocinela signata* (*Isopoda*, *Flabellifera*) off Brazil. *Bolm. Inst. Oceanogr.* 26, 293–301. doi: 10.1590/s0373-55241977000200007

Myers, A. A. (1986). *Amphipoda* from the South Pacific: Niue Island. *J. Nat. Hist.* 20, 1381–1392. doi: 10.1080/00222938600770921

Nixon, K. C. (2002). *Winclada (Beta) (Version 1.00.08)*. Avaliable at: http://cladistics.com/about_winc.html. (accessed 26 July 2020).

Nixon, K. C., and Carpenter, J. M. (1993). On outgroups. *Cladistics* 9, 413–426.

O'Leary, M. A., and Kaufman, S. G. (2012). *MorphoBank 3.0: Web Application for Morphological Phylogenetics and Taxonomy*. Avaliable at: http://www.morphobank.org (accessed July 7, 2020).

Oliveira, L. P. H. (1951). The genus *Elasmopus* on the coast of Brazil with description of *Elasmopus besnardi* n. sp., and *E. fusimanus* n. sp. (*Crustacea*, *Amphipoda*). *Bolm. Inst. Paul. Oceanogr.* 2, 1–17. doi: 10.1590/s0100-42391951000200001

Oliveira, L. P. H. (1953). *Crustacea Amphipoda* do Rio de Janeiro. *Mem. Inst. Oswaldo Cruz* 51, 289–376. doi: 10.1590/s0074-02761953000100009

Ortiz, M., and Lalana, R. (1994). Two new species of the genus *Elasmopus* (*Amphipoda*, *Gammaridea*), from the Cuban marine waters. *Trav. du Muséum Natl. d'Histoire Nat. 'Grigore Antipa'* 34, 293–302.

Ortíz, M., Martín, A., and Díaz, Y. J. (2007). Lista y referencias de los crustáceos anfípodos (*Amphipoda*: *Gammaridea*) del Atlántico occidental tropical. *Rev. Biol. Trop.* 55, 479–498. doi: 10.15517/rbt.v55i2.6026

Pachelle, P. P. G., and Tavares, M. (2020). Axiidean ghost shrimps (*Decapoda*: *Axiidae*, *Callianassidae*, *Callichiridae*, *Micheleidae*) of the Trindade and Martin Vaz Archipelago, Vitória-Trindade Seamounts Chain and Abrolhos, off southeastern Brazil. *Zootaxa* 4758, 103–126. doi: 10.11646/zootaxa.4758.1.4

Paiva, P. C. (2005). "Soft-bottom polychaetes of the Abrolhos Bank," in *A Rapid Marine Biodiversity Assessment of the Abrolhos Bank, Bahia, Brazil. The RAP Bulletin of Biological Assessment*, eds G. Dutra, G. Allen, T. Werner, and S. McKenna (Washington, DC: Conservation International), 87–90.

Paz-Ríos, C. E., Simões, N., and Ardisson, P.-L. (2013a). Intertidal and shallow water amphipods (*Amphipoda* : *Gammaridea* and *Corophiidea*) from Isla Pérez, Alacranes Reef, southern Gulf of Mexico. *Nauplius* 21, 179–194. doi: 10.1590/S0104-64972013000200005

Paz-Ríos, C. E., Simões, N., and Ardisson, P.-L. (2013b). Records and observations of amphipods (*Amphipoda* : *Gammaridea* and *Corophiidea*) from fouling assemblages in the Alacranes Reef, southern Gulf of Mexico. *Mar. Biodiv. Rec.* 6, 1–16. doi: 10.1007/978-3-319-23534-9_1

Pereira-Filho, G. H., Amado-Filho, G. M., Guimarães, S. M., Moura, R. L., Sumida, P. Y., Abrantes, D. P., et al. (2011). Reef fish and benthic assemblages of the Trindade and Martin Vaz island group, southwestern Atlantic.Braz. *J. Oceanogr.* 59, 201–212. doi: 10.1590/s1679-87592011000300001

Pinheiro, H. T., Bernardi, G., Simon, T., Joyeux, J. C., Macieira, R. M., and Gasparini, J. L. (2017). Island biogeography of marine organisms. *Nature* 549, 82–85. doi: 10.1038/nature23680

Pinheiro, H. T., Mazzei, E., Moura, R. L., Amado-Filho, G. M., Carvalho-Filho, A., Braga, A. C., et al. (2015). Fish biodiversity of the Vitória-Trindade Seamount Chain, southwestern Atlantic: an updated database. *PLoS One* 10:e0118180. doi: 10.1371/journal.pone.0118180

Rathke, H. (1836). Zur Fauna der Krym. *Mém. Acad. Imp. Sci. Saint Pétersbourg* 3, 291–454.

Riggio, S. (1973). Segnalazione del genere *Synapseudes* Miller, 1940 (*Crustacea Peracarida Anisopoda*) nel Mediterraneo con la Descrizione preliiminare di *Synapseudes shiinoi* n. sp. *Mem. Biol. Mar. Oceanogr. Mess. N.S.* 3, 11–19.

Ronquist, F., and Huelsenbeck, J. P. (2003). MrBayes3: bayesian phylogenetic inference undermixed models. *Bioinformatics* 19, 1572–1574. doi: 10.1093/bioinformatics/btg180

Rosenzweig, M. L. (1995). *Species Diversity in Space and Time*. Cambridge: Cambridge University Press.

Ruffo, S. (1954). Studi sui crostacei anfipodi. XL. Nuovi anfipodi raccolti nel Venezuelan dal Prof. G. Marcuzzi. *Mem. Mus. Civ. Storia Nat. Ver. ona* 4, 117–125.

Ruffo, S. (1959). Contributions to the knowledge of the Red Sea No. 13. Contributo alia conoscenze degli anfipodi del Mar Rosso (1) (Materiali raccolti a Ghardaqa e nel Golfo di Aqaba). *Bull. Sea Fish. Res. Stat. Haifa* 20, 1–26. doi: 10.1080/11250003809436977

Santos, J. P., and Soares, C. M. A. (1999). Crustacea Amphipoda Gammaridea da Praia de Piedade – Jaboatão dos Guararapes – Pernambuco – Brasil. *Trab. Oceanog. Univ. Fed.* 27, 61–72. doi: 10.5914/tropocean.v27i2.2818

Savigny, J. C. (1816). Observations generales sur la bouche des arachnides, des crustaces et des entomostraces, Memories sur les Animaux sans Vertebres. *Second Memorie* 1, 39–117.

Schellenberg, A. (1928). Report on the *Amphipoda*. *Trans. Zool. Soc. London* 22, 633–692.

Senna, A. R., and Souza-Filho, J. F. (2011). A new species of the *Elasmopus rapax* complex (*Crustacea*: *Amphipoda*: *Maeridae*) from Brazilian waters. *Cah. Biol. Mar.* 52:57.

Serejo, C. S. (1999). "Taxonomy and distribution of the family Hyalidae (*Amphipoda*, Talitroidea) on the Brazilian coast," in *Crustaceans and the Biodiversity Crisis. Proceedings of the Fourth International Crustacea Congress. Crustacean Issues*, eds F. R. Schram and J. C. V. Klein (Leiden: Brill), 591–616.

Serejo, C. S., and Licínio, M. V. S. (2002). The genus *Ampithoe* (*Crustacea*, *Amphipoda*, *Ampithoidae*) from the Brazilian coast. *Arq. Mus. Nac.* 60, 41–60.

Serejo, C. S., and Siqueira, S. G. L. (2018). Catalogue of the Order *Amphipoda* from Brazil (*Crustacea*, *Peracarida*): suborders amphilochidea, senticaudata and order ingolfiellida. *Zootaxa* 4431, 1–139. doi: 10.11646/zootaxa.4431.1.1

Shiino, S. M. (1951). On two new species of the family Apseudidae found at Seto. *Rep. Facul. Fish. Prefect. Univ. Mie* 1, 11–25.

Shoemaker, C. R. (1933). *Two New Genera and Six New Species of Amphipoda From Tortugas. Papers of the Tortugas Laboratory*. Washington, DC: Carnegie Institute of Washington, 245–256.

Shoemaker, C. R. (1938). Three new species of the amphipod genus *Ampithoe* from the west coast of America. *J. Wash. Acad. Sci.* 28, 15–25.

Sieg, J. (1980). Sind die Dikonophora eine polyphyletische Gruppe? *Zool. Anzieger* 205, 401–416.

Sieg, J. (1986). "*Crustacea Tanaidacea* of the antarctic and the subantarctic. 1. On material collected at tierra del Fuego, Isla de los Estados, and the west coast of the Antarctic Peninsula," in *Biology of the Antarctic Seas 18*, Vol. 45, ed. L. S. Korniker (Washington, D.C: American Geophysical Union). the Antarctic Research Series.

Simone, L. R. L., and Cavallari, D. C. (2020). A new species of *Macrocypraea* (*Gastropoda*, *Cypraeidae*) from Trindade Island, Brazil, including phenotypic differentiation from remaining congeneric species. *PLoS One* 15:e0225963. doi: 10.1371/journal.pone.0225963

Siqueira, S. G. L. (2012). *Alga parda Sargassum Furcatum e Anfípodes Ampitoídeos Associados como Potenciais Bioindicadores de Poluição por Hidrocarbonetos de Petróleo*. Ph. D. Thesis, Universidade Estadual de São Paulo, São Paulo, 126.

Sivaprakasam, T. E. (1970). A new species and a new record of *Amphipoda* (*Crustacea*) from the Gulf of Mannar. *J. Mar. Biol. Assoc. India* 10, 274–282.

Soledade, G. O., Fonseca, M. S., and Almeida, A. O. (2015). Shallow-water stenopodidean and caridean shrimps from Abrolhos Archipelago, Brazil: new records and updated checklist. *Zootaxa* 3905, 52–68.

Soledade, G. O., Santos, G. G., Pinheiro, U., and Almeida, A. O. (2017). New records of association between caridean shrimps (Decapoda) and sponges (Porifera) in Abrolhos Archipelago, northeastern Brazil. *Nauplius* 25. doi: 10.1590/2358-2936e2017027

Sotka, E. E., Bell, T., Hughes, L. E., Lowry, J. K., and Poore, A. G. (2017). A molecular phylogeny of marine amphipods in the herbivorous family *Ampithoidae*. *Zool. Scr.* 46, 85–95. doi: 10.1111/zsc.12190

Souza, L. L., Azevedo, H. J. C. C., Vargas, A. B., Senna, A. R., and Souza, L. A. (2013). First record of *Porcellionides pruinosus* (Brandt, 1833)(*Oniscidea*: *Porcellionidae*) from Trindade Island, off Espírito Santo state coast, Brazil. *Bol. Mus. Biol. Mello Leitão* 32, 71–78.

Souza-Filho, J. F., and Serejo, C. S. (2012). Redescription and designation of a neotype for *Eudevenopus capuciatus* (Oliveira, 1955) (*Crustacea*: *Amphipoda*: *Platyschnopidae*) from Brazilian waters, with comments on its cuticular ultrastructures. *Cah. Biol. Mar.* 53, 469–484.

Stebbing, T. R. R. (1888). Report on the *Amphipoda* collected by H.M.S. Challenger during the years 1873–76. Report on the Scientific Results of the Voyage of H.M.S. Challenger during the Years 1873–1876. *Zool.* 29, 1–1737.

Stebbing, T. R. R. (1899). *Amphipoda* from the copenhagen museum and other sources. *Part II. Trans. Linn. Soc. Lond. Zool.* 8, 395–432. doi: 10.1111/j.1096-3642.1899.tb00202.x

Stebbing, T. R. R. (1906). *Amphipoda* I. Gammaridea. *Das Tierreich* 21, 1–806. doi: 10.11646/zootaxa.646.1.1

Tanaka, M. O., and Leite, F. P. P. (2003). Spatial scaling in the distribution of macrofauna associated with *Sargassum stenophyllum* (Mertens) Martius: analyses of faunal groups, gammarid life habits, and assemblage structure. *J. Exp. Mar. Biol. Ecol.* 293, 1–22. doi: 10.1016/s0022-0981(03)00233-8

Tavares, M., Carvalho, L., and Mendonça, J. B. (2017). Towards a review of the decapod *Crustacea* from the remote oceanic Archipelago of Trindade and Martin Vaz, South Atlantic Ocean: new records and notes on ecology and zoogeography. *Pap. Avulsos Zool. Mus. Zool. Univ. São Paulo* 57, 157–176. doi: 10.11606/0031-1049.2017.57.14

Thiel, M. (2003). "Rafting of benthic macrofauna: important factors determining the temporal succession of the assemblage on detached macroalgae," in *Migrations and Dispersal of Marine Organisms*, eds M. B. Jones, A. Ingólfsson, E. Ólafsson, G. V. Helgason, K. Gunnarsson, and J. Svavarsson (Dordrecht: Springer), 49–57. doi: 10.1023/b:hydr.0000008486.37391.60

Thomas, J. D. (1993). *Identification manual for marine Amphipoda (Gammaridea): I. Common coral Reef and Rocky Bottom Amphipods of South Florida*. Tallahassee, FL: Florida Department of Environmental Protection, 1–83. Final Report, Contract No. SP290.

Vanhöffen, E. (1914). Die Isopoden der deutschen Südpolar-Expedition 1901-1903. Deutsche Südpolar-Expedition, *Zoologie* 15, 447–598.

Wheeler, W. C., Schuh, R. T., and Bang, R. (1993). Cladistic relationships among higher groups of Heteroptera: congruence between morphological and molecular data sets. *Insect Syst. Evol.* 24, 121–137. doi: 10.1163/187631293x00235

Whittaker, R. J., Triantis, K. A., and Ladle, R. J. (2008). A general dynamic theory of oceanic island biogeography. *J. Biogeogr.* 35, 977–994. doi: 10.1111/j.1365-2699.2008.01892.x

Young, P. S., and Serejo, C. S. (2005). "*Crustacea* of the Abrolhos Region, Brazil," in *A Rapid Marine Biodiversity Assessment of the Abrolhos Bank, Bahia, Brazil*, Vol. 38, eds G. F. Dutra, G. R. Allen, T. Werner, and S. A. McKenna (Washington, DC: Conservation International), 91–95.

Yu, Y., Harris, A. J., Blair, C., and He, X. (2015). RASP (Reconstruct Ancestral State in Phylogenies): a tool for historical biogeography. *Mol. Phylogenet. Evol.* 87, 46–49. doi: 10.1016/j.ympev.2015.03.008

Conflict of Interest: The authors declare that the research was conducted in the absence of any commercial or financial relationships that could be construed as a potential conflict of interest.

frontiers in Marine Science

ORIGINAL RESEARCH
published: 13 April 2021
doi: 10.3389/fmars.2021.642659

Conservation Implications of *Sabellaria spinulosa* Reef Patches in a Dynamic Sandy-Bottom Environment

Karin J. van der Reijden[1], Leo Koop[2], Sebastiaan Mestdagh[3], Mirjam Snellen[2,4], Peter M. J. Herman[5,6], Han Olff[1] and Laura L. Govers[1,7]*

[1] Conservation Ecology Group, Groningen Institute for Evolutionary Life Sciences, University of Groningen, Groningen, Netherlands, [2] Acoustics Group, Faculty of Aerospace Engineering, Delft University of Technology, Delft, Netherlands, [3] Department of Estuarine and Delta Systems, NIOZ Royal Netherlands Institute for Sea Research, Yerseke, Netherlands, [4] Department of Applied Geology and Geophysics, Deltares, Utrecht, Netherlands, [5] Marine and Coastal Systems, Deltares, Delft, Netherlands, [6] Department of Hydraulic Engineering, Faculty of Civil Engineering and Geosciences, Delft University of Technology, Delft, Netherlands, [7] Department of Coastal Systems, NIOZ Royal Netherlands Institute for Sea Research, Den Burg, Netherlands

OPEN ACCESS

Edited by:
Puri Veiga, University of Porto, Portugal

Reviewed by:
Daniele Ventura, Sapienza University of Rome, Italy
Maria Flavia Gravina, University of Rome "Tor Vergata", Italy

***Correspondence:**
Karin J. van der Reijden
k.j.van.der.reijden@rug.nl; karinvdreijden@hotmail.com

Specialty section:
This article was submitted to Marine Evolutionary Biology, Biogeography and Species Diversity, a section of the journal Frontiers in Marine Science

Received: *16 December 2020*
Accepted: *22 March 2021*
Published: *13 April 2021*

Citation:
van der Reijden KJ, Koop L, Mestdagh S, Snellen M, Herman PMJ, Olff H and Govers LL (2021) Conservation Implications of Sabellaria spinulosa Reef Patches in a Dynamic Sandy-Bottom Environment. Front. Mar. Sci. 8:642659. doi: 10.3389/fmars.2021.642659

Biogenic reefs form biodiversity hotspots and are key components of marine ecosystems, making them priority habitats for nature conservation. However, the conservation status of biogenic reefs generally depends on their size and stability. Dynamic, patchy reefs may therefore be excluded from protection. Here, we studied epibenthos and epifauna density, richness, and community composition of patchy, dynamic *Sabellaria spinulosa* (ross worm) reefs in the North Sea. This study was conducted by comparing boxcore (endobenthos) and video transect (epifauna) data from two research campaigns in 2017 and 2019 to the Brown Bank area on the Dutch Continental Shelf, where *S. spinulosa* reefs were first discovered in 2017. The Brown Bank area is characterized by dynamic, migratory bedforms at multiple scales which potentially affect biogenic reef stability. We showed that *S. spinulosa* habitats had a patchy distribution and alternated with habitats comprised of plain sand. Average *S. spinulosa* habitat patch size was 5.57 ± 0.99 m and 3.94 ± 0.22 m in 2017 and 2019, respectively (mean ± SE), which especially in 2019 closely resembled the small-scale megaripple bedforms. Contrary to the endobenthos communities that were unaffected by *S. spinulosa*, epifauna density and species richness were at least two times higher in *S. spinulosa* habitats compared to sandy habitats, resulting in different community compositions between the two habitat types. We showed that *S. spinulosa* persisted in the area for almost 2 years. Although the stability of individual patches remained unclear, we demonstrated that even patchy biogenic reefs may promote density and local biodiversity of mobile, epibenthic species, very likely as a result of increased habitat heterogeneity provided by reef habitat patches. This indicates that patchy biogenic reefs that occur in dynamic environments may also have high ecological value and their conservation status should be (re)considered to ensure their protection.

Keywords: biogenic reefs, patchiness, habitat heterogeneity, marine management, ecosystem engineering, megaripples, ross worm, North Sea

INTRODUCTION

Biogenic reefs are physical benthic structures formed by ecosystem engineering species. Key examples are coral reefs (Roberts et al., 2002; Plaisance et al., 2011; Ferrario et al., 2014) and oyster beds (Lenihan, 1999; van der Zee et al., 2012; Donadi et al., 2013). By their physical presence, biogenic reefs modify their surroundings to such an extent that resource availability for other species is positively altered (Jones et al., 1994). They engineer a new habitat that can provide suitable settlement substrate (Coolen et al., 2015), increase refuge possibilities (Ryer et al., 2004) and food sources (van der Zee et al., 2012) for associated species, and decrease turbidity due to attenuation of waves and currents (Lenihan, 1999; van der Heide et al., 2011). Such effects of biogenic reefs can stretch well beyond the actual physical extent of these organisms (van der Zee et al., 2012; Donadi et al., 2013). As a result, biogenic reefs often form biodiversity hotspots and can be considered key components of marine ecosystems (Roberts et al., 2002; Christianen et al., 2016; van der Zee et al., 2016). Unfortunately, biogenic reefs are generally assumed to be vulnerable to (external) physical disturbances, due to their emergent structures (Collie et al., 2000; Sciberras et al., 2018) and the time required for these reef structures to recover (Hiddink et al., 2019). Biogenic reefs are therefore prioritized in nature conservation. Various legislative bodies exist to protect biogenic reefs, for instance by the designation of protected areas that locally restrict anthropogenic use and thus prevent any anthropogenic disturbance (Costello and Ballantine, 2015; Boonzaier and Pauly, 2016; Fariñas-Franco et al., 2018). However, there is no real consensus as to what characteristics are required for biogenic reefs in order to become protected. Within the European Habitats Directive (European Commission, 1992), for instance, these characteristics are limited to the general statement that reefs (1) arise from the seafloor and (2) support a zonation of benthic communities (European Commission, 2013). As a result, the more stable reefs with persistent associated communities are generally favored for conservation (Hendrick and Foster-Smith, 2006).

The ross worm (*Sabellaria spinulosa*) is a biogenic reef builder in soft-sediment environments (OSPAR Commission, 2013; Fariñas-Franco et al., 2014). This polychete builds strong, cohesive tubes by cementing sand particles, which can form biogenic reefs when they aggregate in high densities (Hendrick and Foster-Smith, 2006; Lisco et al., 2017). *S. spinulosa* has a widespread distribution, with observations in the northeast Atlantic, the greater North Sea including the Skagerrak, Kattegat and English Channel, the Mediterranean, and the Indian Ocean (Pearce, 2014; Gravina et al., 2018). Reef structures are dominantly formed in areas with a continuous supply of suspended sand particles and nutrients (Lisco et al., 2017). In the North Sea, most reefs are located near the British coast (Fariñas-Franco et al., 2014; Gibb et al., 2014; Pearce, 2014). They are often encountered on rocky substrates (Pearce, 2014), but are also observed on sandy bottoms (Pearce et al., 2014; Jenkins et al., 2018). The worms excrete fecal matter that may increase local food availability (Pearce, 2014), while the reefs increase habitat complexity and provide refugia and settlement substrate (Hendrick and Foster-Smith, 2006; Pearce et al., 2013; van der Reijden et al., 2019). The long-clawed porcelain crab (*Pisidia longicornis*), for instance, is well-known to hide between the individual tubes of *S. spinulosa* reefs (Fariñas-Franco et al., 2014; Pearce, 2014; van der Reijden et al., 2019). The reefs form biodiversity hotspots (Gravina et al., 2018), with locally distinct endobenthos and epifauna communities (Fariñas-Franco et al., 2014). As such, *S. spinulosa* reefs are included as priority habitats under both the Habitats Directive (European Commission, 1992) and the OSPAR convention (OSPAR Commission, 2013). Hendrick and Foster-Smith (2006) introduced a scoring system to evaluate the "reefiness" of *S. spinulosa* reefs under the Habitats Directive. They propose to assess a reef on physical, biological and temporal characteristics, such as elevation, biodiversity, and stability, respectively, on a continuous scale from low to high. In addition, they state that some threshold values could be set in place for specific characteristics, like a minimal total extent. However, multiple characteristics are difficult to assess as they require detailed information over a longer time period, resulting in the need for multiple surveys with advanced sampling techniques. Whereas several advanced methods have been developed to study intertidal or shallow subtidal reefs at the required spatiotemporal scales (Collin et al., 2019; Ventura et al., 2020), the application of these methods is less suitable in deep or turbid waters.

In 2017, *S. spinulosa* reefs were discovered for the first time on the Dutch Continental Shelf, in the Brown Bank area (van der Reijden et al., 2019). This area is characterized by large-scale (5–10 km) tidal ridges, superimposed with dynamic, migrating bedforms at smaller scales: sand waves with wavelengths of ∼200 m, and megaripples with wavelengths of ∼10 m (Knaapen, 2009; van Dijk et al., 2012; Koop et al., 2019). In addition, the area is fished at least once a year by demersal fisheries (van der Reijden et al., 2018, 2019). The multi-scale seafloor morphology potentially offers *S. spinulosa* small-scale safe sites to these fisheries, allowing them to persist and form reef patches in this area (van der Reijden et al., 2019). At the same time, the highly dynamic environment is likely to limit reef stability and therewith promote patchy reef formation. As a result, the protection status of these reefs may also be limited.

In this study, we aimed to determine the ecological relevance of these patchy, dynamic *S. spinulosa* reefs and the implications for the conservation of such reefs. During two research campaigns in autumn 2017 and May 2019, we investigated *S. spinulosa* reef patches in the dynamic Brown Bank area on the Dutch Continental Shelf. By means of acoustic, videographic and boxcore data, we assessed their spatial extent and associated endobenthic and epifaunal assemblages. We subsequently discuss the implications of our observations for reef conservation policy.

MATERIALS AND METHODS

Study Area

This study focused on the Brown Bank area within the Dutch sector of the North Sea (52°36′09.461″ N, 3°18′54.884″ E; **Figure 1A**). This region is characterized by stable north-south

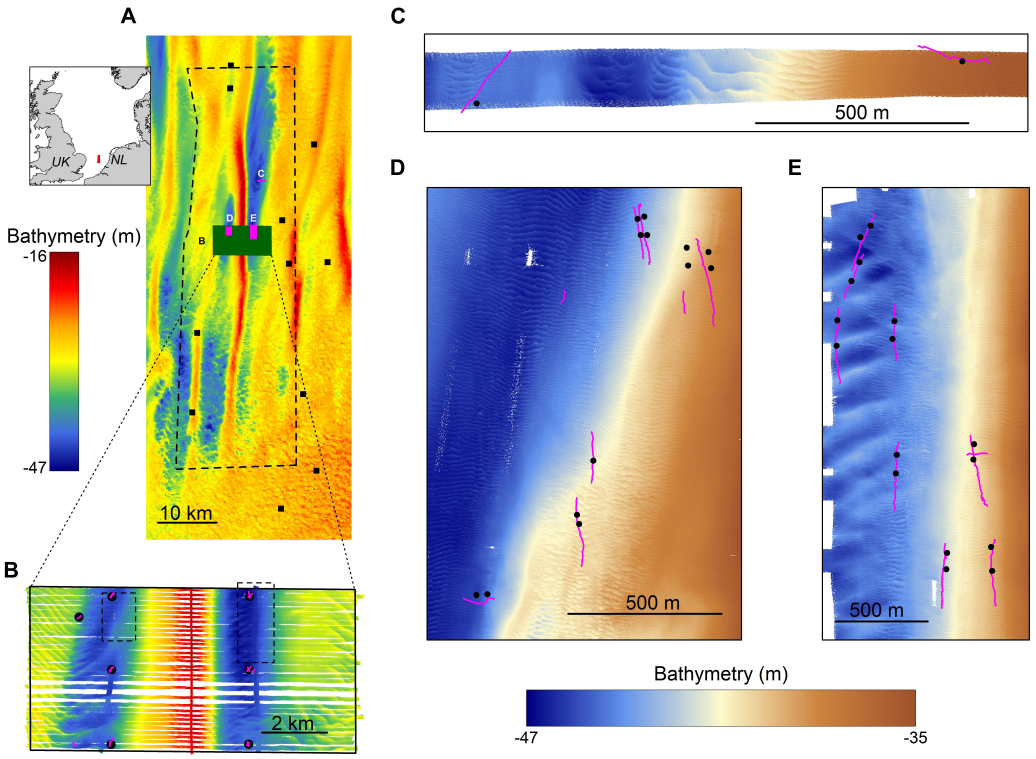

FIGURE 1 | The study area. **(A)** an overview of the Brown Bank area including bathymetry, sampling locations for the MWTL- survey (squares) and the locations of more intensively studied areas displayed in other panels. Inset shows the location of the study area within the North Sea. **(B)** an overview of data gathered in the research campaign of 2017, showing bathymetry data (background), boxcores (black circles) and video transect locations (pink lines) and the locations of panels **(C,D)** (dotted lines). **(C–E)** close-up of the three survey areas in the 2019 campaign, showing bathymetry data, boxcore and video transect locations. Note the differences in bathymetry color scales used for panels **(A,B)** and **(C–E)**.

oriented tidal ridges, with amplitudes ranging from 7.5 to 29 m for the Brown Bank tidal ridge (Knaapen, 2009; van Dijk et al., 2012). Sand waves are superimposed on these ridges, with average wave lengths of ∼200 m, amplitudes of several meters and orientated in a northwest to southeast direction. Smaller scaled megaripples are found superimposed on the sand waves. These megaripples have wavelengths of ∼10 m, amplitudes of ∼0.5 m, and an east-west orientation (Koop et al., 2019). Both sand waves and megaripples are known to migrate. Sand waves migrate several meters a year (Knaapen, 2005; Knaapen et al., 2005), whereas the migration speed of megaripples is not entirely clear but assumed to be site-specific with speeds up to 1 m h^{-1} reported for megaripples in the Dover Straits (Idier et al., 2002).

Research Campaigns

For this study, two research campaigns were conducted on board of the *RV Pelagia*; one in October-November 2017 and one in May 2019. The 2017 campaign aimed to study the spatial effects of the large-scale tidal ridge on benthic communities. It covered a study area of 5 × 10 km with sampling positions determined by the structure of the tidal ridge (**Figure 1B**). Only the stations located in the troughs have been included for this particular study, as the *S. spinulosa* reefs have been observed in the troughs exclusively (Mestdagh et al., 2020). The 2019 campaign was a dedicated survey aimed to study the ecological relevance of the *S. spinulosa* reefs discovered in 2017. For this, three smaller, separate survey areas were selected, in which the locations of videographic and boxcore samples were determined based on a preliminary analysis of freshly acquired acoustic data (**Figures 1C–E**). In addition, the sampling design was furthermore focused to have minimal impact on the reefs, by minimizing the number of boxcores and using a drop camera that hovered above the seafloor. To summarize, acoustic, videographic and boxcore data were gathered during both campaigns, but with slightly different methods. These will therefore be described separately for both years.

Acoustics

Data Collection

During both campaigns acoustic data were gathered with a hull-mounted Kongsberg EM 302 multibeam echosounder (MBES), which was operated at 30 kHz. In the 2019 campaign, acoustic data was also collected using the multi-spectral R2Sonic MBES, operating at 90, 200, and 400 kHz. This second MBES was mounted on a pole on the vessels' portside. Because the R2Sonic

was newly installed, a patch test was performed prior to survey operations, using a shipwreck as a ground object. This patch test validated that the MBES was correctly installed by acquiring validation data while sailing a standard set of survey lines designed for such a test (R2Sonic LLC, 2017). Location data was provided by a Kongsberg Seapath 360 global positioning system and motion reference unit. The 2017 acoustic data was cleaned and processed as described in Koop et al. (2019), while more details on cleaning and processing of the R2Sonic data can be found in Koop et al. (2020).

Data Processing

The acoustic surveys yielded nearly 60 km^2 of surveyed seabed (2017: 41.18 km^2; 2019: 17.23 km^2), with a resolution of $\sim$1 $\times$ 1 m for 2017 and 0.75 $\times$ 0.75 m in 2019. Small-scale (10 m) Bathymetric Position Indices (BPIs) were then derived from the bathymetry, using the Benthic Terrain Modeler toolbox add-in for ArcGIS[1] (ESRI, 2018; Walbridge et al., 2018). These BPIs represent the local depth relative to the average depth of the surroundings and is therefore a suitable method to identify the positioning of morphological structures. We classified our BPI in 3 classes that represented the crests, slopes and troughs of megaripples, by applying visually verified cut-off values of $-$10 and 10 cm. This means that all pixels $\geq$10 cm below the average surrounding depth were classified as a trough and all pixels $\geq$10 cm above were defined as a crest. Pixels between these values are considered to be on a slope. To determine BPI-habitat patch sizes along the video transects, we computed straight line segments at the video locations. These line segments were determined by performing a linear regression on the camera coordinates, with a similar direction as applied in the video transect. Cross-sections of BPI-habitats along these straight video lines were then made, which enabled the calculation of the observed patch sizes.

[1] ArcGIS, Version 10.5.1

Videographic Data

Video transects were conducted on both campaigns. During the video transects, vessel speed was kept at $\sim$0.1 m s^{-1} with respect to the seabed. The towed camera frames were attached to the starboard side winch, which was located centrally on the vessel. Both systems comprised of a full HD-camera, a set of scaled lasers, and underwater lights attached to a frame. Main differences between the video devices were caused by the differences in the positioning of the camera and the construction of towing cables (**Figure 2**).

2017 Campaign

A video sledge was used in the 2017 campaign. The frame was designed to float in the water, at a stable height above the seafloor. This was achieved as a result of two specific construction aspects (Barker et al., 1999; Sheehan et al., 2010). Firstly, three towing cables were attached to the front of the frame at the left and right side of the bottom, and in the middle on top (**Figure 2A**). After 6.5 m, these were combined into one towing cable, which was connected to the winch. At the conjunction point, a drop weight (55 kg) was added to ensure the horizontal position of the three towing cables. A live-view enabled manual adjustments of the towing cable length if needed. Secondly, the camera frame itself had a slightly positive buoyancy which was neutralized by two drag chains attached to both sides of the frame. The ends of these drag chains touched the seafloor, and stabilized the frame at a specific height. The video sledge is described in more detail in Koop et al. (2019) and Mestdagh et al. (2020). During the $\sim$200 m long video transects, the video sledge hovered around 0.5–1 m above the seafloor, with the camera set to view an area of $\sim$0.25 m^2 just in front of the frame. At both the eastern and

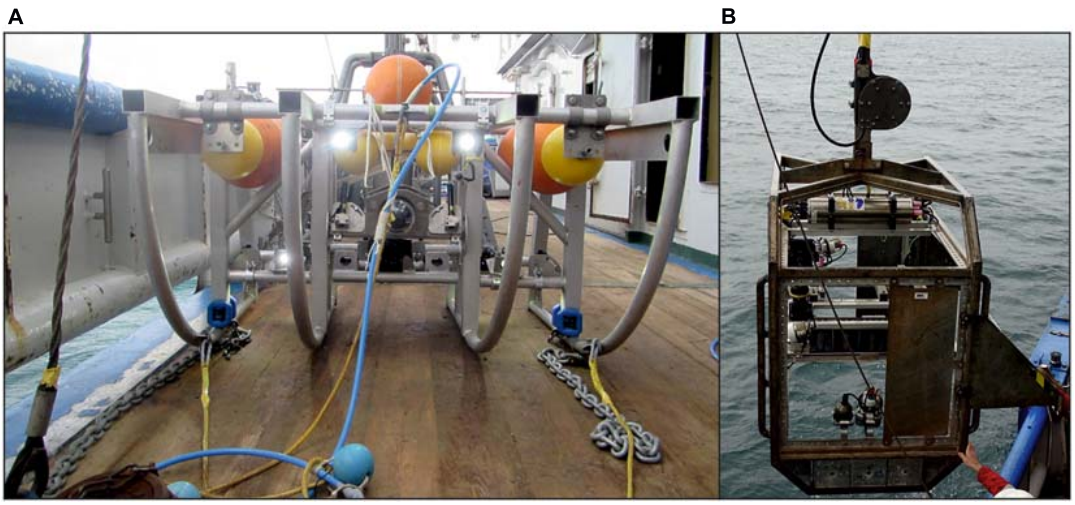

FIGURE 2 | The different camera frames used in this study, showing the towed video frame **(A)** and the drop camera **(B)**. Note the differences in towing construction and camera set-up. The towed video frame **(A)** has three (yellow) towing cables on the front of the frame, and a forward-facing camera. For the drop camera **(B)**, the towing cable is attached to the top of the frame, and has a downward-facing camera. Photo credits to Danielle Prins-de Jonge **(A)** and Jip Vrooman **(B)**.

western trough, two replicate video transects were performed at three different latitudes (**Figure 1B**. Top: 52°37′22.897″ N, middle: 52°36′11.210″ N, bottom: 52°34′55.329″ N). In addition to these 6 stations, three extra stations were picked based on observations within the acoustic data, at which a total of four video transects were conducted.

2019 Campaign

In the 2019 campaign, a hopper camera was used to perform the video transects. A Kevlar cable was centrally attached on top of the frame, which resulted in a vertical drop of the camera from the winch (**Figure 2B**). Height above the seabed was manually controlled based on a live-view, and was estimated to be around 1.5–2 m. The downward facing camera recorded an area of ∼1 m^2. More details on the camera specifics can be found in Damveld et al. (2018). A total of 19 video transects was conducted. The location of each transect was chosen based on a preliminary analysis of acoustic data.

Data Processing

All footage with unclear visibility of the seabed was classified as invalid. Analysis of all valid footage comprised the recording of observed organisms and prevailing habitats. Specimens were identified to the lowest taxonomic level possible. Habitats were defined by their sediment features, resulting in three different habitats: (1) Sand, (2) Rubble, and (3) Sabellaria (**Figure 3**). Sand habitats classified all seafloors that were comprised of plain sand without any deviating features apart from some small shell fragments. Rubble and Sabellaria habitats were comprised of seafloor habitats that both contained a sandy seafloor, with coarser material like small stones and/or many shell fragments (Rubble) or Sabellaria reef fragments (Sabellaria). As a consequence, Sabellaria habitats do not necessarily have a 100% coverage of *S. spinulosa* reefs. For both research campaigns, an example screenshot of each habitat is shown in **Figure 3**.

The camera location was derived from the vessels' GPS logging system, which registered the vessels' location every 30 s. These locations were linearly interpolated to obtain a GPS position for every second. The interpolated vessel positions were then time-matched to camera locations. Depending on the prevailing depth, currents and waves, the distance between the camera and the vessel varied, causing for a positioning error of the camera. Because both cameras were deployed approximately in the middle of the vessel, not far from the GPS receivers, and with as little towing cable as possible, we expect this positioning error to be >10 m and <100 m. Moreover, we assume this error to be larger in 2017 compared to 2019 (but still within the given range), due to the horizontal component of the towed camera sledge used in 2017 that the drop camera does not have.

We determined the surveyed area by matching all camera positions to a grid. The grid resolution was 0.5 × 0.5 m in 2017, and 1 × 1 m in 2019, corresponding to the average area observed by the camera. We then summed the number of unique grid cells per habitat type per transect, and calculated the total observed area per habitat type. Habitat patch size was determined as the physical distance between the camera location at the first and last recording of each habitat patch. Large interruptions (>10 s) of the video transects, due to invalidity of footage, were included as patch boundaries.

Boxcores

Data Collection

Endobenthos samples were collected with a boxcorer (30 cm diameter) during both cruises. During the 2017 campaign, triplicate samples were taken at seven sampling stations. In 2019, 31 single boxcores were taken. All samples were sieved over a 0.5 mm sieve in 2017 and a 1 mm sieve in 2019, after which the organisms were stored in 4–6% formaldehyde. Subsequently,

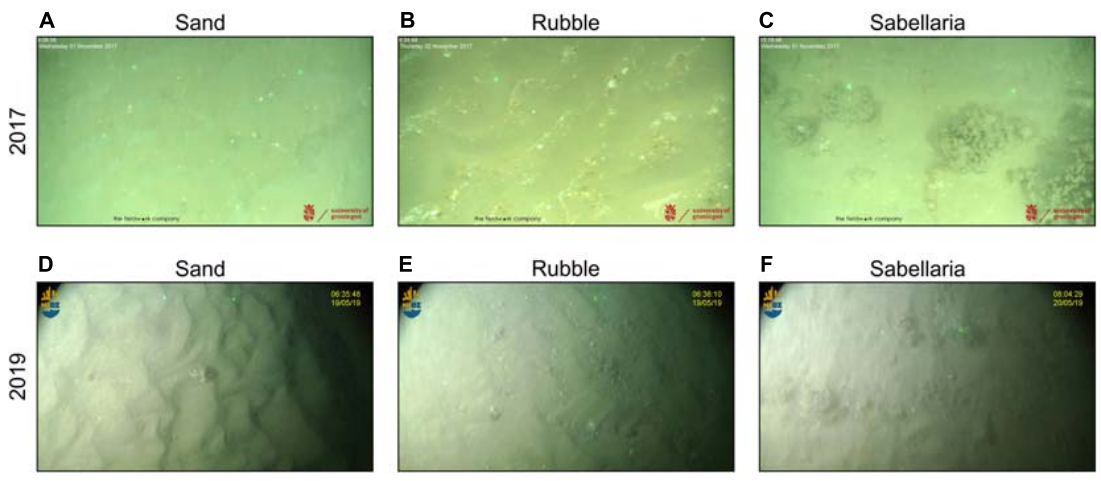

FIGURE 3 | Habitat types observed in video transects. **(A)** sand habitat in 2017. **(B)** rubble habitat in 2017. **(C)** sabellaria habitat in 2017, with several *S. spinulosa* reef fragments, two starfish (*Asterias rubens*) and a dragonet (Callionymidae). **(D)** sand habitat in 2019, showing a hermit crab (*Pagurus bernhardus*). **(E)** rubble habitat in 2019. **(F)** sabellaria habitat in 2019, showing several *S. spinulosa* reef fragments, and three starfish (*A. rubens*). Green dots are lasers, set to a distance of 35 cm and 30 cm for 2017 **(A–C)** and 2019 **(D–F)**, respectively.

organisms were counted and identified to the lowest taxonomic level possible in the laboratory.

We additionally used boxcore data collected by the Directorate General for Public Works and Water Management of the Dutch Ministry of Infrastructure and Water Management for their MWTL-program ("Monitoring Waterstaatkundige Toestand des Lands"). This monitoring program samples endobenthos over the entire Dutch Continental Shelf with a similar methodology as applied in the 2019 research campaign. For this study, we selected the stations within 15 km of the Brown Bank Area, sampled in the summer of 2018. This yielded 11 stations (**Figure 1A**). Endobenthos densities (N m^{-2}) and species richness (N m^{-2}) were determined and compared to the data gathered at the 2019 research campaign.

Data Processing

Boxcore stations for the 2017 and 2019 research campaigns were spatially linked to video observations. For this, boxcore areas were created by extending the station location with a radius of 50 m. All valid video footage within these boxcore areas were then assigned to that specific boxcore station. Stations without any assigned video observations were removed from the dataset. Remaining boxcores were classified as "*Sabellaria*" or "*no-Sabellaria,*" depending on whether any *Sabellaria* habitat was assigned to that station.

Species nomenclature was checked against the World Register of Marine Species (WoRMS) to ensure validity and similarity of taxonomic names (Holstein, 2018). Then, a taxonomic leveling exercise was performed to increase similarity of species' taxonomic levels. With this leveling, we specifically wanted to (1) exclude single observations at higher taxonomic levels while the majority of similar specimens was identified to lower taxonomic levels, and to (2) account for the higher taxonomic precision of only a small subset of related observations. An example of the first event is the recording of two amphipods at order level, while all other amphipods were identified to species or genus level. The leveling removed the two registrations at the order level. The second event comprised, for example, the merging of *Ensis ensis* recordings with the recordings of *Ensis sp.* as the majority of the observations were made on a genus level. For this leveling exercise, we determined the number of observations for all species, genera, families and orders observed. We then calculated the percentage of observations at each lower taxonomic level with respect to the total number of observations at the corresponding higher taxonomic levels. Within this taxonomic ranking, lower taxonomic levels were merged with a higher taxonomic level if that higher level contributed to more than 50% of the observations. Higher taxonomic records were removed if they contributed to less than 15% of the total observations within the associated ranking. After this species leveling, species richness (N m^{-2}) was determined for all stations, in which the triplicates of 2017 were merged and divided by the total sampled area.

Data Analysis

All data processing and analysis was performed in R, version 3.6.2 (R Development Core Team, 2014).

Epifauna

The video analysis yielded registrations of organism observations and their associated habitat type. For each transect separately, we determined both the habitat-specific epifauna densities (N m^{-2}) and the overall density (N m^{-2}). Epifauna densities represent the observed species densities, determined by the total number of observations for each species within a certain habitat, divided by the total observed surface of that habitat. Overall density represents the total number of organisms per square meter of observed habitat. This resulted in two datasets that represent the epifauna and overall density for each combination of habitat type and transect. A non-Metric Multi-Dimensional Scaling (nMDS) was applied in order to visually determine differences in community composition between habitats separately for both research campaigns. Bray-Curtis dissimilarities were determined based on the epifauna densities and were used as input for this nMDS.

Differences in overall density between habitats were tested for with linear mixed models (LMM) from the lme4-package (Bates et al., 2015), taking the transects as separate sampling locations. These models included "habitat type" as fixed effects, and one of either random factors "station" (2017) and "survey area" (2019) to limit spatial autocorrelation. Pairwise comparisons between habitat types were determined using an a *post hoc* Tukey test from the emmeans-package (Lenth, 2020). Model assumptions of homogeneity of variance and normality were visually checked by plotting the model residuals.

We also determined differences in species richness between habitats. However, the three habitat types differed in their total observed area, and their ratios were also unequally distributed over the transects. We had to correct for this in our calculations of species richness. Hence, we determined the number of species and the observed area (m^2) for each individual habitat patch encountered in the video transects. We then modeled species-area curves using the *specaccum*-function in the vegan package (Oksanen et al., 2019). These curves represent the total number of species observed over an increasing sampling effort. The presented species-area curves are based on 1,000 permutations comprising random resampling of the different patches, in which each patch was weighted for their sampled surface.

Endobenthos

Both research campaigns were analyzed separately, because the different methods used impacted the results. Community composition was compared between the MWTL survey and the 2019 campaign, for which similar sampling methods were used. For this, Bray-Curtis dissimilarities were determined on fourth root transformed endobenthos densities at the stations sampled in both the MTWL-survey and the 2019 campaign (Reiss et al., 2010). A nMDS was subsequently applied in order to assess distinctions between the MWTL-stations and the *Sabellaria* and *no-Sabellaria* stations of the 2019 campaign. A similar analysis was performed for the 2017 campaign. A pairwise PERMANOVA, based on Bray-Curtis dissimilarities, was used to test for significant differences in community composition between stations. Both the nMDS and the PERMANOVA used the vegan-package (Oksanen et al., 2019).

In addition, total species richness was compared between habitat types. Differences in richness were tested with an ANOVA and a subsequent *post hoc* Tukey test. Model assumptions were visually checked.

RESULTS

Habitat Patchiness

The 35 video transects covered a total area of 6295.75 m^2 (2017: 1050.75 m^2; 2019: 5,245 m^2), with three types of habitat: Sand (4674.25 m^2), Rubble (767 m^2), and Sabellaria (854.50 m^2). For 2017, 73% was comprised of Sand habitat, with the remaining area being ascribed to 9% Sabellaria (95.50 m^2) and 18% Rubble (190 m^2) habitat. In 2019, a similar percentage of Sand habitat was observed (75%), but slightly more Sabellaria habitat was observed, with 14% (759 m^2) and 11% (577 m^2) for Sabellaria and Rubble habitat, respectively.

Video transects revealed a patchy distribution of the different habitats, with alternating patterns. In 2017, Sand habitats often alternated with Rubble habitats (**Figure 4A**). The limited Sabellaria habitat observed in 2017 (24 patches) showed a similar alternating pattern with Sand habitat, but consisted generally of larger patches than the Rubble habitat (**Figure 4B**). Habitat patches were 5.57 ± 0.99 m (mean ± SE) for Sabellaria, 4.13 ± 0.35 m for Rubble, and 9.13 ± 0.81 m for Sand habitat. In 2019, a similar alternating habitat pattern was observed (**Figures 4D,E**). Patch sizes of the Sabellaria and Rubble habitats, however, were smaller than in 2017 (Sabellaria: 3.94 ± 0.22 m, Rubble: 3.58 ± 0.29 m, Sand:11.12 ± 1.10 m).

The seabed was shown to have multiple morphological structures, at various scales (**Figure 1**). The seafloor structure, created by the small-scale megaripples, closely resembled the observed alternating habitat pattern (**Figures 4A,B,D,E**). The troughs of these megaripples had a mean size of 3.69 ± 0.33 m and 2.98 ± 0.12 m in 2017 and 2019, respectively. The histograms

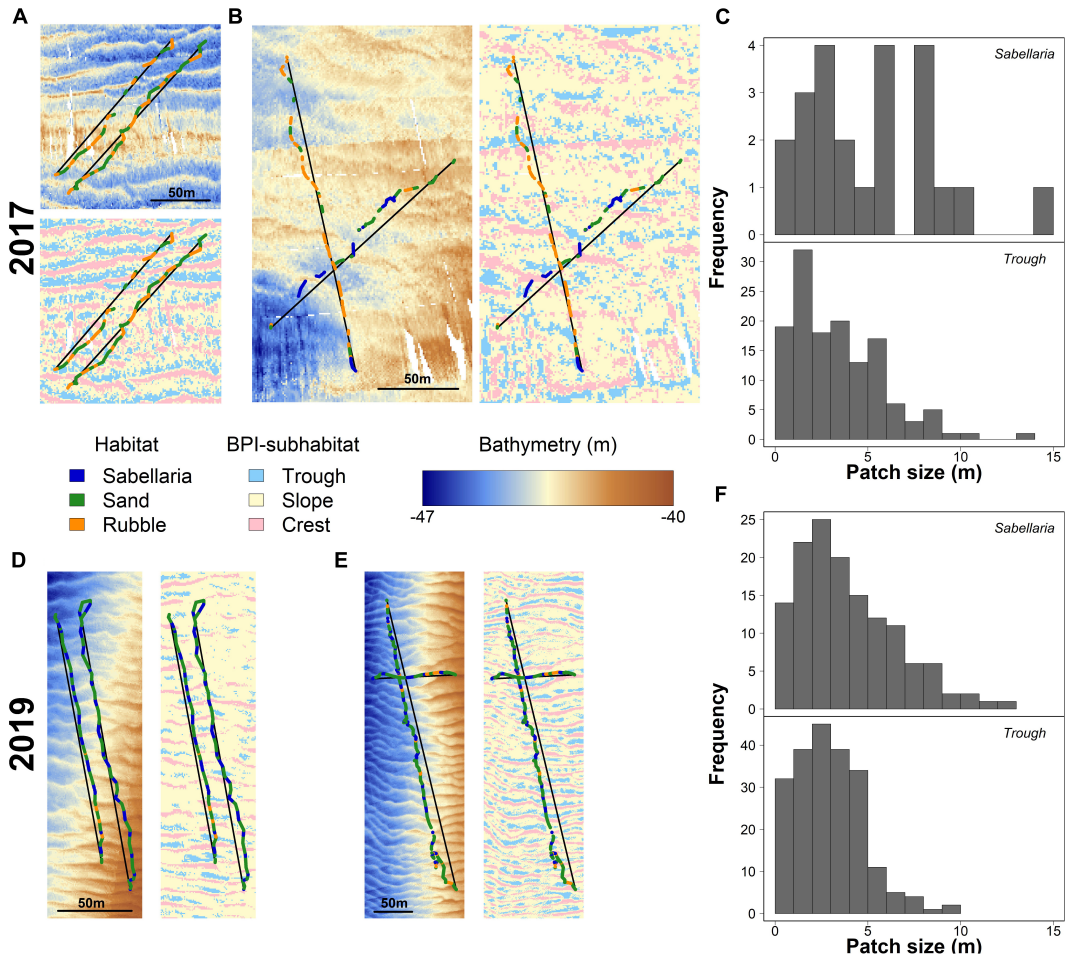

FIGURE 4 | Habitat patch distributions and their link to seafloor morphology for 2017 **(A–C)** and 2019 **(D–F)**. **(A)** detailed maps showing the bathymetry and BPI-subhabitats surrounding the video-observed habitat patches (Sabellaria in blue, Sand in green, and Rubble in Orange) for two representative video transects gathered in 2017 in the western trough. Black lines represent the line segments used to determine BPI-subhabitat sizes. Similar maps of bathymetry and BPI-subhabitat overlayed with video-observed habitats are shown for **(B)** 2017, eastern trough, **(D)** 2019, western trough, and **(E)** 2019, eastern trough. Histograms show the absolute frequency of the sizes for the video-observed Sabellaria habitat patches and BPI-subhabitats "trough" for 2017 **(C)** and 2019 **(F)**.

in **Figures 4C,F** show a strong similarity in Sabellaria patch sizes and megaripple trough sizes. For 2017, this pattern showed less similarities, probably as a result of the low number of Sabellaria habitat patches encountered, their slightly larger sizes (2017: 5.57 ± 0.99 m; 2019: 3.94 ± 0.22 m), and the lower resolution of the bathymetry data (**Figure 4C**). A similar size comparison could also be made for Sabellaria habitat patches and megaripple crests, as the latter had a comparable mean size (2017: 3.76 ± 0.21 m; 2019: 2.75 ± 0.10 m). However, at multiple occasions during the video analysis, we observed that the seafloor dropped directly before a Sabellaria habitat patch started, indicating *S. spinulosa* reef presence in the troughs rather than on crests.

Endobenthos

A total of 105 and 121 species were observed in the 2017 and 2019 research campaigns, respectively, which amounted to the observation of 176 species in total. In contrast, only 50 species were observed in the MWTL- survey, of which 10 were exclusively observed in this dataset. Most abundant species in all three datasets were ribbon worms (Nemertea), sand-dwelling amphipods (*Bathyporeia elegans*, *Bathyporeia guiliamsoniana,* and *Nototropis swammerdamei*), the white catworm (*Nephthys cirrosa*), and a bristleworm (*Ophelia borealis*) (**Supplementary Table 1**). The endobenthos community composition did not differ significantly between boxcores classified as Sabellaria and *no-Sabellaria* for 2019 (**Figure 5A**). In 2017, the limited number of samples prohibit any firm conclusion on community composition differences (**Figure 5B**). However, there was a difference in community composition at the landscape-scale (**Figure 5A**). Community compositions of the small survey areas of the 2019 campaign were shown to deviate from the community composition found in the MWTL survey, representing the wider surrounding area of the Brown Bank (PERMANOVA, $p = 0.041$). The subsequent pairwise PERMANOVA demonstrated a significant difference between the MWTL survey and the boxcores in the south eastern trough (pair-wise PERMANOVA, $p = 0.024$).

In addition, some interesting observations could be made with regard to species richness of the samples (**Figure 5C**). For 2017, a significant higher species richness was observed in *Sabellaria*, compared to *no-Sabellaria* (*Sabellaria*: 50 ± 3.5; *no-Sabellaria*: 30 ± 3.7; ANOVA: $p = 0.038$). Such a significant difference was not observed for the 2019 campaign (Sabellaria: 20.9 ± 1.9; *no-Sabellaria*: 25.5 ± 2.4: Tukey emmeans: $p = 0.305$). A significant twofold of species richness compared to the MWTL survey was observed for *no-Sabellaria* in 2019 (Tukey emmeans: $p = 0.004$), while a trend toward higher species richness was observed for Sabellaria (Tukey emmeans: $p = 0.065$). Species richness in 2017 should not be compared to species richness of 2019 and MWTL samples, as different methods were used (smaller sieve and larger sampled surface).

Epifauna

A total of 4,947 epibenthic organisms were observed, comprising 21 species. Dominant species was the common star fish (*Asterias rubens*). The hermit crab (*Pagurus bernhardus*) and several demersal fish species were also frequently observed (**Supplementary Table 2**). Different community compositions were observed between Sand and Sabellaria habitat types (**Figures 6A,B**). Moreover, overall density was at least twice as high within the Sabellaria habitat compared to the Sand habitat (**Figure 6C**. LMM 2017 & 2019: $p < 0.0001$). In 2019, Sabellaria and Rubble habitats had a similar community composition (**Figure 6A**) and overall density (**Figure 6C**). An opposite pattern was observed in 2017. Then, Sabellaria and Rubble habitats differed in community composition (**Figure 6B**). Rubble habitat strongly resembled Sand habitat, with lower overall densities than in the Sabellaria habitat (**Figure 6C**). The species-area curves of both campaigns show that species richness of the Sabellaria habitat was higher than the Sand and Rubble habitats (**Figure 6D**).

DISCUSSION

We here studied the effects of *S. spinulosa* habitat patches on associated endo- and epibenthic communities in the dynamic Brown Bank area in the North Sea. We showed that within this area, *S. spinulosa* reef habitats have a highly patchy distribution that may be linked to seafloor megaripple morphology. These migratory bedforms are commonly abundant in dynamic sand-bottom environments (Knaapen, 2009; Koop et al., 2019). The patchy Sabellaria habitats had similar endobenthic community compositions compared to surrounding habitats and showed slightly higher species richness in 2017, but not in 2019. In contrast, species richness and overall density of mobile epifauna was higher near *S. spinulosa* reefs, suggesting that especially the mobile, epifauna community is positively affected by the presence of *S. spinulosa* reef patches. Our study demonstrates that patchy biogenic reefs have a relevant positive impact on benthic biodiversity even in morphologically dynamic sandy-bottom environments.

Compared with the surrounding Sand habitat, Sabellaria habitat patches showed 2 and 12 times higher epifauna densities for 2019 and 2017, respectively. Moreover, species richness of mobile, epifaunal organisms was higher. Similar patterns have been observed in *S. spinulosa* reefs elsewhere, showing higher local species densities than in surrounding habitats (Pearce et al., 2013; Fariñas-Franco et al., 2014; Pearce, 2014). We did not observe clear effects of the *S. spinulosa* patches on endobenthic organisms, contrary to observations described in literature. They show that biogenic reefs can locally exclude soft-sediment endobenthic species due to their physical structure, and promote higher endobenthic densities in their direct surroundings as a consequence of altered hydrodynamics or fecal output (Rees et al., 2008; van der Zee et al., 2012; Donadi et al., 2013). Potentially, the investigated *S. spinulosa* patches were too small to produce such effects. It may, however, also demonstrate the methodological challenge to adequately sample a patchy reef feature. Contrary to our intentions, no boxcore samples were taken within *S. spinulosa* reef patches themselves, but in their surroundings. This underlines that –when small-scale habitat heterogeneity is expected– more precise sampling methods should be deployed, such as scuba-diving or ROV-directed sampling (Parry et al., 2003; Rees et al., 2008; Coolen et al., 2015). The results also demonstrated that it is necessary to

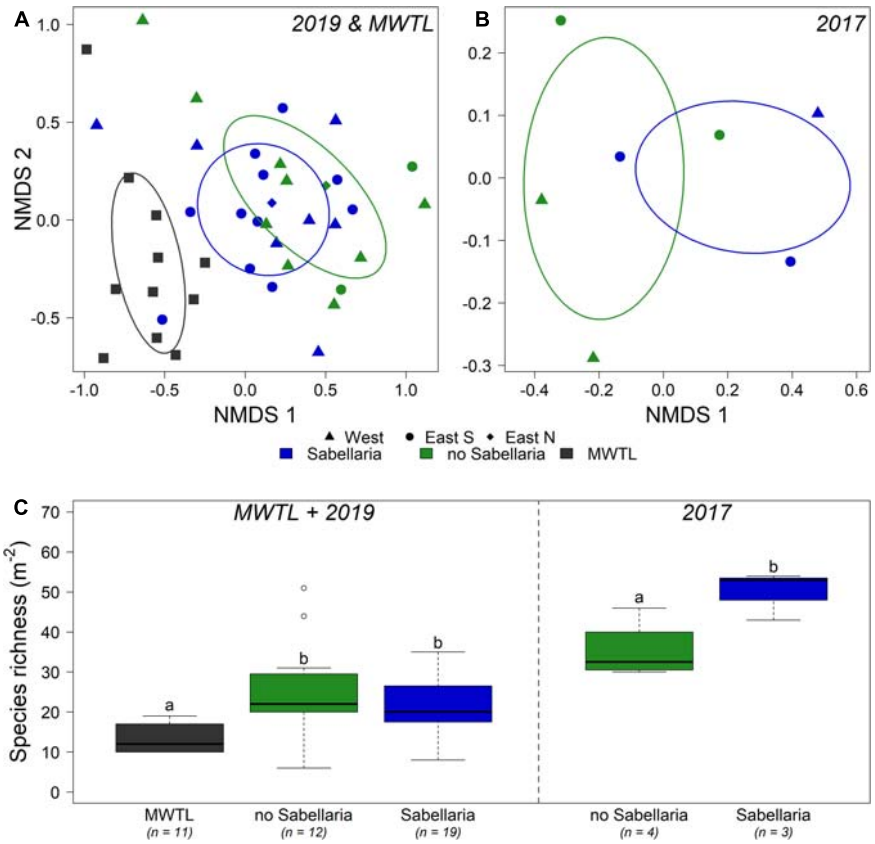

FIGURE 5 | Comparison of endobenthos data between both research campaigns and the MWTL survey. **(A)** NMDS of endobenthos data gathered in the joint MWTL survey and the 2019 campaign, and for **(B)** the 2017 campaign. Samples with video-based observed Sabellaria habitat within a 50 m distance are blue; samples without Sabellaria habitat are green. Circles show the western trough, triangles the eastern trough south, and diamonds the eastern trough north. **(C)** species richness (Nm^{-2}) is shown per habitat for the MWTL survey and 2019 campaign combined, and separately for the 2017 campaign. n represents the number of boxcores included. Significant differences are represented by different letters. Note that the 2017 campaign data are analyzed separately from the MWTL survey and 2019 campaign data.

apply multiple sampling methods that target different ecological components and different spatial scales. Only the combination of these techniques provides a comprehensive overview of, in this case, the ecological relevance of *S. spinulosa* reefs (Tiano et al., 2020). In addition, our multi-scale design of acoustics, video transects, and boxcores enabled the integration of prevailing habitat heterogeneity in the interpretation of local observations.

The importance of this small-scale habitat heterogeneity was further investigated at a landscape-scale. Slightly different endobenthos communities were observed between boxcore samples taken in the wider surroundings and boxcores gathered in the 2019 campaign. These differences could have resulted from the large-scale morphological seabed structure alone (van Dijk et al., 2012; Mestdagh et al., 2020). However, it is very likely that the *S. spinulosa* reef patches contributed to this difference in endobenthos communities. The reef patches produce a high level of small-scale habitat heterogeneity, which has proven important for overall biodiversity (Hewitt et al., 2005; Sanderson et al., 2008). We demonstrated that *S. spinulosa* patch size is very likely related to small-scale heterogeneity created by dynamic, morphological bedforms, as the mean patch size of Sabellaria habitats matches the average size of megaripple throughs (Knaapen et al., 2005; Koop et al., 2019; van der Reijden et al., 2019). Similarly, in Dorset (SW England), a *S. spinulosa* reef appeared to be constrained by mobile sand waves, which periodically overwhelmed the reef (Collins, 2003). Most likely, sand wave migration has limited effect on our *S. spinulosa* reefs, as sand waves were almost absent in the tidal sand bank throughs (Knaapen, 2005; Koop et al., 2019). Megaripple migration, however, could considerably affect *S. spinulosa* reef patchiness and stability. Migration patterns are thought to be site-specific (Knaapen et al., 2005) and affected by morphological bedforms at larger scales (Leenders et al., 2021). Intertidal megaripples with similar amplitude and wavelength as encountered in the Brown Bank area were shown to migrate around 1 m $week^{-1}$ (van der Wal et al., 2017). Together with the high burial tolerance of *S. spinulosa* (Hendrick et al., 2016), this migration speed might pose a tolerable stress for the reefs. However, it does not explain the observed patchy distribution of Sabellaria habitats. Another possibility is that megaripple migration opposingly is altered by reef presence since biogenic reefs are known for their

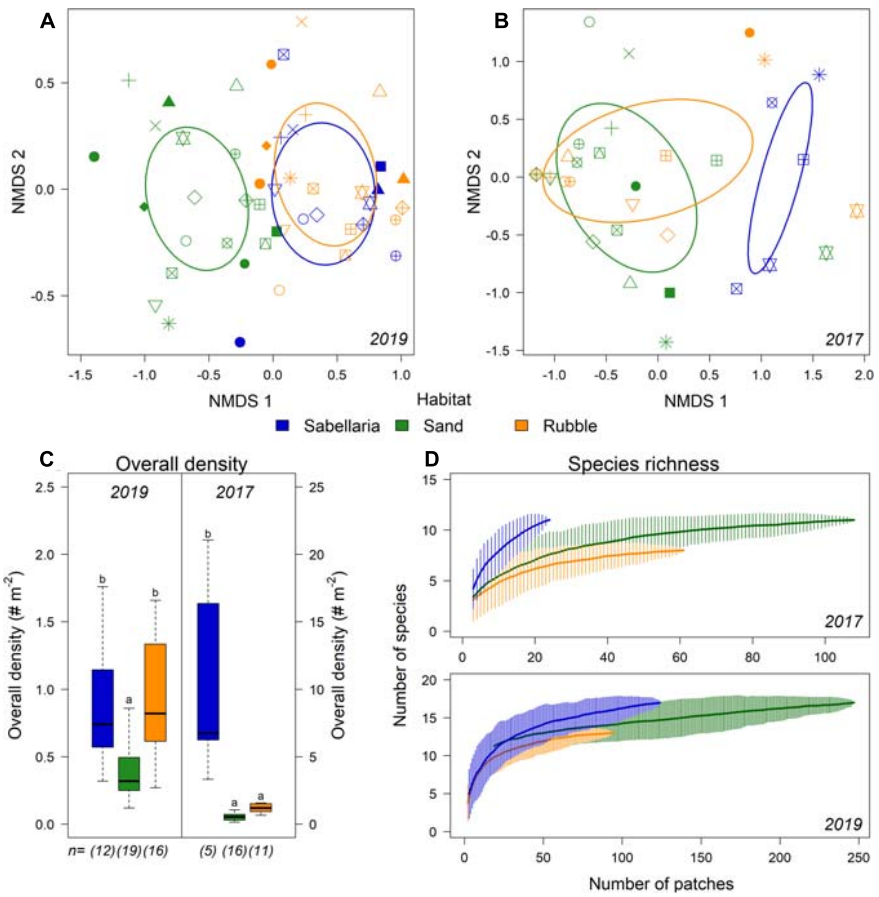

FIGURE 6 | Differences in community composition between the different habitat types Sabellaria (blue), Sand (green), and Rubble (orange). **(A)** NMDS of epifauna data gathered in the 2019 campaign and **(B)** in the 2017 campaign. Each habitat type observed within a transect is displayed separately, with the different symbols representing the video transects. **(C)** overall density (# Nm^{-2}) and species richness (Nm^{-2}) per habitat type for 2019 and **(D)** for 2017. n represents the number of different transects with this habitat type. Significant differences are represented by different letters.

sediment stabilization effects (Rabaut et al., 2009; Paul et al., 2012). Modeling studies show that artificial tubes mimicking the sand mason worm (*Lanice conchilega*) affect near-bed flow velocities, which result in sediment trapping (Borsje et al., 2014) and affect sand wave morphology (Damveld et al., 2019, 2020). A preliminary model run showed that the presence of tube-worm patches can decrease sand wave migration speed (Damveld, 2020). Hence, *S. spinulosa* reef patches might be able to reduce megaripple dynamics to levels they can cope with, enabling them to persist. To test these hypotheses, detailed studies on the mechanistic link between *S. spinulosa* reefs and megaripples should be conducted. Such a study would also provide insights in the stability of the studied *S. spinulosa* reef patches.

Our observations, however, pose an interesting case with respect to marine habitat conservation. Despite the patchiness and dynamics of the observed *S. spinulosa* reefs, their persistence in the area has been demonstrated over a time period of almost 2 years. The preference of *S. spinulosa* larvae to settle on conspecifics (Wilson, 1970; Fariñas-Franco et al., 2014), especially in combination with the hypothesized small-scale refugia created by the megaripples (van der Reijden et al., 2019), can potentially explain this persistence. The reef patches increased both local diversity and density of mobile epifauna. We therefore argue that the observed *S. spinulosa* reef patches definitely have conservation value. Many other biogenic reefs are characterized by patchy distributions or small-scale variation of sub-habitats as well. Aggregations of the sand mason worm (*Lanice conchilega*) for example, form patchy mounts that are elevated from the seabed (van Hoey et al., 2008; Rabaut et al., 2009). Similarly, horse mussels (*Modiolus modiolus*) can form distinct beds that are typified by ridges of mussels with muddy patches in between (Rees et al., 2008). The positive impact on biodiversity and ecosystem functioning has been demonstrated for both examples of patchy biogenic reefs (Sanderson et al., 2008; van Hoey et al., 2008; Cook et al., 2013; Coolen et al., 2015). Together with our observations, we therefore argue that conservation status of patchy, dynamic reefs should be reconsidered to ensure their protection.

The assessment of biogenic reef habitats, for instance under the European Habitats Directive, should hence include dynamic and patchy reefs that currently have low conservation status.

Often, it is stated that communities in dynamic environments are less vulnerable to anthropogenic disturbances, like demersal fisheries, than those in stable environments (Collie et al., 2000; Hiddink et al., 2006; van Denderen et al., 2015). However, migrating bedforms and high hydrodynamics pose a different stress on the reef fragments than the physical disturbance of demersal fishing gears. For *S. spinulosa*, multiple studies indicate that demersal fisheries pose a threat to the reefs, which could result in reef damage, fragmentation, and ultimately disappearance (Fariñas-Franco et al., 2014; Gibb et al., 2014; van der Reijden et al., 2019). In addition, a sliding scale is introduced when anthropogenic activities cause reef fragmentation, which in turn results in patchy reef habitats with little conservation status (Cook et al., 2013). Assessments of reef conservation value should therefore focusing dominantly on the contribution of reef structures to ecosystem functioning in addition to the physical dimensions of these structures (Hendrick and Foster-Smith, 2006; Sheehan et al., 2013). Moreover, the physical dimensions assessed should be considered at the right scale and with respect to the entire landscape. For a patchy reef like the one described here, dimensions of individual reef fragments or habitat patches contain little information. It is the extent of the area in which the reef habitat patches are found that is of importance for the ecosystem, including the non-reef habitats (Sheehan et al., 2013). The subsequent conservation of such patchy, dynamic reef habitats should allow a continuity of natural dynamic processes, without anthropogenic disturbances at the seafloor, at scales relevant to the dynamics of both reef patches and morphological bedforms.

DATA AVAILABILITY STATEMENT

The original contributions presented in this study are available at https://doi.org/10.34894/TNXNX2.

ETHICS STATEMENT

Ethical review and approval were not required for the animal study because field sampling was limited to box coring and video transects to estimate abundance of any species present. As such, no animal experiments were performed.

AUTHOR CONTRIBUTIONS

KR: conceptualization, methodology, validation, formal analysis, investigation, data curation, writing – original draft, and visualization. LK: conceptualization, methodology, investigation, data curation, writing, review, and editing. SM: writing, review, and editing. MS: supervision, project administration, funding acquisition, writing, review, and editing. PH: methodology, resources, writing, review, and editing. HO: conceptualization, methodology, project administration, funding acquisition, writing, review, and editing. LG: conceptualization, methodology, writing, review, editing, and supervision. All authors contributed to the article and approved the submitted version.

FUNDING

This work was funded by the Gieskes-Strijbis Fonds, Netherlands. LG was funded by NWO grant 016.Veni.181.087. The funders had no involvement in the execution of the study.

ACKNOWLEDGMENTS

We would like to thank the crew of RV *Pelagia* for their assistance during the fieldwork campaigns, and Rob Witbaard and Jip Vrooman for their role as cruise leaders. Joël Cuperus of the Directorate General for Public Works and Water Management of the Dutch Ministry of Infrastructure and Water Management was so kind to share the MWTL- survey dataset. We further thank Loran Kleine Schaars and his colleagues from the NIOZ benthos laboratory for the processing of endobenthos samples of the 2019 campaign, and Matthew Parsons and Maria Bacelar Martinez for processing the endobenthos samples from the 2017 campaign. We also would like to thank two reviewers that substantially improved the manuscript with their comments.

SUPPLEMENTARY MATERIAL

The Supplementary Material for this article can be found online at: https://www.frontiersin.org/articles/10.3389/fmars.2021.642659/full#supplementary-material

REFERENCES

Barker, B. A. J., Helmond, I., Bax, N. J., Williams, A., Davenport, S., and Wadley, V. A. (1999). A vessel-towed camera platform for surveying seafloor habitats of the Continental Shelf. *Cont. Shelf Res.* 19, 1161–1170. doi: 10.1016/S0278-4343(99)00017-5

Bates, D., Mächler, M., Bolker, B. M., and Walker, S. C. (2015). Fitting linear mixed-effects models using lme4. *J. Stat. Softw.* 67, 1–48. doi: 10.18637/jss.v067.i01

Boonzaier, L., and Pauly, D. (2016). Marine protection targets: an updated assessment of global progress. *Oryx* 50, 27–35. doi: 10.1017/S0030605315000848

Borsje, B. W., Bouma, T. J., Rabaut, M., Herman, P. M. J., and Hulscher, S. J. M. H. (2014). Formation and erosion of biogeomorphological structures: a model study on the tube-building polychaete *Lanice conchilega*. *Limnol. Oceanogr.* 59, 1297–1309. doi: 10.4319/lo.2014.59.4.1297

Christianen, M. J. A., van der Heide, T., Holthuijsen, S. J., van der Reijden, K. J., Borst, A. C. W., and Olff, H. (2016). Biodiversity and food web indicators of community recovery in intertidal shellfish reefs. *Biol. Conserv.* 213, 317–324. doi: 10.1016/j.biocon.2016.09.028

Collie, J. S., Hall, S. J., Kaiser, M. J., and Poiner, I. A. N. R. (2000). A quantitative analysis of fishing impacts on shelf-sea benthos. *J. Anim. Ecol.* 69, 785–798. doi: 10.1046/j.1365-2656.2000.00434.x

Collin, A., Dubois, S., James, D., and Houet, T. (2019). Improving intertidal reef mapping using UAV surface, red edge, and near-infrared data. *Drones* 3:67. doi: 10.3390/drones3030067

Collins, K. (2003). *Dorset Marine Habitat Surveys: Maerl, Worm Reefs, Bream Nests, Sea Fans and Brittlestars. 2003 survey results. Report to Dorset Wildlife Trust and English Nature from the School of Ocean and Earth Science*. Southampton: University of Southampton.

Cook, R., Fariñas-Franco, J. M., Gell, F. R., Holt, R. H. F., Holt, T., Lindenbaum, C., et al. (2013). The substantial first impact of bottom fishing on rare biodiversity hotspots: a dilemma for evidence-based conservation. *PLoS One* 8:e69904. doi: 10.1371/journal.pone.0069904

Coolen, J. W. P., Bos, O. G., Glorius, S., Lengkeek, W., Cuperus, J., van der Weide, B., et al. (2015). Reefs, sand and reef-like sand: a comparison of the benthic biodiversity of habitats in the Dutch Borkum Reef Grounds. *J. Sea Res.* 103, 84–92. doi: 10.1016/j.seares.2015.06.010

Costello, M. J., and Ballantine, B. (2015). Biodiversity conservation should focus on no-take Marine Reserves: 94% of marine protected areas allow fishing. *Trends Ecol. Evol.* 30, 507–509. doi: 10.1016/j.tree.2015.06.011

Damveld, J. H. (2020). *The Feedbacks Among Tidal Sand Waves, benthic Organisms and Sediment Sorting Processes*. Enschede: University of Twente. doi: 10.3990/1.9789036550000

Damveld, J. H., Borsje, B. W., Roos, P. C., and Hulscher, S. J. M. H. (2020). Biogeomorphology in the marine landscape: modelling the feedbacks between patches of the polychaete worm *Lanice conchilega* and tidal sand waves. *Earth Surf. Process. Landforms* 45, 2572–2587. doi: 10.1002/esp.4914

Damveld, J. H., van der Reijden, K. J., Cheng, C., Koop, L., Haaksma, L. R., et al. (2018). Video transects reveal that tidal sand waves affect the spatial distribution of benthic organisms and sand ripples. *Geophys. Res. Lett.* 45, 11837–11846. doi: 10.1029/2018GL079858

Damveld, J. H., Roos, P. C., Borsje, B. W., and Hulscher, S. J. M. H. (2019). Modelling the two-way coupling of tidal sand waves and benthic organisms: a linear stability approach. *Environ. Fluid Mech.* 19, 1073–1103. doi: 10.1007/s10652-019-09673-1

Donadi, S., van der Heide, T., van der Zee, E. M., Eklöf, J. S., van de Koppel, J., Weerman, E. J., et al. (2013). Cross-habitat interactions among bivalve species control community structure on intertidal flats. *Ecology* 94, 489–498. doi: 10.1890/12-0048.1

ESRI (2018). *ArcGIS*. Redlands, CA: ESRI.

European Commission (1992). *Council Directive 92/43/ECC on the Conservation of Natural Habitats and of Wild Fauna and Flora*. Brussels: European Commission.

European Commission (2013). *Interpretation Manual of European Union Habitats. EU28*. Available online at: http://scholar.google.com/scholar?hl=en&btnG=Search&q=intitle:INTERPRETATION+MANUAL+OF+EUROPEAN+UNION+HABITATS#0 (accessed September 14, 2020).

Fariñas-Franco, J. M., Allcock, A. L., and Roberts, D. (2018). Protection alone may not promote natural recovery of biogenic habitats of high biodiversity damaged by mobile fishing gears. *Mar. Environ. Res.* 135, 18–28. doi: 10.1016/j.marenvres.2018.01.009

Fariñas-Franco, J. M., Pearce, B., Porter, J., Harries, D., Mair, J. M., Woolmer, A. S., et al. (2014). *Marine Strategy Framework Directive Indicators for Biogenic Reefs formed by Modiolus modiolus, Mytilus edulis and Sabellaria spinulosa. Part 1: Defining and Validating the Indicators*. Peterborough: JNCC.

Ferrario, F., Beck, M. W., Storlazzi, C. D., Micheli, F., Shepard, C. C., and Airoldi, L. (2014). The effectiveness of coral reefs for coastal hazard risk reduction and adaptation. *Nat. Commun.* 5:3794. doi: 10.1038/ncomms4794

Gibb, N., Tillin, H., Pearce, B., and Tyler-Walters, H. (2014). *Assessing the Sensitivity of Sabellaria spinulosa Reef Biotopes to Pressures Associated with Marine Activities*. Peterborough: JNCC.

Gravina, M. F., Cardone, F., Bonifazi, A., Bertrandino, M. S., Chimienti, G., Longo, C., et al. (2018). *Sabellaria spinulosa* (Polychaeta, Annelida) reefs in the Mediterranean Sea: habitat mapping, dynamics and associated fauna for conservation management. *Estuar. Coast. Shelf Sci.* 200, 248–257. doi: 10.1016/j.ecss.2017.11.017

Hendrick, V. J., and Foster-Smith, R. L. (2006). Sabellaria spinulosa reef: a scoring system for evaluating 'reefiness' in the context of the Habitats Directive. *J. Mar. Biol. Assoc. U.K.* 86, 665–677. doi: 10.1017/S0025315406013555

Hendrick, V. J., Hutchison, Z. L., and Last, K. S. (2016). Sediment burial intolerance of marine macroinvertebrates. *PLoS One* 11:e0149114. doi: 10.1371/journal.pone.0149114

Hewitt, J. E., Thrush, S. F., Halliday, J., and Duffy, C. (2005). The importance of small-scale habitat structure for maintaining beta diversity. *Ecology* 86, 1619–1626. doi: 10.1890/04-1099

Hiddink, J. G., Jennings, S., Kaiser, M. J., Queirós, A. M., Duplisea, D. E., and Piet, G. J. (2006). Cumulative impacts of seabed trawl disturbance on benthic biomass, production, and species richness in different habitats. *Can. J. Fish. Aquat. Sci.* 63, 721–736. doi: 10.1139/F05-266

Hiddink, J. G., Jennings, S., Sciberras, M., Bolam, S. G., Cambiè, G., McConnaughey, R. A., et al. (2019). Assessing bottom trawling impacts based on the longevity of benthic invertebrates. *J. Appl. Ecol.* 56, 1075–1084. doi: 10.1111/1365-2664.13278

Holstein, J. (2018). *Worms: Retriving Aphia Information from World Register of Marine Species. R package version* 0.2.2. Available online at: https://cran.r-project.org/package=worms (accessed September 14, 2020).

Idier, D., Ehrhold, A., and Garlan, T. (2002). Morphodynamique d'une dune sous-marine du détroit du pas de Calais. *Comptes Rendus Geosci.* 334, 1079–1085. doi: 10.1016/s1631-0713(02)01852-7

Jenkins, C., Eggleton, J., Barry, J., and O'Connor, J. (2018). Advances in assessing *Sabellaria spinulosa* reefs for ongoing monitoring. *Ecol. Evol.* 8, 7673–7687. doi: 10.1002/ece3.4292

Jones, C. G., Lawton, J. H., and Shachak, M. (1994). Organisms as ecosystem engineers. *Oikos* 69, 373–386. doi: 10.2307/3545850

Knaapen, M. A., van Bergen Henegouw, C. N., and Hu, Y. Y. (2005). Quantifying bedform migration using multi-beam sonar. *Geo Mar. Lett.* 25, 306–314. doi: 10.1007/s00367-005-0005-z

Knaapen, M. A. F. (2005). Sandwave migration predictor based on shape information. *J. Geophys. Res. Earth Surf.* 110, 1–9. doi: 10.1029/2004JF000195

Knaapen, M. A. F. (2009). Sandbank occurrence on the Dutch continental shelf in the North Sea. *Geo Mar. Lett.* 29, 17–24. doi: 10.1007/s00367-008-0105-7

Koop, L., Amiri-Simkooei, A., van der Reijden, K. J., O'Flynn, S., Snellen, M., and Simons, D. G. (2019). Seafloor classification in a sand wave environment on the Dutch continental shelf using multibeam echosounder backscatter data. *Geosciences* 9:142. doi: 10.3390/geosciences9030142

Koop, L., van der Reijden, K. J., Mestdagh, S., Ysebaert, T., Laura, L., Olff, H., et al. (2020). Measuring centimeter scale sand ripples using multibeam echosounder backscatter data on the Brown Bank of the Dutch Continental Shelf. *Geosciences* 10:495. doi: 10.3390/geosciences10120495

Leenders, S., Damveld, J. H., Schouten, J., Hoekstra, R., Roetert, T. J., and Borsje, B. W. (2021). Numerical modelling of the migration direction of tidal sand waves over sand banks. *Coast. Eng.* 163:103790. doi: 10.1016/j.coastaleng.2020.103790

Lenihan, H. S. (1999). Physical-biological coupling on oyster reefs: How habitat structure influences individual performance. *Ecol. Monogr.* 69, 251–275. doi: 10.2307/2657157

Lenth, R. (2020). *Emmeans: Estimated Marginal Means, aka Least-Squares Means. R package version* 1.5.2-1. Available online at: https://cran.r-project.org/package=emmeans (accessed September 14, 2020).

Lisco, S., Moretti, M., Moretti, V., Cardone, F., Corriero, G., and Longo, C. (2017). Sedimentological features of *Sabellaria spinulosa* biocontructions. *Mar. Pet. Geol.* 87, 203–212. doi: 10.1016/j.marpetgeo.2017.06.013

Mestdagh, S., Amiri-Simkooei, A., van der Reijden, K. J., Koop, L., O'Flynn, S., Snellen, M., et al. (2020). Linking the morphology and ecology of subtidal soft-bottom marine benthic habitats: a novel multiscale approach. *Estuar. Coast. Shelf Sci.* 238:106687. doi: 10.1016/j.ecss.2020.106687

Oksanen, J., Blanchet, F. G., Friendly, M., Kindt, R., Legendre, P., McGlinn, D., et al. (2019). *Vegan: Community Ecology package. R package version* 2.5-6. Available online at: https://cran.r-project.org/package=vegan (accessed September 14, 2020).

OSPAR Commission (2013). *Background Document on Sabellaria spinulosa Reefs*. Available online at: http://www.ospar.org/documents?v=7342 (accessed September 14, 2020).

Parry, D. M., Kendall, M. A., Pilgrim, D. A., and Jones, M. B. (2003). Identification of patch structure within marine benthic landscapes using a remotely operated vehicle. *J. Exp. Mar. Bio. Ecol.* 285–286, 497–511. doi: 10.1016/S0022-0981(02)00546-4

Paul, M., Bouma, T. J., and Amos, C. L. (2012). Wave attenuation by submerged vegetation: combining the effect of organism traits and tidal current. *Mar. Ecol. Prog. Ser.* 444, 31–41. doi: 10.3354/meps09489

Pearce, B. (2014). *The Ecology of Sabellaria Spinulosa Reefs*. Available online at: https://pearl.plymouth.ac.uk/bitstream/handle/10026.1/10098/2017Pearce736123phd.pdf?sequence=1 (accessed September 14, 2020).

Pearce, B., Fariñas-franco, J. M., Wilson, C., Pitts, J., and Somer, P. J. (2014). Repeated mapping of reefs constructed by *Sabellaria spinulosa* Leuckart 1849 at an offshore wind farm site. *Cont. Shelf Res.* 83, 3–13. doi: 10.1016/j.csr.2014.02.003

Pearce, B., Hill, J. M., Wilson, C., Griffin, R., Earnshaw, S., and Pitts, J. (2013). *Sabellaria spinulosa Reef Ecology and Ecosystem Services*. London: The Crown Estate. doi: 10.13140/2.1.4856.0644

Plaisance, L., Caley, M. J., Brainard, R. E., and Knowlton, N. (2011). The diversity of coral reefs: What are we missing? *PLoS One* 6:e0025026. doi: 10.1371/journal.pone.0025026

R Development Core Team (2014). *R: A Language and Environment for Statistical Computing*. Available online at: https://www.r-project.org/ (accessed September 14, 2020).

R2Sonic LLC (2017). *Operational Manual V6.3*. Austin, TX: R2Sonic LLC.

Rabaut, M., Vincx, M., and Degraer, S. (2009). Do *Lanice conchilega* (sandmason) aggregations classify as reefs? Quantifying habitat modifying effects. *Helgol. Mar. Res.* 63, 37–46. doi: 10.1007/s10152-008-0137-4

Rees, E. I. S., Sanderson, W. G., Mackie, A. S. Y., and Holt, R. H. F. (2008). Small-scale variation within a *Modiolus modiolus* (Mollusca: Bivalvia) reef in the Irish Sea: III. Crevice, sediment infauna and epifauna from targeted cores. *J. Mar. Biol. Assoc. U.K.* 88, 151–156. doi: 10.1017/S0025315408000374

Reiss, H., Degraer, S., Duineveld, G. C. A., Kröncke, I., Aldridge, J., Craeymeersch, J. A., et al. (2010). Spatial patterns of infauna, epifauna, and demersal fish communities in the North Sea. *ICES J. Mar. Sci.* 67, 278–293. doi: 10.1093/icesjms/fsp253

Roberts, C. M., McClean, C. J., Veron, J. E. N., Hawkins, J. P., Allen, G. R., McAllister, D. E., et al. (2002). Marine biodiversity hotspots and conservation priorities for tropical reefs. *Science* 295, 1280–1284. doi: 10.1126/science.1067728

Ryer, C. H., Stoner, A. W., and Titgen, R. H. (2004). Behavioral mechanisms underlying the refuge value of benthic habitat structure for two flatfishes with differing anti-predator strategies. *Mar. Ecol. Prog. Ser.* 268, 231–243. doi: 10.3354/meps268231

Sanderson, W. G., Holt, R. H. F., Kay, L., Ramsay, K., Perrins, J., Mcmath, A. J., et al. (2008). Small-scale variation within a *Modiolus modiolus* (Mollusca: Bivalvia) reef in the Irish Sea. II. Epifauna recorded by divers and cameras. *J. Mar. Biol. Assoc. U.K.* 88, 143–149. doi: 10.1017/S0025315408000040

Sciberras, M., Hiddink, J. G., Jennings, S., Szostek, C. L., Hughes, K. M., Kneafsey, B., et al. (2018). Response of benthic fauna to experimental bottom fishing: a global meta-analysis. *Fish Fish.* 19, 698–715. doi: 10.1111/faf.12283

Sheehan, E. V., Cousens, S. L., Nancollas, S. J., Stauss, C., Royle, J., and Attrill, M. J. (2013). Drawing lines at the sand: evidence for functional vs. visual reef boundaries in temperate Marine Protected Areas. *Mar. Pollut. Bull.* 76, 194–202. doi: 10.1016/j.marpolbul.2013.09.004

Sheehan, E. V., Stevens, T. F., and Attrill, M. J. (2010). A quantitative, non-destructive methodology for habitat characterisation and benthic monitoring at offshore renewable energy developments. *PLoS One* 5:e14461. doi: 10.1371/journal.pone.0014461

Tiano, J. C., van der Reijden, K. J., O'Flynn, S., Beauchard, O., van der Ree, S., van der Wees, J., et al. (2020). Experimental bottom trawling finds resilience in large-bodied infauna but vulnerability for epifauna and juveniles in the Frisian Front. *Mar. Environ. Res.* 159:104964. doi: 10.1016/j.marenvres.2020.104964

van Denderen, P. D., Bolam, S. G., Hiddink, J. G., Jennings, S., Kenny, A., Rijnsdorp, A. D., et al. (2015). Similar effects of bottom trawling and natural disturbance on composition and function of benthic communities across habitats. *Mar. Ecol. Prog. Ser.* 541, 31–43. doi: 10.3354/meps11550

van der Heide, T., van Nes, E. H., van Katwijk, M. M., Olff, H., and Smolders, A. J. P. (2011). Positive feedbacks in seagrass ecosystems - Evidence from large-scale empirical data. *PLoS One* 6:e16504. doi: 10.1371/journal.pone.0016504

van der Reijden, K. J., Hintzen, N. T., Govers, L. L., Rijnsdorp, A. D., and Olff, H. (2018). North Sea demersal fisheries prefer specific benthic habitats. *PLoS One* 13:e0208338. doi: 10.1371/journal.pone.0208338

van der Reijden, K. J., Koop, L., O'Flynn, S., Garcia, S., Bos, O., Sluis, C., et al. (2019). Discovery of *Sabellaria spinulosa* reefs in an intensively fished area of the Dutch Continental Shelf, North Sea. *J. Sea Res.* 144, 85–94. doi: 10.1016/j.seares.2018.11.008

van der Wal, D., Ysebaert, T., and Herman, P. M. J. (2017). Response of intertidal benthic macrofauna to migrating megaripples and hydrodynamics. *Mar. Ecol. Prog. Ser.* 585, 17–30. doi: 10.3354/meps12374

van der Zee, E. M., Angelini, C., Govers, L. L., Christianen, M. J. A., Altieri, A. H., van der Reijden, K. J., et al. (2016). How habitat-modifying organisms structure the food web of two coastal ecosystems. *Proc. R. Soc. B.* 283:20152326. doi: 10.1098/rspb.2015.2326

van der Zee, E. M., van der Heide, T., Donadi, S., Eklöf, J. S., Eriksson, B. K., Olff, H., et al. (2012). Spatially extended habitat modification by intertidal reef-building bivalves has implications for consumer-resource interactions. *Ecosystems* 15, 664–673. doi: 10.1007/s10021-012-9538-y

van Dijk, T. A., van Dalfsen, J. A., van Lancker, V., van Overmeeren, R. A., van Heteren, S., and Doornenbal, P. J. (2012). "Benthic habitat variations over tidal ridges, North Sea, The Netherlands," in *Seafloor Geomorphology as Benthic Habitat*, eds P. T. Harris and E. K. Baker (London: Elsevier Inc), 241–249. doi: 10.1016/b978-0-12-385140-6.00013-x

van Hoey, G., Guilini, K., Rabaut, M., Vincx, M., and Degraer, S. (2008). Ecological implications of the presence of the tube-building polychaete *Lanice conchilega* on soft-bottom benthic ecosystems. *Mar. Biol.* 154, 1009–1019. doi: 10.1007/s00227-008-0992-1

Ventura, D., Dubois, S. F., Bonifazi, A., Jona Lasinio, G., Seminara, M., Gravina, M. F., et al. (2020). Integration of close-range underwater photogrammetry with inspection and mesh processing software: a novel approach for quantifying ecological dynamics of temperate biogenic reefs. *Remote Sens. Ecol. Conserv* 2:178. doi: 10.1002/rse2.178

Walbridge, S., Slocum, N., Pobuda, M., and Wright, D. J. (2018). Unified geomorphological analysis workflows with Benthic Terrain Modeler. *Geosciences* 8:94. doi: 10.3390/geosciences8030094

Wilson, D. P. (1970). The larvae of *Sabellaria spinulosa* and their settlement behaviour. *J. Mar. Biol. Assoc. U.K.* 50, 33–52. doi: 10.1017/S0025315400000588

Conflict of Interest: The authors declare that the research was conducted in the absence of any commercial or financial relationships that could be construed as a potential conflict of interest.

frontiers in Marine Science

ORIGINAL RESEARCH
published: 07 May 2021
doi: 10.3389/fmars.2021.648197

Integrative Description of Cryptic *Tigriopus* Species From Korea Using MALDI-TOF MS and DNA Barcoding

Jisu Yeom[1†], Nayeon Park[1†], Raehyuk Jeong[2] and Wonchoel Lee[1]*

[1] Laboratory of Biodiversity, Department of Life Science, Hanyang University, Seoul, South Korea, [2] Big Data Biology Lab, Department of Life Science, Chung-Ang University, Seoul, South Korea

OPEN ACCESS

Edited by:
Carlos Navarro Barranco, Autonomous University of Madrid, Spain

Reviewed by:
Samuel Gómez, National Autonomous University of Mexico, Mexico
Sven Rossel, German Centre for Marine Biodiversity Research, Germany
Janna Peters, University of Hamburg, Germany
Nikolaos V. Schizas, University of Puerto Rico at Mayagüez, Puerto Rico

***Correspondence:**
Wonchoel Lee
wlee@hanyang.ac.kr

[†] These authors have contributed equally to this work and share first authorship

Specialty section:
This article was submitted to Marine Evolutionary Biology, Biogeography and Species Diversity, a section of the journal Frontiers in Marine Science

Received: 31 December 2020
Accepted: 12 April 2021
Published: 07 May 2021

Citation:
Yeom J, Park N, Jeong R and Lee W (2021) Integrative Description of Cryptic Tigriopus Species From Korea Using MALDI-TOF MS and DNA Barcoding. Front. Mar. Sci. 8:648197. doi: 10.3389/fmars.2021.648197

MALDI Time-of-Flight Mass Spectrometry (MALDI-TOF MS) provides a fast and reliable alternative method for species-level identification of pathogens and various metazoans. Compared to the commonly used mitochondrial cytochrome *c* oxidase subunit I (mtCOI) barcoding, advantages of MALDI-TOF MS are rapid species identifications and low costs. In this study, we used MALDI-TOF MS to determine whether spectra patterns of different species can be used for species identification. We obtained a total of 138 spectra from individual specimens of *Tigriopus*, which were subsequently used for various cluster analyses. Our findings revealed these spectra form three clear clusters with high AU value support. This study validates the viability of MALDI-TOF MS as a methodology for higher-resolution species identification, allowing detection of cryptic species of harpacticoida. In addition, we propose a new species, *Tigriopus koreanus* sp. nov. by utilizing integrative methods such as morphological comparison, mtCOI barcoding, and MALDI-TOF MS.

Keywords: copepoda, MALDI-TOF MS, cryptic species, protein, identification

INTRODUCTION

Intertidal copepods of the genus *Tigriopus* Norman, 1869 are widely distributed in high-shore intertidal rockpools across several continents (Tsuboko-Ishii and Burton, 2018). The genus consists of 17 species and is known to be easily bred under laboratory conditions, as it tolerates abrupt changes in environmental factors such as temperature and salinity (Kwok and Leung, 2005). *Tigriopus californicus* (Baker, 1912), a well-known representative of the genus, shows extensive population divergence and is a model for understanding allopatric speciation (Barreto et al., 2018). Reproductive isolation and molecular information have confirmed cryptic speciation in *T. californicus* (Peterson et al., 2013), but it remains unresolved.

Similarly, *Tigriopus*, which can be found also in the coast of Korea, is represented by *T. japonicus* Mori, 1938 and has been the subject study of several contributions. However, it has long been recognized that the Korean populations of *T. japonicus* are molecularly different from those of Japan (e.g., Jung et al., 2006; Ki et al., 2009).

In Karanovic et al. (2018), it was shown that the populations of *T. japonicus* inhabiting Korean coasts are actually two different species: *Tigriopus west* Karanovic et al., 2018 and *Tigriopus east* Karanovic et al., 2018. These three species are morphologically similar, making it nearly impossible to separate them through optical microscopy. Their cryptic nature was unraveled by Karanovic et al. (2018) through molecular and morphological comparisons. For morphological comparison,

they selected landmarks on somitic sensilla and segments of different appendages, which were used for two-dimensional geometric morphometrics. In addition, average Kimura 2-parameter (K2P) pairwise distance of mtCOI partial sequences between the two Korean species were revealed to be 0.226, confirming that *Tigriopus* in the west-south coasts and east coasts of Korea are two different species.

MALDI-TOF MS (Matrix-Assisted Laser Desorption/Ionization Time of Flight Mass Spectrometry) initially hits the sample with a pulsed laser to ionize it. This procedure is known as laser desorption ionization. Using a matrix—which is a small material that can absorb laser wavelengths—the sample collapses when the temperature of the sample-matrix rises rapidly by absorption of the laser. Fundamentally, MALDI is an ionization technique that uses a laser energy absorbing matrix to emit ions from large molecules with minimal fragmentation (Hillenkamp et al., 1991). The protein mass is analyzed with a TOF analyzer that measures the flight time of the ion emitted.

The representative protein spectra obtained by MALDI-TOF MS are used as a kind of barcode that can distinguish different species. This identification method was initially used for the identification of species of bacteria, fungi, and viruses (e.g., Claydon et al., 1996; Fenselau and Demirev, 2001), and is still widely used (e.g., Seng et al., 2010; Chalupová et al., 2014; Singhal et al., 2015). In addition, MALDI-TOF MS has been used for species identification of microalgae (Baumeister et al., 2020), microorganisms (Maier et al., 2006) and various metazoan taxa including insects (Feltens et al., 2010), fish (Volta et al., 2012; Shao and Bi, 2020), and calanoid copepods (Riccardi et al., 2012; Laakmann et al., 2013; Bode et al., 2017). Previous studies with several taxa as study subjects confirmed that MALDI-TOF MS is a reliable and fast alternative method for species identification.

Recently, Rossel and Martínez Arbizu (2019) suggested that the identification of species through protein mass measurement is a faster and cheaper method compared to mtCOI barcoding. In general, barcoding takes at least a day or more to obtain the sequencing result following DNA extraction of the target organism, and additional hours to complete PCR, electrophoresis, and purification. Most importantly, barcoding method varies highly in success rates depending on the primer sets used and requires prior knowledge on the target organism to find a suitable primer set. On the other hand, the protein spectrum used for MALDI-TOF MS can be obtained immediately by incubating the individual in a matrix for several minutes after drying the sample and measuring it with a MALDI-TOF MS machine. Rossel and Martínez Arbizu (2019) argued that the results could be obtained relatively quickly, at a lower cost. They (Rossel and Martínez Arbizu, 2019) used MALDI-TOF for the assessment of 75 species and confirmed that cryptic species *Leptastacus* can be separated using this approach (Rossel et al., 2019). In this study, we used MALDI-TOF MS to obtain spectra of *Tigriopus* from Korea and determine whether their varying peaks can be used to detect and differentiate cryptic species. In addition, a new species of *Tigriopus* is proposed based on approaches such as mtCOI barcoding, clustering of protein spectra, and morphological comparative analysis.

MATERIALS AND METHODS

Collecting and Morphological Comparison

Specimens of *Tigriopus* inhabiting intertidal rock pools were collected with a spuit at seven different coastal areas of Korea (**Figure 1** and **Table 1**) and brought to the laboratory in plastic container with seawater. In the absence of other animals, specimens of *Tigriopus* were kept alive in a 20℃ incubator under a photoperiod of 12 h light: 12 h dark, for 2–3 months after being brought to the laboratory. As food source for copepods, a small amount of Tetra Bits was provided.

Several individuals of *Tigriopus* were sorted under a dissecting microscope and stored in 99% ethyl alcohol. The descriptive terminology of Huys et al. (1996) was adopted. Abbreviations used in the text are as follows: Mxp, maxilliped; exp, exopod; enp, endopod; P1–P5, first to fifth thoracopod; exp (enp)-1 (2, 3) to denote the proximal (middle, distal) segment of a three-segmented ramus. BN, Baengnyeong island; DB, Daebu island; BR, Boryeong; SGP, Seogwipo; BS, Busan; JMJ, Jumunjin; GS, Goseong.

For morphological observation, slides were prepared using the sandwich method of 20 adult females of each species (total 60 individuals). Figure works for morphological comparison of each appendage (Mxp, P1 enp-1, P1 enp-2, P4 exp-3, P5 exp) were completed through observation at 400x magnification with an Olympus BX51 differential interference contrast microscope equipped with a drawing tube. First, length of each segment was measured to calculate the length/width ratio. Based on the ratio, analyses were conducted to compare the differences between the mean of the three species in SPSS. Normal distribution was tested, and while some Mxp's data were below significance, because the number of samples was sufficient, the data were kept for analysis. In addition, Bonferroni correction was performed, and ANOVA test determined which features showed significant morphological differences between species ($p < 0.05$).

Scanning Electron Microscopy (SEM)

In total, 18 specimens from BS were prepared for Scanning electron microscopy (SEM). For SEM preparation, specimens were transferred into hexamethyldisilazane (HMDS) for drying (Shively and Miller, 2009), mounted on stubs, and finally coated with gold in an ion coater, SPT-20 (COXEM, Korea). Coated stub was observed under SEM on the in-lens detector at an accelerating voltage of 15.0 Kv. The specimens were photographed using a COXEM EM-30 SEM at the Biodiversity laboratory in Hanyang University. Digital photographs were processed and combined into plates using Adobe Photoshop CS6.

MALDI-TOF MS

Pretreatment for MALDI-TOF MS

Total of 143 individual harpacticoids (138 *Tigriopus* and 5 *Schizopera*) were transferred to a 6-well plate a day before and fasted. On the day of the experiment, copepods were fixed in 99% ethyl alcohol for approximately 30 min, and then transferred to a 1.5 ml tube containing small amount of ethyl alcohol (0.5

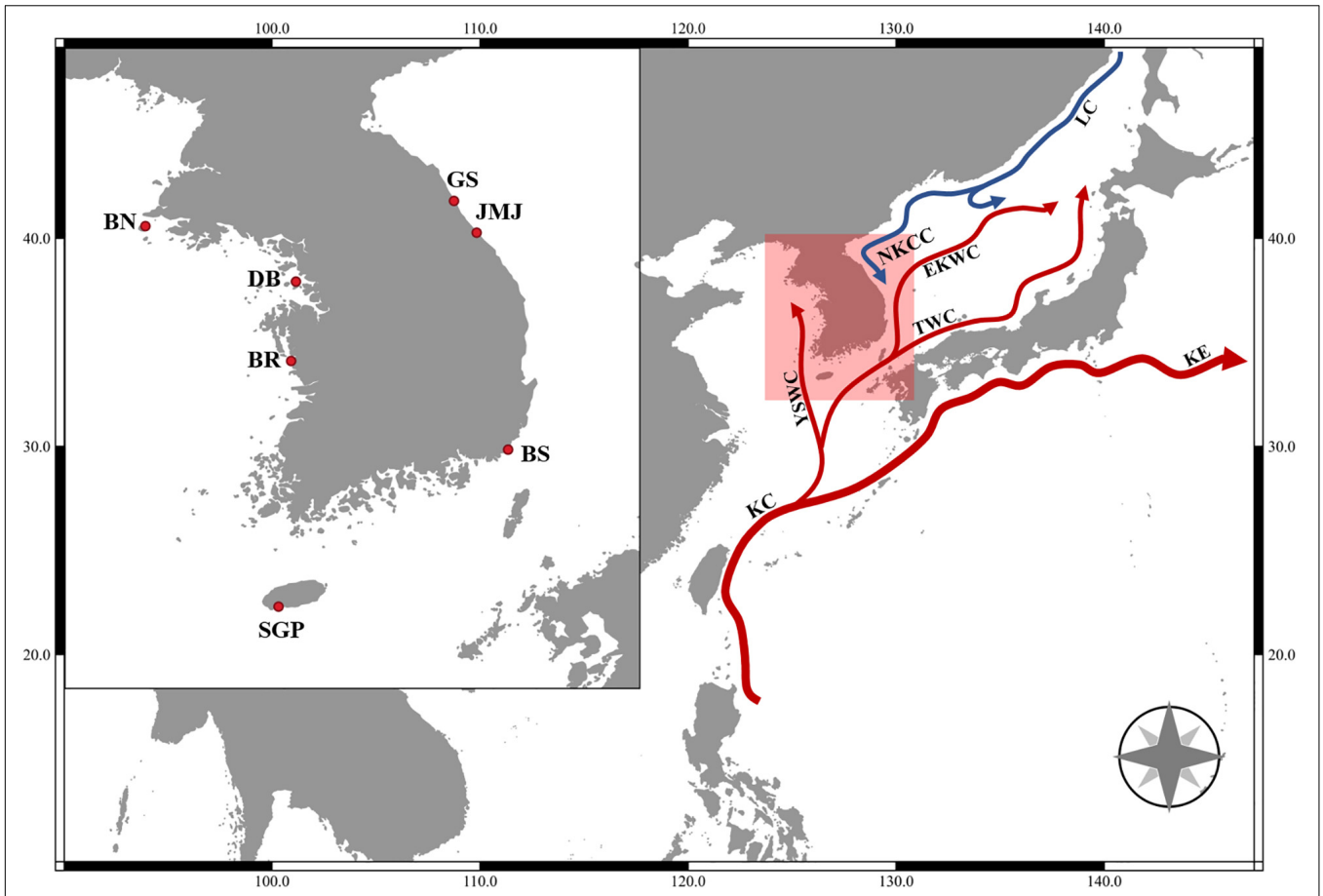

FIGURE 1 | Map of collecting locations. BN, Gobong port, Baengnyeong island, Incheon; BR, Daecheon beach, Boryeong; SGP, Daepyeong port, Seogwipo, Jeju island; JMJ, Jumunjin, Gangneung, Gangwon; BS, Gijang, Busan; GS, Munam, Goseong, Gangwon; DB, Bangameori beach, Daebu island, Ansan; KC, Kuroshio Current; KE, Kuroshio Extension; LC, Liman Current; NKCC, North Korea Cold Current; EKWC, East Korea Warm Current; TWC, Tsushima Warm Current; YSWC, Yellow Sea Warm Current.

TABLE 1 | Collecting information and the number of harpacticoids by region used in the MALDI-TOF MS experiment.

Collecting site	Abbr.	GPS coordinates	Date (2020)	Female (*egg)	Male	**Fixed	Total individuals
Bangameori beach, Daebu island, Ansan	DB	37°17′26.1″N 126°34′37.5″E	09-Apr	*5 (1)-Miraciidae*			*5-Miraciidae*
Gobong port, Baengnyeong island, Incheon	BN	37°58′57.5″N 124°41′55.3″E	13-Aug	18 (4)	7		25
Daecheon beach, Boryeong	BR	36°18′00.0″N 126°31′02.0″E	26-Apr	11 (1)	9	6	20
Daepyeong port, Seogwipo, Jeju island	SGP	33°14′11.1″N 126°21′35.5″E	04-Aug	15 (4)	13		28
Gijang, Busan	BS	35°11′40.6″N 129°13′29.2″E	06-Aug	25 (2)	4		29
Jumunjin, Gangneung, Gangwon	JMJ	37°54′′02.7″N 128°49′56.2″E	26-Jul	23 (1)	8		31
Munam, Goseong, Gangwon	GS	38°17′48.1″N 128°32′57.8″E	29-Jun	5		5	5
Total (*Tigriopus*)				97	41	11	138

**Egg- the number of female individual(s) with egg sac, **Fixed- directly fixed with ethanol when collected at field.*

μl). Once all ethyl alcohol in the tube evaporated, leaving the copepod in completely dried state, 4 μl of α-Cyano-4-hydroxy-cinnamic acid (HCCA) matrix [Acetonitrile 50%; U.P. Water 47.5%; Trifluoroacetic acid 2.5%; supersaturated HCCA (30 mg for total 1 ml matrix)] was added to each tube and incubated at room temperature for at least 20 min.

Two microliter of this solution was placed on the target plate of the MALDI-TOF MS equipment (AXIMA Confidence MALDI TOF—Mass Spectrometer; Shimadzu) and once the solution dried completely to crystalize, the plate was placed in the instrument to be analyzed.

Protein mass spectra were measured between 2k to 20k Dalton on a MALDI-MS Application Launchpad 2.9.2 (Shimadzu Biotech) software using linear mode with laser power 80. To create a sum spectrum, 150 profiles were summed up. Each profile was measured 10 times, and the obtained individual protein

spectra were exported to ASCII format files after range editing in Data Explorer (TM) software version 4.3.

Workflow in R

The ASCII files were imported to RStudio using the R package MALDIquantForeign (ver. 0.12) (Gibb, 2015) and the subsequent data processing and analysis of the data was achieved using MALDIquant (ver. 1.19.3) (Gibb and Strimmer, 2012) and MALDIrppa (ver. 1.0.5) (Palarea-Albaladejo et al., 2018). For general methods to obtain the featureMatrix mentioned below, we referred to Species Identification using MALDIquant manual[1].

The range of all protein mass spectra were trimmed to 2,000–15,000 m/z. We conducted a basic quality control with raw data and tested whether all spectra contain the same number of data points and are not empty before overall analysis. Spectra were square root transformed and smoothed with the Savitzky-Golay method. The baseline was removed based on SNIP baseline estimation method and spectra were normalized using the Total-Ion-Current-calibration (TIC) method implemented in MALDIquant. Peak detection was applied with a signal-to-noise ratio (SNR) of 8 and a half window size of 18. Peaks were repeatedly binned with the "binpeaks" command from MALDIquant with a tolerance of 0.002. Through this process a feature matrix was created, which was then Hellinger transformed for further analysis. Results of the Hellinger transformed matrix were visualized through clustering analysis, diagonal discriminant analysis (DDA), and non-metric multi-dimensional scaling analysis.

Cluster analysis was performed using 138 spectra of data obtained from adult individuals of *Tigriopus*. Dendrogram was produced with pvclust (ver. 2.2) R package (Suzuki and Shimodaira, 2006) using Ward's 2D clustering algorithm with Euclidean distances and 10,000 bootstrapping replications. Approximately unbiased (AU) p-value and bootstrap probability (BP) values were provided alongside the dendrogram, of which AU values of $\geq$ 85% were considered strong evidence of a cluster for the analysis.

Non-Metric Multidimensional Scaling Plot (NMDS) was generated with the vegan (ver. 2.5.6) R package (Oksanen et al., 2018) based on Bray-Curtis Dissimilarity distance with k = 2. To test multivariate homogeneity of group dispersion, ANOVA test was performed utilizing betadisper function provided with the vegan (ver. 2.5.6) package. PERMANOVA test was also performed using Adonis tool to test the fit of the data with 999 permutations.

Diagonal discriminant analysis (DDA) was performed using Hellinger transformed featurematrix with sda (Ahdesmäki and Strimmer, 2010) function to find peaks with the highest variation among three different species. Total of 196 variables, 138 observations and 3 classes (species) were used to compute t-score for feature ranking. **Figure 6** was generated by peakPatterns function in MALDIrppa (ver. 1.0.5). Peaks were filtered with minimum frequency of 0.7.

[1]http://www.strimmerlab.org/software/maldiquant/

MtCOI

DNA Extraction and Amplification

For DNA extraction and amplification, specimens were transferred to a well of ultrapure water for 2 h to remove ethanol or seawater. Non-destructive DNA extraction was then carried out by utilizing worm lysis buffer (Williams et al., 1992). Specimens were transferred to microcentrifuge tubes containing 25 μl lysis buffer and placed in a Takara thermocycler (Takara, Otsu, Shiga, Japan) with the following settings: 65℃ for 15 min, 95℃ for 20 min and 15℃ for 2 min. After this, specimens were kept for morphological identification. Unpurified total DNA was kept at −20℃ for long-term storage.

MtCOI genes were amplified using PCR premix (LaboPass, COSMOgenetech, Korea) and 3 μl of DNA template with Cop-COI-2189 and jgLCO or LCO1490 primers (Bucklin et al., 2010). The amplification protocol consisted of an initial denaturation at 94℃ for 5 min followed by 40 cycles of denaturation at 94℃ for 1 min, annealing at 45℃ for 2 min, and extension at 72℃ for 3 min; this was followed by a final extension step at 72℃ for 10 min (Bucklin et al., 2010). Successful amplification was confirmed by electrophoresis on a 1% agarose gel. PCR products were sent to Bionics (Seoul, Korea) for purification and DNA sequencing. For sequencing, an ABI automatic capillary sequencer was used with the same set of primers used for amplification. All obtained sequences were visualized using Finch TV (ver. 1.4.0)[2] (Geospiza Inc., United States). The quality of each sequence was evaluated, and low-resolution peaks were checked by comparing forward and reverse strands. BLAST search confirmed the obtained sequences as copepods without contaminants. Sequence information from this study was deposited in the NCBI database (MW429840–MW429844).

Phylogenetic Analyses

Thirty two additional sequences were downloaded from GenBank and included in our analyses (**Supplementary Table 1**). Sequences were aligned with the ClustalW algorithm (Thompson et al., 1994) in MEGA version 7.0 (Kumar et al., 2016). Average pairwise distances were also computed in MEGA version 7.0 using the K2P model. Phylogenetic analyses were performed using Neighbor-Joining (NJ), Maximum parsimony (MP), Maximum Likelihood (ML), and Bayesian Inference (BI) approaches.

NJ analysis used the Kimura two-parameter model (K2P) (Kimura, 1980; Nei and Kumar, 2000) with uniform rates. ML analysis used the TrN + I + G model based on the model test result in jModelTest 2.1.10 (Darriba et al., 2012). 1,000 bootstrap replicates were performed to obtain a relative measure of node support for the resulting trees. A BI tree was constructed with MrBayes (ver. 3.2.6) (Ronquist et al., 2012) based on the following model parameters obtained using jModelTest 2.1.10: nst = 6, rates = gamma, ncat = 4, Lset base = (0.2320, 0.1835, 0.2216, 0.3629), rmat = (1, 6.9644, 1, 1, 12.3900, 1), gamma shape = 0.7700 and pinvar = 0.4730. Markov Chain Monte Carlo (MCMC) was run with the following parameters: nchains = 4, ngen = 1,000,000, samplefreq = 100, savebrlens = yes, and

[2]https://digitalworldbiology.com/FinchTV

printfreq = 1,000. The BI trees were constructed using the "sump" command with burnin = 250 to summarize parameters and the "sumt" command with burnin = 250 to summarize the tree. ML and BI trees were visualized using FigTree (ver. 1.4.2). Average pairwise distances were also computed in MEGA version 7.0 using the K2P model. All trees were rooted with *Calanus glacialis* sequence.

RESULTS

MALDI-TOF MS

Protein Mass Spectrum Pattern

Spectra data obtained from a total of 138 *Tigriopus* and 5 Miraciidae specimens were used for the analysis (**Table 1**). In the protein spectra obtained from raw data (**Figure 2**), the x-axis represents protein mass, and the y-axis is intensity, showing how much protein is present for each mass value corresponding to the x-axis. Similar spectra peak patterns were observed among species collected from the same region. Prominent peak values were also confirmed to be similar by region. Protein spectra pattern did not seem to differ by body parts (prosome/urosome), or by sex (**Figure 2**). Presence of eggs did not seem to effect ability to obtain spectra. Even specimens fixed in 99% ethyl alcohol stored at 4℃ for several months yielded spectra without a problem (**Table 1**, marked with "-fix"), but when only female egg sacs were used for the analysis, accurate protein spectra data could not be obtained.

Cluster Dendrogram With *p*-values (%)

Cluster analysis of 138 adult individuals of *Tigriopus* collected from six different regions in Korea are shown in **Figure 3**. Analysis using Hellinger transformed matrix confirm that species are divided into three clusters (Busan, *T. east* and *T. west*) with fairly strong support (AU *p*-values = 91, 84, and 92%, respectively). Of the two *p*-values, AU is considered to be superior to BP in terms of bias by using multiscale bootstrap resampling as opposed to ordinary bootstrap resampling (Suzuki and Shimodaira, 2006).

It is worth mentioning that clustering analysis was attempted with both raw spectra feature matrix as well as Hellinger transformed matrix. Results from the Hellinger transformed matrix yielded a dendrogram with higher AU and BP values. While optimal combination of data transformation has been documented by Rossel and Martínez Arbizu (2018), they recommended Hellinger transformed data in most cases. Other MALDI-TOF MS studies conducted on copepods also utilized Hellinger transformed datasets (Rossel and Martínez Arbizu, 2018; Rossel et al., 2019).

The indication of a third new species of the cryptic species *Tigriopus* spp. is further supported below via NMDS analysis.

Non-metric Multi-Dimensional Scaling (NMDS)

Non-Metric Multi-Dimensional Scaling (NMDS) analysis of all 138 spectra of *Tigriopus* used in the experiment are shown in **Figure 4**. This is the result of visualizing a two-dimensional space by measuring similarities between spectra.

In the West Sea cluster, spectra from Jeju, Boryeong, and Baengnyeong island are mixed. Based on this, all of them are *T. west*, although there is a considerable geographical difference between Baengnyeong island and Jeju. In addition, it was confirmed that only the Busan cluster was gathered separately above. Therefore, it was determined that *Tigriopus* in six regions in Korea were divided into three groups.

It is quite clear from the NMDS plot that three groups are visibly distinguishable from one another (homogeneity test, $P < 0.05$, PERMANOVA test, $P = 0.001$). Stress value of this plot was 0.1518 which is in usable range according to Clarke (1993), who suggested stress value < 0.20 to be usable. Considering that our dataset contains 138 samples of different variables, and since stress value increases with the number of samples and variables, the stress value of 0.15 is quite acceptable.

Diagonal Discriminant Analysis

In **Figure 5**, the numbers on the left show top 40 protein masses that differed greatly among species. Simply put, in the case of *T. koreanus* sp. nov., they have a relatively large amount of 2,986−2,988 m/z compared to the other species, followed by *T. west* with a relatively large amount of 2,958 m/z. Such inferring peaks with high variation among different species can thus be considered when delimitating Korean species of *Tigriopus*. **Figure 6** illustrates variation in important peaks shown in **Figure 5**. It is evident individuals exhibit similar peak patterns for each species. The parts not marked in blue mean that they are the peaks below the SNR criteria and have lower intensity compared to other species.

MtCOI Distance

Partial mtCOI sequences were successfully obtained from five specimens of the three putative different species (JMJ; BN, BR, SGP; BS). As a result of calculating the average pairwise distance with the mtCOI sequences obtained from each cluster, the mtCOI distances within each species are shown in **Table 2**. In the case of *T. californicus*, the average intra-species distance was 0.222, which is considered to reflect the fact that it is a cryptic species complex.

Busan population differs from the West coast and Jeju population by about 5–8% (mean = 0.063, S.E. = 0.011) and differs from the East population by about 31–38% (mean = 0.341, S.E. = 0.037) (**Supplementary Tables 2**, **3**). These divergence values exceed the range of mean distances within *T. east, T. japonicus*, and *T. west* (0.014–0.037) (**Table 2**).

Mean distance within *Tigriopus* was 0.298 (S.E. = 0.022) (**Supplementary Table 2**). The topologies of the Bayesian inference tree and maximum likelihood tree (**Figure 7**), maximum parsimony tree (**Supplementary Figure 1**), and neighbor joining tree (**Supplementary Figure 2**) were different.

Taxonomy

Family Harpacticidae Dana, 1846

Genus *Tigriopus* Norman, 1869

Tigriopus koreanus sp. nov.

(**Figures 8**, **9**)

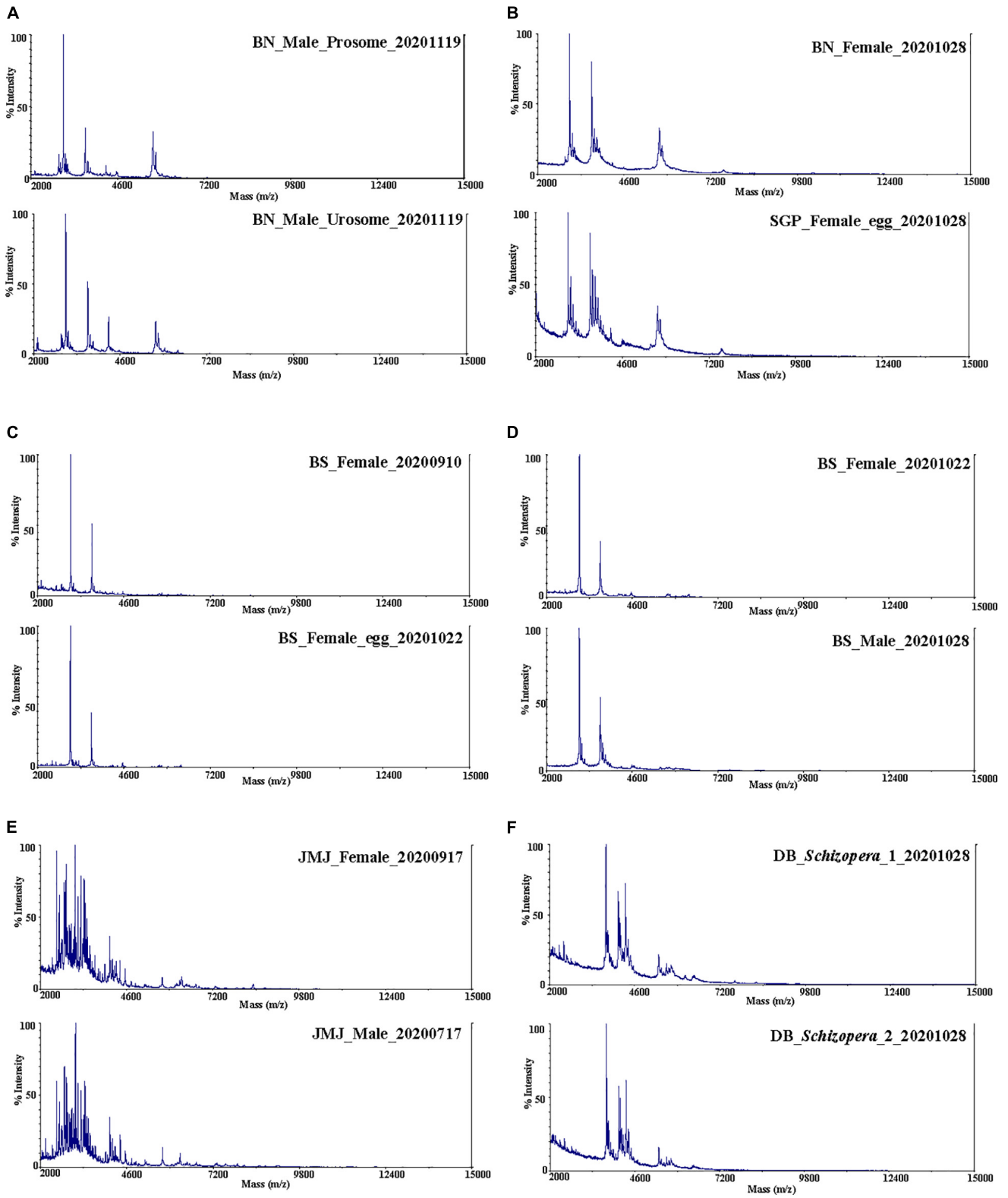

FIGURE 2 | Protein mass spectra. *T. west* **(A,B)**; **(A)** prosome and urosome, **(B)** BN and SGP. *T. koreanus* sp. nov. **(C,D)**; **(C)** female and female with egg sac, **(D)** female and male. **(E)** *T. east* female and male, **(F)** *Schizopera* sp.

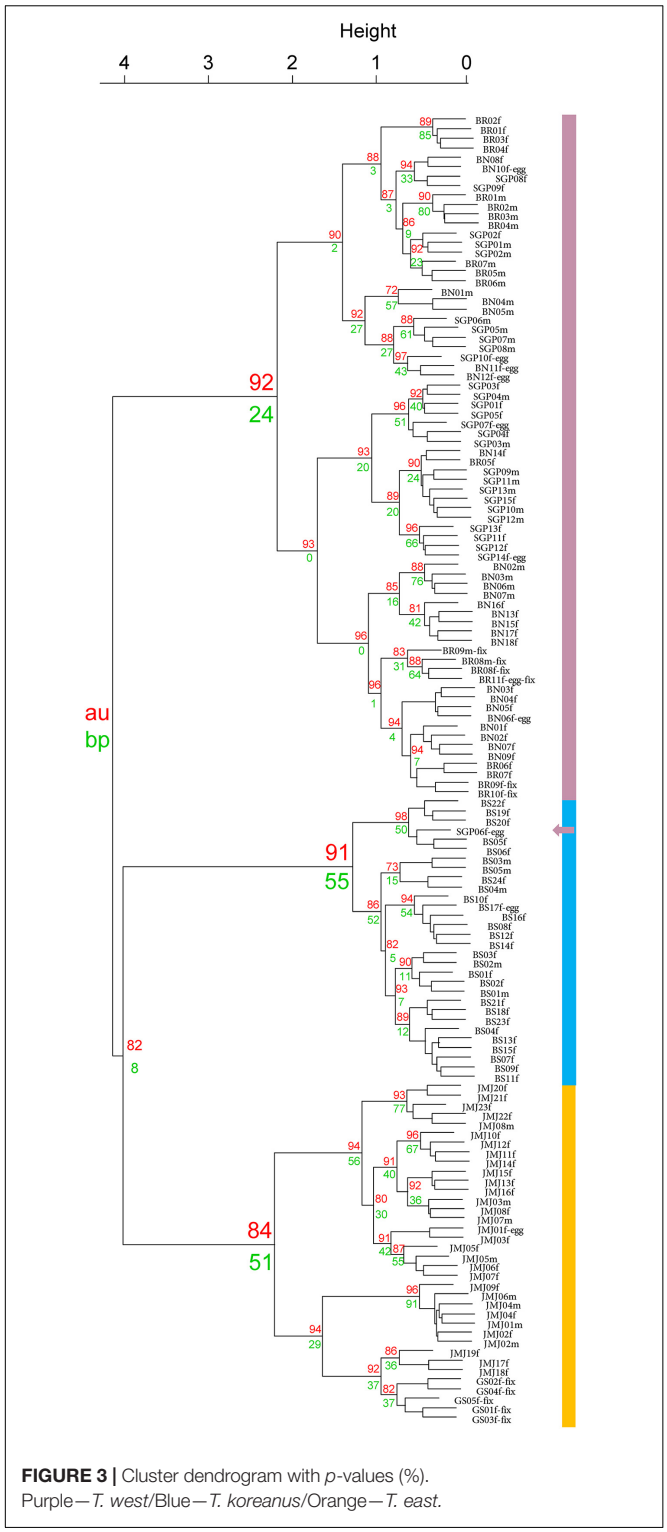

FIGURE 3 | Cluster dendrogram with *p*-values (%).
Purple—*T. west*/Blue—*T. koreanus*/Orange—*T. east*.

urn:lsid:zoobank.org:act:9F568FAE-D7A0-4439-8BED-0B72056C494C

Type locality – Rock pool, Gijang, Busan, South Korea, 35°11′40.6″N 129°13′29.2″E

Type material – Holotype; 1 female on slide (NIBRIV0000880626). Allotype; 1 male on slide (NIBRIV0000880627). Paratypes; 3 females and 3 males on a SEM stub (NIBRIV0000880628), 2 females and 2 males in a vial (NIBRIV0000880629).

Other material examined – 17 females on slides (for morphological observation). 12 individuals on a SEM stub

Description – Total body length of female 1000.06 μm (n = 10) (**Figures 8A,B**), male 720.12 μm (*n* = 9) (**Figures 8D,E**); Habitus, segmentation, armature, and general ornamentation of somites and appendages as given by Ito (1969) for the redescription of *T. japonicus*.

Based on female, Mxp basis (**Figure 9A**) has a maximum length of 63.9–80.6 μm (mean = 73.5; *SD* = 4.2), a maximum width of 34.7–45.8 μm (mean = 40.6; *SD* = 2.9), and the ratio average between length and width is 1.8. P1 enp-1 (**Figure 9B**) has a maximum length of 66.7—91.7 μm (mean = 80.2; *SD* = 7.6), a maximum width of 25.0—38.9 μm (mean = 33.1; *SD* = 3.5), and the ratio average between length and width is 2.4. The maximum length of P1 exp-1 is 94.4—121.0 μm (mean = 106.5; *SD* = 7.5), and the maximum length of P1 exp-2 is 65.3—88.9 μm (mean = 78.5; *SD* = 6.3). P4 exp-3 (**Figure 9C**) has a maximum length of 55.6—68.1 μm (mean = 61.5; *SD* = 3.7), a maximum width of 18.1—26.4 μm (mean = 22.4; *SD* = 1.7), and the ratio average between length and width is 2.7. Female P5 exp (**Figure 9D**) has a maximum length of 45.8—58.3 μm (mean = 51.7; *SD* = 3.1), a maximum width of 27.8—34.7 μm (mean = 31.1; *SD* = 2.0), and the ratio average between length and width is 1.7 (**Supplementary Table 4**).

Sexual dimorphism of male expressed in A1 (**Figure 8F**), P2 enp (**Figure 8G**), P5, and P6 (**Figure 8H**).

Remarks – From measuring and comparing the morphological features of 20 females of each species, subtle morphological differences in the length:width ratio (l/w) of the Mxp basis, l/w ratio of the P1 enp-1, P4 exp-3, and P5 exp (**Table 3** and **Figures 9**, **10**) among the Korean species of *Tigriopus* were revealed.

T. koreanus sp. nov. and *T. west* showed significant differences in Mxp basis l/w ($P < 0.001$), P1 enp-1 l/w ($P < 0.001$). The difference between *T. koreanus* sp. nov. and *T. east* showed significant differences in all four morphological features ($P < 0.001$). The Mxp basis l/w of *T. koreanus* sp. nov. was about 1.8, which was stouter than the other two species (l/w = 2). For P1 enp-1 l/w, *T. west* is about 2.8, the longest, *T. east* is 2.6, and *T. koreanus* sp. nov. is 2.4, which is different in all three species. On the contrary, P4 exp-3 l/w showed the narrowest trend at *T. east* at about 2.9, followed by *T. koreanus* sp. nov. with 2.7 and *T. west* with 2.6. P5 exp l/w was similar in *T. west* and *T. koreanus* sp. nov., but both species showed significant differences from *T. east*.

According to DDA, compared to the other two species, *T. koreanus* sp. nov. showed strong intensity at 2,986—2,988, 3,066—3,067, and 3,026 m/z, and these peaks can be regarded as representative peaks of this species (**Figure 5**). In the case of *T. west*, ten representative peaks were identified, including 2,958, 3,036—3,037, 3,617—3,618, and 4,242. *Tigriopus east* showed

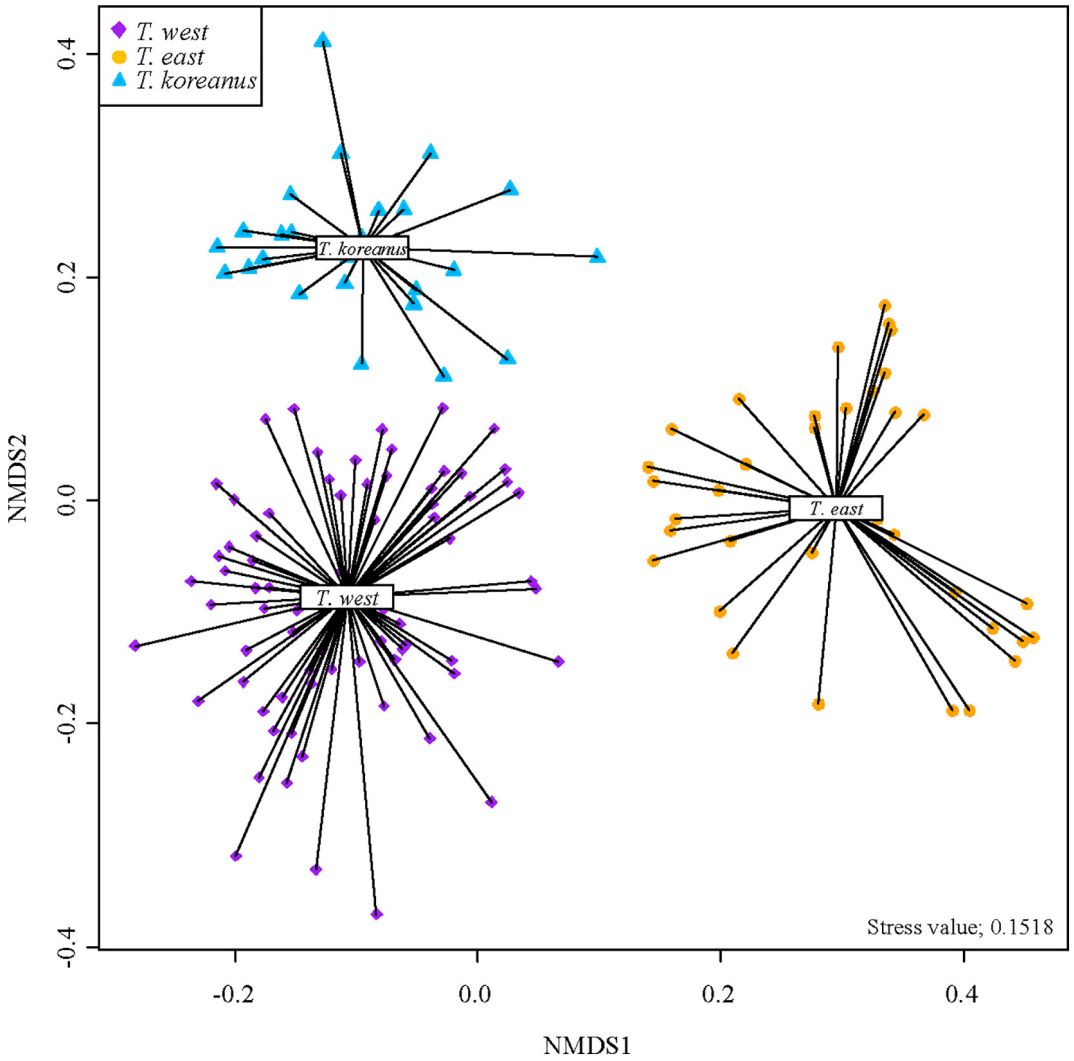

FIGURE 4 | NMDS plot of 138 *Tigriopus* spectra from Hellinger transformed matrix.

distinct differences from the other two species in 22 mass, including 2,950, 3,310−3,312, and 3,287−3,288.

Computing the distance by comparing the mtCO1 partial sequences of three species, the mtCO1 distance between each species is as follows: *T. west*—*T. koreanus* sp. nov.; 0.063 (0.045–0.081), *T. west*—*T. east*; 0.301 (0.261−0.346), *T. east*—*T. koreanus* sp. nov.; 0.341 (0.308−0.379) (**Supplementary Tables 2**, **3**).

Etymology – Species name refers to the type locality (i.e., Republic of Korea).

DISCUSSION

MALDI-TOF MS

There was no difference in raw spectra (**Figure 2A**) when an individual specimen was cut in half by prosome and urosome, processed in separate tubes by body parts. The protein spectra of *Schizopera* sp. (Miraciidae) were also obtained in order to observe spectra variation from species not belonging to *Tigriopus* (**Figure 2F**). The protein spectra of *Schizopera* sp. were significantly different from *Tigriopus* spp. (**Figures 2A–E**).

Figure 5 shows relative difference between peaks when the three species are compared together, and it is sufficient to find the difference between the three Korean species of *Tigriopus*. Until now, various factors which could affect difference in spectra such as fixative solution and storage period after fixation have been investigated (Rossel and Martínez Arbizu, 2018). Usefulness of MALDI-TOF MS in cryptic species identification such as bacteria, mosquitoes, fish and sandflies have also been documented (Müller et al., 2013; Dieme et al., 2014; Paauw et al., 2015; Chavy et al., 2019; Maasz et al., 2020). This study further expands on the usefulness of MALDI-TOF MS, confirming that higher-resolution species identification (identification of cryptic species) is possible for copepods as well.

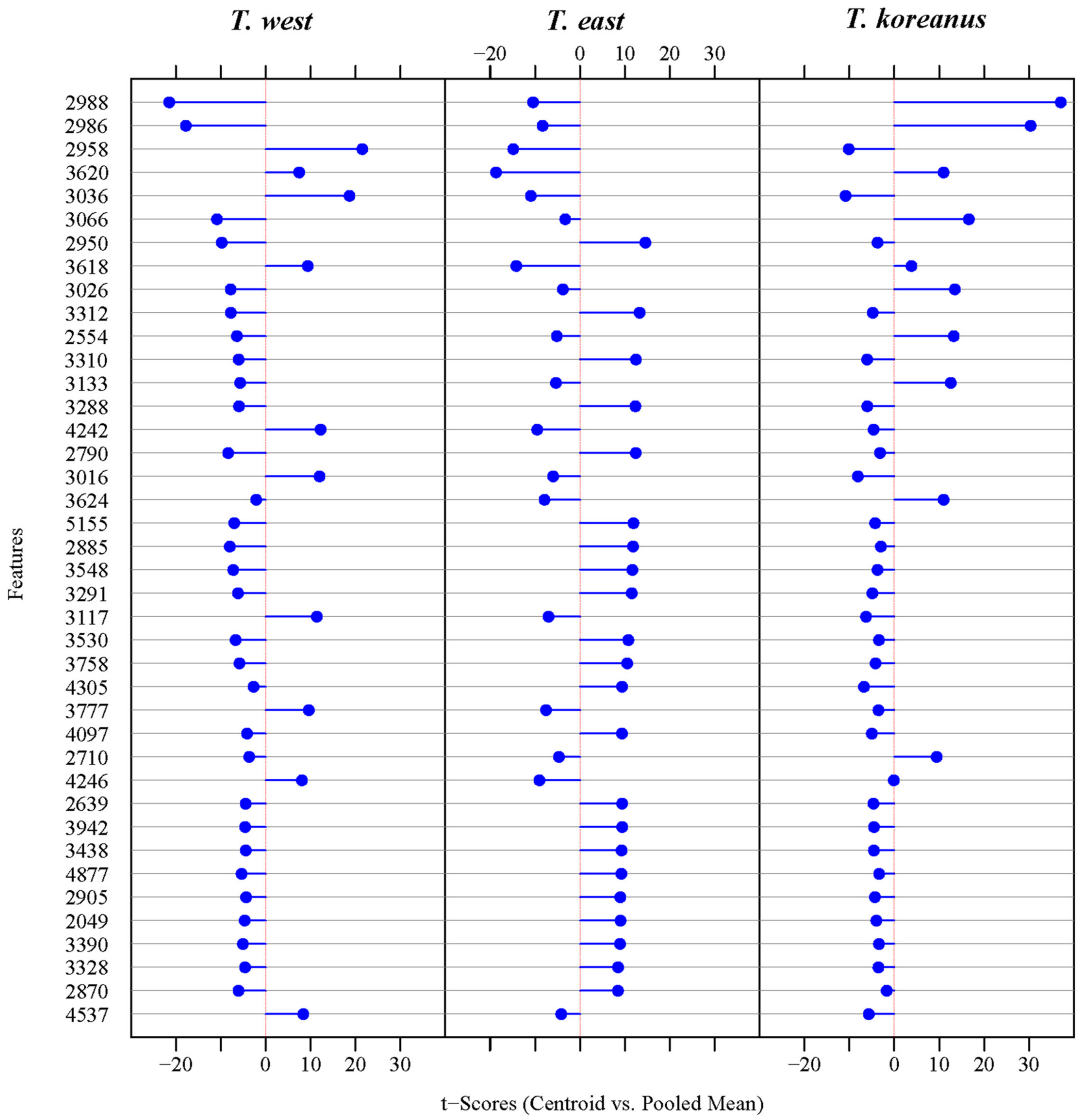

FIGURE 5 | Diagonal discriminant analysis for protein mass. (The 40 Ranking Features).

Despite its ability to identify cryptic species, there are several limitations. First, closely related species have similar protein composition, so the aspects of mass spectra patterns may appear similar. In such case, using only the overall pattern of mass spectra may lead to insignificant results. We expect that increasing the SNR to focus specifically on peaks with strong signal difference help detect cryptic species better. Just as DNA barcoding varies in resolution by different gene markers, and markers are chosen depending on the specific study purpose, parameters such as SNR, halfwindow, minfrequency for MALDI-TOF methodology must be adjusted accordingly.

Secondly, MADLI-TOF MS does not provide insight on the phylogenetic relationships between species. Because this method simply compares the overall protein pattern for species identification, protein molecules, composition, or function is not considered. Granted, if there is a difference in genetic distance, it is reflected on protein composition, resulting in mass spectra difference. However, this does not reflect proportional difference in the genetic distance. As such, to gain insight on phylogenetic relationship whilst discerning species complex, MALDI-TOF MS should be used complementally with DNA barcoding method.

Thirdly, it can be misleading to delimit species solely using MALDI-TOF without any prior knowledge about the species being investigated. In such case, cluster result obtained from the dendrogram may be difficult to interpret, since the number of clusters (or in this case, species) differ depending on the criterion setting of the y-axis. However, since this study presented three pieces of evidence (morphology, molecule, and protein) together, other evidences allowed us to present species classification criterion in MALDI-TOF. What this study can suggest is that Korean species of *Tigriopus* can be classified based on the height

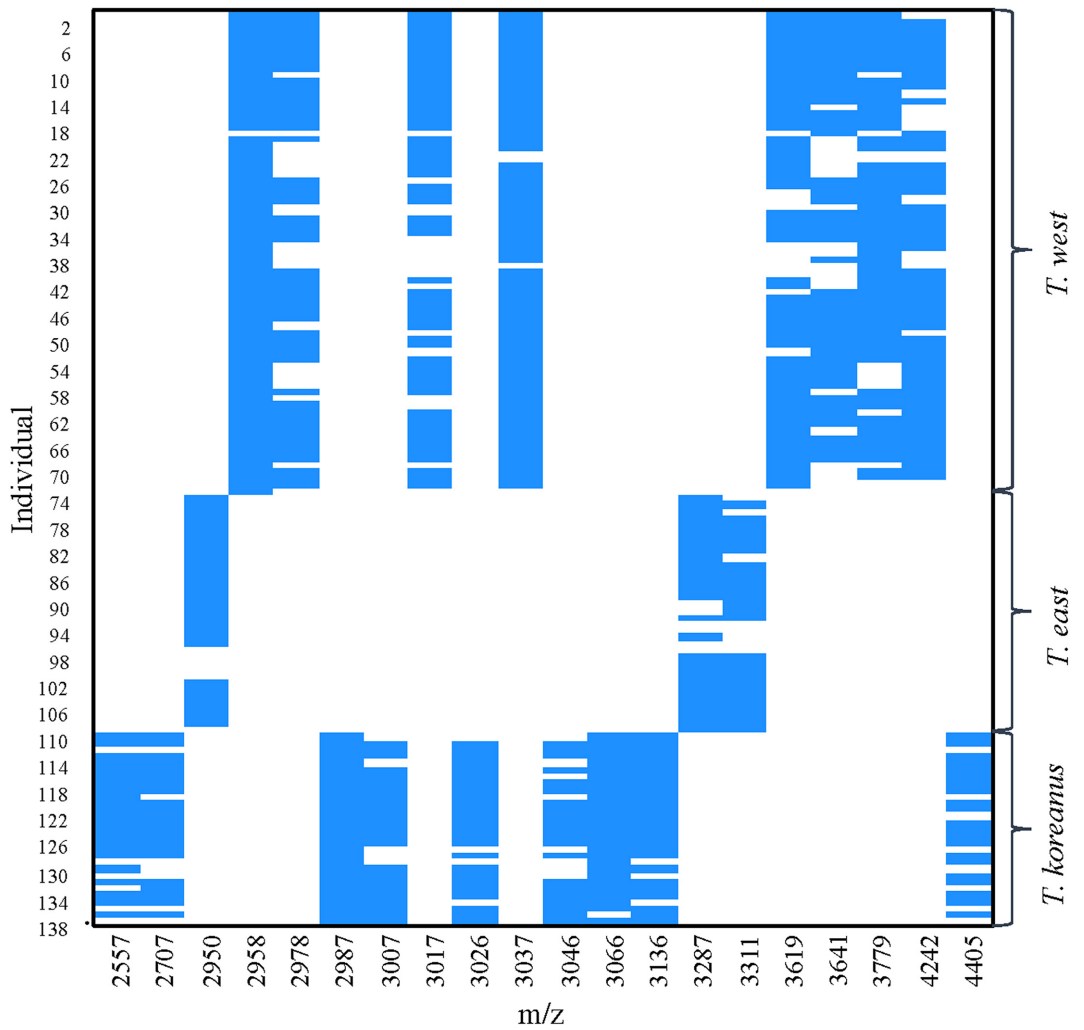

FIGURE 6 | PeakPatterns plot of 138 *Tigriopus* spectra. X-axis; peaks with the highest variation among three *Tigriopus* species, Y-axis; individual numbers were displayed in 4 intervals.

value of 3 in the dendrogram through protein mass comparison. Since criteria vary depending on the taxa, in order to use MALDI-TOF for species identification, a library must be established through further studies dealing with many taxa. To achieve this, role of taxonomists to confirm morphology while building on curated spectra, or molecular data would be essential.

TABLE 2 | Estimates of average evolutionary divergence over sequence pairs within *Tigriopus* species based on mitochondrial cytochrome oxidase I (mtCOI) data.

Species	Distance	S.E.	N	Range
T. east	0.021	0.004	4	0.008–0.027
T. japonicus	0.037	0.007	3	0.016–0.047
T. koreanus	0.019	0.006	2	–
T. west	0.014	0.002	15	0.001–0.026
T. californicus	0.222	0.021	6	0.009–0.349

Finally, MALDI-TOF MS can be affected by other factors, such as environmental factors (Karger et al., 2019; Chac et al., 2020). Karger et al. (2019) suggest that subtle differences within mass spectra can occur depending on habitat type, season, and region. This means environmental factors can directly influence differences in clusters, resulting differentiation of species. To improve the aforementioned limitations, sufficient accumulation of data from various species and habitats is required.

As is the case with other methods, it is still difficult to accurately identify a species with MALDI-TOF MS alone, so it is necessary to accumulate data library by morphological taxonomists, and in the beginning, it will be necessary to verify the species identification through other methods.

MtCOI Distance

Based solely on this result (**Supplementary Table 3**), it could be confirmed that the Busan community differs from the West coast and Jeju communities by about 6%. According to a study

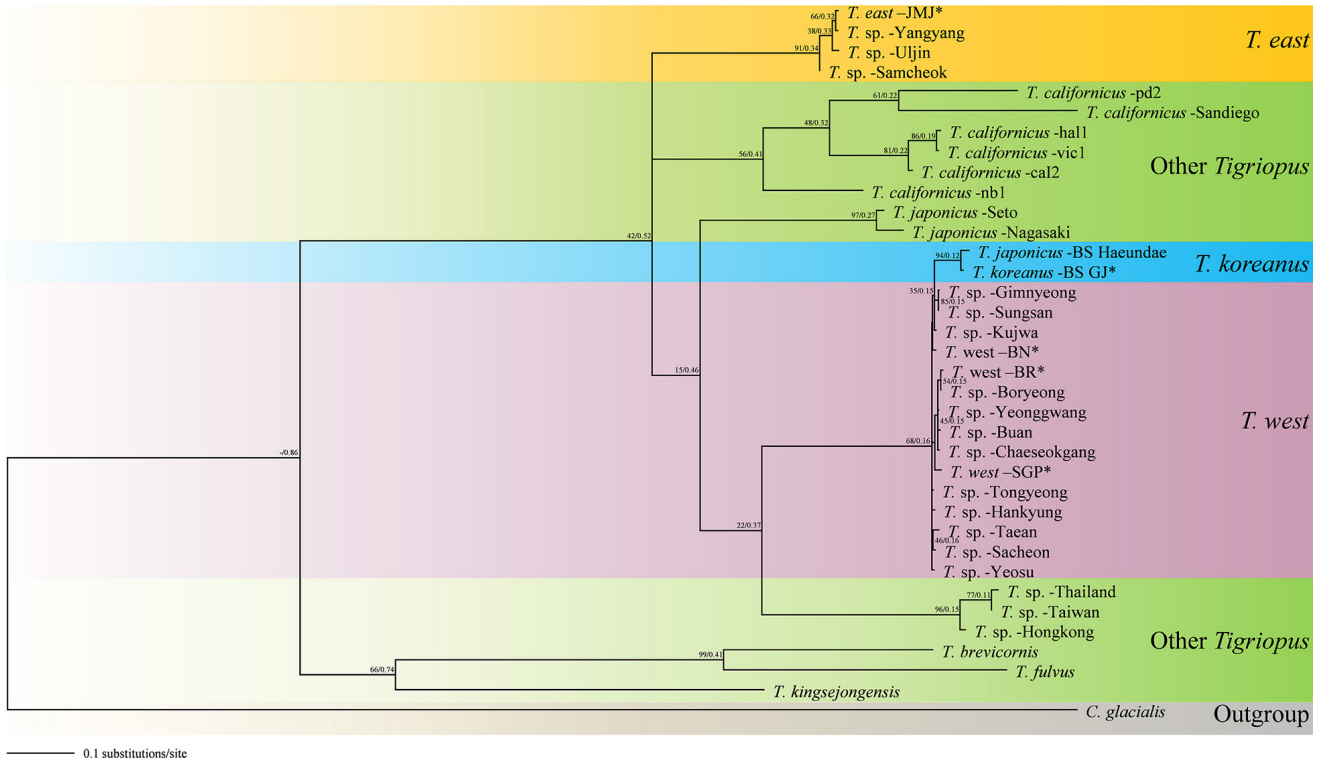

FIGURE 7 | Molecular phylogenetic Maximum Likelihood (ML) and Bayesian Inference (BI) tree of *Tigriopus* species based on 36 mtCOI sequences. All positions containing gaps and missing data were eliminated. The first number along the branches represents ML, the second number represents BI bootstrap values, and * indicates sequence obtained from this study.

on copepod DNA barcoding (Baek et al., 2016), the mean interspecific distance of harpacticoida was 1.6%, which is similar to the results of the three Korean *Tigriopus* species obtained in this study (**Table 2**). Also, in other copepod orders, there were cases where the mtCOI sequences between congeners differed only by 0.26−1.1%. Therefore, the difference of 6% is considered to be one of the supporting evidences for the species classification. As such, it is evident from existing studies, that range of intraspecific and interspecific distance varies for each copepoda order. The fact that the range of distance always vary among taxa is an indication that classification of species using only fragment sequence of one molecular marker is with limitations.

With DNA templates, researchers can obtain sequences of different lengths and locations depending on the primers used. Therefore, distinguishing cryptic species with just mtCOI barcode may prove to be an ambiguous task, and there is a possibility that they will result in the same species, although they are in fact different species. In accordance with this, in several studies (e.g., Huys et al., 2007; Thum and Harrison, 2009; Wyngaard et al., 2010; Blanco-Bercial et al., 2011; Marrone et al., 2013; Vakati et al., 2019) suggest that multigene analyses are required for more accurate results when identifying species through molecular information. Therefore, rather than using only one marker such as mtCOI for species identification, providing protein analysis alongside can strengthen the support for the overall results.

In a previous study, Rossel and Martínez Arbizu (2019) showed that *Leptastacus* cf. *laticaudatus* can be separated through MALDI TOF-MS experiments in three putative cryptic species. The mtCOI distances of the three cryptic species included in this *L.* cf. *laticaudatus* complex ranged from 15.32 to 31.15%. Although mtCOI distance between *T. koreanus* sp. nov. and *T. west* was less (6%) compared to distances reported by Rossel and Martínez Arbizu (2019), results from protein analysis showed that they were indeed different clusters.

Clusters observed from the protein data are different from clusters from phylogenetic trees based on mtCOI data. Therefore, it is difficult to extract evolutionary and systematic relationships based solely from these results. It is also challenging to interpret whether *T. east* and *T. west* clusters are closer to the *T. koreanus* sp. nov. clusters.

It is predicted that the reason that a Jeju individual had a high similarity to Busan community is because Busan and Jeju are relatively closer than other West Sea regions. In the same vein, when comparing the mtCOI data uploaded to the NCBI, there was only 4.5−6.3% difference from the data known as *T. west* on the South Sea coast (Yeosu, Sacheon, Tongyeong) or on the northeast coast of Jeju (Gimnyeong, Seongsan), which are adjacent to Busan.

Although the East sea community is relatively close to Busan in geographic distance, the molecular distance differs as much as the distance from the Japanese species. A probable explanation

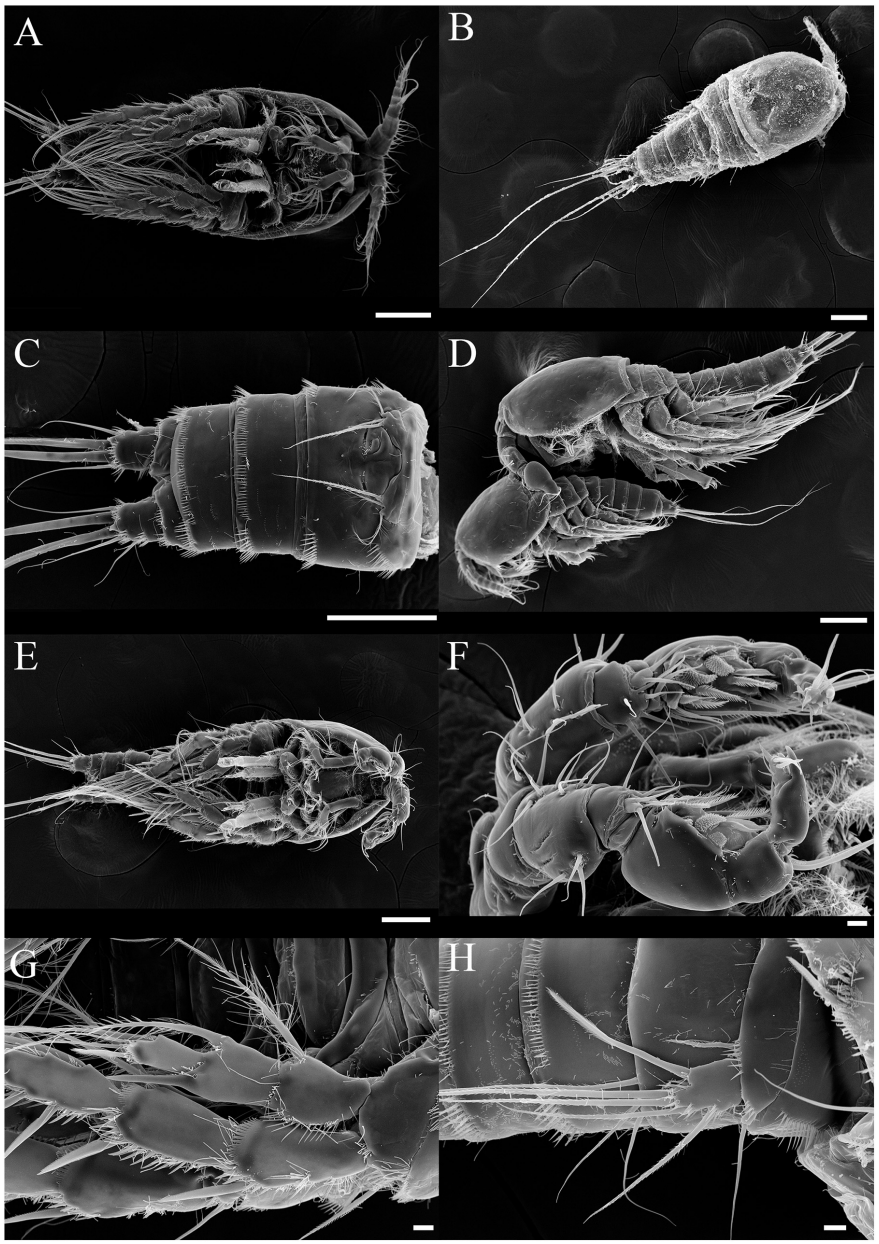

FIGURE 8 | SEM photos of *Tigriopus koreanus* sp. nov. Female **(A–C)**; **(A)** Habitus, ventral. **(B)** Habitus, dorsal. **(C)** Urosome and P6, ventral. **(D)** Precopulatory mate-guarding behavior. Male **(E–H)**; **(E)** Habitus, ventral. **(F)** A1, **(G)** P2, **(H)** P5. **(A–E)**; Scale bars = 100 μm, **(F–H)**; Scale bars = 10 μm.

for this is that *T. east* in the East Sea region have been influenced by the North Korea Cold Current coming from the north, rather than the Kuroshio Current coming from the south. If samples of *Tigriopus* from South Sea coast and North Korea are obtained in the future, it would be possible to verify this hypothesis through protein spectra measurements. In the BI and ML tree (**Figure 7**), the topology supports this hypothesis. Because the origin of *T. east* is different, it appears as a clade different from the species in the region related to the Kuroshio Current.

On the other hand, according to the MP tree (**Supplementary Figure 1**) and NJ tree (**Supplementary Figure 2**), the Korean species form one clade (bootstrap; 23, 67%, respectively). This supports the possibility that individuals originating from the same species by the Kuroshio Current were geographically divided, resulting in speciation. Considering the geological aspect, according to a previous study (Knowlton and Weigt, 1998), it was estimated that millions of years would have passed per 1.5−2.6% of mtCOI mutation rates in crustaceans. According to this result, the estimated timing of speciation of *T. east* and *T. west* from their most recent common ancestor would be between 20 and 11.6 mya (Miocene).

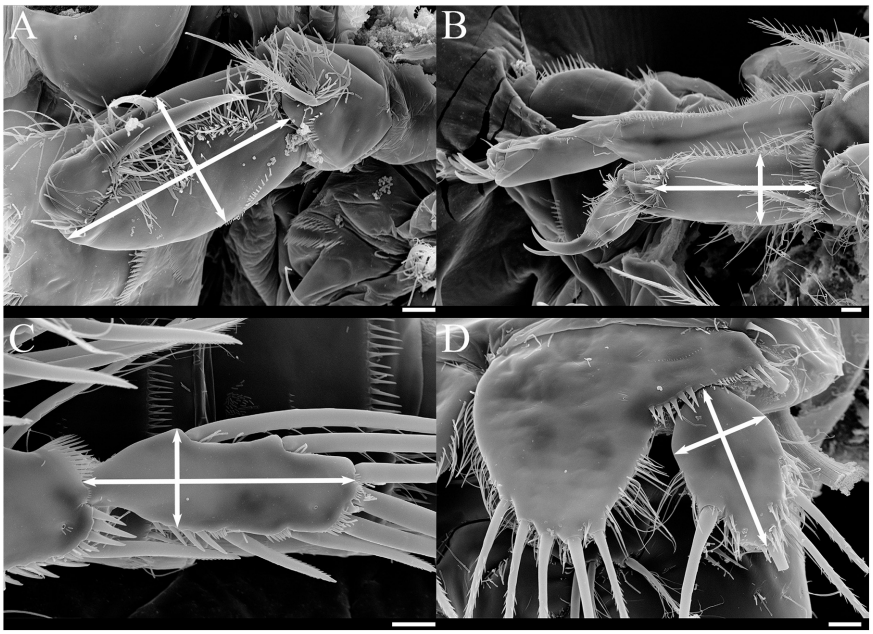

FIGURE 9 | SEM photos of female *Tigriopus koreanus* sp. nov.; Appendages that length/width measured (white arrow lines) for morphological comparison. **(A)** Maxilliped, **(B)** P1, **(C)** P4 exp-3, **(D)** P5 exp. Scale bars = 10 μm.

TABLE 3 | The result of multiple comparison (Bonferroni) for morphological comparisons between Korean *Tigriopus* species.

Dependent variable	(I) species	(J) species	Mean difference (I-J)	Standardization error	*p*-value	95% confidence interval	
						Lower limit	Upper limit
P1 enp-1 l/w	*T. west*	*T. koreanus*	0.39728*	0.08131	0.000	0.1967	0.5978
		T. east	0.19241	0.08131	0.064	−0.0082	0.3930
	T. koreanus	*T. west*	−0.39728*	0.08131	0.000	−0.5978	−0.1967
		T. east	−0.20487*	0.08131	0.044	−0.4054	−0.0043
	T. east	*T. west*	−0.19241	0.08131	0.064	−0.3930	0.0082
		T. koreanus	0.20487*	0.08131	0.044	0.0043	0.4054
Mxp basis l/w	*T. west*	*T. koreanus*	0.16019*	0.03142	0.000	0.0827	0.2377
		T. east	0.02366	0.03142	1.000	−0.0538	0.1012
	T. koreanus	*T. west*	−0.16019*	0.03142	0.000	−0.2377	−0.0827
		T. east	−0.13653*	0.03142	0.000	−0.2140	−0.0590
	T. east	*T. west*	−0.02366	0.03142	1.000	−0.1012	0.0538
		T. koreanus	0.13653*	0.03142	0.000	0.0590	0.2140
P4 exp-3 l/w	*T. west*	*T. koreanus*	−0.10502	0.04822	0.101	−0.2240	0.0139
		T. east	−0.27812*	0.04822	0.000	−0.3971	−0.1592
	T. koreanus	*T. west*	0.10502	0.04822	0.101	−0.0139	0.2240
		T. east	−0.17310*	0.04822	0.002	−0.2921	−0.0541
	T. east	*T. west*	0.27812*	0.04822	0.000	0.1592	0.3971
		T. koreanus	0.17310*	0.04822	0.002	0.0541	0.2921
P5 exp l/w	*T. west*	*T. koreanus*	0.02193	0.03056	1.000	−0.0534	0.0973
		T. east	0.12402*	0.03056	0.000	0.0486	0.1994
	T. koreanus	*T. west*	−0.02193	0.03056	1.000	−0.0973	0.0534
		T. east	0.10209*	0.03056	0.004	0.0267	0.1775
	T. east	*T. west*	−0.12402*	0.03056	0.000	−0.1994	−0.0486
		T. koreanus	−0.10209*	0.03056	0.004	−0.1775	−0.0267

**The mean difference is significant at the 0.05 level.*

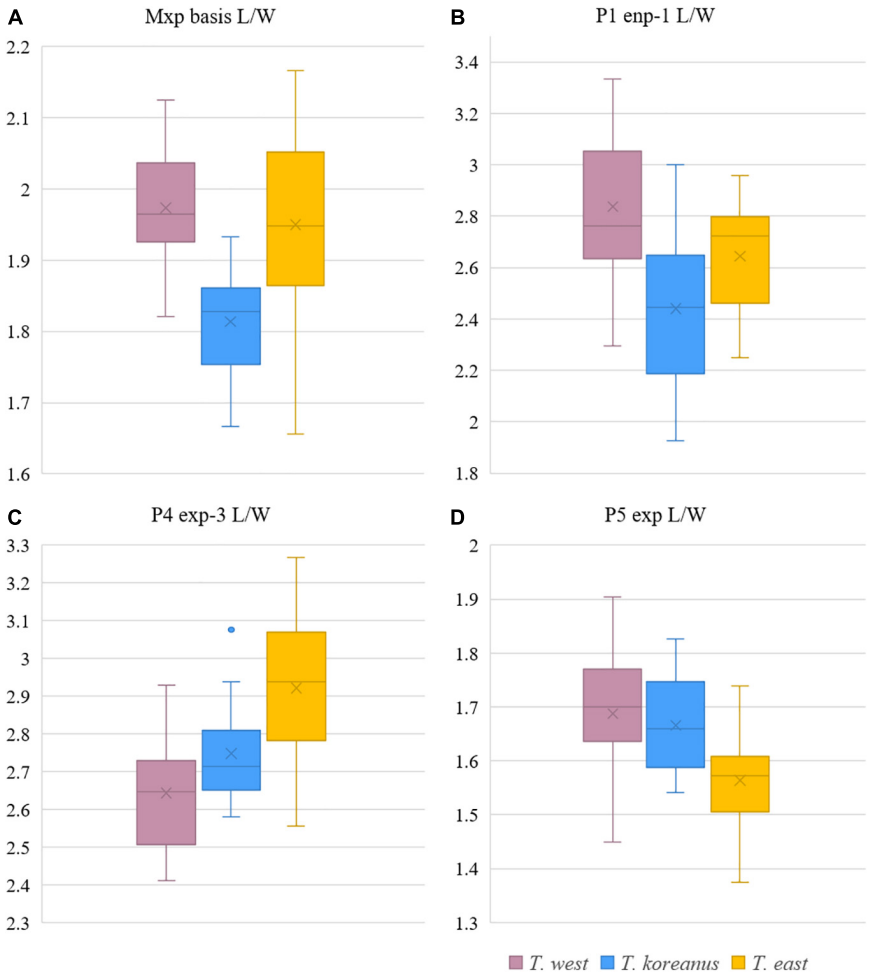

FIGURE 10 | Boxplot of morphological comparisons data between Korean *Tigriopus* species (*n* = 20). **(A)** Mxp basis L/W, **(B)** P1 enp-1 L/W, **(C)** P4 exp-3 L/W, **(D)** P5 exp L/W.

The two trees obtained in this study were similar to the topologies of the trees suggested in previous studies. The topologies of MP tree and NJ tree in this study were similar to that of Karanovic et al. (2018), which also used mtCOI gene marker. In these cases, *T. east* and *T. west* formed the same clade. On the other hand, the topologies of the BI tree and ML tree in this study (**Figure 7**) were similar to those of the BI tree in Ki et al. (2009) and Karanovic et al. (2018). Although the markers used were different in Ki et al. (2009), based on ITS-5.8S rDNA, the topology was corresponding.

As can be seen from different topologies depending on the marker, method, and model, in fact, no one knows what evolutionary histories remain veiled. Naturally, there are only a few hypotheses that we can infer from these results.

However, the second hypothesis is difficult to support since *Tigriopus* is a fast-evolving genus, and Miocene may be too old as time for speciation. Therefore, in this study, topological results of the BI tree and ML tree were deemed more reliable, and we suggest that *T. east* had different origin from *T. koreanus* and *T. west*.

Nevertheless, it is evident that *Tigriopus* species from Busan is different from the previously known *T. west* and *T. east*. The mtCOI barcodes further support that the population of *Tigriopus* inhabiting Korea consists of at least three different species.

Morphology

When comparing the morphological differences, the microscopic morphological features that distinguish the new species and other two species of *Tigriopus* were found in the length-width ratio of the P1 enp-1 and Mxp. Karanovic et al. (2018) found the differences between *T. west* and *T. east* by geometric morphometrics in P4 exp-3, female P5 exp, and male P2 enp. In this study, differences in P4 exp-3 l/w and P5 exp l/w of the two species were also confirmed, but when comparing the P5 exp l/w of the three species together, it was confirmed that it was difficult to clearly distinguish the three species by these morphological features as *T. koreanus* shows overlap, the mid-level characteristics of the other two species.

Geometric morphometrics is a good tool to find significant differences in morphological characteristics, but it requires a lot of time and effort. Therefore, based on the results of this study, we recommend MALDI-TOF MS as a simple and efficient method for species identification rather than these time-consuming methods.

Furthermore, studies that are likely to be conducted in the future should include experiments to confirm the difference between nauplii and copepodites of the species of *Tigriopus*. It would also be meaningful to apply this method to other sibling species complexes such as *T. californicus* (**Table 2**; mtCO1 distance within genus; 0.22, S.E.; 0.02) to clear its convoluted taxonomic status.

CONCLUSION

Various identification tools such as mtCOl barcoding and geometric morphometry were utilized alongside morphological analysis to test the usefulness of MALDI-TOF for the identification of species of *Tigriopus*. Based on our findings, we conclude that identification of cryptic species can be made simpler, faster, and more cost-effective with MALDI-TOF MS than with mtCOI barcoding.

Through MALDI-TOF MS experiments on harpacticoid copepods of *Tigriopus,* we showed that the separation of specimens, fixation, presence of egg sac, and gender did not have a fatal effect on the clustering results. In addition, it was confirmed that the populations of *Tigriopus* from Baengnyeong island, Boryeong, and Jeju are in fact *Tigriopus west*, although there is a considerable geographical difference between Baengnyeong island and Jeju.

Although it has been known as one species for a long time due to the difficulty of morphological distinction even with optical microscopes, results from protein analysis in this study supported that *Tigriopus*, which inhabits rock pools in Korea's coastal intertidal zone, actually consists of three species, and that the Busan population is a third distinct species different from the previously reported two species.

DATA AVAILABILITY STATEMENT

The datasets presented in this study can be found in online repositories. The names of the repository/repositories and accession number(s) can be found below: NCBI (accession: MW429840—MW429844) and **Supplementary Materials**.

AUTHOR CONTRIBUTIONS

JY, NP, and WL designed the study and collected samples. JY and NP carried out measurements, DNA barcoding and analyses of the data. RJ analyzed of the protein data. All authors contributed to the writing of the manuscript.

FUNDING

This research was supported by Basic Science Research Program through the National Research Foundation of Korea (NRF) funded by the Ministry of Education (2018R1D1A1B07050117), the National Institute of Biological Resources (NIBR) funded by the Ministry of Environment of the Republic of Korea (MOE, NIBR202102108), and the National Marine Biodiversity Institute of Korea (2021M01100).

ACKNOWLEDGMENTS

We would like to express our sincere gratitude to Prof. Jinwon Lee and Ms. Yourae Kim for providing technical support to obtain the protein mass spectra. Also, we would like to express our deep appreciation to Dr. Seunghan Lee for his helpful information regarding *Tigriopus* culture and molecular experiments.

SUPPLEMENTARY MATERIAL

The Supplementary Material for this article can be found online at: https://www.frontiersin.org/articles/10.3389/fmars.2021.648197/full#supplementary-material

Supplementary Figure 1 | Molecular phylogenetic Maximum parsimony (MP) tree of *Tigriopus* species based on 36 mtCOI sequences. All positions containing gaps and missing data were eliminated. The number along the branches represents bootstrap values, and "*" indicates sequence obtained from this study.

Supplementary Figure 2 | Molecular phylogenetic Neighbor-Joining (NJ) tree of *Tigriopus* species based on 36 mtCOI sequences. All positions containing gaps and missing data were eliminated. The number along the branches represents bootstrap values, and "*" indicates sequence obtained from this study.

Supplementary Table 1 | GenBank numbers of mtCOI sequences used in phylogenetic analyses in this study.

Supplementary Table 2 | Estimates of evolutionary divergence between mtCOI sequences of *Tigriopus* species.

Supplementary Table 3 | Between *Tigriopus* species distance and S.E. (blue text).

Supplementary Table 4 | Length and width measurement data of appendages of *Tigriopus* species (μm).

REFERENCES

Ahdesmäki, M., and Strimmer, K. (2010). Feature selection in omics prediction problems using cat scores and false nondiscovery rate control. *Ann. Appl. Statist.* 4, 503–519.

Baek, S., Jang, K., Choi, E., Ryu, S., Kim, S., Lee, J., et al. (2016). DNA Barcoding of Metazoan Zooplankton Copepods from South Korea. *PLoS One* 11:e0157307. doi: 10.1371/journal.pone.0157307

Barreto, F. S., Watson, E. T., Lima, T. G., Willett, C. S., Edmands, S., Li, W., et al. (2018). Genomic signatures of mitonuclear coevolution across populations of

Tigriopus californicus. *Nat. Ecol. Evolut.* 2, 1250–1257. doi: 10.1038/s41559-018-0588-1

Baumeister, T. U. H., Vallet, M., Kaftan, F., Guillou, L., Svatoš, A., and Pohnert, G. (2020). Identification to species level of live single microalgal cells from plankton samples with matrix-free laser/desorption ionization mass spectrometry. *Metabolomics* 16, 1–10.

Blanco-Bercial, L., Bradford-Grieve, J., and Bucklin, A. (2011). Molecular phylogeny of the Calanoida (Crustacea: Copepoda). *Mol. Phylogenet. Evolut.* 59, 103–113. doi: 10.1016/j.ympev.2011.01.008

Bode, M., Laakmann, S., Kaiser, P., Hagen, W., Auel, H., and Cornils, A. (2017). Unravelling diversity of deep-sea copepods using integrated morphological and molecular techniques. *J. Plankton Res.* 39, 600–617. doi: 10.1093/plankt/fbx031

Bucklin, A., Ortman, B. D., Jennings, R. M., Nigro, L. M., Sweetman, C. J., Copley, N. J., et al. (2010). A "Rosetta Stone" for metazoan zooplankton: DNA barcode analysis of species diversity of the Sargasso Sea (Northwest Atlantic Ocean). *Deep Sea Res. Part II Topic. Stud. Oceanogr.* 57, 2234–2247. doi: 10.1016/j.dsr2.2010.09.025

Chac, D., Kordahi, M., Brettner, L., Verma, A., McCleary, P., Crebs, K., et al. (2020). Proteomic changes in bacteria caused by exposure to environmental conditions can be detected by Matrix-Assisted Laser Desorption/Ionization–Time of Flight (MALDI-ToF) Mass Spectrometry. *bioRxiv* 918938. [preprint].

Chalupová, J., Raus, M., Sedlářová, M., and Šebela, M. (2014). Identification of fungal microorganisms by MALDI-TOF mass spectrometry. *Biotechnol. Adv.* 32, 230–241. doi: 10.1016/j.biotechadv.2013.11.002

Chavy, A., Nabet, C., Normand, A. C., Kocher, A., Ginouves, M., Prévot, G., et al. (2019). Identification of French Guiana sand flies using MALDI-TOF mass spectrometry with a new mass spectra library. *PLoS Neglec. Trop. Dis.* 13:e0007031. doi: 10.1371/journal.pntd.0007031

Clarke, K. R. (1993). Non-parametric multivariate analyses of changes in community structure. *Austral. J. Ecol.* 18, 117–143. doi: 10.1111/j.1442-9993.1993.tb00438.x

Claydon, M. A., Davey, S. N., Edwards-Jones, V., and Gordon, D. B. (1996). The rapid identification of intact microorganisms using mass spectrometry. *Nat. Biotechnol.* 14, 1584–1586. doi: 10.1038/nbt1196-1584

Darriba, D., Taboada, G. L., Doallo, R., and Posada, D. (2012). jModelTest 2: more models, new heuristics and parallel computing. *Nat. Methods* 9, 772–772. doi: 10.1038/nmeth.2109

Dieme, C., Yssouf, A., Vega-Rúa, A., Berenger, J.-M., Failloux, A.-B., Raoult, D., et al. (2014). Accurate identification of Culicidae at aquatic developmental stages by MALDI-TOF MS profiling. *Parasites Vectors* 7, 1–14.

Feltens, R., Görner, R., Kalkhof, S., Gröger-Arndt, H., and von Bergen, M. (2010). Discrimination of different species from the genus *Drosophila* by intact protein profiling using matrix-assisted laser desorption ionization mass spectrometry. *BMC Evolution. Biol.* 10:95. doi: 10.1186/1471-2148-10-95

Fenselau, C., and Demirev, P. A. (2001). Characterization of intact microorganisms by MALDI mass spectrometry. *Mass Spectrometry Rev.* 20, 157–171. doi: 10.1002/mas.10004

Gibb, S. (2015). *MALDIquantForeign: Import/Export routines for MALDIquant*. Vienna: R Core Team.

Gibb, S., and Strimmer, K. (2012). MALDIquant: a versatile R package for the analysis of mass spectrometry data. *Bioinformatics* 28, 2270–2271. doi: 10.1093/bioinformatics/bts447

Hillenkamp, F., Karas, M., Beavis, R. C., and Chait, B. T. (1991). Matrix-assisted laser desorption/ionization mass spectrometry of biopolymers. *Analyt. Chem.* 63, 1193–1203.

Huys, R., Gee, J. M., Moore, C. G., and Hamond, R. (1996). *Marine and brackish water harpacticoid copepods*. London: Published for the Linnean Society of London and the Estuarine and Coastal Sciences Association.

Huys, R., Llewellyn-Hughes, J., Conroy-Dalton, S., Olson, P. D., Spinks, J. N., and Johnston, D. A. (2007). Extraordinary host switching in siphonostomatoid copepods and the demise of the Monstrilloida: integrating molecular data, ontogeny and antennulary morphology. *Mol. Phylogenet. Evolut.* 43, 368–378. doi: 10.1016/j.ympev.2007.02.004

Jung, S., Lee, Y., Park, T., Park, H., Hagiwara, A., Leung, K. M. Y., et al. (2006). The complete mitochondrial genome of the intertidal copepod *Tigriopus* sp. (Copepoda, Harpactidae) from Korea and phylogenetic considerations. *J. Exp. Mar. Biol. Ecol.* 333, 251–262. doi: 10.1016/j.jembe.2005.12.047

Karanovic, T., Lee, S., and Lee, W. (2018). Instant taxonomy: choosing adequate characters for species delimitation and description through congruence between molecular data and quantitative shape analysis. *Invertebrate Systemat.* 32, 551–580. doi: 10.1071/is17002

Karger, A., Bettin, B., Gethmann, J. M., and Klaus, C. (2019). Whole animal matrix-assisted laser desorption/ionization time-of-flight (MALDI-TOF) mass spectrometry of ticks–Are spectra of *Ixodes ricinus* nymphs influenced by environmental, spatial, and temporal factors? *PLoS One* 14:e0210590. doi: 10.1371/journal.pone.0210590

Ki, J., Lee, K., Park, H., Chullasorn, S., Dahms, H.-U., and Lee, J. (2009). Phylogeography of the copepod *Tigriopus japonicus* along the Northwest Pacific rim. *J. Plankton Res.* 31, 209–221. doi: 10.1093/plankt/fbn100

Kimura, M. (1980). A simple method for estimating evolutionary rates of base substitutions through comparative studies of nucleotide sequences. *J. Mol. Evolut.* 16, 111–120. doi: 10.1007/bf01731581

Knowlton, N., and Weigt, L. A. (1998). New dates and new rates for divergence across the Isthmus of Panama. *Proc. R. Soc. London Ser. B Biol. Sci.* 265, 2257–2263. doi: 10.1098/rspb.1998.0568

Kumar, S., Stecher, G., and Tamura, K. (2016). MEGA7: molecular evolutionary genetics analysis version 7.0 for bigger datasets. *Mol. Biol. Evolut.* 33, 1870–1874. doi: 10.1093/molbev/msw054

Kwok, K. W. H., and Leung, K. M. Y. (2005). Toxicity of antifouling biocides to the intertidal harpacticoid copepod *Tigriopus japonicus* (Crustacea, Copepoda): effects of temperature and salinity. *Mar. Pollut. Bull.* 51, 830–837. doi: 10.1016/j.marpolbul.2005.02.036

Laakmann, S., Gerdts, G., Erler, R., Knebelsberger, T., Martínez Arbizu, P., and Raupach, M. J. (2013). Comparison of molecular species identification for North Sea calanoid copepods (Crustacea) using proteome fingerprints and DNA sequences. *Mol. Ecol. Resour.* 13, 862–876. doi: 10.1111/1755-0998.12139

Maasz, G., Zrínyi, Z., Fodor, I., Boross, N., Vitál, Z., Kánainé Sipos, D. I., et al. (2020). Testing the Applicability of MALDI-TOF MS as an Alternative Stock Identification Method in a Cryptic Species Complex. *Molecules* 25:3214. doi: 10.3390/molecules25143214

Maier, T., Klepel, S., Renner, U., and Kostrzewa, M. (2006). Fast and reliable maldi-tof ms–based microorganism identification. *Nat. Methods* 3, i–ii.

Marrone, F., Brutto, S. L., Hundsdoerfer, A. K., and Arculeo, M. (2013). Overlooked cryptic endemism in copepods: systematics and natural history of the calanoid subgenus *Occidodiaptomus Borutzky* 1991 (Copepoda, Calanoida, Diaptomidae). *Mol. Phylogenet. Evolut.* 66, 190–202. doi: 10.1016/j.ympev.2012.09.016

Müller, P., Pflüger, V., Wittwer, M., Ziegler, D., Chandre, F., Simard, F., et al. (2013). Identification of cryptic *Anopheles* mosquito species by molecular protein profiling. *PLoS One* 8:e57486. doi: 10.1371/journal.pone.0057486

Nei, M., and Kumar, S. (2000). *Molecular evolution and phylogenetics*. Oxford: Oxford university press.

Oksanen, J., Blanchet, F. G., Friendly, M., Kindt, R., Legendre, P., McGlinn, D., et al. (2018). *vegan: Community Ecology Package. R package version 2.5-2. 2018*. Vienna: R Core Team.

Paauw, A., Jonker, D., Roeselers, G., Heng, J. M., Mars-Groenendijk, R. H., Trip, H., et al. (2015). Rapid and reliable discrimination between *Shigella* species and *Escherichia coli* using MALDI-TOF mass spectrometry. *Int. J. Medical Microbiol.* 305, 446–452. doi: 10.1016/j.ijmm.2015.04.001

Palarea-Albaladejo, J., McLean, K., Wright, F., and Smith, D. G. E. (2018). MALDIrppa: quality control and robust analysis for mass spectrometry data. *Bioinformatics* 34, 522–523. doi: 10.1093/bioinformatics/btx628

Peterson, D. L., Kubow, K. B., Connolly, M. J., Kaplan, L. R., Wetkowski, M. M., Leong, W., et al. (2013). Reproductive and phylogenetic divergence of tidepool copepod populations across a narrow geographical boundary in Baja California. *J. Biogeogr.* 40, 1664–1675. doi: 10.1111/jbi.12107

Riccardi, N., Lucini, L., Benagli, C., Welker, M., Wicht, B., and Tonolla, M. (2012). Potential of matrix-assisted laser desorption/ionization time-of-flight mass spectrometry (MALDI-TOF MS) for the identification of freshwater zooplankton: a pilot study with three *Eudiaptomus* (Copepoda: Diaptomidae) species. *J. Plankton Res.* 34, 484–492. doi: 10.1093/plankt/fbs022

Ronquist, F., Teslenko, M., Van Der Mark, P., Ayres, D. L., Darling, A., Höhna, S., et al. (2012). MrBayes 3.2: efficient Bayesian phylogenetic inference and

model choice across a large model space. *Systemat. Biol.* 61, 539–542. doi: 10.1093/sysbio/sys029

Rossel, S., and Martínez Arbizu, P. (2018). Effects of sample fixation on specimen identification in biodiversity assemblies based on proteomic data (MALDI-TOF). *Front. Mar. Sci.* 5:149. doi: 10.3389/fmars.2018.00149

Rossel, S., and Martínez Arbizu, P. (2019). Revealing higher than expected diversity of Harpacticoida (Crustacea: Copepoda) in the North Sea using MALDI-TOF MS and molecular barcoding. *Sci. Rep.* 9, 1–14.

Rossel, S., Khodami, S., and Martinez Arbizu, P. (2019). Comparison of rapid biodiversity assessment of meiobenthos using MALDI-TOF MS and Metabarcoding. *Front. Mar. Sci.* 6:659. doi: 10.3389/fmars.2019.00659

Seng, P., Rolain, J.-M., Fournier, P. E., La Scola, B., Drancourt, M., and Raoult, D. (2010). MALDI-TOF-mass spectrometry applications in clinical microbiology. *Future Microbiol.* 5, 1733–1754.

Shao, M., and Bi, H. (2020). Direct identification of fish species by surface molecular transferring. *Analyst* 145, 4055–4374.

Shively, S., and Miller, W. R. (2009). The use of HMDS (hexamethyldisilazane) to replace critical point drying (CPD) in the preparation of tardigrades for SEM (scanning electron microscope) imaging. *Transact. Kansas Acad. Sci.* 112, 198–200. doi: 10.1660/062.112.0407

Singhal, N., Kumar, M., Kanaujia, P. K., and Virdi, J. S. (2015). MALDI-TOF mass spectrometry: an emerging technology for microbial identification and diagnosis. *Front. Microbiol.* 6:791. doi: 10.3389/fmicb.2015.00791

Suzuki, R., and Shimodaira, H. (2006). Pvclust: an R package for assessing the uncertainty in hierarchical clustering. *Bioinformatics* 22, 1540–1542. doi: 10.1093/bioinformatics/btl117

Thompson, J. D., Higgins, D. G., and Gibson, T. J. (1994). CLUSTAL W: improving the sensitivity of progressive multiple sequence alignment through sequence weighting, position-specific gap penalties and weight matrix choice. *Nucleic Acids Res.* 22, 4673–4680. doi: 10.1093/nar/22.22.4673

Thum, R. A., and Harrison, R. G. (2009). Deep genetic divergences among morphologically similar and parapatric *Skistodiaptomus* (Copepoda: Calanoida: Diaptomidae) challenge the hypothesis of Pleistocene speciation. *Biol. J. Linnean Soc.* 96, 150–165. doi: 10.1111/j.1095-8312.2008.01105.x

Tsuboko-Ishii, S., and Burton, R. S. (2018). Individual culturing of *Tigriopus* copepods and quantitative analysis of their mate-guarding behavior. *J. Visualiz. Exp.* 139:e58378.

Vakati, V., Eyun, S., and Lee, W. (2019). Unraveling the intricate biodiversity of the benthic harpacticoid genus *Nannopus* (Copepoda, Harpacticoida, Nannopodidae) in Korean waters. *Mol. Phylogenet. Evolut.* 130, 366–379. doi: 10.1016/j.ympev.2018.10.004

Volta, P., Riccardi, N., Lauceri, R., and Tonolla, M. (2012). Discrimination of freshwater fish species by matrix-assisted laser desorption/ionization-time of flight mass spectrometry (MALDI-TOF MS): a pilot study. *J. Limnol.* 71:e17.

Williams, B. D., Schrank, B., Huynh, C., Shownkeen, R., and Waterston, R. H. (1992). A genetic mapping system in *Caenorhabditis elegans* based on polymorphic sequence-tagged sites. *Genetics* 131, 609–624. doi: 10.1093/genetics/131.3.609

Wyngaard, G. A., Hołyńska, M., and Schulte, J. A. II (2010). Phylogeny of the freshwater copepod *Mesocyclops* (Crustacea: Cyclopidae) based on combined molecular and morphological data, with notes on biogeography. *Mol. Phylogenet. Evolut.* 55, 753–764. doi: 10.1016/j.ympev.2010.02.029

Conflict of Interest: The authors declare that the research was conducted in the absence of any commercial or financial relationships that could be construed as a potential conflict of interest.

frontiers in Marine Science

ORIGINAL RESEARCH
published: 11 May 2021
doi: 10.3389/fmars.2021.654141

Musical Chairs on Temperate Reefs: Species Turnover and Replacement Within Functional Groups Explain Regional Diversity Variation in Assemblages Associated With Honeycomb Worms

Alexandre Muller[1†], Camille Poitrimol[1,2†], Flávia L. D. Nunes[1†], Aurélien Boyé[1†], Amelia Curd[1†], Nicolas Desroy[3†], Louise B. Firth[4†], Laura Bush[5], Andrew J. Davies[6†], Fernando P. Lima[7†], Martin P. Marzloff[1†], Claudia Meneghesso[7,8†], Rui Seabra[7†] and Stanislas F. Dubois[1†]*

[1] Ifremer, Centre de Bretagne, DYNECO, Laboratory of Coastal Benthic Ecology, Plouzané, France, [2] Sorbonne Université, Station Biologique de Roscoff, UMR 7144, Adaptation et Diversité en Milieu Marin, Roscoff, France, [3] Ifremer, Laboratoire Environnement et Ressources Bretagne Nord, Dinard, France, [4] School of Biological and Marine Sciences, University of Plymouth, Plymouth, United Kingdom, [5] FUGRO GB Marine Limited, Heriot-Watt University, Edinburgh, United Kingdom, [6] Department of Biological Sciences, University of Rhode Island, Kingston, RI, United States, [7] CIBIO-InBIO, Centro de Investigação em Biodiversidade e Recursos Genéticos, Universidade do Porto, Vairão, Portugal, [8] Departamento de Biologia, Faculdade de Ciências da Universidade do Porto, Porto, Portugal

Reef-building species are recognized as having an important ecological role and as generally enhancing the diversity of benthic organisms in marine habitats. However, although these ecosystem engineers have a facilitating role for some species, they may exclude or compete with others. The honeycomb worm *Sabellaria alveolata* (Linnaeus, 1767) is an important foundation species, commonly found from northwest Ireland to northern Mauritania, whose reef structures increase the physical complexity of the marine benthos, supporting high levels of biodiversity. Local patterns and regional differences in taxonomic and functional diversity were examined in honeycomb worm reefs from 10 sites along the northeastern Atlantic to explore variation in diversity across biogeographic regions and the potential effects of environmental drivers. While taxonomic composition varied across the study sites, levels of diversity remained relatively constant along the European coast. Assemblages showed high levels of species turnover compared to differences in richness, which varied primarily in response to sea surface temperatures and sediment content, the latter suggesting that local characteristics of the reef had a greater effect on community composition than the density of the engineering species. In contrast, the functional composition of assemblages was similar regardless of taxonomic composition or biogeography, with five functional groups being observed in all sites and only small differences in abundance in these groups being detected. Functional groups represented primarily filter-feeders and deposit-feeders, with the notable absence of herbivores, indicating that

OPEN ACCESS

Edited by:
Carlos Navarro Barranco, Autonomous University of Madrid, Spain

Reviewed by:
Cristián E. Hernández, University of Concepcion, Chile
James Davis Reimer, University of the Ryukyus, Japan

***Correspondence:**
Stanislas F. Dubois
sdubois@ifremer.fr

†ORCID:
Alexandre Muller
orcid.org/0000-0002-5495-2862
Camille Poitrimol
orcid.org/0000-0002-0878-1855
Flávia L. D. Nunes
orcid.org/0000-0002-3947-6634
Aurélien Boyé
orcid.org/0000-0002-5692-7660
Amelia Curd
orcid.org/0000-0003-3260-7192
Nicolas Desroy
orcid.org/0000-0002-9047-5637
Louise B. Firth
orcid.org/0000-0002-6620-8512
Andrew J. Davies
orcid.org/0000-0002-2087-0885
Fernando P. Lima
orcid.org/0000-0001-9575-9834
Martin P. Marzloff
orcid.org/0000-0002-8152-4273
Claudia Meneghesso
orcid.org/0000-0003-0144-022X
Rui Seabra
orcid.org/0000-0002-0240-3992
Stanislas F. Dubois
orcid.org/0000-0002-3326-4892

Specialty section:
This article was submitted to Marine Evolutionary Biology, Biogeography and Species Diversity, a section of the journal Frontiers in Marine Science

Received: *15 January 2021*
Accepted: *29 March 2021*
Published: *11 May 2021*

the reefs may act as biological filters for some species from the local pool of organisms. Redundancy was observed within functional groups that may indicate that honeycomb worm reefs can offer similar niche properties to its associated assemblages across varying environmental conditions. These results highlight the advantages of comparing taxonomic and functional metrics, which allow identification of a number of ecological processes that structure marine communities.

Keywords: biodiversity, taxonomic diversity, functional diversity, ecosystem engineer, reef, turnover

INTRODUCTION

Unraveling the processes that control how biodiversity is distributed over space and time are central objectives in macroecology and biogeography (Addo-Bediako et al., 2000; Ricklefs, 2004). While biodiversity was first observed to increase from the poles toward the tropics over 200 years ago (Hawkins, 2001), it is now recognized that latitude *per se* is not the main driver of spatial gradients in biodiversity, but rather a combination of variables and mechanisms that include ecological, evolutionary and historical processes (Hawkins and Diniz-Filho, 2004; D'Amen et al., 2017). For example, the rates of species diversification are thought to be greater in the tropics due to higher mutation rates in warmer regions (Rohde, 1992; Mittelbach et al., 2007). In addition, regions that have greater environmental stability over time may also host higher species diversity than areas that have suffered major environmental change, such as glaciations (Fine, 2015; but see also Fordham et al., 2019). Other variables shown to influence biodiversity include habitat or organism types, and organism properties, such as biomass, dispersal rates and physiology (Addo-Bediako et al., 2000; Hillebrand, 2004; Buckley et al., 2010; Rolland et al., 2015; Gaucherel et al., 2018). Given the multitude of factors that can affect diversity, understanding and predicting spatial and temporal patterns in biodiversity is challenging.

An important factor that influences biodiversity is whether a community is found on geogenic (of geological origin: sedimentary or rocky) or biogenic (of biological origin) substrate. Many communities co-exist in habitats that are altered by another living organism, and these are called foundation species or ecosystem engineers. Foundation species not only build habitat (Dayton, 1972) but also control the availability of resources for other organisms (Sarà, 1986; Jones et al., 1994). Through habitat modification, foundation species can alter the realized niche of species, at times facilitating niche expansion by buffering environmental conditions so that they continue to be favorable within the engineered habitat (Bulleri et al., 2016). Heterogeneity in the engineered habitat can promote facilitation of a greater number of species, while dominance of the engineering species or homogeneity in the habitat can enhance competition and limit the number of associated taxa (Schöb et al., 2012; Bulleri et al., 2016). Given that community composition can vary greatly within biogenic habitats across environmental gradients (Boström et al., 2006; Boyé et al., 2017), investigating within-habitat diversity is essential for guiding conservation actions (Airoldi et al., 2008) and enhances our understanding of biodiversity over broad geographical scales.

Although the northeast Atlantic is amongst the most studied marine regions on Earth (Hawkins et al., 2019), spatial structure in its coastal marine assemblages remains poorly understood. Variation in diversity over broad spatial scales may be related to species distributions, but even broad biogeographic delimitations continue to be contentious. For example, broadly accepted marine biogeographic frameworks consider two biogeographic provinces in the northeastern Atlantic: Boreal and Lusitanian (Briggs and Bowen, 2012), or Northern European Seas and Lusitania (Spalding et al., 2007), separated by "Forbes' Line" (*sensu* Firth et al., 2021, after Forbes and Godwin-Austen, 1859). They differ, however, on boundary positions between provinces, and whether or not the southern province includes the Mediterranean Sea. Further biogeographic subdivision has been proposed for the northeastern Atlantic such that four provinces could be recognized: Boreal, Boreal-Lusitanian, Lusitanian-Boreal, and Lusitanian (Dinter, 2001), but these finer-scale subdivisions are less often considered or employed in macroecology. Lack of consensus on biogeographic delimitations are partially due to competing criteria used for setting boundaries but may also reflect incomplete distributional knowledge of many marine species, especially for poorly studied invertebrates. If the majority of species have restricted distributions, then species turnover might be expected to be higher over a given spatial scale. Community structure may therefore be related to some extent to biogeographic partitioning, such that communities may be more similar within rather than between biogeographic regions.

To examine diversity in marine ecosystems, it is important to consider how diversity is quantified and described. Biodiversity is a multifaceted concept that includes several components (Whittaker, 1972). In order to better understand what mechanisms influence biodiversity, it may be helpful to consider each of these different facets. While local patterns in diversity (α diversity; Whittaker, 1972) are most commonly assessed, regional differences in diversity due to variation in richness or species composition (β diversity; Whittaker, 1972; Airoldi et al., 2008) can also provide important insights into the mechanisms driving community structure (Hewitt et al., 2005; Anderson et al., 2011; Villéger et al., 2013). Focusing on β diversity is especially important in the context of global change, where ecological communities are subject to large environmental fluctuations and disturbances (Mori et al., 2018). Furthermore, it is now widely recognized that the integration of functional information based on species traits provides a better understanding of

community functioning (Díaz and Cabido, 2001; Anderson et al., 2011; Pavoine and Bonsall, 2011; Münkemüller et al., 2012; Mouillot et al., 2014). Thus, comparing taxonomic with functional diversity (α and β) provides a better understanding of the ecological processes that shape community composition (Swenson et al., 2011; Villéger et al., 2013; Mori et al., 2018) and the impact of biodiversity loss on ecosystem functioning (Cadotte et al., 2011; Burley et al., 2016). For example, selective processes, such as environmental filtering, lead to homogenization of traits in communities, since only species with a specific set of traits could survive and develop under certain abiotic conditions. As a result, the loss of species with unique functional characteristics may have significant consequences for ecosystem functioning than the loss of species with characteristics that are more commonly expressed in the community (O'Connor and Crowe, 2005; Queirós et al., 2013). Nevertheless, the comparison of taxonomic and functional β diversity alone may not reveal the underlying ecological processes that structure communities (Baselga, 2010; Villéger et al., 2013; Legendre, 2014). This is in part because variation in species composition among sites (β diversity) is the resultant of two components: species turnover (i.e., replacement of species or functional strategies) and nestedness (i.e., dissimilarity associated with the loss of species or functional strategies, in which an assemblage is a strict subset of another). Partitioning β diversity into turnover and nestedness thus provides an additional facet for dissecting community assembly rules. In sum, a combination of tools and metrics, including taxonomic and functional α and β diversity (and their components) are essential for better understanding biodiversity in marine ecosystems.

The honeycomb worm, *Sabellaria alveolata* (Linnaeus, 1767), is a physical ecosystem engineer (Berke, 2010) commonly found along the European coast from northwest Ireland to northern Mauritania (Curd et al., 2020), where it builds biogenic structures of varying extent in the intertidal and shallow subtidal zones. Honeycomb worms build what are considered Europe's largest biogenic reefs (Noernberg et al., 2010) and support a unique and rich assemblage of species (Dias and Paula, 2001; Dubois et al., 2006; Jones et al., 2018). Honeycomb worms play key functional roles in the ecosystems they support, by creating new three-dimensional habitat, which increases the physical complexity of the initial substrate, increases local biodiversity (Dubois et al., 2006; Jones et al., 2018), limits coastal erosion (Noernberg et al., 2010) and fashions biogenic structures (ranging from crusts and veneers to large reefs, hereafter "reefs" for simplicity) with high esthetic and recreational fishing value (Plicanti et al., 2016). Honeycomb worm reefs are broadly distributed across temperate Europe, however diversity investigations have only been carried out at local scales (Dias and Paula, 2001; Dubois et al., 2002, 2006; Schlund et al., 2016; Jones et al., 2018). It is therefore currently unknown how biodiversity supported by these reefs varies over its range.

The present study examined the patterns of diversity of benthic marine macrofauna associated with honeycomb worm reefs from sites spanning the entire European distribution of the species (but excluding North Africa), in order to address the following questions: (i) Does taxonomic and functional diversity of communities associated with honeycomb worms vary over broad geographical scales, and if so, what environmental drivers best explain this variation? (ii) Does community composition within honeycomb worm reefs vary with respect to currently described biogeographic provinces? (iii) Are there regional differences in taxonomic and functional β diversity in assemblages associated with honeycomb worm reefs? (iv) If so, are they mainly due to differences in species richness or in turnover? Finally, can differences between taxonomic and functional diversity help identify the ecological processes that affect biodiversity on honeycomb worm reefs?

MATERIALS AND METHODS

Study Area and Sampling Methods

Ten sites along the coast of Europe were selected for quantifying the diversity of benthic macrofaunal assemblages: four in the United Kingdom, four in France and two in Portugal (**Figure 1**). Sampling was carried out in the summer (spring tides of June and August 2017) following a standard protocol at each site. The sampling strategy aimed to maximize the number of species collected by sampling in a variety reef phases (prograding and retrograding, *sensu* Curd et al., 2019) within each site, as these are known to harbor different assemblages (Dubois et al., 2002; Jones et al., 2018). Reefs were sampled using eight PVC cores of 5 cm in diameter to a maximum depth of 15 cm. Since honeycomb worms occur within the first 15–20 cm of the reef (Gruet, 1986), only the living portion of the reef was sampled. At UK4, only veneer bio-constructions were available for sampling, and only five cores were collected because veneers were too scarce for further sampling. The contents of each core were preserved in 70% ethanol.

In the laboratory, cores were first weighed (wet weight, after removal of alcohol), then sieved on a 1 mm circular mesh. For a given core volume, the weight of the sediment provides means for comparing porosity or the void fraction of a sample. Macrofauna was then extracted from the sediments and enumerated. Individuals were identified to the lowest taxonomic level, most often to the species level. All species names were used according the World Register of Marine Species[1] and references used for taxonomic identification can be found in **Supplementary Appendix 1**. To ensure consistent taxonomic resolution across samples, the number of operators was limited ($n = 4$) and each uncertain identification was cross-verified by an expert in benthic taxonomy. However, due to the uncertainty regarding the morphological distinction at the species level between *Mytilus edulis* and *Mytilus galloprovincialis*, particularly at the juvenile stage (Jansen et al., 2007) and because hybridization occurs between the two (Daguin et al., 2001), all specimens sampled in the hybridization area (UK1, UK4, FR1, FR2, FR3, and FR4) were considered as *Mytilus* spp. (Wenne et al., 2020). All specimens are stored in the Laboratory of Coastal Benthic Ecology's collections at Ifremer (Plouzané, France).

[1] http://www.marinespecies.org/index.php (accessed January 15, 2021)

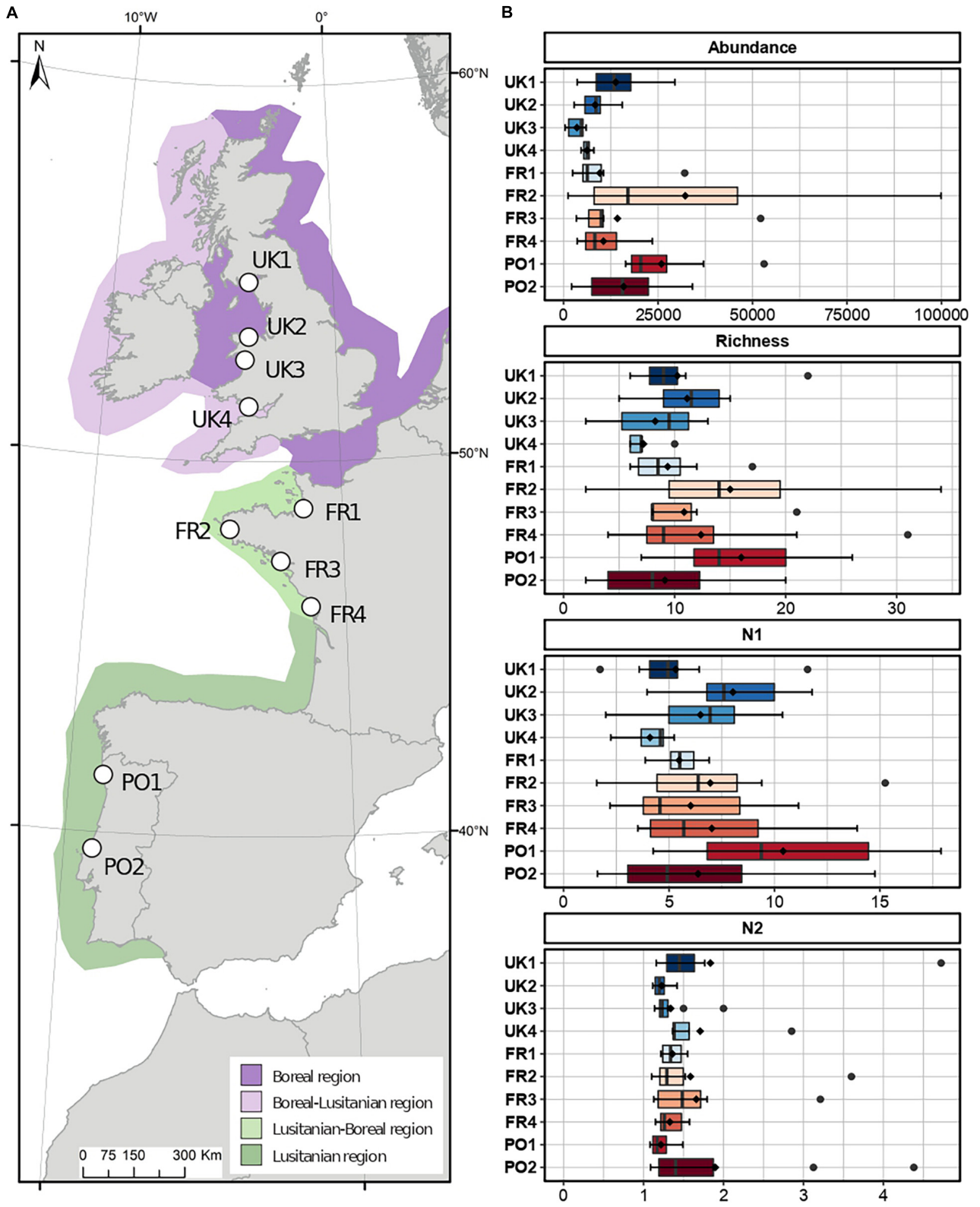

FIGURE 1 | (A) Map indicating the locations of the 10 study sites in the United Kingdom, France, and Portugal within the four biogeographic provinces defined by Dinter (2001). (Eight stations were sampled in each of the ten sites, except for UK4 where five stations were sampled.) **(B)** Abundance (±SD) of the associated macrofauna (in number of individuals.m^{-2}) and taxonomic indices (Richness, Hill diversity indices N1 and N2) per site.

Data Processing and Environmental Variables

Given that the reef-building species *S. alveolata* affects resource availability for the associated community (Dubois et al., 2002), all analyses considered the density of this species as an explanatory variable. Hence, *S. alveolata* abundance was removed from the species (response) matrix. Although some studies exclude rare species (i.e., represented by a single individual in one or two samples) for the calculation of similarity (see Clarke and Warwick, 2001), they may represent a non-negligible portion of a functional group, and are likely to have an impact on ecosystem functioning (Leitão et al., 2016). Rare species were therefore retained in the analysis in order to avoid reducing the functional richness of the communities (Mouillot et al., 2013; Jain et al., 2014).

To obtain information on the environmental conditions at each site, water and air temperature data were recorded using iButton® temperature loggers (accuracy ±0.5°C, hourly measurements) (Lima and Wethey, 2009), deployed between August and October 2016 for a period of approximately 1 year prior to the sampling campaign. In order to mimic temperatures similar to those experienced within the reefs, the loggers were coated with sand from the reefs and fixed onto rocky substrate at a constant shore level (corresponding approximately to the mid-tide level where the majority of reefs develop).

Taxonomic Diversity

Multivariate analyses were used to test for differences in macrofaunal assemblages across four biogeographic provinces (as delimited by Dinter, 2001). Non-metric multidimensional scaling (nMDS) was used to plot sample stations on a two-dimensional ordination plane based on taxa composition dissimilarities and labeled with the corresponding collection site. nMDS was also run using species abundances averaged across all stations sampled in a given site. In addition, a hierarchical cluster analysis (HCA) was run on all samples using the Ward method (Ward, 1963). All analyses were carried out on the basis of Bray–Curtis similarity matrices. Abundance data were transformed by the log $(x + 1)$ function to reduce the weight of the most abundant species.

In order to examine regional variation in α diversity, each site was coded as belonging to one of four biogeographic regions: Boreal, Boreal-Lusitanian, Lusitanian-Boreal, and Lusitanian (**Figure 1**; Dinter, 2001). Differences in community composition within and among regions were tested using PERMANOVA with a two-factor design (4999 residual permutations under a reduced model), with region as the fixed factor and site as the nested random factor. The weight of sediment was included as a co-variable in all analyses. Paired tests between regions were performed where the main effect was significant ($P < 0.05$). Prior to the PERMANOVA, differences in within-site multivariate dispersion were examined using the PERMDISP routine. When significant differences in assembly structure between regions were detected, a SIMPER analysis was performed to determine and rank the taxa responsible for the dissimilarities among sites and biogeographic regions. Variation of univariate assemblage metrics (i.e., abundance, species richness, the exponential of Shannon entropy (N1), and the inverse Simpson concentration (N2); Hill, 1973; Jost, 2006) were examined with permutational ANOVA, using the Euclidean distance in the PERMANOVA procedure (Anderson, 2017).

To qualify the link between the environment and macrobenthic community structure at each site, a distance-based redundancy analysis (dbRDA; Legendre and Andersson, 1999) was carried out. In addition to the variables recorded in the field (density of the engineering species *S. alveolata*, weight of sediment, maximum water and air temperatures), mean monthly values spanning 2000–2014 were obtained for 30 variables from BioORACLE[2] (Tyberghein et al., 2012; Assis et al., 2018). In order to eliminate multicollinearity among these environmental variables, Spearman rank correlations were calculated for all pairs of variables. Pairs with a Spearman correlation coefficient >0.7 were considered highly correlated. Only the following uncorrelated variables were kept in the analysis, in addition to the variables recorded in the field: mean surface water temperature (°C), mean chlorophyll *a* concentration ($mg.m^{-3}$) and maximum current speed ($m.s^{-1}$) (Dormann et al., 2013). Prior to analysis, all values for the environmental variables were standardized, then a DISTLM routine was used to obtain the most parsimonious model using a stepwise selection procedure and adjusted R^2 selection criterion (McArdle and Anderson, 2001).

Functional Diversity

To characterize the functional diversity at each site, a biological trait analysis (BTA) was conducted (Statzner et al., 1994). Eight biological traits (divided into 32 modalities) were selected (**Table 1**), providing information linked to the ecological functions performed by the associated macrofauna. The selected traits provide information on: (i) resource use and availability (by the trophic group of species, e.g., Thrush et al., 2006); (ii) secondary production and the amount of energy and organic matter (OM) produced based on the life cycle of the organisms (including longevity, maximum size, and mode of reproduction, e.g., Cusson and Bourget, 2005; Thrush et al., 2006); and (iii) the behavior of the species in general (i.e., how these species occupy the environment and contribute to biogeochemical fluxes through habitat, movement, and bioturbation activity at different bathymetric levels, e.g., Solan et al., 2004; Thrush et al., 2006; Queirós et al., 2013). Species were scored for each trait modality based on their affinity using a fuzzy coding approach (Chevenet et al., 1994), where multiple modalities can be attributed to a species if appropriate, and allowed for the incorporation of intraspecific variability in trait expression. The information concerning polychaetes was derived primarily from Fauchald and Jumars (1979) and Jumars et al. (2015). Information on other taxonomic groups was obtained either from databases[3] of biological traits, publications (Caine, 1977; Leblanc et al., 2011; Rumbold et al., 2012; Jones et al., 2018) and publications listed in **Supplementary Appendix 1**.

[2]https://www.bio-oracle.org/

[3]www.marlin.ac.uk/biotic

TABLE 1 | Selected biological traits and modalities for analysis of biological traits (BTA).

Traits	Modalities	Definition	Information
Maximum size (mm)	<10	Very small	Breathing, excretion, and carbon degradation (Thrush et al., 2006).
	(10–50)	Small	
	(50–100)	Medium	
	>100	Large	
Longevity	<1 year	Annual	Secondary production (Cusson and Bourget, 2005).
	1–2 years	Short	
	2–5 years	Average	
	>5 years	Long	
Movement	None <1 m 1–10 m >10 m	Daily capacity of adult movement	Breathing, excretion, anaerobic mineralization, remineralization of the organic matter (Solan et al., 2004; Queirós et al., 2013).
Habitat	tdw	Tube	Biogeochemical trophic dynamic fluxes (Lam-Gordillo et al., 2020).
	bdw	Burrow dwelling	
	att	Fixed	
	fl	Free	
Trophic group	SusP	Suspensivore	Respiration, excretion, and carbon degradation (Thrush et al., 2006).
	SurF	Surface deposit-feeders	
	SubS	Sub-surface deposit-feeders	
	PreDScaV	Predator/scavenger	
	GraZ	Grazers	
Reproduction	asx	Asexual reproduction	Colonization, recolonization, and resilience potential (Lam-Gordillo et al., 2020).
	bsp	Gamete emitter in the water column (broadcast spawner)	
	ind	Laying or brooding eggs with larval phase (indirect)	
	dir	Egg laying or brooding without a larval phase (direct)	
Bioturbation	EpiF	Epifauna	Anaerobic mineral regenerator, remineralization of organic matter (Solan et al., 2004; Thrush et al., 2006; Queirós et al., 2013).
	OnMod	Surface modifier	
	UpDown	Vertical transporter	
	BioD	Biodiffuser	
	ReG	Regenerator	
Bathymetric level	InterT	Intertidal species	Resistance to climatic variation and temperature changes (Costello et al., 2015; Martini et al., 2020).
	SubT	Subtidal species	

Ordination of the functional trait data was done using a Fuzzy coded multiple Correspondence Analysis (FCA) (Chevenet et al., 1994). Then, a hierarchical clustering analysis based on the Ward algorithm (Ward, 1963) was carried out using Euclidean distances (Usseglio-Polatera et al., 2000) to define homogeneous functional groups comprising species with similar biological trait associations. The frequencies of the modalities of each trait were calculated in order to visualize the biological profiles of identified functional groups.

Partitioning of Taxonomic and Functional β Diversity

Regional differences in diversity (β diversity) were estimated from presence-absence data using Sørensen's (1948) dissimilarity. For each pair of cores, taxonomic β diversity and its two components, turnover and nestedness, were computed using the Baselga partitioning scheme (Baselga, 2017; Schmera et al., 2020). Functional β diversity was computed based on the multidimensional functional space from the Fuzzy Correspondence Analysis, where axes were synthetic components summarizing functional traits (Villéger et al., 2010). The first four axes were used for calculating Sørensen dissimilarity according to Villéger et al.'s (2013) equation for all pairwise comparisons between samples (1) belonging to the same region (within bioregion), or (2) belonging to different regions (among bioregion). Correlations between taxonomic and functional β diversity as well as between their respective components were tested using Mantel permutational tests (Villéger et al., 2013).

All index calculations and statistical analyses were performed using the "betapart" (Baselga, 2012), "ade4" (Dray and Dufour, 2007) and "vegan" (Oksanen et al., 2020) packages in R 3.4.4 (R Development Core Team, 2008) as well as using PRIMER 7

(Clarke and Gorley, 2015) for PERMANOVA, PERMDISP, SIMPER and DISTLM analyses.

RESULTS

Taxonomic Diversity

A total of 129 taxa were observed in association with honeycomb worm reefs across the 10 sampled sites (77 stations, **Supplementary Table 1**). Taxon richness varied from two taxa (core from UK3, FR2, and PO2) to 34 taxa per station (core from FR2). In all sites except FR3, *S. alveolata* was the dominant species, with densities ranging from 6,450 ind.m^{-2} at UK2 to 80,000 ind.m^{-2} at FR2 (**Supplementary Figure 1A**). In all sites except FR3, *S. alveolata* was the dominant species, with densities ranging from 6,450 ind.m^{-2} at UK2 to 80,000 ind.m^{-2} at FR2 (**Supplementary Figure 1A**). The highest densities were observed in UK4 (130,000 ind.m^{-2}) but this most likely corresponds to a recent recruitment event, as individuals were on average much smaller (diameter of the opercular crown less than 2 mm; Gruet, 1986). The ratio of individuals of *S. alveolata* to individuals of associated macrofauna showed a clear dominance of the engineering species at UK4 and UK3 (94 and 87%), while at other sites, this ratio varied from 43 to 68% (**Supplementary Figure 1B**). It was also at these two sites that the number of individuals of the associated macrofauna were the lowest, reaching up to 5,820 ind.m^{-2} at UK3 (with an average of 3,507 $\pm$ 2,313 ind.m^{-2}) and 7,500 ind.m^{-2} 283 at UK4 (with an average of 6,194 $\pm$ 1,304 ind.m^{-2}; **Supplementary Figure 1A**). The fauna associated with honeycomb worm reefs were primarily of annelids and arthropods and to a lesser extent, mollusks and nematodes (**Supplementary Figure 2**). However, community composition varied significantly among sites. Annelids were dominant in UK2, UK3, FR4, and PO2, where they represented between 36 and 56% of individuals. At UK1 and PO4, arthropods dominated the community, representing 47 and 51% of individuals, respectively. For the other sites, mollusks were dominant (53% of individuals in UK4 and 39% in FR2) as well as nematodes (36% of individuals in FR1 and 39% in FR3). Sites FR1 and FR3 had a higher abundance of nematodes and mollusks compared to other sites.

Taxon richness and abundance did not show any significant variation between sites within the same region but showed significant differences between regions (**Table 2**). As for N1 and N2 indices, honeycomb worm reef communities were characterized by low values (**Figure 1**). For both metrics, there was no significant effect of site or region. Sediment weight had a significant effect, but only on the N2 index (**Table 2**). The PERMANOVA also detected a significant effect of sediment weight on taxon richness but not on abundance (**Table 2**).

Hierarchical cluster analysis based on species composition and abundances per station defined four groups of assemblages (**Figure 2B**). Group I included stations sampled in UK1 and UK4, plus two stations from UK3 and one station from FR1. Group II included all stations in UK2 and the remaining stations from UK3. Group III included all but one station in France (FR1, FR2, FR3, and FR4) and Group IV included stations in Portugal (PO1 and PO2). The nMDS indicated some degree of partitioning among sites, with two of the British sites (UK1 and UK4) being distinct from two of the southern sites (nMDS1 and nMDS2; **Figure 2A**). However, much overlap was observed in community composition among sites found in the center of the distribution, particularly FR1, FR3, and UK3, which exhibited considerable variability among stations within each site ($F = 7.98$, $P < 0.001$; PERMDISP; **Figure 2A**). PERMANOVA detected significant variability between regions and between sites within regions, as well as a significant effect of the sediment covariate (**Table 2**). Regional differences were driven by differences in

TABLE 2 | Results of PERMANOVA to test for differences in benthic macrofaunal assemblages between bioregions (fixed) and sites (random, nested within bioregion).

	Benthic macrofaunal assemblages			
Source	**df**	**MS**	***F***	***P***
Sediment	1	19,830	2.3015	**0.0088**
Bioregion	3	16,974	2.0381	**0.0072**
Site (bioregion)	6	10,124	5.9491	**0.0002**
Residuals	66	1701.8		
Total	76			
Taxon abundance				
Sediment	1	3.7823E+8	1.7416	0.2258
Bioregion	3	2.1007E+9	9.7396	**0.0062**
Site (bioregion)	6	2.2494E+8	1.239	0.2934
Residuals	66	1.8155E+8		
Total	76			
Taxon richness				
Sediment	1	168.05	9.1909	**0.0112**
Bioregion	3	327.53	17.508	**0.0026**
Site (bioregion)	6	16.07	0.56507	0.7518
Residuals	66	28.438		
Total	76			
N1 index				
Sediment	1	9.7505E−2	2.0997	0.1758
Bioregion	3	3.6729E−2	0.80318	0.5312
Site (bioregion)	6	5.015E−2	1.7046	0.126
Residuals	66	2.942E−2		
Total	76			
N2 index				
Sediment	1	6.3026E−2	6.1914	**0.0312**
Bioregion	3	1.016E−2	1.0022	0.4522
Site (Bioregion)	6	1.0396E−2	1.1316	0.3606
Residuals	66	9.1871E−3		
Total	76			

Sediment weight provides a proxy for the porosity of the bioconstructions and was included as a covariable in the analysis. Permutations were based on a Bray–Curtis dissimilarity matrix generated from log (x + 1) abundance data. Results of univariate PERMANOVA to test for differences in assemblage-level univariate metrics in macrofaunal assemblages (taxon richness and total abundance) are also shown. Permutations for univariate analysis were based on the Euclidean distance matrix generated from untransformed diversity data. All tests used a maximum of 4999 permutations under a reduced model; significant effects (P < 0.05) are shown in bold. An underlined P-value indicates that PERMDISP detected significant differences in within-group dispersion between levels of that factor (P < 0.05). df, degrees of freedom; MS, mean squares; F, pseudo F-statistic; P, P-value.

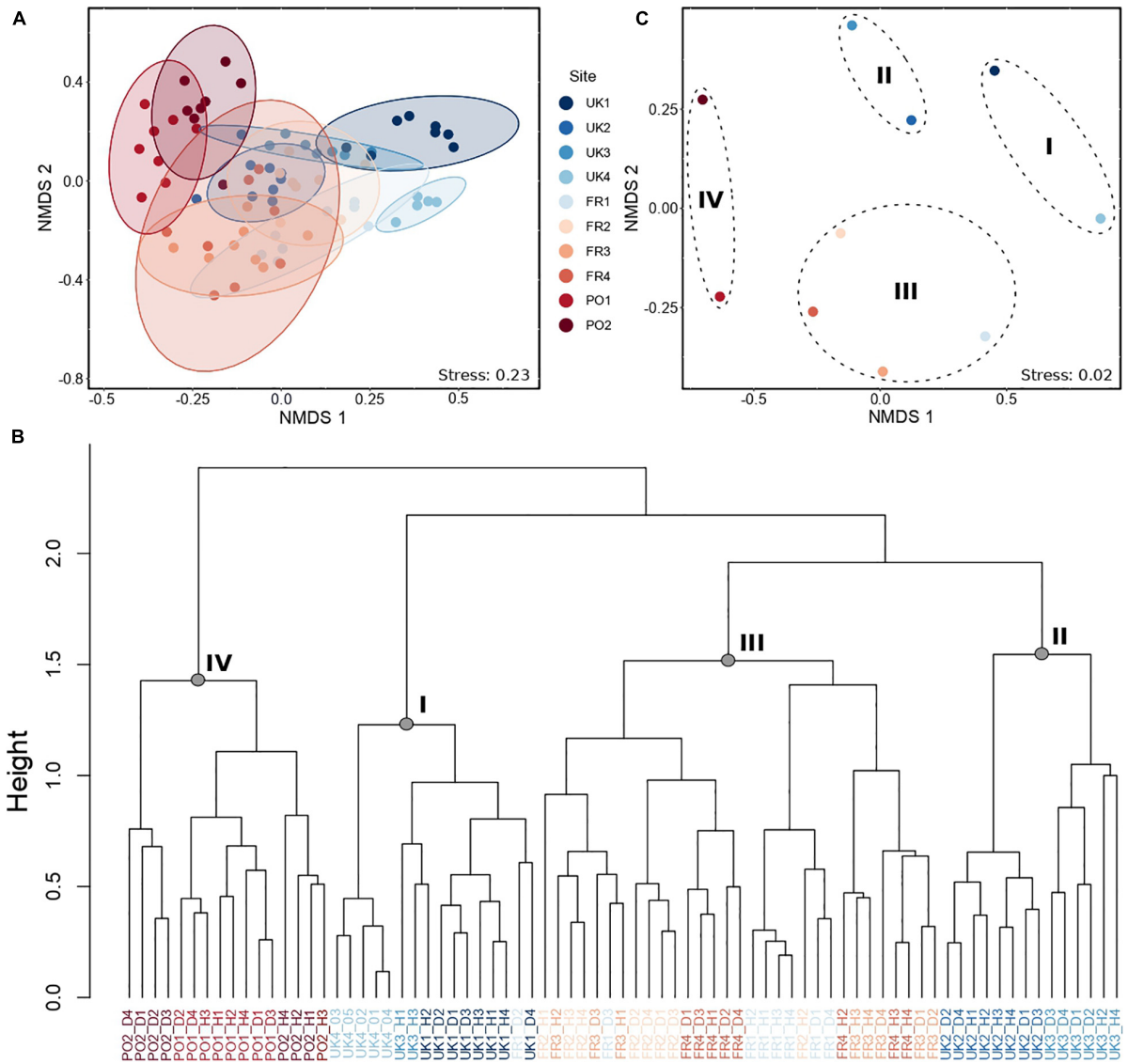

FIGURE 2 | (A) nMDS representing the variability across sites and stations within sites. **(B)** Cluster constructed using the "Ward D2"' method, showing the four groups of replicates. Height indicates the order in which the clusters were joined. **(C)** nMDS constructed from data averaged for each site, grouped by cluster groups. **A–C** were derived from a Bray–Curtis dissimilarity matrix constructed from log (x + 1) abundance data transformed.

intra-regional variability (F = 18.08, P < 0.001; PERMDISP; **Figure 2A**) but also by changes in mean species composition (**Figures 2A,C**). Paired tests between regions showed that assemblages from the Lusitanian Province (PO1 and PO2) were distinct from those from the Boreal province (UK1, UK2, and UK3) and the Lusitanian-Boreal province (FR1, FR2, FR3, and FR4) (**Supplementary Table 2**). SIMPER analysis indicated that the differences observed between regions were mainly due to a higher abundance of the polychaete *Syllis armillaris* (Müller, 1776) and the mussel *M. galloprovincialis* (Lamarck, 1819) in the Lusitanian Province compared to the Lusitanian-Boreal and Boreal Provinces (**Supplementary Table 2**).

Distance-based redundancy analysis analyses indicated some degree of partitioning between regions. The first two axes represent 12.4 and 10.5% of the explained total variance, respectively (**Figure 3**). The species assemblages were structured along two gradients. The first was driven by the mean chlorophyll *a* and mean water temperature variables, which were negatively correlated, highlighting the differences between the northern and the southern assemblages. The second was driven by the amount of sediment in the cores and the maximal temperature of the air, which separated the middle range sites from the southern and northern sites, with higher values in the middle range sites (**Figure 3**). Note that the amount of sediment in the cores was also negatively correlated with maximal current velocity, which was higher in the northern sites. The DISTLM routine was used to determine links between environmental predictor variables and variability in assemblage structure (**Table 3**). Marginal

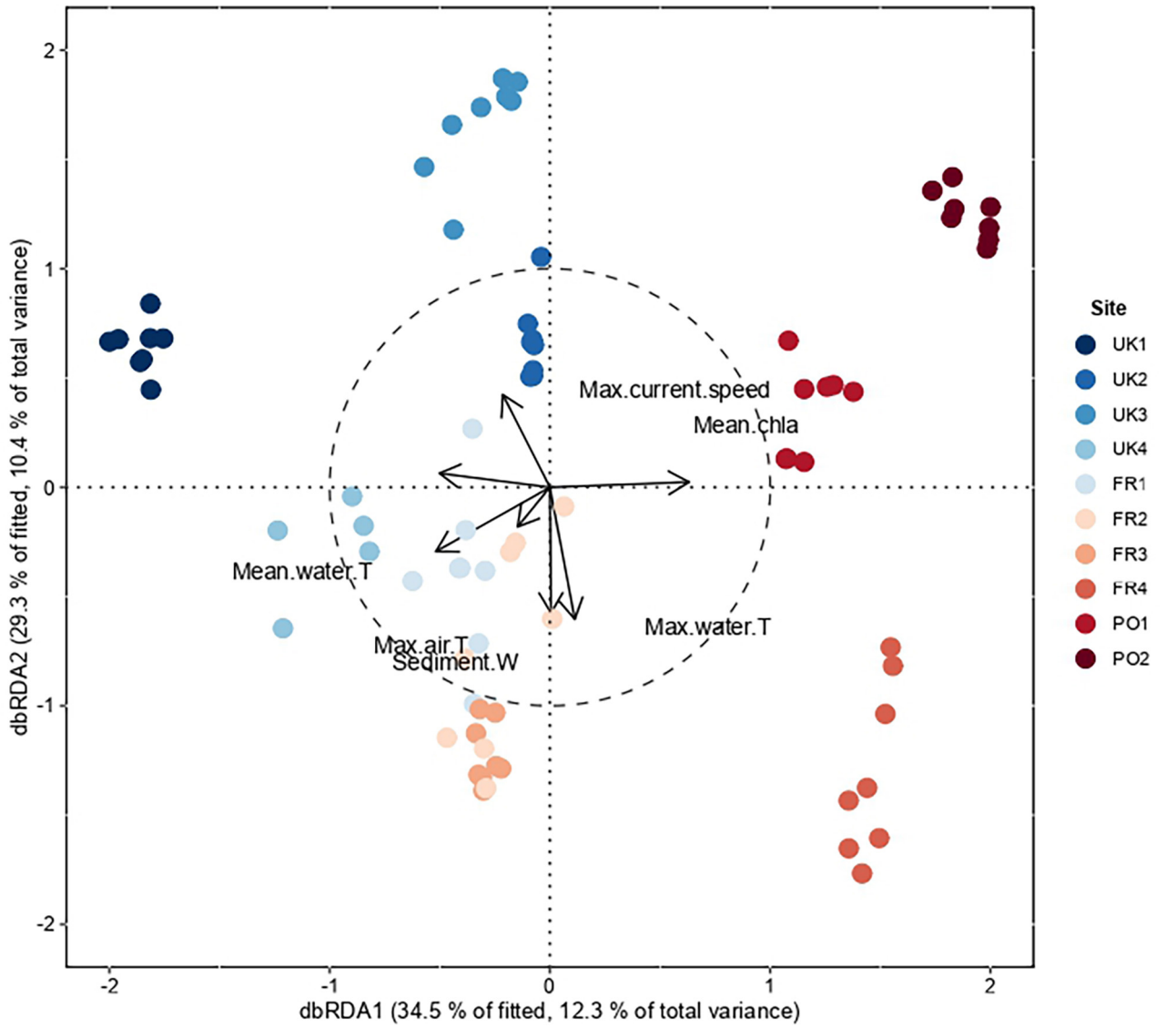

FIGURE 3 | Result of the distance-based redundancy analysis (dbRDA) using the Bray–Curtis dissimilarity matrix computed on the log-transformed abundance data and the seven selected environmental variables. Field data: "Water" and "Air (T°C max)" = maximum air and water temperature, "Sediment" = amount of sediment in $g.m^{-2}$, "Density SA" = density of *S. alveolata* ($ind.m^{-2}$). Data extracted from BioORACLE: "Chla" = average chlorophyll level ($mg.m^{-3}$), "Water (T°C avg.)" and "Current (max)" = average maximum current velocity ($m.s^{-1}$). The first two axes capture 22.9% of the variation explained by these seven variables.

tests showed that mean water temperature and the amount of sediment in the cores were, individually, the most important predictor variables. Surprisingly, the density of *S. alveolata* did not appear to be a structuring factor for these intertidal communities. The stepwise selection procedure indicated that the most parsimonious model included all environmental variables, explaining 0.38% (adjusted R^2 = 0.31) of the total observed variation in this assemblage structure.

Functional Diversity

Changes in community structure were also analyzed in terms of functional diversity. Cluster analysis carried out on the FCA axes revealed five main groups of taxa with distinct trait combinations (**Figure 4A**). The most clearly delineated group (Group 1) was composed mostly of intertidal, suspension-feeding, small, long-lived organisms that live mostly fixed or in tubes and release their gametes into the water column (**Figure 4B**). This group was represented by 14 taxa, the majority of which were bivalve mollusks, sabellidae polychaetes, and barnacles. The four other groups were largely composed of infaunal taxa. Group 2 was composed of very small, free-living and tube-dwelling, short-lived, sometimes annual, organisms. Most species in this group lay or incubate eggs and have no larval phase. Their contribution to sediment reworking was mainly at the sediment surface. This group was composed of 47 taxa that included amphipods and isopods but also pycnogonids and

TABLE 3 | DISTLM marginal test results for each environmental predictor variable selected for the most parsimonious model for macrofaunal assemblages.

Variable	Adj. R^2	SS	*F*	*P*	Prop
Mean water temperature	0.89369	24,711	8.4587	0.0002	0.10135
Sediment weight	0.16155	20,056	7.4563	0.0002	0.082260
Maximum water temperature	0.19959	11,598	4.5169	0.0002	0.047571
Density of *Sabellaria alveolata*	0.22953	9484	3.837	0.0002	0.038898
Maximum current speed	0.258562	9083.8	3.8189	0.0002	0.037257
Maximum air temperature	0.29764	11,154	4.9502	0.0002	0.045748
Mean chlorophyll concentration	0.31250	5544.1	2.5137	0.0036	0.022739

The best solution based on stepwise selection and adjusted R^2 is shown. Adj. R^2, adjusted R^2; SS, sum of squares (trace); F, pseudo F-statistic; P, P-value; Prop, proportion of variation explained.

nematodes. Group 3 comprised large, average-lived organisms, that freely release their gametes into the water column, with feeding modes mostly associated to scavenging and sub-surface deposit-feeding, living free or in burrows, and participating to sediment reworking, either as biodiffusors or through vertical sediment transport. This group included 23 taxa, belonging to the polychaete annelids Eunicidae, Lumbrinereidae, and Oenonidae (formerly part of Eunicidae) and Terebellidae. Group 4 and Group 5 comprised species with heterogeneous and intermediate trait characteristics relative to the more functionally homogeneous Groups 2 and 3, the former being represented by 14 taxa, mainly polychaete annelids belonging to the Spionidae, Capitellidae, and Cirratulidae families, while the latter included 23 taxa, most of them being polychaetes belonging to different families of the order Phyllodocida (Phyllodocidae, Nereidae, Syllidae, Glyceridae, and Polynoidae). It also included decapod crustaceans, gastropods, and oligochaetes (all groups are detailed in **Supplementary Figure 3**). The relative frequencies of each group did not show a significant difference in the proportion of each functional group with latitude (**Supplementary Figure 4**).

Taxonomic and Functional β Diversity

Taxonomic β diversity values for macrofauna associated with honeycomb worm reefs showed greater similarity on average within regions (19–51%; **Figure 5A** and **Table 4**) compared to among regions (9–33%; **Figure 5B** and **Table 4**). However, levels of similarity within regions remained low, indicating important heterogeneity across sites of a given region. On average, when considering pairs of assemblages within regions, 60% of the species were found in only one assemblage: 50% of them changed in terms of species identity (turnover) and 10% were unique to the richest assemblage (nestedness) (**Figure 5A** – within region, **Table 4**). For pairwise comparisons among different regions, differences were even more pronounced, with an average of 80% of species being found in only one assemblage, with 70% due to species turnover and 10% linked to nestedness (**Figure 5B** – among bioregion, **Table 4**; for all pairwise comparisons among regions, see **Supplementary Figure 5** and **Table 4**). The contributions of nestedness to β diversity were on average similar within and among regions. Overall, variation in species composition within and between bioregions were primarily due to changes in species identity.

Functional β diversity values for macrofauna associated with honeycomb worm reefs showed a comparable range in similarity within regions (38–88%; **Figure 5A** and **Table 4**) and among regions (34–84%; **Figure 5B** and **Table 4**). This similarity within and among regions, indicates high levels of overlap in functional space. On average, two assemblages shared 40% of their functional space, while functional β diversity was mostly driven by nestedness (i.e., by difference in the volume of the functional space filled by the assemblages; 24%) rather than by turnover (i.e., functional spaces not shared by the two assemblages; 15%) (**Figures 5C,D** and **Table 4**). The contributions of nestedness to functional β diversity were similar within and between regions (for all pairwise comparisons among bioregions, see **Supplementary Figure 6**).

DISCUSSION

Influence of Honeycomb Worm Reefs on Local Diversity

Honeycomb worm reefs host diverse invertebrate assemblages. Here we examined how multiple facets of diversity, including taxonomic and functional α and β diversity, vary over much of the Atlantic coast of Europe. In terms of local levels of diversity, no significant differences were observed in Hill diversity indices (including richness) over the 10 study sites. Only the abundances of macrofauna were relatively higher in the southern sites compared to the northern sites. Our results are in agreement with a growing number of examples that show that there are many exceptions to the latitudinal diversity gradient described by Brown and Lomolino (1998) and Gaston and Chown (1999). Recent investigations have shown little or no relationship of diversity with latitude for the European marine benthos (Renaud et al., 2009; Hummel et al., 2017), particularly for soft sediment communities (Kendall and Aschan, 1993; Wilson et al., 1993; Kendall, 1996). Latitude is not a unidimensional environmental variable but a proxy for a number of primary environmental

TABLE 4 | Taxonomic and functional β diversity and its two components; mean ± standard deviation.

	Taxonomic			Functional		
	β diversity	Turnover	Nestedness	β diversity	Turnover	Nestedness
Within bioregion	0.65 ± 0.16	0.53 ± 0.21	0.12 ± 0.11	0.37 ± 0.25	0.13 ± 0.20	0.24 ± 0.20
Among bioregion	0.78 ± 0.12	0.70 ± 0.16	0.08 ± 0.08	0.39 ± 0.24	0.15 ± 0.21	0.24 ± 0.20

Contributions were calculated for comparisons between pairs of samples belonging: to the same bioregion (within bioregion), or to different bioregions (among bioregion).

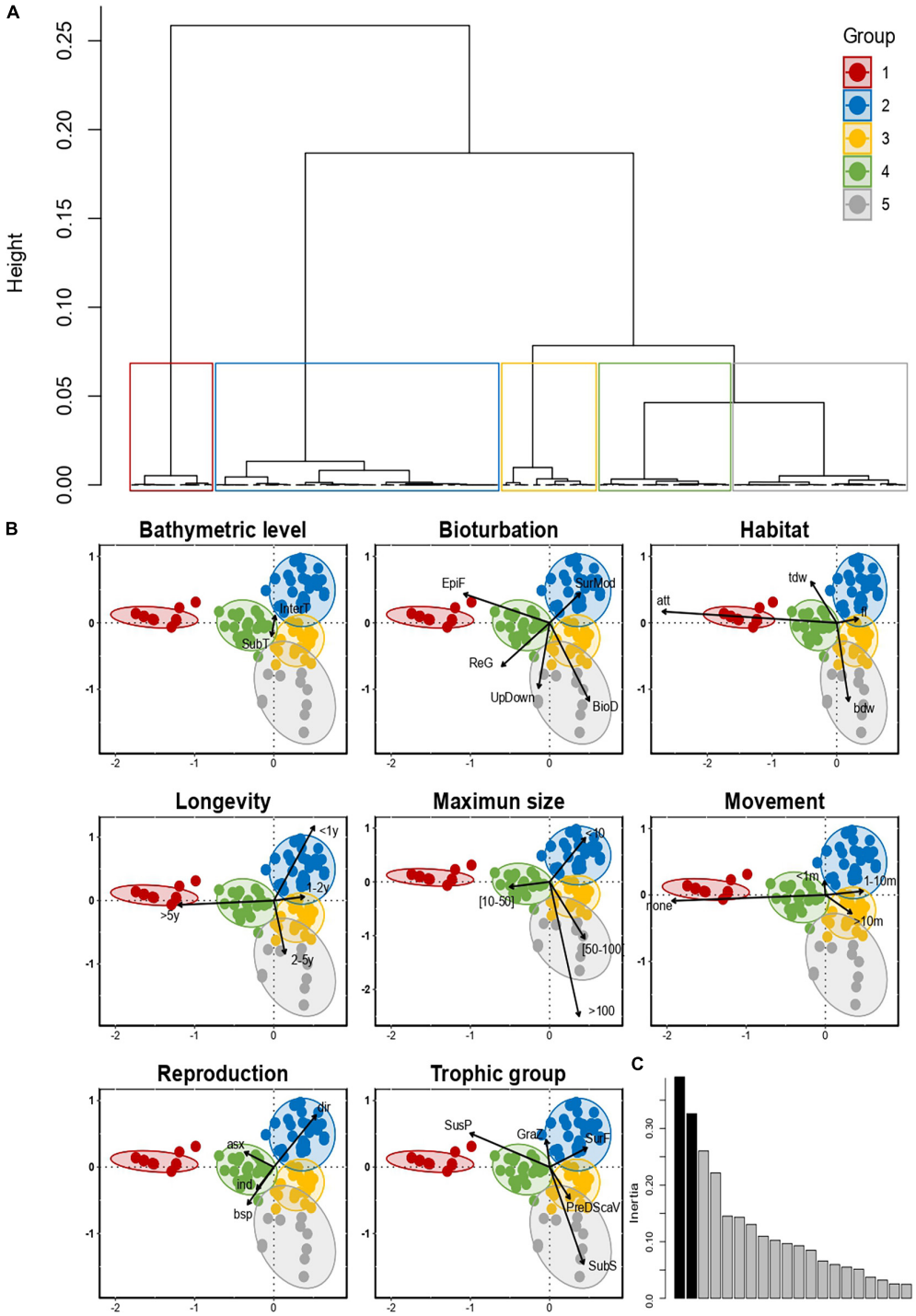

FIGURE 4 | (A) Cluster constructed using the "Ward D2"' method performed from the Fuzzy Correspondence Analysis (FCA) results. **(B)** Projection of modalities and taxa by biological traits on the first two axes of the FCA. **(C)** Histogram of eigenvalues. The first two axes (in black) were kept in the FCA.

factors that interact and correlate with each other (Hawkins, 2003). For honeycomb worms, it appears that biotic and abiotic factors associated with the reef environment have contributed to maintaining constant levels of diversity over broad geographical scales, as discussed further below.

The assemblages sampled in our study showed a high diversity of macrofaunal organisms and are typical of the honeycomb worm reef assemblages reported in previous studies (Gruet, 1986; Dias and Paula, 2001; Dubois et al., 2002, 2006; Schlund et al., 2016). Mean species richness was comparable, but notably lower

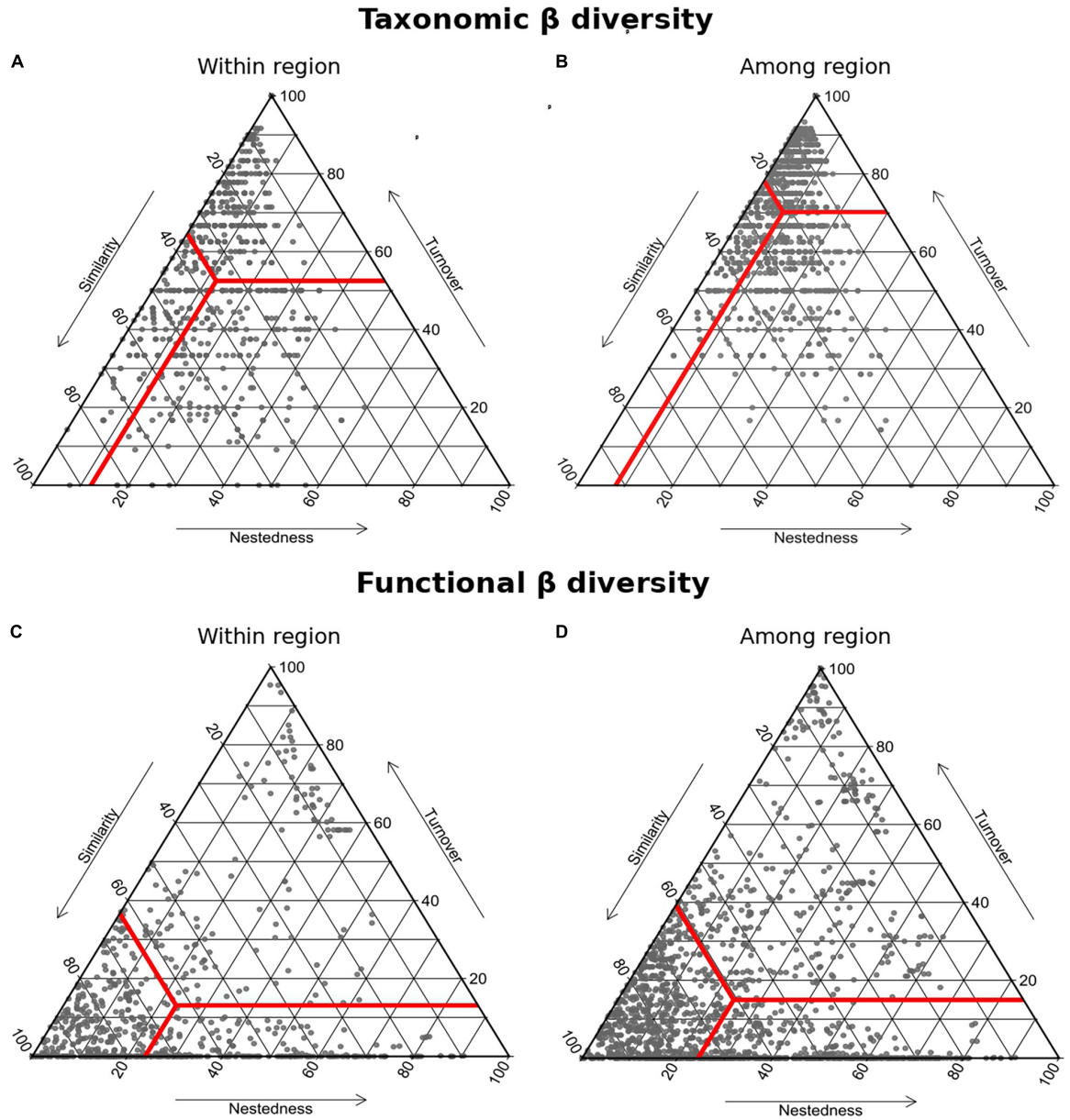

FIGURE 5 | Triangular plots illustrating the geographical pattern of **(A,B)** taxonomic and **(C,D)** functional β diversity Sorensen dissimilarity between the species composition (presence/absence data) of the 10 study sites was used to quantify their similarity, and the two components of their beta diversity nestedness (i.e., influenced by the difference in number of species between the two communities) and turnover (i.e., species replacement between two communities). Contributions were calculated for comparisons between samples belonging either to **(A,C)** the same bioregion (within bioregion) or to **(B,D)** different bioregions (among bioregion). Red lines indicate the centroid value for each graph with its associated mean values for the three components of the Sorensen dissimilarity.

(7–16 species), than most previous reports for honeycomb worm reef richness (7–33 species; Holt et al., 1998; Dubois et al., 2002, 2006; Schlund et al., 2016; Jones et al., 2018). These values are also comparable to the values reported for epifauna from macroinvertebrate assemblages associated with *Laminaria hyperborea* (Gunnerus) Foslie, 1884 kelp holdfasts (10–30 species; Teagle et al., 2018) but lower than infaunal assemblages reported for the eelgrass *Zostera marina* Linnaeus, 1753 (10–60 species; Blanchet et al., 2004; Boström et al., 2006) in the northeast Atlantic. In terms of richness, maerl beds (composed of at least two species: *Lithothamnion corallioides* and *Phymatolithon calcareum*; Riosmena-Rodríguez et al., 2017) hosted, by far, the richest assemblages sampled thus far, with an average richness of 53 species (32–73 species; Boyé et al., 2019). Our results confirm that habitats engineered by honeycomb worms, as with other bioengineered habitats, host higher species richness than geogenic habitats (8–12 species; Jones et al., 2018; Boyé et al., 2019).

While species richness in assemblages associated with honeycomb worms remained within a narrow range throughout the coast of Europe, faunal composition did vary among sites. Two environmental variables were found to significantly structure assemblages: mean annual water temperature and the quantity of sediment in the cores. Mean annual temperature distinguished the United Kingdom sites and France sites from the Portugal sites and one site (FR4) in the Bay of Biscay. Thermal regimes affecting faunal composition appear to change within the Bay of Biscay, south of the Brittany peninsula, consistent with higher sea surface temperatures in the Bay of Biscay than in the surrounding areas connected by the Gulf Stream (Jenkins et al., 2008; Hummel et al., 2017). Sediment content was a key variable that structured communities, with sites that had higher sediment content, typically the France sites, being distinct from sites with lower sediment content, namely the United Kingdom and Portugal sites. Sediment content was negatively correlated with current velocity, such that sites that had lower hydrodynamics accumulated more sediment, while sites with higher hydrodynamics had higher porosity within the reef. In areas with high current velocities, the reef-building activity of *S. alveolata* is challenged by wave erosion, generating higher porosity within reefs. Conversely, low current velocities allow reefs to grow homogeneously but also allows unconsolidated particles to settle within fissures in the reefs. Previous studies have reported that within the same site, dense sections of reef, where *S. alveolata* is in an active growth phase (prograding reef, *sensu* Curd et al., 2019) tend to host assemblages with lower abundances and diversity than parts of the reef that are more fragmented (retrograding reef) (Dubois et al., 2002; Jones et al., 2018).

Sediment content has been found to be an important variable structuring communities at local scales. In the Bay of Mont-Saint-Michel, for example, higher sediment content in retrograding reefs explained the presence of many species typically belonging to muddy sandy bottom communities (Dubois et al., 2002, 2006). At the regional level, differences in hydrodynamic and sediment accumulation regimes may therefore lead to differences in reef density, which in turn affect assemblage compositions over the Atlantic coast of Europe. Unlike other engineering species such as haploops (gregarious tube-dwelling amphipods) (Rigolet et al., 2014), the density of *S. alveolata* was not the main factor structuring communities. Unlike haploops, the reef structures developed by *S. alveolata* persist after the death of the individuals, such that characteristics of the reef (here sediment content) better explain variation in communities than the density of the engineering species. Our results are consistent with other studies that have shown that reef structure is more important for explaining community composition than density of the engineer, such as in habitats built by *Owenia fusiformis* Delle Chiaje, 1841 (Fager, 1964); *Spiochaetopterus bergensis* Gitay, 1969 (Munksby et al., 2002; Hastings et al., 2007), and *Lanice conchilega* (Pallas, 1766) (Zühlke et al., 1998; Zühlke, 2001; Callaway, 2006; Rabaut et al., 2007; Van Hoey et al., 2008; De Smet et al., 2015).

We found five functional groups in association with honeycomb worm reef formations. Our results show that changes in taxonomic composition did not result in changes in ecological role, but rather that the same functional groups were found in association with honeycomb worm reefs throughout the coasts of Europe. Foundation species greatly influence the structure and functioning of species assemblages (Bruno et al., 2003). However, the effects of foundation species on biodiversity are not necessarily positive for all species, providing resources for some but excluding others (Rigolet et al., 2014). Through tube building activity, honeycomb worms transform unconsolidated sediment into a complex three-dimensional structure with properties that differ from both rocky shores or bare sediment. The reefs attract mostly soft sediment infauna (other polychaetes) and provide pockets of soft sediment for burrowers, but exclude taxa that require rocky substrate to settle upon or that compete for space with *S. alveolata*, such as barnacles and mussels (Holt et al., 1998; Dubois et al., 2002, 2006). Brown and red macroalgae cover on honeycomb worm reefs is reduced compared to rocky shores (Dubois et al., 2006), hence, excluding a large set of herbivores, and favoring deposit-feeders, as can be seen in the functional groups recovered here. Honeycomb worm reefs may therefore act as a biological filter for a given local pool of organisms. Similar results have been reported in different bioengineered habitats such as the communities associated with haploops in the bay of Concarneau, France (Rigolet et al., 2014). Contrary to adjacent sandy and muddy bottom communities, the establishment of haploops communities excluded or limited the colonization of other burrowers and tube-dwelling suspension-feeders, but attracted small mobile predators which possibly predate on haploops or other small associated organisms. The biological filtering that occurs in honeycomb worm and haploops habitats may therefore be applicable to other bioengineered habitats.

Relationship Between Taxonomic and Functional β Diversity

Our results show that while the taxonomic composition of the fauna associated with honeycomb worm reefs varied over broad geographical scales, species were replaced by another with the same functional role, such that only few differences in functional groups occurred across the reefs of the northeastern Atlantic. Despite high species turnover observed between biogeographic regions (70% on average), functional turnover was only 15% on average. As a result, high functional similarity was observed between regions and most functional changes across regions were due to one assemblage being a subset of another (24% of functional nestedness). For instance, the functional role performed by the isopod *Lekanesphaera levii* (Argano and Ponticelli, 1981) sampled in the northern reefs is the same as another isopod, *Dynamene bidentata* (Adams, 1800) in the southern reefs. This is also the case for two species of Phyllodocidae: *Eulalia clavigera* (Audouin and Milne Edwards, 1833) and *Eulalia ornata* (Saint-Joseph, 1888). *E. ornata* is more abundant at Boreal and Boreal-Lusitanian sites but tends to be replaced by *E. clavigera* at Lusitanian-Boreal and Lusitanian sites.

Biogenic habitats tend to show little variation in functional groups over broad spatial scales with high levels of redundancy within each group (Hewitt et al., 2008; Barnes and Hamylton, 2015), although this depends somewhat on the foundation

species (Boyé et al., 2019). High species turnover accompanied by constant taxonomic richness has also been observed in eelgrass assemblages (Boyé et al., 2017). Similarly, variation in taxonomic composition associated with eelgrass beds, mangroves, maerl beds, and coral reefs did not result in differences in functional trait composition across approximately 500 km of coastline from both sides of the Atlantic and from the Caribbean and coral seas (Hemingson and Bellwood, 2018; Boyé et al., 2019). Our results support previous work that has shown that biogenic habitats are important in structuring benthic assemblages at the regional scale. And as with other biogenic habitats, communities supported by honeycomb worms show high functional redundancy that is thought to provide spatial insurance for benthic ecosystem functioning at local and broad spatial scales (Boyé et al., 2019). In addition, high functional redundancy may indicate that honeycomb worm reefs can offer similar niche properties to its associated assemblages across varying environmental conditions, as has been found for North Atlantic eelgrass, Caribbean mangroves or Indo-Pacific coral reefs (Cornell and Lawton, 1992; Boyé et al., 2017; Hemingson and Bellwood, 2018; Storch and Okie, 2019). Indeed, the reefs themselves provide protection from the physical elements, such as wind, waves, sun exposure, and desiccation, which may mean that they also act as environmental filters, buffering extremes in temperature or other environmental variables as is observed for many foundation species (Bertness and Callaway, 1994; Bruno et al., 2003; Bouma et al., 2009). As such, they may override the effect of large environmental gradients such as latitudinal temperature gradients (Jurgens and Gaylord, 2018), with important consequences for the spatial and temporal variation of their associated communities (Bulleri et al., 2018; Boyé et al., 2019).

Biogeographic Regions

Taxonomic differences were observed in macrobenthic faunal assemblages associated with honeycomb worm reefs along the coast of Europe. Hierarchical clustering analyses showed that assemblages were grouped together into four main clusters, two of which were found in the United Kingdom, a third represented by all assemblages in France, and a fourth represented the assemblages from Portugal. These clusters suggest there may be greater regional differences in macrobenthic communities than is currently recognized in biogeographic frameworks which consider only two main provinces in the northeastern Atlantic (Spalding et al., 2007; Briggs and Bowen, 2012). The assemblages observed in our study suggest important differences in species composition within both Lusitanian (Portugal vs. France sites) and the Boreal/Northern European Seas provinces (UK1 + UK4 vs. UK2 + UK3). While our results show good agreement with assemblage differences that could correspond to differences in species distributions associated with Lusitanian-Boreal and Lusitanian province subdivisions (defined by Dinter, 2001), it is less clear whether the northern assemblages found in honeycomb worms support a Boreal and Boreal-Lusitanian subdivision. Nevertheless, the differentiation observed here does suggest a higher degree of partitioning of species within the northeastern Atlantic that may be in part related to biogeography, with many species having restricted distributions. Our findings for the four United Kingdom study sites are in agreement with patterns of community composition associated with another important temperate foundation species, the kelp *L. hyperborea* (Teagle et al., 2018). While communities associated with holdfasts were fairly variable throughout the study area, six sites collected in northern and southern Scotland (Boreal province) were distinct from six sites in northwestern Wales and Southern England, supporting partitioning within the Boreal/Northern European Seas province.

In honeycomb worm assemblages, differences in Boreal and Boreal-Lusitanian regions were mainly driven by the occurrence or absence of *M. edulis* and potential hybrids of *M. edulis* × *M. galloprovincialis* in the two studied regions. Given the morphological similarities among the three taxa, identification to the species level was uncertain in UK1 and UK4, with most identifications being kept to the genus level. This may partly explain the similarity among the Scottish and southern England sites in our dataset. Molecular identification was not attempted here, but could help resolve some of these taxonomic uncertainties in future work, as has been done for *Mytilus* spp. (Wenne et al., 2020). Similarly, nematodes were identified only to the phylum level, but did contribute significantly to the observed differences in assemblages between the Lusitanian and Lusitanian-Boreal regions. Identification to the species level would likely further differentiate these two regions (Bhadury et al., 2006). Overall, our results indicate strong differences in community composition that are related to taxonomic turnover, which in turn indicates that species ranges may better correspond with finer-scale biogeographic partitioning within the northeastern Atlantic, as proposed by Dinter (2001). Future studies that take into consideration more extensive species inventories across phyla and habitats may help refine our understanding of marine biogeography in the northeastern Atlantic, and resolve some of the current discord in various frameworks.

CONCLUSION

Our results highlight the importance of considering various aspects of diversity in order to have a more comprehensive understanding of the ecological processes that shape marine communities, which will ultimately better inform conservation strategies (Meynard et al., 2011; Villéger et al., 2013; Loiseau et al., 2017). In the case of honeycomb worm reefs, the environmental filtering that excludes some functional groups from the reefs would not have been detected if only patterns in taxonomic diversity had been examined. Similarly, the high level of taxonomic turnover observed among and within biogeographic regions would have been overlooked if functional diversity had been considered alone. Examining multiple facets of community diversity has enhanced our understanding of the factors that shape assemblages associated with *S. alveolata*. Preserving taxonomic diversity is and will continue to be valuable for maintaining regional levels of species diversity (De Juan and Hewitt, 2011). However, while many conservation programs

prioritize the conservation of local taxonomic community diversity (Socolar et al., 2016), considering the functional complementarity of communities across broader spatial scales in addition may prove to be more efficient in maintaining healthy ecosystems (Mori et al., 2018). The results presented here show that honeycomb worm reefs support high taxonomic diversity, but functional diversity is more limited, with some key functional groups (such as grazers) being absent from the community. Adjacent habitats may therefore host very different sets of species with equally important ecological roles. Benthic homogenization and loss of complexity of the sea floor may reduce overall functional diversity in the marine benthos (Airoldi et al., 2008). Protecting a diversity of benthic habitats may therefore be necessary for ensuring good ecosystem functioning in marine communities.

DATA AVAILABILITY STATEMENT

The original contributions presented in the study are included in the article/**Supplementary Material**. The functional trait dataset for this study can be found in SEANOE (https://www.seanoe.org/; https://doi.org/10.17882/79817). Further inquiries can be directed to the corresponding author/s.

AUTHOR CONTRIBUTIONS

SD, LF, and FN conceived the study. AM led analysis and drafting of the manuscript. LB, AC, AD, SD, LF, FL, CM, FN, and RS carried out the field work. CP, AM, SD, and ND conducted species and trait identification. AB, CP, MM, and SD contributed to data analysis. All authors contributed to editing the final manuscript.

FUNDING

This work was supported by the Total Foundation (Grant No. 1512 215 588/F, 2015). AM and AC were funded by Ph.D. grants from Ifremer, Region Bretagne, and the ISblue project (the Interdisciplinary graduate school for the blue planet, ANR-17-EURE-0015, co-funded by the "Investissements d'Avenir" program).

ACKNOWLEDGMENTS

The authors would like to thank Céline Cordier, Mickael Vasquez, and Anthony Knights for assistance with field collections. The authors would also like to thank Maïwenn Lescop, Gautier Sourimant, and Jean-Dominique Gaffet for their help with sorting through reef samples and measuring worms. This study forms part of the REEHAB (REEf HABitat) project (www.honeycombworms.org).

SUPPLEMENTARY MATERIAL

The Supplementary Material for this article can be found online at: https://www.frontiersin.org/articles/10.3389/fmars.2021.654141/full#supplementary-material

REFERENCES

Adams, J. (1800). Description of some marine animals found on the coast of Wales. *Trans. Linn. Soc. Lon.* 5, 7–13.

Addo-Bediako, A., Chown, S. L., and Gaston, K. J. (2000). Thermal tolerance, climatic variability and latitude. *Proc. R. Soc. B Biol. Sci.* 267, 739–745. doi: 10.1098/rspb.2000.1065

Airoldi, L., Balata, D., and Beck, M. W. (2008). The Gray Zone: relationships between habitat loss and marine diversity and their applications in conservation. *J. Exp. Mar. Bio. Ecol.* 366, 8–15. doi: 10.1016/j.jembe.2008.07.034

Anderson, M. J., Crist, T. O., Chase, J. M., Vellend, M., Inouye, B. D., Freestone, A. L., et al. (2011). Navigating the multiple meanings of β diversity: a roadmap for the practicing ecologist. *Ecol. Lett.* 14, 19–28. doi: 10.1111/j.1461-0248.2010.01552.x

Anderson, M. J. (2017). Permutational multivariate analysis of variance (PERMANOVA). *Wiley StatsRef Stat. Ref. Online* 1–15. doi: 10.1002/9781118445112.stat07841

Argano, R., and Ponticelli, A. (1981). Nomenclature e geonemia di Sphaeroma monodi Arcangeli, 1934, del Mediterraneo e del Mar Nero (*Crustacea*, *Isopoda Flabellifera*). *Bolletino del Mus. Civ. di Stor. Nat. di Verona* 1980, 227–234.

Assis, J., Tyberghein, L., Bosch, S., Verbruggen, H., Serrão, E. A., and De Clerck, O. (2018). Bio-ORACLE v2.0: extending marine data layers for bioclimatic modelling. *Glob. Ecol. Biogeogr.* 27, 277–284. doi: 10.1111/geb.12693

Audouin, J. V., and Milne Edwards, H. (1833). [Part 3.] Classification des Annélides et description de celles qui habitent les côtes de la France. *Ann. des Sci. Nat. Paris* 28, 195–269.

Barnes, R. S. K., and Hamylton, S. (2015). Uniform functional structure across spatial scales in an intertidal benthic assemblage. *Mar. Environ. Res.* 106, 82–91. doi: 10.1016/j.marenvres.2015.03.006

Baselga, A. (2010). Partitioning the turnover and nestedness components of beta diversity. *Glob. Ecol. Biogeogr.* 19, 134–143. doi: 10.1111/j.1466-8238.2009.00490.x

Baselga, A. (2012). The relationship between species replacement, dissimilarity derived from nestedness, and nestedness. *Glob. Ecol. Biogeogr.* 21, 1223–1232. doi: 10.1111/j.1466-8238.2011.00756.x

Baselga, A. (2017). Partitioning abundance-based multiple-site dissimilarity into components: balanced variation in abundance and abundance gradients. *Methods Ecol. Evol.* 8, 799–808. doi: 10.1111/2041-210X.12693

Berke, S. K. (2010). Functional groups of ecosystem engineers: a proposed classification with comments on current issues. *Integr. Comp. Biol.* 50, 147–157. doi: 10.1093/icb/icq077

Bertness, M. D., and Callaway, R. (1994). Positive interactions in communities. *Trends Ecol. Evol.* 9, 191–193. doi: 10.1016/0169-5347(94)90088-4

Bhadury, P., Austen, M., Bilton, D., Lambshead, P., Rogers, A., and Smerdon, G. (2006). Development and evaluation of a DNA-barcoding approach for the rapid identification of nematodes. *Mar. Ecol. Prog. Ser.* 320, 1–9. doi: 10.3354/meps320001

Blanchet, H., De Montaudouin, X., Lucas, A., and Chardy, P. (2004). Heterogeneity of macrozoobenthic assemblages within a *Zostera noltii* seagrass bed: diversity, abundance, biomass and structuring factors. *Estuar. Coast. Shelf Sci.* 61, 111–123. doi: 10.1016/j.ecss.2004.04.008

Boström, C., Jackson, E. L., and Simenstad, C. A. (2006). Seagrass landscapes and their effects on associated fauna: a review. *Estuar. Coast. Shelf Sci.* 68, 383–403. doi: 10.1016/j.ecss.2006.01.026

Bouma, T. J., Ortells, V., and Ysebaert, T. (2009). Comparing biodiversity effects among ecosystem engineers of contrasting strength: macrofauna diversity in *Zostera noltii* and *Spartina anglica* vegetations. *Helgol. Mar. Res.* 63, 3–18. doi: 10.1007/s10152-008-0133-8

Boyé, A., Legendre, P., Grall, J., and Gauthier, O. (2017). Constancy despite variability: local and regional macrofaunal diversity in intertidal seagrass beds. *J. Sea Res.* 130, 107–122. doi: 10.1016/j.seares.2017.06.004

Boyé, A., Thiébaut, É, Grall, J., Legendre, P., Broudin, C., Houbin, C., et al. (2019). Trait-based approach to monitoring marine benthic data along 500 km of coastline. *Divers. Distrib* 25, 1879–1896. doi: 10.1111/ddi.12987

Briggs, J. C., and Bowen, B. W. (2012). A realignment of marine biogeographic provinces with particular reference to fish distributions. *J. Biogeogr.* 39, 12–30. doi: 10.1111/j.1365-2699.2011.02613.x

Brown, J. H. and Lomolino, M. V. (1998). *Biogeography. Sinaur.*

Bruno, J. F., Stachowicz, J. J., and Bertness, M. D. (2003). Inclusion of facilitation into ecological theory. *Trends Ecol. Evol.* 18, 119–125. doi: 10.1016/S0169-5347(02)00045-9

Buckley, L. B., Jonathan Davies, T., Ackerly, D. D., Kraft, N. J. B., Harrison, S. P., Anacker, B. L., et al. (2010). Phylogeny, niche conservatism and the latitudinal diversity gradient in mammals. *Proc. R. Soc. B Biol. Sci.* 277, 2131–2138. doi: 10.1098/rspb.2010.0179

Bulleri, F., Bruno, J. F., Silliman, B. R., and Stachowicz, J. J. (2016). Facilitation and the niche: implications for coexistence, range shifts and ecosystem functioning. *Funct. Ecol.* 30, 70–78. doi: 10.1111/1365-2435.12528

Bulleri, F., Eriksson, B. K., Queirós, A., Airoldi, L., Arenas, F., Arvanitidis, C., et al. (2018). Harnessing positive species interactions as a tool against climate-driven loss of coastal biodiversity. *PLoS Biol.* 16:e2006852. doi: 10.1371/journal.pbio.2006852

Burley, H. M., Mokany, K., Ferrier, S., Laffan, S. W., Williams, K. J., and Harwood, T. D. (2016). Macroecological scale effects of biodiversity on ecosystem functions under environmental change. *Ecol. Evol.* 6, 2579–2593. doi: 10.1002/ece3.2036

Cadotte, M. W., Carscadden, K., and Mirotchnick, N. (2011). Beyond species: functional diversity and the maintenance of ecological processes and services. *J. Appl. Ecol.* 48, 1079–1087. doi: 10.1111/j.1365-2664.2011.02048.x

Caine, E. A. (1977). Feeding mechanisms and possible resource partitioning of the Caprellidae (*Crustacea*: *Amphipoda*). *Mar. Biol.* 42, 331–336. doi: 10.1007/BF00402195

Callaway, R. (2006). Tube worms promote community change. *Mar. Ecol. Prog. Ser.* 308, 49–60. doi: 10.3354/meps308049

Chevenet, F., Dolédec, S., and Chessel, D. (1994). A fuzzy coding approach for the analysis of long-term ecological data. *Freshw. Biol.* 31, 295–309. doi: 10.1111/j.1365-2427.1994.tb01742.x

Clarke, K. R., and Warwick, R. M. (2001). A further biodiversity index applicable to species lists: variation in taxonomic distinctness. *Mar. Ecol. Prog. Ser.* 216, 265–278. doi: 10.3354/meps216265

Clarke, K. R., and Gorley, R. N. (2015). *PRIMER v7: User Manual/Tutorial.* Plymouth: PRIMER-E, Plymouth, 296.

Cornell, H. V., and Lawton, J. H. (1992). Species interactions, local and regional processes, and limits to the richness of ecological communities: a theoretical perspective. *J. Anim. Ecol.* 61, 1–12. doi: 10.2307/5503

Costello, M. J., Claus, S., Dekeyzer, S., Vandepitte, L., Tuama, É, Lear, D., et al. (2015). Biological and ecological traits of marine species. *PeerJ* 3:e1201. doi: 10.7717/peerj.1201

Curd, A., Cordier, C., Firth, L. B., Bush, L., Gruet, Y., Le Mao, P., et al. (2020). A broad-scale long-term dataset of *Sabellaria alveolata* distribution and abundance curated through the REEHAB (REEf HABitat) Project. *SEANOE.* doi: 10.17882/72164

Curd, A., Pernet, F., Corporeau, C., Delisle, L., Firth, L. B., Nunes, F. L. D., et al. (2019). Connecting organic to mineral: how the physiological state of an ecosystem-engineer is linked to its habitat structure. *Ecol. Indic.* 98, 49–60. doi: 10.1016/j.ecolind.2018.10.044

Cusson, M., and Bourget, E. (2005). Global patterns of macroinvertebrate production in marine benthic habitats. *Mar. Ecol. Prog. Ser.* 297, 1–14.

Daguin, C., Bonhomme, F., and Borsa, P. (2001). The zone of sympatry and hybridization of *Mytilus edulis* and *M. galloprovincialis*, as described by intron length polymorphism at locus mac-1. *Heredity* 86, 342–354. doi: 10.1046/j.1365-2540.2001.00832.x

D'Amen, M., Rahbek, C., Zimmermann, N. E., and Guisan, A. (2017). Spatial predictions at the community level: from current approaches to future frameworks. *Biol. Rev.* 92, 169–187. doi: 10.1111/brv.12222

Dayton, P. K. (1972). "Toward an understanding of community resilience and the potential effects of enrichments to the benthos at McMurdo Sound, Antarctica," in *Proceedings of the Colloquium on Conservation Problems in Antarctica*, Lawrence, KS, 81–96.

De Juan, S., and Hewitt, J. (2011). Relative importance of local biotic and environmental factors versus regional factors in driving macrobenthic species richness in intertidal areas. *Mar. Ecol. Prog. Ser.* 423, 117–129. doi: 10.3354/meps08935

De Smet, B., D'Hondt, A. S., Verhelst, P., Fournier, J., Godet, L., Desroy, N., et al. (2015). Biogenic reefs affect multiple components of intertidal soft-bottom benthic assemblages: the *Lanice conchilega* case study. *Estuar. Coast. Shelf Sci.* 152, 44–55. doi: 10.1016/j.ecss.2014.11.002

Delle Chiaje, S. (1841). *Descrizione e notomia degli animali invertebrati della Sicilia citeriore: osservati vivi negli anni 1822–1830/da S. delle Chiale*. 2nd editi. Naples.

Dias, A. S., and Paula, J. (2001). Associated fauna of *Sabellaria alveolata* colonies on the central coast of Portugal. *J. Mar. Biol. Assoc. U. K.* 81, 169–170. doi: 10.1017/S0025315401003538

Díaz, S., and Cabido, M. (2001). Vive la différence: plant functional diversity matters to ecosystem processes. *Trends Ecol. Evol.* 16, 646–655. doi: 10.1016/S0169-5347(01)02283-2

Dinter, W. (2001). *Biogeography of the OSPAR Maritime Area*. Bonn: German Federal Agency for Nature Conservation.

Dormann, C. F., Elith, J., Bacher, S., Buchmann, C., Carl, G., Carré, G., et al. (2013). Collinearity: a review of methods to deal with it and a simulation study evaluating their performance. *Ecography* 36, 27–46. doi: 10.1111/j.1600-0587.2012.07348.x

Dray, S., and Dufour, A. B. (2007). The ade4 package: implementing the duality diagram for ecologists. *J. Stat. Softw.* 22, 1–20. doi: 10.18637/jss.v022.i04

Dubois, S., Commito, J. A., Olivier, F., and Retière, C. (2006). Effects of epibionts on *Sabellaria alveolata* (L.) biogenic reefs and their associated fauna in the Bay of Mont Saint-Michel. *Estuar. Coast. Shelf Sci.* 68, 635–646. doi: 10.1016/j.ecss.2006.03.010

Dubois, S., Retière, C., and Olivier, F. (2002). Biodiversity associated with *Sabellaria alveolata* (*Polychaeta*: Sabellariidae) reefs: effects of human disturbances. *J. Mar. Biol. Assoc. U. K.* 82, 817–826. doi: 10.1017/S0025315402006185

Fager, E. W. (1964). Marine sediments: effects of a tube-building polychaete. *Science* 143, 356–359. doi: 10.1126/science.143.3604.356

Fauchald, K., and Jumars, P. A. (1979). The diet of worms: a study of polychaete feeding guilds. *Oceanogr. Mar. Biol. Annu. Rev.* 17, 193–284.

Fine, P. V. A. (2015). Ecological and evolutionary drivers of geographic variation in species diversity. *Annu. Rev. Ecol. Evol. Syst.* 46, 369–392. doi: 10.1146/annurev-ecolsys-112414-054102

Firth, L. B., Harris, D., Blaze, J. A., Marzloff, M. P., Boyé, A., Miller, P. I., et al. (2021). Specific niche requirements underpin multi-decadal range edge stability, but may introduce barriers for climate change adaptation. *Divers Distrib.* 27, 668–683. doi: 10.1111/ddi.13224

Forbes, E., and Godwin-Austen, R. A. C. (1859). *The Natural History of the European Seas. By the late Prof. Edw. Forbes…* London: J. Van Voorst.

Fordham, D. A., Brown, S. C., Wigley, T. M. L., and Rahbek, C. (2019). Cradles of diversity are unlikely relics of regional climate stability. *Curr. Biol.* 29, R356–R357. doi: 10.1016/j.cub.2019.04.001

Gaston, K. J., and Chown, S. L. (1999). Why Rapoport's rule does not generalise. *Oikos* 84, 309–312. doi: 10.2307/3546727

Gaucherel, C., Tramier, C., Devictor, V., Svenning, J. C., and Hély, C. (2018). Where and at which scales does the latitudinal diversity gradient fail? *J. Biogeogr.* 45, 1905–1916. doi: 10.1111/jbi.13355

Gruet, Y. (1986). Spatio-temporal changes of Sabellarian reefs built by the sedentary polychaete *Sabellaria alveolata* (Linné). *Mar. Ecol.* 7, 303–319. doi: 10.1111/j.1439-0485.1986.tb00166.x

Hastings, A., Byers, J. E., Crooks, J. A., Cuddington, K., Jones, C. G., Lambrinos, J. G., et al. (2007). Ecosystem engineering in space and time. *Ecol. Lett.* 10, 153–164. doi: 10.1111/j.1461-0248.2006.00997.x

Hawkins, B. A. (2001). Ecology's oldest pattern? *Trends Ecol. Evol.* 16:470.

Hawkins, B. A. (2003). Energy, water and broad-scale geographic patterns of species richness. *Ecology* 84, 3105–3117.

Hawkins, B. A., and Diniz-Filho, J. A. F. (2004). "Latitude" and geographic patterns in species richness. *Ecography* 27, 268–272. doi: 10.1111/j.0906-7590.2004.03883.x

Hawkins, S. J., Pack, K. E., Firth, L. B., Mieszkowska, N., Evans, A. J., Martins, G. M., et al. (2019). "The intertidal zone of the north-east atlantic region," in *Interactions in the Marine Benthos*, eds S. J. Hawkins, K. Bohn, L. B. Firth,

and G. A. Williams (Cambridge: Cambridge University Press), doi: 10.1017/9781108235792.003

Hemingson, C. R., and Bellwood, D. R. (2018). Biogeographic patterns in major marine realms: function not taxonomy unites fish assemblages in reef, seagrass and mangrove systems. *Ecography* 41, 174–182. doi: 10.1111/ecog.03010

Hewitt, J. E., Thrush, S. F., and Dayton, P. D. (2008). Habitat variation, species diversity and ecological functioning in a marine system. *J. Exp. Mar. Bio. Ecol.* 366, 116–122. doi: 10.1016/j.jembe.2008.07.016

Hewitt, J. E., Thrush, S. F., Halliday, J., and Duffy, C. (2005). The importance of small-scale habitat structure for maintaining beta diversity. *Ecology* 86, 1619–1626. doi: 10.1890/04-1099

Hill, M. O. (1973). Diversity and evenness: a unifying notation and its consequences. *Ecology* 54, 427–432.

Hillebrand, H. (2004). On the generality of the latitudinal diversity gradient. *Am. Nat.* 163, 192–211. doi: 10.1126/science.26.678.918

Holt, T. J., Rees, E. I., Hawkins, S. J., and Seed, R. (1998). *Biogenic Reefs. An Overview of Dynamic and Sensitivity Characteristics for Conservation Management of Marine SACs*, vol. IX (United Kingdom: Scottish Association for Marine Science (UK Marine SACs Project)), 1–169.

Hummel, H., Van Avesaath, P., Wijnhoven, S., Kleine-Schaars, L., Degraer, S., Kerckhof, F., et al. (2017). Geographic patterns of biodiversity in European coastal marine benthos. *J. Mar. Biol. Assoc. U. K.* 97, 507–523. doi: 10.1017/S0025315416001119

Jain, M., Flynn, D. F. B., Prager, C. M., Hart, G. M., Devan, C. M., Ahrestani, F. S., et al. (2014). The importance of rare species: a trait-based assessment of rare species contributions to functional diversity and possible ecosystem function in tall-grass prairies. *Ecol. Evol.* 4, 104–112. doi: 10.1002/ece3.915

Jansen, J. M., Pronker, ÆA. E., Kube, ÆS., Sokolowski, ÆA., Sola, J. C., Marquiegui, ÆM. A., et al. (2007). Geographic and seasonal patterns and limits on the adaptive response to temperature of European *Mytilus* spp . and *Macoma balthica* populations. *Oecologia* 154, 23–34. doi: 10.1007/s00442-007-0808-x

Jenkins, S. R., Moore, P., Burrows, M. T., Garbary, D. J., Hawkins, S. J., Ingólfsson, A., et al. (2008). Comparative ecology of North Atlantic shores: do differences in players matter for process? *Ecology* 89, S3–S23. doi: 10.1890/07-1155.1

Jones, A. G., Dubois, S. F., and Desroy, N. (2018). Interplay between abiotic factors and species assemblages mediated by the ecosystem engineer *Sabellaria alveolata* (*Annelida*: *Polychaeta*). *Estuar., Coast. Shelf Sci.* 200, 1–18. doi: 10.1016/j.ecss.2017.10.001

Jones, C. G., Lawton, J. H., and Shachak, M. (1994). *Organisms as Ecosystem Engineers*.

Jost, L. (2006). Entropy and diversity. *Oikos* 113, 363–375.

Jumars, P. A., Dorgan, K. M., and Lindsay, S. M. (2015). Diet of worms emended: an update of polychaete feeding guilds. *Ann. Rev. Mar. Sci.* 7, 497–520. doi: 10.1146/annurev-marine-010814-020007

Jurgens, L. J., and Gaylord, B. (2018). Physical effects of habitat-forming species override latitudinal trends in temperature. *Ecol. Lett.* 21, 190–196. doi: 10.1111/ele.12881

Kendall, M. A. (1996). Are Arctic soft-sediment macrobenthic communities impoverished? *Polar Biol.* 16, 393–399. doi: 10.1007/BF02390421

Kendall, M. A., and Aschan, M. (1993). Latitudinal gradients in the structure of macrobenthic communities: a comparison of Arctic, temperate and tropical sites. *J. Exp. Mar. Bio. Ecol.* 172, 157–169. doi: 10.1016/0022-0981(93)90095-6

Lamarck, J.-B. M. (1819). *Histoire naturelle des animaux sans vertèbres . . . précédée d'une introduction offrant la détermination des caractères essentiels de l'animal, sa distinction du végétal et des autres corps naturels, enfin, l'exposition des principes fondamentaux de la zool.*. Paris: Verdière.

Lam-Gordillo, O., Baring, R., and Dittmann, S. (2020). Establishing the South Australian Macrobenthic Traits (SAMT) database: a trait classification for functional assessments. *Ecol. Evol.* 10, 14372–14387. doi: 10.1002/ece3.7040

Leblanc, C., Schaal, G., Cosse, A., Destombe, C., Valero, M., Riera, P., et al. (2011). Trophic and biotic interactions in *Laminaria digitata* beds: which factors could influence the persistence of marine kelp forests in northern Brittany? *Cah. Biol. Mar.* 52, 415–427.

Legendre, P. (2014). Interpreting the replacement and richness difference components of beta diversity. *Glob. Ecol. Biogeogr.* 23, 1324–1334. doi: 10.1111/geb.12207

Legendre, P., and Andersson, M. J. (1999). Distance-based redundancy analysis: testing multispecies responses in multifactorial ecological experiments. *Ecol. Monogr.* 69, 1–24.

Leitão, R. P., Zuanon, J., Villéger, S., Williams, S. E., Baraloto, C., Fortune, C., et al. (2016). Rare species contribute disproportionately to the functional structure of species assemblages. *Proc. R. Soc. B Biol. Sci* 283:20160084. doi: 10.1098/rspb.2016.0084

Lima, F. P., and Wethey, D. S. (2009). Robolimpets: measuring intertidal body temperatures using biomimetic loggers. *Limnol. Oceanogr. Methods* 7, 347–353. doi: 10.4319/lom.2009.7.347

Linnaeus, C. (1753). *Species Plantarum, Exhibentes Plantas rite Cognitas ad Genera Relatas cum Differentiis Specificis, Nominibus Trivialibus, Synonymis Selectis, Locis Natalibus, Secundum Systema Sexuale Digestas*. Stockholm: Salvius, doi: 10.5962/bhl.title.59734

Linnaeus, C. (1767). *Systema Naturae per Regna tria Naturae: Secundum Classes, Ordines, Genera, Species, cum Characteribus, Differentiis, Synonymis, locis. Ed. 12. 1., Regnum Animale. 1 & 2*. Stockholm: Laurentii Salvii.

Loiseau, N., Legras, G., Kulbicki, M., Mérigot, B., Harmelin-Vivien, M., Mazouni, N., et al. (2017). Multi-component β-diversity approach reveals conservation dilemma between species and functions of coral reef fishes. *J. Biogeogr.* 44, 537–547. doi: 10.1111/jbi.12844

Martini, S., Larras, F., Boyé, A., Faure, E., Aberle, N., Archambault, P., et al. (2020). Functional trait-based approaches as a common framework for aquatic ecologists. *Limnol. Oceanogr.* 66, 965–994. doi: 10.1002/lno.11655

McArdle, B. H., and Anderson, M. J. (2001). Fitting multivariate models to community data: a comment on distance-based redundancy analysis. *Ecology* 82, 290–297.

Meynard, C. N., Devictor, V., Mouillot, D., Thuiller, W., Jiguet, F., and Mouquet, N. (2011). Beyond taxonomic diversity patterns: how do α, β and γ components of bird functional and phylogenetic diversity respond to environmental gradients across France? *Glob. Ecol. Biogeogr.* 20, 893–903. doi: 10.1111/j.1466-8238.2010.00647.x

Mittelbach, G. G., Schemske, D. W., Cornell, H. V., Allen, A. P., Brown, J. M., Bush, M. B., et al. (2007). Evolution and the latitudinal diversity gradient: speciation, extinction and biogeography. *Ecol. Lett.* 10, 315–331. doi: 10.1111/j.1461-0248.2007.01020.x

Mori, A. S., Isbell, F., and Seidl, R. (2018). β-Diversity, community assembly, and ecosystem functioning. *Trends Ecol. Evol.* 33, 549–564. doi: 10.1016/j.tree.2018.04.012

Mouillot, D., Bellwood, D. R., Baraloto, C., Chave, J., Galzin, R., Harmelin-Vivien, M., et al. (2013). Rare species support vulnerable functions in high-diversity ecosystems. *PLoS Biol.* 11:e1001569. doi: 10.1371/journal.pbio.1001569

Mouillot, D., Villéger, S., Parravicini, V., Kulbicki, M., Arias-González, J. E., Bender, M., et al. (2014). Functional over-redundancy and high functional vulnerability in global fish faunas on tropical reefs. *Proc. Natl. Acad. Sci. U.S.A.* 111, 13757–13762. doi: 10.1073/pnas.1317625111

Müller, O. F. (1776). *Zoologiæ Danicæ Prodromus, seu Animalium Daniæ et Norvegiæ Indigenarum Characteres, Nomina, et Synonyma Imprimis Popularium*. Copenhagen: Hallageri, doi: 10.5962/bhl.title.13268

Muller, A., Poitrimol, C., Nunes, F. L. D., Curd, A., Desroy, N., Firth, L. B., et al. (2021). Functional traits of benthic marine invertebrates associated with honeycomb worm reefs in Europe. *SEANOE*. doi: 10.17882/79817

Münkemüller, T., de Bello, F., Meynard, C. N., Gravel, D., Lavergne, S., Mouillot, D., et al. (2012). From diversity indices to community assembly processes: a test with simulated data. *Ecography* 35, 468–480. doi: 10.1111/j.1600-0587.2011.07259.x

Munksby, N., Benthien, M., and Glud, R. N. (2002). Flow-induced flushing of relict tube structures in the central Skagerrak (Norway). *Mar. Biol.* 141, 939–945. doi: 10.1007/s00227-002-0874-x

Noernberg, M. A., Fournier, J., Dubois, S., and Populus, J. (2010). Using airborne laser altimetry to estimate *Sabellaria alveolata* (*Polychaeta*: Sabellariidae) reefs volume in tidal flat environments. *Estuar. Coast. Shelf Sci.* 90, 93–102. doi: 10.1016/j.ecss.2010.07.014

O'Connor, N. E., and Crowe, T. P. (2005). Biodiversity loss and ecosystem functioning: distinguishing between number and identity of species. *Ecology* 86, 1783–1796. doi: 10.1890/04-1172

Oksanen, A. J., Blanchet, F. G., Friendly, M., Kindt, R., Legendre, P., Mcglinn, D., et al. (2020). *Package ' vegan .'*.

Pallas, P. S. (1766). *Miscellanea Zoologica. Quibus Novae Imprimis Atque Obscurae Animalium Species Describuntur et Observationibus Iconibusque Illustrantur. Petrum van Cleef.*

Pavoine, S., and Bonsall, M. B. (2011). Measuring biodiversity to explain community assembly: a unified approach. *Biol. Rev.* 86, 792–812. doi: 10.1111/j.1469-185X.2010.00171.x

Plicanti, A., Domínguez, R., Dubois, S. F., and Bertocci, I. (2016). Human impacts on biogenic habitats: effects of experimental trampling on *Sabellaria alveolata* (Linnaeus, 1767) reefs. *J. Exp. Mar. Bio. Ecol.* 478, 34–44. doi: 10.1016/j.jembe.2016.02.001

Queirós, A. M., Birchenough, S. N. R., Bremner, J., Godbold, J. A., Parker, R. E., Romero-Ramirez, A., et al. (2013). A bioturbation classification of European marine infaunal invertebrates. *Ecol. Evol.* 3, 3958–3985. doi: 10.1002/ece3.769

R Development Core Team (2008). *R: A Language and Environment for Statistical Computing*. Vienna, Austria: R Foundation for Statistical Computing. Available online at: http://www.R-project.org.

Rabaut, M., Guilini, K., Van Hoey, G., Vincx, M., and Degraer, S. (2007). A bio-engineered soft-bottom environment: the impact of *Lanice conchilega* on the benthic species-specific densities and community structure. *Estuar. Coast. Shelf Sci.* 75, 525–536. doi: 10.1016/j.ecss.2007.05.041

Renaud, P. E., Webb, T. J., Bjørgesaeter, A., Karakassis, I., Kędra, M., Kendall, M. A., et al. (2009). Continental-scale patterns in benthic invertebrate diversity:: insights from the MacroBen database. *Source Mar. Ecol. Prog. Ser.* 382, 239–252. doi: 10.2307/24873169

Ricklefs, R. E. (2004). A comprehensive framework for global patterns in biodiversity. *Ecol. Lett.* 7, 1–15. doi: 10.1046/j.1461-0248.2003.00554.x

Rigolet, C., Dubois, S. F., and Thiébaut, E. (2014). Benthic control freaks: effects of the tubiculous amphipod *Haploops nirae* on the specific diversity and functional structure of benthic communities. *J. Sea Res.* 85, 413–427. doi: 10.1016/j.seares.2013.07.013

Riosmena-Rodríguez, R., Nelson, W., and Aguirre, J. (2017). *Rhodolith / Maërl Beds: A Global Perspective*. Berlin: Springer.

Rohde, K. (1992). Latitudinal gradients in species diversity: the search for the primary cause. *Oikos* 65, 514–527.

Rolland, J., Condamine, F. L., Beeravolu, C. R., Jiguet, F., and Morlon, H. (2015). Dispersal is a major driver of the latitudinal diversity gradient of Carnivora. *Glob. Ecol. Biogeogr.* 24, 1059–1071. doi: 10.1111/geb.12354

Rumbold, C. E., Obenat, S. M., and Spivak, E. D. (2012). Life history of *Tanais dulongii* (*Tanaidacea*: *Tanaidae*) in an intertidal flat in the Southwestern Atlantic. *J. Crustac. Biol.* 32, 891–898. doi: 10.1163/1937240X-00002094

Saint-Joseph, A. (1888). Les annélides polychètes des côtes de Dinard. Seconde partie. *Ann. des Sci. Nat. Zool. Paléontol. Paris Sér.* 5, 141–338. plates VI-XIII.,

Sarà, M. (1986). Sessile macrofauna and marine ecosystem. *Bolletino di Zool.* 53, 329–337. doi: 10.1080/11250008609355518

Schlund, E., Basuyaux, O., Lecornu, B., Pezy, J., Baffreau, A., and Dauvin, J. C. (2016). Macrofauna associated with temporary *Sabellaria alveolata* reefs on the west coast of Cotentin (France). *Springerplus* 5, 1–21. doi: 10.1186/s40064-016-2885-y

Schmera, D., Podani, J., and Legendre, P. (2020). What do beta diversity components reveal from presence-absence community data? Let us connect every indicator to an indicandum! *Ecol. Indic.* 117:106540. doi: 10.1016/j.ecolind.2020.106540

Schöb, C., Butterfield, B. J., and Pugnaire, F. I. (2012). Foundation species influence trait-based community assembly. *New Phytol.* 196, 824–834. doi: 10.1111/j.1469-8137.2012.04306.x

Socolar, J. B., Gilroy, J. J., Kunin, W. E., and Edwards, D. P. (2016). How should beta-diversity inform biodiversity conservation? *Trends Ecol. Evol.* 31, 67–80. doi: 10.1016/j.tree.2015.11.005

Solan, M., Cardinale, B. J., Downing, A. L., Engelhardt, K. A. M., Ruesink, J. L., and Srivastava, D. S. (2004). Extinction and ecosystem function in the marine benthos. *Science* 306, 1177–1180. doi: 10.1126/science.1103960

Sørensen, T. J. (1948). A method of establishing groups of equal amplitude in plant sociology based on similarity of species content and its application to analyses of the vegetation on Danish commons. *Biologiske Skrifter/Kongelige Danske Videnskabernes Selskab* 5, 1–34.

Spalding, M. D., Fox, H. E., Allen, G. R., Davidson, N., Ferdaña, Z. A., Finlayson, M. A. X., et al. (2007). Marine ecoregions of the world: a bioregionalization of coastal and shelf areas. *Bioscience* 57, 573–583.

Statzner, B., Resh, V. H., and Roux, A. L. (1994). The synthesis of long-term ecological research in the context of concurrently developed ecological theory: design of a research strategy for the Upper Rhône River and its floodplain. *Freshw. Biol.* 31, 253–263. doi: 10.1111/j.1365-2427.1994.tb01739.x

Storch, D., and Okie, J. G. (2019). The carrying capacity for species richness. *Glob. Ecol. Biogeogr.* 28, 1519–1532. doi: 10.1111/geb.12987

Swenson, N. G., Anglada-Cordero, P., and Barone, J. A. (2011). Deterministic tropical tree community turnover: evidence from patterns of functional beta diversity along an elevational gradient. *Proc. R. Soc. B Biol. Sci.* 278, 877–884. doi: 10.1098/rspb.2010.1369

Teagle, H., Moore, P. J., Jenkins, H., and Smale, D. A. (2018). Spatial variability in the diversity and structure of faunal assemblages associated with kelp holdfasts (*Laminaria hyperborea*) in the northeast Atlantic. *PLoS One* 13:e0200411. doi: 10.1371/journal.pone.0200411

Thrush, S. F., Hewitt, J. E., Gibbs, M., Lundquist, C., and Norkko, A. (2006). Functional role of large organisms in intertidal communities: community effects and ecosystem function. *Ecosystems* 9, 1029–1040. doi: 10.1007/s10021-005-0068-8

Tyberghein, L., Verbruggen, H., Pauly, K., Troupin, C., Mineur, F., and De Clerck, O. (2012). Bio-ORACLE: a global environmental dataset for marine species distribution modelling. *Glob. Ecol. Biogeogr.* 21, 272–281. doi: 10.1111/j.1466-8238.2011.00656.x

Usseglio-Polatera, P., Bournaud, M., Richoux, P., and Tachet, H. (2000). Biological and ecological traits of benthic freshwater macroinvertebrates: relationships and definition of groups with similar traits. *Freshw. Biol.* 43, 175–205. doi: 10.1046/j.1365-2427.2000.00535.x

Van Hoey, G., Guilini, K., Rabaut, M., Vincx, M., and Degraer, S. (2008). Ecological implications of the presence of the tube-building polychaete *Lanice conchilega* on soft-bottom benthic ecosystems. *Mar. Biol.* 154, 1009–1019. doi: 10.1007/s00227-008-0992-1

Villéger, S., Grenouillet, G., and Brosse, S. (2013). Decomposing functional β-diversity reveals that low functional β-diversity is driven by low functional turnover in European fish assemblages. *Glob. Ecol. Biogeogr.* 22, 671–681. doi: 10.1111/geb.12021

Villéger, S., Miranda, J. R., Hernández, D. F., and Mouillot, D. (2010). Contrasting changes in taxonomic vs. functional diversity of tropical fish communities after habitat degradation. *Ecol. Appl.* 20, 1512–1522. doi: 10.1890/09-1310.1

Ward, J. H. (1963). Hierarchical grouping to optimize an objective function. *J. Am. Stat. Assoc.* 58, 236–244.

Wenne, R., Zbawicka, M., Bach, L., Strelkov, P., Gantsevich, M., Kukliński, P., et al. (2020). Trans-Atlantic distribution and introgression as inferred from single nucleotide polymorphism: mussels *Mytilus* and environmental factors. *Genes* 11:530. doi: 10.3390/genes11050530

Whittaker, R. H. (1972). Evolution and measurement of species diversity. *Taxon* 21, 213–251. doi: 10.2307/1218190

Wilson, R. S., Cohen, B. F., and Poore, G. C. B. (1993). *The Role of Suspension-Feeding and Deposit-Feeding Benthic Macroinvertebrates in Nutrient Cycling in Port Phillip Bay*. Melbourne: CSIRO.

Zühlke, R. (2001). Polychaete tubes create ephemeral community patterns: *Lanice conchilega* (Pallas, 1766) associations studied over six years. *J. Sea Res.* 46, 261–272. doi: 10.1016/S1385-1101(01)00091-0

Zühlke, R., Blome, D., Van Bernem, K. H., and Dittmann, S. (1998). Effects of the tube-building polychaete *Lanice conchilega* (Pallas) on benthic macrofauna and nematodes in an intertidal sandflat. *Senckenbergiana Maritima* 29, 131–138. doi: 10.1007/BF03043951

Conflict of Interest: LB was employed by the company Fugro GB Marine Limited.

The remaining authors declare that the research was conducted in the absence of any commercial or financial relationships that could be construed as a potential conflict of interest.

Citation: Muller A, Poitrimol C, Nunes FLD, Boyé A, Curd A, Desroy N, Firth LB, Bush L, Davies AJ, Lima FP, Marzloff MP, Meneghesso C, Seabra R and Dubois SF (2021) Musical Chairs on Temperate Reefs: Species Turnover and Replacement Within Functional Groups Explain Regional Diversity Variation in Assemblages Associated With Honeycomb Worms. Front. Mar. Sci. 8:654141. doi: 10.3389/fmars.2021.654141

frontiers in Marine Science

ORIGINAL RESEARCH
published: 31 May 2021
doi: 10.3389/fmars.2021.642764

Impacts of Pervasive Climate Change and Extreme Events on Rocky Intertidal Communities: Evidence From Long-Term Data

Nova Mieszkowska[1,2], Michael T. Burrows[3], Stephen J. Hawkins[2,4,5] and Heather Sugden[6]*

[1] School of Ocean and Earth Science, University of Liverpool, Liverpool, United Kingdom, [2] Marine Biological Association, Plymouth, United Kingdom, [3] Scottish Association for Marine Science, Oban, United Kingdom, [4] School of Ocean and Earth Science, University of Southampton, Southampton, United Kingdom, [5] School of Biological and Marine Sciences, University of Plymouth, Plymouth, United Kingdom, [6] The Dove Marine Laboratory, School of Natural and Environmental Sciences, Newcastle University, Newcastle, United Kingdom

OPEN ACCESS

Edited by:
Marcos Rubal, University of Porto, Portugal

Reviewed by:
Angus Jackson, Marine Conservation Society, United Kingdom
Camilla Bertolini, Ca' Foscari University of Venice, Italy
Paul Robert Brooks, University College Dublin, Ireland

***Correspondence:**
Nova Mieszkowska
nova@liverpool.ac.uk;
nova@MBA.ac.uk

Specialty section:
This article was submitted to Marine Evolutionary Biology, Biogeography and Species Diversity, a section of the journal Frontiers in Marine Science

Received: *16 December 2020*
Accepted: *12 March 2021*
Published: *31 May 2021*

Citation:
Mieszkowska N, Burrows MT, Hawkins SJ and Sugden H (2021) Impacts of Pervasive Climate Change and Extreme Events on Rocky Intertidal Communities: Evidence From Long-Term Data. Front. Mar. Sci. 8:642764. doi: 10.3389/fmars.2021.642764

Annual surveys of the abundance of intertidal invertebrates and macroalgae have been made at between 70 and 100 rocky intertidal time-series sites around the United Kingdom coastline since 2002 under the MarClim project. The data provide a unique opportunity to investigate the impacts of both pervasive climate change and their punctuation by extreme events on intertidal species. After the extreme storm events in the 2013/2014 winter season and the record heatwaves in the summers of 2018 and 2020, MarClim surveys recorded both physical and biological changes to rocky shore habitats. Subsequent surveys reassessed the effects on community structure via analysis of those species that resisted storm damage, those species that returned after the extreme storm events, and species that opportunistically occupied vacant habitat after storm-induced species loss. In addition, biannual storm damage surveys documenting communities recovery were carried out in the spring and winter of each year from 2014 to 2020 at three MarClim sites in north Cornwall (Crackington Haven, Trevone, and St. Ives), which experienced different types of abiotic and biotic damage resulting from these storms. Impacts of heatwaves and cold spells on the abundance of species were determined by regression on frequencies of event per year. Species of invertebrates and macroalgae generally declined in years of more frequent winter cold spells and summer heatwaves, while winter heatwaves and summer cold spells had similar numbers of positive and negative effects across species. Winter warm spells tended to have a more negative effect on cold-affinity species than on warm-affinity species. No abrupt shift was recorded after the 2013/2014 storms. Whilst a short-term change in some species was recorded in quantitative quadrat surveys, the biological communities returned to the long-term species composition and abundance within 2 years. The heatwave events caused sublethal heat damage in macroalgae, evidenced as dried areas of tissue on many individuals, with mortality-induced reductions in the abundance of only a few invertebrate species, recorded in Scotland and southwest

England after the heatwave events in 2018 and 2020. MarClim and storm-damage surveys indicate that there have been no sustained impacts from either extreme thermal or storm events across the rocky intertidal communities, and biodiversity has not been significantly altered as a result. The abundance and biogeographical distributions of rocky intertidal species and communities around the United Kingdom are being driven by longer-term, large scale, pervasive change in environmental conditions, with a gradual shift towards dominance of Lusitanian species from the early 2000s in responses to warming of the marine climate.

Keywords: climate change, intertidal, invertebrate, biogeography, range shift, time-series, Species Thermal Index, extreme event

INTRODUCTION

Storms and heatwaves are becoming more frequent as a result of climate warming (Oliver et al., 2018; IPCC, 2019) with significant impacts on the coastal ecosystems of the world (Smale et al., 2019). Long-term sustained observing programmes have shown evidence of community-wide shifts in composition from cold to warm affinity species (Simpson et al., 2011; Burrows et al., 2019) as long-term trends, but such studies neglect the short-term effects of extreme events.

The marine climate of the British Isles and Ireland has undergone oscillations throughout the 20th century, with the onset of global climate change first becoming evident in the late 1980s (Hawkins et al., 2003; Philippart et al., 2011). The warming trend has slowed down over the last decade (NOAA OISST; Reynolds et al., 2007) due to the climate-driven slowdown in the Atlantic Meridional Overturning Circulation (AMOC) causing a colder patch of surface water to the northwest of the United Kingdom[1] This has been reflected in changes in intertidal communities (Burrows et al., 2020). Despite the recent slowing of the warming trend in the United Kingdom, the impacts of climate change are still being experienced, especially the punctuation of pervasive climate change by extreme events (Firth et al., 2015). There has been an increase in both winter and summer extreme events, with 2020 being recently announced as the warmest year on record (NOAA OISST; Reynolds et al., 2007; Madge, 2020; National Oceanic Atmospheric Administration, 2020). Thus it is important to improve understanding of the impacts of climate by extreme events, or climate-driven disturbances on the natural environment and the resultant persistence of the associated communities, rather than just focusing on average annual sea temperatures.

Biological responses to climate change in natural systems are variable, non-linear, and difficult to interpret (Harris et al., 2018). Climate change exerts complex, interacting influences on organismal physiology, with species-specific responses due to different functional traits, sensitivity, and adaptive and acclimatory capacities (Huey et al., 2012). Shifts in the temporal dynamics of recruitment and the abundance of ecosystem engineers in response to environmental changes can modify interaction networks and change the vulnerability of entire communities to disturbance, although the degree of potential change is poorly understood (Mrowicki et al., 2016). Biological responses include aphasic and idiosyncratic shifts in species distributions (Hawkins et al., 2009) that are likely to result in novel ecological conditions in future climates that have no previous analogue (Elith and Leathwick, 2009; Kuo and Sanford, 2009; Pearson et al., 2009). This results in non-analogous communities for which there is no contemporary equivalent in terms of species composition, abundance, community structure, and hence ecosystem processes. In the face of environmental changes in marine and terrestrial systems, there is a need for accurate forecasts of composition and structure of communities and likely consequences for functioning of ecosystems and hence delivery of services to society.

The effects of long-term trends in temperature on changes in the distribution and abundance of marine species are becoming better understood, with range limits shifting polewards (Poloczanska et al., 2013) and a shifting balance of species with colder thermal tolerance ranges (cold-affinity species) and species with warmer thermal tolerance ranges (warm affinity species) within communities (Burrows et al., 2019, 2020). Impacts of short-term variation in temperature, particularly marine heatwaves (Hobday et al., 2016), however, are less well understood. Positive and negative changes in abundance, as well as range expansions and contractions are associated with marine heatwaves (Smale et al., 2019), with species at locations in the warmer half of their distribution ranges tending to be more negatively impacted. Heatwaves are becoming more frequent, longer, and more intense (Oliver et al., 2018), with increasing ecological impacts expected for the rest of this century (Frölicher and Laufkötter, 2018; Oliver et al., 2018, 2019).

The British Isles and Ireland along with much of the North-East Atlantic have rich rocky intertidal habitats (Lewis, 1964; Hawkins et al., 2019b) due to a complex coastline with sharp wave exposure gradients, a broad spectrum of tidal ranges and diverse geologies contributing to differing topographic complexities. There are also mesoscale differences in the fetch and aspect of the coastline and gradients between oceanic and more neritic waters into the Irish and North Seas and along the English Channel. The complex coastline also contributes to differences in larval retention and dispersal. All the above occur across a broader environmental gradient of warmer waters to the south and west and colder waters to the north and east, creating a biogeographic boundary zone region where boreal, lusitanian, and invasive species with different thermal affinities mix (Forbes,

[1]https://www.ncdc.noaa.gov/cdo-web/

1858; Southward et al., 1995; Simkanin et al., 2005; Helmuth et al., 2006; Mieszkowska et al., 2006; Burrows et al., 2020).

Winter storm events are common, exerting both hydrodynamic pressure in the form of bottom currents, and wind driven storm disturbance (Birchenough et al., 2015). Storm events represent a natural disturbance event in United Kingdom intertidal habitats with impacts including smothering by sediment and displacement by hydrodynamic shear or scouring by wave driven cobbles and finer sediments (Sugden et al., 2008; Birchenough et al., 2015). There is differential adaptation of intertidal species to wave-generated disturbance along wave exposure gradients (Raffaelli and Hawkins, 1996). Changes to the frequency and intensity of extreme storm events may have a greater impact on species survival, communities composition to ephemeral early successional species (Sousa, 1979), with implications for stability, functioning, and resilience of rocky shore communities (Posey et al., 1996; Sugden et al., 2007; Machado et al., 2016; Dzwonkowski et al., 2020). Extreme events including storm events and heat waves are predicted to increase in frequency and intensity (IPCC, 2013) as a consequence of climate change (Machado et al., 2016), with an increase in North Atlantic storms already recorded since the end of the 20th Century (Wolf et al., 2020).

The 2013/2014 winter was meteorologically classified as "highly unusual" (Met Office, 2014), with "very severe" storms periods and associated wave conditions characterised. The combination of high cyclone frequency and above-average cyclone intensity resulted in exceptional storminess, with a succession of major storm events occurring between mid-December 2013 and January 2014. The sequence of storms affecting the United Kingdom was caused by a powerful jet stream driving a succession of low-pressure systems across the Atlantic. Twelve significant storms occurred between December 2013 and February 2014. These storm events reported in this winter period were said to be unmatched in terms of intensity and duration for over 50 years, causing this winter to be ranked as the stormiest on record for the Ireland–United Kingdom domain (Matthews et al., 2014). These conditions resulted in the bulk of the ocean wave energy from the North Atlantic being driven onto the coastlines of southwest England and Wales repeatedly between December 2013 and February 2014. The geomorphical storm response along the southwest coast of England displayed considerable spatial variability; this is mainly attributed to the embayed nature of the coastline and the associated variability in coastal orientation (Masselink et al., 2016). The size and intensity of the storms generated some of the largest waves ever recorded to hit land in Western Europe, reaching 16 m in height. These storms coincided with some of the highest spring tides of the year and record-breaking precipitation levels for the United Kingdom dating back 248 years, leading to saturated coastal ecosystems and an exacerbation of the physical impacts of storm wave forces. The "highly unusual" conditions reported in the 2013/2014 winter period were due to the intense storm events, whereas extreme storms did not occur the following two winters (2014/2015 and 2015/2016), however, these were two of the warmest on record thereby resulting in abnormally mild conditions.

Rocky shores provide an important role in the functioning of nearshore habitats and contribute a wide range of ecosystem services including natural erosion resilience, protection from coastal storms and flooding, habitat provision, economic value, aesthetic, and wellbeing provision as well as scientific research benefits (Hawkins et al., 2010; Corte et al., 2017). Despite their importance and accessibility, the response of these communities to extreme events remains poorly understood, partly due to a lack of long-term contextual data describing the ecological patterns of an area prior to the storm events. Extreme storm events are unpredictable and therefore studies in this area need to be responsive to an event (Harris et al., 2011). The MarClim time series provides a unique opportunity to investigate the impact of the two detailed extreme storm events on rocky shore communities by providing this contextual data, enabling the attribution of ecological patterns to the quantified disturbance event.

The rocky intertidal zone has long been used to examine relationships between abiotic stressors and biological interactions determining ecological (Raffaelli and Hawkins, 1996 for review; updated in chapters in Hawkins et al., 2019a, 2020) and biogeographical patterns (Fischer-Piette, 1934; Crisp and Southward, 1958; Forbes, 1858; Southward et al., 1995; Helmuth et al., 2006; Mieszkowska et al., 2006). High spatio-temporal variation in environmental and anthropogenic stressors occurs both at the local scale of the individual shore, leading to differential population structure, but also large latitudinal gradients in environmental conditions from the tropics to the poles (Mieszkowska and Sugden, 2016a). Rocky intertidal habitats around the United Kingdom coastline have been studied throughout the last century, providing a rich legacy of biological and biogeographical data unrivalled across the globe (see Southward et al., 2004 for review). The United Kingdom straddles the boreal-lusitanian biogeographic transition zone (Forbes, 1858; Lewis, 1964), providing a rich tapestry of habitats, communities and species with which to study the effects of pervasive climate change and extreme events on organisms from a range of evolutionary origins (Vye et al., 2020), including invasive non-native invasive species (NIS) (Mieszkowska et al., 2014a; Firth et al., 2020).

Understanding the spatio-temporal scales over which climate driven changes will impact marine systems is key to producing accurate forecasts of future changes and effective management actions to mitigate the effects of climate change where possible (United Nations, 2020). Here we examine the impacts of extreme events and pervasive climate change to better understand the effects of short-term extreme events and long-term pervasive climate change on rocky intertidal biodiversity. We tested the following hypotheses: (a) cold-affinity species with colder thermal tolerance ranges would be more negatively impacted by heatwaves than warm-affinity species with warmer thermal tolerance ranges, (b) cold spells would have a greater negative effect on warm-affinity species, and (c) summer heatwaves and winter cold spells would have greater impacts than winter warm spells and summer cold spells. Given the highly disturbed nature of rocky shores we also hypothesised that recovery from storm damage would be rapid by core foundation species

such as mussels in the *Mytilus* species complex but would be prefaced by more ephemeral species. We have also considered important habitat-forming canopy seaweeds on, under and amongst which many invertebrates live (e.g., Thompson et al., 1996; Teagle et al., 2017).

MATERIALS AND METHODS

United Kingdom Rocky Intertidal Long-Term Time-Series

The MarClim project annually surveys between 70 and 100 long-term time-series sites, with each site being surveyed in the same season of each year. These surveys record the abundance and geographic distribution of 82 species of invertebrates and macroalgae of boreal, lusitanian and invasive biogeographic origins, many of which have a distributional limit on, or close to the United Kingdom coastline. The original species list comprising 55 ecologically important and easy to identify species was developed from historical surveys carried out by Southward and Crisp in the 1950s (Crisp and Southward, 1958; Southward et al., 2004), Lewis and team from the 1970s (Lewis et al., 1982; Lewis, 1986) plus monitoring and experimental work by Hawkins and colleagues from the 1970s to the 2000s (Hawkins and Hartnoll, 1983; Hartnoll and Hawkins, 1985; Southward et al., 1995; all featured in Hawkins and Jones, 1992); these were added to over the years with the rise in number of NIS and lusitanian species colonizing rocky shores in the United Kingdom assisted by better field identification guides (e.g., Bunker et al., 2010). The surveys use the rank categorical SACFOR scale, derived from Crisp and Southward (1958) (amended by JNCC, 1990) to assess the abundance of all 82 species, combined with quadrat-based counts for limpets and barnacles, and timed searches for trochids.

Species Thermal Affinities

Thermal affinities for species in surveys were represented by the median temperatures of their known geographical ranges (Species Temperature Index, STI), obtained by overlaying distribution polygons on maps of average sea surface temperature (SST, see Burrows et al., 2020 for details). Average SST values from 1982 to 2011 were calculated using the same NOAA OISST dataset used to express heatwaves and cold spells in daily temperatures for within-range coastal 0.25° latitude/longitude grid cells.

Extreme Events

The *RmarineHeatWaves* package in R (Hobday et al., 2016; Smit et al., 2018) was used to detect abnormally hotter and colder events or spells in regional daily SSTs from the NOAA Optimal Interpolated Sea Surface Temperature dataset (OISSTv2 HR; Reynolds et al., 2007). Data were extracted and expressed as daily average temperatures for the whole of the region 49-53°N 6-0°W for the period January 1, 1982 to December 31, 2019. These regional average daily temperatures were used for hot and cold spell detection. The period from January 1, 1983 to December 31, 2012 was used as the reference period for calculation of day of the year temperature percentiles. Warm events were detected as those periods in which temperatures exceeded the 90th percentile temperature for that day of the year for five or more days (Hobday et al., 2016). Cold spells followed a similar definition; those periods where temperatures were below the 10th percentile for that day of the year for five or more days. We also obtained yearly maxima and minima and 5 and 95 percentile temperatures from the same daily time series. Warm and cold events were characterised by their intensity, as maximum and mean temperature above the 90th percentile, duration and cumulative intensity (days × mean intensity).

Changes in Average Annual Abundance and Annual Frequency of Heatwaves and Cold Spells

Species abundance time series were taken as average annual abundance grouped across all sites surveyed annually from 2002 to 2018 (Burrows et al., 2020). For each species, differences in abundance from the preceding year were related to the frequency of heatwaves and cold spells occurring in the winters and summers using trends derived from linear regression [lm () call in R 4.0.2] to test the hypotheses outlined in the introduction.

Heatwave Damage Surveys

Visual assessments of heat damage were recorded during MarClim annual surveys at all sites around the United Kingdom coastline, with digital photographic images taken of damaged organisms. The broadscale abundance of organisms was then recorded, using the SACFOR scale (Mieszkowska et al., 2014b), to place into a long-term context. Temporal patterns of abundance of intertidal communities were visualised using multidimensional scaling (MDS) ordination to show the recovery trajectories predicted for each site. MDS were based on Bray Curtis similarity coefficient calculated from non-standardised, square root transformed data. This biannual dataset is placed into context alongside the sustained time-series monitoring of MarClim intertidal community data at these locations dating back to the early 2000s.

Storm Damage Surveys

Biological impacts of the extreme storm events were initially surveyed at all MarClim sites in England 4 months afterwards, and at all MarClim sites in Wales 6 months after the storms during the annual surveys. Subsequent annual surveys have reassessed the effects on community structure following the 2013/2014 storms via analysis of: those species that were undamaged, those species that were able to return after the extreme storm events and invasive non-native species that opportunistically occupied vacant habitat after storm-induced species loss, colonising those shores affected by storm damage.

In addition, biannual surveys to document damage and potential recovery to rocky intertidal communities were carried out in the spring and winter of 2014 and 2020 at three sites on the north coast of Cornwall, Crackington Haven (50.7417N, −4.6405W), Trevone (50.5450N, −4.9850W) and St. Ives (50.2187N, −5.4751W) (**Figure 3**). Five replicate 50 cm × 50 cm

quadrats were randomly placed in the lowshore and midshore regions at each of these sites (defined biologically) across a distance of approximately 50 m and the percentage cover of sessile species and the abundance of mobile species recorded within each quadrat. Storm damage was evident across large areas of these shores, and these quadrat surveys were carried out in addition to MarClim surveys to provide additional quantitative data specifically focusing on biological damage and recovery. Data were analysed using the PRIMER Version 7 Software and MDS ordination produced (as above) for each survey period and each site (Clarke and Gorley, 2015).

RESULTS

Extreme Events

Several extreme weather events occurred in 2018. Between late February and early March, Britain experienced a severe spell of winter weather with notable extremenes in air temperature. Known as the "Beast from the East," anticyclone Hartmut coincided with storm Emma to cause some of the worst weather conditions in decades. These events caused a mass mortality of subtidal biota along the east coast of England (Pinnegar et al., 2020), however, no observed changes in the abundance of any of the 50 species of invertebrate surveyed by MarClim were recorded at any long-term monitoring site along the North Sea coastline during 2018 (Mieszkowska et al., 2020). Repeat surveys at a frequently studied site, Heybrook Bay in southwest England found some damage to calcareous algae (crustose corallines and habitat forming *Corallina officinalis*) around the rim of rockpools, but no obvious signs of death of marine invertebrates including warm-water lusitanian species (e.g., *Chthamalus* species, *Phorcus lineatus, Patella depressa*).

Cold spells such as those caused by the extreme event of 2018 can occur at any time of the year, but are more frequent in the first half of the year in the region, with 30 cold spells occurring between January – June over the period of analysis (1982–2020) compared with 19 in the second half of the year between July – December around the southwest UK coastline (**Table 1**). Notably the cold spells of 2013, although short in duration, were the most intense event for 17 years and since this time there have been no cold spells for the past 7 years (**Figure 1**).

Marine warm spells have become more frequent in both summer (heatwaves) and winter (anomalously warm temperatures) since 1982, whereas cold spells are becoming less frequent in both summer and winter across the same period. This evidences a shift away from seasonal patterns of extreme cold temperature in the marine environment towards a more widespread set of warmer events throughout the year (**Table 1**).

In addition to the extreme cold weather, 2018 was one of the warmest years on record, with the joint hottest summers on record recorded in 2018 and 2020[2]. Five of the warmest years ever recorded in the United Kingdom occurred since 2010. The Marine heatwaves are becoming more frequent since the 1980s, and possibly longer and more intense. The heatwave of 2018 stands out as being the longest (60 days) if not the most intense on record, and with the biggest cumulative degree × days score in excess of 19°C (**Figure 2**). Heatwaves occur most frequently in June (11 events between 1982 and 2020), July (13 events) and August (10 events) with the Met Office reporting an average air temperature of 1.5°C above the long-term average in 2018 (Met Office, 2020).

MarClim surveys across the British Isles in 2018 and 2020 after hot weather in July and August found evidence of heat damage to the highshore habitat-forming fucoid species *Pelvetia canaliculata, Fucus spiralis*, and *Fucus vesiculosus* (**Figure 3**). This heat damage was probably caused by exposure to hot air temperatures during low tides. It did not, however, affect the overall abundance of these species at long-term sites compared to previous years, with no decrease in abundances recorded in surveys the following years, suggesting sub-lethal impacts of the heatwave at this time. The only evidence of negative impacts of heatwaves on invertebrates was recorded for the boreal barnacle *Semibalanus balanoides,* with patchy but total mortality recorded after the 2018 event at some sites in Oban, southwest Scotland, at the upper vertical limit of the species (Burrows, personal observation). A severe impact on invertebrates was also observed by SJH at Port Gaverne in July 2004 when amphipods (*Ampithoe rubricata*, and *Hyale* spp.) usually associated with fucoids, were observed at Port Gaverne, north Cornwall being baked red on the shore. This was not, however, observed during the heatwaves of 2018 or 2020.

TABLE 1 | Summary of frequencies of heatwaves and cold spells in the southwest Britain (49–53°N, 6–0°W) between 1980 and 2020.

Year	Frequency of marine warm spells		Frequency of marine cold spells	
	Summer	Winter	Summer	Winter
1980–1985	0	2	6	6
1985–1990	2	4	5	8
1990–1995	2	2	2	8
1995–2000	8	3	1	3
2000–2005	8	5	1	0
2005–2010	9	6	0	3
2010–2015	7	3	4	2
2015–2020	13	12	0	0

*Timings of individual events are shown in **Figure 1**.*

Change in Abundance and Extreme Thermal Events

The annual time series for each species was analysed to investigate effects of extreme events on changes in abundance. Changes in abundance since the previous year were related to the number of summer and winter heatwaves in that year using linear regression, with the regression slope expressing the effect of as the response of abundance change to

[2]https://www.metoffice.gov.uk/about-us/press-office/news/weather-and-climate/2019/2020-global-temperature-forecast

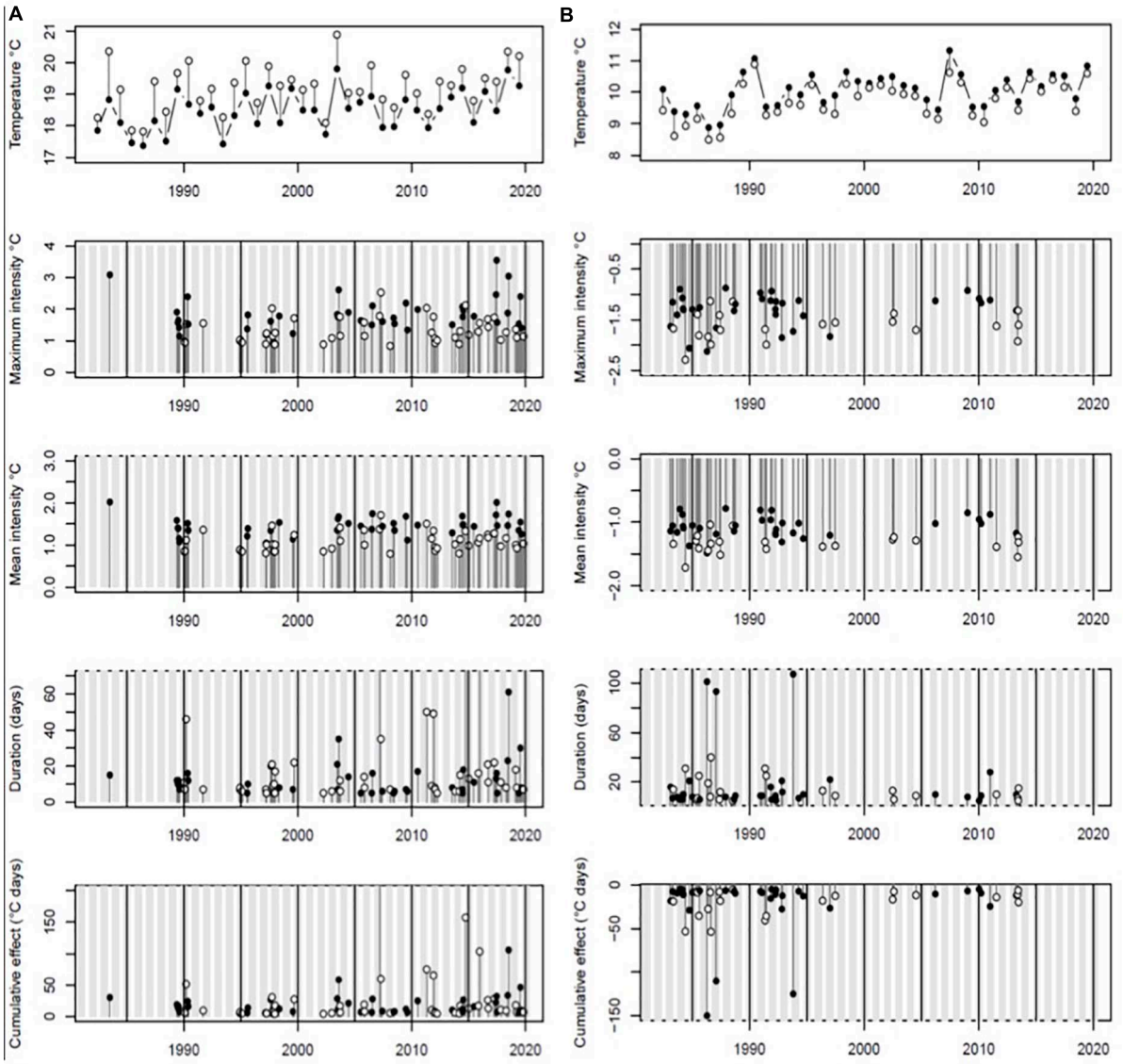

FIGURE 1 | (A) Heatwaves, **(B)** cold spells from 1982 to 2020. Top plots show **(A)** 95th percentile (closed circles) and maximum values (open circles) of daily SSTs per year and **(B)** 5th percentile and minimum daily temperatures per year. Summer heatwaves (May to September) and winter cold spells are shown by filled circles, with winters and summers shown shaded and blank, respectively.

increases in annual frequencies of heatwaves and cold spells (**Figures 4**, **5**). Declines across most species, regardless of thermal affinity, were found in years with more summer heatwaves (**Figure 4A**). The strength of response of abundance change to the frequency of summer heatwaves was not affected by the thermal affinity of the species (**Figure 4A**, $P > 0.05$ for the regression slope of species response on STI; $P = 0.07$ for the intercept). The increase in frequency of winter heatwaves has resulted in the cold-water, boreal species showing a decline in abundance for those years with more winter heatwaves. The impact of winter heatwaves on boreal species was much clearer than the impact of summer heatwaves on species with affinities for both warmer and colder thermal tolerance ranges (**Figure 4B**). Cold-water species clearly decline in years with more winter heatwaves, with a positive significant relationship with thermal affinity ($P = 0.028$).

The negative slopes of abundance change on event frequencies shown in **Figures 3A,B** show that the change in abundance to the previous year becomes more negative with more heatwaves. Most species trends, as regression slope of change in abundance versus frequency of heatwaves per year, were negative ($n = 35$), showing greater decreases in abundance in years with more frequent heatwaves, with only nine species increasing in abundance due to an increase in the number of summer heatwaves. Summer heatwaves more

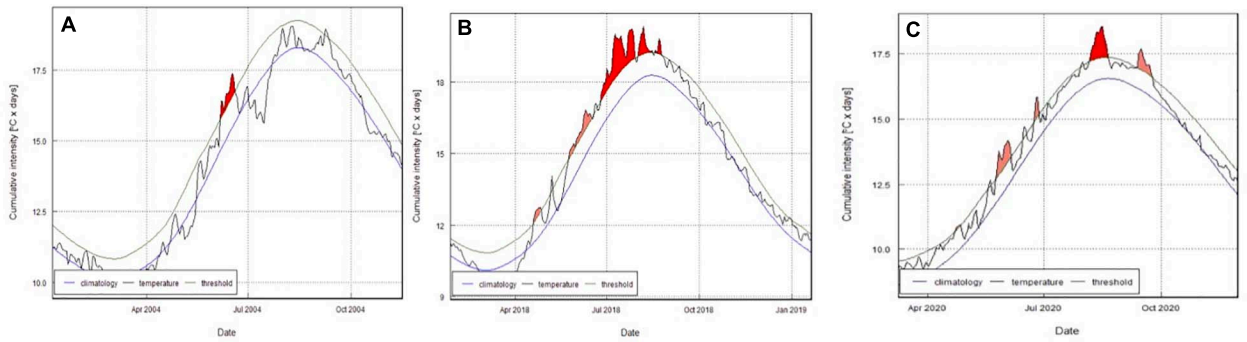

FIGURE 2 | (A) 2004, **(B)** 2018, **(C)** 2020 heatwave events, durations, and cumulative intensities for SST.

FIGURE 3 | (A) Heat damaged *Pelvetia canaliculata*, 2018. **(B)** heat damaged *Fucus spiralis*, 2018.

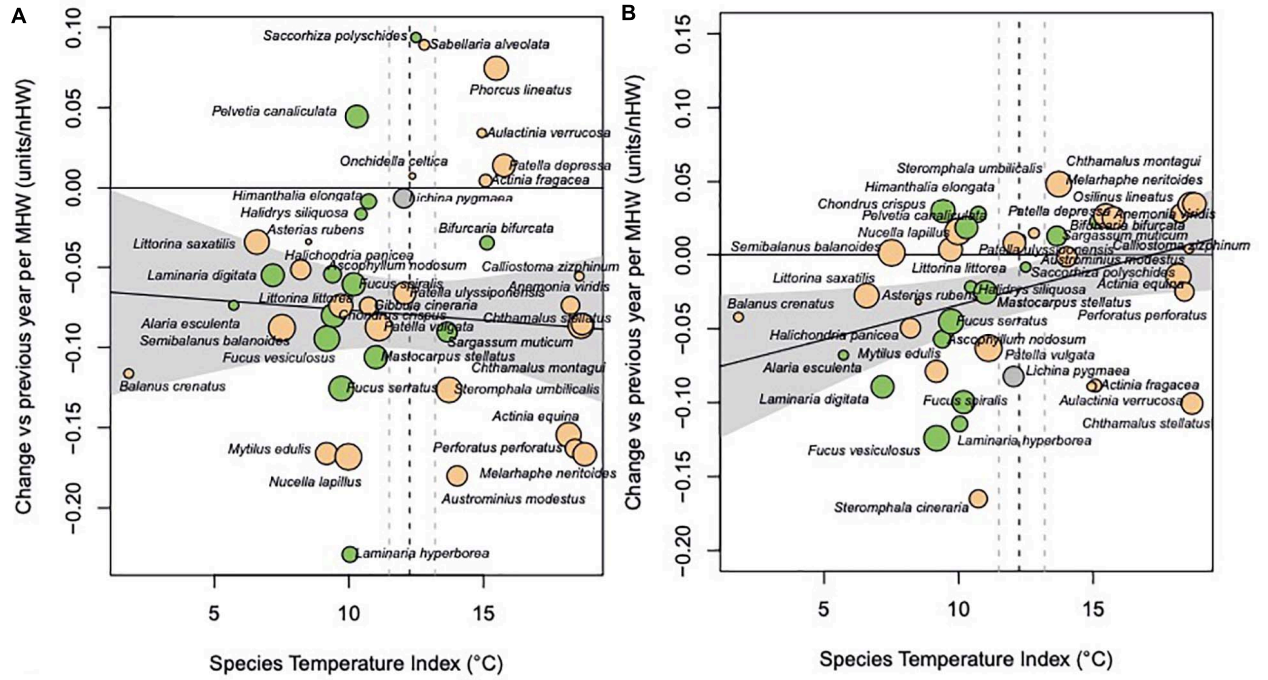

FIGURE 4 | (A) Response to summer heatwaves, shown as the trend in annual abundance change relative to annual frequency of heatwaves. **(B)** Response to winter heatwaves. Regression slopes for **(A)** $Y = -0.064$ (±0.035 SE) – 0.0012.STI (±0.0027 SE), $p = 0.65$; **(B)** $Y = -0.081$ (±0.026 SE) + 0.0047.STI (±0.0021 SE), $p = 0.028$.

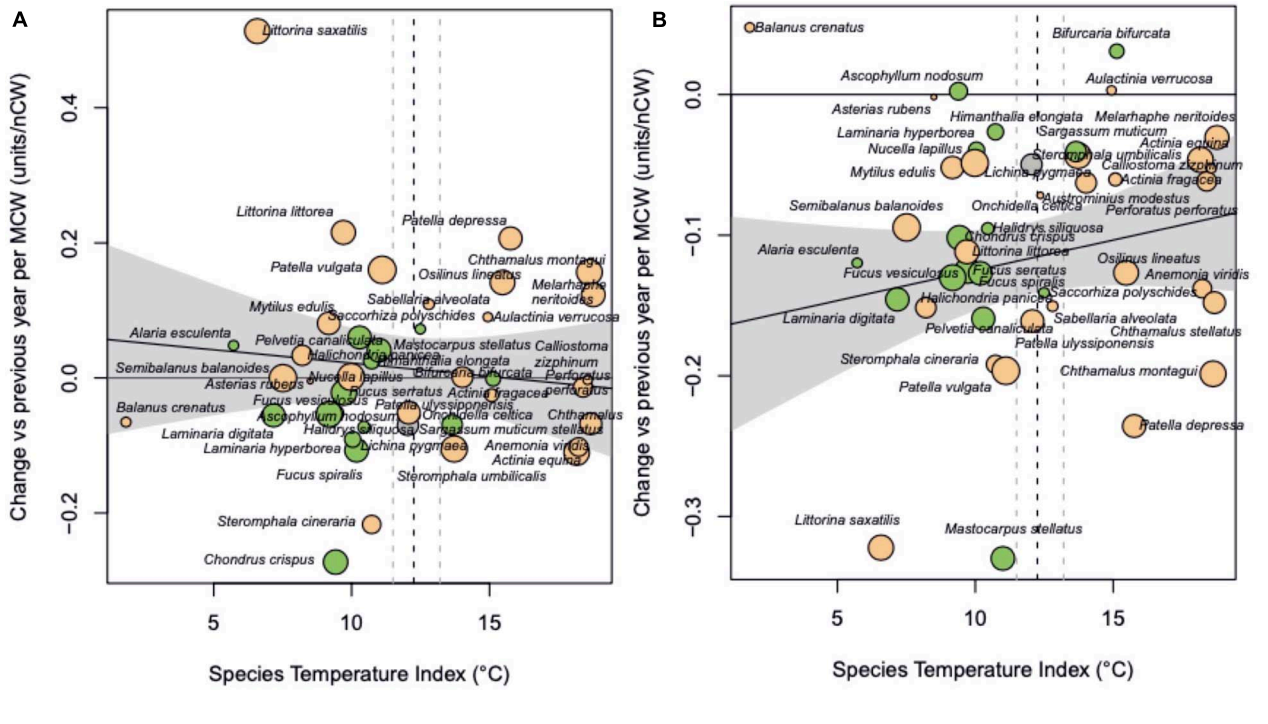

FIGURE 5 | (A) Response to summer cold spells and **(B)** response to winter cold spells. Regression slopes for **(A)** $Y = 0.049$ (±0.076 SE) – 0.0024.STI (±0.0061 SE), $p = 0.70$; **(B)** $Y = -0.160$ (±0.043 SE) + 0.0047.STI (±0.0021 SE), $p = 0.33$. Regression intercept for **(B)** was significantly negative ($p = 0.0005$).

TABLE 2 | Meta-analysis of species responses to frequencies of extreme climatic events, expressed as the sign of the slope of annual change in abundance to the number of extreme events, for time series in abundance of United Kingdom rocky shore species between 2002 and 2019.

Species response to frequency of:	Sign of species slope of annual change on event frequency		Binomial test *p*	Dependence of slope on Species Temperature Index
	−ve	+ve	*p* (−ve = +ve)	
Summer heatwaves	35	8	<0.0001	$p > 0.05$ (**Figure 4A**)
Winter warm spells	24	19	0.27	+ve, $p = 0.03$ (**Figure 4B**)
Summer cold spells	24	19	0.27	$p > 0.05$ (**Figure 5A**)
Winter cold spells	39	4	<0.0001	$p > 0.05$ (**Figure 5B**)

Binomial tests give the likelihood of getting at least n negative slopes out of the total number of species analysed (k = 43). Dependence of slope on Species Temperature Index.

frequently had negative effects but the magnitude of effects was not related to species thermal affinity (**Figure 4A** and **Table 2**).

Effects of summer cold spells on abundance were not consistently positive or negative (**Figure 5A**). There was a higher frequency of negative species responses to winter cold spells (**Table 2**), as expected, but no significant effect of species thermal affinity on responses (**Figure 5B**).

Storm Damage

Storm damage to intertidal habitats during the extreme events of the winter of 2013/2014 was site specific. Alterations to rock substrate were recorded at several sites; Lizard Point, Cornwall (49.9590, −5.2080), Renney Rocks, south Devon (50.3179, −4.1310), and Osmington Mills, Dorset (50.6330, −2.3760) experienced smothering by large amounts of soft sediment transported from nearby beaches, rocky habitat was uncovered by the loss of most of the sediment from the beach at Crackington Haven, north Cornwall (50.7417, −4.6405), a large boulderfield appeared on top of the soft sediment beach at Porth Neigwl, north Wales (52.7908, −4.5404), and large sections of rock cliff face were removed by the storms at Portland Bill (50.5130, −2.4600) (**Figure 6**). The smallest biological impacts of the storm events were seen at St. Ives (**Figures 7A,B**). Variation in the abundance and presence of species was evident between spring and winter each year, but this is in line with natural seasonal cycles at both the lower and mid eulittoral shore zones. No species were entirely removed from the community at this site by the storm events, and there was no change to the rocky habitat.

Crackington Haven had no species present on the rocky habitat that was uncovered by the storm events in the lower and eulittoral zones in 2014 and 2015. Species had begun to colonise these vacant rock habitats in 2016, with increasing species diversity in 2017 and 2018. There was a seasonal signal as for St. Ives which is related to natural seasonal cycles (**Figures 8A,B**).

The largest biological responses were recorded at Trevone. At this site the complete removal of adult mussels (*Mytilus edulis*, *Mytilus galloprovincialis* and hybrids) from the lower eulittoral zone impacted the wider intertidal community (**Figure 9A**). Spring 2014 and spring and autumn 2015 were visually different to subsequent years, as biological recovery had not occurred. The low eulittoral took longer to stabilise than the mid eulittoral zone due to almost all adult mussels in the low eulittoral zone being removed by the storms (**Figure 9B**), and did not show signs of recovery until 2016, when juvenile *M. edulis* settlement had occurred in this zone. Similar to St. Ives and Crackington Haven, seasonal cycles were evident in the data.

At all three sites where storm damage occurred, the community abundance and composition showed a gradual shift from the early 2000s, but no abrupt shift after the winter 2013/2014 storms (**Figure 10**). These sustained observations surveys demonstrate how the extreme storm events did not drive significant impacts across the rocky intertidal communities, with biodiversity not being significantly affected. Whilst a short-term change in some species was recorded in the quadrat surveys, the biological communities returned to the long-term composition within a few years as colonisation and succession occurred at all three sites.

DISCUSSION

Year-to-year changes in occupancy-derived measures of abundance for rocky intertidal species are a sensitive metric with which to track the vulnerability of species to extreme thermal events occurring in the marine climate. Declines in abundance were seen for the majority of invertebrates and macroalgae, regardless of their biogeographic origin, to anomalously warm conditions whenever they occurred during the year, with only responses to winter warm events influenced by thermal affinity. Thermal affinity of species also influenced responses to intense cold spells in winter, but not to the anomalous cooler spells in summer months, reflecting the seasonal acclimatory ability of temperate intertidal species (Vinagre et al., 2016), which are more cold-tolerant during the winter period where environmental temperatures are lower (Bourget, 2011). The negative responses of most species to summer heatwave frequencies again supports the occurrence of seasonal acclimation including drought hardening in upper shore algae (e.g., Schonbeck and Norton, 1979), and suggests that whilst temperate intertidal species are able to tolerate short periods of extreme heat or cold, they are more responsive to pervasive changes in the climate that occur across decadal timescales ultimately influencing performance in terms of growth and reproductive output leading to recruitment. The responses of intertidal species in the British Isles match global-scale analyses, indicating a general relationship between

FIGURE 6 | MarClim sites where storm damage was recorded in England and Wales, and biannual storm damage survey locations at Crackington Haven, Trevone, and St. Ives.

species thermal affinity and responses to marine climate change across the world (Webb et al., 2020), supporting the value of thermal affinity calculations in advancing the ability to accurately forecast population abundances and future distributional shifts (Sunday et al., 2012).

Our work has focused on analysing SST, rather than air temperature. In coastal waters, warm anomalies in summer sea temperatures are associated with heatwave summer air temperatures and very mild winter air temperatures; anomalously cold events in both winter and summer similarly follow air temperatures. Thus sea temperatures can indicate what is happening when the tide is out (e.g., Poloczanska et al., 2008) Extreme heat events, especially when the tide is out, will trim back the upper limits of species of both algae and animals, especially high on the shore (e.g., *F. spiralis* and *P. canaliculata*; Schonbeck and Norton, 1979; Hawkins and Hartnoll, 1985; see **Figure 4**), but do not seem to cause damage throughout the whole zone of a species. Those species that span the lower water mark such as *Laminaria digitata* are also highly susceptible. Interestingly as reported previously (Schonbeck and Norton, 1979; Hawkins and Hartnoll, 1985) mid and low shore fucoids showed much less damage than high shore fucoids, although in contrast to the 1970s and 1980s, some slight but not fatal damage was noticed in 2018–2020 across many locations in southwest England in *F. vesiculosus, Ascophyllum nodosum* and *Fucus serratus* at their upper zonal limits. Thus zones may be shifted downshore if physical factors act at the top of the zone and squeezed if biological interactions intensify at the bottom of a zone, as recently shown with a combination of observations of upper limit heat damage to *Fucus guiryi* (recently split from *F. spiralis*) in Azores, coupled with increased grazing damage lower in the zone due to spread of herbivorous fish from further south – showing

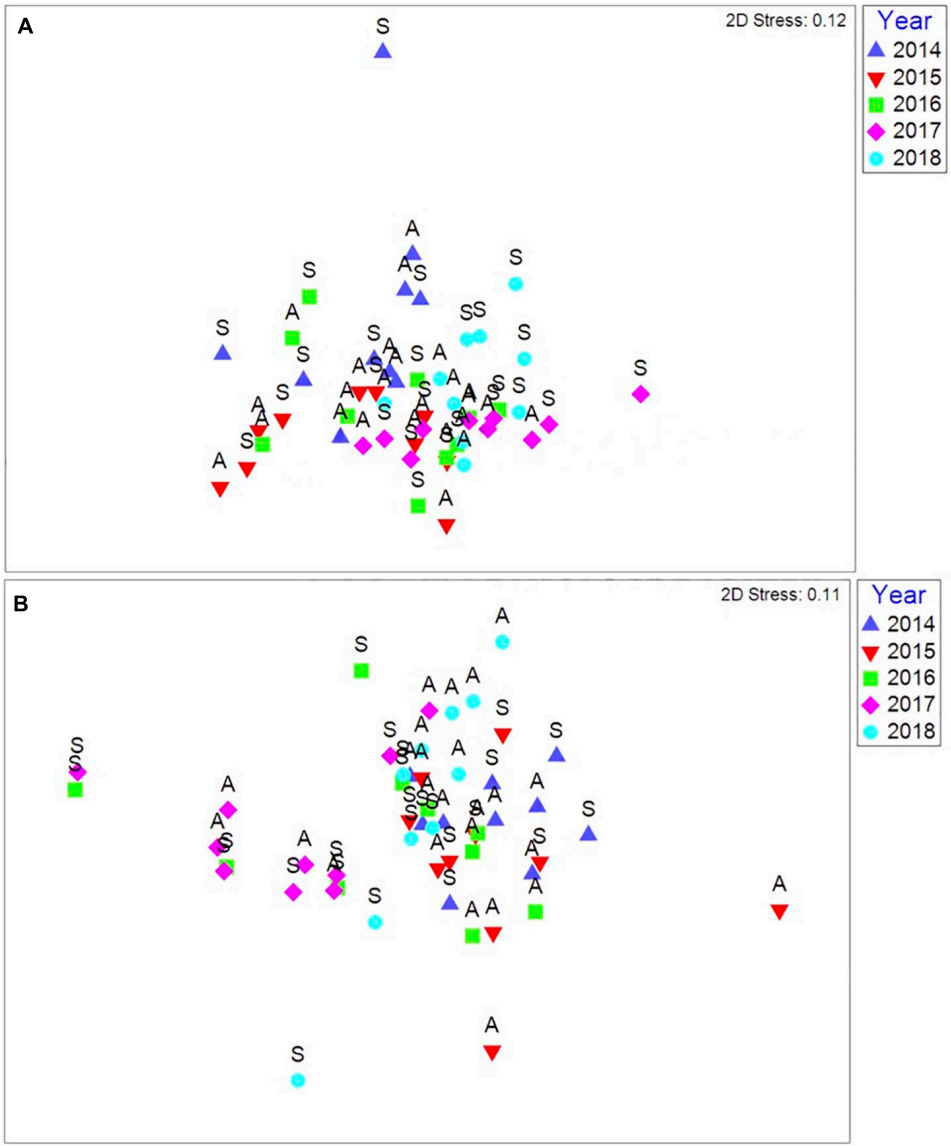

FIGURE 7 | (A) Multi-dimensional scaling ordination of communities diversity per season (S, Spring; A, Autumn) from immediately after the storm events in spring 2014 until autumn 2018 in the low eulittoral at St. Ives, **(B)** Multi-dimensional scaling ordination of communities diversity per season (S, Spring; A, Autumn) from immediately after the storm events in spring 2014 until autumn 2018 in the mid eulittoral at St. Ives. Based on Bray Curtis similarity coefficient, non-standardised data and square root transformed abundances.

a combination of direct and indirect effects of climate change (Martins et al., 2019).

The extreme storm events of winter 2013/2014 caused physical and ecological damage to intertidal ecosystems around the coastlines of England and Wales. These storms were unprecedented in terms of their wave height and magnitude in combination with high winds and heavy precipitation. They occurred during periods of large tides, exacerbating the impacts on intertidal habitats and ecosystems. The time-series surveys showed that the storm impacts were site-specific, with locations on the same stretch of coastline experiencing either biological removal, physical habitat damage, or the removal or deposition of soft sediment from neighbouring beaches. Some sites at exposed locations showed little biological variation from long-term trends in biodiversity and abundance, as species inhabiting these areas have evolved to tolerate rough sea conditions.

Biological impacts were site specific and species specific, with loss of the blue mussel *M. edulis*/*M. galloprovincialis* hybrids at Trevone, north Cornwall, with slow recovery due to new recruits taking a few years to attain the body size similar to those individuals removed during the storms. Damage to kelp beds was also recorded at many sites around southwest England, however, these species have evolved to survive in areas of high wave exposure and no reduction in SACFOR abundance of the six main species was recorded in subsequent years. Whilst declines in abundance in species of kelp were recorded immediately

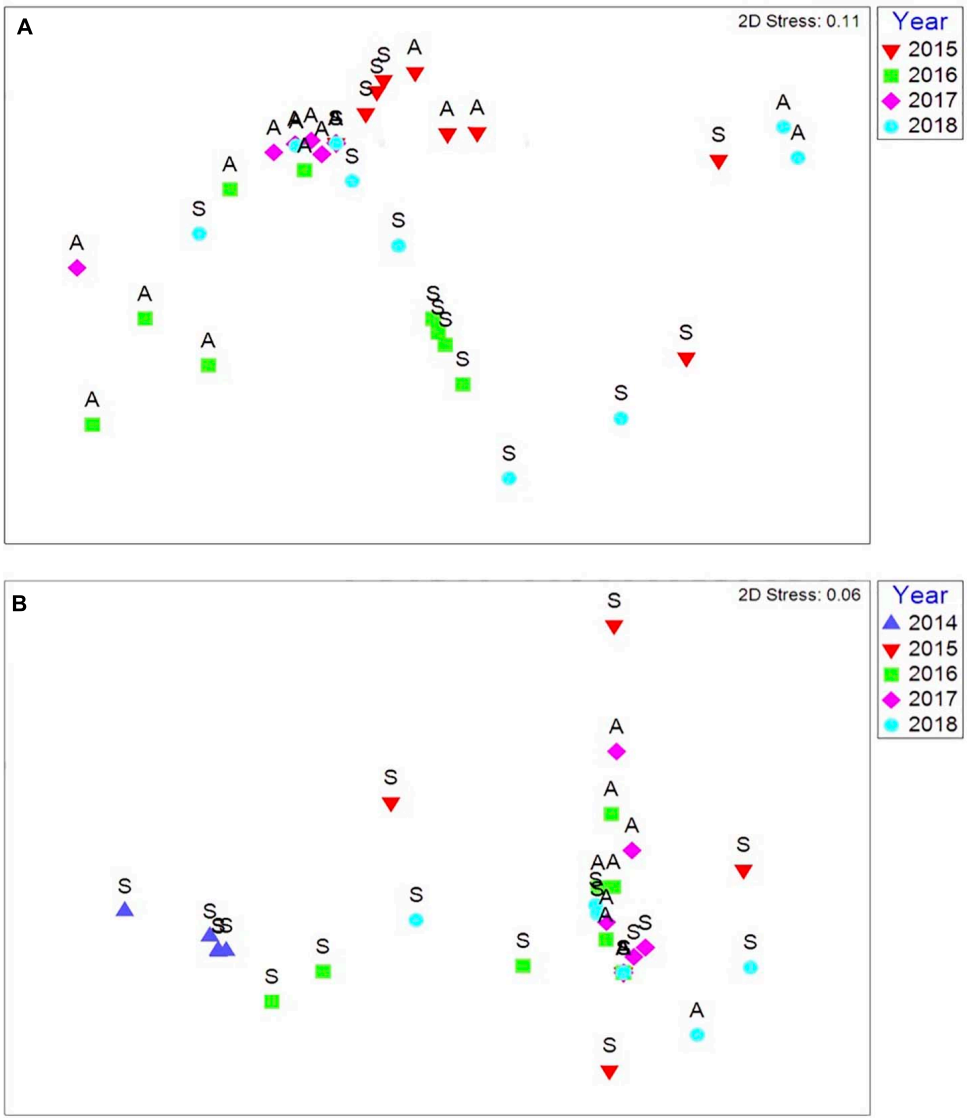

FIGURE 8 | (A) Multi-dimensional scaling ordination of communities diversity per season (S, Spring; A, Autumn) from immediately after the storm events in 2015 until autumn 2018 in the low eulittoral at Crackington Haven, **(B)** Multi-dimensional scaling ordination of communities diversity per season (S, Spring; A, Autumn) from immediately after the storm events in spring 2014 until autumn 2018 in the mid eulittoral at Crackington Haven. Based on Bray Curtis similarity coefficient, non-standardised data and square root transformed abundances.

after the storm events (Smale and Vance, 2016), the lack of subsequent surveys by these authors meant that they did not record the recovery that occurred within a year or so of these storms as species abundance, composition and extent of kelp forests rapidly returned to pre-storm conditions (Mieszkowska and Sugden, 2016b, 2017, 2018). Rapid recovery has previously been found in experimental clearances of seaweed canopies in both the intertidal and shallow subtidal zone, with recovery within 2 years of laminarian (Hawkins and Harkin, 1985) and *F. serratus* canopies (Jenkins et al., 1999a), but not *A. nodosum* (Jenkins et al., 1999b, 2004) that recovers much more slowly. The biannual quadrat surveys demonstrated how species loss and subsequent recovery occurred at one site, Trevone. In contrast colonisation of "new" habitat after the beach sediments were washed away at Crackington Haven showed typical biological succession, with little biological impact recorded at St. Ives. These data echo the lack of significant long-term impacts recorded in the MarClim time-series surveys, and highlight the range of impacts occurring along the same stretch of coastline.

The site-specific effects of these events show how difficult it will be to accurately predict future impacts for intertidal ecosystems. Regardless of the type of impact, communities returned to their long-term species composition within a few years, although the biogenic habitat created by blue mussels will require several years for the newly settled organisms to grow and mature sufficiently for the communities to regain their previous structure and functional capacity. These findings support the importance of considering both the mean and

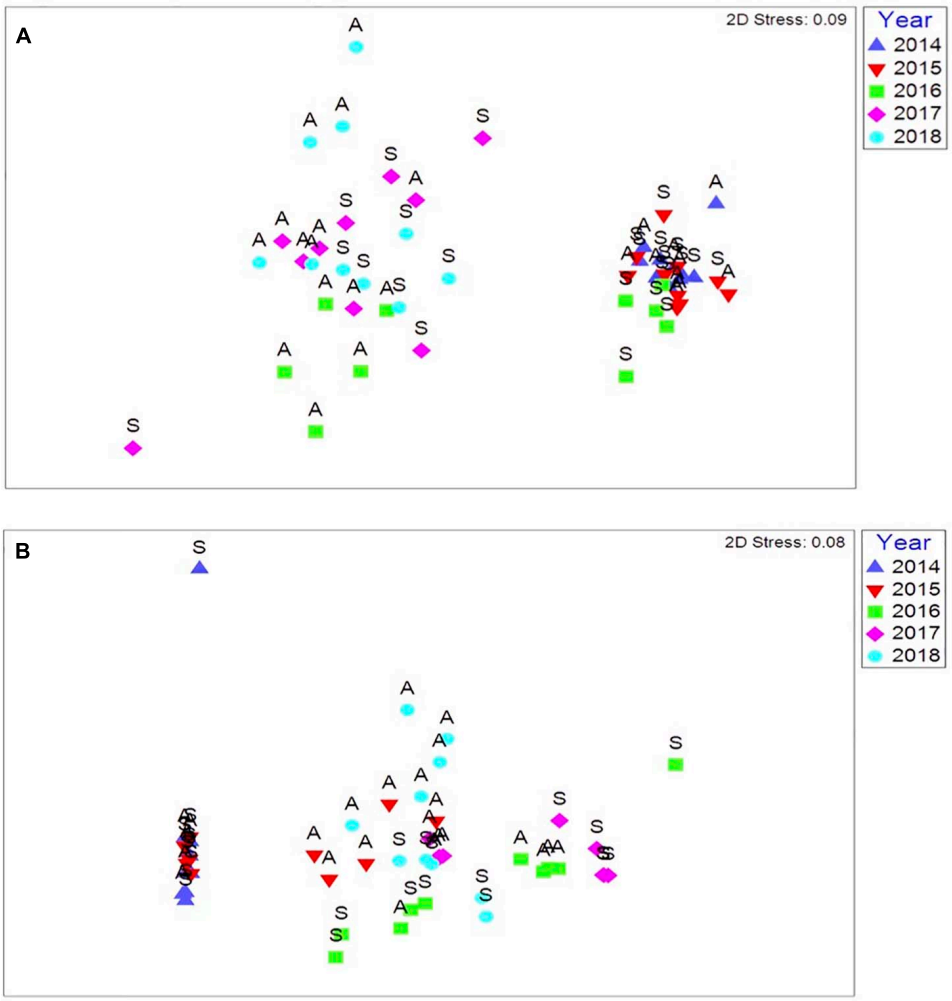

FIGURE 9 | (A) Multi-dimensional scaling ordination of communities diversity per season (S, Spring; A, Autumn) from immediately after the storm events in spring 2014 until autumn 2018 in the low eulittoral at Trevone, **(B)** MDS plot showing communities diversity per season (S, Spring; A, Autumn) from immediately after the storm events in spring 2014 until autumn 2018 in the mid eulittoral at Trevone. Based on Bray Curtis similarity coefficient, non-standardised data and square root transformed abundances.

variance when assessing climate change impacts (Benedetti-Cecchi, 2001, 2003; Bertocci et al., 2005; Vasseur et al., 2014) and the role of both weather and climate in shaping the distribution of species, as has also been shown for intertidal species across the Pacific (Harley and Paine, 2009; Mislan et al., 2009; Williams et al., 2016), Atlantic (Birchenough et al., 2015), and Mediterranean (Sarà et al., 2014). These studies support the hypothesis that heterogeneous performance is linked to latitude for intertidal systems around the world (Kingsolver et al., 2013; Mangano et al., 2020).

Long-term sustained observing of rocky intertidal species of macroalgae and invertebrates in the British Isles has put both the extreme temperatures and the storm damage with subsequent recovery into a longer-term context. Across the 2000s there was a species-specific increase in abundance of many Lusitanian species at many time-series sites around the United Kingdom, with extensions in the leading range edges of several gastropods and cirripedes (Mieszkowska et al., 2006; Mieszkowska and Sugden, 2016a). This general increasing trend stopped in 2010 when SST began to cool around the United Kingdom in response to the slowdown in the AMOC, but continued again after 2014; no obvious impacts of extreme thermal or storm events lasting more than a few years were apparent (Burrows et al., 2020). Our data show how pervasive climate change is ultimately driving the abundance and distribution of these species. In contrast short-term changes caused by proximate direct extreme events are much less long-lasting. These can, however, influence abundance along sharp local environmental gradients such as zonation patterns on rocky shores and could contribute to decreases in abundance and local extinctions – especially high on the shore should their frequency of occurrence increase and return time shorten (Benedetti-Cecchi, 2001; Bertocci et al., 2005). Moreover, climate change is more than just temperature and storm driven disturbance events can be important – especially in

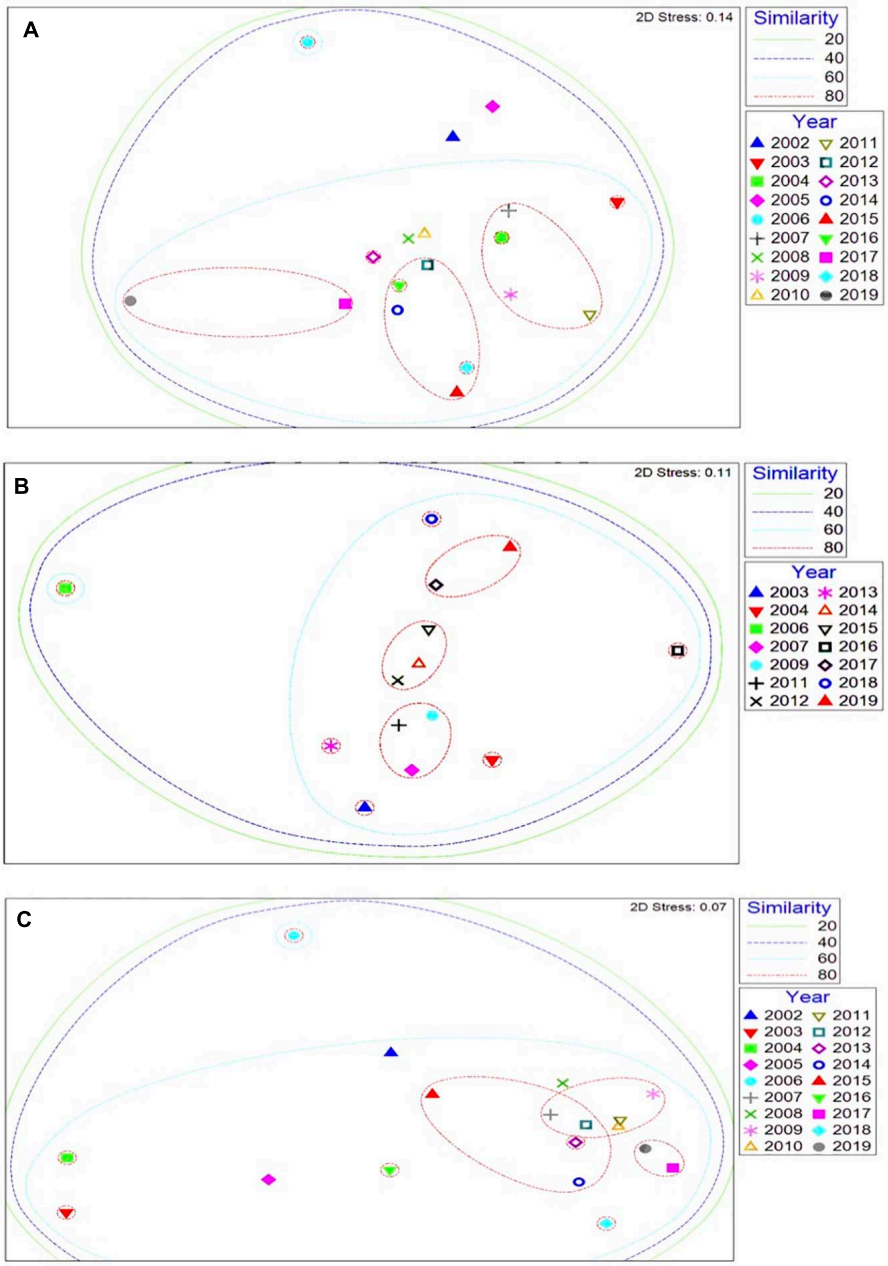

FIGURE 10 | Multi-dimensional scaling ordination of MarClim community data at **(A)** St. Ives, **(B)** Crackington Haven, and **(C)** Trevone over the long-term time-series 2002–2019. Based on Bray Curtis similarity coefficient, non-standardised data and square root transformed abundances.

the North-east Atlantic where they tend to occur in anomalously warm, wet and windy NAO positive winters such as 2013/2014.

The data provide support for hypothesis (a), as cold-affinity species were more negatively impacted by heatwaves than warm-affinity species with warmer thermal tolerance ranges, and partial support for hypothesis (b), because cold spells in winters had greater negative effects on warm-affinity species, although this was not supported for summer cold spells. Summer heatwaves and winter cold spells did have greater impacts on species abundances, regardless of thermal affinity, than winter warm spells and summer cold spells, providing support for hypothesis (c).

Our study shows that the impacts of heatwaves, cold weather events, and extreme storm events can be seen in annual sustained observing spanning long timescales over large spatial scales. Time-series data such as these allow the impacts of extreme events to be placed into context of long-term pervasive trends in the environment and resultant impacts on biodiversity. With better understanding of the role of species traits and thermal tolerances in shaping responses to short-term events

(Helmuth et al., 2015; Mieszkowska et al., 2019), we can make more robust predictions of future impacts of climate-driven change.

DATA AVAILABILITY STATEMENT

The raw data supporting the conclusions of this article will be made available by the authors, without undue reservation.

AUTHOR CONTRIBUTIONS

NM led the field data collection and manuscript writing. SH, MB, and HS contributed to the field data collection. MB led the statistical analysis. HS carried out the PRIMER analyses. All authors contributed to the article and approved the submitted version.

FUNDING

Natural Resources Wales, Natural England, NM was part-funded by a Marine Biological Association Fellowship.

ACKNOWLEDGMENTS

The authors would like to thank Natural Resources Wales, Natural England, Scottish Natural Heritage for funding the MarClim time-series, Louise Firth, Leoni Adams, Katrin Bohn, and Catherine Scott for assistance on fieldwork.

REFERENCES

Benedetti-Cecchi, L. (2001). Variability in abundance of algae and invertebrates at different spatial scales on rocky sea shores. *Mar. Ecol. Prog. Ser.* 215, 79–92. doi: 10.3354/meps215079

Benedetti-Cecchi, L. (2003). The importance of the variance around the mean effect size of ecological processes. *Ecology* 84, 2335–2346. doi: 10.1890/02-8011

Bertocci, I., Maggi, E., Vaselli, S., and Benedetti-Cecchi, L. (2005). Contrasting effects of mean intensity and temporal variation of disturbance on a rocky seashore. *Ecology* 86, 2061–2067. doi: 10.1890/04-1698

Birchenough, S. N., Reiss, H., Degraer, S., Mieszkowska, N., Borja, Á, and Buhl-Mortensen, L. (2015). Climate change and marine benthos: a review of existing research and future directions in the North Atlantic. Wiley interdisciplinary reviews: climate change. *Wires Clim. Change* 6, 203–223. doi: 10.1002/wcc.330

Bourget, E. (2011). Seasonal variations of cold tolerance in intertidal mollusks and relation to environmental conditions in the St. Lawrence Estuary. *Can. J. Zool.* 61, 1193–1201. doi: 10.1139/z83-162

Bunker, F. StP. D., Brodie, J. A., Maggs, C. A., and Bunker, A. R. (2010). *Guide to Seaweeds of Britain and Ireland*. Ross-on-Wye: Marine Conservation Society.

Burrows, M. T., Bates, A. E., Costello, M. J., Edwards, M., Edgar, G. J., Fox, C. J., et al. (2019). Ocean community warming responses explained by thermal affinities and temperature gradients. *Nat. Clim. Chang.* 9, 959–963. doi: 10.1038/s41558-019-0631-5

Burrows, M. T., Moore, J., Hawkins, S. J., Adams, L., Sugden, H., Firth, L., et al. (2020). Global-scale species distributions predict temperature-related changes in species composition of rocky shore communities in Britain. *Glob. Change Biol.* 25, 2093–2105. doi: 10.1111/gcb.14968

Clarke, K. R., and Gorley, R. N. (2015). *PRIMER v6: User Manual/Tutorial*. Plymouth: PRIMER-E.

Corte, G. N., Schlacher, T. A., Checon, H. H., Barboza, C. A. M., Siegle, E., Coleman, R. A., et al. (2017). Storm effects on intertidal invertebrates: increased beta diversity of few individuals and species. *PeerJ* 5:e3360. doi: 10.7717/peerj.3360

Crisp, D. J., and Southward, A. J. (1958). The distribution of intertidal organisms along the coasts of the English channel. *J. Mar. Biol. Assoc. UK* 37, 157–208. doi: 10.1017/s0025315400014909

Dzwonkowski, B., Coogan, J., Fournier, S., Lockridge, G., Park, K., and Lee, T. (2020). Compounding impact of severe weather events fuels marine heatwave in the coastal ocean. *Nat. Commun.* 11:4623. doi: 10.1038/s41467-020-18339-2

Elith, J., and Leathwick, J. R. (2009). Species distribution models: ecological explanation and prediction across space and time. *Annu. Rev. Ecol. Evol. Sci.* 40, 677–697. doi: 10.1146/annurev.ecolsys.110308.120159

Firth, l. B., Duff, L., Gribben, P. E., and Knights, A. M. (2020). Do positive interactions between marine invaders increase likelihood of invasion into natural and artificial habitats? *Oikos* 130, 453–463. doi: 10.1111/oik.07862

Firth, L. B., Mieszkowska, N., Grant, L. M., Bush, L. E., Davies, A. J., and Frost, M. T. (2015). Historical comparisons reveal multiple drivers of decadal change of an ecosystem engineer at the range edge. *Ecol. Evol.* 5, 3210–3222. doi: 10.1002/ece3.1556

Fischer-Piette, E. (1934). Sur la distribution verticale des organismes fixes dans la zone de fluctuation des marees. *CR Acad. Sci. Paris* 198, 1721–1723.

Forbes, E. (1858). *The Distribution of Marine Life, Illustrated Chiefly by Fishes and Molluscs and Radiata*. Edinburgh: William Blackwood and Sons.

Frölicher, T. L., and Laufkötter, C. (2018). Emerging risks from marine heat waves. *Nat. Commun.* 9:650. doi: 10.1038/s41467-018-03163-6

Harley, C. D., and Paine, R. T. (2009). Contingencies and compounded rare perturbations dictate sudden distributional shifts during periods of gradual climate change. *Proc. Natl. Acad. Sci.* 106, 11172–11176. doi: 10.1073/pnas.0904946106

Harris, L., Nel, R., Smale, M., and Schoeman, D. (2011). Swashed away? Storm impacts on sandy beach macrofaunal communities. *Estuar. Coast. Shelf Sci.* 94, 210–221. doi: 10.1016/j.ecss.2011.06.013

Harris, R. M. B., Beaumont, L. J., Vance, T. R., Tozer, C. R., Remenyi, T. A., and Perkins-Kirkpatrick, S. E. (2018). Biological responses to the press and pulse of climate trends and extreme events. *Nat. Clim. Chang.* 8, 579–587. doi: 10.1038/s41558-018-0187-9

Hartnoll, R. G., and Hawkins, S. J. (1985). Patchiness and fluctuations on moderately exposed rocky shores. *Ophelia* 24, 53–64. doi: 10.1080/00785236.1985.10426619

Hawkins, S. J., and Harkin, E. (1985). Preliminary canopy removal experiments in algal dominated communities low on the shore and in the shallow subtidal on the Isle of Man. *Bot. Mar.* 28, 223–230. doi: 10.1515/botm.1985.28.6.223

Hawkins, S. J., and Hartnoll, R. G. (1983). Changes in a rocky shore community: an evaluation of monitoring. *Mar. Environ. Res.* 9, 131–181. doi: 10.1016/0141-1136(83)90051-x

Hawkins, S. J., and Hartnoll, R. G. (1985). Factors determining the upper limits of intertidal canopy-forming algae. *Mar. Ecol. Prog. Ser.* 20, 265–271. doi: 10.3354/meps020265

Hawkins, S. J., and Jones, H. D. (1992). *Marine Conservation Society Marine Field Course Guide 1*. London: Immel.

Hawkins, S. J., Bohn, K., Firth, L. B., and Williams, G. A. (2019a). *Interactions in the Marine Benthos: Global Patterns and Processes*. Cambridge: Cambridge University Press. doi: 10.1017/9781108235792

Hawkins, S. J., Pack, K. E., Firth, L. B., Mieszkowska, N., Evans, A. J., and Martins, G. M. (2019b). "The intertidal zone of the north-east atlantic region: pattern and process," in *Interactions in the Marine Benthos: Global Patterns and Processes*, eds S. J. Hawkins, K. Bohn, L. B. Firth, and G. A. Williams (Cambridge: Cambridge University Press).

Hawkins, S. J., Pack, K. E., Hyder, K., Benedetti-Cecchi, L., and Jenkins, S. R. (2020). *Rocky Shores as Tractable Test Systems for Experimental Ecology*. Cambridge: Cambridge University Press. doi: 10.1017/S0025315420001046

Hawkins, S. J., Southward, A. J., and Genner, M. J. (2003). Detection of environmental change in a marine ecosystem – evidence from the western English Channel. *Sci. Total Environ.* 310, 245–256. doi: 10.1016/s0048-9697(02)00645-9

Hawkins, S. J., Sugden, H. E., Mieszkowska, N., Moore, P. J., Poloczanska, E., and Leaper, R. (2009). Consequences of climate-driven biodiversity changes for ecosystem functioning of North European rocky shores. *Mar. Ecol. Prog. Ser.* 396, 245–259. doi: 10.3354/meps08378

Hawkins, S. J., Sugden, H. E., Moschella, P. S., Mieszkowska, N., Thompson, R. C., and Burrows, M. T. (2010). "The Seashore", in *Silent Summer: The State of Wildlife in Britain and Ireland*, ed. N. Maclean (Cambridge: Cambridge University Press), 591–614.

Helmuth, B. T., Russell, B. D., Connnell, S., Dong, Y., Harley, C. D. G., Lima, F. P., et al. (2015). Beyond long-term averages: making biological sense of long term averages in a changing world. *Clim. Chang. Responses* 1:6. doi: 10.1186/s40665-014-0006-0

Helmuth, B., Mieszkowska, N., Moore, P., and Hawkins, S. J. (2006). Living on the edge of two changing worlds: forecasting the impacts of climate change on rocky intertidal ecosystems. *Annu. Rev. Ecol. Evol. Sci.* 37, 373–404. doi: 10.1146/annurev.ecolsys.37.091305.110149

Hobday, A. J., Alexander, L. V., Perkins, S. E., Smale, D. A., Straub, S. C., and Oliver, E. C. J. (2016). A hierarchical approach to defining marine heatwaves. *Prog. Oceanogr.* 141, 227–238. doi: 10.1016/j.pocean.2015.12.014

Huey, R. B., Kearney, M. R., Krockenberger, A., Holtum, J. A. M., Jess, M., Stephen, E., et al. (2012). Predicting organismal vulnerability to climate warming: roles of behaviour, physiology and adaptation. *Philos. Trans. R. Soc. B.* 367, 1665–1679. doi: 10.1098/rstb.2012.0005

IPCC (2013). "Summary for policymakers," in *Climate Change 2013: the Physical Science Basis. Contribution of Working Group I to the Fifth Assessment Report of the Intergovernmental Panel on Climate Change*, eds T. F. Stocker, D. Qin, and G.-K. Plattner (Cambridge: Cambridge University Press).

IPCC (2019). *IPCC Special Report on the Ocean and Cryosphere in a Changing Climate*. Geneva: IPCC.

Jenkins, S., Hawkins, S., and Norton, T. (1999a). Interaction between a fucoid canopy and limpet grazing in structuring a low shore intertidal community. *J. Exp. Mar. Biol. Ecol.* 233, 41–63. doi: 10.1016/S0022-0981(98)00128-2

Jenkins, S., Hawkins, S., and Norton, T. (1999b). Direct and indirect effects of a macroalgal canopy and limpet grazing in structuring a sheltered inter-tidal community. *Mar. Ecol. Prog. Ser.* 188, 81–92.

Jenkins, S. R., Norton, T., and Hawkins, S. J. (2004). Long term effects of *Ascophyllum nodosum* canopy removal on mid shore community structure. *J. Mar. Biol. Assoc. UK* 84, 327–329. doi: 10.1017/S0025315404009221h

JNCC (1990). *SACFOR Abundance Scale used for Both Littoral and Sublittoral Taxa from 1990 Onwards*. Available online at: https://mhc.jncc.gov.uk/media/1009/sacfor.pdf [accessed December 2, 2020].

Kingsolver, J. G., Diamond, S. E., and Buckley, L. B. (2013). Heat stress and the fitness consequences of climate change for terrestrial ectotherms. *Funct. Ecol.* 27, 1415–1423. doi: 10.1111/1365-2435.12145

Kuo, E. S., and Sanford, E. (2009). Geographic variation in the upper thermal limits of an intertidal snail: implications for climate envelope models. *Mar. Ecol. Prog. Ser.* 388, 37–146. doi: 10.3354/meps08102

Lewis, J. R. (1964). *The Ecology of Rocky Shores*. London: English Universities Press.

Lewis, J. R. (1986). Latitudinal trends in reproduction, recruitment and population characteristics of some rocky littoral molluscs and cirripedes. *Hydrobiologia* 142, 1–13. doi: 10.1007/978-94-009-4049-9_1

Lewis, J. R., Bowman, R. S., Kendall, M. A., and Williamson, P. (1982). Some geographical components in population dynamics: possibilities and realities in some littoral species. *Neth. J. Sea Res.* 16, 18–28. doi: 10.1016/0077-7579(82)90013-8

Machado, P. M., Costa, L. L., Suciu, M. C., Tavares, D. C., and Zalmon, I. R. (2016). Extreme storm wave influence on sandy beach macrofauna with distinct human pressures. *Mar. Pollut. Bull.* 107, 125–135. doi: 10.1016/j.marpolbul.2016.04.009

Madge, G. (2020). *2020 Set to Extend Series of Earth's Warmest Years*. Available online at: https://www.metoffice.gov.uk/about-us/press-office/news/weather-and-climate/2019/2020-global-temperature-forecast [accessed November 25, 2020]

Mangano, M. C., Mieszkowska, N., Helmuth, B., Domingos, T., Sousa, T., and Baiamonte, G. (2020). Moving towards a strategy for addressing climate displacement of marine resources: a proof-of-concept. *Front. Mar. Sci.* 7:408. doi: 10.3389/fmars.2020.00408

Martins, G. M., Harley, C. D. G., Faria, J., Vale, M., Hawkins, S. J., Neto, A. I., et al. (2019). Direct and indirect effects of climate change squeeze the local distribution of a habitat-forming seaweed. *Mar. Ecol. Prog. Ser.* 626, 43–52. doi: 10.3354/meps13080

Masselink, G., Scott, T., Poate, T., Russell, P., Davidson, M., and Conley, D. (2016). The extreme 2013/2014 winter storms: hydrodynamic forcing and coastal response along the southwest coast of England. *Earth Surf. Proc. Land.* 41, 378–391. doi: 10.1002/esp.3836

Matthews, T., Murphy, C., Wilby, R. L., and Harringan, S. (2014). Stormiest winter on record for Ireland and UK. *Nat. Clim. Chang.* 4, 738–740. doi: 10.1038/nclimate2336

Met Office (2014). Avaialble at: https://www.metoffice.gov.uk/binaries/content/assets/metofficegovuk/pdf/weather/learn-about/uk-past-events/interesting/2013/winter-storms-december-2013-to-january-2014---met-office.pdf (accessed November 25, 2020).

Met Office (2020). Available online at: https://www.metoffice.co.uk/about-us/press-office/news/weather-and-climate/2018/end-of-summer-stats (accessed November 25, 2020).

Mieszkowska, N., and Sugden, H. (2016a). Climate-driven range shifts within benthic habitats across a marine biogeographic transition zone. *Adv. Ecol. Res.* 55, 325–369. doi: 10.1016/bs.aecr.2016.08.007

Mieszkowska, N., and Sugden, H. (2016b). *Marine Biodiversity and Climate Change Monitoring in the UK: Final Report to Natural England on the MarClim Annual Survey 2015*. York: Natural England.

Mieszkowska, N., and Sugden, H. (2017). *Marine Biodiversity and Climate Change Monitoring in the UK: Final Report to Natural England on the MarClim Annual Survey 2016*. York: Natural England.

Mieszkowska, N., and Sugden, H. (2018). *Marine Biodiversity and Climate Change Monitoring in the UK: Final Report to Natural England on the MarClim annual survey 2017*. York: Natural England.

Mieszkowska, N., Benedetti-Cecchi, L., Burrows, M. T., Cristina Mangano, M., Queirós, A., Seuront, L., et al. (2019). Multinational, integrated approaches linking organismal to biogeographic impacts of climate change. *Mar. Ecol. Prog. Ser.* 613, 247–252.

Mieszkowska, N., Burrows, M. T., and Sugden, H. (2020). Impacts of climate change on intertidal habitats relevant to the coastal and marine environment around the UK. *MCCIP Sci. Rev.* 2020, 256–271.

Mieszkowska, N., Burrows, M., Pannacciulli, F., and Hawkins, S. J. (2014b). Multidecadal signals within co-occuring intertidal barnacles *Semibalanus balanoides* and *Chthamalus* spp. linked to the Atlantic Multidecadal Oscillation. *J. Mar. Syst.* 133, 70–76. doi: 10.1016/j.jmarsys.2012.11.008

Mieszkowska, N., Kendall, M. A., Hawkins, S. J., Leaper, R., Williamson, P., Hardman-Mountford, N. J., et al. (2006). Changes in the range of some common rocky shore species in Britain - a response to climate change? *Hydrobiologia* 555, 241–251. doi: 10.1007/1-4020-4697-9_20

Mieszkowska, N., Sugden, H., Firth, L., and Hawkins, S. J. (2014a). The role of sustained observations in tracking impacts of environmental change on marine biodiversity and ecosystems. *Philos. Trans. R. Soc. A* 372:20130339. doi: 10.1098/rsta.2013.0339

Mislan, K. A. S., Wethey, D. S., and Helmuth, B. (2009). When to worry about the weather: role of tidal cycle in determining patterns of risk in intertidal ecosystems. *Glob. Change Biol.* 15, 3056–3065. doi: 10.1111/j.1365-2486.2009.01936.x

Mrowicki, R. J., O'Connor, N. E., and Donohue, I. (2016). Temporal variability of a single population can determine the vulnerability of communities to perturbations. *J. Ecol.* 104, 887–897. doi: 10.1111/1365-2745.12533

National Oceanic Atmospheric Administration (2020). Available online at: https://www.ncdc.noaa.gov/cdo-web/ (accessed December 7, 2020).

Oliver, E. C. J., Burrows, M. T., Donat, M. G., Sen Gupta, A., Alexander, L. V., and Perkins-Kirkpatrick, K. (2019). Projected marine heatwaves in the 21st

century and the potential for ecological impact. *Front. Mar. Sci.* 6:734. doi: 10.3389/fmars.2019.00734

Oliver, E. C. J., Donat, M. G., Burrows, M. T., Moore, P. J., Smale, D. A., and Alexander, L. V. (2018). Longer and more frequent marine heatwaves over the past century. *Nat. Commun.* 9:1324. doi: 10.1038/s41467-018-03732-9

Pearson, G. A., Lago-Leston, A., and Mota, C. (2009). Frayed at the edges: selective pressure and adaptive response to abiotic stressors are mismatched in low diversity edge populations. *J. Ecol.* 97, 450–462. doi: 10.1111/j.1365-2745.2009.01481.x

Philippart, C. J., Anadón, R., Danovaro, R., Dippner, J. W., Drinkwater, K. F., Hawkins, S. J., et al. (2011). Impacts of climate change on European marine ecosystems: observations, expectations and indicators. *J. Exp. Mar. Biol. Ecol.* 400, 52–69. doi: 10.1016/j.jembe.2011.02.023

Pinnegar, J. K., Wright, P. D., Maltby, K., and Garrett, A. (2020). The impact of climate change on fisheries, relevant to the coastal and marine environment around the UK. *MCCIP Sci. Rev.* 456–481.

Poloczanska, E. S., Brown, C. J., Sydeman, W. J., Kiessling, W., Schoeman, D. S., Moore, P. J., et al. (2013). Global imprint of climate change on marine life. *Nat. Clim. Chang.* 3, 919–925. doi: 10.1038/nclimate1958

Poloczanska, E. S., Hawkins S. J., Southward, A. J., and Burrows, M. T., (2008). Modelling the response of populations of competing species to climate change. *Ecology* 89, 3138–3149. doi: 10.1890/07-1169.1

Posey, M., Lindberg, W., Alphin, T., and Vose, F. (1996). Influence of Storm Disturbance on an Offshore Benthic Community. *Bull. Mar. Sci.* 59, 523–529.

Raffaelli, D., and Hawkins, S. J. (1996). *Intertidal Ecology*. New York, NY: Kulwer Academic Publishers.

Reynolds, R. W., Smith, T. M., Lui, C., Chelton, D. B., Casey, K. S., and Schlax, M. G. (2007). Daily high-resolution-blended analysis for sea surface temperature. *J. Clim.* 20, 5473–5496. doi: 10.1175/2007jcli1824.1

Sarà, G., Milanese, M., Prusina, I., Sara, A., Angel, D. L., and Glamuzina, B. (2014). The impact of climate change on mediterranean intertidal communities: losses in coastal ecosystem integrity and services. *Reg. Environ. Chang.* 14, 5–17. doi: 10.1007/s10113-012-0360-z

Schonbeck, M. W., and Norton, T. A. (1979). Drought-hardening in the upper-shore seaweeds *Fucus spiralis* and *Pelvetia canaliculata*. *J. Ecol.* 67, 687–696. doi: 10.2307/2259120

Simkanin, C., Power, A.-M., Myers, A., McGrath, D., Southward, A. J., Mieszkowska, N., et al. (2005). Using historical data to detect temporal changes in the abundances of intertidal species on Irish shores. *J. Mar. Biol. Assoc. U.K.* 85, 1329–1340. doi: 10.1017/s0025315405012506

Simpson, S. D., Jennings, S., Johnson, M. P., Blanchard, J. L., Schön, P.-J., Sims, D. W., et al. (2011). Continental shelf-wide response of a fish communities to rapid warming of the sea. *Curr. Biol.* 21, 1565–1570. doi: 10.1016/j.cub.2011.08.016

Smale, D. A., and Vance, T. (2016). Climate-driven shifts in species' distributions may exacerbate the impacts of storm disturbances on North-east Atlantic kelp forests. *Mar. Freshw. Res.* 67, 65–74. doi: 10.1071/MF14155

Smale, D. A., Wernberg, T., Oliver, E. C. J., Thomsen, M., Straub, S. C., and Burrows, M. T. (2019). Marine heatwaves threaten global biodiversity and the provision of ecosystem services. *Nat. Clim. Chang.* 9, 306–312. doi: 10.1038/s41558-019-0412-1

Smit, A. J., Hobday, A. J., Alexander, L. V., Perkins, S. E., Smale, D. A., and Straub, S. C. (2018). *RmarineHeatWaves: Package for the Calculation of Marine Heat Waves Version 0.17.0*. Bellville: South Africa: University of the Western Cape.

Sousa, W. P. (1979). Disturbance in marine intertidal boulder fields: the nonequilibrium maintenance of species diversity. *Ecology* 60, 1225–1239. doi: 10.2307/1936969

Southward, A. J., Hawkins, S. J., and Burrows, M. T. (1995). Seventy years' observations of changes in distribution and abundance of zooplankton and intertidal organisms in the western English Channel in relation to rising sea temperature. *J. Therm. Biol.* 20, 127–155. doi: 10.1016/0306-4565(94)00043-i

Southward, A. J., Langmead, O., Hardman-Mountford, N. J., Aiken, J., Boalch, G. T., and Dando, P. R. (2004). Long-term biological and environmental researches in the western English Channel. *Adv. Mar. Biol.* 47, 1–105. doi: 10.1016/j.pocean.2014.07.004

Sugden, H., Lenz, M., Molis, M., Wahl, M., and Thomason, J. C. (2008). The interaction between nutrient availability and disturbance frequency on the diversity of benthic marine communities on the north-east coast of England. *J. Anim. Ecol.* 77, 24–31. doi: 10.1111/j.1365-2656.2007.01323.x

Sugden, H., Panusch, R., Lenz, M., Wahl, M., and Thomason, J. C. (2007). Temporal variability of disturbances: is this important for diversity and structure of marine fouling communitiess? *Mar. Ecol.* 28, 368–376. doi: 10.1111/j.1439-0485.2007.00184.x

Sunday, J. M., Bates, A. E., and Dulvy, N. K. (2012). Thermal tolerance and the global redistribution of animals. *Nat. Clim. Chang.* 2, 686–690. doi: 10.1038/nclimate1539

Teagle, H., Hawkins, S. J., Moore, P. J., and Smale, D. A. (2017). The role of kelp species as biogenic habitat formers in coastal marine ecosystems. *J. Exp. Mar. Biol. Ecol.* 492, 81–98. doi: 10.1016/j.jembe.2017.01.017

Thompson, R. C., Wilson, B. J., Tobin, M. L., Hill, A. S., and Hawkins, S. J. (1996). Biologically generated habitat provision and diversity of rocky shore organisms at a hierarchy of spatial scales. *J. Exp. Mar. Biol. Ecol.* 202, 73–84. doi: 10.1016/0022-0981(96)00032-9

United Nations (2020). Available online at: https://www.un.org/sustainabledevelopment/sustainable-development-goals/ (accessed November 21, 2020).

Vasseur, D. A., DeLong, J. P., Gilbert, B., Greig, H. S., Harley, C. D., McCann, K. S., et al. (2014). Increased temperature variation poses a greater risk to species than climate warming. *Proc. R. Soc. B Biol. Sci.* 281:20132612. doi: 10.1098/rspb.2013.2612

Vinagre, C., Leal, I., Mendonça, V., Madeira, D., Narciso, L., Diniz, M. S., et al. (2016). Vulnerability to climate warming and acclimation capacity of tropical and temperate coastal organisms. *Ecol. Ind.* 62, 317–327. doi: 10.1016/j.ecolind.2015.11.010

Vye, S. R., Dickens, S., Adams, L., Bohn, K., Chenery, J., Dobson, N., et al. (2020). Patterns of abundance across geographical ranges as a predictor for responses to climate change: evidence from UK rocky shores. *Divers. Distrib.* 26, 1357–1365. doi: 10.1111/ddi.13118

Webb, T. J., Lines, A., and Howarth, L. M. (2020). Occupancy-derived thermal affinities reflect known physiological thermal limits of marine species. *Ecol. Evol.* 10, 7050–7061. doi: 10.1002/ece3.6407

Williams, G. A., Helmuth, B., Russell, B. D., Dong, Y. W., Thiyagarajan, V., and Seuront, L. (2016). Meeting the climate change challenge: pressing issues in southern China and SE Asian coastal ecosystems. *Reg. Stud. Mar. Sci.* 8, 373–381. doi: 10.1016/j.rsma.2016.07.002

Wolf, J., Woolf, D., and Bricheno, L. (2020). Impacts of climate change on storms and waves relevant to the coastal and marine environment around the UK. *MCCIP Sci. Rev.* 2020, 132–157.

Conflict of Interest: The authors declare that the research was conducted in the absence of any commercial or financial relationships that could be construed as a potential conflict of interest.

frontiers in Marine Science

ORIGINAL RESEARCH
published: 06 October 2021
doi: 10.3389/fmars.2021.688316

Species That Fly at a Higher Game: Patterns of Deep–Water Emergence Along the Chilean Coast, Including a Global Review of the Phenomenon

Vreni Häussermann[1,2], Stacy Anushka Ballyram[2,3†], Günter Försterra[4†], Claudio Cornejo[5], Christian M. Ibáñez[6], Javier Sellanes[7], Aris Thomasberger[8], Juan Pablo Espinoza[2,3] and Francine Beaujot[2]*

[1] Departamento de Vinculación con el Medio, Facultad de Economía y Negocios, Universidad San Sebastian, Puerto Montt, Chile, [2] Huinay Foundation, Puerto Montt, Chile, [3] Programa de Magíster en Oceanografía, Facultad de Recursos Naturales, Escuela de Ciencias del Mar, Pontificia Universidad Católica de Valparaíso, Valparaíso, Chile, [4] Facultad de Recursos Naturales, Escuela de Ciencias del Mar, Pontificia Universidad Católica de Valparaíso, Valparaíso, Chile, [5] Programa de Doctorado en Sistemática y Biodiversidad, Departamento de Zoología, Facultad de Ciencias Naturales y Oceanográficas, Universidad de Concepción, Concepción, Chile, [6] Departamento de Ecología y Biodiversidad, Facultad de Ciencias de la Vida, Universidad Andres Bello, Santiago, Chile, [7] Departamento de Biología Marina and MN ESMOI, Universidad Católica del Norte, Coquimbo, Chile, [8] Section for Coastal Ecology, National Institute of Aquatic Resources, Technical University of Denmark, Kongens Lyngby, Denmark

OPEN ACCESS

Edited by:
Marcos Rubal, University of Porto, Portugal

Reviewed by:
Clara F. Rodrigues, University of Aveiro, Portugal
Astrid Brigitta Leitner, Monterey Bay Aquarium Research Institute (MBARI), United States

***Correspondence:**
Vreni Häussermann
v.haussermann@gmail.com

† These authors have contributed equally to this work

Specialty section:
This article was submitted to Marine Evolutionary Biology, Biogeography and Species Diversity, a section of the journal Frontiers in Marine Science

Received: *30 March 2021*
Accepted: *19 July 2021*
Published: *06 October 2021*

Citation:
Häussermann V, Ballyram SA, Försterra G, Cornejo C, Ibáñez CM, Sellanes J, Thomasberger A, Espinoza JP and Beaujot F (2021) Species That Fly at a Higher Game: Patterns of Deep–Water Emergence Along the Chilean Coast, Including a Global Review of the Phenomenon. Front. Mar. Sci. 8:688316. doi: 10.3389/fmars.2021.688316

Deep-water emergence (DWE) is the phenomenon where marine species normally found at great depths (i.e., below 200 m), can be found locally occurring in significantly shallower depths (i.e., euphotic zone, usually shallower than 50 m). Although this phenomenon has been previously mentioned and deep-water emergent species have been described from the fjord regions of North America, Scandinavia, and New Zealand, local or global hypotheses to explain this phenomenon have rarely been tested. This publication includes the first literature review on DWE. Our knowledge of distribution patterns of Chilean marine invertebrates is still very scarce, especially from habitats below SCUBA diving depth. In our databases, we have been gathering occurrence data of more than 1000 invertebrate species along the Chilean coast, both from our research and from the literature. We also distributed a list of 50 common and easily *in situ*-identifiable species among biologically experienced sport divers along the Chilean coast and recorded their sighting reports. Among other findings, the analysis of the data revealed patterns from 28 species and six genera with similar longitudinal and bathymetric distribution along the entire Chilean coast: along the Chilean coast these species are typically restricted to deep water (>200 m) but only in some parts of Chilean Patagonia (>39°S–56°S), the same species are also common to locally abundant at diving depths (<30 m). We found 28 of these 'deep' species present in shallow-water of North Patagonia, 32 in Central Patagonia and 12 in South Patagonia. The species belong to the phyla Cnidaria (six species), Mollusca (four species), Arthropoda (two species) and Echinodermata (16 species). We ran several analyses comparing depth distribution between biogeographic regions (two-way ANOVA) and comparing abiotic parameters of shallow and deep sites to search for correlations of distribution with environmental variables (Generalized Linear Models). For the analyses, we used a total of

3328 presence points and 10635 absence points. The results of the statistical analysis of the parameters used, however, did not reveal conclusive results. We summarize cases from other fjord regions and discuss hypotheses of DWE from the literature for Chilean Patagonia.

Keywords: Norway, British Columbia, Alaska, New Zealand, Chile, fjord region, marine invertebrates, deep-water emergence

INTRODUCTION

Vertical changes in the physical and chemical properties of the ocean divide the benthic environment into six depth zones: (1) the intertidal, which is exposed during low tide; (2) the littoral or photic zone (0–200 m) which extends from the high tide line down to about 200 m at the edge of the continental shelf and includes the euphotic zone (0–50 m) and the oligophotic zone (50–200 m); the sublittoral or deep-sea, which is lightless and cold, and is sub-dived into (3) the archibenthic zone (200–1000 m) at the continental slope, which is often oxygen-deficient and also called dysphotic, mesophotic or twilight zone (there is <1% of light left, but it is not enough for primary production); (4) the bathybenthic zone or bathyal (1000–4000 m), which is aphotic, includes most of the continental rise and usually has a greater oxygen-content than the overlaying layer; (5) the abyssobenthic zone or abyssal (4000–6000 m), which includes the deep ocean floor and has little nutrient import; and (6) the hadobenthic zone or hadal (>6000 m) which is usually found in deep-sea trenches (Sutton, 2013; Pinet, 2019).

The deep-sea was considered an azoic environment until the mid-nineteenth century when Norwegian naturalist Michael Sars listed hundreds of invertebrate species collected from the deep-sea. Nowadays it is known as the largest biome on earth, distinct from other ecosystems and comparably diverse (Ramirez-Llodra et al., 2010). The origin and possible antiquity of the surprisingly diverse modern deep-sea fauna has been debated since the beginning of deep-sea research. Based on material collected during the HMS Challenger Expedition from 1872 to 1876, Murray (1895) concluded that the animals recovered from the deep-sea were similar to the taxa found in shallow-water high-latitude habitats, and thus the origin of this life was in shallow waters. Subsequently, papers discussed the two possible pathways explaining the origin of deep-sea species: shallow-water submergence versus an origin in deep water. Most studies compared the southern ocean littoral fauna to deep-sea fauna. Examples for both pathways have been published. Research that supports the DWE pathway include those by Hessler and Thistle (1975) that suggests an *in situ* evolution for parasseloidean deep-sea isopods, also Thuy and Schulz (2012) described an ancient echinoderm assemblage from the NE Atlantic deep-sea and Quattro et al. (2001) showed the upper bathyal zone of the North Atlantic to be an active site of population differentiation for mollusks. In support of the shallow-water submergence pathway, Riehl and Kaiser (2012) described a deep-sea isopod originating from the Antarctic shelf. Some relationships between shallow and deep-water fauna, however, could not be explained by either scenario, e.g., for the echinoid genus *Sterechinus* (Dıaz et al., 2010) and for foraminiferans (Lipps and Hickman, 1982); and for some groups of deep-sea octopuses, both pathways have been shown (Strugnell et al., 2011). Discussions on the origin of deep-sea fauna are ongoing.

Deep-water benthic research in Chile started with the Challenger (1872–1876) and Lund University Chile Expeditions (1948/49). Since then, advances in the knowledge of deep-sea benthos have been sparse, including mainly occasional samples of US research vessels transiting to Antarctica between the 1960s and early 1980s (e.g., R/V Hero and USNS Eltanin), as well as surveys onboard the R/V Anton Bruun in 1965–1966, to mention a few (reviewed in Sievers-Czischke, 2018). Major national expeditions started in the 1960s, mainly with the MarChile program, highlighting benthic studies at the shelf break and upper slope in northern Chile during the MarChile II expedition in 1962 (Gallardo, 1963). However, the first comprehensive bathymetric and latitudinal study of the upper-bathyal benthos (∼200 to 2000 m depth) was performed during the Oceanographic Expedition PUCK (R/V Sonne, SO-156 cruise) in 2001 (Quiroga et al., 2009; Sellanes et al., 2010). In this cruise, the emphasis was put on studying the role of the SE Pacific Oxygen Minimum Zone (OMZ) in shaping the patterns of benthic assemblages along the Chilean continental margin.

Methane-seep environments were discovered in 2003 and later studied on the upper slope off Concepción (∼36°S, ∼800 m depth), leading to the description of many new species and new records of existing species for the area (see Sellanes et al., 2004, 2008). Subsequent findings of methane seep communities include areas from off the Taitao Peninsula (∼45°S, ∼500 m depth) (Zapata-Hernández et al., 2014), to off El Quisco (∼33°S; ∼300 m depth) (Krylova et al., 2014), and more recently off Huasco (∼28°S, ∼1500 m depth) (Kobayashi and Araya, 2018).

Benthic surveys conducted using remotely operated vehicles (ROVs), are quite scarce on the continental slope off Chile. An advantage of using ROVs is that benthic communities can be observed *in situ* before being altered by the sampling procedure, and characteristics of the living animal are lost. Probably the most important ROV survey was on the R/V Sonne cruise SO-210, in which the ROV Kiel 6000 was used (Treude et al., 2011). Another ROV survey led to the first report of antipatharian black corals on the shelf break off La Higuera (∼29°S, 70–107 m depth) (Gorny et al., 2018). Other methods of benthic studies in the area include studying species collected as bycatch from deep-water Patagonian Toothfish and crustacean fisheries (e.g., Ibáñez et al., 2006, 2011, 2012, 2016; Araya, 2013, 2016).

The deep-water emergence (DWE) hypothesis has been mentioned in the literature since 1970 (Hessler, 1970). Since this phenomenon is more common in higher latitudes, it has also been

called "polar emergence" or "high-latitude emergence." Hessler (1970) and Hessler et al. (1979) argued that specialized deep-sea isopods evolved *in situ* and their presence at shallow high latitudes is a result of subsequent emergence. In the following decades, other deep-water species have been described from shallow waters in several places. Some Chilean species with deep-water records off northern and central Chile as well as Patagonia are well known in shallow waters of Chilean Patagonia (Häussermann and Försterra, 2009). Other deep-water species have been described in shallow waters of New Zealand, Alaska, and Norway (summarized in this paper), from nearshore marine caves in the Mediterranean and the Atlantic (e.g., Grigg, 1965; Stock and Vermeulen, 1982) and from the turbid waters between Trinidad and Venezuela (Warner, 1981).

In the present paper, we list 28 species and six genera from the phyla Cnidaria, Mollusca, Arthropoda, and Echinodermata that have been recorded in deep waters between 200 and 1800 m off the coast of Chile, restricted to these deep waters in central and northern Chile, while in addition, present at diving depth in fjords and channels of Chilean Patagonia. Biogeographically there is a break at about 30°S, which separates the Peruvian Province (north of ∼30°S) from the Intermediate Area (∼30°S to ∼40–42°S) (Tellier et al., 2009). Chilean Patagonia is part of the Magellan Province and is subdivided into North Patagonia (NP; ∼40–42°S to Golfo de Penas, ∼47–48°S), Central Patagonia (CP; ∼47–48°S to Straight of Magellan, ∼53–54°S) and South Patagonia (SP; ∼53–54°S to Cape Horn, 56°S). We summarize the latitudinal and bathymetric distribution of the listed species and genera, their type of larvae and mode of reproduction, as far as it is known. We compared depth distribution between biogeographic regions and searched for correlations between distribution and environmental variables. Our paper also includes the first review on the DWE phenomenon: we list deep-water emergent species described in the literature from other parts of the world and summarize and discuss the hypotheses used to explain this phenomenon.

MATERIALS AND METHODS

Database

The PAtagonia MArine DAtabase (PAMADA) includes nearly 2,000 identified benthic species and more than 20,000 presence points collected during 43 SCUBA expeditions and six ROV expeditions at more than 500 study sites during the years 1997 and 2020, and from the literature. The Biological Collection of Universidad Católica del Norte UCN (SCBUCN) currently keeps more than 6,000 samples of preserved marine organisms, mainly from the continental slope and oceanic islands of Chile, as well as from seamounts within the Chilean Exclusive Economic Zone (**Figure 1** and **Supplementary Figure 1**). The SCBUCN database is available through the Global Biodiversity Information Facility (Sellanes, 2018) and for the current study, 144 of these records were used. During data searches to complement the

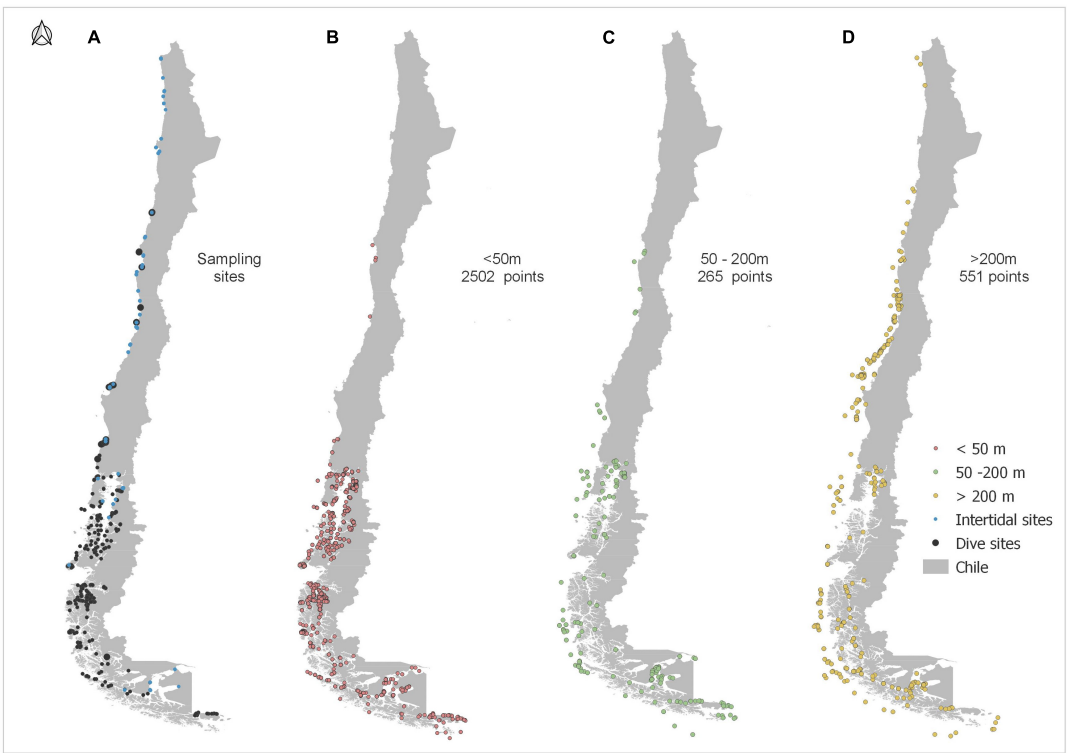

FIGURE 1 | (A) Sampling sites. Black points represent dive sites and blue points intertidal study sites. **(B–D)** Sites of invertebrate presence data along the Chilean coast from both PAMADA and SCBUCN (total 3331 points). **(B)** Presence data <50 m depth. **(C)** Presence data 50–200 m depth. **(D)** Presence data >200 m depth.

PAMADA database from SCBUCN and OBIS, V. Häussermann (see also Häussermann, 2006) detected some species with unusual distribution patterns which led to an extensive search for species present in both shallow waters of Chilean Patagonia and deep waters off Central and Northern Chile. To complete the existing Patagonian shallow-water records (a coastline of > 100,000 km) for the Central and Northern Chilean coast, we distributed a list of common and easily *in situ*-identifiable species, including the 28 species and six genera, among biologically experienced sport divers along the Chilean coast between Bahía Mansa (40.77°S; 73.84°W) and Caldera (27.05°S; 70.82°W) (a coastline of 1500 km). We used data from the 24 dive sites they regularly visit. Christian Ibáñez added data from 40 intertidal sites along the exposed coast of North and Central Chile. We could not find any diving biologists or sports divers who dive at sites north of 27°S.

Statistical Analyses

We compared the depth distribution of 34 genera between biogeographic regions (Peruvian Province and Intermediate Area to Magellan Province) by means of two-way ANOVA using R ver. 4.0.5 (R Core Team, 2021).

We also tested the correlations of abiotic factors (where data were available) with species presence data. The sea bottom temperature (SBT), sea bottom salinity (SBS), molecular dissolved oxygen at bottom (SBO), primary productivity (PP), Chlorophyll-a, silicate and current velocity were obtained from the BioOracle v2 (Assis et al., 2018) based on monthly averages from 2000 to 2017. Environmental variables were extracted from each presence/absence point. The BioOracle web platform[1] (Tyberghein et al., 2012; Assis et al., 2018) was used to obtain these data using QGIS (QGIS Development Team, 2012).

Three Generalized Linear Models (GLM) with a binomial distribution error type were run to establish the existence of linear patterns between the presence/absence data and the predictor variables (depth, temperature, salinity, primary production, chlorophyll-a, oxygen, silicate, current velocity). The first GLM was run with all presence/absence data (>13,000 records). To detect the common predictors responsible for shallow water presence points in the south and deep water presence points in the north, we ran two more GLMs, one for those records shallower than 50 m and one with those records deeper than 200 m. The predictor variables were set over 250 models (for each GLM), executed using the "glmulti" function of the 'GLMULTI' package (Calcagno and de Mazancourt, 2010) implemented in the software R, this function examines all possible combinations of predictor variables, and the best model for each analysis was selected based on Bayesian information criterion (BIC). To establish which predictor variables contribute to a total variance, an ANOVA was used over the GLM coefficients. The most important variable for each GLM was obtained based on the *t*-statistic, using the "varImp" function from the "caret" package (Kuhn, 2008) implemented in the software R.

[1]https://www.bio-oracle.org

RESULTS

Deep-Water Emergent and Eurybathic Species in Chilean Patagonia

Based on the data search described above, we compiled a list of 28 species and six genera that are restricted to deep waters off Central and Northern Chile but reach into shallow water in Chilean Patagonia, a pattern first mentioned in Häussermann (2006). The listed taxa are from the phyla Cnidaria (six species, four genera), Mollusca (four species, one genus), Arthropoda (two species, one genus) and Echinodermata (16 species) and include three sea anemones (Cnidaria, Actiniaria), three stony corals (Cnidaria, Scleractinia), three gorgonians and one soft coral (Cnidaria, Alcyonacea), three snails (Mollusca, Gastropoda), one mussel (Mollusca, Bivalvia), one chiton (Mollusca, Polyplacophora), two crabs (Arthropoda, Decapoda), one sea spider (Arthropoda, Pycnogonida), six starfish (Echinodermata, Asteroidea), five brittle stars (Echinodermata, Ophiuroidea), two sea urchins (Echinodermata, Echinoidea), two sea cucumbers (Echinodermata, Holothuroidea) and one feather star (Echinodermata, Crinoidea) (**Table 1**). The search resulted in a total of 3331 presence (**Supplementary Table 1**) and 10842 absence points. For typical distributions of some selected deep-water emergent species, see **Figure 2**. In addition to these 28 species and six genera we found more species that present a eurybathic distribution within Chilean Patagonia (from the deep-sea to diving depth) but so far have not been observed north of Patagonia. These species are typical members of deep-water genera, which within the Chilean fiord region extend into shallow water: the sea anemones *Bolocera kerguelensis* (25–485 m; possibly 3329 m at 38.10°S if the suggested synonymy with *B. patens* is correct) and *Isotealia antarctica* (25–420 m) (Häussermann and Försterra, 2005), the gorgonian *Convexella magelhaenica* (12–1666 m) (Häussermann et al., 2016) and the hydrocoral *Errina antarctica* (18–771 m) (Häussermann and Försterra, 2007b).

Cnidaria

Actinostola intermedia (=*A. chilensis*) and *Hormathia pectinata* (described down to 1220 m) are sea anemone species from typical deep-water genera; along the Chilean coast they have been collected between 30 and 34°S from 350 to 400 m depth and between 34 and 36°S from 744 to 936 m. In Chilean Patagonia, south of 41°S, both are regularly found below 20 and 25 m, respectively (*H. pectinata* to 53°S, *A. chilensis* to 55°S). Single specimens of *A. intermedia* were even found at 9 m depth, and *H. pectinata* at 12 m. *A. intermedia* inhabits current-exposed sites and can also be found in groups of up to 15–25 individuals. *H. pectinata* is rarely found in water shallower than 30 m, specimens were found on near vertical walls with little sedimentation. *Dactylanthus antarcticus* (described down to 610 m) was sighted on a video from the SONNE expedition in 700 m depth at 36°S. South of 45°S it is regularly found below 20 m depth in channels, becoming more abundant south of 49°S.

The cosmopolitan stony corals *Desmophyllum dianthus* (described down to 2460 m depth) and the recently described

TABLE 1 | List of deep-water emergent species from Chilean Patagonia: geographic and bathymetric distribution (bd) for North and Central Chile (N-C), North Patagonia (NP), Central Patagonia (CP), and South Patagonia (SP) main citation for Chile and first citation of deep-water emergence (DWE), typical deep-water species, type of reproduction and larvae.

Species	Phylum	Main citation for Chile	Distribution within Chile (°S)	First DWE mention	Distribution outside of Chile	Typical deep-water genus	bd (m)	bd (N-C)	bd (NP)	bd (CP)	bd (SP)	type of reproduction	type of larvae
Acanthogorgia spp.	Cnidaria, Octocorallia	Häussermann and Försterra, 2009	36–53	Häussermann and Försterra, 2007a	British Columbia coast	Species-specific	18-1920	940	20–30	18-1920	NA	Sexual and asexual	Pelagic planula Larvae
Acesta patagonica	Mollusca, Bivalvia	Osorio, 1968	29 - 53	Cairns et al., 2005	Atlantic SW, Falkland Islands	Yes	15-880	250-761	20 - 215	15-880	NA	Sexual	Pelagic Larvae
Actinostola intermedia	Cnidaria, Actiniaria	Häussermann, 2004	30 - 56	Häussermann, 2006	Atlantic SW, Desembocadura Rio La Plata	Yes	9 - 936	350-936	9 - 35	17 - 34	14 - 32	Sexual (probably spawning; Chilean species not brooding)	Pelagic planula Larvae
Alcyonium spp.	Cnidaria, Octocoralia	van Ofwegen et al., 2007	29 - 59	This paper	Worldwide	Species-specific	12-1800	257-764	12-36.6	18-35	14-1800	Sexual and asexual (broadcast spawning and brooding, species-dependent)	Planktonic planula larva
Arbacia dufresnii	Echinodermata, Echinoidea	Häussermann and Försterra, 2009	18 - 56	This paper	Antartic peninsula, Atlantic SW, Falkland Islands	No	0-1300	(55)223-1300	2-345	0-682	6-476	Sexual (spawning)	Planktonic larvae
Astrotoma agassizii	Echinodermata, Ophiuroidea	Häussermann and Försterra, 2009; Manso, 2010	18 -56	This paper	Antartica, Subantartic Islands, Atlantic SW,	Yes	20-1300	327-1300	33-861	20-680	88-420	Sexual (brooding)	Planktotrophic larvae
Bathyplotes moseleyi	Echinodermata, Holothuroidea	Häussermann and Försterra, 2009	32 - 53	This paper	Pacific NW (Japan), Sub antartic Islands, Pacific E (Perú)	Yes	24-2454	580-960	2454	30-675	NA	Sexual and asexual	Planktotrophic larvae
Capulus ungaricoides	Mollusca, Gastropoda	Häussermann and Försterra, 2009	18 - 56	This paper	Atlantic SW, USA, Perú	Yes	30 - 636	209-450	30-252	32-636	522	Sexual	Pelagic Larvae
Caryophyllia huinayensis	Cnidaria, Scleractinia	Cairns et al., 2005	35 - 54	Cairns et al., 2005	Pacific SE (Perú, Ecuador, Colombia)	Yes	11-870	870	11-36.6	12-320	275 - 447,5	Sexual (probably spawning)	Pelagic Larvae
Colossendeis macerrima	Arthropoda, Pycnogonida	Araya, 2016	26 - 52	Försterra et al., 2013	Cosmopolitan	Yes	18 - 4306	1800	582	18-472	NA	PA	PA
Cosmasterias lurida	Echinodermata, Asteroidea	Häussermann and Försterra, 2009	29 - 55	This paper	Subantartic islands, South Georgia, Atlantic SW		0-906	(30)143-906	0-697	0-638	5-675	Sexual (spawning)	Planktonic larvae
Dactylanthus antarcticus	Cnidaria, Actiniaria	Häussermann and Försterra, 2009	45 - 54	This paper	Atlantic SW, Falkland Islands		10-700	700	10-831	25 - 33	21-571	Sexual (probably spawning)	Pelagic planula Larvae
Desmophyllum dianthus	Cnidaria, Scleractinia	Cairns et al., 2005	35- 54	Försterra and Häussermann, 2003	Cosmopolitan	Yes	8 - 2500 m	500-1300	8-831	18-923	267-1900	Sexual (broadcast spawning)	Pelagic Larvae
Florometra magellanica	Echinodermata, Crinoidea	Catalán et al., 2020	19 - 55	This paper	North of Panamá, Perú	Yes	20-949	275-949	574-687	20-574	22-485	Sexual (spawning)	Planktonic larvae
Fusitriton magellanicus	Mollusca, Gastropoda	Häussermann and Försterra, 2009	30 - 56	This paper	Atlantic SW, Central Argentina, New Zealand		0 - 960	200 - 960	3-334	0-607	0-869	Sexual (egg-laying)	Planktonic Larvae
Gorgonocephalus chilensis	Echinodermata, Ophiuroidea	Häussermann and Försterra, 2009; Manso, 2010	29 - 55	This paper	South Africa, Subantartic islands, Pacific SW,	Yes	4 - 3648m	349-3648	20-435	4-622	90-378	Sexual (spawning)	Planktotrophic larvae
Henricia studeri	Echinodermata, Asteroidea	Häussermann and Försterra, 2009	29 - 53	This paper	Pacific SW, New Zealand, Atlantic S, Atlantic SW, Falkland Islands		5-450	256-450	5-31	32-116	288	Sexual and asexual	Planktonic larvae
Hormathia pectinata	Cnidaria, Actiniaria	Häussermann and Försterra, 2009	30 - 53	Häussermann, 2006	Atlantic SW, Falkland Islands	Yes	12-1220	350-836	25-324	12-675	NA	Sexual (probably spawning)	Pelagic planula Larvae

(Continued)

TABLE 1 | (Continued)

Species	Phylum	Main citation for Chile	Distribution within Chile (°S)	First DWE mention	Distribution outside of Chile	Typical deep-water genus	Bd (m)	bd (N-C)	bd (NP)	bd (CP)	bd (SP)	type of reproduction	type of larvae
Labidiaster radiosus	Echinodermata, Asteroidea	Häussermann and Försterra, 2009	35 - 55	This paper	SW Atlantic, Pacific SW, Falkland Islands		3-1300	1300	14-29.2	10-95	3-385	Sexual and asexual	Planktonic larvae
Lithodes spp.	Arthropoda, Decapoda	Häussermann and Försterra, 2009	31 - 55	This paper	Atlantic SW (Argentina and Uruguay)	Yes	0-769	108-769	1-149	0-236	2-160	Sexual	Pelagic Larvae
Lophaster stellans	Echinodermata, Asteroidea	Häussermann and Försterra, 2009	29 - 55	This paper	Antartic and subantartic ocean, SW Atlantic, SE Pacific, New Zealand		15-510	(73)280-450	20 - 510	15-247	450	Sexual and asexual	Planktonic larvae
Ophiocten amitinum	Echinodermata, Ophiuroidea	Häussermann and Försterra, 2009; Manso, 2010	22 - 56	This paper	Antartica, subantartic islands, Atlantic SW,	Yes	23-3566	129-1300	NA	23-485	135-182	Sexual and asexual	Planktotrophic larvae
Ophiomitrella chilensis	Echinodermata, Ophiuroidea	Mortensen, 1952	33 - 42	This paper	NA	Yes	25-848	382-848	25-275	NA	NA	Sexual, simultaneous hermaphrodite	Planctonic Larvae
Ophiura lymani	Echinodermata, Ophiuroidea	Dahm, 1999; Häussermann and Försterra, 2009; Manso, 2010	31 - 54	This paper	Antartica, Atlantic SW, Rio la Plata, Subantartic islands (South Georgia, Falkland Islands)	Yes	23-940	346-940	130-861	23-642	448	Sexual (spawning, absence of annual periodicity)	Planktotrophic larvae
Pagurus comptus	Arthropoda, Decapoda	Häussermann and Försterra, 2009	29 - 56	This paper	SW Atlantic	No	0 - 746	400	5-30	12 - 263	6-360	Sexual	4 larva states
Poraniopsis echinaster	Echinodermata, Asteroidea	Häussermann and Försterra, 2009	26 - 54	This paper	S Atlantic, South Africa, Gough Island		5-651	(25)143 -502	5-490	5-651	66	Sexual and asexual	Planktonic larvae
Psolus squamatus	Echidermata, Holothuroidea	Häussermann and Försterra, 2009	31 - 49	This paper	N, SW Atlantic (Argentina, Falkland Islands)		7-1087	400	7-27	27.1-256	NA	Sexual	Planktotrophic larvae
Solaster regularis	Echinodermata, Asteroidea	Häussermann and Försterra, 2009	29 - 55	This paper	SW Atlantic (Brasil, Islas Malvinas, Uruguay)		5-1660	370-850	21-646	9-638	158-514	Sexual and asexual	Planktonic larvae
Stenosemus exaratus	Mollusca, Polyplacophora	Häussermann and Försterra, 2009; Schwabe and Sellanes, 2010	36 - 54	This paper	Artic ocean, Subantartic ocean, Norway, Atlantic SE	Yes	0-2850	467 - 934	0-225	23-732	NA	Sexual (egg-laying)	Lecitotrophic planktonic larvae
Swiftia spp.	Cnidaria, Octocorallia	Breedy et al., 2015	30 - 53	Häussermann and Försterra, 2007a	Worldwide	NA	15-906	320-906	15-55	31-329	NA	Sexual	Planktonic larvae
Tethocyathus endesa	Cnidaria, Scleractinia	Cairns et al., 2005	36 - 49	Cairns et al., 2005	Pacific SE (Perú, Ecuador, Colombia)	NA	11-240	240	11 - 37	12 - 31	NA	Sexual (probably spawning)	Probably pelagic Larvae
Thouarella spp.	Cnidaria, Octocorallia	Taylor et al., 2013	20 - 56	T. Koellikeri and T. brucei: T. n. sp.: Cairns and Häussermann, in press	Worldwide (especially Southern Ocean)	Yes	18-1920	761-960	20-765	18-770	494-1920	Sexual (some species brooding)	Planktonic planula larva
Tripylaster philippi	Echinodermata, Echinoidea	Häussermann and Försterra, 2009	35 - 55	This paper	Atlantic SW (Argentina), Subantartic islands	Yes	0-1300	714-1300	30-461	9-290	30-634	Sexual	Planktotrophic larvae
Trophon spp.	Mollusca, Gastropoda	Häussermann and Försterra, 2009	30 - 56	This paper	Atlantic SW (Argentina, Falkland Islands)	Species-dependent	0-607	(88)280-450	5-33	6-607	2-351	Sexual (egg-laying)	Planktonic larvae

For information on distribution within and outside of Chile, general bathymetric distribution, type of reproduction and larvae, data from the literature were used; information on reproduction, if not known for Chilean species, refers to genera; for information on bathymetric distribution in Chilean regions, data from both databases were used.

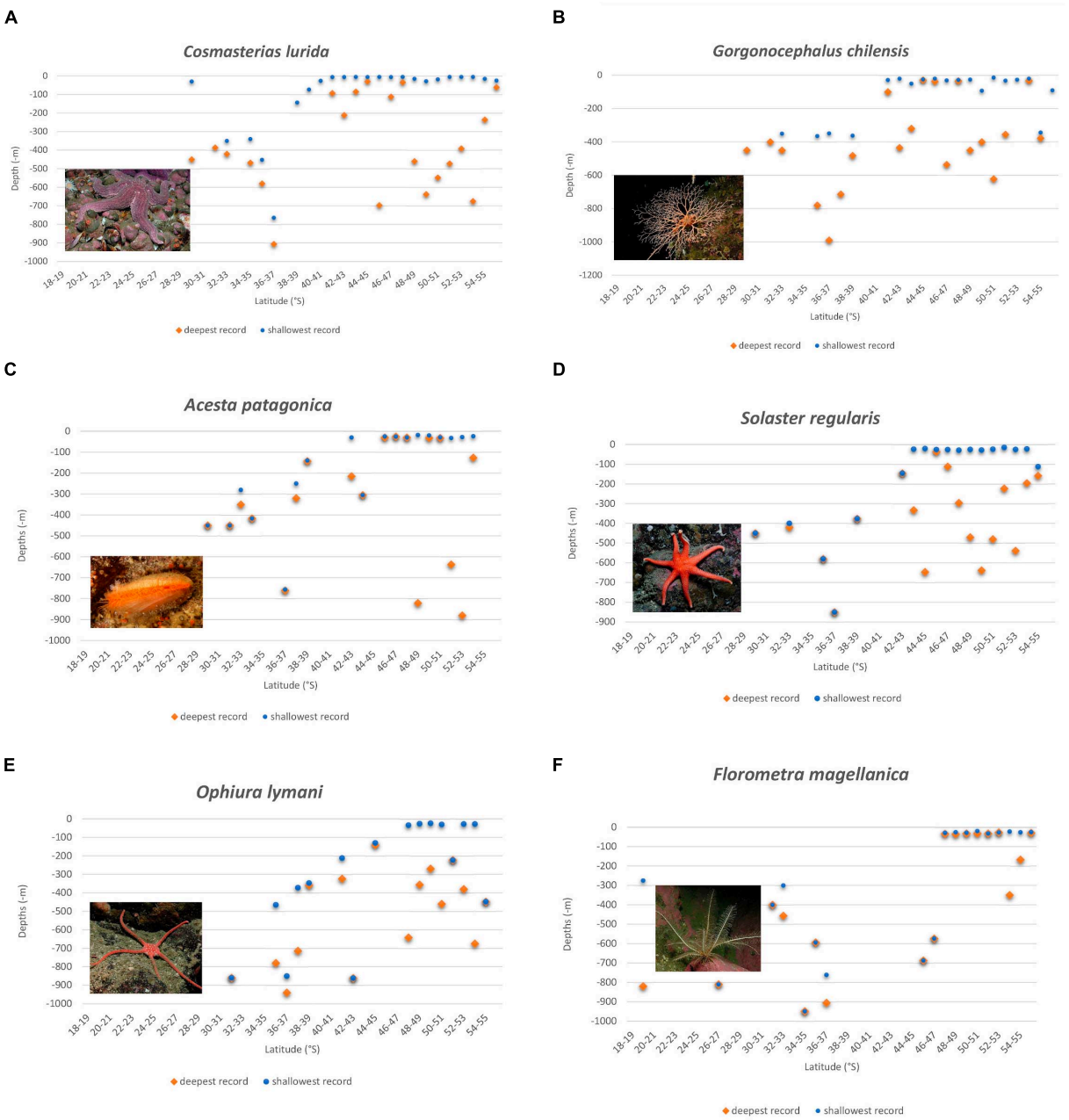

FIGURE 2 | Depth distribution of six typical deep-water emergent species with above-average number of records throughout Chile and appearance in shallow water of North Patagonia **(A–D)** and Central Patagonia **(E–F)**, sorted by appearance from north to south. A trend is visible with the upper depth distribution limit (deep-water emergence phenomenon) rising toward the south. **(A)** *Cosmasterias lurida* (Asteroidea), **(B)** *Gorgonocephalus chilensis* (Ophiuroidea), **(C)** *Acesta patagonica* (Bivalvia); **(D)** *Solaster regularis* (Asteroidea); **(E)** *Ophiura lymani* (Ophiuroidea); **(F)** *Florometra magellanica* (Crinoidea).

Caryophyllia huinayensis have been collected at about 750 m depth at 36.4°S. *Desmophyllum dianthus* was also collected at 35.5°S from 1100 to 1300 m, and *C. huinayensis* at 29.4°S from 256 to 276 m. Both species live on near vertical to overhanging rocky walls in Chilean Patagonia, south of 41°S, with little sediment (*D. dianthus* below 8 m down to 52.8°S, *C. huinayensis* below 11 m depth down to 53.4°S). *D. dianthus* was also found on a shipwreck at the exposed coast slightly north of the fjord region at 40.6°S in 11 m depth. The recently described *Tethocyathus endesa* was collected at 36.5°S in 240 m depth in a methane seep area. It is described from Patagonian fjords between 42°S and 48.4°S below 11 m depth on rocky substratum, withstands some sedimentation and is rarely found south of 47°S (Taitao Peninsula). All three species belong to the family Caryophylliidae.

Specimens of the gorgonian genus *Swiftia* were collected between 29 and 38°S from 320 to 906 m and in NP (42–46°S)

between 20 and 31 m. Specimens of the primnoid gorgonian genus *Thouarella* were collected at 20 and 36°S from 761 and 960 m respectively, and between 41.6 and 53.4°S while diving below 18 m. South of 50°S there are nine deep records, the deepest at 53°S from 1666 and 1920 m. The two records south of 53.4°S were from 269 and 1666 m. The gorgonian genus *Acanthogorgia* has one record from 940 m (36.3°S) and was found diving below 18–20 m between 45.3 and 53°S. The two records further south (53.1 and 53.8°S) were 1920 and 269 m. The soft coral genus *Alcyonium* has 14 records between 29.5 and 36.4°S from 250 to 764 m, and was found between 41.6°S (common south of 45.4°S) and 55°S while diving below 12 m. The record at 56°S is from 1800 m.

Mollusca

The deep-water bivalve *Acesta patagonica* (described down to 820 m) was found between 31°S and 34°S from 280 to 450 m and at 36.4°S from 751 to 763 m depth. At 38.8°S it was found in 137 m and at 42.5°S below 88 m depth (with two records from 20 to 30 m in Comau Fjord), associated with the scleractinian coral banks of *D. dianthus*. Further records lie south of 45°S with shallow-water specimens being more common between 48 and 49°S where it was found diving below 15 m depth; we have no records south of 53.4°S (**Figure 2C**).

The gastropod *Fusitriton magellanicus* has 12 records between 30 and 39°S where it was found from 200 to 960 m. South of 42°S in Patagonia it is found below 5 m, being more common in shallow water south of 48°S. *Capulus ungaricoides* is a poorly known species, it was found twice between 30 and 32°S at 300 and 450 m depth, at 41°S in 212 m depth, at 53°S in 522 m depth, and at 42.5 and 49°S in 30 m depth.

The chiton *Stenosemus exaratus* is a deep-water inhabiting species described down to 2580 m depth; most Chilean records are between 36 and 52°S from approximately 700–900 m depth; in Chilean Patagonia the species was collected at three sites in the intertidal and shallow subtidal.

Specimens of the gastropod genus *Trophon* have eight records between 30°S and 34.5°S from 280 to 450 m between (one record at 30°S is from 88 m), and can be found south of 39.9°S (down to 55°S) within diving depths. The southernmost record at 55.8°S is from 115 m depth.

Arthropoda

The decapod crab *Pagurus comptus* was collected once at 30°S at 400 m depth; it is common below 5 m depth throughout Chilean Patagonia. The cosmopolitan deep-sea spider *Colossendeis macerrima* (described from 141 to 4000 m) was collected at 26.7°S from 1500 to 1800 m depth and at 45.9°S in 510 m depth. In Chilean Patagonia it was found during a diving expedition at 48.5°S in 18 m depth.

Specimens of the decapod genus *Lithodes* have two records at 31.9°S and 36.4°S in 108 m and 769 m depth and can be found south of 41.5°S down to 55.3°S within diving depths.

Echinodermata

The sea stars *Lophaster stellans* and *Solaster regularis* (both Family Solasteridae) have been collected in Northern and Central Chile between 29 and 33°S from 260 to 420 m depth and between 32 and 39°S from 376 to 850 m. Both have been collected between 39 and 42°S in the littoral zone below diving depth (*L. stellans* at 39°S in 73 m and *S. regularis* at 42.5°S in 146 m) and appear within diving depths south of approximately 44°S, becoming much more abundant in shallow water between 48 and 50°S while there is only one (*L. stellans*) or no record (*S. regularis*) south of 53°S (**Figure 2D**). *Labidiaster radiosus* was found at 35.5°S in 1300 m depth. It is known from shallow water of Patagonia south of 42.6°S. *Cosmasterias lurida* presents 10 records between 29 and 37°S from 200 to 400 m depth. At 38.7°S it was collected in 140 m and at 39.1°S from 36 to 90 m. Between 41°S and 55°S it is very common, especially in fjords and inner channels from 5 m down to 460 m depth (**Figure 2A**). *Henricia studeri* has three records between 29 and 33°S from 256 to 450 m, it is known from shallow water south of 41°S with the shallowest record being from 5 m depth. *Poraniopsis echinaster* has 25 records between 26 and 39°S from 200 to 450 m. It was also found four times at 29, 30, and 33°S at the lower limit of diving depth from 25 to 40 m. It is very common in shallow water south of 41.6°S, with the shallowest record being from 5 m depth.

The feather star *Florometra magellanica* has 10 records between 19 and 37°S from 275 to 949 m depth. Between 45 and 47°S it was collected from 574 to 687 m; south of 47°S it was found regularly within diving depths (**Figure 2F**). The sea cucumber *Bathyplothes moseleyi* has two records at 32°S (580, 960 m). it was found at 42°S in 454 m and between 48 and 53.4°S within diving depths. The sea cucumber *Psolus squamatus* was found once at 31°S in 400 m depth and is common between 42 and 48°S within diving depths.

The brittle star *Gorgonocephalus chilensis* (Family Gorgonocephalidae) has 25 records between 35 and 39°S from 354 to 990 m depth. Between 41.7 and 53.8°S it was regularly seen in shallow water, being more abundant south of 48°S (**Figure 2B**). *Astrotoma agassizi* (Family Gorgonocephalidae) was found 30 times between 18.7 and 38.2°S from 327 to 1300 m and six times between 42 and 43°S from 85 to 860 m. Between 41.7 and 53°S there are 12 records from diving depth, most from 30 to 35 m, the shallowest being 20 m at 48.6°S. The brittle stars *Ophiura lymani* and *Ophiocten aminitum* belong to the family Ophiuridae. *Ophiura lymani* was collected 15 times between 31.7 and 43°S from 212 to 940 m, *O. amitinum* four times between 22.8 and 36.5°S from approximately 200–1300 m. Both species were found regularly in shallow water between approximately 47.8°S and 53.7/53.8°S, respectively, and were not found in shallow water south of 54°S; *O. lymani* being more common (25 records versus 11 records) (**Figure 2E**). *Ophiomitrella chilensis* has four records between 33°S and 39°S from 344 m to 843 m and was collected at 41°S in 100 m and at 42°S between 25 and 70 m.

The sea urchins *Arbacia dufresnei* has eleven records between 28.4 and 38.9°S from 223 to 1300 m and two recent records at 30°S from 55 and 60 m. In Chilean Patagonia south of 40.6°S it is very common from the intertidal to diving depths. *Tripylaster philippi* was found four times between 35.5 and 37.8°S from 714 to 1300 m, between 41.7 and 42.1°S from 230 to 460 m, and eight times between 42.3 and 54.9°S within diving depths.

Deep-Water Emergence Patterns Throughout Chilean Patagonia

Seven of the 34 deep-water species/genera from Northern and Central Chile appear at diving depth between 39.9°S (Valdivia) and 41.5°S (the northern end of the fjord region), further 16 species/genera appear between 41.6 and 43°S (the region around Chiloé Island, corresponding to the northern section of NP), six between 43 and 47°S (the Guaitecas and Chonos Archipelago, corresponding to the southern section of NP), and five between 47°S and 49°S (CP) (**Table 2** and **Figure 2**). This pattern results in 28 deep-water emergent species being present in NP (12 Echinodermata, nine Cnidaria, five Mollusca, two Arthropoda), 32 in CP (15 Echinodermata, nine Cnidaria, five Mollusca, three Arthropoda) and 12 in SP (five Echinodermata, three Cnidaria, two Gastropoda, two Arthropoda). Although also recorded in NP, the species *Lophaster stellans, Labidiaster radiosus, Solaster regularis* (all Echinodermata), and *Dactylanthus antarcticus* and the genera *Thouarella* and *Acanthogorgia* (all Cnidaria) were found only rarely in NP but were common in CP. This results in 22 common deep-water emergent species/genera in diving depth in NP; 32 in CP and 12 in SP (**Table 2**).

Twenty-eight of the 34 deep-water emergent species/genera have been registered from fjords, 34 from channels and only 11 from the exposed coast: one specimen of the coral *Desmophyllum dianthus*, however, was registered once at the exposed coast at 40°S (**Table 2**).

Single specimens of the species *Acesta patagonica* and *Tripylaster philippi* were found in Comau Fjord, a comparably well-studied fjord in NP, while specimens were only recorded more frequently south of 46 – 47°S. The species (*Ophiomitrella chilensis*), which was recorded in shallow water of NP, but not in CP, has only nine records in Patagonia. *Colossendeis macerrina* (Arthropoda) was only recorded once with diving depths in CP (Försterra et al., 2013). For one species (*Porianopsis echinaster*) around 29/30°S and 33°S four shallow-water records (25–40 m) were found during the last years, however most records are from sites deeper than 293 m. Two shallow-water records from *Arbacia dufresnei* (55 and 60 m) come from 29.8 and 30°S; all other northern records are from depth greater than 223 m. North of Chilean Patagonia, the genus *Trophon* has one record at 88 m (30°S), all other records lie between 280 and 450 m. The three stony coral species *Desmopyhllum dianthus, Caryophyllia huinayensis,* and *Tethocyathus endesa,* described for Chilean Patagonia, are much more common in NP than in CP. In NP they form dense banks in the fjords of the Los Lagos Region (Försterra and Häussermann, 2003) and a patch in the Pitipalena Fjord. The genus *Swiftia* was only found within diving depths in NP.

Deep-Water Emergent Species in Other Areas

Twenty-eight deep-water emergent species have been described from other fjord regions, from near-shore marine caves and turbid waters (**Table 3**): in New Zealand fjords, the black coral *Antipathes fiordensis* was found at depths as shallow as 5 m (Grange, 1985), the hydrocoral *Errina novezelandiae* below 15 m (Grange et al., 1981), and some deep-water fish species (Perciformes, Scorpaeniformes) below 6–15 m (Roberts, 2001; Wing and Jack, 2013). On the western Canadian shelf, the hexactinellid sponge *Aphrocallistes vastus* can be found as shallow as 10 m depth (Leys et al., 2004; Austin et al., 2007), in Alaska the hexactinellid sponge *Heterchone calyx* below 22 m. In south-eastern Alaskan fjords, the octocoral *Primnoa pacifica* occurs as shallow as 25 m (Stone et al., 2005), and two *Sebastes* (Scorpaeniformes) species were described below 6 and 20 m, respectively (Stone and Mondragon, 2018). In Norwegian fjords, the stony coral *Lophelia pertusa* inhabits the sill inside Trondheimsfjorden below 39 m (Mortensen and Fosså, 2006), and two Alcyonacea can be found as shallow as 25–32 m (Strömgren, 1970, 1971). Examples of DWE are described from nearshore marine caves in the Mediterranean and Atlantic (e.g., Grigg, 1965; Stock and Vermeulen, 1982) and from the turbid waters between Trinidad and Venezuela (Warner, 1981).

Environmental Factors From the Literature Suggested to Explain Deep-Water Emergence

A variety of mainly physical factors have been proposed in the literature to explain the phenomenon of DWE into shallower waters, such as low light levels, and low temperature (**Table 4**).

Although not discussed inter-regionally, several hypotheses of DWE were mentioned independently in the literature for the different regions. The factors or combinations of factors used to explain this phenomenon differ between regions (**Table 4**). The factor "low light levels" was mentioned in eight publications for all regions, followed by "low temperature" which was mentioned in five publications for all regions except New Zealand. Factors such as "less wave action" were mentioned in three publications for three regions. The following factors were only mentioned for two regions each: "less interspecific competition" (Alaska, New Zealand), "stenohaline conditions" (Alaska, Norway), "low sedimentation rates" (British Columbia, New Zealand), "upwelling of cold deep water" (New Zealand, Sweden) and "narrow continental shelf" (Alaska, Sweden). Other factors were mentioned for one region only: "low nutrient levels" (caves), "high levels of dissolved silica (important for Hexactinellidae)" (British Columbia), "tidewater glaciers (resulting in deep-sea like conditions)" (Alaska) and "fjord bathymetry (e.g., sills, resulting in deep-sea like conditions" (Alaska).

Environmental Variables Along the Chilean Coast

Our analysis, based on the best available information, indicates that marine invertebrates inhabiting the Chilean coast have a wide bathymetric distribution, but exhibit marked depth preferences or depth distribution limits that differ across latitudes. Most of the listed species occurred only at deep-sea depths north of 39°S but extended into shallower water south of 39°S (**Figure 3**). In the same way, all studied genera show the same significant pattern ($P < 0.001$, **Table 5** and **Supplementary Table 2**) of deeper distribution at northern locations, mostly down to 500 m depth, and reaching significantly shallower at southern locations. Most of the genera in the data set did not

TABLE 2 | Deep-water emergent species within diving depths in Chilean Patagonia (nl, northern limit; sl, southern limit), sorted by appearance from north to south, including summary of their presence in North Patagonia (NP), Central Patagonia (CP), and South Patagonia (SP), and in fjords, channels and at the exposed coast.

Species Name	Distribution in Chile (°S)	Diving depth: nl	Diving depth: sl	NP	CP	SP	fjords	channels	exp. coast	Comment
Trophon spp.	30-55.8	39.9	54.9	1	1	1	2-3	2-3	2-3	
Poraniopsis echinaster	26.1-54.9	40 (29.3; 30.1; 33.2)	53.4	1	1	0	2	2	1	
Arbacia dufresnii	28.4-56.2	40.6	56.2	1	1	1	3	3	2	
Cosmasterias lurida	30-55.2	40.6	55.2	1	1	1	3	2-3	1	
Desmophyllum dianthus	35.5-56.5	40.6	52.8	1 C	1	0	4 (NP)	1 (loc. 2)	0 (1)	only present at sediment-protected sites
Pagurus comptus	30-55.9	40.6	55.8	1	1	1	2	2	1	
Lithodes spp.	31.9-55.3	41.5	55.3	1	1	1	2-3	2-3	1	
Actinostola intermedia	30-55	41.6	55	1	1	1	2	2	0	supports little sedimentation
Alcyonium spp.	29.5-56.3	41.6	55	1	1	1	2	0-2	0	
Caryophyllia huinayensis	36.4-53.8	41.6	53.8	1 C	1	0	2 (NP)	1	0	only present at sediment-protected sites
Hormathia pectinata	30-53	41.6	51	1	1	0	1	1	0	supports some sedimentation
Thouarella spp.	20.2-56.1	41.6	53.4	1	1 C	0	1-2	2-3,4 (esp. CP)	0	supports little sedimentation
Fusitriton magellanicus	30-55.9	41.7	55.9	1	1 C	1	2	2	2	
Gorgonocephalus chilensis	30-55.5	41.8	53.9	1	1	0	1	1-2	0	on elevated spots of epizoic
Lophaster stellans	30-55.7	41.8	53.7	1	1 C	0	1	2	1	
Ophiomitrella chilensis	33.4-42.4	41.8	41.8	1	0	0	0	1	0	
Swiftia spp.	30-52.9	42.2	46.3	1 C	0	0	1	1	0	supports little sedimentation
Tethocyathus endesa	36.5-48.5	42.2	48.5	1 C	1	0	2 (NP)	1	0	tolerates some sedimentation
Capulus ungaricoides	30.4-53.7	42.4	49	1	1	0	0	1	0	
Henricia studeri	30-53.8	42.4	49	1	1	0	2	2	1-2	
Psolus squamatus	31.9-49.4	42.4	48.1	1	1	0	2, loc 3	2	0	
Labidiaster radiosus	35.5-55	42.6	55	1	1 C	1	0	Loc. 2	Loc. 2	
Stenosemus exaratus	36-53.8	43	53.8	1	1	0	1	1	0	
Solaster regularis	30-54.9	43.8	53.9	1	1 C	0	1	2	0	
Astrotoma agassizi	18.7-56.7	44.0 (41.6)	50.5	1	1 C	0	0	1	0	on gorgonians
Dactylanthus antarticus	36.3-55.1	45	55	1	1 C	1	0 (1)	Loc. 2	0	on gorgonians
Acanthogorgia spp.	36.3-53.8	45.3	53.8	1	1 C	0	1-2 (CP)	2-3 (CP)	0	tolerates some sedimentation
Acesta patagonica	30-53.3	45.9 (42.3)	53.3	1	1 C	0	2	1	0	
Tripylaster philippi	35.5-55.8	46.7 (42.3)	54.9	0	1 C	1	1	1	0	buried
Ophiura lymani	31.6-54.1	47.8	53.9	0	1 C	0	1	1	0	
Florometra magellanica	19.1-55.1	47.8	55	0	1 C	1	1	1-2	0	on gorgonians
Ophioctena mitinum	22.8-56.7	48.2	53.7	0	1 C	0	1	1	0	
Bathyplothes moseleyi	32.2-53.6	48.4	53.4	0	1 C	0	1	1	0	
Colossendeis macerrima	26.7-51.2	48.5	48.5	0	1	0	0	1	0	
Summary				28	32	12	28	34	11	

C: common; 1: present; 0: absent. Latitude(s) in parenthesis are sites where single specimen was found within diving depths outside of usual range.

TABLE 3 | List of deep-water emergent species from other parts of the world: geographic and bathymetric distribution, main citation and first citation of deep-water emergence (DWE), typical deep-water species, type of reproduction and larvae.

Species	Phylum	DWE Region	Main citation	First mention of DWE	Distribution	typical deep-water genus	Bathymetric distribution (m)	Type of reproduction	Type of larvae
Gesiella jameensis	Annelida, Phyllodocida	Cave (Lanzarote, Canary Islands)	Hartmann-Schröder, 1974	Iliffe et al., 1984	Lanzarote, Atlantic Ocean	Only in shallow, but close affinities to deep sea organisms	endemic to shallow marine cave	Broadcast spawning	Pelagic larvae
Spelaeonicippe buchi	Arthropoda, Amphipoda	Cave	Andres, 1975	Stock and Vermeulen, 1982	Lanzarote, Atlantic Ocean	yes	sublittoral/bathyal	Brooding	No larval stage
Spelaeonicippe provo	Arthropoda, Amphipoda	Cave	van der Ham, 2002	Stock and Vermeulen, 1982	Caicos Islands, Atlantic Ocean	yes	sublittoral/bathyal	Brooding	No larval stage
Munidopsis polymorpha	Arthropoda, Decapoda	Cave	Wilkens et al., 1990	Stock and Vermeulen, 1982	Lanzarote, Atlantic Ocean	Only in shallow, but close affinities to deep sea organisms	endemic to shallow marine cave	Brooding	Pelagic larvae
Lepidoperca tasmanica	Chordata, Perciformes	New Zealand	Roberts, 1989	Roberts, 2001	New Zealand, Southwest Pacific	yes	6-400 m	Batch spawning	Pelagic larvae
Parapercis gilliesi	Chordata, Perciformes	New Zealand	Paulin et al., 1989	Wing and Jack, 2013	New Zealand, Southwest Pacific	yes	< 15–350 m	Broadcast spawning	Pelagic larvae
Pseudolabrus miles	Chordata, Perciformes	New Zealand	Russell, 1988	Wing and Jack, 2013	New Zealand, Southwest Pacific (endemic)	Only in shallow, but close affinities to deeper living species	shallow water	Broadcast spawning	Pelagic larvae
Helicolenus percoides	Chordata, Scorpaeniformes	New Zealand	Paulin, 1989	Wing and Jack, 2013	New Zealand, Southwest Pacific	Yes	<15–750 m	Broadcast spawning	Pelagic larvae
Sebastes melanostictus	Chordata, Scorpaeniformes	Alaska	Orr and Hawkins, 2008	Stone and Mondragon, 2018	Pacific Ocean	Yes	20–1000 m	Broadcast spawning	Pelagic larvae
Sebastes variabilis	Chordata, Scorpaeniformes	Alaska	Orr and Blackburn, 2004	Stone and Mondragon, 2018	North Pacific	Yes	6–675 m	Broadcast spawning	Pelagic larvae
Antipathes atlantica	Cnidaria, Antipatharia	Trinidad	Warner, 1981	Warner, 1981	Western Central Atlantic	No	15–152 m	Broadcast spawning or pseudo-brooding	Pelagic larvae
Antipathes barbadensis	Cnidaria, Antipatharia	Trinidad	Warner, 1981	Warner, 1981	Western Central Atlantic	No	<30–500 m	Broadcast spawning or Pseudo-brooding	Pelagic larvae
Antipathes fiordensis	Cnidaria, Antipatharia	New Zealand	Grange, 1990	Grange, 1985	New Zealand, Southwest Pacific	No	5–100 m	Broadcast spawning or Pseudo-brooding	Pelagic larvae (negatively buoyant and weak swimmers)
Antipathes furcata	Cnidaria, Antipatharia	Trinidad	Opresko et al., 2016	Warner, 1981	Western Central Atlantic	Yes	15–340 m	Broadcast spawning or pseudo-brooding	Pelagic larvae
Antipathes gracilis	Cnidaria, Antipatharia	Trinidad	Opresko and Sanchez, 2005	Warner, 1981	North Atlantic & New Zealand, Pacific Ocean	No	20–100 m	Broadcast spawning or pseudo-brooding	Pelagic larvae
Antipathes grandis	Cnidaria, Antipatharia	Cave	Wagner et al., 2010	Grigg, 1965	New Zealand, Pacific Ocean	No	30–120 m	Broadcast spawning or pseudo-brooding	Pelagic larvae
Antipathes pennacea	Cnidaria, Antipatharia	Trinidad	Opresko, 2001	Warner, 1981	Western Central Atlantic	No	20–330 m	Broadcast spawning or pseudo-brooding	Pelagic larvae
Antipathes thamnea	Cnidaria, Antipatharia	Trinidad	Warner, 1981	Warner, 1981	Western Central Atlantic	No	15–350 m	Broadcast spawning or pseudo-Brooding	Pelagic larvae
Stichopathes luetkeni	Cnidaria, Antipatharia	Trinidad	Opresko et al., 2016	Warner, 1981	Western Central Atlantic	No	20–70? m	Broadcast spawning or pseudo-brooding	Pelagic larvae
Paramuricea placomus	Cnidaria, Alcyonacea	Norway	Simpson et al., 2005	Strömgren, 1971	Atlantic and Mediterranean	Yes	25–1600 m	Broadcast spawning	Pelagic larvae
Primnoa pacifica	Cnidaria, Alcyonacea	Alaska	Choy et al., 2020	Stone et al., 2005	Pacific Ocean	Yes	<25–900 m	Broadcast spawning (maybe external brooding?)	Pelagic larvae
Primnoa resedaeformis	Cnidaria, Alcyonacea	Norway	Roberts et al., 2009	Strömgren, 1970	Atlantic and Mediterranean	Yes	32–1000 m	Broadcast spawning	Pelagic larvae

(Continued)

TABLE 3 | (Continued)

Species	Phylum	DWE Region	Main citation	First mention of DWE	Distribution	typical deep-water genus	Bathymetric distribution (m)	Type of reproduction	Type of larvae
Ernina novaezelandiae	Cnidaria, Anthoathecata	New Zealand	Cairns et al., 2009	Grange et al., 1981	New Zealand, Southwest Pacific	No	15–177 m	Brooding	No pelagic stage
Lophelia pertusa	Cnidaria, Scleractinia	Norway/ Sweden	Cairns, 1994	Mortensen and Fossâ, 2006	Atlantic and Mediterranean	Yes	39–3300 m	Broadcast spawning	Pelagic larvae
Asbestopluma hypogea	Porifera, Poecilosclerida	Cave	Vacelet and Boury-Esnault, 1996	Bakran-Petricioli et al., 2015	Mediterranean Sea	Yes	20–8840 m	Brooding	Pelagic larvae
Aphrocallistes vastus	Porifera, Sceptrulophora	Alaska/Canada	Brown et al., 2017	Leys et al., 2004	Northern Pacific Ocean	Yes	10–1600 m	Brooding	Pelagic larvae
Heterchone calyx	Porifera, Sceptrulophora	Alaska	Leys et al., 2007	Stone and Mondragon, 2018	Northern Pacific Ocean	No	22–240 m	Brooding	Pelagic larvae
Oopsacas minuta	Porifera, Lyssacinosida	Cave	Boury-Esnault and Vacelet, 1994	Bakran-Petricioli et al., 2015	Mediterranean Sea	Yes	18–2912 m	Brooding	Pelagic larvae

?, doubtful because of poor data.

reveal significant positive or negative coefficients related to depth occurrences (**Supplementary Table 2**). Only 9 of 33 genera (27%) showed positive associations with depth at northern sites. Similarly, 11 of 33 genera (33%) showed negative coefficients related to depth at southern localities (**Supplementary Table 2**).

Using the entire data set, the GLM revealed significant differences in species presence/absence ($P < 0.001$) related to depth, temperature, primary production, silica, salinity and oxygen but with a low deviance (<12%, **Tables 6**, **7** and **Supplementary Figure 2**), and temperature was considered the most important variable for this model. The GLM that only used records up to 50 m depth followed a similar pattern, revealing significant differences in species presence/absence related to depth, primary production (**Supplementary Figure 3**), temperature (**Supplementary Figure 4**), salinity (**Supplementary Figure 5**), oxygen (**Supplementary Figure 6**), and velocity, with low deviance explained (<11%, **Table 7**), and temperature was the most important variable (**Table 6**). In both GLMs, temperature is inversely related to presence probability, in other words, presence probability is high at lower temperatures, and declines when temperatures increases. The GLM with records deeper than 200 m depth revealed a significant effect of depth, silica (**Supplementary Figure 7**), salinity, oxygen and clorophyll-a on the presence/absence of species, with an explained deviance close to 25% (**Table 7**). In this case, oxygen is considered to be the most important variable and is inversely related to presence probability (**Table 6**).

DISCUSSION

Analysis of Environmental Factors Along the Chilean Coast

In general, the statistical analyses searching for correlations between species distribution and seven environmental parameters (**Supplementary Figure 8**) suggest that several of these factors (primary production, salinity, oxygen and temperature, see **Table 6** and **Supplementary Figures 3–7, 8A,B,D,E**) were significantly associated to the bathymetric distribution of the studied taxa of benthic invertebrates, but temperature was the most important environmental driver (**Supplementary Figure 8D**). In the intertidal areas of northern and central Chile species composition, abundance and diversity are influenced by temperature and salinity (Broitman et al., 2001, 2011; Rivadeneira et al., 2002; Ibáñez et al., 2019). This study shows the same pattern at deep-sea communities (below the OMZ), where bottom temperature and salinity have a strong influence on bathymetric distribution. The sea surface temperature is the most conspicuous gradient along the Chilean coast ranging from 19.5 to 6.9°C, however bottom temperature in the top 100 m is similar at northern and southern localities (mean 10.5 and 9.7°C, respectively); a similar pattern is observed at 500 m depth (mean 4.1 and 3.8°C, respectively). Salinity shows little variation at latitudinal and bathymetric scales along the exposed coast but may have strong gradients within the fjords and channels where a Low Salinity Layer (LSL) and further haloclines may be present with surface salinities below 10 psu

TABLE 4 | Literature overview on deep-water emergence theories from different regions: North America (Alaska and British Columbia), Chilean Patagonia, New Zealand, Scandinavia (Norway, Sweden), caves and turbid waters (Trinidad).

DWE factor Region	Low light levels	Less interspecific competition	Less wave action	Low nutrient levels	Low temperature	Stenohaline conditions	Low sedimentation rates	Upwelling of cold deep water	Narrow continental shelf	High levels of dissolved silica (important for Hexactinellida)	Tidewater glaciers (resulting in deep-sea like conditions)	Fjord bathymetry (e.g., sills) (resulting in deep-sea like conditions)	Positive correlation with precipitation and negative correlation with abundance of macroalgae
Alaska	Stone et al., 2005	Stone et al., 2005			Stone et al., 2005	Stone et al., 2005			Weingartner et al., 2009; Waller et al., 2011		Stone and Mondragon, 2018	Stone and Mondragon, 2018	
British Columbia	Leys et al., 2004				Leys et al., 2004		Leys et al., 2004			Leys et al., 2004			
Chilean Patagonia	Not always present where DWE occurs.	Does not apply	Wave action generally plays no role in depths of DWE., Certain positive correlation cannot be negated but with many exceptions.	No correlation and if, rather a negative one	Certain large scale correlation visible, but with many smaller scale exceptions	Not present in all areas with DWE species	Does not apply in some areas with DWE species, very species-dependent	Does not apply in most areas with DWE species	Does not apply	Present in fjords but no direct importance for DWE species, possibly indirect through food chain	Not present in most areas with DWE species	Not present in many areas with DWE species	This paper (see section "Discussion")
New Zealand	Grange et al., 1981; Grange and Singleton, 1988	Grange and Singleton, 1988	Grange and Singleton, 1988				Grange and Singleton, 1988	Cairns, 1995					
Norway	Rogers, 1999; Mortensen et al., 2001		Rogers, 1999; Mortensen et al., 2001		Rogers, 1999; Mortensen et al., 2001	Mortensen et al., 2001							
Sweden								Wisshak et al., 2005	Wisshak et al., 2005				
Caves	Iliffe et al., 1984		Iliffe et al., 1984	Iliffe et al., 1984	Iliffe et al., 1984								
Turbid water (Trinidad)	Warner, 1981				Warner, 1981								

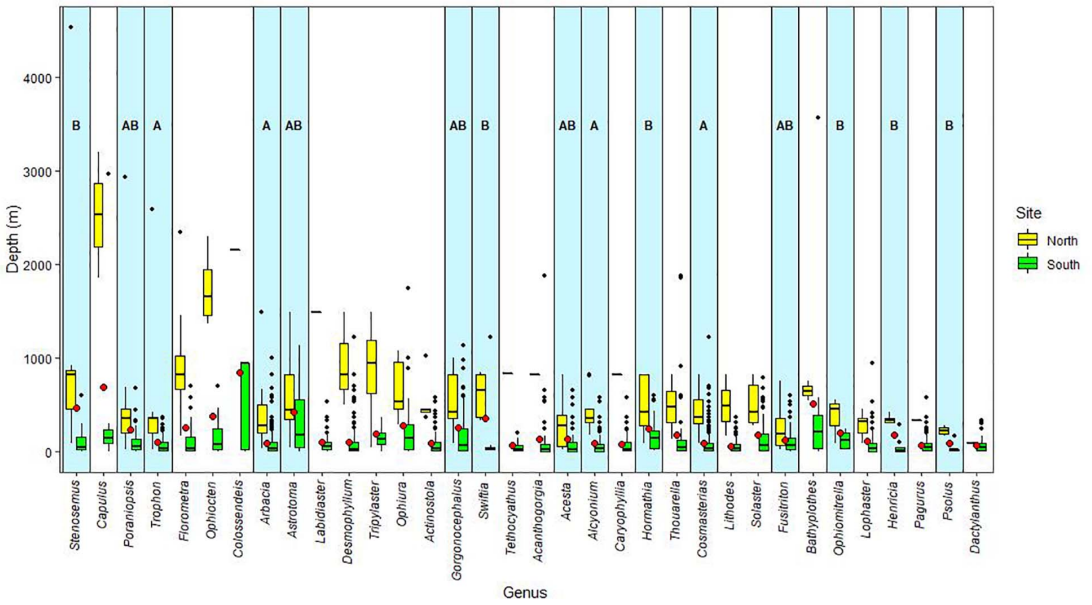

FIGURE 3 | Average depth of analyzed species and genera north ("North" corresponding to 18–40°S) and south of 40°S ("South," corresponding to 40–56°S). A: genera with significant positive coefficient for depth in "North"; B: genera with significant negative coefficient for depth in "South"; AB: genera with pattern A and B.

(see Häussermann and Försterra, 2009). The OMZ has a powerful effect on the bathymetric distribution of benthic communities along the Chilean coast (Thiel et al., 2007). In the southern fjords and channels the high oxygen concentration in shallow water promotes the occurrence of deep-water species, living below the OMZ at northern localities (>200 m). Nevertheless, the results of the analyses do not allow us to conclude if the parameters that show significant correlations with distribution represent minimum or sufficient conditions for triggering DWE, and the negative correlation of oxygen levels with presence probability seems counter-intuitive (**Supplementary Figure 2**). It is possible that at least some of the detected correlations are indirect effects of other parameters we have not looked at so far.

TABLE 5 | Two-way ANOVA results for comparison of mean bathymetric distribution by genus and biogeographic regions.

	df	SS	Mean	*F*	*P*
Genus	33	24337985	737515	36.151	<0.001
Site	1	33488804	33488804	1641.551	<0.001
Genus:site	33	5745539	174107	8.534	<0.001
Residuals	3261	66526728	20401		

df, degree of freedom; SS, sum of squares; F, F statistics; P, p-value.

TABLE 6 | Coefficients and most important variable for the best GLM of each data (all data; <50 m; >200 m).

	All data	<50 m	>200 m
		Coefficients	
α	28.794	28.072	739.606
Depth	0.002*	−0.012*	0.004*
Oxygen	−0.003*	−0.007*	**−0.039***
Salinity	−0.788*	−0.703*	−21.387*
Silica	−0.008*	−0.012*	0.025*
Temperature	**−0.263***	**−0.337***	–
Primary production	**−37.774***	−32.09*	–
Velocity	–	−5.318*	–
Chlorophyll-a	–	–	29.877*

α represents the intercept of the pendent when dependent variables values = 0, the coefficient values in all variables represent the pendent (β). Significative coefficients are noted with asterisk (*), and the most important variable for each GLM is shown in bold letters. Variables not included in the best model are represented with a hyphen (–).

Environmental Factors Explaining Deep-Water Emergence and Their Potential to Explain This Phenomenon in Chile

Most species mentioned in the literature for DWE and 18 of the genera mentioned in this article for Chile belong to typical deep-water genera (**Table 1**) and are only at some special locations found in shallow water. Therefore at least for most, if not all of

TABLE 7 | Deviance and degree of freedom for the best GLM for each data (all data; <50 m; >200 m).

	All Data	< 50 m	> 200 m
Residual deviance	13897	8863	1204
Null deviance	15150	7952	900.4
df Total	13897	9267	937
Residual df	13891	9260	932
BIC	13412.86	8024.93	937.65

df, degree of freedom; BIC, Bayesian Information Criterium.

the analyzed species, we are observing DWE and not shallow-water submergence.

Light Levels

Low light level is the most frequently mentioned factor hypothesized to trigger DWE (**Table 4**). In some regions of DWE, these low light levels are caused by cave habitats (e.g., in the Mediterranean), light absorbing tannin-stained surface water (e.g., in New Zealand) and/or high particle load in the upper column either from glaciers, rivers or other sources. Looking at light attenuation (**Supplementary Figure 9**), areas with lower water clarity coincide with areas with strong DWE (inner fjords and channels); see also turbid estuarine plume in Aysén Fjord (Figure 3 in Cáceres, 2004). But values fluctuate strongly within the fjords and channels of Patagonia. Due to the extremely high precipitation in the Chilean fjord region (more than 5000 mm between 42 and 51°S, see Alvarez-Garreton et al., 2019, and even to 6700 mm, see Häussermann and Försterra, 2009), tannin-stained run-off in most fjords is so diluted that the light-absorbing effect of the surface layer is negligible and average visibility within the Chilean fjords and channels is generally even higher than along large sections of the exposed coast. The highest values of light-absorbing turbidity are often measured in summer when radiation is at maximum and lowest in winter when cloud coverage and low sun angles reduce radiation. This has a leveling effect throughout the year and reduces longer phases of low light conditions at the surface. In some Chilean fjords on the other hand (e.g., Tempano Fjord; 48°43′07″S; 74°14′19.3″W) with extremely turbid glacial run-off or tannin-stained surface layer (e.g., Seno Farquhar; 48°29′18.7″S; 74°12′25.7″W), the low-salinity surface layer blocks most of the light causing night-like conditions below. Nevertheless, the number of deep-water emergent species in these fjords are not higher than in neighboring fjords with clear water and high light levels (e.g., Paso Schlucht; 48°8′3.84″S; 74°47′25.44″S) where deep-water gorgonians can even be seen through the surface.

Kregting and Gibbs (2006) showed that salinity rather than light levels controlled the upper limit of black corals in Doubtful Sound, New Zealand and proved a hypothesis wrong that was used for decades to explain DWE in NZ fjords.

Thus any correlation between light levels and DWE is either a coincidence, or low light is a factor that could be enhancing conditions for DWE but is not enough to trigger DWE.

Wave Action

The wave energy (**Supplementary Figure 10**) to a large extent has a negative correlation with DWE and suggests a connection. While wave energy decreased from the exposed coast and islands in the west toward the protected channels and fjords in the east, the number of deep-water emergent species is higher in the protected areas (e.g., none of the listed anthozoans were recorded in shallow water of the exposed Patagonian coast). The current velocity data (**Supplementary Figure 8G**) decreases from northern and central Chile toward Patagonia, but the resolution is not high enough to see differences between areas within Patagonia. Although most fjord shores are indeed protected from open ocean waves, there are many examples of areas with several deep-water emerging species present despite their exposure to waves and surge (e.g., Isla Millar at the entrance to Penas Gulf 47°58′45.4″S, 74°40′47.0″W). In fact, in most fjord regions, some fjords and channels can be found that act as funnels for wave action from the ocean with a pronounced discharge of wave energy at their entrance, but which still exhibit DWE. Since a hypothesized connection fails to explain the exceptions, again, low wave energy may create favorable but alone does not provide sufficient conditions for DWE. Most DWE takes place in depths where wave energy is negligible anyway. Only in special locations (e.g., in caves) where deep-water emergent species reach into extremely shallow depths, the absence of wave energy may play a role.

Low Nutrient Levels

For DWE in Mediterranean caves, Iliffe et al. (1984) proposed low nutrient levels to be the cause. While this factor may be valid for the studied caves, there are many examples of high-nutrient habitats that show strong DWE. In fact, fjord water due to strong terrestrial runoff is generally rich in nutrients and thus highly productive (Iriarte et al., 2014). For the Comau fjord in Chilean Patagonia, high nutrient levels have been hypothesized to be the main reason why the deep-water emergent coral species *Desmophyllum dianthus* can thrive in shallow water with Aragonite-corrosive pH levels as low as 7.4 (Höfer et al., 2018; Martínez-Dios et al., 2020). Interestingly, based on data from BioOracle, chlorophyll-a (**Supplementary Figures 3, 8F**) show the highest levels for the inner fjords and channels while primary production (**Supplementary Figure 8E**) shows a different, more patchy, and seemingly more erratic pattern. The maps reveal strong fluctuations in both parameters, which makes it hard to hypothesize any correlation with DWE.

Low Temperature

Since DWE is also called high-latitude emergence, the phenomenon is often correlated with comparably low average water temperatures. Nevertheless, DWE can also be found in regions that do not have low temperatures at all. In the Caribbean Sea between Trinidad and Venezuela, several examples of DWE are described (**Tables 3**, **4**) while the average temperature in shallow water is significantly above deep-sea values. The same is valid for Mediterranean caves. Average water temperature in Comau fjord (42°30′S) in southern Chile, in depths where 14 deep-water emergent species can be found, varies throughout the year between 8 and 12°C (Häussermann and Försterra, 2009), which is not colder than average water temperatures from the exposed coast at the same latitude where less deep-water emerging species were observed (e.g., only the sea urchin *Arbacia dufresnei* down to 15 m at Puñihuil, 41°55.743′S; 74°02.202′W and a total of eight species at the three sites down to 30 m around Guafo Island, 43°36.269′S; 74°42.911′W: the echinoderms *A. dufresnei*, *Cosmasterias lurida*, *Poraniopsis echinaster*, *Labidiaster radiosus*, *Henricia* sp., the gastropod *Fusitriton magellanicus* and the decapods *Pagurus comptus* and *Lithodes santolla*). These temperatures are significantly higher than those from the deep-sea environments where these species are normally found (**Supplementary Figure 8D**).

The temperature data (**Supplementary Figures 4, 8D**) reveal that along the Chilean coast shallow-water temperature is gradually and significantly decreasing from north to south, with shallow-water temperatures approaching deep-water values from northern latitudes at the southern tip of South America. The statistical analyses (**Tables 6, 7**) suggest a negative correlation of the occurrence of the selected species with temperature (**Supplementary Figure 2**). But the number of deep-water emergent species is highest in CP, followed by NP while fewer species were recorded in SP (**Table 2**). The temperature hypothesis fails to explain this pattern, which again suggests that low temperatures may be an enhancing factor or even a necessary requirement for DWE, but alone are not sufficient to trigger DWE.

Low Sedimentation Rates

Low sedimentation rates have been proposed to allow for DWE in British Columbia by Leys et al. (2004) and in New Zealand fjords by Grange and Singleton (1988). While this may be the case for the studied areas, in other regions, DWE was explained by light absorption from highly turbid water off Trinidad (**Table 4**) with a consequently high sedimentation load. Furthermore, even in extremely high sediment-loaded glacial fiords of Alaska (Stone and Mondragon, 2018) and Chilean Patagonia (own data, e.g., Tempano Fjord) DWE was observed. Nevertheless, sedimentation indeed may be a stressor for passive suspension feeders (e.g., the listed anthozoans), which are absent from highly sediment-laden places. In Tempano Fjord, however, the bivalve *Acesta patagonica* was recorded at a slightly overhanging wall at the unusual shallow depth of 15 m.

Upwelling of Cold Deep Water and Narrow Continental Shelf

Cairns (1995) proposed the upwelling of colder deep-water was triggering DWE in New Zealand Fjords. The same was suggested by Wisshak et al. (2005) for DWE off the Swedish coast. While temperature alone has already been shown to be an insufficient factor for causing DWE, the upwelling of deep-water could in fact transport larvae from deeper habitats into shallower zones. Most fjords show internal circulations that are driven by an outflow of low-saline surface water and a density-driven inflow of deep salty water (Stigebrandt, 2012). Nevertheless, for significant larvae transport into shallow water, the deep water must come directly from deep-water supply site populations. Within the Chilean fjord region, there are many examples of fjords where extended and comparably shallow bays and gulfs lie between the deeper ocean and the fjords (**Supplementary Figure 1**). Actually, within the Chilean fjord region the only location with a narrow shelf is off Peninsula Taitao (∼47°S), where relatively few deep-water emerging species were present (**Supplementary Figure 1** and **Table 3**). It is highly unlikely that the larvae transport from the deep-sea into the shallow water of these fjords is stronger than at upwelling zones along the exposed Chilean coast where no or less DWE is observed. In addition, the hypothesis suggests that the shallow-water populations are sinks that depend on the constant supply of larvae from the deep. However, several studies show reproductive success of the deep-water emergent species in the shallow habitats (Rossin et al., 2017; Feehan et al., 2019), which suggests that these populations can sustain themselves. Stone et al. (2005) suggest that the deep-water emergent tree coral population in Alaskan fjords is a disjunct population with little connection to tree coral populations outside the fjords.

High Levels of Silica

The highest abundance of glass sponges in British Columbia was correlated with fjords that exhibited high dissolved silicate, low light, temperatures between 9 and 10°C and low suspended sediments (Leys et al., 2004). While high levels of silica are in fact typical for fjord water (Silva, 2008), especially in areas with high glacial freshwater run off (Cuevas et al., 2019), and may be beneficial or even indispensable for glass sponges, silica is of minor to no importance for other deep-water emerging species. Silica concentration on the other hand affects phytoplankton communities and thus may have an effect on the food web (Cuevas et al., 2019) and consequently also on benthic species composition. However, the maps of silica concentrations within the fjord region based on BioOracle data do not coincide with the pattern of DWE (**Supplementary Figures 7, 8C**), which is probably due to a lack of spatial resolution of the data.

Tidewater Glaciers

Stone and Mondragon (2018) proposed tidewater glaciers and typical fjord bathymetry (e.g., sills) to be triggers for DWE of tree corals in Alaskan fjords. Many fjords in Chilean Patagonia have no sill, or at least no pronounced sill (Pickard and Stanton, 1980). In addition, due to the large inland icefields located in CP, the fjords of CP, and only some fjords of SP, possess glaciers at their heads, while there are no glaciers reaching the ocean in NP (Häussermann and Försterra, 2009). However, DWE in Patagonia is also present in channels. Again, these factors coincide with DWE in many fjords but not in all fjords and fail to explain DWE outside of fjords.

Less Interspecific Competition

Grange and Singleton (1988) and Stone et al. (2005) proposed low interspecific competition for promoting DWE in Alaskan and New Zealand fjords, respectively. In Chilean fjords, average benthic coverage and species diversity are higher than at the exposed coast north of Patagonia (Fernández et al., 2000; Häussermann and Försterra, 2009). In fact, the additional presence of deep-water emerging species is one factor to explain the extremely high benthic diversity in Chilean fjords. Here, the deep-water emerging species live intermingled with typical shallow-water species and form part in different stages of succession after disturbance (own data).

Special Salinity Conditions

Stable salinity in zones with DWE was proposed to mimic deep-water conditions and thus create a suitable habitat for deep-water emergent species (**Table 4**). While salinity levels are a key factor for marine species distribution (Broitman et al., 2001), places with stable salinity are much more frequent than places with DWE. At the same time, Kregting and Gibbs (2006) could show that the deep-water emergent black corals in Doubtful Sound,

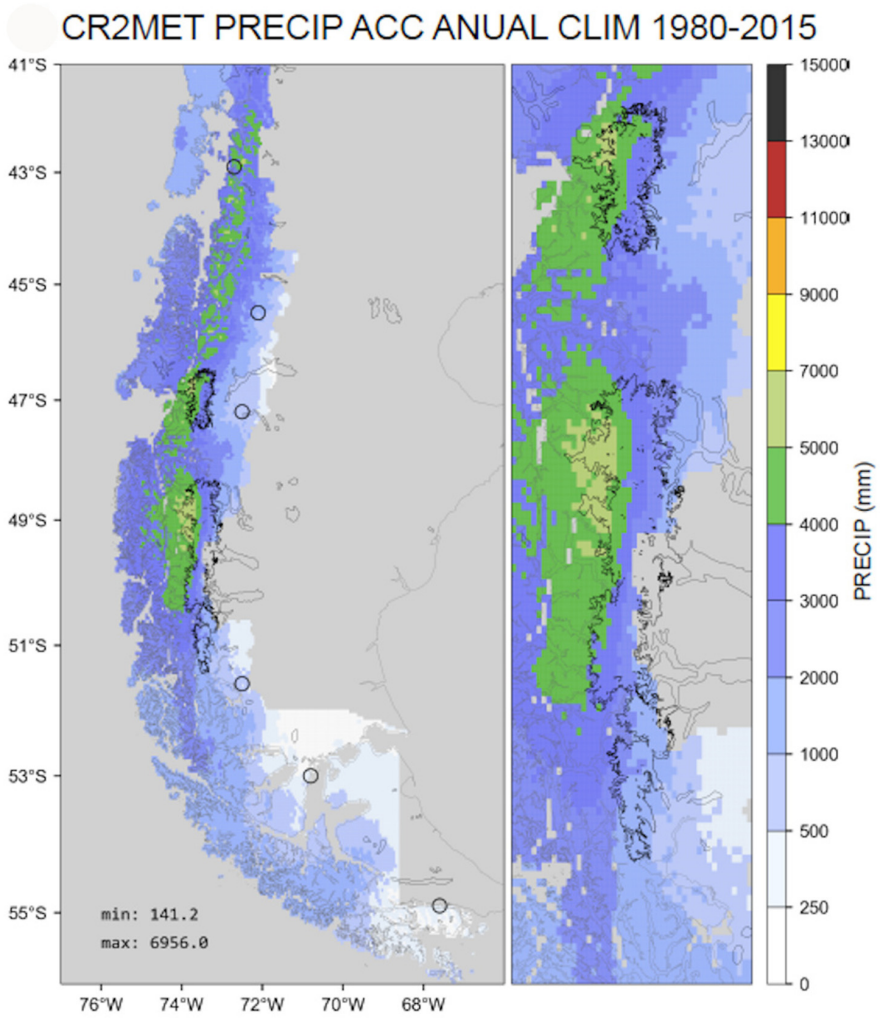

FIGURE 4 | Mean annual precipitation of Chilean Patagonia 1980–2015, R. Garreaud (personal communication), see Alvarez-Garreton et al. (2019).

New Zealand, withstand drops in salinity down to 20 psu when the exposure to low salinity is restricted to less than 6 h (a medium diurnal tide cycle) and when they are followed by salinities above 32 psu. Chilean fjords generally possess a superficial LSL with salinities down to approximately 2–10 psu and a thickness of up to 10 m (Häussermann and Försterra, 2009). But even below this LSL, fluctuations in salinity are present and stronger than in most marine regions without DWE: at three sites in Comau and Reñihué Fjords (NP) at depth where *Desmophyllum dianthus* was habitat-forming, monthly average salinities varied between 25 and 31.5 psu during a 13 months cycle, and spikes at the site Morro Gonzalo in Reñihué Fjord (42°32′46″S; 72°37′7″W) at 27 m even reached 10 psu (Feehan et al., 2019). So stable salinity alone, although a possibly enhancing factor, cannot explain the occurrence of DWE.

In Chilean Patagonia, the deepest reach of the LSL sharply marks the highest extension of many deep-water emerging species [the sea star *Cosmasterias lurida* (**Figure 2A**) regularly migrates close to the surface in fjords but was regularly found dead in large numbers after strong rainfall events when the LSL grows faster than the star fish can retreat into safe higher saline depths]. However, data from the superficial LSLs are not present in the BioOracle database and thus not available for statistical analyses and thus the magnitude of the LSL is not revealed by the salinity data (**Supplementary Figures 5, 7B**). In addition, this LSL is very dynamic and is varying on several time scales since its depth, horizontal extension, and time of persistence depend on precipitation, glacial run-off, currents and mixing events. Hence, low salinity may explain the upper limitation for DWE in some areas. On the other hand, the magnitude of DWE along the Chilean fjord region with high numbers of species in NP and CP shows a positive correlation with precipitation which peaks between 42 and 51°S (**Figure 4** and **Table 2**). The latter determines the magnitude of the LSL. In addition, most deep-water emergent species are found in channels (34) followed by fjords (28), with least species at the exposed coast (11) (**Table 2**), where salinity is highest. Since DWE takes place below the LSL, the positive effect of low a LSL on DWE, if present, must be

indirect. One effect of a LSL is the suppression of macroalgae. This suggests that the lack of dense kelp forests may have a positive influence on the phenomenon of DWE. In fact, most areas with DWE worldwide have in common a lower abundance or the absence of macroalgae (fjords, caves and turbid waters, see **Table 4**). The reasons for that may vary between regions, and besides low salinity, low light levels may also cause a scarcity of macroalgae. The presence or absence of macroalgae on the other hand may have a significant influence on the primary production regime, the quality and quantity of food for filter- and detritus-feeders and the annual dynamics in their availability. However, the role of kelp as a trophic resource is still not well understood (Miller and Page, 2012). How far the conditions created by the absence of macroalgae may allow deep-water species to emerge into shallow water remains to be studied. Unfortunately, our own macro-algae data set is relatively poor, does not include abundances, and sampling-effort was biased (**Supplementary Figure 11**) and the models for macroalgae-presence in the Chilean fjord region have too many false positives, due to the presence of *Ulva* species and shore vegetation to make them useful for statistical analyses (see Mora-Soto et al., 2020). Nevertheless, the positive correlation of precipitation, and the negative correlation of the abundance of macroalgae with DWE is eye-catching and justifies hypothesizing a connection.

Summarizing Considerations on the Parameters That Could Explain DWE

None of the factors hypothesized in the literature to explain DWE alone seems to be able to explain this phenomenon in all areas around the world where it occurs. This leaves several alternative explanations or combinations of those: (1) In each region where DWE occurs, unique factors or combinations of factors cause this phenomenon, (2) not one single factor, but a combination of widely common factors is triggering DWE or (3) there are other factors that have not been looked at so far that cause or significantly contribute to DWE. (4) There is not one factor or a combination of factors that trigger DWE for a variety of species, but each species or phylum requires its own specific set of factors to deep-water emerge that are only met in specific locations. For example, the mentioned anthozoans, ophiurids, the holothurian, the crinoid, the bivalve and the pycnogonid are restricted to fjords and channels, while some of the mentioned sea stars, gastropods and decapods can also be found at more exposed sites. Fjord regions are very diverse in their near-shore oceanographic conditions (Pickard and Stanton, 1980). As a consequence, a high number of strong gradients interfere within comparably small areas, producing a large number of possible combinations of parameters (Häussermann and Försterra, 2009). This increases the probability that certain combinations of factors are met that are required for certain species to deep-water emerge. As a result, in these regions, a comparably high number of deep water emerging species can be found in a given area. (5) Rather than looking for DWE-triggering factors, we would need to look for the absence of DWE-inhibiting factors. This latter hypothesis is based on the assumption that factors or factor combinations enabling DWE are widely common, but do not have an effect due to single or few inhibiting factors. These inhibiting factors may be difficult to detect since the coastal marine systems are often dynamic and the "knock-out" criteria are most likely rare extreme or peak values of otherwise unproblematic factors (e.g., drops in oxygen after die offs of algae blooms or sedimentation peaks near river mouths after extreme weather events that occur only very sporadically).

Although the statistical analyses for the Chilean coast show some significant influence of some factors on the presence of the mentioned species, by looking at the distribution maps, the correlation of the analyzed factors with the magnitude of DWE within Patagonia is not completely clear, or at least there seem to be too many mismatches to justify a rule. This basically rules out the possibility that a single factor is responsible for the frequent DWE in Chilean Patagonia. We could neither find combinations of the mentioned factors that would work to explain the depth-dependent pattern. This suggests that the factors that showed statistical significance rather represent minimum prerequisites for DWE than actual triggers for this phenomenon. For example salinities that do not drop below certain minima, lower temperatures and less wave action most likely make it easier for deep-water species to persist in shallow water. Upwelling and larval support from deep-water populations are also factors that help to establish and/or maintain shallow-water populations. However, none of these factors alone nor the combination of them seem to be the crucial trigger for DWE.

Possible Present and Future Effects of Climate Change on DWE and on Species Distribution in Chile

Eight records of deep-water species from Central and Northern Chile are from depths shallower than 100 m; four from the sea star *Poraniopsis echinaster* (29, 30, and 33°S) in 20–30 m depth, two from the sea urchin *Arbacia dufresnei* (30°S) in 55 and 60 m depth, one from the sea star *Cosmasterias lurida* in 30 m depth (30°S), and one from the gastropod *Trophon* sp. in 88 m depth (30°S). All records are from the last decade, which for records below diving depths (30 m) can be explained by the time frame these ROV surveys have taken place. However, it is interesting that three of the five records from diving depths are from the last year. Since all mentioned records are situated in known upwelling areas (around 30°S and around 33°S) (Aravena et al., 2014) and upwelling is getting stronger due to climate change (Bakun et al., 2015), it is possible that these species appeared and will become more abundant in shallow water with climate change advancing. The southern distribution limits of other species from Central and Northern Chile are moving southward (e.g., the sea star *Heliaster helianthus* was originally described to Valparaiso, approximately 32.5°S, and is now frequently seen in Concepcion, approximately 37°S), and also within Patagonia species described from further north are expending southward (e.g., the sea stars *Patiria chilensis* and *Meyenaster gelatinosus* formerly described to 44°S were spotted down to 53 and 50°S, respectively, the temperate sunfish *Mola mola* has been observed at 47°S, tuna at 50°S, etc.; our own observations). Thus, one should expect to see

important changes in the composition of benthic species of Chilean Patagonia with advancing climate change. In particular, it would be interesting if to note if, with a general southward shift of habitats and distributions, the phenomenon of DWE also shifts southward.

Resolution of the Analyzed Data

The dataset from deep-water habitats along the Chilean coast is still extremely poor, with only nine of 34 species having more than 10 records, and only three having more than 20 records. The poor sampling in deep-water habitats, in general, leads to biased and statistically non-significant analyses. Taking into account a coastline of more than 100,000 km, the data we have on Patagonian shallow-water habitats are also poor; gaps are located especially between 50° and 52°S and 54–56°S. In addition, even species that are well-known by local divers along the Northern and Central Chilean coast are lacking published records in the literature, thus more and continuous species inventories along the entire Chilean coast are needed.

Since many of the abiotic data available for Chilean Patagonia are derived from satellite imagery and/or models, the resolution in the finely structured maize of the Chilean Fjord Region is poor and does not reflect the diversity and patchiness of the small-scale mosaic of oceanographic conditions (**Supplementary Figures 3–8**).

CONCLUSION

(1) Twenty-eight species and six genera show a distinct distribution pattern with deep-water records off northern and central Chile and a continuous rise of the shallowest records into diving depths along Chilean Patagonia. On a north-south gradient, the highest number of deep-water emergent species in the upper 30 m can be found in CP (32), followed by NP (28) and SP (12), while on an east–west gradient, most species occur in channels (34) followed by fjords (28) and the exposed coast (11).

(2) None of the factors proposed in the literature alone, nor combinations of them, can satisfyingly explain the phenomenon of DWE in some places and its absence in other places, where the same combination of abiotic factors are present.

(3) Besides some basic requirements, most likely, DWE requires a combination of factors and this combination may vary between areas and or species. There may be factors involved that have not been hypothesized so far. The fresh-water input and associated absence of macroalgae may be one of them. More studies of this phenomenon are needed to understand the observed patterns.

(3) Through the phenomenon of DWE climate change may not only cause latitudinal but also bathymetric species shifts.

(4) More sampling in deep and poorly known areas and inventorying efforts, even in better-known areas, are strongly recommended to be able to carry out significant analyses to understand phenomena like DWE. More data of abiotic environmental variables, especially from the inner fjords and channels, are required for statistically sound analyses. The data provided, and analysis carried out can only be the first step toward a better knowledge of Chilean benthic invertebrates.

DATA AVAILABILITY STATEMENT

The data analyzed in this study is subject to the following licenses/restrictions: The database of the collection of the Universidad Catolica del Norte is available at GBIF (Sellanes, 2018). The PAMADA database includes data from other scientists who do not agree with their publication. Requests to access these datasets should be directed to VH, v.haussermann@gmail.com.

AUTHOR CONTRIBUTIONS

VH and GF: design of the project, collection of data, analysis and interpretation of data, and writing of the manuscript. SB: preparation of data and discussion of the manuscript. CC: preparation and analysis of data, writing of the manuscript. CC and CI: preparation and analysis of data and writing of the manuscript. JS: collection of data and writing of the manuscript. AT and JE: background research, collection of data, and discussion of the manuscript. FB: collection of data and discussion of the manuscript. All authors: contributed to the article and approved the submitted version.

FUNDING

This research was supported by the Fondecyt project 1201717 to GF, Fondecyt project 1161699 to VH, and Fondecyt project 1181153 to JS and CI. CC was supported by the ANID project "ANID-PCHA/Doctorado Nacional/2019-21191261".

ACKNOWLEDGMENTS

Many thanks to all the former assistants, volunteers, and employees who supported the work at Huinay Scientific Field Station, and to the Huinay Foundation.

SUPPLEMENTARY MATERIAL

The Supplementary Material for this article can be found online at: https://www.frontiersin.org/articles/10.3389/fmars.2021.688316/full#supplementary-material

Supplementary Figure 1 | Bathymetry map of Chile showing 50 and 200 m isobaths. **(A)** Chile, **(B)** North Patagonia, **(C)** Central Patagonia, **(D)** South Patagonia. The bathymetry of fjords and channels is very poor, thus many deep areas are not shown; e.g. Comau fjord, NP (left of blue asterisk) reaches nearly 500 m depth and Messier Channel, CP (orange asterisk) reaches 1300 m depth.

Supplementary Figure 2 | Relationship between each variable and presence probability calculated during GLM analysis **(A)** complete dataset. **(B)** <50 m; **(C)** >200 m.

Supplementary Figure 3 | Spatial variation of mean Chlorophyll-a concentration at different depths. **(A)** surface and **(B)** bottom waters.

Supplementary Figure 4 | Spatial variation of mean temperature at different depths. **(A)**Surface and **(B)** bottom waters.

Supplementary Figure 5 | Spatial variation of mean salinity at different depths. **(A)** surface and **(B)** bottom waters.

Supplementary Figure 6 | Spatial variation of mean dissolved molecular oxygen concentration at different depths. **(A)** Bottom and **(B)** Surface waters.

Supplementary Figure 7 | Spatial variation of silica concentration at different depths. **(A)** Surface and **(B)** bottom waters.

Supplementary Figure 8 | Latitudinal variation of parameters along the Chilean coast (18–56°S) at two depths. The blue line represents surface water while the orange line represents deep water (>200 m). The points are the mean for each latitudinal band while the whiskers represent minimum and maximum values at each latitudinal band. **(A)** oxygen, **(B)** salinity, **(C)** silica, **(D)** temperature, **(E)** primary production, **(F)** chlorophyll *a*. **(G)** current velocity.

Supplementary Figure 9 | Turbidity (Kd_490) for Chilean Patagonia based on southern hemisphere winter average for Kd_490 for the year 2009, as derived from NASA MODIS Aqua and Terra Satellites. Darker areas indicate a higher incidence of Kd_490 and thus a smaller attenuation depth and lower clarity of ocean water (Zhong-Ping et al., 2005).

Supplementary Figure 10 | Wave Exposure Model for Chilean Patagonia, showing areas of high (red) to low (blue) energy wave action. Wave exposure is a derived product of wave fetch and wave energy, that calculates the wind energy as a function of wind speed average occurrence and direction, and wave fetch as a derivative of distance and direction of energy to the coastline, with the maximum wave fetch set at 200 km. Model produced by M. T. Burrows, Department of Ecology, Scottish Association for Marine Science (Burrows et al., 2008).

Supplementary Figure 11 | Presence of macroalgae based on Huinay Fiordos Expeditions. Abundances of macroalgae strongly rise with elevated surface salinity values which, in Patagonia, can be found along the exposed coast and in some channels, but usually not inside fjords (for model, see https://biogeoscienceslaboxford.users.earthengine.app/view/kelpforests).

Supplementary Table 1 | Presence points of the 28 species and six genera used during the present study: number of presence points in: North and Central Chile (N-C: < 40°S); North Patagonia (NP: 40–47/48°S), Central Patagonia (CP: 47/48–53/54°S), and South Patagonia (SP: 53/54–56°S).

Supplementary Table 2 | Relationship of the occurrence probability with depth, site and genus. SE, standard error; z, Z-statistics; P, *p*-value.

REFERENCES

Alvarez-Garreton, C., Mendoza, P., Boisier, J. P., Addor, N., Galleguillos, M., Zambrano-Bigiarini, M., et al. (2019). The CAMELS-CL dataset: catchment attributes and meteorology for large sample studies – Chile dataset. *Hydrol. Earth Syst. Sci.* 22, 5817–5846. doi: 10.5194/hess-22-5817-2018

Andres, H. V. (1975). Nicippe buchi, n. sp., ein Pardaliscide aus einem Lavatunnel auf Lanzarote (Amphipoda, Crustacea). *Mitteilungen aus dem Hamburgischen Zool. Museum Institut* 72, 91–95.

Aravena, G., Broitman, B., and Stenseth, N. C. (2014). Twelve years of change in coastal upwelling along the central-northern coast of Chile: spatially heterogeneous responses to climatic variability. *PLoS One* 9:e90276. doi: 10.1371/journal.pone.0090276

Araya, J. F. (2013). A new species of aeneator finlay, 1926 (Mollusca, Gastropoda, Buccinidae) from northern Chile, with comments on the genus and a key to the Chilean species. *ZooKeys* 89–101. doi: 10.3897/zookeys.257.4446

Araya, J. F. (2016). New records of deep-sea sea spiders (Chelicerata: Pycnogonida) in the southeastern Pacific. *Mar. Biodiversity* 46, 725–729. doi: 10.1007/s12526-015-0416-7

Assis, J., Tyberghein, L., Bosch, S., Verbruggen, H., Serrão, E. A., and De Clerck, O. (2018). Bio-ORACLE V2.0: extending marine data layers for bioclimatic modelling. *Glob. Ecol. Biogeogr.* 27, 277–284. doi: 10.1111/geb.12693

Austin, W. C., Conway, K. W., Barrie, J. V., and Krautter, M. (2007). Growth and morphology of a reef-forming glass sponge, *Aphrocallistes vastus* (Hexactinellida), and implications for recovery from widespread trawl damage. *Por. Res. Biod. Inn. Sustain.* 2007, 139–145.

Bakran-Petricioli, T., Vacelet, J., Zibrowius, H., Petricioli, D., and Chevaldonné, P. (2007). New data on the distribution of the "deep-sea" sponges Asbestopluma hypogea and Oopsacas minuta in the Mediterranean Sea. *Mar. Ecol.* 28, 10–23. doi: 10.1111/j.1439-0485.2007.00179.x

Bakun, A., Black, B. A., Bograd, S. J., Garcia-Reyes, M., Miller, A. J., Rykaczewski, R. R., et al. (2015). Anticipated effects of climate change on coastal upwelling ecosystems. *Curr. Climate Change Rep.* 1, 85–93. doi: 10.1007/s40641-015-0008-4

Boury-Esnault, N., and Vacelet, J. (1994). "Preliminary studies on the organization and development of a hexactinellid sponge from a Mediterranean cave, Oopsacas minuta," in *Sponges in Time and Space*, eds R. W. M. van Soest, Th.M.G. van Kempen, and J.-C. Braekman, (Rotterdam: Balkema).

Breedy, O., Cairns, S., and Häussermann, V. (2015). A new alcyonian octocoral (Cnidaria, Anthozoa, Octocorallia) from Chilean fjords. *Zootaxa* 3919, 327–334. doi: 10.11646/zootaxa.3919.2.5

Broitman, B. R., Navarrete, S. A., Smith, F., and Gaines, S. D. (2001). Geographic variation of southeastern Pacific intertidal communities. *Mar. Ecol. Prog. Series* 224, 21–34. doi: 10.3354/meps224021

Broitman, B. R., Veliz, F., Manzur, T., Wieters, E. A., Finke, G. R., Fornes, P. A., et al. (2011). Geographic variation in diversity of wave exposed rocky intertidal communities along central Chile. *Revista Chilena de Historia Nat.* 84, 143–154. doi: 10.4067/s0716-078x2011000100011

Brown, R. R., Davis, C. S., and Leys, S. P. (2017). Clones or clans: the genetic structure of a deep-sea sponge, *Aphrocallistes vastus*, in unique sponge reefs of British Columbia, Canada. *Mol. Ecol.* 26, 1045–1059. doi: 10.1111/mec.13982

Burrows, M.T., Harvey, R., and Robb, L. (2008). Wave exposure indices from digital coastlines and the prediction of rocky shore community structure. *Mar. Ecol. Prog. Ser.* 353, 1–12. doi10.3354/meps07284

Cáceres, M. (2004). Surface features of the circulation in fjords of southern Chile observed in ERS and LANDSAT images. *Gayana (Concepción)* 68, 71–76. doi: 10.4067/S0717-65382004000200014

Cairns, S., Häussermann, V., and Försterra, G. (2005). A review of the Scleractinia (Cnidaria: Anthozoa) of Chile, with the description of two new species. *Zootaxa* 1018, 15–46. doi: 10.11646/zootaxa.1018.1.2

Cairns, S. D. (1994). Scleractinia of the temperate North Pacific. *Smiths. Contrib. Zool.* 557, 1–150.

Cairns, S. D. (1995). *The Marine Fauna of New Zealand: Scleractinia (Cnidaria: Anthozoa)*. New Zealand: New Zealand Oceanographic Institute Memoir.

Cairns, S. D., Gerhswin, L. A., Brook, F., Pugh, P. R., Dawson, E. W., Ocaña, V. O., et al. (2009). *Phylum Cnidaria; Corals, MEDUSAE, HYDROIDS, MYXOZOA. New Zealand Inventory of Biodiversity*. Kingdom Animalia: Radiata,.

Cairns, S. D., and Häussermann, V. (in press). A new species of *Thouarella* (Anthozoa: Octocorallia: Primnoidae) from off Chile. *Spixiana*.

Calcagno, V., and de Mazancourt, C. (2010). glmulti: an R package for easy automated model selection with (generalized) linear models. *J. Statist. Softw.* 34, 1–29.

Catalán, J., Merino-Yunnissi, C., Martínez, A., Sellanes, J., and Ibáñez, C. M. (2020). New records of crinoids (Echinodermata: Crinoidea) in the continental slope of Chile. *Rev. Biol. Mar. Oceanogr.* 55, 68–72. doi: 10.22370/rbmo.2020.55.1.2395

Choy, E., Watanabe, K., Williams, B., Stone, R., Etnoyer, P., Druffel, E., et al. (2020). Understanding growth and age of red tree corals (*Primnoa pacifica*) in the North Pacific Ocean. *PLoS One* 15:e0241692. doi: 10.1371/journal.pone.0241692

Cuevas, L. A., Tapia, F. J., Iriarte, J. L., González, H. E., Silva, N., and Vargas, C. A. (2019). Interplay between freshwater discharge and oceanic waters modulates

phytoplankton size-structure in fjords and channel systems of the Chilean Patagonia. *Prog. Oceanography* 173, 103–113. doi: 10.1016/j.pocean.2019.02.012

Dahm, C. (1999). Ophiuroids (Echinodermata) of southern Chile and the Antarctic: taxonomy, biomass, diet and growth of dominant species. *Sci. Mar.* 63(Suppl. 1), 427–432.

Dıaz, J.-P., Feral, B., David, T., and Saucede, E. P. (2010). Evolutionary pathways among shallow and deep-sea echinoids of the genus *Sterechinus* in the Southern Ocean. *Deep. Sea Res. II.* 58, 205–211. doi: 10.1016/j.dsr2.2010.10.012

Feehan, K. A., Waller, R. G., and Häussermann, V. (2019). Highly seasonal reproduction in deep-water emergent *Desmophyllum dianthus* (Scleractinia: Caryophylliidae) from the Northern Patagonian Fjords. *Mar. Biol.* 166, 1–13.

Fernández, M., Jaramillo, E., Marquet, P. A., Moreno, C. A., Navarrete, S. A., Ojeda, P. F., et al. (2000). Diversity, dynamics and biogeography of Chilean benthic nearshore ecosystems: an overview and guidelines for conservation. *Revista Chilena de Historia Natural* 73, 797–830.

Försterra, G., and Häussermann, V. (2003). First report on large scleractinian (Cnidaria: Anthozoa) accumulations in cold-temperate shallow water of south Chilean fjords. *Zool. Verhandelingen* 345, 117–128.

Försterra, G., Häussermann, V., Melzer, R. R., and Weis, A. (2013). A deep water pycnogonid close to the beach: *Colossendeis macerrima* Hoek, 1881 spotted at 18 m in the Chilean fjords. *Spixiana* 36:20.

Gallardo, V. A. (1963). Notas sobre la densidad de la fauna bentónica en el sublitoral del norte de Chile. *Gayana* 10, 3–15.

Gorny, M., Easton, E. E., and Sellanes, J. (2018). First record of black corals (Antipatharia) in shallow coastal waters of northern Chile by means of underwater video. *Latin Am. J. Aquatic Res.* 46, 457–460. doi: 10.3856/vol46-issue2-fulltext-20

Grange, K. R. (1985). Distribution, standing crop, population structure, and growth rates of black coral in the southern fiords of New Zealand. *New Zealand J. Mar. Freshwater Res.* 19, 467–475. doi: 10.1080/00288330.1985.9516111

Grange, K. R. (1990). Antipathes fiordensis, a new species of black coral (Coelenterata: Antipatharia) from New Zealand. *New Zealand J. Zool.* 17, 279–282. doi: 10.1080/03014223.1990.10422603

Grange, K. R., Singleton, R. I., Richardson, J. R., Hill, P. J., and Main, W. D. (1981). Shallow rock-wall biological associations of some southern fiords of New Zealand. *New Zealand J. Zool.* 8, 209–227. doi: 10.1080/03014223.1981.10427963

Grange, K. R., and Singleton, R. J. (1988). Population structure of black coral. *Antipathes aperta*, in the southern fiords of New Zealand. *New Zealand J. Zool.* 15, 481–489. doi: 10.1080/03014223.1988.10422628

Grigg, R. W. (1965). Ecological studies of black coral in Hawaii. *Pacific Sci.* 19, 244–260.

Hartmann-Schröder, G. (1974). Die Unterfamilie Macellicephalinae Hartmann-Schröder, 1971. *Mittheilungen aus dem Hamburgischen Zoologischen Museum und Institut* 71, 75–85.

Häussermann, V. (2004). The sea anemone genus *Actinostola Verrill*, 1883: variability and utility of traditional taxonomic features; and a re-description of *Actinostola chilensis* McMurrich, 1904. *Pol. Biol.* 28, 26–28. doi: 10.1007/s00300-004-0637-x

Häussermann, V. (2006). Biodiversity of Chilean sea anemones (Cnidaria: Anthozoa): distribution patterns and zoogeographic implications, including new records for the fjord region. *Latin Am. J. Aquatic Res.* 34, 23–35.

Häussermann, V., and Försterra, G. (2005). Distribution patterns of Chilean shallow-water sea anemones (Cnidaria: Anthozoa: Actiniaria, Corallimorpharia); with a discussion of the taxonomic and zoogeographic relationships between the actinofauna of the South East Pacific, the South West Atlantic and the Antarctic. *Sci. Mar.* 69, 91–102. doi: 10.3989/scimar.2005.69s291

Häussermann, V., and Försterra, G. (2007a). "Large assemblages of cold-water corals in Chile: a summary of recent findings and potential impacts," in *Conservation and Adaptive Management of Seamount and Deep-sea Coral Ecosystems*, eds R. Y. George and S. D. Cairns (Miami: Rosenstiel School of Marine and Atmospheric Science, University of Miami), 324.

Häussermann, V., and Försterra, G. (2007b). Extraordinary abundance of hydrocorals (Cnidaria, Hydrozoa, Stylasteridae) in shallow water of the Patagonian fjord region. *Pol. Biol.* 30, 487–492. doi: 10.1007/s00300-006-0207-5

Häussermann, V., and Försterra, G. (2009). *Marine Benthic Fauna of Chilean Patagonia*. Santiago: Nature in Focus.

Häussermann, V., Försterra, G., and Cairns, S. D. (2016). New record of the primnoid gorgonian *Primnoella* delicatissima Kükenthal, 1909 for Chilean waters. *Spixiana* 39, 147–148.

Hessler, R. R. (1970). High-latitude emergence of deep-sea isopods. *U. S. Antarctic Res. J.* 5, 133–134.

Hessler, R. R., and Thistle, D. (1975). On the place of origin of deep-sea lsopods. *Mar. Biol.* 32, 155–165. doi: 10.1007/bf00388508

Hessler, R. R., Wilson, G. D., and Thistle, D. (1979). The deep-sea isopods: a biogeographic and phylogenetic overview. *Sarsia* 64, 67–75. doi: 10.1080/00364827.1979.10411365

Höfer, J., González, H. E., Laudien, J., Schmidt, G. M., Häussermann, V., and Richter, C. (2018). All you can eat: the functional response of the cold-water coral *Desmophyllum dianthus* feeding on krill and copepods. *PeerJ* 6:e5872. doi: 10.7717/peerj.5872

Ibáñez, C. M., Pardo-Gandarillas, M. C., Párraga, D., Ziruelello, M., and Sellanes, J. (2011). Cefalópodos recolectados en el talud continental de Chile. *Amici Molluscarum* 19, 37–40.

Ibáñez, C. M., Pardo-Gandarillas, M. C., Peña, F., Gleadall, I. G., Poulin, E., and Sellanes, J. (2016). Phylogeny and biogeography of *Muusoctopus* (Cephalopoda: Enteroctopodidae). *Zool. Scripta* 45, 494–503. doi: 10.1111/zsc.12171

Ibáñez, C. M., Pardo-Gandarillas, M. C., Poulin, E., and Sellanes, J. (2012). Morphological and molecular description of a new record of *Graneledone* (Cephalopoda, Octopodidea) in the southeastern Pacific ocean. *Revista de Biol. Mar. y Oceanografía* 47, 439–450. doi: 10.4067/s0718-19572012000300007

Ibáñez, C. M., Sepúlveda, R. D., and Chong, J. (2006). A new species of *Benthoctopus* Grimpe 1921 (Cephalopoda: Octopodidae) from the southeastern Pacific Ocean. *Proc. Biol. Soc. Washington* 119, 355–364. doi: 10.2988/0006-324x(2006)119[355:ansobg]2.0.co;2

Ibáñez, C. M., Waldisperg, M., Torres, F. I., Carrasco, S. A., Sellanes, J., Pardo-Gandarillas, M. C., et al. (2019). Environmental and ecological factors mediate taxonomic composition and body size of polyplacophoran assemblages along the Peruvian Province. *Sci. Rep.* 9, 1–11.

Iliffe, T. M., Wilkens, H., Parzefall, J., and Williams, D. (1984). Marine lava cave fauna: composition, biogeography, and origins. *Science* 225, 309–311. doi: 10.1126/science.225.4659.309

Iriarte, J. L., Pantoja, S., and Daneri, G. (2014). Oceanographic processes in Chilean fjords of Patagonia: from small to large-scale studies. *Prog. Oceanogr.* 129, 1–7. doi: 10.1016/j.pocean.2014.10.004

Kobayashi, G., and Araya, J. F. (2018). Southernmost records of *Escarpia* spicata and *Lamellibrachia* barhami (Annelida: Siboglinidae) confirmed with DNA obtained from dried tubes collected from undiscovered reducing environments in northern Chile. *PLoS One* 13:e0204959. doi: 10.1371/journal.pone.0204959

Kregting, L. T., and Gibbs, M. T. (2006). Salinity controls the upper depth limit of black corals in Doubtful Sound, New Zealand. *New Zealand J. Mar. Freshwater Res.* 40, 43–52. doi: 10.1080/00288330.2006.9517402

Krylova, E. M., Sellanes, J., Valdes, F., and D'Elía, G. (2014). *Austrogena*: a new genus of chemosymbiotic bivalves (Bivalvia; Vesicomyidae; Pliocardiinae) from the oxygen minimum zone off central Chile described through morphological and molecular analyses. *Systematics Biodiversity* 12, 225–246. doi: 10.1080/14772000.2014.900133

Kuhn, M. (2008). Building predictive models in R using the caret package. *J. Statist. Softw.* 28, 1–26.

Leys, S. P., Mackie, G. O., and Reiswig, H. M. (2007). The biology of glass sponges. *Adv. Mar. Biol.* 52, 1–145. doi: 10.1016/s0065-2881(06)52001-2

Leys, S. P., Wilson, K., Holeton, C., Reiswig, H. M., Austin, W. C., and Tunnicliffe, V. (2004). Patterns of glass sponge (Porifera, Hexactinellida) distribution in coastal waters of British Columbia, Canada. *Mar. Ecol. Prog. Ser.* 283, 133–149. doi: 10.3354/meps283133

Lipps, J. H., and Hickman, C. S. (1982). *Origin, age and evolution of Antarctic and Deep-Sea Faunas. The Environment of the Deep-Sea*. Englewood Cliffs, NJ: Prentice-Hall.

Manso, C. (2010). Deep-water Ophiuroidea (Echinodermata) from off Chile in the Eastern South Pacific. *Biota Neotropica (Brasil)* 2: 185–199.

Martínez-Dios, A., Pelejero, C., López-Sanz, A., Sherrell, R., Ko, S., Häussermann, V., et al. (2020). Effects of low pH and feeding on calcification rates of the cold-water coral *Desmophyllum dianthus*. *PeerJ* 8:e8236. doi: 10.7717/peerj.8236

Miller, R. J., and Page, H. M. (2012). Kelp as a trophic resource for marine suspension feeders: a review of isotope-based evidence. *Mar. Biol.* 159, 1391–1402. doi: 10.1007/s00227-012-1929-2

Mora-Soto, A., Palacios, M., Macaya, E. C., Gómez, I., Huovinen, P., Pérez-Matus, A., et al. (2020). A high-resolution global map of giant kelp (*Macrocystis pyrifera*) forests and intertidal green algae (Ulvophyceae) with Sentinel-2 Imagery. *Remote Sens.* 12:694. doi: 10.3390/rs12040694

Mortensen, P. B., and Fossså, J. H. (2006). "Species diversity and spatial distribution of invertebrates on deep-water *Lophelia* reefs in Norway," in *Proceedings of 10th International Coral Reef Symposium*, (Okinawa).

Mortensen, P. B., Hovland, T., Fossså, J. H., and Furevik, D. M. (2001). Distribution, abundance and size of Lophelia pertusa coral reefs in mid-Norway in relation to seabed characteristics. *J. Mar. Biol. Ass.* 81, 581–597. doi: 10.1017/s002531540100426x

Mortensen, T. (1952). Echinoidea and Ophiuroidea. Reports of the Lund University Chile Expedition 1948-49, 3. *Lunds Universitets årsskrift N.F. avd.* 47, 1–22. doi: 10.1080/00364827.1970.10411156

Murray, J. (1895). *A Summary of the Scientific Results Obtained at the Sounding, Dredging and Trawling Stations of HMS Challenger*. London: HM Stationery Office.

Opresko, D. M. (2001). Revision of the Antipatharia (Cnidaria: Anthozoa). Part I. Establishment of a new family, Myriopathidae. *Zool. Meded.* 75, 343–370.

Opresko, D. M., Nuttall, M. F., and Hickerson, E. L. (2016). Black corals of the flower garden banks national marine sanctuary. *Gulf Mexico Sci.* 33:5.

Opresko, D. M., and Sanchez, J. A. (2005). Caribbean shallow-water black corals (Cnidaria: Anthozoa: Antipatharia). *Caribbean J. Sc.* 41, 492–507.

Orr, J. W., and Blackburn, J. E. (2004). The dusky rockfishes (Teleostei: Socrpaeniformes) of the North Pacific Ocean: resurrection of *Sebastes* variabilis (Pallas, 1814) and a redescription of *Sebastes ciliatus* (Tilesius, 1813). *Fish. Bull.* 102, 328–348.

Orr, J. W., and Hawkins, S. (2008). Species of the rougheye rockfish complex: resurrection of *Sebastes melanostictus* (Matsubara, 1934) and a redescription of *Sebastes aleutianus* (Jordan and Evermann, 1898)(Teleostei: Scorpaeniformes). *Fish. Bull.* 106, 111–134.

Osorio, C. (1968). Lima (Acesta) patagonica (Dall), en Chile (Mollusca Lamellibranchiata, Limidae). *Noticiario Mensual del Museo Nacional de Historia Natural, Chile* 143, 3–5.

Paulin, C. D. (1989). Redescription of *Helicolenus percoides* (Richardson) and *H. barathri* (Hector) from New Zealand (Pisces, Scorpaenidae). *J. Roy. Soc.New Zealand* 19, 319–325. doi: 10.1080/03036758.1989.10427185

Paulin, C., Stewart, A., Roberts, C., and McMillan, P. (1989). *New Zealand Fish: a Complete Guide*. Wellington: Museum of New Zealand. National Museum of New Zealand Miscellaneous Series No. 19.

Pickard, G., and Stanton, B. (1980). "Pacific fjords-A review of their water characteristics," in *Proceedings of the Conference on Fjord Oceanography, Victoria, 1979*. New York, NY: Plenum Press.

Pinet, P. R. (2019). "The physiography of the Ocean Floor," in *Invitation to Oceanography*. Burlington, MA: Jones & Bartlett Learning.

QGIS Development Team (2012). *QGIS Geographic Information System. Open Source Geospatial Foundation Project*. Available online at: http://qgis.osgeo.org (accessed March 31, 2021).

Quattro, J., Chase, M., Rex, M., Greig, T., and Etter, R. (2001). Extreme mitochondrial DNA divergence within populations of the deep-sea gastropod *Frigidoalvania brychia*. *Mar. Biol.* 139, 1107–1113. doi: 10.1007/s002270100662

Quiroga, E., Sellanes, J., Arntz, W. E., Gerdes, D., Gallardo, V. A., and Hebbeln, D. (2009). Benthic megafaunal and demersal fish assemblages on the Chilean continental margin: the influence of the oxygen minimum zone on bathymetric distribution. *Deep Sea Res. Part II: Top. Stud. Oceanography* 56, 1112–1123. doi: 10.1016/j.dsr2.2008.09.010

R Core Team (2021). *R A Language and Environment for Statistical Computing*. Vienna: R Foundation for Statistical Computing.

Ramirez-Llodra, E., Brandt, A., Danovaro, R., Mol, B. D., Escobar, E., German, C. R., et al. (2010). Deep, diverse and definitely different: unique attributes of the world's largest ecosystem. *Biogeosciences* 7, 2851–2899. doi: 10.5194/bg-7-2851-2010

Riehl, T., and Kaiser, S. (2012). Conquered from the deep sea? a new deep-sea isopod species from the Antarctic shelf shows pattern of recent colonization. *PLoS One* 7:e49354. doi: 10.1371/journal.pone.0049354

Rivadeneira, M. M., Fernández, M., and Navarrete, S. A. (2002). Latitudinal trends of species diversity in rocky intertidal herbivore assemblages: spatial scale and the relationship between local and regional species richness. *Mar. Ecol. Prog. Ser.* 245, 123–131. doi: 10.3354/meps245123

Roberts, C. D. (1989). A revision of New Zealand and Australian orange perches (Teleostei; Serranidae) previously referred to *Lepidoperca pulchella* (Waite) with description of a new species of *Lepidoperca* from New Zealand. *J. Nat. Hist.* 23, 557–589. doi: 10.1080/00222938900770321

Roberts, C. D. (2001). Survey of deepwater emergence in New Zealand fiord fishes. *NZ J. Mar. Freshwater Res.* 35:661.

Roberts, J. M., Wheeler, A., Freiwald, A., and Cairns, S. (2009). *Cold-water Corals: the Biology and Geology of Deep-sea Coral Habitats*. Cambridge: Cambridge University Press.

Rogers, A. D. (1999). The Biology of *Lophelia pertusa* (Linnaeus 1758) and other deep-water reef-forming corals and impacts from human activities. *Int. Rev. Hydrobiol.* 84, 315–406. doi: 10.1002/iroh.199900032

Rossin, A. M., Waller, R. G., and Försterra, G. (2017). Reproduction of the cold-water coral *Primnoella chilensis* (Philippi, 1894). *Continental Shelf Res.* 144, 31–37. doi: 10.1016/j.csr.2017.06.010

Russell, B. C. (1988). Revision of the labrid genus *Pseudolabrus* and allied genera. *Rec. Aust. Mus. Suppl.* 9, 1–72. doi: 10.3853/j.0812-7387.9.1988.95

Schwabe, E., and Sellanes, J. (2010). Revision of Chilean bathyal chitons (Mollusca: Polyplacophora) associated with cold-seeps, including description of a new species of Leptochiton (Leptochitonidae). *Org. Divers. Evol.* 10, 31–55. doi: 10.1007/s13127-009-0002-6

Sellanes, J. (2018). *Base de Datos de la Sala de Colecciones Biológicas de la Universidad Católica del Norte (SCBUCN). Version 1.2. Universidad Católica del Norte. Occurrence Dataset.* Available online at: https://doi.org/10.15468/d3auf9 (accessed August 6, 2021).

Sellanes, J., Neira, C., Quiroga, E., and Teixido, N. (2010). Diversity patterns along and across the Chilean margin: a continental slope encompassing oxygen gradients and methane seep benthic habitats. *Mar. Ecol.* 31, 111–124. doi: 10.1111/j.1439-0485.2009.00332.x

Sellanes, J., Quiroga, E., and Gallardo, V. A. (2004). First direct evidence of methane seepage and associated chemosynthetic communities in the bathyal zone off Chile. marine biological association of the United Kingdom. *J. Mar. Biol. Assoc. U K* 84:1065. doi: 10.1017/s0025315404010422h

Sellanes, J., Quiroga, E., and Neira, C. (2008). Megafauna community structure and trophic relationships at the recently discovered Concepción Methane Seep Area, Chile, 36 S. *ICES J. Mar. Sci.* 65, 1102–1111. doi: 10.1093/icesjms/fsn099

Sievers-Czischke, H. (2018). "La oceanografía en Chile: historia de un desarrollo imperativo," in *Servicio Hidrográfico y Oceanográfico de la Armada de Chile,* Valparaíso, 266.

Silva, N. (2008). "Dissolved oxygen, pH, and nutrients in the austral Chilean channels and fjords," in *Progress in the Oceanographic Knowledge of Chilean Interior Waters, from Puerto Montt to Cape Horn*, eds N. Silva and S. Palma (Valparaíso: Comité Oceanográfico Nacional - Pontificia Universidad Católica de Valparaíso), 37–43.

Simpson, A. W., Eckelbarger, J., and Watling, L. (2005). "Some aspects of the reproductive biology of *Paramuricea placomus* (Octocorallia) from the Gulf of Maine. Integr. Comp. Biol. 45," in *Proceedings of the 3rd International Symposium on Deep-sea Coral*, (Miami).

Stigebrandt, A. (2012). "Hydrodynamics and Circulation of Fjords," in *Encyclopedia of Lakes and Reservoirs. Encyclopedia of Earth Sciences Series*, eds L. Bengtsson, R. W. Herschy, and R. W. Fairbridge (Dordrecht: Springer), doi: 10.1007/978-1-4020-4410-6_247

Stock, J. H., and Vermeulen, J. J. (1982). A representative of the mainly abyssal family Pardaliscidae (Crustacea, Amphipoda) in cave waters of the Caicos Islands. *Bijdragen tot de Dierkunde* 52, 3–12. doi: 10.1163/26660644-05201002

Stone, R. P., Andrews, A., and Mondragon, J. (2005). "Deepwater emergence of red tree coral (*Primnoa sp.*) in Glacier Bay, Alaska," in *Proceedings of the 3rd International Symposium on Deep Water Corals*, (Miami, FL).

Stone, R. P., and Mondragon, J. (2018). *Deep-sea Emergence of Red Tree Corals (Primnoa pacifica) in Southeast Alaska Glacial Fjords*. Washington, DC: NOAA.

Strömgren, T. (1970). Emergence of *Paramuricea placomus* (L.) and *Primnoa resedaeformis* (Gunn.) in the inner part of Trondheimsfjorden (Western coast of Norway). *Det Kongelige Norske Videnskabers Selskabs Skrifter* 4, 1–6.

Strömgren, T. (1971). Vertical and horizontal distribution of *Lophelia pertusa* (Linné) in Trondheimsfjordan on the West Coast of Norway. *K. Nor. Vidensk. Selsk. Skr.* 6, 1–9.

Strugnell, J. M., Cherel, Y., Cooke, I. R., Gleadall, I. G., Hochberg, F. G., Ibáñez, C. M., et al. (2011). The Southern Ocean: source and sink? *Deep Sea Res. Part II: Top. Stud. Oceanography* 58, 196–204.

Sutton, T. T. (2013). Vertical ecology of the pelagic ocean: classical patterns and new perspectives. *J. Fish Biol.* 83, 1508–1527. doi: 10.1111/jfb.12263

Taylor, M. L., Cairns, S. D., Agnew, D. J., and Rogers, A. D. (2013). A revision of the genus *Thouarella Gray*, 1870 (Octocorallia: Primnoidae), including an illustrated dichotomous key, a new species description, and comments on Plumarella Gray, 1870 and Dasystenella, Versluys, 1906. *Zootaxa* 3602, 1–105. doi: 10.11646/zootaxa.3602.1.1

Tellier, F., Meynard, A. P., Correa, J. A., Faugeron, S., and Valero, M. (2009). Phylogeographic analyses of the 30° S south-east Pacific biogeographic transition zone establish the occurrence of a sharp genetic discontinuity in the kelp *Lessonia nigrescens*: vicariance or parapatry? *Mol. Phylogenet. Evol.* 53, 679–693. doi: 10.1016/j.ympev.2009.07.030

Thiel, M., Castilla, J. C., Fernández, M., and Navarrete, S. (2007). The Humboldt current system of northern and central Chile. oceanographic processes, ecological interactions and socioeconomic feedback. *Ocean. Mar. Biol. Annu. Rev.* 45, 195–344. doi: 10.1201/9781420050943.ch6

Thuy, B., and Schulz, H. (2012). The oldest representative of a modern deep-sea ophiacanthid brittle-star clade from Jurassic shallow-water coral reef sediments. *Acta Palaeontologica Polonica* 58, 525–531.

Treude, T., Kiel, S., Linke, P., Peckmann, J., and Goedert, J. L. (2011). Elasmobranch egg capsules associated with modern and ancient cold seeps: a nursery for marine deep-water predators. *Mar. Ecol. Prog. Series* 437, 175–181. doi: 10.3354/meps09305

Tyberghein, L., Verbruggen, H., Pauly, K., Troupin, C., Mineur, F., and De Clerck, O. (2012). Bio-ORACLE: a global environmental dataset for marine species distribution modelling. *Global Ecol. Biogeography* 21, 272–281. doi: 10.1111/j.1466-8238.2011.00656.x

Vacelet, J., and Boury-Esnault, N. (1996). A new species of carnivorous sponge (Demospongiae: Cladorhizidae) from a mediterranean cave. *Bull. Inst. R. Sci. Nat. Belg.* 66, 109–115.

van der Ham, J. L. (2002). Addition to the description of *Spelaeonicippe provo* (Amphipoda, Pardaliscidae). *Crustaceana* 75, 1271–1274. doi: 10.1163/156854002321518199

van Ofwegen, L., Häussermann, V., and Försterra, G. (2007). The genus *Alcyonium* (Octocorallia: Alcyonacea: Alcyoniidae) in Chile. *Zootaxa* 1607, 1–19. doi: 10.11646/zootaxa.1607.1.1

Wagner, D., Brugler, M. R., Opresko, D. M., France, S. C., Montgomery, A. D., and Toonen, R. J. (2010). Using morphometrics, in situ observations and genetic characters to distinguish among commercially valuable Hawaiian black coral species; a redescription of *Antipathes grandis* Verrill, 1928 (Antipatharia: Antipathidae). *Invert. Syst.* 24, 271–290. doi: 10.1071/is10004

Waller, R. G., Stone, R. P., Mondragon, J., and Clark, C. E. (2011). "Reproduction of red tree corals in the southeastern Alaskan fjords: implications for conservation and population turnover," in *Proceedings of the American Academy of Underwater Sciences 30th Scientific Symposium*, (Dauphin Island, AL), 29.

Warner, G. F. (1981). Species descriptions and ecological observations of black corals (Antipatharia) from Trinidad. *Bull. Mar. Sci.* 31, 147–163.

Weingartner, T., Eisner, L., Eckert, G. L., and Danielson, S. (2009). Southeast Alaska: oceanographic habitats and linkages. *J. Biogeogr.* 36, 387–400. doi: 10.1111/j.1365-2699.2008.01994.x

Wilkens, H., Parzefall, J., and Ribowski, A. (1990). Population biology and larvae of the anchialine crab *Munidopsis polymorph*a (Galatheidae) from Lanzarote (Canary Islands). *J. Crust. Biol.* 10, 667–675. doi: 10.2307/1548411

Wing, S. R., and Jack, L. (2013). Marine reserve networks conserve biodiversity by stabilizing communities and maintaining food web structure. *Ecosphere* 4, 1–14.

Wisshak, M., Freiwald, A., Lundälv, T., and Gektidis, M. (2005). "The physical niche of the bathyal *Lophelia pertusa* in a non-bathyal setting: environmental controls and palaeoecological implications," in *Cold-water Corals and Ecosystems*, eds A. Freiwald and J. M. Roberts (Berlin: Springer).

Zapata-Hernández, G., Sellanes, J., Thurber, A. R., and Levin, L. A. (2014). Trophic structure of the bathyal benthos at an area with evidence of methane seep activity off southern Chile (45° S). *J. Mar. Biol. Assoc. U K.* 94, 659–669. doi: 10.1017/s0025315413001914

Zhong-Ping, L, Darecki, M., Carder, K., Davis, C., Stramski, D. and William, R. (2005). Diffuse Attenuation Coefficient of Downwelling Irradiance: An Evaluation of Remote Sensing Methods. *J. Geophys. Res.* 110, 1–9. doi: 10.1029/2004JC002573

Conflict of Interest: The authors declare that the research was conducted in the absence of any commercial or financial relationships that could be construed as a potential conflict of interest.

Publisher's Note: All claims expressed in this article are solely those of the authors and do not necessarily represent those of their affiliated organizations, or those of the publisher, the editors and the reviewers. Any product that may be evaluated in this article, or claim that may be made by its manufacturer, is not guaranteed or endorsed by the publisher.

frontiers in Marine Science

ORIGINAL RESEARCH
published: 08 October 2021
doi: 10.3389/fmars.2021.720710

Detection of Ecological Thresholds and Selection of Indicator Taxa for Epibenthic Communities Exposed to Multiple Pressures

Laurie Isabel[1,2], David Beauchesne[1], Chris McKindsey[2] and Philippe Archambault[1]*

[1] ArcticNet, Québec-Océan, Takuvik, Département de Biologie, Université Laval, Québec, QC, Canada, [2] Fisheries and Oceans Canada, Maurice Lamontagne Institute, Mont-Joli, QC, Canada

The estuary and the Gulf of St. Lawrence (EGSL), eastern Canada form a vast inland sea that is subjected to numerous anthropogenic pressures. Management tools are needed to detect and quantify their effect on benthic communities. The aims of this study are to analyze the spatial distribution of epibenthic communities in the EGSL and quantify the impact of important pressures on them to identify indicator taxa. Epibenthic communities were sampled at 1314 EGSL sites between 2011 and 2018 by bottom trawling. Cluster analyses revealed the presence of six distinct epibenthic communities that seem to be strongly influenced by oxygen concentration. Threshold analyses confirm that oxygen is an important predictor of epibenthic community composition and distribution. A major oxygen threshold is observed around 50–100 μmol O_2 L^{-1}, resulting in a shift of community type. At these concentrations and below, opportunistic taxa dominate the community while sensitive taxa are absent or present at very low abundance. Biomass of the latter only starts to increase when oxygen concentrations reach 150 μmol O_2 L^{-1}. The species *Actinostola callosa*, *Actinauge cristata*, *Ctenodiscus crispatus*, and *Brisaster fragilis* were identified as good indicators for detecting this impact threshold forepibenthic communities. This study provides threshold-based indicator species that help to establish and monitor the ecological state of epibenthic communities in a marine ecosystem exposed to multiple pressures.

Keywords: biodiversity, ecological thresholds, epibenthic communities, estuary and Gulf of St. Lawrence, multiple pressures, climate change, indicator taxa

OPEN ACCESS

Edited by:
Jose Manuel Guerra-García, Seville University, Spain

Reviewed by:
Thadickal V. Joydas, King Fahd University of Petroleum and Minerals, Saudi Arabia
Pål Buhl-Mortensen, Norwegian Institute of Marine Research (IMR), Norway

****Correspondence:***
Laurie Isabel
Laurie.Isabel@dfo-mpo.gc.ca

Specialty section:
This article was submitted to Marine Evolutionary Biology, Biogeography and Species Diversity, a section of the journal Frontiers in Marine Science

Received: *04 June 2021*
Accepted: *20 September 2021*
Published: *08 October 2021*

Citation:
Isabel L, Beauchesne D, McKindsey C and Archambault P (2021) Detection of Ecological Thresholds and Selection of Indicator Taxa for Epibenthic Communities Exposed to Multiple Pressures. Front. Mar. Sci. 8:720710. doi: 10.3389/fmars.2021.720710

INTRODUCTION

Marine ecosystems are changing faster than ever, causing profound changes to communities of living organisms (Walther et al., 2002; Myers and Worm, 2003; Worm et al., 2006). Increasing types and intensities of human activities over the last century have been identified as the main cause for these rapid changes (Halpern et al., 2015; Jouffray et al., 2020). Increasing human activities concomitantly increases pressures that may affect marine species. Moreover, Anthropocene-related climate changes are occurring and interacting with other long-term trends (Hoegh-Guldberg and Bruno, 2010). Together, these pressures dominate the human footprint on marine ecosystems, with the potential for significant overlap between pressures (Halpern et al., 2008, 2015). Overlaps may

lead to biological interactions and non-linear effects that are difficult to predict and interpret (Crain et al., 2008; Côté et al., 2016; Carrier-Belleau et al., 2021). Cumulative or not, increasing numbers of pressures on marine ecosystems makes ecological management increasingly challenging. Although the number and types of pressures have increased tremendously in recent decades, little is known about which are having the greatest impacts on communities and how they interact over space and time (Halpern et al., 2015).

Benthic communities are likely to be greatly affected by these environmental changes as they are located at the convergence of these pressures—the bottom. Moreover, many benthic taxa are sessile or have limited mobility, and therefore have limited ability to avoid pressures that can reduce their chances of reproduction and survival (Dauer, 1993; Weisberg et al., 1997). Benthic communities play a major role in marine ecosystems and their degradation could affect the entire ecosystem. Several taxa, such as corals, sea pens, and sponges, form biogenic structures that create habitats that serve as protection for benthic and demersal taxa (Buhl-Mortensen et al., 2010). Benthic organisms living in sediments also play an important role in the transport and circulation of water and particles through sediments and at the water-sediment interface (Rhoads, 1974; Aller, 1982). Benthic communities are also involved in biogeochemical cycles through feeding by filtering taxa such as bivalves, which play a crucial role in benthic-pelagic coupling (Newell, 2004).

The need to develop tools to capture the complexity of ecological responses to pressures has become essential for environmental management (Landres et al., 1988; Groom et al., 1997). Ecological thresholds are particularly useful in ecosystem management as they represent transition points where small changes to ecological conditions could greatly impact the diversity, structure, and function of marine communities (Toms and Lesperance, 2003; Huggett, 2005; Groffman et al., 2006; Brenden et al., 2008; Andersen et al., 2009; Sonderegger et al., 2009; Baker and King, 2010). Incorporating thresholds in ecological management can further address the increased non-linear responses (Kelly et al., 2014). Such rapid changes could generate undesirable shifts in ecological conditions, resulting in drastic impacts on communities. Indicators able to detect these thresholds can be developed and serve as a proxy of these tipping points. Indicators are quantifiable measures of an ecological parameter that can be followed over time to establish the ecological state (Jamieson et al., 2001; Large et al., 2015). Identifying relevant indicators or major ecological thresholds has been shown to strengthen ecological monitoring and assessment programs (Suding and Hobbs, 2009; Samhouri et al., 2011; Large et al., 2015).

The estuary and Gulf of St. Lawrence (EGSL) in eastern Canada is an inland sea characterized by heterogeneic oceanographic and geological conditions, and high productivity (El-Sabh and Silverberg, 1990; Therriault, 1991; Benoît et al., 2012; Moritz et al., 2013). The EGSL has attracted human settlement for centuries to the benefit of the socio-economic development of its adjacent lands (Alexander et al., 2010). Combined with global changes, this intense human use has concomitantly exposed this ecosystem to multiple environmental changes. Like many inland seas, the EGSL has internal dynamics that restrict flushing and are subject to a convergence of pressures from land-based and marine disturbances as well as climatic changes (MacCraken et al., 2008; Beauchesne et al., 2020). Deep waters of the EGSL are warming, reaching new temperature records in 2019 due to altered ocean circulation dynamics (Claret et al., 2018; Galbraith et al., 2020). Increasing temperatures has also decreased bottom oxygen levels (Poitevin et al., 2019). Indeed, oxygen concentration has decreased by more than half the 1930 value over the last century (Gilbert et al., 2005). While two-thirds of the oxygen depletion observed can be attributed to this altered ocean circulation, the remaining third is a result of higher bacterial activity due to increased particulate matter in the water column and sediments (Lehmann et al., 2009). Land-based human activities are responsible for the increased organic matter inputs in the EGSL (Gilbert et al., 2005, 2007; Thibodeau et al., 2006). A permanent hypoxic zone is now present in the estuary (Gilbert et al., 2007). These changes have also resulted in acidification, with the pH of bottom waters dropping by 0.2–0.3 over the past 75 years (Mucci et al., 2011).

Several studies have examined the impacts of environmental pressures on the distribution of benthic communities in the EGSL (Bourget et al., 2003; Lévesque, 2009; Belley et al., 2010; Moritz et al., 2013, 2015). Current trawl fisheries in the EGSL appear to have very little impact on epibenthic communities (Moritz et al., 2015). Depth, bottom current, temperature, and oxygen saturation have been shown to influence the distribution of benthic communities. Canonical analyses suggested a strong relationship between oxygen concentrations and benthic community structure (Lévesque, 2009). A strong relationship between oxygen and the level of bioturbation traces on the seafloor has also been observed (Belley et al., 2010), suggesting that the infaunal community may also be affected by hypoxia in the estuary. Similar taxa richness was observed between hypoxic and normoxic sites, which was likely the result of different community compositions along the studied oxygen gradient. Notwithstanding these studies, the quantitative impacts of pressures on benthic communities remain largely unknown. To this end, this study explores the spatial variation of EGSL epibenthic communities, identifies thresholds of community composition, and further quantifies the impact of oxygen to select indicator species. The hypothesis is that sensitive and tolerant epibenthic taxa will be negatively and neutrally or positively affected by the presence of pressures, respectively. It is expected that the type and intensity of pressures will vary spatially in the EGSL with corresponding effects on benthic communities and that ecologically relevant thresholds may be identified.

MATERIALS AND METHODS

Study Area

The EGSL covers an area of 116,115 km^2, excluding the coastal area, with depth varying between 37 and 550 m (**Figure 1**; Bourdages et al., 2018). Its topography includes three deep channels: the Laurentian, Anticosti, and Esquiman channels (Saucier et al., 2003). The seabed topography of this region is

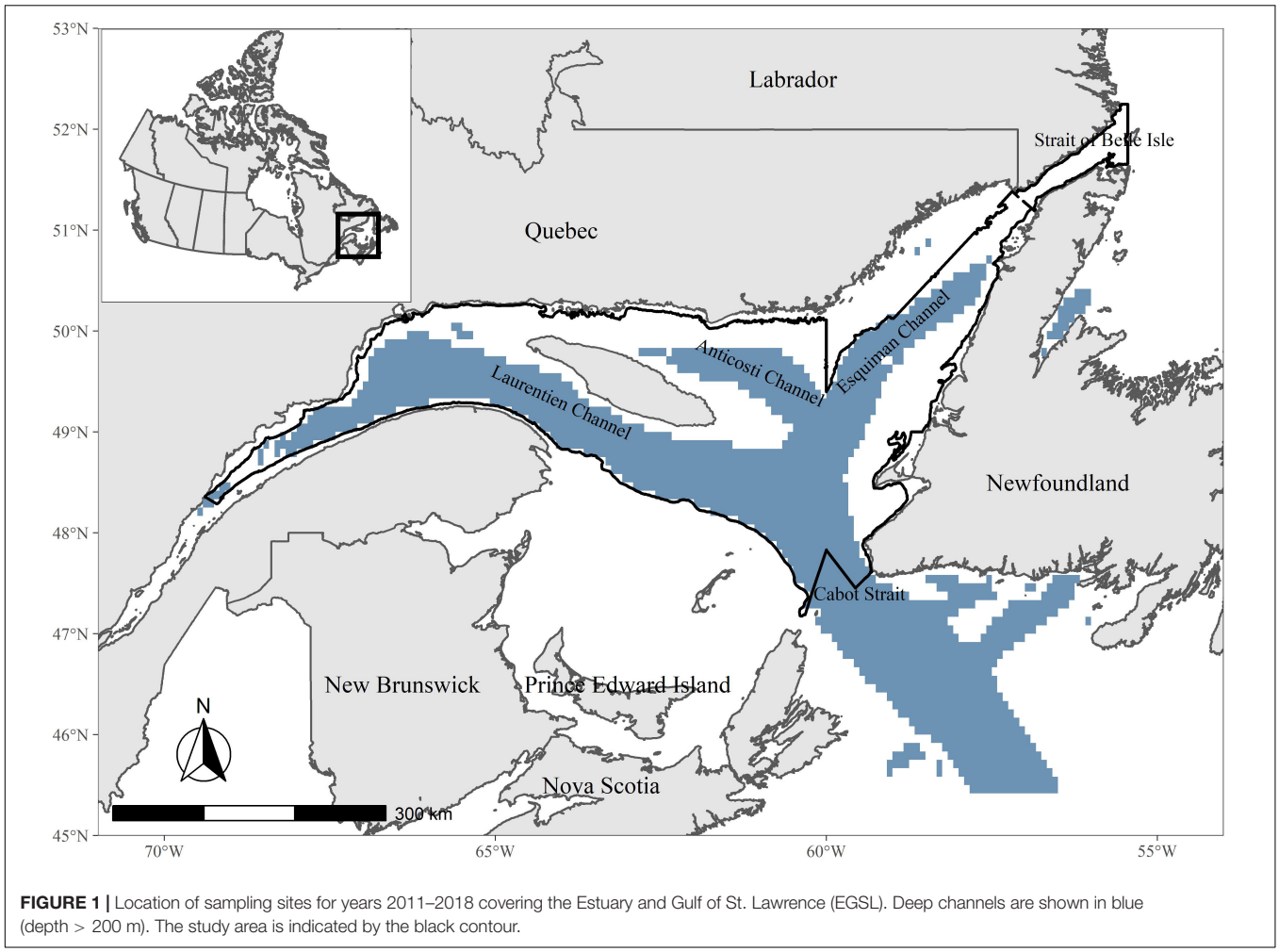

FIGURE 1 | Location of sampling sites for years 2011–2018 covering the Estuary and Gulf of St. Lawrence (EGSL). Deep channels are shown in blue (depth > 200 m). The study area is indicated by the black contour.

complex and strongly influences water circulation (Dufour and Ouellet, 2007). Waters are stratified with two layers during winter and spring and three layers in the summer and fall (Galbraith, 2006). Deep waters are formed by two water masses: the Labrador Current, which is cold and well-oxygenated and enters the Gulf through Strait of Belle Isle to the north, and Atlantic continental shelf water, which is warmer with less dissolved oxygen, entering the Gulf from the east through Cabot Strait (Galbraith et al., 2019).

Benthic Data

Benthic taxa data were collected onboard the CCGS Teleost during the Fisheries and Ocean Canada multidisciplinary research survey, each August (Moritz et al., 2013; Bourdages et al., 2018). The data used in the present study covers the years 2011–2018. Sampling was done within depth-specific strata using a random sampling design (Gagnon, 1991). Samples were collected by bottom trawling with a four-sided Campelen 1800 shrimp trawl equipped with Rockhopper footgear (Walsh and McCallum, 1997). The trawl had a knotless nylon lining with 12.7 mm mesh size, allowing most epibenthic macroinvertebrates to be collected (Bourdages et al., 2018). Trawling lasted around 15 min but was shorter if a very large amount of fish was expected, to prevent overloading the trawl net or if the bottom was rocky.

Catches were sorted at each sampling site and benthic taxa identified to the lowest possible taxonomic level. Sorted invertebrates were then photographed, one taxon at a time, weighed, and counted to obtain population density and biomass. When > 30 individuals of a given taxon were collected, the mass of the total capture and of 30 random individuals was recorded to estimate the total number of individuals collected. Since trawl lengths and times were not standardized, biomass estimates were standardized relative to the catch effort (catch per unit effort (CPUE)—$kg.km^{-2}$).

Environmental Data

Data on environmental predictors were obtained from two datasets: the fisheries multidisciplinary research survey and *eDrivers*, an open-knowledge data platform (Beauchesne et al., 2020). For the fisheries survey data, an SBE19plusTM CTD mounted on the outside of the top of the trawl recorded temperature, salinity, and oxygen concentration on the bottom during the trawling at each site (Bourdages et al., 2018). Depth was also recorded at the beginning and end of each trawl to

provide a mean for each site. The second set of predictors was extracted from the *eDrivers* platform for EGSL environmental data (Beauchesne et al., 2020). Selected drivers were aragonite (indicating acidification) and positive temperature anomalies (posAnom), as described in Galbraith et al. (2019). Data on fishing intensity were created from raw data (fishing vessel log book) provided by DFO for *eDrivers* (DFO, 2016; Beauchesne et al., 2020). Intensities of demersal non-destructive high-by-catch fisheries (DNH) and demersal destructive fisheries (DD) are expressed as the number of fishing events in a 1 km^2 area in a year. Acidification and posAnom were normalized (0–1) to obtain an index of the intensity for each driver.

Data Analysis

Epibenthic Community Structure

Sites were classified based on taxonomic composition similarity using hierarchical cluster analysis performed using Ward's hierarchical agglomeration method to identify compact, spherical clusters (Ward, 1963). The analysis was applied to a Bray-Curtis dissimilarity matrix of taxa biomass to define distinct communities based on co-distributions of individual taxa (Bray and Curtis, 1957). Data on shrimp biomass were not included in the analyses. Although shrimps are considered as "benthic" organisms, they are not permanently located on the seabed, undertaking vertical migrations, and thus limiting their link to the benthic habitat (DFO, 2002; Savenkoff et al., 2017). Indeed, only 30% of shrimp diets come from the benthos with the remaining 70% originating from pelagic food webs (Bundy et al., 2000). Moreover, northern shrimp *Pandalus borealis* represents 75% of the invertebrate catch of all EGSL surveys and its inclusion in the analyses could mask trends for other epibenthic taxa (Savenkoff et al., 2017). All data analyses were done using R version 3.5.1. The vegan package was used for species clustering (Oksanen et al., 2019).

Environmental Regimes

Clustering of environmental variables was done to establish if different environmental regimes existed through the study area and could explain the clustering of benthic communities. The similarity of sites in terms of environmental predictors was evaluated using *k*-means clustering to group sites characterized by similar environmental conditions. This clustering method works by creating *k* numbers of clusters with the aim to minimize the sum of residual sums-of-squares (Legendre and Legendre, 2012). The number of clusters selected was defined using the elbow method, an optimization method to select the smallest number of clusters which account for the largest proportion of variation in the data (Bholowalia and Kumar, 2014). This method consists of plotting the explained variation as a function of the number of clusters. To select the number of clusters to use, one picks the elbow of the curve. The function *kmeans* from the stats package was used for the environmental clustering (R Core Team, 2018).

Random Forest and Gradient Forest

Thresholds of epibenthic community assemblage were evaluated with a gradient forest analysis using the "gradientForest" package in R (Ellis et al., 2012). A gradient forest (GF) is created by combining multiple random forests (RF) to establish the response of the whole community to environmental gradients (Ellis et al., 2012). It is an automated learning algorithm used for classification and regression problems based on Breiman's algorithm (Breiman, 2001). The RF algorithm works by combining several (n) decision trees, each created by recursive data partitioning, with bootstrap techniques to minimize the variance of a single model. Each tree is created from a bootstrapped sample of the whole dataset. At each node during the data partitioning, a fixed number of predictors (*mtry*) is randomly selected from all available predictors. GF combines the cross-validated R^2 and accuracy importance measures of every taxa's RF to give a global R^2-value. The overall result is a monotonic function for every predictor representing the turnover of taxonomic composition along the gradient of a predictor. The analysis identified where community composition changes along predictor gradients. RF models were run for taxa individually to determine the directionality of their responses to variation in oxygen concentration with partial dependence plots; this was done solely for taxa with a strong reaction at the previously identified thresholds (from GF models). Partial dependence plots use the biomass regression function generated by each random forest model to show trends in biomass of a taxon as a function of oxygen concentration, while other predictors are kept at their average observed value (Murillo et al., 2016). Models were built with the "randomForest" package in R (Liaw and Wiener, 2002). Default parameters were used except for *mtry*, which was tuned for each taxon, and *ntree* was fixed at 150 trees following Oshiro et al. (2012). RF and GF have many advantages for modeling taxa and community distributions. They can identify which predictors are most important for the observed patterns as multiple trees are grown with different combinations of predictors; this is very useful for ecosystems exposed to multiple pressures. In addition, there are no *a priori* distributional assumptions about the frequency of response variables, as opposed to other methods such as generalized linear models or generalized additive models. RF and its extensions are also good for handling non-linear patterns between predictors and the response variable (Breiman, 2001).

Indicator Taxa

Indicator taxa that characterized groups of sites were identified using the IndVal method (Dufrêne and Legendre, 1997). This approach identifies indicator taxa by combining taxon abundance and frequency of occurrence to create an index representing the association of taxa to groups identified with the Ward clustering method (see section "Epibenthic Community Structure"). Indicator taxa are useful to detect taxa that are characteristic to specific habitats and correspond to a certain set of environmental conditions (Dufrêne and Legendre, 1997; De Cáceres et al., 2010; Legendre and Legendre, 2012). In this analysis, an indicator value is calculated for each taxon in each community cluster based on their specificity and fidelity to each cluster. Specificity measures if a taxon is distributed across many groups (low specificity) or only present in the group of interest (high specificity); fidelity measures if a taxon is present in all (high

fidelity) or few (low fidelity) sites within the group of interest. The maximal indicator taxon, having an indicator value of 1, would be found exclusively in one group and would be present at all the sites of this group.

RESULTS

Community Structure and Distribution

Cluster analysis of the taxa matrix revealed six, partially spatially segregated, communities in the EGSL (**Figure 2**). The six most dominant taxa of each community in terms of biomass and taxa richness of each community are presented in **Table 1**. The first community type was found almost exclusively in the St. Lawrence estuary and is composed (biomass and presence) mainly of the anemone *Actinostola callosa*, the sea urchin *Brisaster fragilis*, and the sea star *Ctenodiscus crispatus*. We also found a large biomass of snow crab *Chionoecetes opilio* and the anemone *Actinauge cristata*. The average total mass of invertebrates was 2,190 kg.km^{-2} and the highest mass captured was 18,905 kg.km^{-2}. It was the second most diverse community in terms of the mean number of taxa found at a single site but the least diverse in terms of the total number of taxa recorded across all sites.

The second community type was found in the Esquiman and Anticosti channels and at the border of the Laurentian Channel in the Gulf of St. Lawrence. It was mainly composed of *C. crispatus*, brittle stars *Ophiura* spp. and *A. callosa*. The top six dominant taxa were very similar to community 1, but with different dominant taxa. The average benthic biomass captured per station was ca. 87 kg.km^{-2}, about 25 times lower than for community 1. It was the most diverse community in terms of

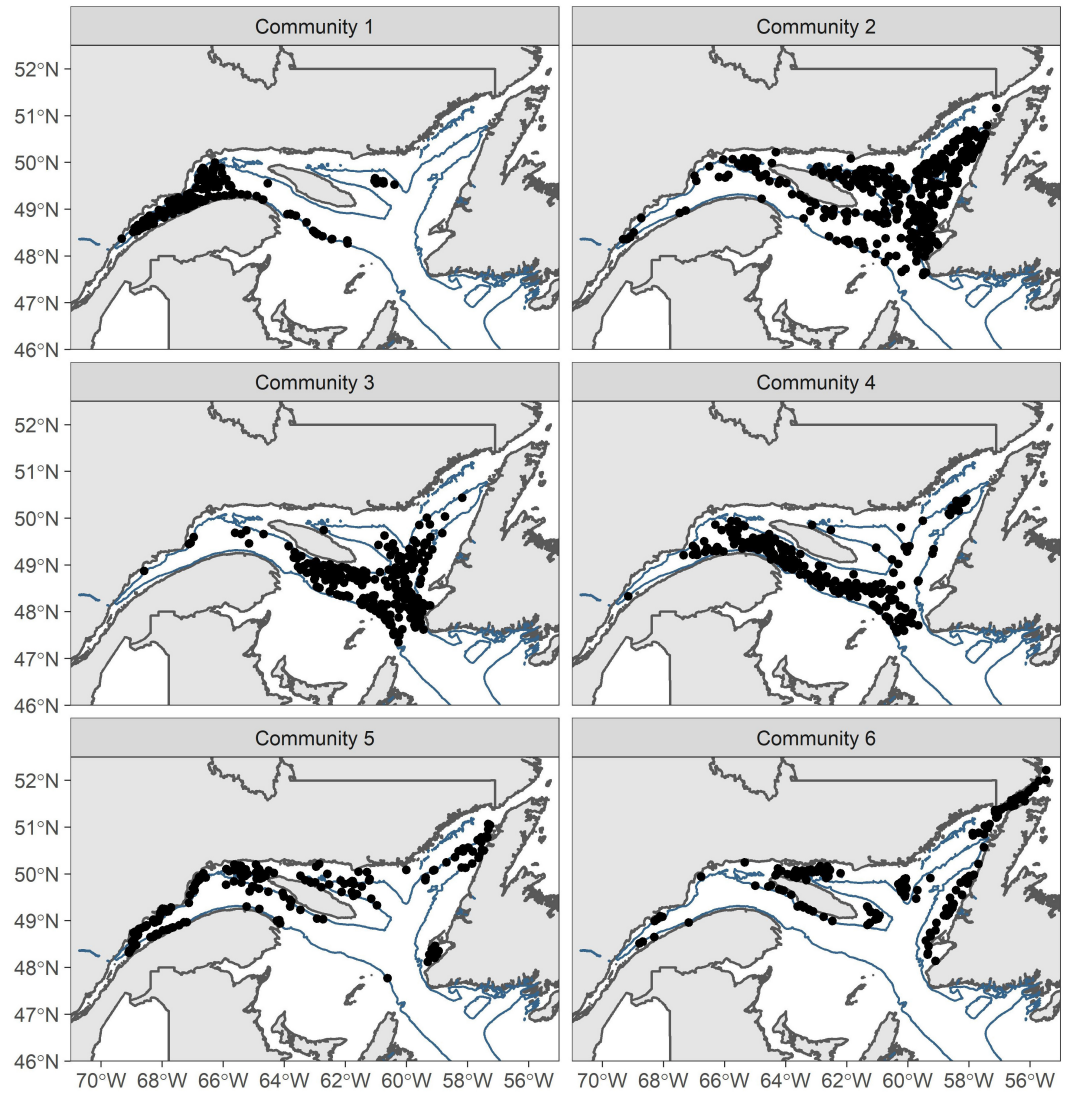

FIGURE 2 | Location of the six epibenthic community types in the Estuary and Gulf of St. Lawrence identified by hierarchical cluster analysis with biomass data collected from 2011 to 2018. Deep channels are shown in blue (depth > 200 m).

TABLE 1 | Summary statistics for six epibenthic community types identified in the estuary and Gulf of St. Lawrence.

Community	N	Total taxa richness	Mean taxa richness per site	Dominant taxa	Biomass ($kg.km^{-2}$)
1	**155**	**80**	**16**	*Actinostola callosa*	1088.04
				Brisaster fragilis	415.89
				Ctenodiscus crispatus	240.68
				Chionoecetes opilio	153.05
				Actinauge cristata	116.14
				Ophiura spp.	61.60
2	**361**	**103**	**11**	*Ctenodiscus crispatus*	25.45
				Ophiura spp.	10.32
				Actinostola callosa	10.15
				Brisaster fragilis	8.29
				Hippasterias phrygiana	6.35
				Chionoecetes opilio	6.34
3	**234**	**92**	**11**	*Lithodes maja*	45.36
				Bolocera tuediae	11.68
				Anthoptilum grandiflorum	9.01
				Actinostola callosa	6.53
				Brisaster fragilis	4.62
				Halipteris finmarchica	4.58
4	**214**	**81**	**13**	*Pennatula grandis*	152.09
				Brisaster fragilis	107.13
				Anthoptilum grandiflorum	100.42
				Bolocera tuediae	73.51
				Lithodes maja	34.95
				Actinostola callosa	27.62
5	**182**	**97**	**11**	*Chionoecetes opilio*	312.03
				Actinostola callosa	17.64
				Ctenodiscus crispatus	16.51
				Strongylocentrotus sp.	11.76
				Gorgonocephalus sp.	8.81
				Ophiura spp.	6.36
6	**168**	**97**	**17**	*Gorgonocephalus* sp.	133.79
				Strongylocentrotus sp.	51.86
				Boltenia ovifera	20.37
				Hyas coarctatus	8.76
				Chionoecetes opilio	7.58
				Crossater papposus	4.72

Data includes identification and biomass of the top six dominant taxa and the total and mean number of taxa in each community type. N refers to the number of sampling sites within each community.

total taxa recorded but among the least diverse in terms of the mean number of taxa found at a single site.

The third community type was also found in deep waters but mainly near the outlets of the three channels. Dominant taxa differed from those of communities 1 and 2 with Norway king crab *Lithodes maja*, the anemone *Bolocera tuediae*, and the sea pen *Anthoptilum grandiflorum* with the highest biomass. *B. tuediae* and *A. callosa* were also dominant taxa present with a similar biomass as that of community 2.

The fourth community type was found almost exclusively in the Laurentian Channel. This community was dominated by a high biomass of the sea pens *Pennatula grandis* and *A. grandiflorum*. Some sites also contained a high biomass of *B. fragilis*.

The fifth community type was mainly located on the edges of the channels. Dominant taxa were similar to community 1 with *C. opilio*, *A. callosa*, and *C. crispatus* being top 3. However, this community also contained high biomasses of sea urchins *Strongylocentrotus* sp. and brittle stars *Gorgonocephalus* sp. that are considered more coastal taxa. Together with community 6, this community ranked second, with a total of 97 taxa.

The sixth community type was scattered throughout the EGSL in sites near the coast. It was dominated by high biomass of *Gorgonocephalus* sp. and *Strongylocentrotus* sp. Other dominant taxa included the sea potato *Boltenia ovifera*, the crab *Hyas coarctatus*, and the sea star *Crossaster papposus*. All these taxa were considered mainly coastal, which suggests that community 6 may represent a coastal community. It was also the most diverse community in terms of the mean number of taxa recorded at each site.

Environmental Clustering

Six environmental clusters were identified as characterized by distinct sets of environmental conditions, using k-means cluster analysis (**Figure 3** and **Table 2**). Habitats 1 and 2 were spatially segregated in deep-water EGSL channels. Habitat 1, restricted to the Laurentian Channel, was characterized by low oxygen concentration and warm water. Habitat 2 bypassed habitat 1 on its edges in the Gulf portion of the EGSL and includes the head of the Laurentian Channel in the estuary and the Anticosti and Esquiman channels in the northern Gulf. Habitat 2 displayed similar conditions to Habitat 1 but with lower oxygen concentrations and a high aragonite index (Acidification). Habitat 3 was concentrated along the slopes of the deep-water channels and had variable temperature, although generally characterized by warm waters and intermediate depths (around 100 m), salinity, and oxygen concentrations. Habitats 4 was characterized by high levels of fisheries activities—especially DNH. In addition to fisheries activities, this habitat was also characterized by heterogeneous environmental conditions. Habitat 5 was concentrated along the coastline, especially in the Gulf, and was characterized by very well-oxygenated water with a mean depth of 92 m; it was thus located either in the surface or intermediate cold layers, as evidenced by temperatures reaching below 0°C in this habitat. Habitat 6 was not characterized by any clearly evident environmental regime.

Detection of Thresholds

Depth, salinity, oxygen, and positive temperature anomalies (posAnom), were the best predictors of taxa assemblages (**Figure 4**). Fisheries predictors (DD and DNH) had very low overall importance. The splits density and the taxa cumulative importance plots (**Figure 5**) showed where the compositional change occurs along predictors ranges and their respective importance (Ellis et al., 2012). The most important predictor was depth. Four important splits were detected for depth from 50 to 100 m, 325 to 350 m, 400 to 425 m, and the strongest from 450 to 525 m, although

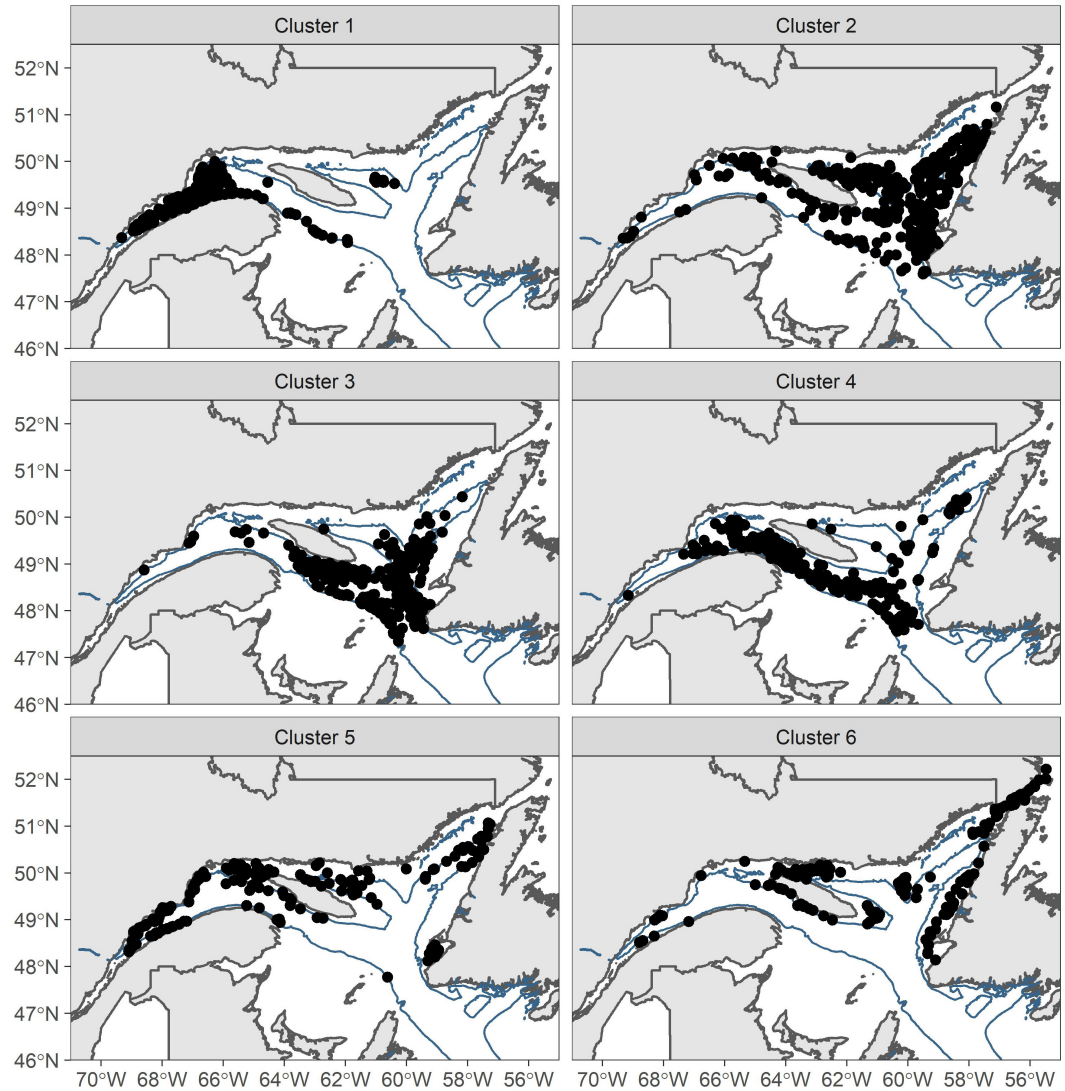

FIGURE 3 | Location of the six habitats in the Estuary and Gulf of St. Lawrence identified by k-means clustering with environmental data ranging from 2011 to 2018. Deep channels are shown in blue (depth > 200 m).

TABLE 2 | Summary of environmental clusters environmental values (mean ± SD).

	Cluster 1	Cluster 2	Cluster 3	Cluster 4	Cluster 5	Cluster 6
Temperature (°C)	5.79 ± 0.29	2.61 ± 1.27	5.58 ± 0.67	4.10 ± 1.14	0.95 ± 1.03	5.80 ± 0.51
Oxygen (μmol L^{-1})	142.4 ± 21.7	204.9 ± 63.8	92.9 ± 18.6	160.5 ± 41.6	300.9 ± 34.7	98.9 ± 26.7
Salinity	34.86 ± 0.07	33.05 ± 0.77	34.4 ± 0.26	33.79 ± 0.41	32.37 ± 0.40	34.56 ± 0.20
Depth (m)	395 ± 52	131 ± 50	253 ± 37	177 ± 34	92 ± 26	282 ± 40
Acidification	0.44 ± 0.06	0.49 ± 0.06	0.57 ± 0.04	0.48 ± 0.05	0.39 ± 0.07	0.59 ± 0.05
DD	20 ± 56	221 ± 756	3, 273 ± 1, 299	93 ± 251	35 ± 177	170 ± 265
DNH	5 ± 72	2, 262 ± 206	23 ± 117	70 ± 192	61 ± 178	3 ± 25
posAnom	3.67 ± 0.48	1.58 ± 0.42	2.27 ± 0.46	1.64 ± 0.40	0.88 ± 0.53	2.47 ± 0.53

sample size was small for this latter split (**Figure 5A**). This last split was caused by relatively few taxa reacting strongly to this depth change; it also showed that many taxa have a threshold reaction between 50 and 100 m, but that the response was relatively weak for all taxa (**Figure 5B**). Splits around 325–350 m and 400–425 m seemed to indicate a continuous split with a high concentration of taxa thresholds between 300 and 400 m.

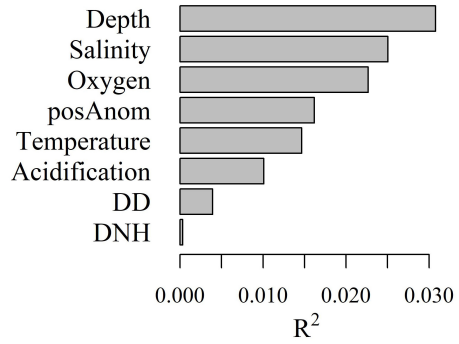

FIGURE 4 | Overall importance, R^2_p, of each predictor p included in the gradient forest analysis.

Salinity was the second most important predictor. Multiple successive splits were observed (**Figure 5A**). The first three splits had similar strength and represented little of the data and are observed between 31 and 33. No clear distinction between these three splits was observed; rather, few taxa react strongly to variable salinities within this range. Two further splits were observed around 34.3 and 35. They represented much of the data and were stronger than the first set of three splits. Indeed, most of the taxa had their threshold between these values and exhibited strong responses to variations in salinity (**Figure 5B**).

Oxygen was the third most important predictor and displayed three splits (**Figure 5A**). A major split occurred around 50–100 μmol O_2 L^{-1}. This strong threshold was caused by the response of approximately ten taxa, including *A. callosa*, *A. cristata*, *C. crispatus*, *Aphroditella hastata*, *Buccinum* sp., *B. fragilis*, and *C. opilio* (**Figure 5B**). Three much smaller splits occurred at higher oxygen concentrations: one around 175–200 μmol O_2 L^{-1} and three successive ones between 250 and 375 μmol O_2 L^{-1}. Many taxa had thresholds at these ranges of oxygen concentration although the strength of the thresholds was much lower than for taxa at the 50–100 μmol O_2 L^{-1} split (**Figure 5B**).

Positive temperature anomalies were also an important predictor. The density plot showed multiple successive strong splits. The first one was observed around −1 to 0°C but represents little of the total data. Two thresholds occur between 1.5 and 2.5°C. and around 4°C. The taxa cumulative importance plot showed that all splits seemed to be caused by the strong reaction of a few taxa. The strength of the response varied between taxa but was generally weak.

Taxa Reactions to Oxygen Thresholds

There was an important increase in the biomass of 8 taxa at and below the first oxygen threshold (50–100 μmol O_2 L^{-1}) as indicated by partial dependence plots (**Figure 6**): *A. callosa* (% variance explained by the model: 58.15%), *A. cristata* (35.33%), *C. crispatus* (36.25%), *A. hastata* (26.03%), *Buccinum* sp. (23.06%), *B. fragilis* (41.65%), *C. opilio* (21.72%), and *Ophiura* spp. (12.88%). All taxa at this threshold displayed low biomass at higher oxygen concentrations but it increased drastically when oxygen concentration approaches the hypoxic condition threshold of 62.5 μmol O_2 L^{-1} (Gilbert et al., 2005). In contrast, the biomass of several other species showed the opposite pattern as O_2 levels approach 125–150 and 275–325 μmol O_2 L^{-1} increasing as oxygen levels increase. The taxa *P. andromeda* (25.01%), *M. curvirostra* (32.86%), *Flabellum alabastrum* (25.07%), *Ciliatocardium ciliatum* (14.18%), *H. coarctatus* (27.02%), Porifera (25.10%), *Rhachotropis aculeata* (10.54%), and *Strongylocentrotus* sp. (21.44%) were absent at low oxygen concentration but increased in biomass as oxygen concentration increases (**Figure 7**). The oxygen concentrations at which biomass begins to increase varied among taxa, ranging from 125 to 325 μmol O_2 L^{-1}.

Indicator Taxa

There is no established threshold for what indicator values should be for a given taxon to be considered a good indicator of a community. In this study, we selected taxa with indicator values of 0.50 or greater, considering values below this as weak. Taxa selected as potential indicators (**Table 3**) for community 1 were the anemones *A. cristata* and *A. callosa*, the sea star *C. crispatus*, the sea urchin *B. fragilis*, and the brittle star *Ophiura* spp. No taxa met the 0.50 threshold for communities 2 and 3, whereas a single taxon was identified for community 4: the sea pen *A. grandiflorum*. For community 5, the crab *C. opilio* was the only taxa that met the 0.5 threshold. For community 6, 5 taxa were selected as potential indicators: *Strongylocentrotus* sp., *H. coarctatus*, *C. papposus*, *O. aculeata*, and *Gorgonocephalus* sp. The four following taxa were selected by the analysis as indicator species and display strong reactions to hypoxic conditions: *A. cristata*, *A. callosa*, *C. crispatus*, and *B. fragilis*. They were thus retained as indicator taxa of benthic conditions for EGSL epibenthic communities potentially exposed to hypoxia.

DISCUSSION

The great heterogeneity of oceanographic and geological conditions in the EGSL creates diverse habitats that are favorable to diverse benthic communities. This study identified distinct communities that seem to be in some way structured by their environment. Depth, salinity, oxygen, and positive temperature anomalies were the main predictors of community composition and distribution. A strong threshold influencing community structure was observed around 50–100 μmol O_2 L^{-1}, which corresponds to a hypoxic condition threshold (Gilbert et al., 2005). A great biomass of opportunistic taxa with fast growth and high reproductive rates was observed below this threshold; sensitive taxa, meanwhile, were largely absent in those conditions and became abundant only when oxygen concentration increased to greater levels. Temperature and oxygen levels in the ESGL are predicted to increase and decrease, respectively, in the future, which may impact EGSL benthic communities if the hypoxic threshold is reached (Lavoie et al., 2019). *Actinostola callosa*, *Actinauge cristata*, *Ctenodiscus crispatus*, and *Brisaster fragilis* were identified as indicator taxa because their relationship with hypoxia conditions reflects the

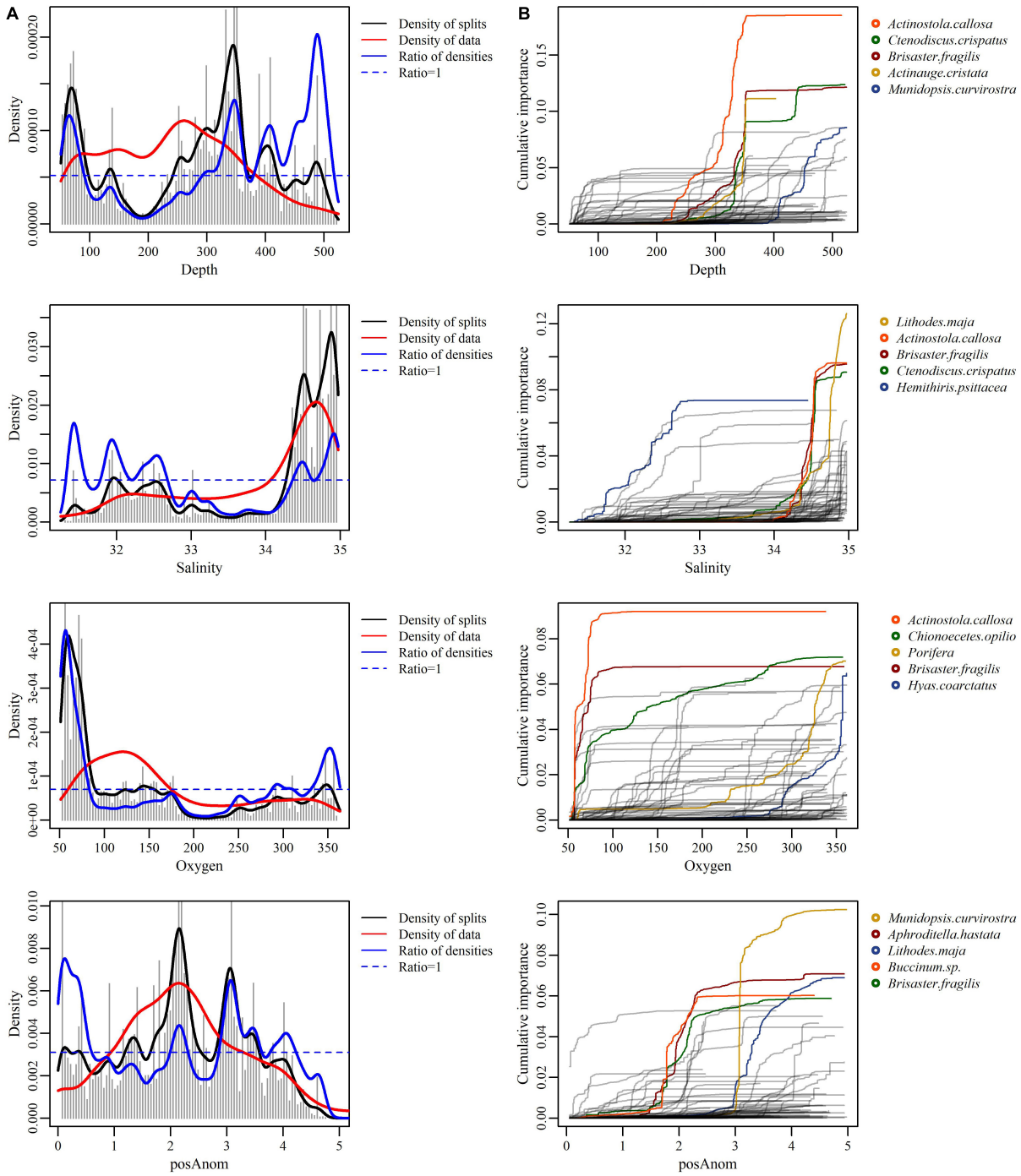

FIGURE 5 | Splits density **(A)** and cumulative distributions of the standardized splits importance **(B)** for each taxon scaled by R^2 of the four most important predictors of the distribution of epibenthic taxa in the estuary and Gulf of St. Lawrence. **(A)** Each curve represents an individual taxon (number of taxa = 104). Only the 5 species the most responsive to each predictor are displayed in color. **(B)** Density plots contain four components: gray vertical bars represent the binned raw importance of a predictor, the black line shows the density of splits estimated by kernel density, the red line indicates the density of actual predictor values (Beazley et al., 2015). The blue line is a combination of these two last components—the expected density of splits if the predictor had been sampled in uniform density, calculated as the density of splits standardized by the density of predictor values (i.e., the black line standardized by the red line) (Beazley et al., 2015).

response of the whole community. Detection of these thresholds and the identification of indicator taxa are essential to help monitor important changes in community composition; one that could lead to important structural changes in the ecosystem, since other taxa may be affected by these pressures as their habitat is modified.

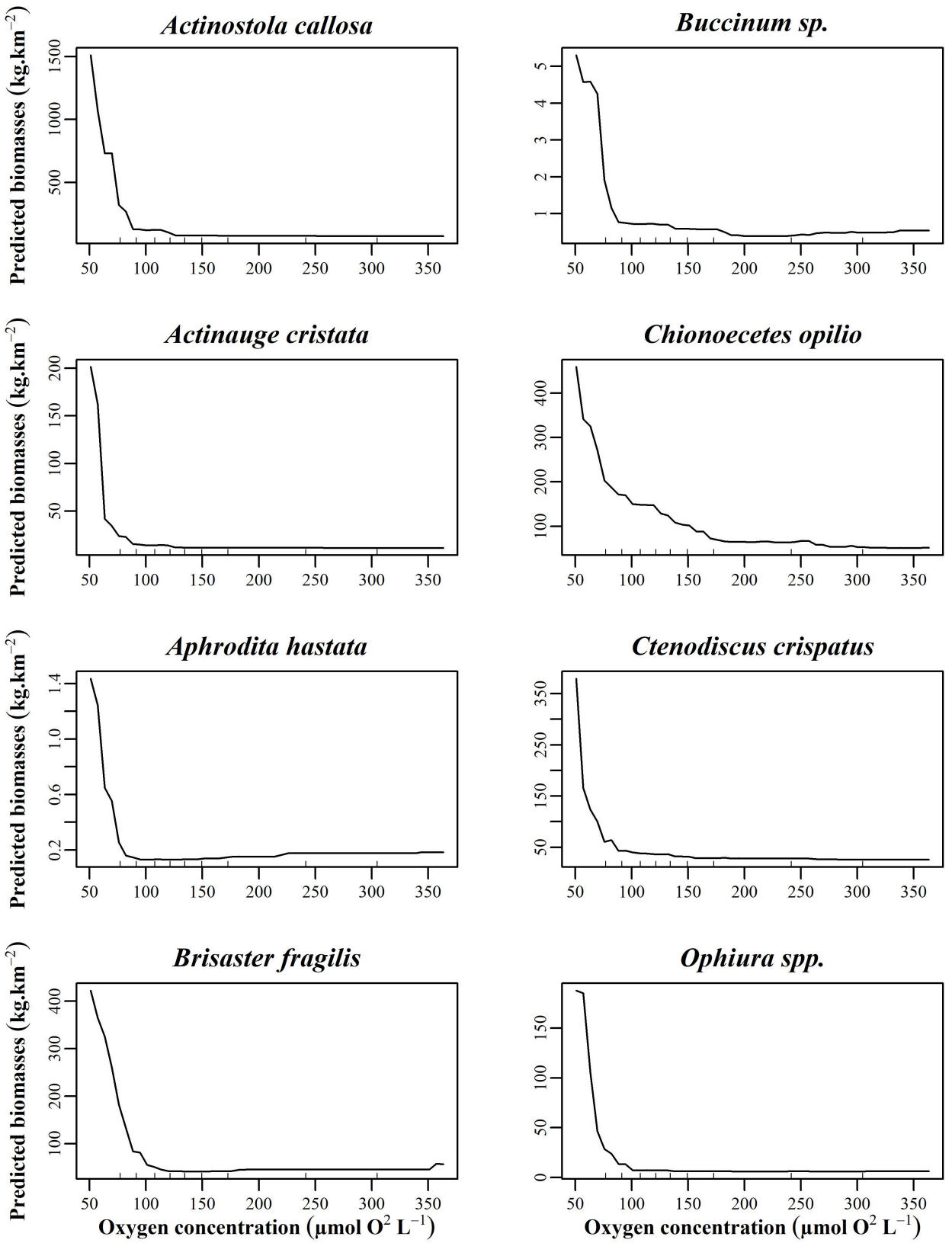

FIGURE 6 | Partial dependence plots of the top eight taxa with the highest R^2 at the 50–100 µmol O_2 L^{-1} threshold build from the random forest biomass regressions of taxa for oxygen.

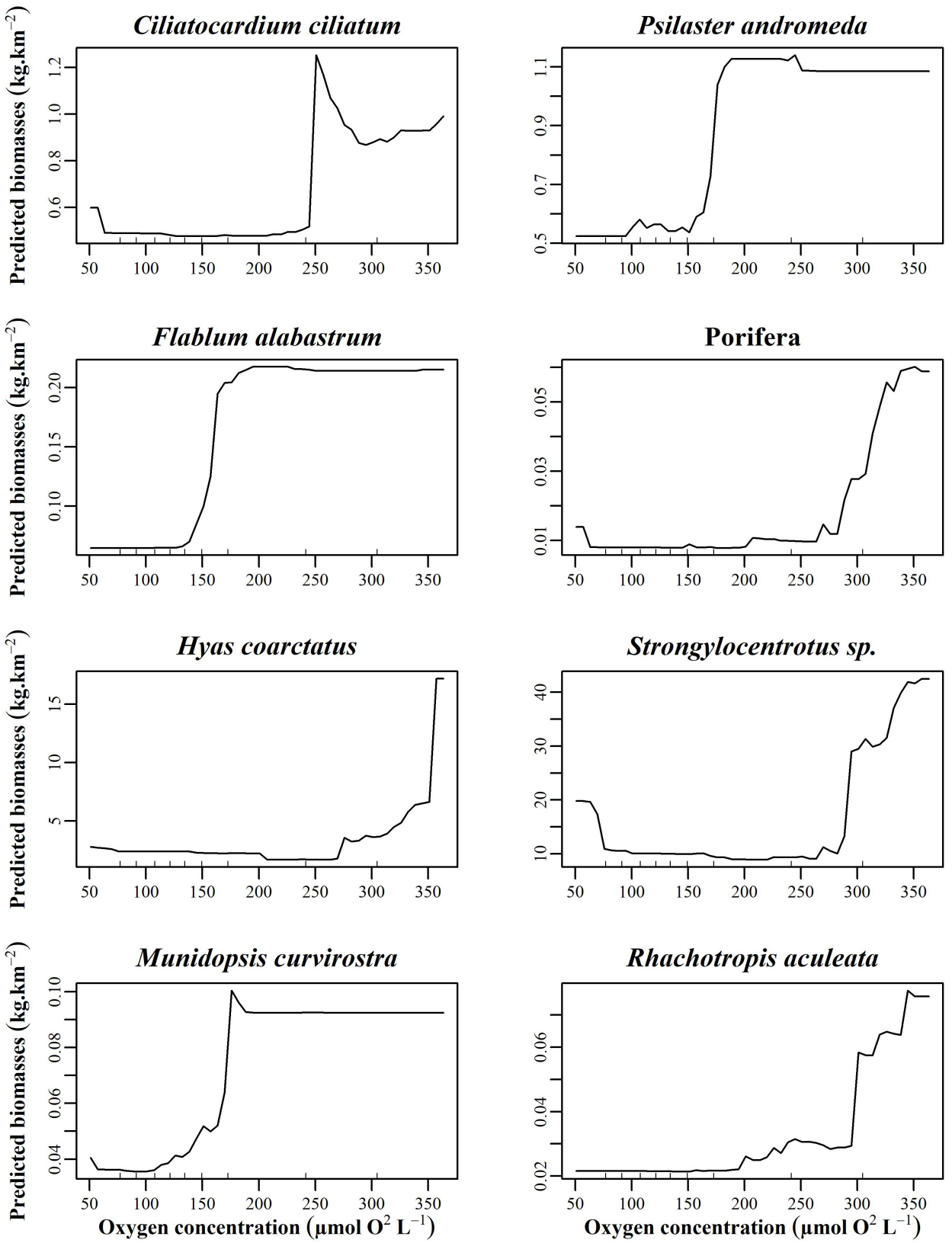

FIGURE 7 | Partial dependence plots of the top eight taxa with the highest R^2 from oxygen concentrations of 175–300 µmol O_2 L^{-1} thresholds build from the random forest biomass regressions of taxa for oxygen.

TABLE 3 | Indicative values of taxa with indicator values > 0.5, for each community.

Taxon	Community type	Indicator value
Actinostola callosa	1	0.95
Actinauge cristata	1	0.87
Ctenodiscus crispatus	1	0.78
Brisaster fragilis	1	0.74
Ophiura spp.	1	0.53
Anthoptilum grandiflorum	4	0.53
Chionoecetes opilio	5	0.64
Strongylocentrotus sp.	6	0.73
Hyas coarctatus	6	0.71
Crossaster papposus	6	0.66
Ophiopholis aculeata	6	0.64
Gorgonocephalus sp.	6	0.58

Epibenthic Communities of the Estuary and the Gulf of St. Lawrence

Epibenthic communities of the EGSL are influenced by a variety of environmental conditions (Bourget et al., 2003; Lévesque et al., 2010; Moritz et al., 2013). Six distinct, partially spatially segregated, communities were identified in this study. Moritz et al. (2013) also identified six distinct epibenthic communities in the EGSL based on the results of trawl surveys from 2006 to 2009 using approaches similar to those in the present study. Site groupings were quite similar to those observed in the present study with a clear distinction between deep-water and shallow-water assemblages and the estuary being identified as a unique community in both analyses. In contrast to Moritz et al. (2013), who included the highly dominant shrimp *Pandalus borealis* with specific environmental requirements in the analysis (Ouellet et al., 2007), the present study did not include shrimp, likely, explaining in part differences between the two studies.

The present study defines six distinct habitats using eight predictors. Epibenthic communities identified in the EGSL did not fully match these potential habitats. The grouping reveals distinct communities in the Laurentian Channel relative to those in the Esquiman and Anticosti channels, even though they are all classified as being from the same habitat type. The heads of all EGSL deep-water channels are characterized by low oxygen concentrations, with the Laurentian Channel being the lowest. Deep waters in the EGSL are isolated from the atmosphere by a permanent pycnocline which prevents the renewal of oxygen as it travels from Cabot Strait to the heads of the channels (Petrie et al., 1996). Since the Laurentian Channel is the longest of the three, water residence time is longer, resulting in lower oxygen levels in the estuary. This could indicate that a threshold for the community to react to low oxygen concentration exists between the heads of the three channels. Oxygen concentrations at the head of the Esquiman and Anticosti channels are low but still above the hypoxia threshold (Gilbert et al., 2007; Thibodeau et al., 2013). Taxa may not yet have reacted to decreased oxygen concentrations but may if levels continue to decrease, perhaps becoming similar to community 1. Another explanation could be the human-induced hypoxic condition at the head of the Laurentian Channel. This is due, in part, to high anthropogenic inputs of organic matter resulting in high decomposition rates. Both these factors may influence the benthic community differently than low oxygen concentration alone. It remains poorly known if anthropogenic-induced hypoxia will affect fauna differently than natural hypoxia alone as they often co-occur (Levin et al., 2009). Future monitoring of benthic communities at the head of the Anticosti and Esquiman channels may indicate if these two sources of hypoxia induce similar or distinct changes in epibenthic community composition.

The Gulf of St. Lawrence is characterized by multiple habitats. No distinct communities are present in habitats with high fishing activities. This agrees with Moritz et al. (2015) who found that there was no longer a detectable effect of trawling on EGSL epibenthic communities. They suggested that the recurring passage of fishing gear may have irreversibly damaged epibenthic communities by removing taxa that are sensitive to physical disturbances, thus switching communities to an alternate equilibrium state such that trawling activities no longer have detectable impacts.

Predictor Importance

Four variables seem to be the main predictors of epibenthic assemblage distributions in the EGSL: depth, salinity, oxygen, and to a lesser extent, positive temperature anomalies. These predictors were also identified as being important in past EGSL epibenthic studies (Bourget et al., 2003; Moritz et al., 2013). Habitat suitability models based on 2006–2009 DFO trawl survey data suggested that depth and temperature were the most important variables affecting epibenthic community structure (Lévesque et al., 2010). In contrast, DNH and DD fisheries, and aragonite were identified as weak predictors of EGSL epifaunal assemblage structure.

Collinearity Between Predictors

The most important predictor was depth. Although depth zonation has been observed in multiple studies worldwide, it is difficult to determine which related factor causes this. Strong variation in taxonomic composition due to depth is one of the most difficult problems for ecologists to solve (Gage and Tyler, 1991). Depth correlates with many variables, including primary production, nutrient levels, temperature, oxygen, and salinity, making effects due to depth *per se* difficult to interpret. Thus, the observed zonation is often attributed to variables and their interactions other than depth *per se* (Carney, 2005). In the EGSL, depth is tightly linked with water masses that display a strong coupling between salinity and temperature (Saucier et al., 2003; Blais et al., 2019), the second and fourth most important predictors, respectively. Indeed, the compositional change threshold observed around 50–100 m corresponds roughly to the transition between the surface and the cold intermediate water layers, where many environmental conditions change (Saucier et al., 2003; Galbraith, 2006). Thus, the strong response of EGSL benthic communities to depth could indicate the influence of multiple predictors. Some authors suggest

removing predictors that are strongly correlated from analyses while others prefer to keep all predictors under the assumption that most predictors are in some way correlated and it is unknown which are actually linked to the response evaluated (Murray and Conner, 2009; Ellis et al., 2012). Comparison of taxonomic assemblage thresholds shows that some taxa shift at co-occurring salinity, temperature, and depth thresholds, underlying the difficulty to discriminate between the effects of salinity and temperature from depth on epibenthic assemblages. For example, the depth threshold of *A. callosa* (highest curve in red in **Figure 5**) is located around 350 m, which corresponds to a temperature of 5.5°C and salinity of 34.5. The cumulative importance plots show that the temperature and salinity thresholds for *A. callosa* are located exactly at these values.

Disentangling the individual effects of these correlated predictors on community assemblages is thus difficult. Salinity is known to affect the distribution of benthic taxa in coastal and estuarine ecosystems where strong salinity gradients are found (Dauer et al., 1987; Dauer, 1993; Zettler et al., 2007; Bleich et al., 2011). However, salinity gradients in the EGSL vary between 31 and 35 and are restricted to the euhaline zone of salinity class boundaries (Venice System., 1958). Temperature is also known to have an important influence on benthic community structure (Schiel et al., 2004). Temperature thresholds, however, are not very strong and taxa responses are dispersed along the temperature gradient resulting in multiple small thresholds. Indeed, temperature requirements vary greatly among taxa, depending on physiological and competitive adaptations (Hale et al., 2011).

Thresholds and Indicators for Hypoxia

As observed in previous EGSL studies, oxygen concentration has an important impact on community structure and has often been hypothesized as a key pressure on benthic community structure and function (Rosenberg et al., 2001; Levin, 2003; Lévesque, 2009; Belley et al., 2010; Moritz et al., 2013). Decreased oxygen concentrations and hypoxia may affect entire ecosystems and biogeochemical cycles (Rabalais et al., 2010). It may cause some taxa to avoid areas or face high mortality, which may reduce taxonomic richness and alter community structure and function (Diaz and Rosenberg, 1995, 2008; Wu, 2002; Levin et al., 2009). Low oxygen and hypoxic waters occur naturally in many marine environments but have recently been exacerbated by human activities, resulting in historically high numbers of hypoxic areas (Diaz and Rosenberg, 1995, 2008; Helly and Levin, 2004; Vaquer-Sunyer and Duarte, 2008; Gooday et al., 2009).

Oxygen thresholds observed for benthic communities in the EGSL display two taxa-specific reaction patterns. The first threshold shows taxa biomass increasing substantially below 100 μmol O_2 L^{-1}. Conversely, two other thresholds show very low taxa biomass at oxygen concentrations below 100 μmol O_2 L^{-1} and then increasing biomass as oxygen concentration increases, starting at around 125 μmol O_2 L^{-1}. Alteration of taxa biomass has been observed by Dauer (1993) where "sensitive" and equilibrium taxa add low biomass in hypoxic areas while opportunistic taxa displayed higher dominance of the community composition. Multiple studies have shown that opportunistic taxa often dominate under hypoxic conditions, with taxa-specific responses based on their tolerances (Dauer et al., 1992; Rosenberg et al., 2001; Levin et al., 2009). Taxa exhibit very different responses to hypoxic stress depending on their tolerance and physical requirement (Vaquer-Sunyer and Duarte, 2008). Taxa tolerant to hypoxic conditions may have developed adaptive strategies that allow them to rapidly colonize disturbed areas vacated by sensitive species through high recruitment (Dauer, 1993). Less hypoxia-tolerant taxa, found at the 175–200 and 275–375 μmol O_2 L^{-1} oxygen thresholds, need higher oxygen concentrations to survive and will leave or die if oxygen levels decrease to a point that no longer supports reproduction and survival (Diaz and Rosenberg, 1995; Wu, 2002).

Opportunistic taxa generally display high larval availability, rapid growth, small body sizes, and short generation times that allow them to quickly recolonize disturbed areas (Levinton, 1970; Wu, 2002). As physiological generalists, opportunistic taxa can generally live under a wide range of oxygen concentrations (Levinton, 1970). Opportunistic taxa identified in the present study display a variety of characteristics that make them well suited to hypoxic environments. *Ophiura* spp. and *C. crispatus* are both tolerant to hypoxia (Shick, 1976; Vistisen and Vismann, 1997). Indeed, *C. crispatus* is one of the most tolerant echinoderms to low oxygen concentrations (Shick, 1976). *Ophiura* spp. has previously been observed in high abundance in hypoxic areas of the EGSL (Belley et al., 2010). Further, high abundances of *Ophiura* spp. were linked to eutrophic conditions in European sea areas (Diaz and Rosenberg, 1995). Molluscs and cnidarians are known to be particularly tolerant to decreased oxygen concentrations, perhaps explaining the high abundance of the gastropods *Buccinum* sp. and the sea anemones *A. callosa* and *A. cristata* in the estuary (Vaquer-Sunyer and Duarte, 2008). Belley et al. (2010) only found *Actinauge* sp. at hypoxic sites. Acclimation to hypoxia has been observed for *Buccinum* sp., which increases oxygen-carrying capacity when environmental oxygen concentrations decrease (Brix et al., 1979). Feeding ecology also plays a major role in hypoxic areas, where dominance by deposit-feeders over suspension-feeders is often observed (Wu, 2002; Levin et al., 2009). This dominance was associated with increased food supplies (organic matter) for deposit-feeders caused by organic enrichment-induced hypoxia (Levin, 2003). Indeed, the deposit feeders *C. crispatus* and *B. fragilis* were among the most abundant taxa found in hypoxic areas.

Notwithstanding the clear effects of depth and salinity, EGSL epibenthic communities are clearly impacted by hypoxic conditions. Indicator taxa analysis identified four taxa that are representative of this community that may be potential indicators of hypoxic conditions and gross community changes: *A. callosa*, *A. cristata*, *C. crispatus*, and *B. fragilis*. High densities of these species are observed in the EGSL estuary, which is known for its persistent hypoxic conditions that result from a mix of climate-induced and anthropogenic decreased oxygen concentrations over the last 60 years (Gilbert et al., 2005, 2007). However, the co-occurrence of many pressures in this region of the EGSL may have caused cumulative changes that were not detected by threshold analysis as combinations of

pressures may not account for cumulative changes (Large et al., 2015). Multiple pressures are inclined to combine and push the ecosystem toward the threshold (Foley et al., 2015). Benthic communities may have reacted to a combination of multiple pressures such as increased organic matter, acidification, and hypoxia. Data on organic matter were not available and thus not included in the models, preventing us from evaluating the importance of this pressure on benthic communities. However, it is probably an important predictor of benthic assemblage, as demonstrated by Pearson and Rosenberg (1978). Although aragonite was not identified as an important predictor, values available from *eDrivers* were derived from a single year of data and therefore the interpolation was made from a much more limited coverage of the EGSL than for the other predictors; perhaps explaining its weak ability to predict benthic community assemblages. The indicator taxa selected could reflect not only the impact of hypoxia but more generally the complex impacts of eutrophication of deep waters (Thibodeau et al., 2006). Indicators may provide more information than environmental variables in these cases as the case is too complex to be captured by models. Ecological indicators are generally stronger when multiple taxa that exhibit different life histories are considered, instead of focusing on a single taxon, to be as representative as possible of the whole community (Karr, 1991; Kremen, 1994; Carignan and Villard, 2002). They also provide a cost- and time-effective way to assess the ecological condition of communities facing environmental pressures that would otherwise be too complex to measure directly (Kreisel, 1984; Davis, 1989; di Castri et al., 1992; Hilty and Merenlender, 2000).

CONCLUSION

Our analyses detected an important oxygen threshold link with hypoxia for EGSL epibenthic communities. Hypoxic conditions in the estuary were correlated with a major shift in epibenthic community composition that was clearly visible in the clustering analysis. The estuary seems largely dominated by a high biomass of fast colonizers, quick-growing, small-sized opportunistic taxa. However, multiple pressures overlap in the estuary and it remains difficult to differentiate the individual impact of single pressure since interaction patterns are unknown. Indeed, this threshold is most probably caused by hypoxic conditions and more broadly by pressures related to eutrophication, such as acidification and increased organic loading. This study also fills a major gap in the conservation of benthic communities in the EGSL, namely the absence of indicators to monitor the condition of epibenthic communities. Four taxa, *Actinostola callosa*, *Actinauge cristata*, *Ctenodiscus crispatus*, and *Brisaster fragilis* were identified as good indicators to detect the major threshold in community composition observed in the gradient forest analysis. Indicator species act as sentinels of the state of a community by reducing the complexity of the system under study (Borja et al., 2000). These indicators will allow spatial and temporal monitoring of EGSL epibenthic communities and could be used as part of research, evaluation, or monitoring program to make conservation and preservation decisions. This study is a first step toward obtaining indicators to establish the condition of epibenthic communities in the EGSL. Further development of more complex indicators combining the abundance of several species in a formula would be interesting to ultimately create a chart of the state of benthic communities based on the results obtained for these indicators. As models predict that temperatures of EGSL deep-waters will continue to rise and lead to decreased oxygen concentrations in the near future, indicators will be essential to make informed management decisions and environmental policies to protect the integrity of EGSL epibenthic communities.

DATA AVAILABILITY STATEMENT

Publicly available datasets were analyzed in this study. This data can be found here: https://obis.org/dataset/ce3c5c7d-daa0-42ed-9cdb-7100b1274b55.

AUTHOR CONTRIBUTIONS

PA and CM developed this project for the "Canadian Healthy Ocean Network (CHONe)," a strategic research program funded by NSERC. The sampling campaigns were managed by the Fisheries and Oceans Canada (DFO), Quebec region, onboard the research vessel CCGS Teleost. This mission has taken place every year in August since 2004. LI participated in missions in 2017 and 2018, as a master student. DB contributed to the acquisition of data of environmental variables. All authors contributed to data, analyses, and writing based on their respective expertise and contributed to the revision of the manuscript.

FUNDING

This research was sponsored by the Natural Sciences and Engineering Research Council of Canada attributed to the Canadian Healthy Oceans Network and its Partners: Fisheries and Oceans Canada and INREST (representing the Port of Sept-Îles and City of Sept-Îles). Québec-Océan also provided financial support for workshops, conferences, and research activities.

ACKNOWLEDGMENTS

We thank all the crew members of the CCGS Teleost from Newfoundland and Institut Maurice-Lamontagne for sampling campaigns. We also thank Denis Bernier from DFO Institut Maurice-Lamontagne who provided the data from the fishery surveys.

SUPPLEMENTARY MATERIAL

The Supplementary Material for this article can be found online at: https://www.frontiersin.org/articles/10.3389/fmars.2021.720710/full#supplementary-material

REFERENCES

Alexander, D. W., Sooley, D. R., Mullins, C. C., Chiasson, M. I., Cabana, A. M., Klvana, I., et al. (2010). *Gulf of St. Lawrence: Human Systems Overview Report. Oceans. Habitat and Species at Risk Publication Series, Newfoundland and Labrador Region*. Available online at: https://publications.gc.ca/site/eng/9.619705/publication.html (accessed February 9, 2020).

Aller, R. C. (1982). "The effects of macrobenthos on chemical properties of marine sediment and overlying water," in *Animal-Sediment Relations*, eds P. L. McCall and M. J. S. Tevesz (New York, NY: Plenum Press), 53–102. doi: 10.1007/978-1-4757-1317-6_2

Andersen, T., Carstensen, J., Hernandez-Garcia, E., and Duarte, C. M. (2009). Ecological thresholds and regime shifts: approaches to identification. *Trends Ecol. Evol.* 24, 49–57. doi: 10.1016/j.tree.2008.07.014

Baker, M. E., and King, R. S. (2010). A new method for detecting and interpreting biodiversity and ecological community thresholds. *Methods Ecol. Evol.* 1, 25–37. doi: 10.1111/j.2041-210X.2009.00007.x

Beauchesne, D., Daigle, R. M., Vissault, S., Gravel, D., Bastien, A., Belanger, S., et al. (2020). Characterizing exposure to and sharing knowledge of drivers of environmental change in the St. Lawrence system in Canada. *Front. Mar. Sci.* 7:383. doi: 10.3389/fmars.2020.00383

Beazley, L., Kenchington, E., Yashayaev, I., and Murillo, F. J. (2015). Drivers of epibenthic megafaunal composition in the sponge grounds of the Sackville Spur, northwest Atlantic. *Deep Sea Res. Part I Oceanogr. Res. Pap.* 98, 102–114. doi: 10.1016/j.dsr.2014.11.016

Belley, R., Archambault, P., Sundby, B., Gilbert, F., and Gagnon, J. M. (2010). Effects of hypoxia on benthic macrofauna and bioturbation in the Estuary and Gulf of St. Lawrence, Canada. *Cont. Shelf Res.* 30, 1302–1313. doi: 10.1016/j.csr.2010.04.010

Benoît, H. P., Gagné, J. A., Savenkoff, C., Ouellet, P., and Bourassa, M.-N. (2012). State of the Ocean Report for the Gulf of St. Lawrence Integrated Management (GOSLIM). *Can. Man. Rep. Fish. Aquat. Sci.* 2986, ix+73.

Bholowalia, P., and Kumar, A. (2014). EBK-Means: a clustering technique based on Elbow Method and K-Means in WSN. *Int. J. Comput. Appl.* 105, 17–24.

Blais, M., Galbraith, P. S., Plourde, S., Scarratt, M., Devine, L., and Lehoux, C. (2019). Chemical and biological oceanographic conditions in the estuary and Gulf of St. Lawrence during 2017. *Can. Tech. Rep. Fish. Aquat. Sci.* 2019/009, iv+56.

Bleich, S., Powilleit, M., Seifert, T., and Graf, G. (2011). β-diversity as a measure of species turnover along the salinity gradient in the Baltic Sea, and its consistency with the Venice System. *Mar. Ecol. Prog. Ser.* 436, 101–118. doi: 10.3354/meps09219

Borja, A., Franco, J., and Perez, V. (2000). A marine biotic index to establish the ecological quality of soft-bottom benthos within European estuarine and coastal environments. *Mar. Pollut. Bull.* 40, 1100–1114. doi: 10.1016/S0025-326X(00)00061-8

Bourdages, H., Brassard, C., Desgagnés, M., Galbraith, P., Gauthier, J., Nozères, C., et al. (2018). Preliminary results from the groundfish and shrimp multidisciplinary survey in August 2017 in the Estuary and northern Gulf of St. Lawrence. *DFO Can. Sci. Advis. Sec. Res. Doc.* 2018/036, iv+90.

Bourget, E., Ardisson, P. L., Lapointe, L., and Daigle, G. (2003). Environmental factors as predictors of epibenthic assemblage biomass in the St. Lawrence system. *Estuar. Coast. Shelf Sci.* 57, 641–652. doi: 10.1016/s0272-7714(02)00404-3

Bray, J. R., and Curtis, J. T. (1957). An ordination of the upland forest of Southern Wisconsin. *Ecol. Monogr.* 27, 326–349.

Breiman, L. (2001). Random forests. *Mach. Learn.* 45, 5–32. doi: 10.1023/A:1010933404324

Brenden, T. O., Wang, L. Z., and Su, Z. M. (2008). Quantitative identification of disturbance thresholds in support of aquatic resource management. *Environ. Manage.* 42, 821–832. doi: 10.1007/s00267-008-9150-2

Brix, O., Lykkeboe, G., and Johansen, K. (1979). Reversed bohr and root shifts in hemocyanin of the marine prosobranch, *Buccinum undatum*: adaptations to a periodically hypoxic habitat. *J. Comp. Physiol. A* 129, 97–103. doi: 10.1007/bf00798171

Buhl-Mortensen, L., Vanreusel, A., Gooday, A. J., Levin, L. A., Priede, I. G., Buhl-Mortensen, P., et al. (2010). Biological structures as a source of habitat heterogeneity and biodiversity on the deep ocean margins. *Mar. Ecol.* 31, 21–50. doi: 10.1111/j.1439-0485.2010.00359.x

Bundy, A., Lilly, G. R., and Shelton, P. A. (2000). A mass-balance model of the Newfoundland-Labrador Shelf. *Can. Tech. Rep. Fish. Aquat. Sci.* 2310, 14–157.

Carignan, V., and Villard, M. A. (2002). Selecting indicator species to monitor ecological integrity: a review. *Environ. Monit. Assess.* 78, 45–61. doi: 10.1023/a:1016136723584

Carney, R. S. (2005). Zonation of deep biota on continental margins. *Oceanogr Mar. Biol. Annu. Rev.* 43, 211–278. doi: 10.1201/9781420037449.ch6

Carrier-Belleau, C., Drolet, D., McKindsey, C. W., and Archambault, P. (2021). Environmental stressors, complex interactions and marine benthic communities' responses. *Sci. Rep.* 11:4194. doi: 10.1038/s41598-021-83533-1

Claret, M., Galbraith, E. D., Palter, J. B., Bianchi, D., Fennel, K., Gilbert, D., et al. (2018). Rapid coastal deoxygenation due to ocean circulation shift in the northwest Atlantic. *Nat. Clim. Change* 8, 868–872. doi: 10.1038/s41558-018-0263-1

Côté, I. M., Darling, E. S., and Brown, C. J. (2016). Interactions among ecosystem stressors and their importance in conservation. *Proc. R. Soc. Lond. Ser. B. Biol. Sci.* 283:20152592. doi: 10.1098/rspb.2015.2592

Crain, C. M., Kroeker, K., and Halpern, B. S. (2008). Interactive and cumulative effects of multiple human stressors in marine systems. *Ecol. Lett.* 11, 1304–1315. doi: 10.1111/j.1461-0248.2008.01253.x

Dauer, D. M. (1993). Biological criteria, environmental-health and estuarine macrobenthic community structure. *Mar. Pollut. Bull.* 26, 249–257. doi: 10.1016/0025-326x(93)90063-p

Dauer, D. M., Ewing, R. M., and Rodi, A. J. (1987). Macrobenthic distribution within the sediment along an estuarine salinity gradient - Benthic studies of the Lower Chesapeake Bay. *Int. Rev. Gesamten Hydrobiol.* 72, 529–538. doi: 10.1002/iroh.19870720502

Dauer, D. M., Rodi, A. J., and Ranasinghe, J. A. (1992). Effects of low dissolved-oxygen events on the macrobenthos of the Lower Chesapeake Bay. *Estuaries* 15, 384–391. doi: 10.2307/1352785

Davis, G. E. (1989). Design of a long-term ecological monitoring program for Channel Islands National Park, California. *Nat. Areas J.* 9, 80–89.

De Cáceres, M., Legendre, P., and Moretti, M. (2010). Improving indicator species analysis by combining groups of sites. *Oikos* 119, 1674–1684. doi: 10.1111/j.1600-0706.2010.18334.x

DFO (2002). *Shrimp of the Estuary and Gulf of St. Lawrence*. Mont-Joli, QC: Fisheries and Oceans Canada (DFO)

DFO (2016). *Zonal Interchange File Format (ZIFF) Data. A Compilation of Landing Data From Logbook Data Between 2010 and 2015*. Mont-Joli, QC: Fisheries and Oceans Canada (DFO).

di Castri, F., Vernhes, J. R., and Younés, T. (1992). Inventorying and monitoring biodiversity: a proposal for an international network. *Vegetatio* 103, 1–28.

Diaz, R. J., and Rosenberg, R. (1995). Marine benthic hypoxia: a review of its ecological effects and the behavioural responses of benthic macrofauna. *Oceanogr Mar. Biol. Annu. Rev.* 33, 245–303.

Diaz, R. J., and Rosenberg, R. (2008). Spreading dead zones and consequences for marine ecosystems. *Science* 321, 926–929. doi: 10.1126/science.1156401

Dufour, R., and Ouellet, P. (2007). Estuary and Gulf of St. Lawrence marine ecosystem overview and assessment report. *Can. Tech. Rep. Fish. Aquat. Sci.* 2744E, vii + 112.

Dufrêne, M., and Legendre, R. (1997). Species assemblages and indicator species: the need for a flexible asymmetrical approach. *Ecol. Monogr.* 67, 345–366. doi: 10.2307/2963459

Ellis, N., Smith, S. J., and Pitcher, C. R. (2012). Gradient forests: calculating importance gradients on physical predictors. *Ecology* 93, 156–168. doi: 10.1890/11-0252.1

El-Sabh, M. I., and Silverberg, N. (1990). *Oceanography of a Large-Scale Estuarine System. The St Lawrence*. New York, NY: Springer-Verlag.

Foley, M. M., Marton, R. G., Fox, M. D., Kappel, C. V., Mease, L. A., Erickson, A. L., et al. (2015). Using ecological thresholds to inform resource management: current options and future possibilities. *Front. Mar. Sci.* 2:95. doi: 10.3389/fmars.2015.00095

Gage, J. D., and Tyler, P. A. (1991). *Deep-Sea Biology: A Natural History of Organisms at the Deep-Sea Floor*. Cambridge: Cambridge University Press.

Gagnon, P. (1991). Optimisation des campagnes d'échantillonnage: les programmes REGROUPE et PARTS. *Rapp. Tech. Can. Sci. Halieut. Aquat.* 1818, 3–20.

Galbraith, P. S. (2006). Winter water masses in the Gulf of St. Lawrence. *J. Geophys. Res. Oceans* 111:C06022. doi: 10.1029/2005jc003159

Galbraith, P. S., Chassé, J., Caverhill, C., Nicot, P., Gilbert, D., Lefaivre, D., et al. (2019). Physical oceanographic conditions in the Gulf of St. Lawrence during 2018. *DFO Can. Sci. Advis. Sec. Res. Doc.* 2019/046, 4–79.

Galbraith, P. S., Chassé, J., Shaw, J.-L., Dumas, J., Caverhill, C., Lefaivre, D., et al. (2020). Physical oceanographic conditions in the Gulf of St. Lawrence during 2019. *DFO Can. Sci. Advis. Sec. Res. Doc.* 2020/030, 4–84.

Gilbert, D., Chabot, D., Archambault, P., Rondeau, B., and Hébert, S. (2007). Appauvrissement en oxygène dans les eaux profondes du Saint-Laurent marin: causes possibles et impacts écologiques. *Le Natur. Can.* 131, 67–75.

Gilbert, D., Sundby, B., Gobeil, C., Mucci, A., and Tremblay, G. H. (2005). A seventy-two-year record of diminishing deep-water oxygen in the St. Lawrence estuary: the northwest Atlantic connection. *Limnol. Oceanogr.* 50, 1654–1666. doi: 10.4319/lo.2005.50.5.1654

Gooday, A. J., Jorissen, F., Levin, L. A., Middelburg, J. J., Naqvi, S. W. A., Rabalais, N. N., et al. (2009). Historical records of coastal eutrophication-induced hypoxia. *Biogeosciences* 6, 1707–1745. doi: 10.5194/bg-6-1707-2009

Groffman, P., Baron, J., Blett, T., Gold, A., Goodman, I., Gunderson, L., et al. (2006). Ecological thresholds: the key to successful environmental management or an important concept with no practical application? *Ecosystems* 9, 1–13. doi: 10.1007/s10021-003-0142-z

Groom, M. J., Meffe, G. K., and Carroll, C. R. (1997). *Principles of Conservation Biology*. Sunderland, MA: Sinauer Associates.

Hale, R., Calosi, P., McNeill, L., Mieszkowska, N., and Widdicombe, S. (2011). Predicted levels of future ocean acidification and temperature rise could alter community structure and biodiversity in marine benthic communities. *Oikos* 120, 661–674. doi: 10.1111/j.1600-0706.2010.19469.x

Halpern, B. S., Frazier, M., Potapenko, J., Casey, K. S., Koenig, K., Longo, C., et al. (2015). Spatial and temporal changes in cumulative human impacts on the world's ocean. *Nat. Commun.* 6:7615. doi: 10.1038/ncomms8615

Halpern, B. S., Walbridge, S., Selkoe, K. A., Kappel, C. V., Micheli, F., D'Agrosa, C., et al. (2008). A global map of human impact on marine ecosystems. *Science* 319, 948–952. doi: 10.1126/science.1149345

Helly, J. J., and Levin, L. A. (2004). Global distribution of naturally occurring marine hypoxia on continental margins. *Deep Sea Res. Part I Oceanogr. Res. Pap.* 51, 1159–1168. doi: 10.1016/j.dsr.2004.03.009

Hilty, J., and Merenlender, A. (2000). Faunal indicator taxa selection for monitoring ecosystem health. *Biol. Conserv.* 92, 185–197. doi: 10.1016/s0006-3207(99)00052-x

Hoegh-Guldberg, O., and Bruno, J. F. (2010). The impact of climate change on the world's marine ecosystems. *Science* 328, 1523–1528. doi: 10.1126/science.1189930

Huggett, A. J. (2005). The concept and utility of 'ecological thresholds' in biodiversity conservation. *Biol. Conserv.* 124, 301–310. doi: 10.1016/j.biocon.2005.01.037

Jamieson, G., O'Boyle, R., Arbour, J., Cobb, D., Courtenay, S., Gregory, R., et al. (2001). Proceedings of the national workshop on objectives and indicators for ecosystem-based management. *DFO Can. Sci. Advis. Sec. Proc. Ser.* 200:140.

Jouffray, J.-B., Blasiak, R., Norström, A., Österblom, H., and Nyström, M. (2020). The Blue Acceleration: the Trajectory of Human Expansion into the Ocean. *One Earth* 2, 43–54. doi: 10.1016/j.oneear.2019.12.016

Karr, J. R. (1991). Biological integrity - A long-neglected aspect of water-resource management. *Ecol. Appl.* 1, 66–84. doi: 10.2307/1941848

Kelly, R. P., Erickson, A. L., and Mease, L. A. (2014). How not to fall off a cliff, or using tipping points to improve environmental management. *Ecol. Law Q.* 41, 843–886.

Kreisel, W. E. (1984). Representation of the environmental-quality profile of a metropolitan area. *Environ. Monit. Assess.* 4, 15–33. doi: 10.1007/bf01047618

Kremen, C. (1994). Biological inventory using target taxa: a case study of the butterflies of Madagascar. *Ecol. Appl.* 4, 407–422. doi: 10.2307/1941946

Landres, P. B., Verner, J., and Thomas, J. W. (1988). Ecological uses of vertebrate indicator species: a critique. *Conserv. Biol.* 2, 316–328. doi: 10.1111/j.1523-1739.1988.tb00195.x

Large, S. I., Fay, G., Friedland, K. D., and Link, J. S. (2015). Critical points in ecosystem responses to fishing and environmental pressures. *Mar. Ecol. Prog. Ser.* 521, 1–17. doi: 10.3354/meps11165

Lavoie, D., Lambert, N., and Gilbert, D. (2019). Projections of future trends in biogeochemical conditions in the Northwest Atlantic using CMIP5 Earth System Models. *Atmos. Ocean* 57, 18–40. doi: 10.1080/07055900.2017.1401973

Legendre, P., and Legendre, L. (2012). *Numerical Ecology*. Amsterdam: Elsevier Science BV.

Lehmann, M. F., Barnett, B., Gelinas, Y., Gilbert, D., Maranger, R. J., Mucci, A., et al. (2009). Aerobic respiration and hypoxia in the Lower St. Lawrence Estuary: stable isotope ratios of dissolved oxygen constrain oxygen sink partitioning. *Limnol. Oceanogr.* 54, 2157–2169. doi: 10.4319/lo.2009.54.6.2157

Lévesque, M. (2009). *Caractérisation de la Macrofaune Épibenthique de L'estuaire et du Nord du Golfe du Saint-Laurent (Québec-Canada) en Relation avec les Paramètres Environnementaux: Analyses Multivariées et Approche de Géostatistique*. Master's thesis. Rimouski, QC: Université du Québec à Rimouski.

Lévesque, M., Archambault, P., McKindsey, C. W., Vaz, S., and Archambault, D. (2010). Predictive benthic habitat suitability model for the Estuary and the northern Gulf of St. Lawrence (2006). *Can. Tech. Rep. Fish. Aquat. Sci.* 2893, vii+20.

Levin, L. A. (2003). Oxygen minimum zone benthos: adaptation and community response to hypoxia. *Oceanogr. Mar. Biol. Annu. Rev.* 41, 1–45.

Levin, L. A., Ekau, W., Gooday, A. J., Jorissen, F., Middelburg, J. J., Naqvi, S. W. A., et al. (2009). Effects of natural and human-induced hypoxia on coastal benthos. *Biogeosciences* 6, 2063–2098. doi: 10.5194/bg-6-2063-2009

Levinton, J. S. (1970). The paleoecological significance of opportunistic taxa. *Lethaia* 3, 69–78. doi: 10.1111/j.1502-3931.1970.tb01264.x

Liaw, A., and Wiener, M. (2002). Classification and regression by randomForest. *R News* 2, 18–22.

MacCraken, M., Escobar Briones, E., Gilbert, D., Korotaev, G., Naqvi, W., Perillo, G. M. E., et al. (2008). "Vulnerability of semi-enclosed marine systems to environmental disturbances," in *Watersheds, Bays, and Bounded Seas: The Science and Management of Semi-Enclosed Marine Systems*, eds P. M. Rizzoli, J. M. Melillo, B. Sundby, and E. R. Urban Jr. (Washington, DC: Island Press), 8–23.

Moritz, C., Gravel, D., Savard, L., McKindsey, C. W., Brethes, J. C., and Archambault, P. (2015). No more detectable fishing effect on Northern Gulf of St Lawrence benthic invertebrates. *ICES J. Mar. Sci.* 72, 2457–2466. doi: 10.1093/icesjms/fsv124

Moritz, C., Levesque, M., Gravel, D., Vaz, S., Archambault, D., and Archambault, P. (2013). Modelling spatial distribution of epibenthic communities in the Gulf of St. Lawrence (Canada). *J. Sea Res.* 78, 75–84. doi: 10.1016/j.seares.2012.10.009

Mucci, A., Starr, M., Gilbert, D., and Sundby, B. (2011). Acidification of Lower St. Lawrence estuary bottom waters. *Atmos. Ocean* 49, 206–218. doi: 10.1080/07055900.2011.599265

Murillo, F. J., Kenchington, E., Beazley, L., Lirette, C., Knudby, A., Guijarro, J., et al. (2016). Distribution Modelling of sea pens, sponges, stalked tunicates and soft corals from research vessel survey data in the Gulf of St. Lawrence for use in the identification of significant benthic areas. *DFO Can. Sci. Advis. Sec. Res. Doc.* 3170, vi+132.

Murray, K., and Conner, M. M. (2009). Methods to quantify variable importance: implications for the analysis of noisy ecological data. *Ecology* 90, 348–355. doi: 10.1890/07-1929.1

Myers, R. A., and Worm, B. (2003). Rapid worldwide depletion of predatory fish communities. *Nature* 423, 280–283. doi: 10.1038/nature01610

Newell, R. I. E. (2004). Ecosystem influences of natural and cultivated populations of suspension-feeding bivalve molluscs: a review. *J. Shellfish Res.* 23, 51–61.

Oksanen, J., Blanchet, F. G., Friendly, M., Kindt, R., Legendre, P., McGlinn, D., et al. (2019). *vegan: Community Ecology Package*. Available online at: https://CRAN.R-project.org/package=vegan (accessed January 16, 2020).

Oshiro, T. M., Perez, P. S., and Baranauskas, J. A. (2012). "How many trees in a random forest?," in *Machine Learning and Data Mining in Pattern Recognition*, ed. P. Perner (New York, NY: Springer), 154–168. doi: 10.1007/978-3-642-31537-4_13

Ouellet, P., Savard, L., and Larouche, P. (2007). Spring oceanographic conditions and northern shrimp Pandalus borealis recruitment success in the northwestern Gulf of St. Lawrence. *Mar. Ecol. Prog. Ser.* 339, 229–241. doi: 10.3354/meps339229

Pearson, T. H., and Rosenberg, R. (1978). Macrobenthic succession in relation to organic enrichment and pollution of the marine environment. *Oceanogr. Mar. Biol. Annu. Rev.* 16, 229–234.

Petrie, B., Drinkwater, K., Sandstrom, A., Pettipas, R., Gregory, D., Gilbert, D., et al. (1996). Temperature, salinity and sigma-t atlas for the Gulf of St. Lawrence. *DFO Can. Tech. Rep. Hydrogr. Ocean Sci.* 178, v+256.

Poitevin, P., Thebault, J., Siebert, V., Donnet, S., Archambault, P., Dore, J., et al. (2019). Growth response of Arctica Islandica to North Atlantic oceanographic conditions Since 1850. *Front. Mar. Sci.* 6:483. doi: 10.3389/fmars.2019.00483

R Core Team (2018). *R: A Language and Environment for Statistical Computing*. Available online at: https://www.R-project.org/ (accessed December 8, 2020).

Rabalais, N. N., Diaz, R. J., Levin, L. A., Turner, R. E., Gilbert, D., and Zhang, J. (2010). Dynamics and distribution of natural and human-caused hypoxia. *Biogeosciences* 7, 585–619. doi: 10.5194/bg-7-585-2010

Rhoads, D. C. (1974). Organism-sediment relations on the muddy seafloor. *Oceanogr. Mar. Biol. Annu. Rev.* 12, 263–300.

Rosenberg, R., Nilsson, H. C., and Diaz, R. J. (2001). Response of benthic fauna and changing sediment redox profiles over a hypoxic gradient. *Estuar. Coast. Shelf Sci.* 53, 343–350. doi: 10.1006/ecss.2001.0810

Samhouri, J. F., Levin, P. S., James, C. A., Kershner, J., and Williams, G. (2011). Using existing scientific capacity to set targets for ecosystem-based management: a Puget Sound case study. *Mar. Policy* 35, 508–518. doi: 10.1016/j.marpol.2010.12.002

Saucier, F. J., Roy, F., Gilbert, D., Pellerin, P., and Ritchie, H. (2003). Modeling the formation and circulation processes of water masses and sea ice in the Gulf of St. Lawrence, Canada. *J. Geophys. Res. Oceans* 108:3269. doi: 10.1029/2000jc000686

Savenkoff, C., Gagne, J. A., Gilbert, M., Castonguay, M., Chabot, D., Chasse, J., et al. (2017). Le concept d'approche écosystemique appliqué à l'estuaire maritime du Saint-Laurent (Canada). *Environ. Rev.* 25, 26–96. doi: 10.1139/er-2015-0083

Schiel, D. R., Steinbeck, J. R., and Foster, M. S. (2004). Ten years of induced ocean warming causes comprehensive changes in marine benthic communities. *Ecology* 85, 1833–1839. doi: 10.1890/03-3107

Shick, J. M. (1976). Physiological and behavioral responses to hypoxia and hydrogen sulfide in the infaunal asteroid *Ctenodiscus crispatus*. *Mar. Biol.* 37, 279–289. doi: 10.1007/bf00387613

Sonderegger, D. L., Wang, H. N., Clements, W. H., and Noon, B. R. (2009). Using SiZer to detect thresholds in ecological data. *Front. Ecol. Environ.* 7, 190–195. doi: 10.1890/070179

Suding, K. N., and Hobbs, R. J. (2009). Threshold models in restoration and conservation: a developing framework. *Trends Ecol. Evol.* 24, 271–279. doi: 10.1016/j.tree.2008.11.012

Therriault, J. C. (1991). The Gulf of St. Lawrence: Small ocean or big estuary? *DFO Can. Spec. Publ. Fish. Aquat. Sci.* 113:359.

Thibodeau, B., de Vernal, A., and Limoges, A. (2013). Low oxygen events in the Laurentian Channel during the Holocene. *Mar. Geol.* 346, 183–191. doi: 10.1016/j.margeo.2013.08.004

Thibodeau, B., De Vernal, A., and Mucci, A. (2006). Enhanced primary productivity, organic carbon fluxes and the development of hypoxic bottom waters in the Lower St. Lawrence estuary, eastern Canada: micropaleontological and geochemical evidence. *Mar. Geol.* 231, 37–50. doi: 10.1016/j.margeo.2006.05.010

Toms, J. D., and Lesperance, M. L. (2003). Piecewise regression: a tool for identifying ecological thresholds. *Ecology* 84, 2034–2041. doi: 10.1890/02-0472

Vaquer-Sunyer, R., and Duarte, C. M. (2008). Thresholds of hypoxia for marine biodiversity. *Proc. Natl. Acad. Sci. U.S.A.* 105, 15452–15457. doi: 10.1073/pnas.0803833105

Venice System. (1958). The Venice System for the classification of marine waters according to salinity. *Limnol. Oceanogr.* 3, 346–347. doi: 10.4319/lo.1958.3.3.0346

Vistisen, B., and Vismann, B. (1997). Tolerance to low oxygen and sulfide in *Amphiura filiformis* and *Ophiura albida* (Echinodermata: Ophiuroidea). *Mar. Biol.* 128, 241–246. doi: 10.1007/s002270050088

Walsh, S. J., and McCallum, B. R. (1997). *Performance of the Campelen 1800 shrimp trawl during the 1995 Northwest Atlantic Fisheries Centre autumn Groundfish Survey*. Available online at: https://www.infona.pl/resource/bwmeta1.element.elsevier-9b39731f-fb07-30ea-a6c9-0a69e96714e8/tab/contributors (accessed January 16, 2021).

Walther, G. R., Post, E., Convey, P., Menzel, A., Parmesan, C., Beebee, T. J. C., et al. (2002). Ecological responses to recent climate change. *Nature* 416, 389–395. doi: 10.1038/416389a

Ward, J. H. (1963). Hierarchical grouping to optimize an objective function. *J. Am. Stat. Assoc.* 58, 236–244. doi: 10.2307/2282967

Weisberg, S. B., Ranasinghe, J. A., Schaffner, L. C., Diaz, R. J., Dauer, D. M., and Frithsen, J. B. (1997). An estuarine benthic index of biotic integrity (B-IBI) for Chesapeake Bay. *Estuaries* 20, 149–158. doi: 10.2307/1352728

Worm, B., Barbier, E. B., Beaumont, N., Duffy, J. E., Folke, C., Halpern, B. S., et al. (2006). Impacts of biodiversity loss on ocean ecosystem services. *Science* 314, 787–790. doi: 10.1126/science.1132294

Wu, R. S. S. (2002). Hypoxia: from molecular responses to ecosystem responses. *Mar. Pollut. Bull.* 45, 35–45. doi: 10.1016/s0025-326x(02)00061-9

Zettler, M., Schiedek, D., and Bobertz, B. (2007). Benthic biodiversity indices versus salinity gradient in the southern Baltic Sea. *Mar. Pollut. Bull.* 55, 258–270. doi: 10.1016/j.marpolbul.2006.08.024

Conflict of Interest: The authors declare that the research was conducted in the absence of any commercial or financial relationships that could be construed as a potential conflict of interest.

Publisher's Note: All claims expressed in this article are solely those of the authors and do not necessarily represent those of their affiliated organizations, or those of the publisher, the editors and the reviewers. Any product that may be evaluated in this article, or claim that may be made by its manufacturer, is not guaranteed or endorsed by the publisher.

frontiers in Marine Science

ORIGINAL RESEARCH
published: 08 February 2022
doi: 10.3389/fmars.2021.773437

A Hidden Diversity in the Atlantic and the SE Pacific: Hamatipedidae n. fam. (Crustacea: Tanaidacea)

Marta Gellert[1], Graham Bird[2], Anna Stępień[1], Maciej Studzian[3,4] and Magdalena Błażewicz[1]*

[1] Department of Invertebrate Zoology and Hydrobiology, University of Lodz, Lodz, Poland, [2] Independent Researcher, Waikanae, New Zealand, [3] Department of Molecular Biophysics, University of Lodz, Lodz, Poland, [4] Laboratory of Transcriptional Regulation, Institute of Medical Biology, Polish Academy of Sciences (PAS), Lodz, Poland

A new family of paratanaoidean Tanaidacea, the hamatipedids, formerly part of the Typhlotanaidae, is established to accommodate three genera (*Hamatipeda* and two new). Deep-sea hamatipedids collected from four sites in the Atlantic (Argentine and Guiana basins) and 14 sites from the Southeast coast of Australia were studied using a taxonomic approach combining morphological and morphometric data. Four new species of *Hamatipeda* and one of a new genus are described from different deep-sea areas of the Atlantic and Pacific oceans. *Hamatipeda sima* originally classified within *Hamatipeda*, is transferred to a new genus. We observed that several morphometric characters (i.e., length of the last two pereonites) in different life-stages of one of the new *Hamatipeda* species (neuter, manca-2, and manca-3) are correlated with the total body length (TBL). Applying a morphometric approach, we aimed: (1) to identify those ontogenetic-dependent characters, and (2) to detect the characters, which can be used in discrimination of Hamatipedidae species, regardless their life-stage.

Keywords: Paratanaoidea, *Hamatipeda*, *Rakaduta*, *Yarutanais*, taxonomy, slope, abyssal, diversity

OPEN ACCESS

Edited by:
Marcos Rubal, University of Porto, Portugal

Reviewed by:
Patricia Esquete Garrote, University of Aveiro, Portugal
Catarina Araújo-Silva, Federal University of Pernambuco, Brazil

****Correspondence:***
Marta Gellert
marta.gellert@edu.uni.lodz.pl

Specialty section:
This article was submitted to Marine Evolutionary Biology, Biogeography and Species Diversity, a section of the journal Frontiers in Marine Science

Received: *29 September 2021*
Accepted: *06 December 2021*
Published: *08 February 2022*

Citation:
Gellert M, Bird G, Stępień A, Studzian M and Błażewicz M (2022) A Hidden Diversity in the Atlantic and the SE Pacific: Hamatipedidae n. fam. (Crustacea: Tanaidacea). Front. Mar. Sci. 8:773437. doi: 10.3389/fmars.2021.773437

INTRODUCTION

Intensive exploration of the deep sea since the 1960s has uncovered a remarkable diversity of benthic organisms (Sanders et al., 1965; Sanders, 1968). The large number of new taxa discovered during each expedition unequivocally refute the 19th Century concept of the deep sea as unproductive and devoid of life ecosystem. These studies also revealed that many undescribed deep-sea species are often much smaller than their shallow-water counterparts, a reason why these have been overlooked over the decades of deep-ocean exploration (Larsen, 2005; Błażewicz-Paszkowycz et al., 2012; McCallum et al., 2015; Frutos et al., 2016). The number of new species and their enormous diversity discovered during each deep-sea expedition, confirms that oceanic bottom is the last recognized ecosystem of the Earth (Ramirez-Llodra et al., 2011; Frutos and Sorbe, 2014; Costello and Chaudhary, 2017; Jażdżewska et al., 2018, 2021). A paucity of specialists and awareness of the role taxonomy for understanding and protection of the biodiversity has meant that collections of invertebrates from deep-sea expeditions were shelved in museums awaiting the attention of taxonomists and formal description (Brandt et al., 2007; Appeltans et al., 2012).

Among these organisms is the superfamily Paratanaoidea Lang, 1949, a monophyletic group of the crustacean suborder Tanaidomorpha (Kakui et al., 2011). It is represented by relatively small

peracarids (<4 mm) of high diversity that is still under-recognized and undescribed (Błażewicz-Paszkowycz and Bamber, 2007; Błażewicz et al., 2019). It is currently represented by 19 recent families.

The Typhlotanaidae Sieg (1984) is one of the most diverse paratanaoidean families in the deep sea, comprising 17 genera and 119 species (Gellert et al., unpublished). Before the first phylogenetic approaches (Larsen and Wilson, 2002), typhlotanaids were grouped within the Leptognathiidae Sieg, 1976, although their morphological distinctiveness was often emphasized (Sieg, 1984). The Typhlotanaidae were characterized by a three-articulated antennule, six-articulated antenna (Sieg, 1984), and absence of eyes, which are considered evidence for a deep-water origin of the family (Błażewicz-Paszkowycz, 2007; Gellert et al., unpublished). The morphological distinctness of the ornamentation of their pereopods and their monophyletic origin is still being resolved, with the "true" typhlotanaids being defined by the presence of a "clinging apparatus" on the carpus of pereopods 4–6, which facilitates movement within their tubicolous domiciles. This apparatus includes several specialized sets of hooks, thorns, and pectinate spines rather than simple "bayonet" spines. Additionally, some genera have rounded and minutely spinulate structures called "prickly tubercles" (Błażewicz-Paszkowycz, 2007). Those structures are apparently absent in some genera such as *Aremus* Segadilha et al., 2018 and *Hamatipeda* Błażewicz-Paszkowycz, 2007, leading to their affinity with Typhlotanaidae being questioned (Segadilha et al., 2018).

The basis for this paper is tanaid material collected during the pioneering expedition exploring the abyssal zone of the West Atlantic and slope off southeastern Australia. Those collections were deposited in the Museum of Comparative Zoology (Boston, MA, United States) and in the Melbourne Museum (Australia). The material was initially identified to the genus *Hamatipeda,* but closer identification has revealed a richer diversity allowing us to distinguish several taxa. Four of the species are formally described (three species from the SW Atlantic and one from SE Australia), two new genera are established, and analysis of morphological characteristics confirms that aspects of the attachment of the cheliped to the cephalothorax, pereopod setation, and the shape of the carpus cheliped enable us to define a new family.

MATERIALS AND METHODS

Sampling

The 5,832 typhlotanaids specimens for the research were collected during the expeditions completed in the SW Atlantic (5,771 individuals) and SE Australia (61 individuals). From the Atlantic, the material included: 147 individuals from the expedition organized by Woods Hole Oceanographic Institution during 1971–1972 aboard the RV *Knorr* found in two places, e.g., the Guiana Basin and Argentine Basin at a wide depth range (1,022–3,317 m), and 61 individuals from the slope and abyss off the Australian coasts of New South Wales (off Eden) to Tasmania (off Freycinet Peninsula) at a wide depth range (49–2,900 m) collected during the SLOPE Program during 1979–1988. The distribution of the stations is given in **Supplementary Table 1**.

The samples were preserved in formalin. Distribution maps were prepared for each species using the QGIS 2.18 software (Szczepanek, 2017). The type-material and other materials studied for this research are deposited at Museums Victoria, Melbourne Museum (NMV) (Melbourne, Australia) and the Museum of Comparative Zoology (MCZ), Harvard University (Cambridge, MA, United States).

Morphological Analyses

Initial species identification was based on morphological observations with a dissecting microscope. The whole collection was sorted to several morpho-groups, and 208 individuals were preliminarily identified as *Hamatipeda* and were chosen for further comprehensive morphological study. From each group several individuals were designated for thorough morphological analysis and dissected with chemically sharpened tungsten needles. The dissected cephalothorax, pereon, and pleon appendages were mounted on slides using glycerin and sealed with molten paraffin (Błażewicz et al., 2021). Morphological drawings were prepared using a light microscope (Nikon Eclipse 50*i*) equipped with a *camera lucida*. Digital pictures were completed using a graphic tablet following Coleman (2003).

Total body length (TBL) was measured along the central axis of symmetry, from the rostrum to the tip of the pleotelson. In contrast, body width was assessed perpendicular to the symmetry axis at the widest point (BW). Body width and length of cephalothorax, pereonites, pleonites, and pleotelson were measured on whole specimens. *Hamatipeda mojito* n. sp. (see below) was represented by numerous specimens of different ontogenetic stages. Observed variability of morphometric characters between life stages pose the question if the length of appendages changes proportionally to increasing body size during developmental growth (isometric growth) or not (allometric growth). In total, we measured ninety-seven specimens of *H. mojito* in three life stages: manca-2 (35 individuals), manca-3 (24 individuals) and neuter (38 individuals). For each specimen nine characters i.e., body length, pereonites 1–6 length, uropodal exopod and endopod configuration, were recorded. All measurements were assessed along the axis of symmetry and were made with a camera connected to the microscope (Nikon Eclipse Ci-L) and the NIS-Elements View software[1].

Morphological terminology is largely as in Błażewicz-Paszkowycz (2007). The seta types are recognized as: (1) simple setae—without ornamentation, (2) serrate—with serration or denticulation, (3) penicillate—with a tuft of setules located distally and with a small knob on which a seta is fixed to the tegument and (4) rod setae—slightly inflated distally and with a pore followed Jakiel et al. (2020).

Stout setae (L:W < 5.0) are called spines (= spiniform setae), and the robust pereopod 4–6 carpal spines which are curved and extremely robust are called "hooks" (Błażewicz-Paszkowycz, 2007) and some, which are apically blunt

[1]www.nikoninstruments.com

are described "molariform". Unspecified setae in taxonomic description refer to simple setae by default. Tegumental extension on appendages arranged in combs [comb-like scales in terminology by Garm and Watling (2013)] are called microtrichia (e.g., Błażewicz-Paszkowycz, 2007).

Statistical Analysis

The relationships between body size, body segments, and uropod rami measured at different developmental stages were presented as a power function ($y = ax^b$) and logarithmically linearized ($\log y = \log a + b \log x$). All dimensions were log transformed before computing the regression equation. The slope of the regression line (b) represents the relative growth and was used to test the degree of allometry: isometry ($b = 1$), negative allometry ($b < 1$) or positive allometry ($b > 1$) (Hartnoll, 1982) (**Supplementary Table 2**).

Imaging

The scanning electron microscope work was performed on a Phenom Pro X (Department of Invertebrate Zoology and Hydrobiology, University of Lodz, Poland) to examine fine morphological details in a subset of specimens from the MCZ collection. Specimens were frozen at −10°C and analyzed using a temperature-controlled sample holder. Confocal laser scanning microscopy (CLSM) images were obtained with LSM 780 (Zeiss) microscope equipped with Plan-Apochromat 63x/1.4 objective using InTune tuneable excitation laser system (set to excitation wavelength 555 nm). Specimens were stained for 24 h with equal volume mixture of saturated water solutions of Congo red and acid fuchsin. Before dissection and mounting in 100% glycerol, stained animals were washed thoroughly with 50% aqueous glycerol solution. Fluorescence was registered in single emission channel: 561–695 nm. Images were recorded as Z-stacks with 12.6 µs pixel dwell and two times line averaging with optical cross section of 0.5 µm. Collected data was pseudo-colored in gold and reconstructed into a 3D image stack by maximum intensity projection using ZEN software (Zeiss).

TAXONOMY

Suborder: Tanaidomorpha Sieg, 1980
Superfamily Paratanaoidea Lang, 1949
Family Hamatipedidae Błażewicz, Gellert and Bird, n. fam.
LSID urn:lsid:zoobank.org:act:1F0F139B-5F63-481C-AED2-0C1CEA2B590E.

Diagnosis: Body long > 10 L:W. Pereonite-1 long (subequal or longer than cephalothorax), without hyposphenium. Pereonites 1–5 longer than wide (pereonites 2–3 over 1.5 L:W). Antennule three-articled. Mandible molar process wide, crushing surface and irregular edge, without tubercles and teeth. Cheliped basis not reaching pereonite-1, posterior lobe enfolded by sclerite. Pereopods 1–3 with seta on coxa; pereopods 4–6 coxa fused with body. Pereopod-1 more slender than others. Pereopods 2–3 often robust, with short setae and small spines. Pereopods 4–6 merus and carpus with two (or three*) hooks and one molariform spine, carpus without prickly tubercles; unguis trifurcate (or bifurcate*). Pleopods small, vestigial; setae always plumose. Uropod endopod one or two-articled; exopod one-articled.[2]

Male: Unknown.

Type species: *Hamatipeda trapezoida* Błażewicz-Paszkowycz (2007).

Genera included: *Hamatipeda* Błażewicz-Paszkowycz (2007); *Rakaduta* n. gen.; *Yarutanais* n. gen.

Remarks: The robust carpal hooks of pereopods 4–6 in the absence of a prickly tubercle are an autapomorphy for the new family and the character that distinguishes its members from the Typhlotanaidae. The Hamatipedidae lack both a hyposphenium on the pereonite-1 and the prickly tubercles on the carpus of pereopods 4–6, both characteristic of "true" typhlotanaids. So far, six typhlotanaid genera, i.e., *Paratyphlotanais* Kudinova-Pasternak and Pasternak, 1978, *Meromonakantha* Sieg, 1986, *Obesutanais* Larsen et al., 2006, *Targaryenella* Błażewicz and Segadilha, 2019; *Typhlamia* Błażewicz-Paszkowycz (2007) and *Aremus* lack the prickly tubercles, although they have robust spines or bayonet setae (or "bayonet-like spines," Bird and Holdich, 1988) on the carpus of pereopods 4–6. There are several other features which distinguish the Hamatipedidae from those genera and these genera can be segregated into two groups based on the setation of pereopods 1–3: the first, *Meromonakantha*, *Paratyphlotanais*, and *Targaryenella* differ from all other typhlotanaid and hamatipedid genera in having simple (or bayonet-like) spines on the carpus (and merus to lesser extent). The second group, *Aremus*, *Obesutanais*, and *Typhlamia* share the general setation pattern of the hamatipedids and typhlotanaids (*sensu stricto*) but the first lacks pleopods in females and has an articulated spine on the antennule apex, *Obesutanais* is characterized by a short and compact body (3.0–6.0x L:W) and only a pair of hooks on the carpus of pereopods 4–6, *inter alia*, and *Typhlamia* by its long antennule article-3 (about 14x L:W) and long setae, and more elongate merus, carpus and propodus of pereopods 1–3. Hamatipedidae have elongated pereonites and the cheliped basis posterior lobe separated from the pereonite-1 (**Figure 1**), making it similar to *Typhlamia* at first glance. However, hamatipedids have a shorter antennule than *Typhlamia*, and their carpal clinging apparatus of pereopods 4–6 is different. In hamatipedids it is formed by hooks (naked or serrated), which are sometimes apically flattened (molariform). In *Typhlamia* the spines are small, slender, and only distally flattened (Gellert et al., unpublished). The morphological phylogeny of *Typhlamia* and Hamatipedidae should be corroborated in future analysis implementing molecular techniques.

Hamatipedidae is the seventh paratanaoid family whose females have three-articled antennules. It comprises three genera: *Hamatipeda* that was originally classified in the Typhlotanaidae (Błażewicz-Paszkowycz, 2007), and two newly erected genera (*Rakaduta* n. gen.; *Yarutanais* n. gen.). A taxonomic key for identification of the paratanaoidean families with a three-articled antennule, and Hamatipedidae genera are presented below.

[2](*) See remarks (Kakui and Hiruta, 2021) and **Supplementary Table 3**.

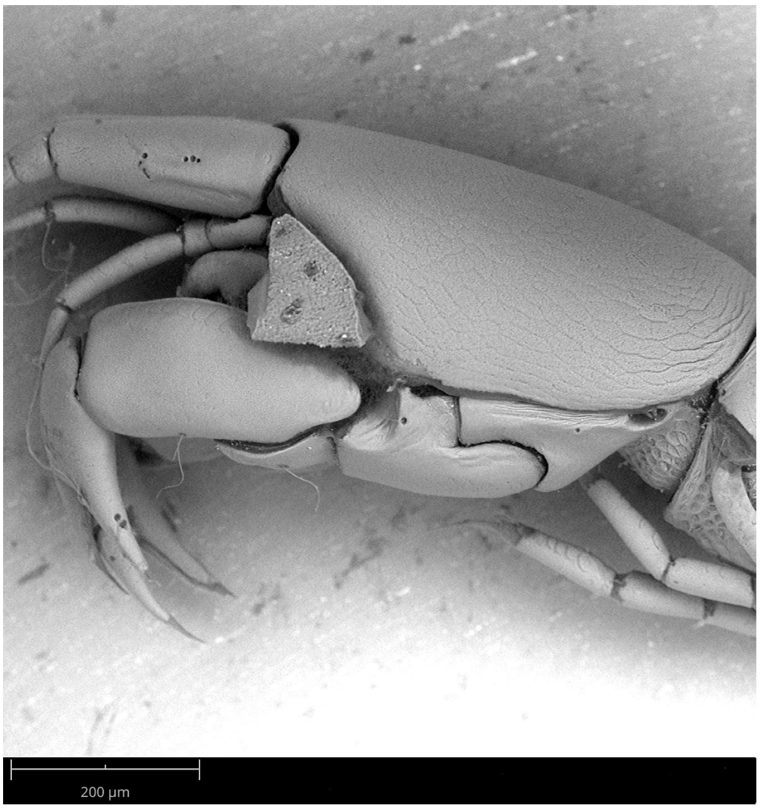

FIGURE 1 | *Hamatipeda mojito* n. sp.: cheliped/cephalothorax details showing sclerite enfolding the posterior lobe of the cheliped basis.

Key for identification of Paratanaoidea with three-articled antennule (neuters) and uropod endopod with one or two articles.

1. Antenna present.....2
 - Antenna with one or two articles..... genus *Agathotanais*
2. Pereonite-1 much shorter than broad; pereopods 2–3 carpus with or without blade-like spine.....Pseudotanaidae
 - Pereonite-1 not much shorter than broad; pereopods 2–3 carpus with setae or simple spines 3
3. Eyes present; pereopods 2–3 carpus with two inferodistal spines.....Nototanaidae
 - Eyes absent; pereopods 2–3 carpus with two inferodistal spines.....4
4. Cephalothorax shape narrower anteriorly, cheliped dactylus clearly more slender than fixed finger, often rugose dorsally.....Tanaissuidae
 - Cephalothorax not narrower anteriorly, dactylus slightly narrower than fixed finger, smooth.....5
5. Pereopods 4–6 carpus with prickly tubercles ....Typhlotanaidae (part)
 - prickly tubercles absent.....6
6. Pereopod 4–6 carpus with distal hooks or molariform spines.....Hamatipedidae n. fam.
 - Pereopod 4–6 carpus with distal spines.....7
7. Cephalothorax shape narrower anteriorly, margin straight.....*Paratyphlotanais*
 - Cephalothorax rounded.....8
8. Pleopods absent..... *Aremus*
 - Pleopods present.....9
9. Antennule article-3 at least 10x L:W.....*Typhlamia*
 - Antennule article-3 clearly less than 10 × LW.....10
10. Body well calcified, cephalothorax rounded; antennule conical, shorter than cephalothorax.....*Meromonakantha*
 - Body weakly calcified, cephalothorax not rounded, antennule longer than cephalothorax.....11
11. Body short (<6.0x L:W); uropodal exopod one- articled .....*Obesutanais*
 - Body long (>7.0x L:W); uropodal exopod two-articled.....*Targaryenella*

Hamatipeda Błażewicz-Paszkowycz (2007)

Diagnosis (after Błażewicz-Paszkowycz, 2007, amended): Pereonite-1 0.7–0.8x pereonite-2. Antennule article-3 long (>3.0x L:W); article-1 ventral microtrichia absent. Antenna articles 2–3 with setae. Cheliped carpal shield absent. Pereopod-1 propodus long (>3.0x L:W). Pereopod-3 carpus with few (2–3) setae. Pereopod-5 propodus seta short.

Type species: *Hamatipeda trapezoida* Błażewicz-Paszkowycz (2007) (by designation).

Species included: *Hamatipeda kohtsukai* Kakui and Hiruta (2021); *H. longa* (Kudinova-Pasternak, 1975); *H. trapezoida* Błażewicz-Paszkowycz (2007); *H. prolata* Segadilha et al. (2019); *H. caipirinha* n. sp.; *H. caipiroska* n. sp.; *H. lelibi* n. sp.; *H. mojito* n. sp.

Remarks: Until this study, *Hamatipeda* included four species[3]. The first to be described, *Hamatipeda longa*, was collected off the Falkland Islands and placed in the genus *Typhlotanais* (Kudinova-Pasternak, 1975). Later, Błażewicz-Paszkowycz (2007) described *Hamatipeda trapezoida* from Drake Passage and assigned it to a new genus, *Hamatipeda*. This genus was supplemented with two other species, *Hamatipeda sima* by Błażewicz-Paszkowycz and Bamber (2012) recovered in SE Australia (Eastern Bass Strait and Flinders Island), and *Hamatipeda prolata* from the SE Brazilian coast (Segadilha et al., 2019). Recently, Kakui and Hiruta (2021) has described another species — *H. kohtsukai*, which was the first record of the genus in the Northern Hemisphere. Because it lacked a trifurcate unguis in the pereopods 4–6 (a key-character for the genus), the definition of the *Hamatipeda* was extended (Kakui and Hiruta, 2021).

During our examination of the SW Atlantic and SE Australia specimens, we observed a high variety of morphological features (character of the antennule, antennule ornamentation, and character of their pereopods) and decided to extract *H. sima* from *Hamatipeda*. It is deposited it in a new genus *Yarutanais* n. gen. (see below). In addition, *Rakaduta* n. gen. is established to accommodate a new hamatipedid species from SE Australia.

Key to identification of Hamatipedidae genera (neuter).

1. Antennule article-3 short (1.0x L:W); antennule article-1 with ornamentation; cheliped carpal shield present... *Yarutanais* n. gen.

- Antennule article-3 long (>3.0x L:W); antennule article-1 ornamentation absent or with weak microtrichia; cheliped carpal shield absent..... 2

2. Antenna articles 2–3 with short and weak setae; pereopod 2–3 propodus with distoventral seta.....*Hamatipeda*

- Antenna articles 2–3 with robust and long setae; pereopod 2–3 propodus with distoventral spine..... *Rakaduta* n. gen.

***Hamatipeda caipirinha* Gellert and Błażewicz n. sp.**

LSID urn:lsid:zoobank.org:act:1AE88054-4248-4020-90B4-

(**Figures 2**, **3**)

Material examined: Holotype: neuter (in tube), MCZ 48366, St. 259A. Paratypes: manca-3 (2.1 mm), MCZ 48350, St. 245A; two neuters (2.6 mm; 2.9 mm—dissected on slide), manca-2 (1.6 mm), one broken (dissected on slide), MCZ 48366, St. 259A.

Diagnosis: Pereonites 1–3 margins narrower posteriorly; pereonites 4–6 margins rounded; pereonites 2–5 proximal margins simple; pereonite-4 long (1.7 L:W). Antennule article-3 long (4.7 L:W). Cheliped carpus 2.2 L:W; fixed finger ventral setae equal length, simple. Pereopod-2 propodus ventrodistal simple seta; pereopod-2 merus with ventrodistal seta. Pereopods 4–6 ischium with seta; carpal molariform spine serrate. Uropod exopod 0.9x endopod; endopod two-articled.

Etymology: The name is given after the popular Brazilian cocktail drink — caipirinha.

Description of neuter with BL 2.9 mm. Paratype. Body (**Figures 2A,B**), slender 9.8 L:W. Cephalothorax narrow, 1.4 L:W, 1.1x pereonite-1, naked. Pereonites smooth, wider anteriorly, margins gently rounded. Pereonites 1–6: 1.3, 1.7, 1.8, 1.7, 1.5 and 0.9 L:W, respectively. Pereonite-1 0.8x pereonite-2; pereonite-2, 0.9x pereonite-3; pereonite-3, 1.2x pereonite-4; pereonite-4, 1.2x pereonite-5; pereonite-5, 1.9x pereonite-6. Pleon 0.1x total body length; pleonites 1–5 same size, 0.1 L:W. Pleotelson 1.2x pereonite-6.

Antennule (**Figure 2E**) 0.7x cephalothorax; article-1, 2.0 L:W, 0.6x of TBL, 4.5x article-2, with three penicillate and two simple middle setae, and distal seta; article-2, 1.0 L:W, 0.4x article-3, with two long simple (0.5x article-3) setae distally; article-3, 5.1 L:W, with distal spur, one aesthetasc, one penicillate and two long simple setae distally.

Antenna (**Figure 2F**) article-1 fused with the cephalothorax; article-2, 1.8 L:W, 2.2x article-3, with two distal setae; article-3, 0.9 L:W, 0.3x article-4, with distal seta; article-4, 4.6 L:W, 2.4x article-5, with three penicillate and three simple distal setae; article-5, 3.1 L:W, 5.0x article-6, with long distal simple seta; article-6 minute, with four simple distal setae.

Mouthparts. Labrum (**Figure 2G**) rounded and distally setose. Left mandible (**Figure 2H**) left incisor distally narrow and smooth; *lacinia mobilis* distally with six rounded projections; molar wide margin irregularly rugose. Right mandible (**Figure 2I**) incisor distally oblique; molar like in left mandible. Maxillule (**Figure 2J**) with nine distal spines (one spine located centrally). Labium and epignath lost during the dissection.

Maxilliped (**Figure 2K**) palp article-1, 1.5 L:W, naked; article-2, 1.3 L:W, with three serrated inner setae (outer seta not seen); article-3, 1.2 L:W, with four serrated inner setae; article-4, 2.6 L:W, with five serrated inner and one outer setae. Basis 0.9 L:W, naked; each endite distal margin almost simple, with two middle setae, 2 minute gustatory cusps, and lateral corners finely setose. Maxilla simple semi-triangular.

Cheliped (**Figure 3A**) basis separated from pereonite-1, 1.4 L:W (**Figure 2D**), naked; merus triangular with seta; carpus 1.6 L:W, with two ventral setae and one dorsodistal seta (dorsoproximal seta not seen); chela distally narrower, 2.0 L:W, 0.9x carpus; palm 1.7x fixed finger, with seta on inner side and seta near dactylus insertion; fixed finger with two ventral rod setae (unequal length); cutting edge with three setae and three strong, blunt small teeth, distal tooth relatively small; dactylus with dorsoproximal seta; unguis slender.

Pereopod-1 (**Figure 3B**) slender; basis and merus broken merus with ventrodistal rod seta; carpus 2.3 L:W, 0.7x propodus, with three short (one fine and two robust) distal setae; propodus

[3]http://www.marinespecies.org

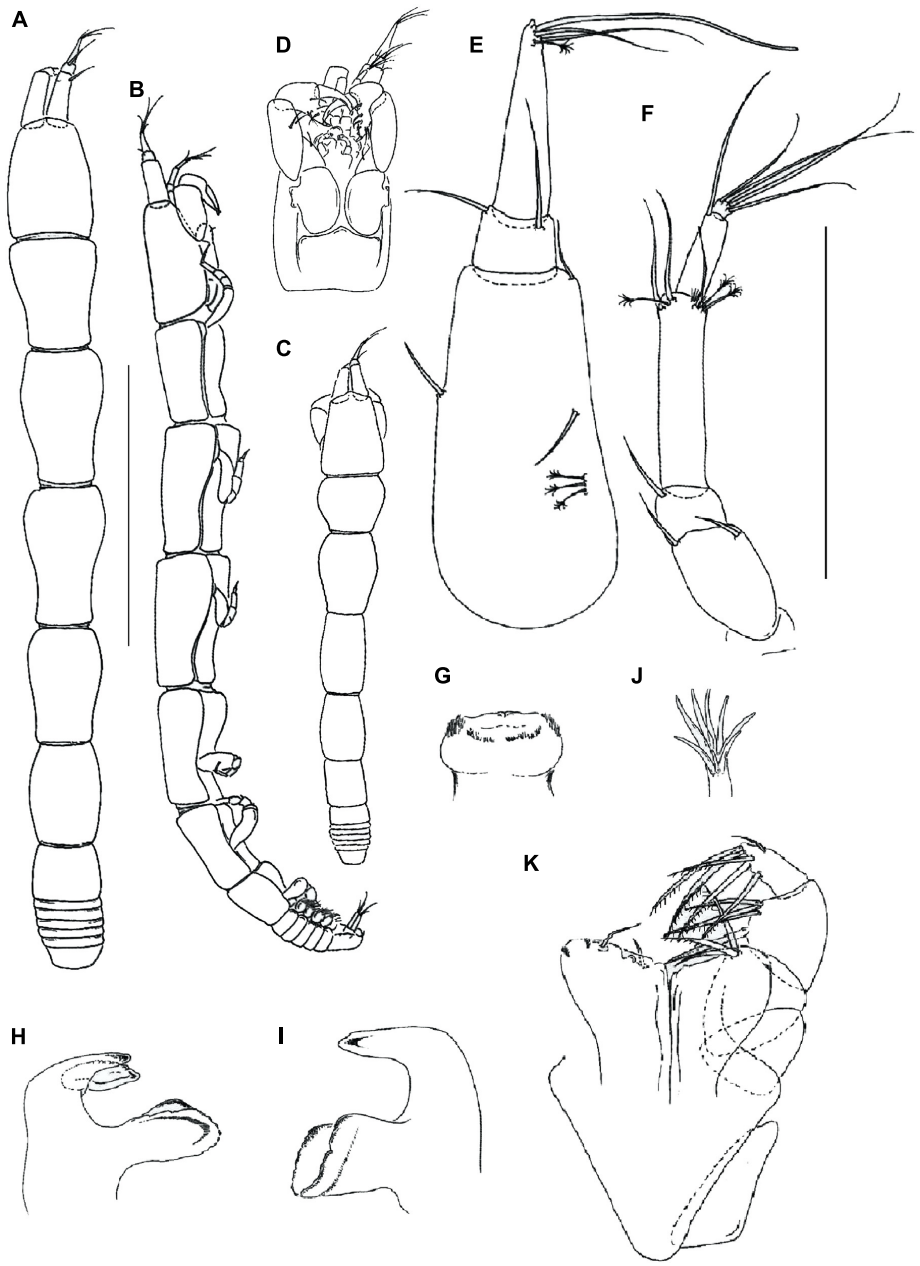

FIGURE 2 | *Hamatipeda caipirinha* n. sp. (MCZ 48366) **(A,B)** neuter; **(C)** manca-3; morphological details: **(D)** cephalothorax ventral side; **(E)** antennule; **(F)** antenna; **(G)**, labrum; **(H,I)**, mandible left and right, respectively; **(J)**, maxillule endite tip; **(K)**, maxilliped and maxilla. Scale: panels **(A,B)** = 1 mm, panels **(E–K)** = 0.1 mm.

3.8 L:W, with one ventrodistal and three dorsodistal setae; dactylus 5.8 L:W, with seta subequal unguis; dactylus and unguis together 0.8x propodus.

Pereopod-2 (**Figure 3C**) robust, overall 10 L:W; basis 4.0 L:W, with short dorsodistal seta; ischium with ventral seta; merus 1.6 L:W, 0.9x carpus, with one dorsodistal seta and two ventrodistal setae; carpus 1.6 L:W, 0.7x propodus, with three simple setae and small spine distally; propodus 2.9 L:W, with rod ventrodistal seta and simple dorsodistal seta; dactylus 4.3 L:W, with seta, 0.7x unguis; dactylus and unguis together 0.7x propodus.

Pereopod-3 (**Figure 3D**) robust, overall 6.0 L:W; basis naked, 2.8 L:W; ischium with ventral seta; merus 1.5 L:W, same length as carpus, with one serrated and two simple setae distally; carpus 1.6 L:W, 0.7x propodus, with spine, one serrated seta, and one simple seta distally; propodus 3.2 L:W, with rod ventrodistal seta and simple dorsodistal seta; dactylus 4.5 L:W, with seta, 0.8x unguis; dactylus and unguis together 0.8x propodus.

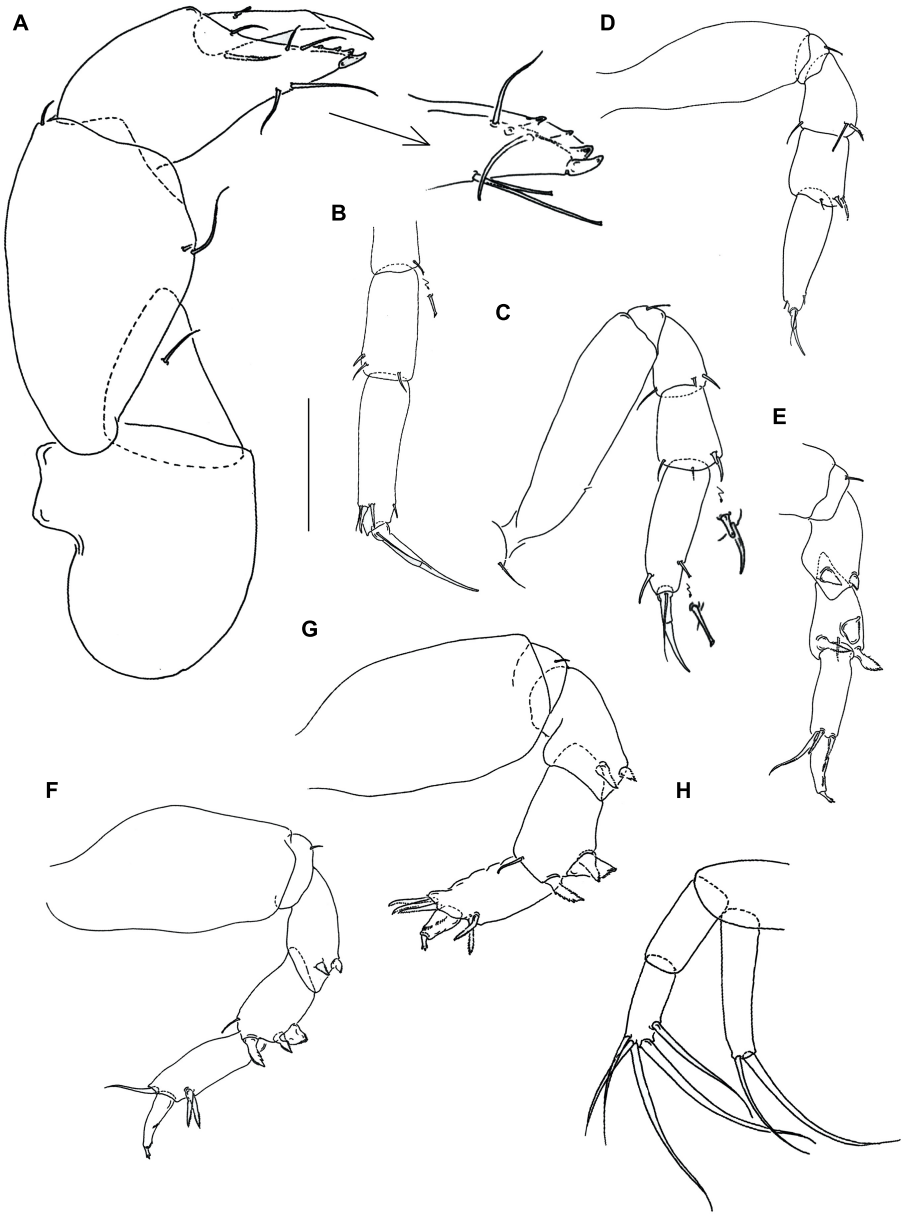

FIGURE 3 | *Hamatipeda caipirinha* n. sp. (MCZ 48366) **(A)** cheliped; **(B)** pereopod-1; **(C)** pereopod-2; **(D)** pereopod-3; **(E)** pereopod-4; **(F)** pereopod-5; **(G)** pereopod-6; **(H)** uropod. Scale: panels **(A–H)** = 0.1 mm.

Pereopod-4 (**Figure 3E**) clinging type; basis broken; ischium with ventral seta; merus 2.0 L:W, the same length as carpus, with two serrated ventrodistal spines; carpus 2.4 L:W, 1.1x propodus, with two serrated, slender (distal and ventrodistal) and one serrated molariform hooks, and simple dorsodistal seta; propodus 2.0 L:W, with two serrated ventrodistal spines and simple dorsodistal seta (longer than dactylus); dactylus 3.3 L:W, 3.3x unguis; dactylus and unguis together 0.8x propodus; unguis trifurcate.

Pereopod-5 (**Figure 3F**) overall 6.0 L:W, as pereonite-4; propodus 2.8 L:W, with two serrated ventrodistal spines and simple dorsodistal seta; dactylus 4.7 L:W, 4.6x unguis; dactylus and unguis together 0.6x propodus; unguis trifurcate.

Pereopod-6 (**Figure 3G**) overall 4.0 L:W, as pereopod-4; propodus 1.9 L:W, with three dorsodistal setae; dactylus 2.5 L:W, 3.0x unguis; dactylus and unguis together 0.5x propodus; unguis trifurcate.

Pleopods 1–5 small (vestigial) with few short, weak setae, destroyed during dissection.

Uropod (**Figure 3H**) basal article 1.3 L:W. Endopod two-articled, article-1 naked 2.3 L:W, 1.1x article-2; article-2, 2.8 L:W, with five long distal (two robust) setae. Exopod one-articled,

5.3 L:W, with one robust and one simple distal setae, almost equal to endopod.

Description of manca-2 with BL 1.7 mm; generally similar to neuter. Body (**Figure 2C**), slender 7.0 L:W. Cephalothorax narrow, 1.4 L:W, 1.5x pereonite-1, naked. Pereonites smooth, wider anteriorly, margins gently rounded. Pereonites 1–6: 0.9, 1.4, 1.7, 1.8, 1.2 and 0.6 L:W, respectively. Pereonite-1 0.6x pereonite-2; pereonite-2, 1.1x pereonite-3; pereonite-3, 1.1x pereonite-4; pereonite-4, 1.5x pereonite-5; pereonite-5, 2.0x pereonite-6. Pleon 0.1x total body length; pleonites 1–5 same size, 0.1 L:W. Pleotelson 1.7x pereonite-6. Pereopods 1–6 similar to neuter, but pereopod-6 absent.

Distribution: Argentine Basin, Atlantic, at depths of 2,707–3,317 m (**Figure 14**).

Remarks: *Hamatipeda caipirinha* n. sp., from the SW Atlantic, can be distinguished from other members of the family by the uropod endopod slightly shorter than exopod. Similar equal-length uropod rami are present in

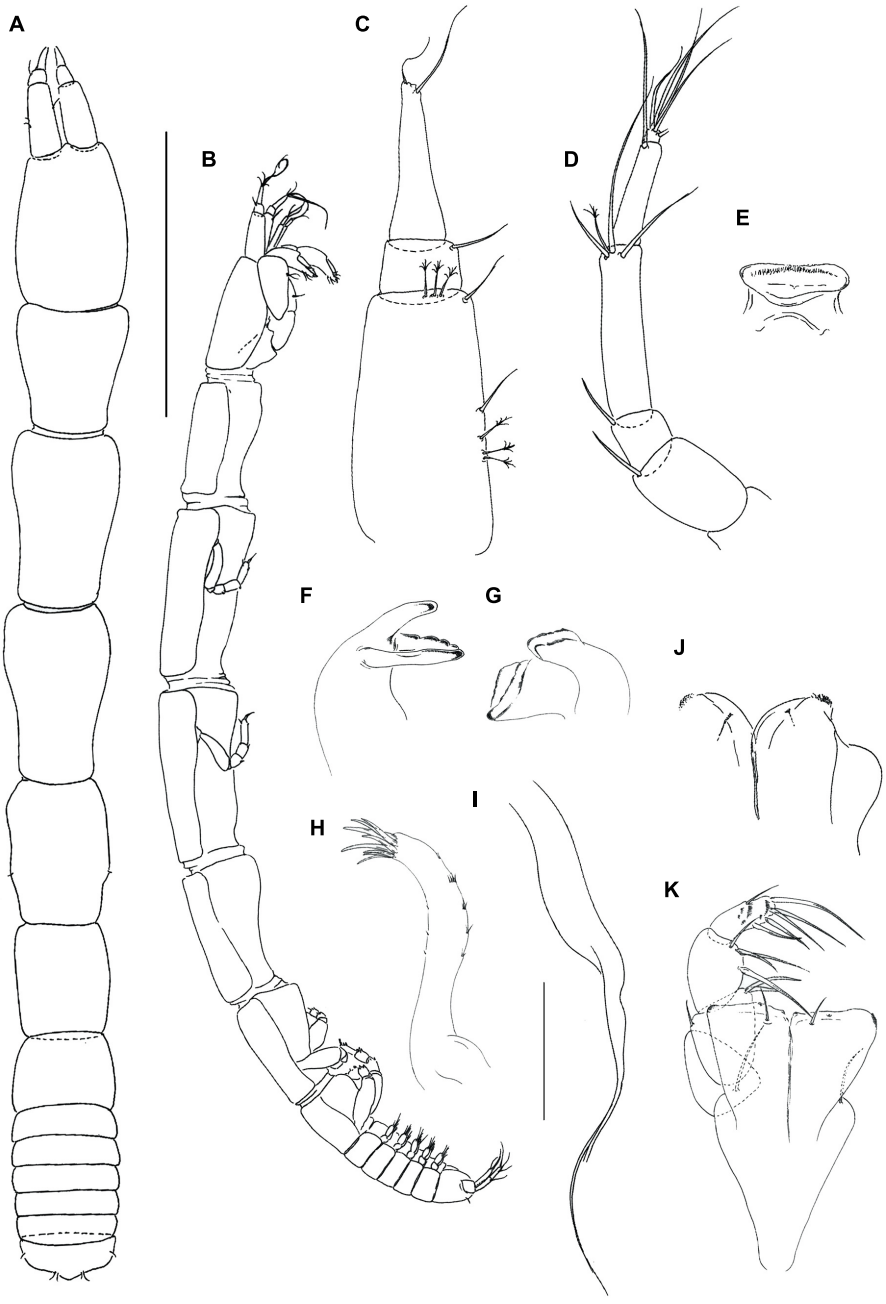

FIGURE 4 | *Hamatipeda caipiroska* n. sp. (MCZ 48350) **(A,B)** neuter; **(C)** antennule; **(D)** antenna; **(E)** labrum; **(F,G)** mandible left and right, respectively; **(H,I)** maxillule endite and palp; **(J)**, labium; **(K)** maxilliped. Scale: panels **(A,B)** = 1 mm, panels **(C–J)** = 0.1 mm.

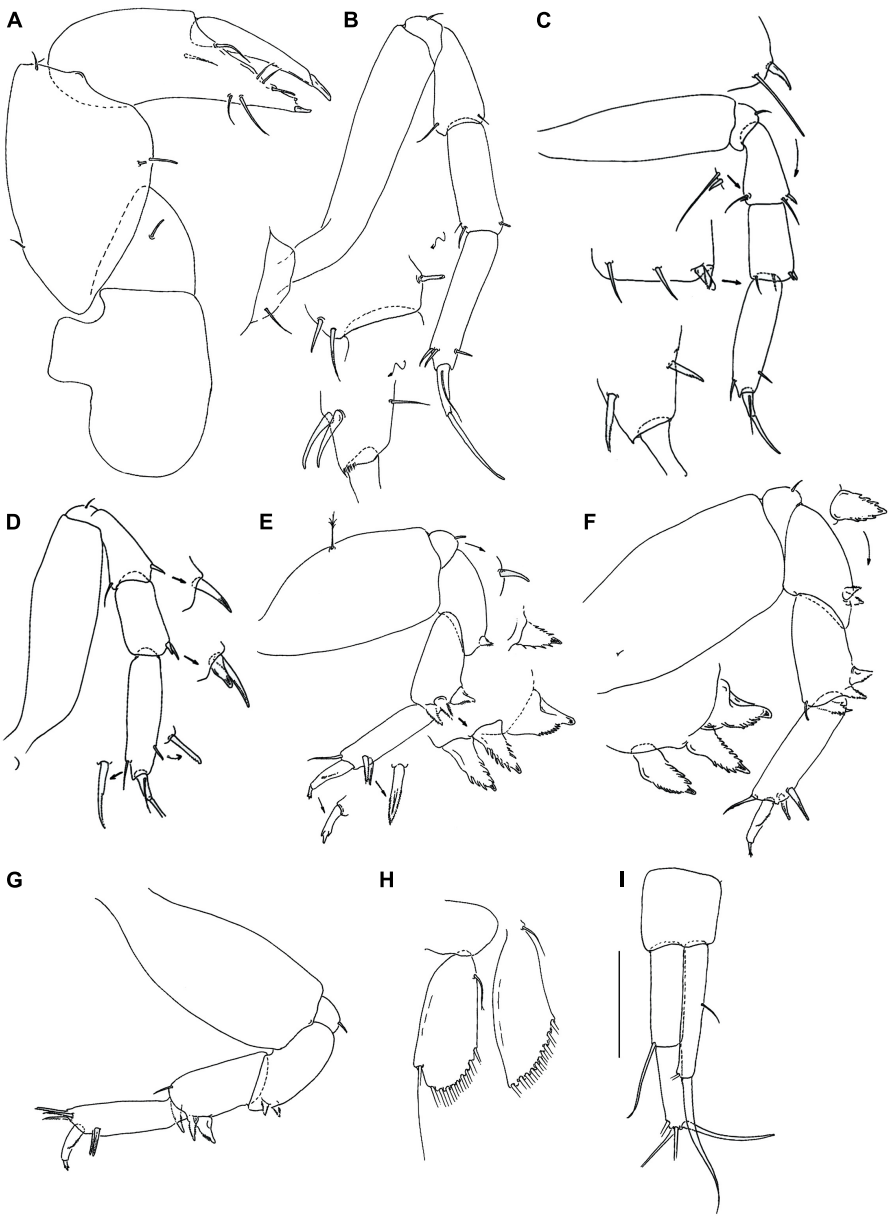

FIGURE 5 | *Hamatipeda caipiroska* n. sp. (MCZ 48350) **(A)** cheliped; **(B)** pereopod-1; **(C)** pereopod-2; **(D)** pereopod-3; **(E)** pereopod-4; **(F)** pereopod-5; **(G)** pereopod-6; **(H)** pleopod; **(I)** uropod. Scale: panels **(A–I)** = 0.1 mm.

H. trapezoida from the Antarctic (Błażewicz-Paszkowycz, 2007), but *H. caipirinha* has a two-articled endopod (one-articled in *H. trapezoida*) and ischial seta on pereopods 4–6 (two in *H. trapezoida*).

H. caipirinha has two rod ventral setae on the cheliped fixed finger (of unequal length) and the ventrodistal part of the pereopod-2 propodus, which are simple in the other members of *Hamatipeda* (**Supplementary Table 1**).

***Hamatipeda caipiroska* Gellert and Błażewicz n. sp.**
LSID urn:lsid:zoobank.org:act:85BCDA06-A8DB-48F2-A34A-
(**Figures 4**, **5**)

Material examined: Holotype: neuter (3.7 mm), MCZ 48369, St. 259A. Paratypes: neuter (4.1 mm, dissected on slide), two mancae-3 (2.1 mm, 2.5 mm), manca-2 (1.6 mm), MCZ 48350, St. 245A; manca-3 (2.0 mm), six mancae-2 (1.3–1.8 mm, 1.6 mm — dissected on slide), MCZ 48366, St. 259A; two mancae-3 (1.8, 2.0 mm), manca-2 (1.8 mm), MCZ 48369, St. 259A.

Diagnosis: Pereonites 1–3 margins narrower posteriorly; pereonites 4–6 margins rectangular; pereonites 2–5 proximal margins simple; pereonite-4 short (1.4 L:W). Antennule article-3 long (5.1 L:W). Cheliped carpus 1.6 L:W; fixed finger ventral setae equal length, simple. Pereopod-2 merus with ventrodistal seta;

propodus with simple ventrodistal seta. Pereopods 4–6 ischium with seta; carpal molariform spine serrate. Uropod exopod 0.7x endopod; endopod two-articled.

Etymology: The name is given after the well-known Brazilian cocktail drink—*caipiroska*.

Description of neuter with BL 4.1 mm. Paratype. Body (**Figures 4A,B**), slender 10.3 L:W. Cephalothorax narrow, 1.5 L:W, 1.3x pereonite-1, naked. Pereonites smooth, wider anteriorly, margins gently rounded. Pereonites 1–6: 1.1, 1.7, 1.8, 1.5, 1.2 and 0.7 L:W, respectively. Pereonite-1 0.7x pereonite-2; pereonite-2 same length as pereonite-3; pereonite-3, 1.3x pereonite-4; pereonite-4, 1.3x pereonite-5; pereonite-5, 1.6x pereonite-6. Pleon 0.1x total body length; pleonites 1–5 same size, 0.3 L:W. Pleotelson 2.5x pereonite-6.

Antennule (**Figure 4C**) 0.6x cephalothorax; article-1, 2.1 L:W, 0.6 × of TBL, 4.1x article-2, with one simple and three penicillate middle setae, and one simple and three penicillate distal setae; article-2, 0.9 L:W, 0.4x article-3, with moderate length distal seta; article-3, 4.7 L:W, with distal spur and two simple distal setae.

Antenna (**Figure 4D**) article-1 fused with the cephalothorax; article-2, 1.5 L:W, 1.7x article-3, with distal seta; article-3, 1.3 L:W, 0.3x article-4, with distal seta; article-4, 4.2 L:W, 1.7x article-5, with one penicillate and three simple distal setae; article-5, 4.6 L:W, 8.0x article-6, with long seta; article-6 minute, with five (one broken) distal setae.

Mouthparts. Labrum (**Figure 4E**) rounded and distally setose. Left mandible (**Figure 4F**) incisor distally narrow and smooth; *lacinia mobilis* distally with five rounded projections; molar wide with margin irregularly rugose. Right mandible (**Figure 4G**) incisor distally oblique; molar like in left mandible. Maxillule (**Figures 4H,I**) with nine distal spines (one spine located centrally); endite with two distal setae. Labium (**Figure 4J**) with two lobes, inner lobe disto-outer margin finely setose, outer lobe feeble, smooth. Maxilla not seen.

Maxilliped (**Figure 4K**) palp article-1, 1.5 L:W, naked; article-2, 1.4 L:W, with three serrated inner setae and one outer seta; article-3, 1.5 L:W, with four serrated inner setae; article-4, 2.8 L:W, with five inner serrated and one outer setae. Basis 1.7 L:W, naked; each endite distal margin almost simple, with middle seta, minute gustatory cusp (second gustatory cusp not seen), and lateral corners finely setose. Epignath not seen.

Cheliped (**Figure 5A**) basis 1.4 L:W, naked; merus triangular with seta; carpus 1.9 L:W, with two ventral setae, dorsodistal and dorsoproximal setae; chela distally narrower, 1.5 L:W, 1.8x carpus; palm 0.8x fixed finger, with seta on inner side and seta near dactylus insertion; fixed finger with two ventral setae (unequal length); cutting edge with three setae and three weak, blunt small spines, distal spine relatively small; dactylus with dorsoproximal seta; unguis slender.

Pereopod-1 (**Figure 5B**) overall slender (15 L:W); basis 5.6 L:W, naked; ischium with ventral seta; merus 2.2 L:W, with ventrodistal and dorsodistal simple setae; carpus 3.1 L:W, 0.8x propodus, with two dorsodistal setae and one ventrodistal spine; propodus 4.8 L:W, with one ventrodistal and two robust dorsodistal setae; dactylus 7.0 L:W, with seta, 0.5x unguis; dactylus and unguis together 0.9x propodus.

Pereopod-2 (**Figure 5C**) robust; overall 9.0 L:W; basis 3.4 L:W, naked; ischium with ventral seta; merus 2.8 L:W, 1.0x carpus, with simple seta and small spine in dorsodistal and ventrodistal corners; carpus 2.1 L:W, 0.7x propodus, with two simple setae and two small spines distally; propodus 4.2 L:W, with one ventrodistal and one dorsodistal setae; dactylus 4.0 L:W, with seta, 0.6x unguis; dactylus and unguis together 0.6x propodus.

Pereopod-3 (**Figure 5D**) robust; basis naked, 3.5 L:W; ischium with ventral seta; merus 2.4 L:W, same length as carpus, with simple dorsodistal seta and ventrodistal spine; carpus 2.0 L:W, 0.6x propodus, with two distal spines; propodus 3.8 L:W, with one rod ventrodistal and one dorsodistal serrated setae; dactylus 4.0 L:W, with seta; unguis broken.

Pereopod-4 (**Figure 5E**) overall 5.0 L:W; basis 2.0 L:W, with ventral penicillate seta; ischium with ventral seta; merus 2.2 L:W, 0.9x carpus, with two serrated ventrodistal spines; carpus 2.3 L:W, 0.9x propodus, with two serrated, slender (distal and ventrodistal) spines and one serrated molariform spine (**Figure 8B**); propodus 3.9 L:W, with two serrated ventrodistal spines and one simple dorsodistal seta (shorter than dactylus); dactylus 3.8 L:W, 3.8x unguis; dactylus and unguis together 0.6x propodus; unguis trifurcate.

Pereopod-5 (**Figure 5F**) overall 5.0 L:W; as pereonite-4, but carpus with dorsodistal seta.

Pereopod-6 (**Figure 5G**) overall 5.0 L:W; as pereopod-4, but propodus with three serrated dorsodistal spines.

Pleopods 1–5 (**Figure 5H**) basal article naked. Endopod 2.3 L:W, with one proximal and nine simple distal setae on outer margin. Exopod 3.1 L:W, with one proximal and ten distal serrated setae on outer margin.

Uropod (**Figure 5I**) basal article 1.1 L:W. Endopod two-articled, article-1, 3.0 L:W, 0.9x article-2, with seta; article-2, 3.4 L:W, with four long distal setae. Exopod one-articled, 6.1 L:W, with one robust and one simple (broken) distal setae.

Distribution: Argentine Basin, Atlantic, at depths of 2,707–3,317 m (**Figure 14**).

Remarks: *Hamatipeda caipiroska* n. sp. is an abyssal species of the SW Atlantic. It can be distinguished from other members of the genus by the presence of a relatively stout cheliped carpus (1.6 L:W) that is more slender in other *Hamatipeda* species (at least 2.0x L:W). Moreover, *H. caipiroska* has a two-articled uropodal endopod, as in *H. longa, H. prolata*, *H. caipirinha*, and *H. mojito*, but only *H. prolata*, known from the Brazilian slope, shares with *H. caipirinha* parallel margins on pereonites 4–6. These two species are also distinguished by the shape of pereonites 1–3, which are rectangular in *H. prolata* and trapezoidal in *H. caipiroska* (**Supplementary Table 1**).

Hamatipeda caipiroska and *H. caipirinha* were collected by dredging at the same station in the abyssal of Argentina Basin. They can be distinguished by the length of the uropod rami (almost equal in *H. caipirinha*, and with exopod clearly shorter 0.7x endopod in *H. caipiroska*), the length of pereonite-4 (long 1.7 L:W) in *H. caipirinha,* and short (1.4 L:W in *H. caipiroska*), and the aspect ratio of the cheliped carpus

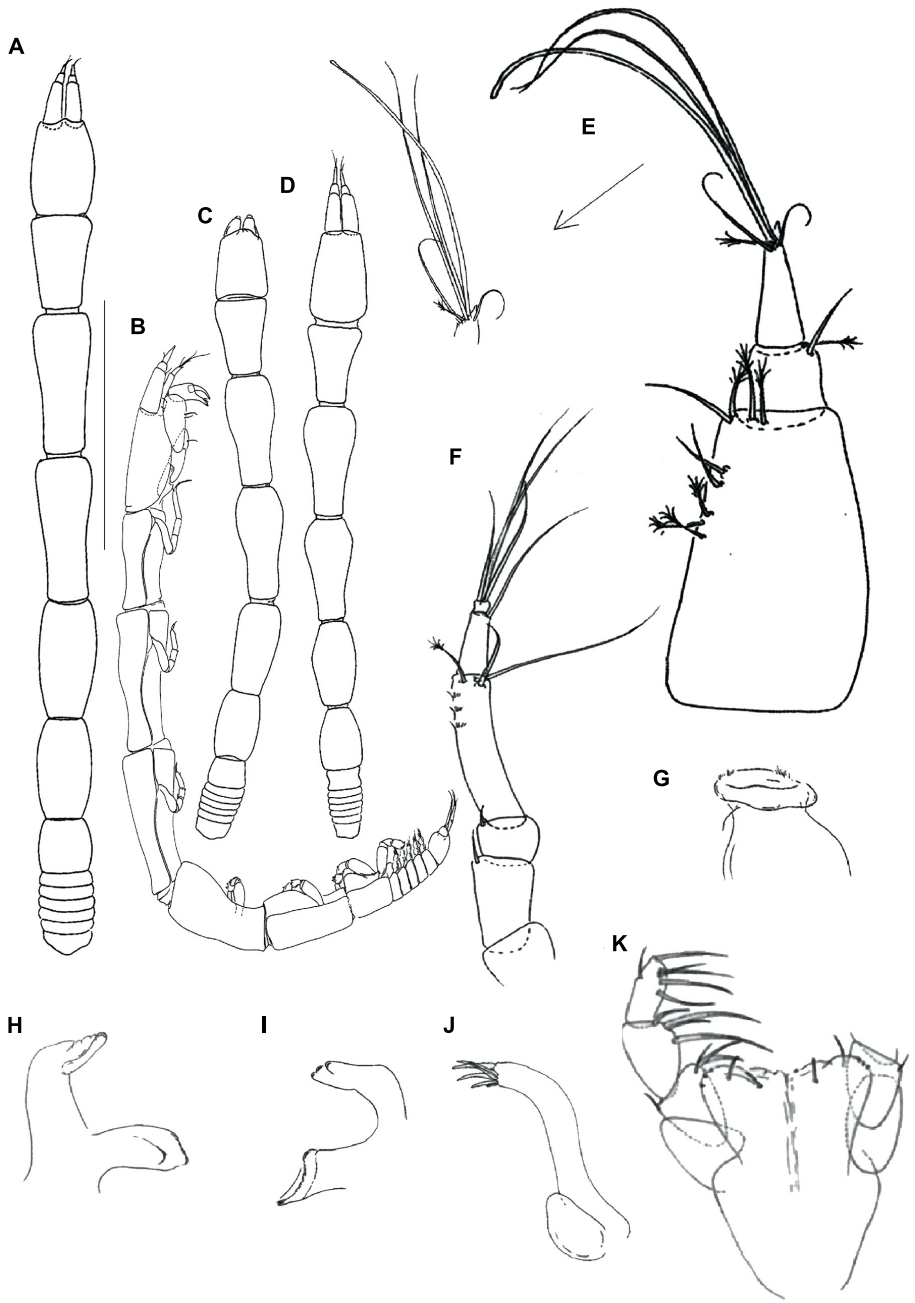

FIGURE 6 | *Hamatipeda mojito* n. sp. (MCZ 49272) **(A,B)** neuter; **(C,D)** manca-2 and 3, respectively; **(E)** antennule; **(F)** antenna; **(G)** labrum; **(H,I)** mandible left and right, respectively; **(J)** maxillule endite and maxilla; **(K)** maxilliped. Scale: panels **(A,B)** = 1 mm, panels **(C–K)** = 0.1 mm.

(slender in *H. caipirinha* (2.2 L:W), and robust (1.6 L:W) in *H. caipiroska*).

Hamatipeda mojito Gellert and Błażewicz n. sp.
LSID urn:lsid:zoobank.org:act:E377CF1D-556E-4B8D-85E9-
(**Figures 6–8**)

Material examined: Holotype: neuter (4.0 mm) (MCZ 49272) St. 293. Paratypes: 35 neuters (2.6–4.56 mm, one broken), neuter (3.44 mm, dissected on slide) 25 mancae-3 (2.1–2.5 mm), 42 mancae-2 (1.6–2.1 mm), six juvenile males (3.9–5.0 mm), 16 individuals broken (two dissected on slide) (MCZ 49272) St. 293; neuter (3 mm), manca-3 (2.1 mm) (MCZ 49288) St. 295.

Diagnosis: Pereonites 1–3 margins narrower posteriorly; pereonites 4–6 margins rounded; pereonites 2–5 proximal margins simple; pereonite-4 very long (2.0 L:W). Antennule article-3 long (4.6 L:W). Cheliped carpus 2.0 L:W; fixed finger ventral setae equal length, simple. Pereopod-2 merus with

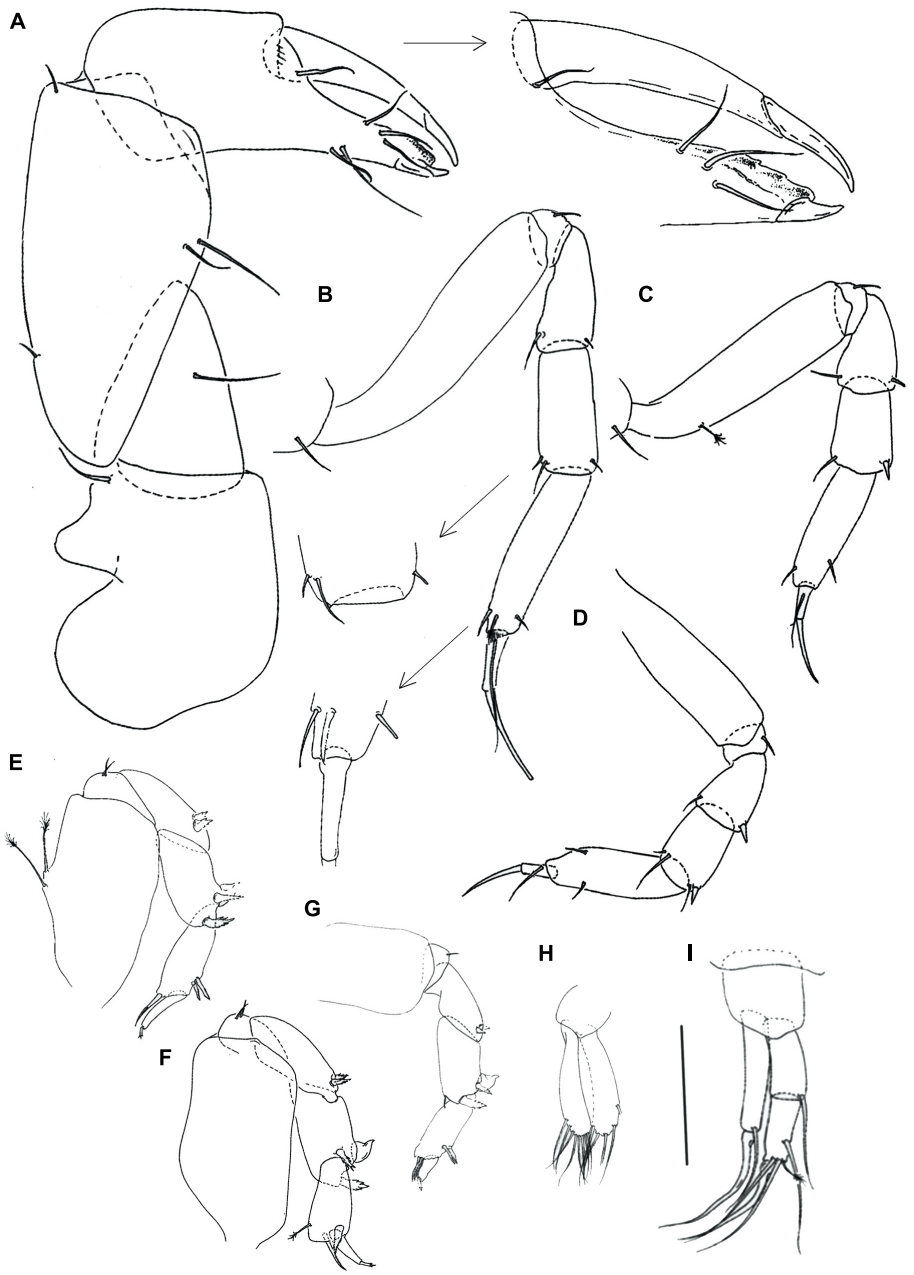

FIGURE 7 | *Hamatipeda mojito* n. sp. (MCZ 49272) **(A)** cheliped; **(B)** pereopod-1; **(C)** pereopod-2; **(D)** pereopod-3; **(E)** pereopod-4; **(F)** pereopod-5; **(G)** pereopod-6; **(H)** pleopod; **(I)** uropod. Scale: panels **(A–I)** = 0.1 mm.

ventrodistal seta; propodus ventrodistal simple seta. Pereopods 4–6 ischium with two setae; carpal molariform spine smooth. Uropod exopod 0.8x endopod; endopod two-articled.

Etymology: The name is given after the famous Cuban cocktail drink — mojito; as noun in apposition.

Description of neuter with 4.0 mm BL. Paratype. Body (**Figures 6A,B**), slender 13.6 L:W. Cephalothorax narrow, 1.6 L:W, same length as pereonite-1, naked. Pereonites smooth, wider anteriorly, margins gently rounded. Pereonites 1–6: 1.4, 2.3, 2.5, 1.9, 1.8 and 1.0 L:W, respectively. Pereonite-1 0.6x pereonite-2; pereonite-2 same length as pereonite-3; pereonite-3, 1.2x pereonite-4; pereonite-4, 1.2x pereonite-5; pereonite-5, 1.8x pereonite-6. Pleon 0.1x of TBL; pleonites 1–5: all same size—0.3 L:W. Pleotelson 1.5x pereonite-6.

Antennule (**Figure 6E**) 0.6x cephalothorax; article-1 2.8 L:W, 1.9x of TBL, 5.8x article-2, with two simple and three penicillate middle setae and three penicillate setae distally; article-2 0.9 L:W, 0.3x article-3, with simple and penicillate distal setae; article-3 5.0 L:W, with distal spur, two short, two long and penicillate setae distally, and one aesthetasc.

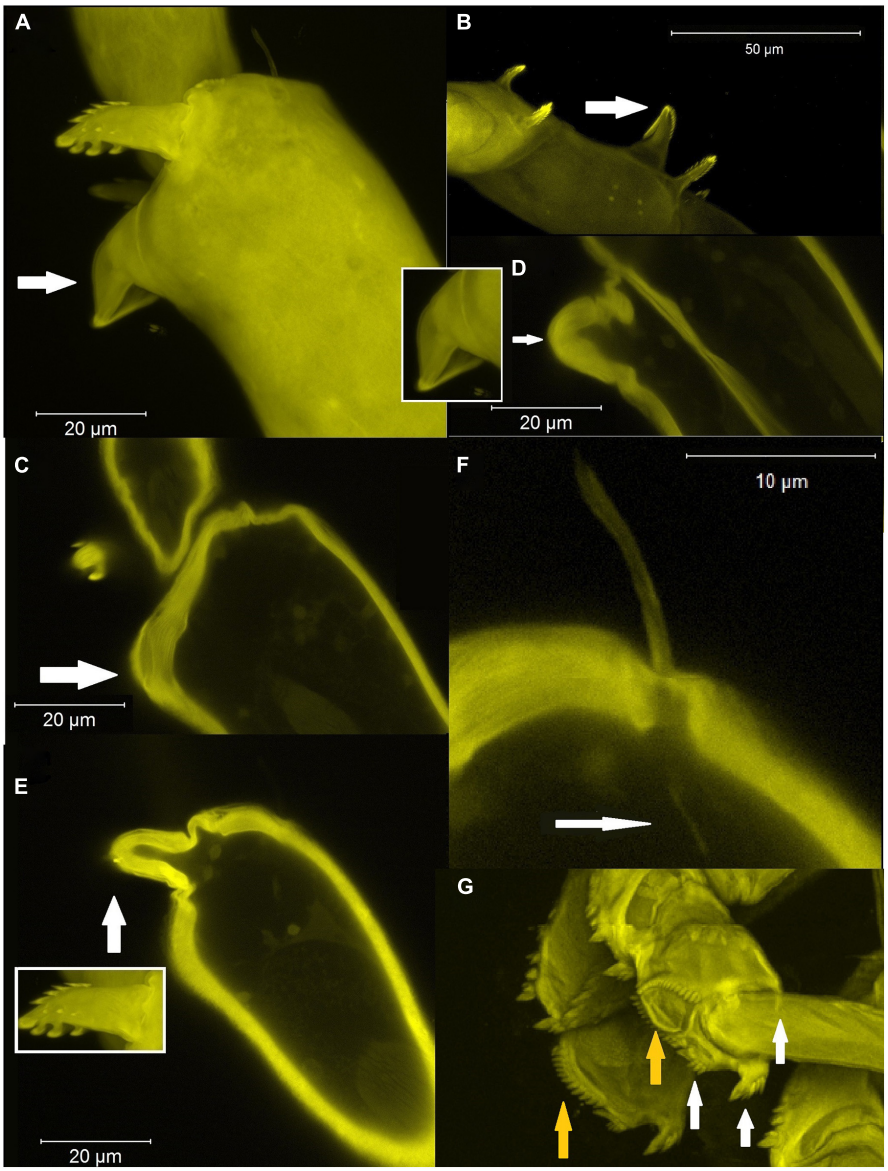

FIGURE 8 | CLSM images of pereopods. Maximum intensity projections [panels **(A,B,G)** and insets] or single optical cross sections **(C–F)** are shown. **(A–E)** Structure and morphology of pereopods 4–6 hooks and setae. **(A)** Ornamentation of the pereopod-4 carpus in *H. mojito* n. sp. (arrow indicates a smooth molariform spine); **(B)** ornamentation of the pereopod-4 carpus in *H. caipiroska* (arrow indicates a serrated molariform spine); **(C–E)** Optical cross section through a smooth **(C,D)** and serrate **(E)** hooks; **(F)** optical cross section through seta (arrow indicates innervation); **(G)** prickly tubercles in *Torquella* sp.—white arrows indicate hooks (dorsodistal seta obscured), orange arrows the separate prickly tubercles.

Antenna (**Figure 6F**) article-1 fused with the cephalothorax; article-2 1.9 L:W, 1.9x article-3, with distal seta; article-3 0.9 L:W, 0.3x article-4, with distal seta; article-4 4.0 L:W, 2.4x article-5, with penicillate and two long simple setae and microtrichia distally; article-5 2.5 L:W, 5x article-6, with long simple seta; article-6 minute, with five simple distal setae.

Mouthparts. Labrum (**Figure 6G**) rounded and distally setose. Left mandible (**Figure 6H**) incisor distally narrow and smooth; *lacinia mobilis* molar wide margin distally with projections. Right mandible right (**Figure 6I**) incisor distally oblique; molar as in left mandible. Maxillule (**Figure 6J**) with eight distal spines; maxilla subtriangular, naked. Labium not seen.

Maxilliped (**Figure 6K**) palp article-1, 1.4 L:W, naked; article-2, 1.3 L:W, with three serrated inner setae and outer simple seta; article-3, 1.6 L:W, with four serrated inner setae; article-4, 2.7 L:W, with five serrated inner and one outer setae; each endite distal margin almost simple, with two middle setae, 2 minute gustatory cusps, and lateral corners finely setose. Basis 1.2 L:W, naked. Epignath not seen.

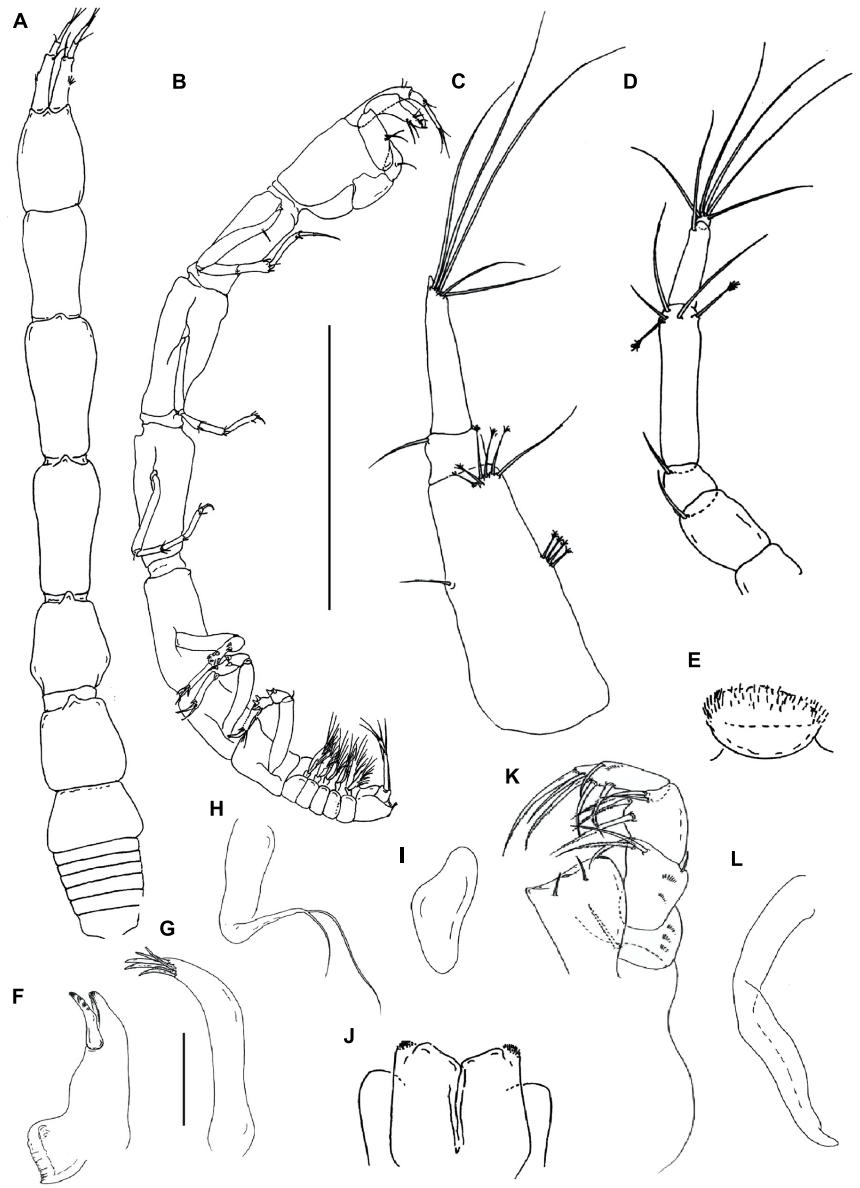

FIGURE 9 | *Hamatipeda lelibi* n. sp. (J57937) **(A,B)** neuter; **(C)** antennule; **(D)** antenna; **(E)** labrum; **(F)** mandible left; **(G,H)** maxilla endite and palp; **(I)** maxilla; **(J)** labium; **(K)** maxilliped; **(L)** epignath. Scale: panels **(A,B)** = 1 mm, panels **(C–L)** = 0.1 mm.

Cheliped (**Figure 7A**) basis 1.3 L:W, naked; merus triangular with seta; carpus 1.4 L:W, with two ventral setae, dorsodistal and dorsoproximal seta; chela distally narrower, 1.1 L:W, 1.9x carpus; palm 2.1x fixed finger, with seta on inner side near dactylus insertion; fixed finger with two ventral setae; cutting edge with three setae and three subtle, blunt small teeth (distal tooth relatively small); dactylus with dorsoproximal seta; unguis slender.

Pereopod-1 (**Figure 7B**) overall slender (14 L:W); basis 5.0 L:W, naked; ischium with ventral seta; merus 2.9 L:W, with ventrodistal and dorsodistal simple setae; carpus 2.4 L:W, 0.7x propodus, with ventrodistal and two dorsodistal setae; propodus 4.1 L:W, with one ventrodistal and two dorsodistal setae; dactylus 4.7 L:W, with long seta; unguis 12.5 L:W; dactylus and unguis together 0.9x propodus.

Pereopod-2 (**Figure 7C**) robust; overall 10 L:W; basis 4.0 L:W, naked; ischium with ventral seta; merus 2.0 L:W, 1.0x carpus, with dorsodistal seta and ventrodistal spine; carpus 1.8 L:W, 0.7x propodus, with two simple setae and two small spines distally; propodus 3.0 L:W, with one ventrodistal and one dorsodistal setae; dactylus 3.3 L:W, with seta; unguis 18.0 L:W; dactylus and unguis together 0.8x propodus.

Pereopod-3 (**Figure 7D**) robust; overall 9.7 L:W; basis naked, 3.7 L:W; ischium with ventral seta; merus 1.5 L:W, 0.9x carpus, with simple distal seta and spine; carpus 1.6 L:W, 0.6x propodus, with two dorsodistal setae and ventrodistal spine and seta;

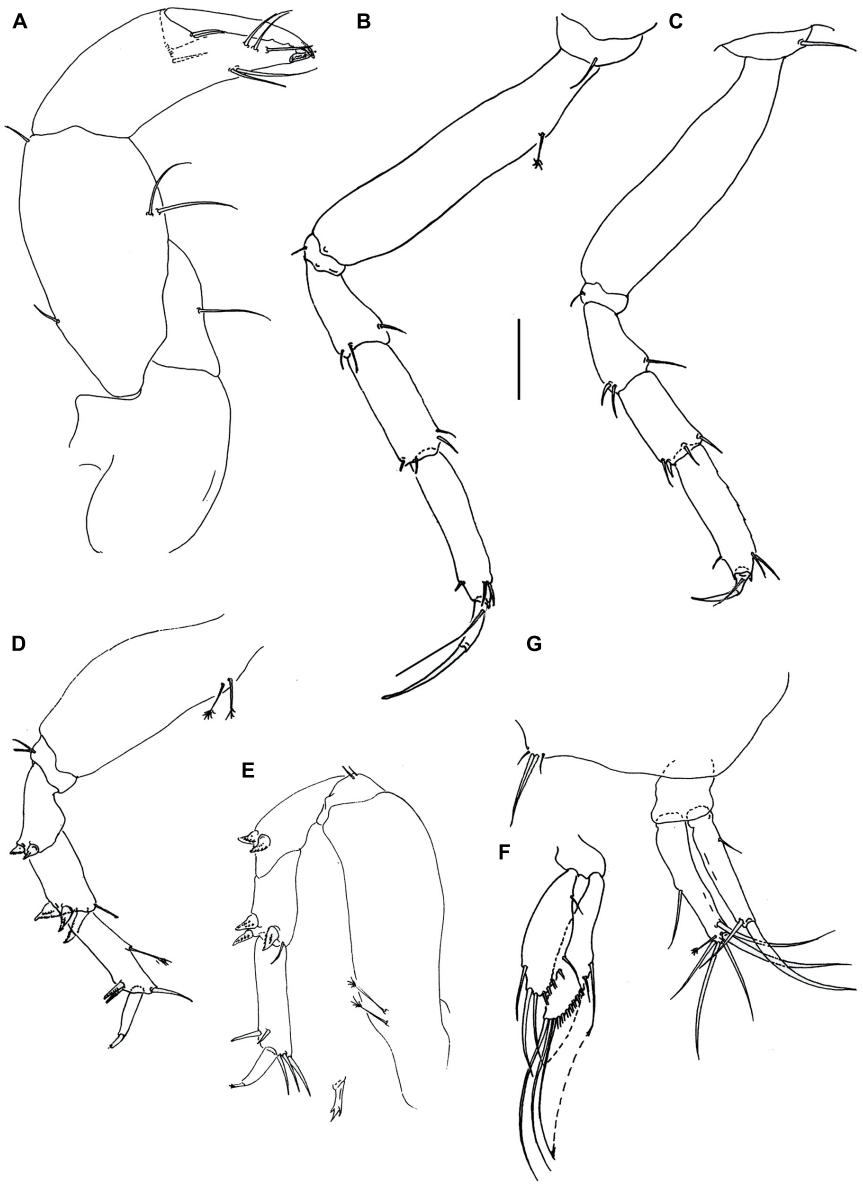

FIGURE 10 | *Hamatipeda lelibi* n. sp. (J57937) **(A)** cheliped; **(B)** pereopod-1; **(C)** pereopod-2; **(D)** pereopod-4; **(E)** pereopod-6; **(F)** pleopod; **(G)** uropod. Scale: panels **(A–G)** = 0.1 mm.

propodus 3.0 L:W, with one ventrodistal and one dorsodistal setae; dactylus 3.0 L:W, with seta; unguis 8.5 L:W; dactylus and unguis together 0.7x propodus.

Pereopod-4 (**Figures 7E**, **8A**) overall 5.2 L:W; basis 2.0 L:W, with two penicillate setae; ischium with two ventral setae; merus 2.2 L:W, 1.1x carpus, with two serrated ventrodistal spines; carpus (**Figure 8A**) 2.0 L:W, 0.9x propodus, with two serrated, slender (distal and ventrodistal) spines and one smooth molariform spine; propodus 3.5 L:W, with two serrated ventrodistal spines and one simple dorsodistal seta (shorter than dactylus); dactylus 7.0 L:W, 3.5x unguis; dactylus and unguis together 0.6x propodus; unguis trifurcate.

Pereopod-5 (**Figure 7F**) overall 5.0 L:W, as pereopod-4, but basis naked; propodus 2.3 L:W, with penicillate dorsal seta; dactylus 3.7 L:W, 2.8x unguis; dactylus and unguis together 0.7x propodus.

Pereopod-6 (**Figure 7G**) as pereopod-4, but basis naked; propodus 2.8 L:W, with three dorsodistal setae; dactylus 2.7 L:W, 2.0x unguis; dactylus and unguis together 0.5x propodus.

Pleopods 1–5 (**Figure 7H**) basal article naked. Endopod 3.5 L:W, with eight simple distal setae on outer margin. Exopod 3.4 L:W, with one proximal and four distal plumose setae on outer margin.

Uropod (**Figure 7I**) basal article 1.1 L:W. Endopod two-articled, article-1, 2.2 L:W, 1.2x article-2, with seta; article-2,

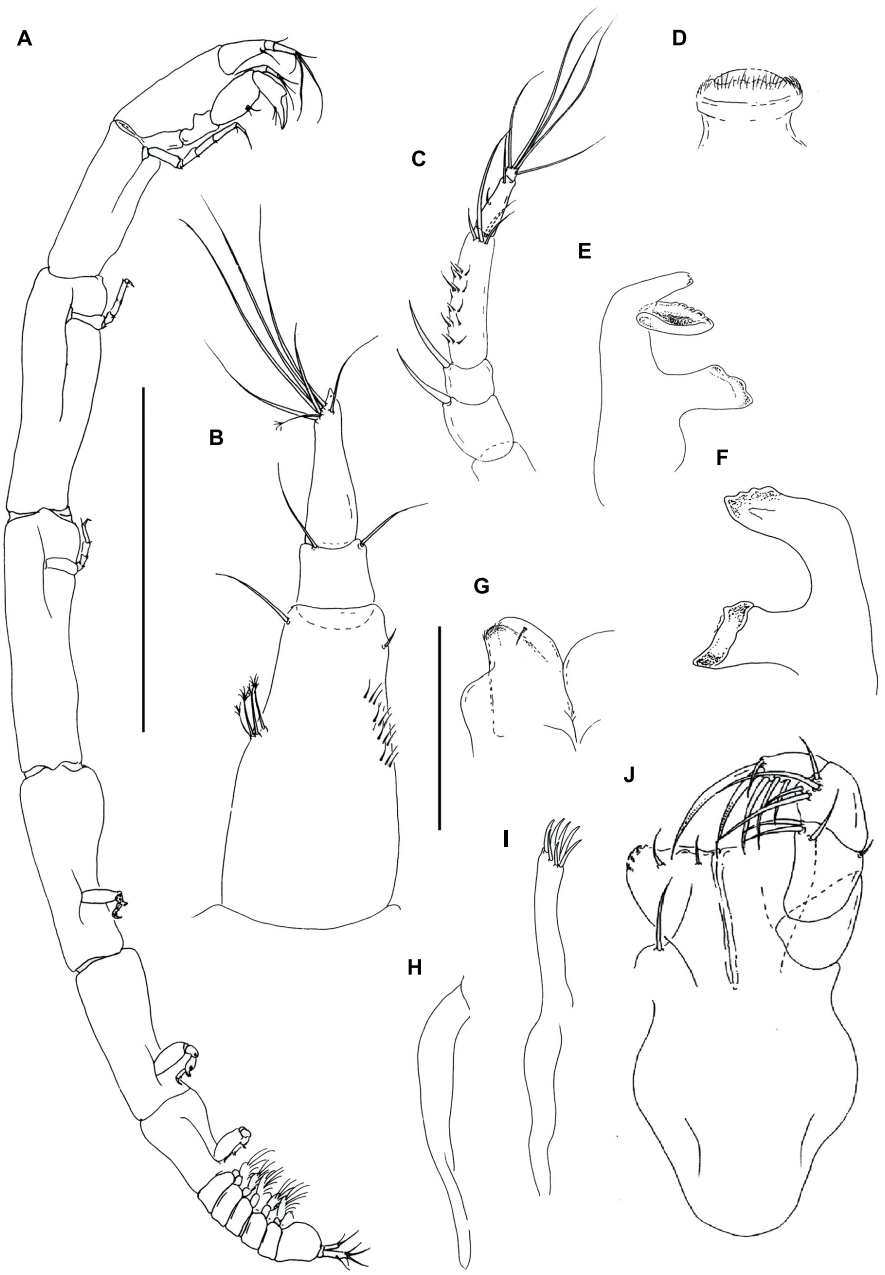

FIGURE 11 | *Rakaduta inexcessis* n. sp. (J57983) **(A)** neuter; **(B)** antennule; **(C)** antenna; **(D)** labrum; **(E,F)** mandible left and right, respectively; **(G)** labium; **(H)** epignath; **(I)** maxillule endite and palp; **(J)** maxilliped. Scale: panel **(A)** = 1 mm, panels **(B–J)** = 0.1 mm.

2.3 L:W, with subdistal seta penicillate seta and three long setae. Exopod one-articled, 5.7 L:W, with one robust and one simple distal setae.

Description of manca-3, BL 3.5 mm. Body similar to neuter (**Figure 6C**), slender 11.4 L:W. Cephalothorax narrow, 1.3 L:W, 0.9x pereonite-1, naked. Pereonites smooth, wider anteriorly, margins gently rounded. Pereonites 1–6: 1.4, 2.1, 2.5, 2.0, 1.5 and 0.8 L:W, respectively. Pereonite-1 1.1x pereonite-2; pereonite-2 same length as pereonite-3; pereonite-3, 1.3x pereonite-4; pereonite-4, 1.3x pereonite-5; pereonite-5, 2.3x pereonite-6. Pleon 0.1x of TBL; pleonites 1–5: all same size—0.2 L:W. Pleotelson 1.8x pereonite-6. Pereopods like neuter, but pereopod-6 undeveloped.

Description of manca-2, BL 3.3 mm. Body similar to neuter (**Figure 6D**), slender 11.1 L:W. Cephalothorax narrow, 1.6 L:W, 1.1x pereonite-1, naked. Pereonites smooth, wider anteriorly, margins gently rounded. Pereonites 1–6: 1.4, 2.0, 2.3, 1.8, 1.3 and

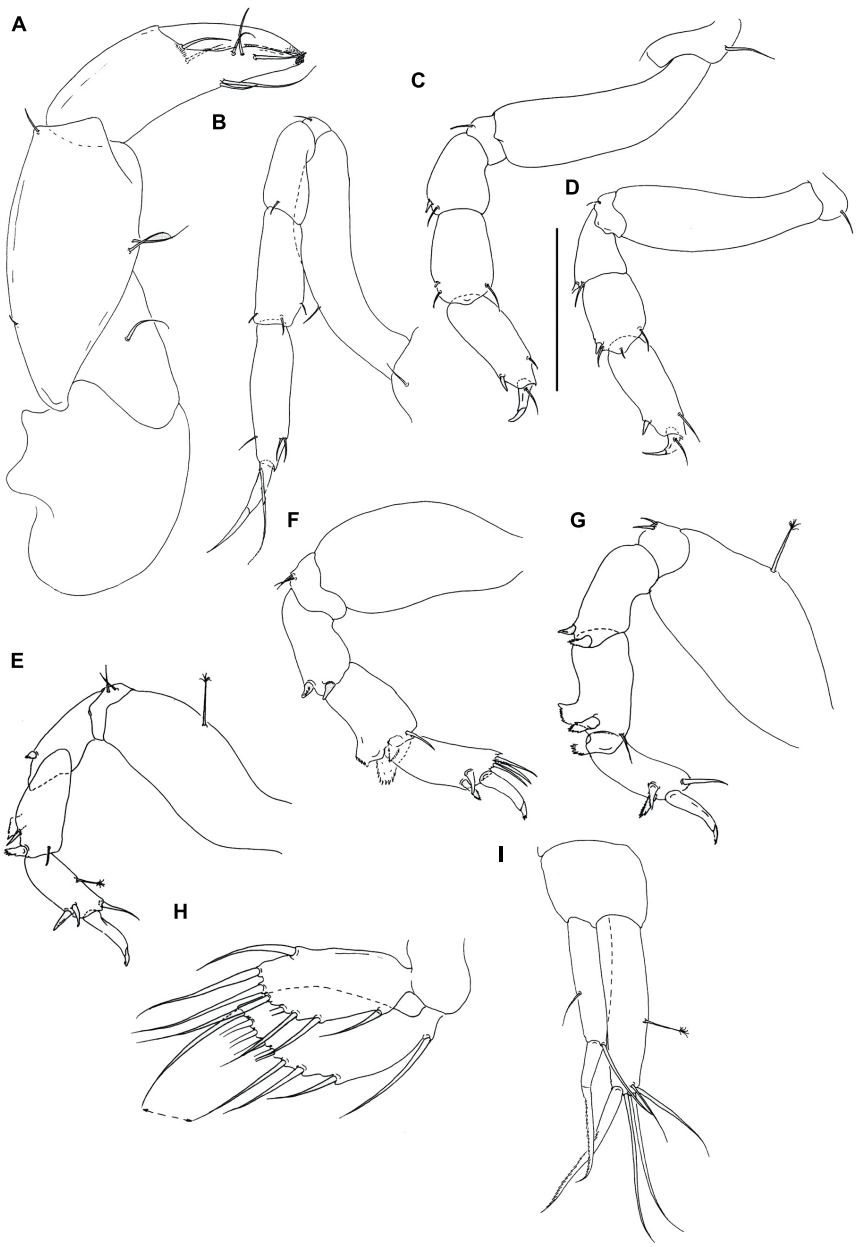

FIGURE 12 | *Rakaduta inexcessis* n. sp. (J57983) **(A)** cheliped; **(B)** pereopod-1; **(C)** pereopod-2; **(D)** pereopod-3; **(E)** pereopod-4; **(F)** pereopod-5; **(G)** pereopod-6; **(H)** pleopod; **(I)** uropod. Scale: panels **(A–I)** = 0.1 mm.

0.8 L:W, respectively. Pereonite-1 0.7x pereonite-2; pereonite-2 same length as pereonite-3; pereonite-3, 1.3x pereonite-4; pereonite-4, 1.4x pereonite-5; pereonite-5, 2.7x pereonite-6. Pleon 0.1x of TBL; pleonites 1–5: all same size—0.2 L:W. Pleotelson 0.8x pereonite-6. Pereopods similar to neuter, but pereopod-6 absent.

Distribution: Guiana Basin, at depths of 1,000–1,518 m (**Figure 14**).

Remarks: *Hamatipeda mojito* n. sp. is the only member of the genus that has a smooth carpal molariform spine on pereopods 4–6 (**Supplementary Table 3** and **Figure 8A**). The other species that has possibly similar smooth molariform spine is *H. longa*, known from the Falkland Islands, although preservation of the holotype of *H. longa* and its long-term storage in formalin did not allow for observation of the minute ornamentation. Nevertheless, *H. longa* has a much shorter uropod exopod (0.5x endopod), that is clearly longer (0.8x endopod) in *H. mojito*.

Currently, four species of *Hamatipeda* are known from the coast of South America. Two of them are deep-sea species (present below 2,500 m, *H. caipirinha* and *H. caipiroska*) and two bathyal taxa, *H. prolata* and *H. mojito*. *H. mojito* has pereopod 4–6 carpal molariform spines smooth, distinguishing

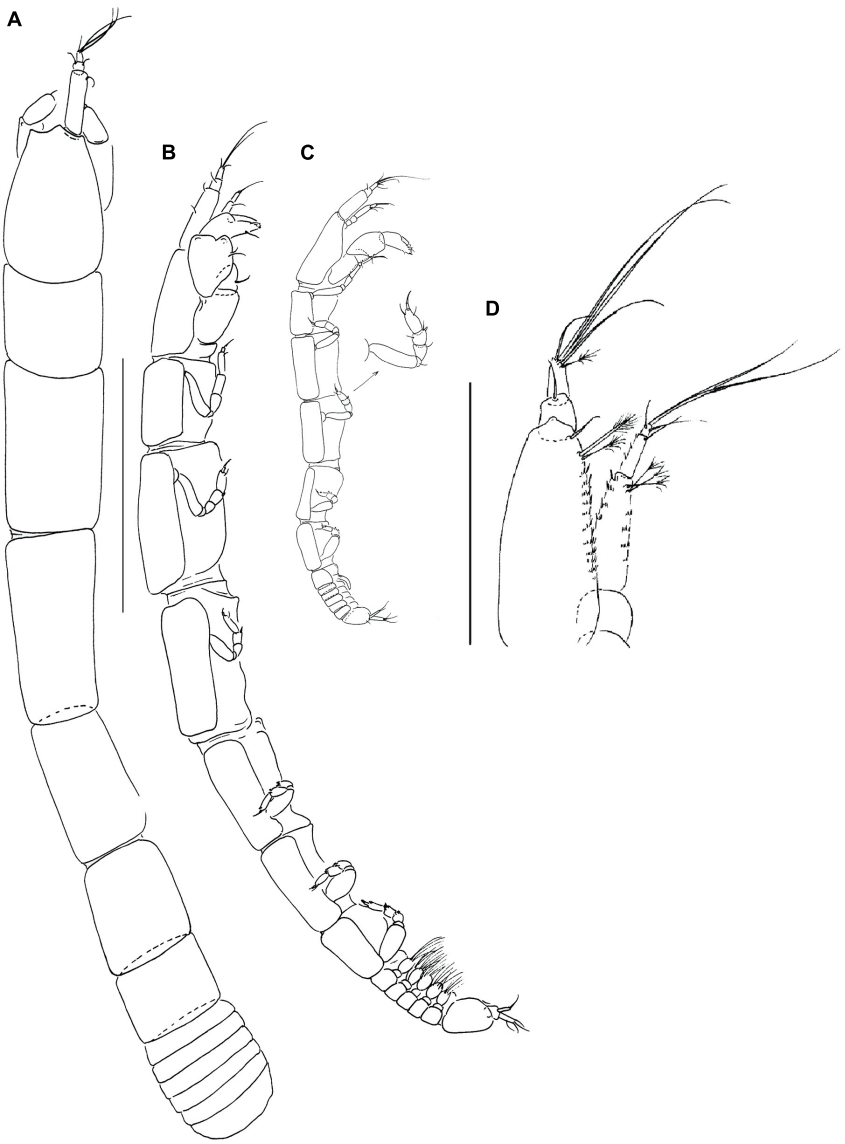

FIGURE 13 | *Yarutanais sima* (Błażewicz-Paszkowycz and Bamber, 2012) **(A,B)** neuter (J69711); **(C)** manca-3; **(D)** antennule (J58902). Scale: panels **(A–C)** = 1 mm, panel **(D)** = 0.1 mm.

it from other species found in the same area, which have serrate molariform spines (*H. caipirinha*, *H. caipiroska* and *H. prolata)*.

Hamatipeda lelibi Gellert and Błażewicz n. sp.

LSID urn:lsid:zoobank.org:act:E4DE8BE7-9C1E-470D-AAA1-6FA7FD3F8A9F

(**Figures 9**, **10**)

Material examined: Holotype: neuter (6.0 mm) (NMV J37857), SLOPE 54. Paratypes: neuter (5.0 mm) (NMV J59671) SLOPE 67; neuter (6.5 mm) (NMV J57828), SLOPE 25; neuter, dissected on slides (NMV J57937), SLOPE 25.

Diagnosis: Pereonites 1–3 margins narrower posteriorly; pereonites 4–6 margins narrower anteriorly; pereonites 2–5 proximal margins with small process; pereonite-4 very short (1.1 L:W). Antennule article-3 long (5.7 L:W). Cheliped carpus 2.2 L:W; fixed finger ventral setae equal length, simple. Pereopod-2 propodus ventrodistal simple seta; pereopod-2 merus with ventrodistal seta. Pereopods 4–6 ischium with two setae; carpal molariform spine serrate. Uropod exopod 0.8 as endopod; endopod one-articled.

Etymology: The name is given after the Australian drink: Lemon, Lime and Bitters (LLB) which is a combination of clear lemonade, lime cordial, and bitters.

Description of neuter with 2.8 mm BL. Paratype. Body (**Figures 9A,B**), slender 12.9 L:W. Cephalothorax narrow, 1.4 L:W, same length as pereonite-1, naked. Pereonites smooth, wider anteriorly, margins gently rounded. Pereonites 1–6: 1.6,

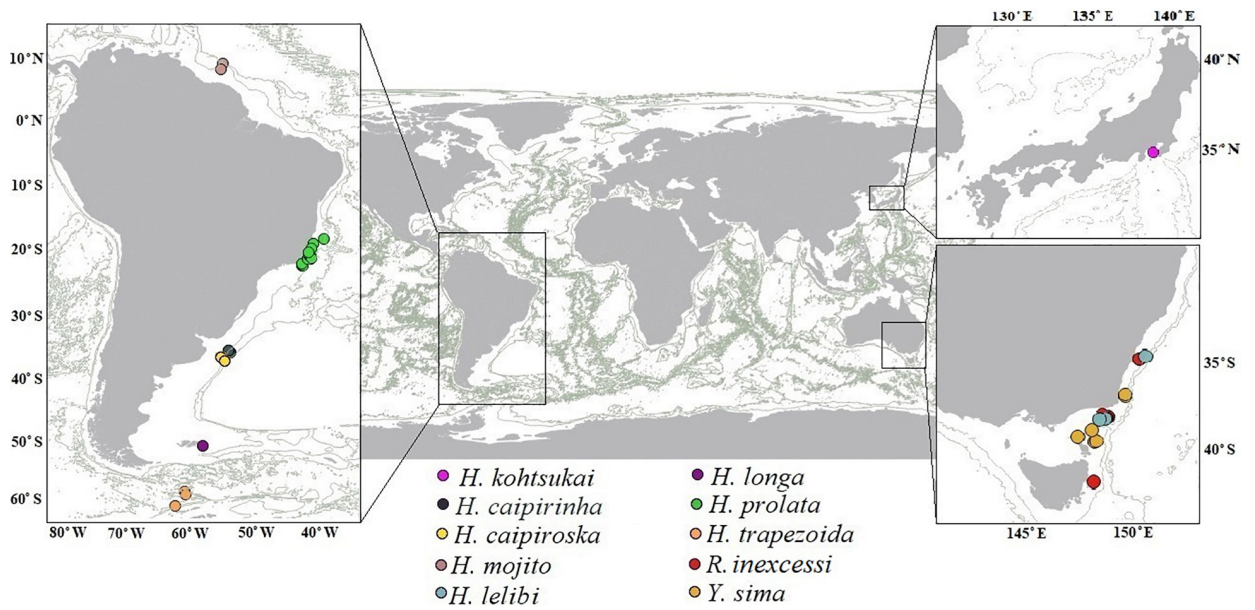

FIGURE 14 | Distribution of Hamatipedidae based on the present study and literature data (Błażewicz-Paszkowycz, 2007; Błażewicz-Paszkowycz and Bamber, 2012; Segadilha et al., 2019; Kakui and Hiruta, 2021).

2.0, 1.9, 1.3, 1.1, and 0.6 L:W, respectively. Pereonite-1 0.7x pereonite-2; pereonite-2, 1.1x pereonite-3; pereonite-3, 1.4x pereonite-4; pereonite-4, 1.1x pereonite-5; pereonite-5, 1.6x pereonite-6. Pleon 0.1x of TBL; pleonites 1–5: all same size—0.2 L:W. Pleotelson 1.7x pereonite-6, with two longer and two short terminal setae.

Antennule (**Figure 9C**) 0.9x cephalothorax; article-1 2.7 L:W, 0.6x of TBL, 5.8x article-2, with one simple and four penicillate middle setae and one long and five penicillate setae distally; article-2 0.9 L:W, 0.3x article-3, with simple distal seta; article-3 5.0 L:W, with distal spur, two short and three long setae distally, aesthetasc not seen.

Antenna (**Figure 9D**) article-1 fused with the cephalothorax; article-2 1.4 L:W, 1.7x article-3, with long (as long as article-3) distal seta; article-3 as long as wide, 0.3x article-4, with distal seta; article-4 5.3 L:W, 1.9x article-5, with two penicillate and three simple setae distally; article-5 3.7 L:W, 5.5x article-6, with long simple seta; article-6 minute, with five simple distal setae.

Mouthparts. Labrum (**Figure 9E**) rounded and distally setose. Left mandible (**Figure 9F**) incisor distally narrow and smooth; *lacinia mobilis* distally with four rounded projections and molar process wide, distally oblique, with a rugose margin. Right mandible not seen. Maxillule (**Figure 9G**) with at least seven distal spines; palp with two distal setae (**Figure 9H**). Maxilla (**Figure 9I**) subtriangular. Labium (**Figure 9J**) with two lobes, inner lobe disto-outer margin finely setose, outer lobe feeble, smooth.

Maxilliped (**Figure 9K**) palp article-1, 1.4 L:W, with numerous microtrichia; article-2, 1.9 L:W, with one outer and three serrated inner setae and numerous microtrichia; article-3, 1.7 L:W, with four inner setae; article-4, 3.2 L:W, with five inner and one outer setae. Basis elongate (damaged during dissection), with distal seta reaching half of the endite; each endite distal margin almost simple, with middle seta, two minute gustatory cusps, and lateral corners finely setose. Epignath (**Figure 9L**) distally narrower, tip rounded.

Cheliped (**Figure 10A**) basis 1.5 L:W; merus wedge-shaped, with ventral seta; carpus 1.9 L:W, with two long ventral setae, two distal and subproximal short setae on the dorsal margin; chela slender, 3.0 L:W, 0.9x carpus; palm 1.2x fixed finger, with seta on inner side, and seta near dactylus insertion; fixed finger with two ventral setae (one longer than the other); cutting edge with three setae and three weak, blunt teeth distally; seta of dactylus not observed.

Pereopod-1 (**Figure 10B**) overall slender (13 L:W); coxa with seta; basis 4.9 L:W, with penicillate seta dorsally; ischium with ventral seta; merus 2.8 L:W, 0.9x carpus, with one dorsodistal and two ventrodistal setae; carpus 2.7 L:W, 0.8x propodus, with four distal setae; propodus 5.3 L:W, with one ventrodistal and two dorsodistal setae; dactylus 7.0 L:W, 0.6x unguis, seta not seen; dactylus and unguis together 0.9x propodus.

Pereopod-2 (**Figure 10C**) overall slender (12 L:W); basis 3.9 L:W, naked; ischium with ventral seta; merus 2.5 L:W, 0.9x carpus, with two ventrodistal and one dorsodistal setae; carpus 2.2 L:W, 0.6x propodus, with three simple setae and spine distally; propodus 4.3 L:W, with ventrodistal seta and two dorsodistal setae; dactylus 3.0 L:W, 0.6x unguis; dactylus and unguis together 0.5x propodus.

Pereopod-3 as pereopod-2 (not illustrated).

Pereopod-4 (**Figure 10D**) overall 6.0 L:W; basis 2.5 L:W, with two proximal penicillate setae; ischium with two ventral seta; merus 2.8 L:W, same length as carpus, with two serrated ventrodistal spines; carpus 2.2 L:W, 0.8x propodus, with two

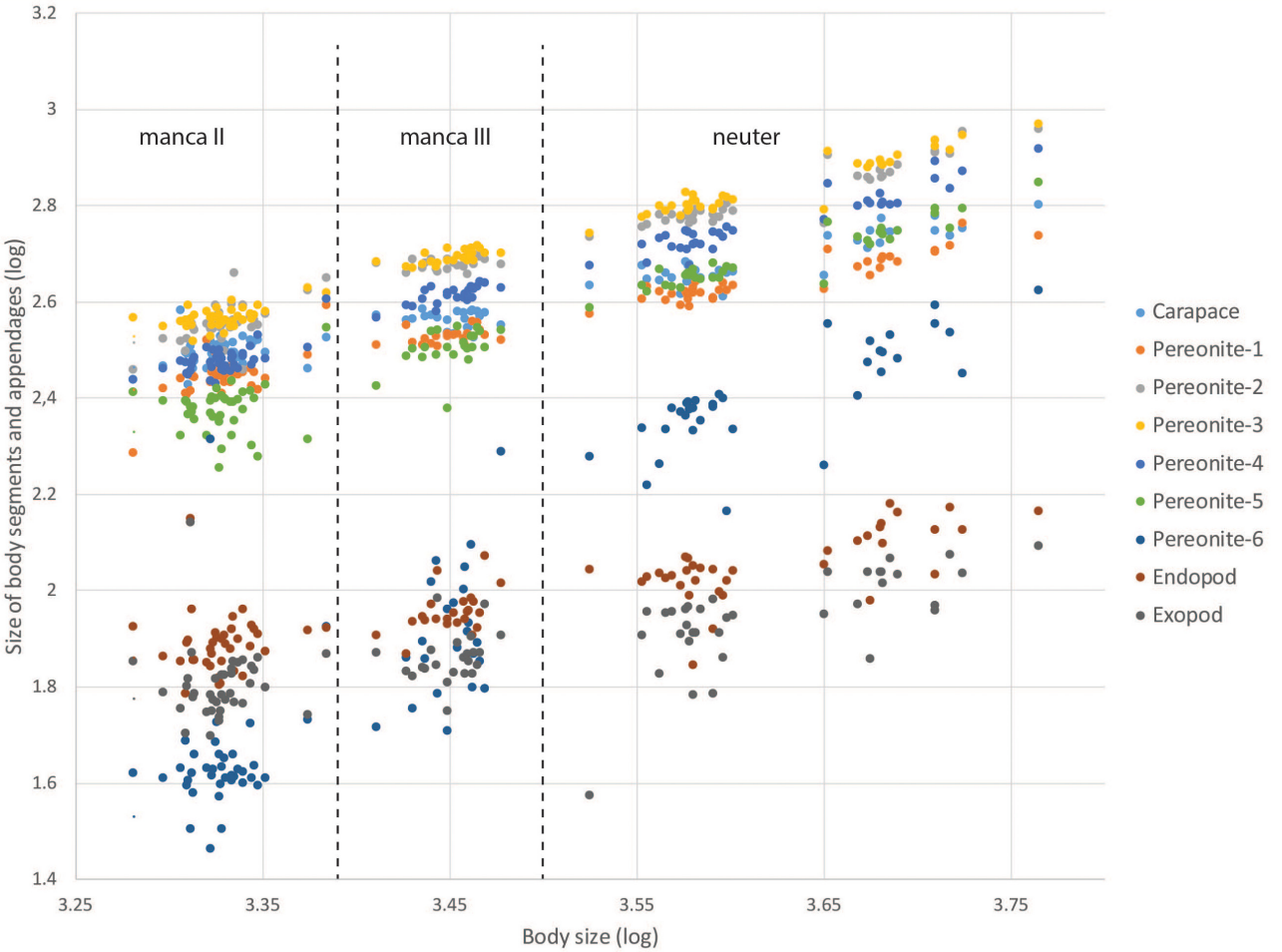

FIGURE 15 | Scatterplot of Spearman correlation of nine morphological characters (body length, pereonites 1–6 length, uropodal exopod and endopod length) of the three developmental stages (manca-2, manca-3, neuter) of *Hamatipeda mojito*.

serrated slender spines, one serrated molariform spine, and simple dorsodistal seta; propodus 3.5 L:W, with two serrated spines ventrodistally, one middle penicillate seta and one simple dorsodistal seta (shorter than dactylus); dactylus 3.0 L:W, 2.0x unguis; dactylus and unguis together 0.6x propodus; unguis trifurcate.

Pereopod-5 as pereopod-4 (not illustrated).

Pereopod-6 (**Figure 10E**) overall 7.0 L:W; as pereopod-4 but propodus with three dorsodistal spines.

Pleopods 1–5 (**Figure 10F**) basal article naked. Endopod 4.8 L:W, with one proximal and ten simple distal setae on outer margin. Exopod 3.3 L:W, with one proximal and seven distal simple setae on outer margin.

Uropod (**Figure 10G**) basal article 0.9 L:W. Endopod one-articled, article-1, 5.7 L:W, 0.9x exopod 3.4 L:W, with one penicillate and five long distal setae. Exopod one-articled, 5.8 L:W, with one robust seta and one simple distal seta.

Distribution: SE Australia, from New South Wales to Victoria, south of Point Hicks, at depths of 1,119–2,600 m (**Figure 14**).

Remarks: *Hamatipeda lelibi* n. sp. from the slope off SE Australia can be distinguished from other *Hamatipeda* species by the distinctive projections on the anterior margins of the tergites of pereonites 2–5 (**Supplementary Table 1**). These are a unique character in the Paratanaoidea, although a similar process is present on the anterior margin of pleonite-1 of the paratanaid *Pseudobathytanais gibberosus* Larsen and Heard, 2001 (p.17, **Figure 8A**).

Hamatipeda lelibi has unarticulated and subequal uropod rami as does the Antarctic *H. trapezoida*, but the lateral margins of pereonites 4–6 of that species are evenly rounded, whereas in *H. lelibi* these are trapezoidal (wider posteriorly).

Key for identification of *Hamatipeda* (neuters). See also **Supplementary Table 3**.

1. Pereopod 4–6 unguis bifurcate.....*Hamatipeda kohtsukai* (NW Pacific, Sagami Sea, 488 m)
- Pereopod 4–6 unguis trifurcate.....2
2. Uropod endopod 5.8 L:W.....*H. lelibi* n. sp. (SW Pacific, SE Australian slope, 1,119–2,600 m)

- Uropod endopod < 5.8 L:W.....3
3. Cheliped carpus short (< 2.0 L:W).....*H. caipiroska* n. sp. (SW Atlantic, Argentinian Basin, 2,707–3,317 m)
- Cheliped carpus long (>2.0 L:W).....4
4. Antennule article-3 4.8 L:W..... .*H. caipirinha* n. sp. (SW Atlantic, Argentinian Basin, 2,707–3,317 m)
- Antennule article-3 < 4.8 L:W.....5
5. Uropod endopod one-articled..... *H. trapezoida* (SW Atlantic, 2372–3876)
- Uropod two-articled.....6
6. Pereopod 2–3 merus with ventrodistal seta..... *H. longa* (SW Atlantic, 720 m)
- Pereopod 2–3 merus with ventrodistal seta and spine.....7
7. Pereopod 4–6 molariform spine smooth..... *H. mojito* n. sp. (W Atlantic, Guiana Basin, 1,000–1,518 m)
- Pereopod 4–6 molariform spine serrate.....*H. prolata* (W Atlantic, Brazilian Basin, 77–1,310 m)

Genus *Rakaduta* Gellert and Błażewicz n. gen.

LSID urn:lsid:zoobank.org:act:03B68010-395E-458B-BA5F-939C86FB5A18

Diagnosis: Pereonite-1 0.5x pereonite-2. Antennule article-3 long (4.0 L:W); article-1 with few microtrichia. Antenna articles 2–3 with spines. Cheliped without carpal shield. Pereopod-1 propodus short (2.3 L:W). Pereopods 2–3 propodus with short ventrodistal spine. Pereopod-3 carpus with few (three) setae. Pereopod-5 propodus seta short. Endopod one-articled.

Type species: *Rakaduta inexcessis* n. sp. (by monotypy).

Etymology: In the Aboriginal language Walpiri, "rakadu" means "deep," which reflects deeper distribution of the genus in relation to *Yarutanais*, which occurs on the continental shelf. The ending "ta" are two first letters from Tanaidacea.

Remarks: The genus is defined by a unique robust and long seta on antenna articles 2–3, where other hamatipedids have a rather short and weak seta. Moreover, *Rakaduta* n. gen. also has a short ventrodistal spine on the propodus of pereopods 2–3 and rather short unguis and dactylus in pereopods 2–3, where all other hamatipedids have a propodal seta (see **Supplementary Table 3**).

Rakaduta inexcessis Gellert and Błażewicz n. sp.

LSID urn:lsid:zoobank.org:act:0B845327-E37F-4F95-9C08-7559913E9040

(**Figures 11**, **12**)

Material examined: Holotype: neuter (4.5 mm) NMV J57938, SLOPE 33. Paratypes: four neuters (3.6 mm, 3.7 mm, 4.0 mm and one damaged) NMV J37878, SLOPE 32; neuter (2.7 mm) NMV J62715, SLOPE 2; three post-ovi. females (3.0 mm, 3.4 mm, and 3.8 mm), manca-3, 2.2 mm, J37862, SLOPE 45; neuter (2.5 mm) NMV J62714, SLOPE 40; three neuters (3.5 mm, one in tube) NMV J37866, one dissected on slides NMV J57939, SLOPE 33; neuter (2.5 mm) NVM J57883, SLOPE 40.

Diagnosis: As for genus (monotypy).

Type species: *Rakaduta inexcessis* n. sp.

Etymology: The name of the species is for the Australian rock band (INXS) formed in Sydney, New South Wales.

Description of neuter with BL 3.9 mm (paratype). Body (**Figure 11A**) slender, 15.3 L:W. Cephalothorax narrow, 2.4 L:W, 0.8x pereonite-1, naked. Pereonites smooth, wider anteriorly, margins gently rounded. Pereonites 1–6: 2.4, 3.3, 3.3, 2.5, 2.0 and 1.7 L:W, respectively. Pereonite-1, 0.7x pereonite-2; pereonite-2 same length as pereonite-3; pereonite-3, 1.3x pereonite-4; pereonite-4, 1.2x pereonite-5; pereonite-5, 1.5x pereonite-6. Pleon 0.1x of total body length; pleonites 1–5 same size, 0.3 L:W. Pleotelson 1.4x pereonite-6.

Antennule (**Figure 11B**) 0.6x cephalothorax; article-1 2.3 L:W, 0.6 of antennule length, with four penicillate ventral setae, several fine midlength seta on dorsal margin, and simple distal seta; article-2, 1.3 L:W, 0.6x article-3, with two long distal setae; article-3, 4.0 L:W, with distal spur, one penicillate and six long setae distally.

Antenna (**Figure 11C**) article-1 fused with the cephalothorax; article-2 1.1 L:W, 1.1x article-3, with dorsodistal long and robust seta (2.0x article-3); article-3, 1.1 L:W, 0.4x article-4, with dorsodistal long and robust setae (0.5x article-4); article-4, 4.0 L:W, 2.0x article-5, with few fine sparsely distributed setae on dorsal margin and four simple distal setae (one longer and three shorter); article-5 4.7 L:W, 7.0x article-6, with distal seta; article-6 minute with distal five setae.

Mouthparts. Labrum (**Figure 11D**) rounded and distally setose. Left mandible (**Figure 11E**) incisor distally with two small and blunt processes; *lacinia mobilis* well developed, distally with five rounded projections; molar process wide, with irregularly undulate margins. Right mandible (**Figure 11F**) incisor distally truncate, with four blunt processes; molar as in left mandible. Maxillule (**Figure 11J**) with at least seven distal spines. Maxilla not seen. Labium (**Figure 11G**) with two lobes, inner lobes finely setose, outer lobe feeble with seta.

Maxilliped (**Figure 11I**) palp article-1 1.6 L:W, naked; article-2 1.6 L:W, with one outer and three serrated inner setae; article-3 1.5 L:W with four inner setae; article-4, slender 2.0 L:W, with five inner and one outer setae. Basis elongated, 2.6 L:W, with distal seta 0.7x endite; each endite distal margin almost simple, with two middle setae, 2 minute gustatory cusps, and lateral corners finely setose. Epignath (**Figure 10H**) distally rounded.

Cheliped (**Figure 12A**) basis naked, 1.5 L:W; merus wedge-shaped, with ventral seta; carpus 2.2 L:W, with two ventral setae and two short dorsal setae (dorsodistal rod and subproximal simple); chela narrow, 2.9 L:W, 0.9x carpus; palm 1.3x fixed finger with seta on inner side and seta near dactylus insertion; fixed finger, with two ventral setae (unequal length); cutting edge weakly calcified, with three setae; dactylus proximal seta not seen.

Pereopod-1 (**Figure 12B**) relatively slender, overall 13 L:W; coxa with seta; basis 5.4 L:W, with middorsal seta; ischium with ventral seta; merus 2.7 L:W, 0.8x carpus, with distal seta; carpus 2.7 L:W, 0.8x propodus, with three fine distal setae; propodus 4.0 L:W, with one ventrodistal and two dorsodistal setae; dactylus 4.5 L:W, 0.5x unguis; dactylus and unguis together 0.9x propodus.

Pereopod-2 (**Figure 12C**) robust, overall 10 L:W; coxa with seta; basis naked 3.5 L:W; ischium with ventral seta; merus 1.4 L:W, 0.9x carpus, with simple seta and spine ventrodistally; carpus 1.5 L:W, 0.8x propodus, with two short distal seta and one ventrodistal spine; propodus 2.7 L:W, with ventrodistal spine and two dorsodistal setae; dactylus 2.0 L:W, 0.5x unguis; dactylus and unguis together 0.5x propodus.

Pereopod-3 (**Figure 12D**) as pereopod-2.

Pereopod-4 (**Figure 12E**) overall 6.0 L:W; basis 2.7 L:W, with penicillate midventral seta; ischium with two ventral setae; merus 2.7 L:W, 1.1x carpus, with two serrated ventrodistal spines; carpus 3.3 L:W, with two robust serrate and one serrate, molariform spines (semifused with the article); propodus 2.2 L:W, with penicillate middorsal seta; two serrated spines ventrodistally and one seta (0.8x dactylus); dactylus 4.0 L:W, 2.7x unguis; dactylus and unguis together 0.8x propodus; unguis trifurcate.

Pereopod-5 (**Figure 12F**), as pereopod-4.

Pereopod-6 (**Figure 12G**) overall 7 L:W; as pereopod-5 but propodus with three setae.

Pleopods 1–5 (**Figure 12H**) basal article naked. Endopod 2.1 L:W, with one proximal and eight distal setae on outer margin. Exopod 2.0 L:W, with one proximal and six distal setae on outer margin.

Uropod (**Figure 12I**) basal article 0.9 L:W. Endopod one-articled, 2.9 L:W, with penicillate seta at mid-length, and one robust serrated and four simple setae distally. Exopod one-articled, 3.2 L:W, with one simple midlength seta, and one robust, serrate and one simple distal setae.

Distribution: Australia, from off Nowra, New South Wales to off Freycinet Peninsula, Tasmania, at depths 400–1,000 m (**Figure 14**).

Remarks: As for the genus because of monotypy.

Genus *Yarutanais* Gellert and Błażewicz n. gen.

LSID urn:lsid:zoobank.org:act:A3D283EB-6C41-4BFD-8BF3-1FAFCFCFFCA3

(**Figure 13**)

Diagnosis: Pereonite-1 little shorter than pereonite-2. Antennule article-3 short (1.0x L:W); article-1 with numerous ventral and ventrolateral microtrichia. Antenna articles 2–3 with setae. Cheliped carpal shield present. Pereopod-1 propodus short (0.8 L:W). Pereopod-3 carpus with several (five) setae. Pereopod-5 propodus seta long. Endopod one-articled.

Type species: *Yarutanais sima* Błażewicz-Paszkowycz and Bamber (2012) n. comb. (by monotypy).

Synonym: *Hamatipeda sima* Błażewicz-Paszkowycz and Bamber (2012)

Etymology: In Aboriginal language Walpiri, "yaru" means "shallow," which reflects its shallow-water distribution.

Distribution: Australia, from off Nowra, New South Wales to Eastern Bass Strait, 50 km NE of Babel Island, Tasmania, at depths 49–1,000 m (**Figure 14**).

Remarks: *Yarutanais sima* is the only *Yarutanais* species on the shelf and slope off SE Australia. It can be distinguished from other members of the Hamatipedidae by the presence of a cheliped carpal shield and five setae on the carpus pereopods 2–3 (Błażewicz-Paszkowycz and Bamber, 2012: figure 116 A,C–D) and short antennule article-3 (only little longer than article-3; **Figure 13E**). Moreover, the antennule article-1 has ventral and ventrolateral robust microtrichia that are absent in other hamatipedids (**Figure 13D**).

RESULTS

Diversity and Distribution

As a result of our study, the Hamatipedidae includes three genera (two new for science) and ten species (five new for science). The most speciose genus is *Hamatipeda*, with the two other genera *Rakaduta* and *Yarutanais* monotypic.

The Hamatipedidae is a wide-spread element of the benthic community in the Southern Hemisphere (**Figure 14**), and underestimated element of benthic deep-sea communities. In the Atlantic, the most northern record of the family is *H. mojito,* found off French Guiana. Except for *Yarutanais sima* that occurs in the shallow Bass Strait, all hamatipedids inhabit greater depths beyond the continental shelf, i.e., on the continental slope (seven species) and only two are known from the abyssal.

Morphometrics

Analysis of the relationships between body size, body segments, and uropod rami measured at different developmental stages of *Hamatipeda mojito* indicates allometric growth. Positive allometry was calculated for pereonite-6, isometry for pereonites 4–5, and negative allometry for the carapace, pereonites 1–3, and uropod endopod and exopod (**Figure 15** and **Supplementary Table 2**). Moreover, two size stages of neuters were observed.

DISCUSSION

The proposed new family is the twentieth recent family of the Paratanaoidea and the eleventh that apparently radiated in light-deprived environments such as the deep-sea. The lack of eyes in many paratanaoideans is suggested as evidence of the place of this origin, although in some cases, e.g., the blind Tanaissuidae Bird and Larsen (2009), Bird (2002, 2012) the lack of eyes is considered an adaptation for tubicolous life-style.

The earliest paratanaoidean families to be recognized were relatively straightforward for taxonomic classification. The presence of the multi-articled uropods (Leptocheliidae Lang, 1973), lateral plumose seta on pleonites 1–4 (Paratanaidae Lang, 1949; Teleotanaidae Bamber, 2008), cheliped attached directly/posteriorly to the cephalothorax (Agathotanaidae Lang, 1971 and Anarthruridae Lang, 1971) or one pair of the oostegites (Pseudotanaidae Sieg, 1976), were sufficiently diagnostic for these families. Later classification of the Paratanaoidea and the definitions of the newly established families were less obvious and required use of morphometry, dissection of the mouthparts and having of at least basic experience in tanaidacean taxonomy to capture specific and often fine details in morphological structures. The definition of more recently erected families based on character of pereopod setation (Jóźwiak et al., 2009; Błażewicz et al., 2019), proportion of the uropods rami (Larsen and Wilson,

2002; Bird and Larsen, 2009; Błażewicz-Paszkowycz and Bamber, 2009) or shape of the sclerite that links the cheliped with cephalothorax (Błażewicz et al., 2021).

The application of molecular data in taxonomic studies can promote the validation of morphological data that, although indispensable for taxonomists, can be deficient for proponents of Linnaean taxonomy. Undeniably, integrative taxonomy, in which morphology supplemented with molecular and other data e.g., biology, ecology; (Kaiser et al., 2018; Jakiel et al., 2019, 2020), allows to reliable "group related species into genealogical trees, which represent the evolutionary lineage of modern organisms from common ancestors" (Paterlini, 2007). It serves an ideal way for establishing any new taxa. Nevertheless, decent quality in molecular data is extremely difficult to obtain when studying small deep-sea crustaceans, as they are often represented by single and small-sized specimens, or when historical collections are inappropriate for molecular analysis, i.e., fixed/preserved with formalin. For this reason, only requisite preservation and processing of the collection warrant successful molecular investigations (Riehl et al., 2014).

The decision here to establish the family Hamatipedidae is based solely on morphological observation and focused primarily on a unique setation of the carpus of pereopods 4–6, that has uniquely short, robust and bent spine that was termed a "hook" when the type-genus *Hamatipeda* was established (Błażewicz-Paszkowycz, 2007) to emphasize their unique character. Here, the three new species, whose ornamentation of these legs clearly indicates close affinity with earlier described species of *Hamatipeda,* are supplemented with two species, related, but sufficiently different to warrant two new genera (*Rakaduta* and *Yarutanais*) and place them in the new family.

Ornamentation and setation of crustacean legs are important components in understanding evolutionary relationships of modern organisms and their ancestors. In the most recent system proposed by Garm and Watling (2013), which simplified earlier setae classification (Garm, 2004; Garm and Watling, 2013), the setae were divided into seven categories depending on the function, ornamentation, articulation and the presence of terminal/subterminal pore that extends to an internal lumen and innervation (**Figure 8D**). The carpal spines (= hooks) which are diagnostic characters for the Hamatipedidae might be classified as cuspidate setae in Garm and Watling's classification since they lack a terminal pore and reveal residual articulation (**Figures 8B,C,E**) unlike setae (**Figure 8F**). Loss of flexibility and articulation of the setae implies their purely mechanical function related for tube-life. Imaging of prickly tubercles (**Figure 8G**) shows that they are a separate structure from the three (spinulate) spines on the carpus and are probably derived from microtrichia and associated region of the carpal cuticle.

The low abundance of deep-sea populations often represented by a few individuals in the samples precludes studying a life cycle of deep-sea Tanaidacea. The knowledge we currently have on life history and reproductive strategies of deep water tanaids comes from observations on only a few shallow-water species that we extrapolate to deep-water species (see Esquete et al., 2012; Rumbold et al., 2014; Gellert and Błażewicz, 2018; Stępień et al., 2021). The material we investigated was unique, as one species — *H. mojito* was represented by 127 individuals at different developmental stages, which allowed us to make a series of measurements of total body length, body segments and uropodal rami. Our results have indicated the presence of two postmarsupial manca stages, as those observed for several shallow-water species (e.g., Bückle Ramírez, 1965; Fonseca and D'Incao, 2003). Although we did not observe females with developed oostegites in our material (neither fully developed nor oostegite buds), some neuters were clearly bigger than others. Without a thorough histological analysis assessing the degree of ovarian development, it is impossible to determine unequivocally the life history of *H. mojito*; however, it can be assumed that this species may breed at least twice in a lifetime, like other shallow-water tanaidomorphs (e.g., Lang, 1952; Bückle Ramírez, 1965; Johnson and Attramadal, 1982; Błażewicz-Paszkowycz, 2001; Toniollo and Masunari, 2007; Bamber, 2014). Our data also demonstrate that the last undeveloped last thoracomere (pereonite-6) of *H. mojito* grows about twice as fast as other pereonites. A similar observation was made for the pereonite-5 although it grows slower than in pereonite-6. Nevertheless, relative length of the last two pereonites cannot serve as a reliable diagnostic character. Conversely, the length of the uropod rami of *M. mojito* is constant during ontogenesis, offering a favorable diagnostic character.

Discovering and understanding the biodiversity of the deepest parts of the ocean is written in the priorities of recent marine biology, that is essential for efficient protection of the fragile deep-sea ecosystems. The pressure to apply modern and sophisticated research methods discourages us from focusing on unworked historical collections. Our results, however, demonstrate that investigation of even a small part of historical materials can substantially increase the knowledge of deep-sea diversity. This serves as a reference point for future analyses crucial for developing conservation strategies, and particularly important in the context of the global warming observed in recent decades, which affects also still unknown deep sea.

DATA AVAILABILITY STATEMENT

This article is registered in ZooBank under 6CA6F1DE-4939-4FEC-9ACF-AEE48310D90A.

AUTHOR CONTRIBUTIONS

MG: taxonomic identification, statistical, and manuscript writing. MB: concept of the manuscript, taxonomic identification, manuscript writing, and discussion. GB: manuscript writing and discussion. AS: statistical analysis and manuscript writing. MS: confocal imaging. All authors contributed to the article and approved the submitted version.

FUNDING

The research was financed by NCN OPUS (2018/31/B/NZ8/03198) and NCN PRELUDIUM (2021/41/N/NZ8/02039).

ACKNOWLEDGMENTS

We would like to thank Joanne Taylor and Melanie Mackenzie (Melbourne Museum, Victoria) and Adam Baldinger (Museum of Comparative Zoology, Cambridge, MA, United States) for making the collection available for our research. We would also like to thank Prof. Mirosław Przybylski (University of Lodz) for help in statistical analysis and to Piotr Jóźwiak (University of Lodz) for help with SEM imaging.

SUPPLEMENTARY MATERIAL

The Supplementary Material for this article can be found online at: https://www.frontiersin.org/articles/10.3389/fmars.2021.773437/full#supplementary-material

REFERENCES

Appeltans, W., Ahyong, S. T., Anderson, G., Angel, M. V., Artois, T., Bailly, N., et al. (2012). The magnitude of global marine species diversity. *Curr. Biol.* 22, 2189–2202. doi: 10.1016/j.cub.2012.09.036

Bamber, R. N. (2008). Tanaidaceans (Crustacea: Peracarida: Tanaidacea) from Moreton Bay, Queensland. *Mem. Queensl. Museum* 54, 143–218.

Bamber, R. N. (2014). Two new species of *Sinelobus* Sieg, 1980 (Crustacea: Tanaidacea: Tanaididae), and a correction to the higher taxonomic nomenclature. *J. Nat. Hist.* 48, 2049–2068. doi: 10.1080/00222933.2014.897767

Bird, G. J. (2002). A re-evaluation of the genus *Tanaissus* (Crustacea, Tanaidacea) in British and adjacent waters. *Sarsia* 87, 152–166. doi: 10.1080/00364820320205238

Bird, G. J. (2012). *Stachyops*, a new nototanaid genus (Crustacea: Peracarida: Tanaidacea) from New Zealand, with remarks on nototanaid and tanaissuid phylogeny. *Zootaxa* 10, 1–10. doi: 10.11646/zootaxa.3572.1.1

Bird, G. J., and Holdich, D. M. (1988). Deep-sea Tanaidacea (Crustacea) of the North-East Atlantic: the tribe Agathotanaini. *J. Nat. Hist.* 22, 1591–1621. doi: 10.1080/00222938800771001

Bird, G. J., and Larsen, K. (2009). Tanaidacean phylogeny – the second step: the basal paratanaoidean families (Crustacea: Malacostraca). *Arthropod Syst. Phylogeny* 67, 137–158.

Błażewicz, M., Jakiel, A., Bamber, R. N., and Bird, G. J. (2021). Pseudotanaidae Sieg, 1976 (Crustacea: Peracarida) from the Southern Ocean: diversity and bathymetric pattern. *Eur. Zool. J.* 88, 994–1070. doi: 10.1080/24750263.2021.1960444

Błażewicz, M., Jóźwiak, P., Jennings, R. M., Studzian, M., and Frutos, I. (2019). Integrative systematics and ecology of a new deep-sea family of tanaidacean crustaceans. *Sci. Rep.* 9:18720. doi: 10.1038/s41598-019-53446-1

Błażewicz-Paszkowycz, M. (2001). Remarks on the population structure of two Antarctic peracarid crustaceans: *Eudorella splendida* Zimmer, 1902 (Cumacea) and *Nototanais antarcticus* (Hodgson, 1902) (Tanaidacea). *Pol. Polar Res.* 22, 35–44.

Błażewicz-Paszkowycz, M. (2007). A revision of the family Typhlotanaidae Sieg, 1984 (Crustacea: Tanaidacea) with the remarks on the Nototanaidae Sieg, 1976. *Zootaxa* 1598, 1–141. doi: 10.11646/zootaxa.1598.1.1

Błażewicz-Paszkowycz, M., and Bamber, R. N. (2007). New apseudomorph tanaidaceans (Crustacea: Peracarida: Tanaidacea) from eastern Australia: Apseudidae, Whiteleggiidae, Metapseudidae and Pagurapseudidae. *Mem. Museum Vic.* 64, 107–148. doi: 10.24199/j.mmv.2007.64.11

Błażewicz-Paszkowycz, M., and Bamber, R. N. (2009). A new genus of a new Austral family of paratanaoid tanaidacean (Crustacea: Peracarida: Tanaidacea), with two new species. *Mem. Museum Vic.* 66, 5–15. doi: 10.24199/j.mmv.2009.66.2

Błażewicz-Paszkowycz, M., and Bamber, R. N. (2012). The shallow-water Tanaidacea (Arthropoda: Malacostraca: Peracarida) of the Bass Strait, Victoria, Australia (other than the Tanaidae). *Mem. Museum Vic.* 69, 1–235. doi: 10.24199/j.mmv.2012.69.01

Błażewicz-Paszkowycz, M., Bamber, R. N., and Anderson, G. (2012). Diversity of Tanaidacea (Crustacea: Peracarida) in the world's oceans – how far have we come? *PLoS One* 7:e33068. doi: 10.1371/journal.pone.0033068

Brandt, A., Gooday, A. J., Brandão, S. N., Brix, S., Brökeland, W., Cedhagen, T., et al. (2007). First insights into the biodiversity and biogeography of the Southern Ocean deep sea. *Nature* 447, 307–311. doi: 10.1038/nature05827

Bückle Ramírez, L. F. (1965). Untersuchungen über die biologie von *Heterotanais oerstendi* Kroyer (Crustacea, Tanaidacea). *Z. Morphol. Ökol. Tiere* 55, 714–782. doi: 10.1007/BF00406235

Coleman, C. O. (2003). "Digital inking": how to make perfect line drawings on computers. *Org. Divers. Evol.* 3, 303–304. doi: 10.1078/1439-6092-00081

Costello, M. J., and Chaudhary, C. (2017). Marine biodiversity, biogeography, deep-sea gradients, and conservation. *Curr. Biol.* 27, 511–527. doi: 10.1016/J.CUB.2017.04.060

Esquete, P., Bamber, R. N., Moreira, J., and Troncoso, J. S. (2012). *Apseudopsis adami*, a new species of tanaidacean (Crustacea: Peracarida) from the NW Iberian Peninsula: postmarsupial development and remarks on morphological characters. *Helgol. Mar. Res.* 66, 601–619. doi: 10.1007/s10152-012-0295-2

Fonseca, D. B., and D'Incao, F. (2003). Growth and reproductive parameters of *Kalliapseudes schubartii* in the estuarine region of the Lagoa dos Patos (southern Brazil). *J. Mar. Biol. Assoc. U. K.* 83, 931–935. doi: 10.1017/S0025315403008087h

Frutos, I., Brandt, A., and Sorbe, J. C. (2016). "Deep-sea suprabenthic communities: the forgotten biodiversity," in *Marine Animal Forests*, eds S. Rossi, L. Bramanti, A. Gori, and C. Orejas Saco del Valle (Cham: Springer International Publishing), 1–29. doi: 10.1007/978-3-319-17001-5_21-1

Frutos, I., and Sorbe, J. C. (2014). Bathyal suprabenthic assemblages from the southern margin of the Capbreton Canyon ("Kostarrenkala" area), SE Bay of Biscay. *Deep Sea Res. II Top. Stud. Oceanogr.* 104, 291–309. doi: 10.1016/j.dsr2.2013.09.010

Garm, A. (2004). Revising the definition of the crustacean seta and setal classification systems based on examinations of the mouthpart setae of seven species of decapods. *Zool. J. Linn. Soc.* 142, 233–252. doi: 10.1111/j.1096-3642.2004.00132.x

Garm, A., and Watling, L. (2013). "The crustacean ontegument: setae, setules, and other ornamentation," in *Functional Morphology and Divresity*, eds L. Watling and M. Thiel (Oxford: Oxford University Press), 167–198. doi: 10.1093/acprof

Gellert, M., and Błażewicz, M. (2018). New species of Anarthruridae (Tanaidacea: Crustacea) of the western Australian slope. *Mar. Biodivers.* 49, 583–601. doi: 10.1007/s12526-017-0826-9

Gellert, M., Palero, F., and Błażewicz, M. (unpublished). Deeper diversity exploration: new Typhlotanaidae (Crustacea: Tanaidacea) from the Kuril–Kamchatka Trench and nearby waters. *Front. Mar. Sci.*

Hartnoll, R. G. (1982). "Growth," in *The Biology of Crustacea, Embryology, Morphology and Genetics*, Vol. 2, eds D. E. Bliss and L. G. Abele (New York, NY: Academic Press), 111–196.

Jakiel, A., Palero, F., and Błażewicz, M. (2019). Deep ocean seascape and Pseudotanaidae (Crustacea: Tanaidacea) diversity at the Clarion-Clipperton Fracture Zone. *Sci. Rep.* 9:17305. doi: 10.1038/s41598-019-51434-z

Jakiel, A., Palero, F., and Błażewicz, M. (2020). Secrets from the deep: Pseudotanaidae (Crustacea: Tanaidacea) diversity from the Kuril–Kamchatka Trench. *Prog. Oceanogr.* 183:102288. doi: 10.1016/j.pocean.2020.102288

Jażdżewska, A. M., Corbari, L., Driskell, A., Frutos, I., Havermans, C., Hendrycks, E., et al. (2018). A genetic fingerprint of Amphipoda from Icelandic waters-the baseline for further biodiversity and biogeography studies. *Zookeys* 731, 55–73. doi: 10.3897/zookeys.731.19931

Jażdżewska, A. M., Horton, T., Hendrycks, E., Mamos, T., Driskell, A. C., Brix, S., et al. (2021). Pandora's box in the deep sea—intraspecific diversity patterns

and distribution of two congeneric scavenging amphipods. *Front. Mar. Sci.* 8. doi: 10.3389/fmars.2021.750180

Johnson, S., and Attramadal, Y. G. (1982). Reproductive behaviour and larval development of *Tanais cavolirrii* (Crustacea: Tanaidacea). *Mar. Biol.* 71, 11–16. doi: 10.1007/BF00396987

Jóźwiak, P., Stępień, A., and Błażewicz-Paszkowycz, M. (2009). A revision of the genus *Paranarthrurella* Lang, 1971a (Crustacea: Tanaidacea). *Zootaxa* 2238, 56–68. doi: 10.11646/zootaxa.2238.1.5

Kaiser, S., Brix, S., Kihara, T. C., Janssen, A., and Jennings, R. M. (2018). Integrative species delimitation in the deep-sea genus *Thaumastosoma* Hessler, 1970 (Isopoda, Asellota, Nannoniscidae) reveals a new genus and species from the Atlantic and central Pacific abyss. *Deep Res. II Top. Stud. Oceanogr.* 148, 151–179. doi: 10.1016/j.dsr2.2017.05.006

Kakui, K., and Hiruta, C. (2021). Description of a new *Hamatipeda* species, with an 18S molecular phylogeny (Crustacea: Tanaidacea: Typhlotanaidae). *Zool. Sci.* 39, 1–7. doi: 10.2108/zs210065

Kakui, K., Katoh, T., Hiruta, S. F., Kobayashi, N., Kajihara, H., Kakui, K., et al. (2011). Molecular systematics of Tanaidacea (Crustacea: Peracarida) based on 18S sequence data, with an amendment of suborder/superfamily-level classification. *Zool. Sci.* 28, 749–757. doi: 10.2108/zsj.28.749

Kudinova-Pasternak, R. K. (1975). Tanaidacea, Atlantic sector, Antarctic and subantarctic. *Akad. Nauk SSSR* 103, 194–229. doi: 10.11646/zootaxa.3630.3.2

Kudinova-Pasternak, R. K., and Pasternak, F. A. (1978). Deep-sea Tanaidacea (Crustacea, Malacostraca) collected in the Caribbean Sea and Puerto-Rico trench during the 16-th cruise of R/V "Akademic Kurchatov" and the resemblance between fauna of deep-sea Tanaidacea of the Caribbean region and the Pacific. *Trudy Inst. Okeanol.* 113, 178–197.

Lang, K. (1949). Contribution to the systematics and synonymics of the Tanaidacea. *Ark. Zool.* 42, 1–14.

Lang, K. (1952). The postmarsupial development of the Tanaidacea. *Ark. Zool.* 4, 409–426.

Lang, K. (1971). Taxonomische und phylogenetische Untersuchungen über die Tanaidaceen 7. Revision der Gattung *Strongylura* G. 0. Sars, 1882, nebst Beschreibung einer neuen Art dieser Gattung. *Ark. Zool.* 23, 403–415.

Lang, K. (1973). Taxonomische und phylogenetische Untersuchungen über die Tanaidaceen (Crustacea). *Zool. Scr.* 2, 197–229. doi: 10.1111/j.1463-6409.1974.tb00752.x

Larsen, K. (2005). *Deep-Sea Tanaidacea (Peracarida) from the Gulf of Mexico*. Leiden: Brill. doi: 10.1163/9789047416883

Larsen, K., Błażewicz-Paszkowycz, M., and Cunha, M. R. (2006). Tanaidacean (Crustacea: Peracarida) fauna from chemically reduced habitats–the Lucky Strike hydrothermal vent system, Mid-Atlantic Ridge. *Zootaxa* 1187, 1–36. doi: 10.11646/zootaxa.1187.1.1

Larsen, K., and Heard, R. W. (2001). A new tanaidacean subfamily, Bathytanaidinae (Crustacea: Paratanaididae), from the Australian continental shelf and slope. *Zootaxa* 19, 1–22. doi: 10.11646/zootaxa.19.1.1

Larsen, K., and Wilson, G. D. F. (2002). Tanaidacean phylogeny, the first step: the superfamily Paratanaidoidea. *J. Zool. Syst. Evol. Res.* 40, 205–222. doi: 10.1046/j.1439-0469.2002.00193.x

McCallum, A. W., Woolley, S., Błażewicz-Paszkowycz, M., Browne, J., Gerken, S., Kloser, R., et al. (2015). Productivity enhances benthic species richness along an oligotrophic Indian Ocean continental margin. *Glob. Ecol. Biogeogr.* 24, 462–471. doi: 10.1111/geb.12255

Paterlini, M. (2007). There shall be order. The legacy of Linnaeus in the age of molecular biology. *EMBO Rep.* 8, 814–816. doi: 10.1038/sj.embor.7401061

Ramirez-Llodra, E., Tyler, P. A., Baker, M. C., Bergstad, O. A., Clark, M. R., Escobar, E., et al. (2011). Man and the last great wilderness: human impact on the deep sea. *PLoS One* 6:e22588. doi: 10.1371/journal.pone.0022588

Riehl, T., Brenken, N., Brix, S., Driskell, A., Kaiser, S., and Brandt, A. (2014). Field and laboratory methods for DNA studies on deep-sea isopod crustaceans. *Pol. Polar Res.* 35, 203–224. doi: 10.2478/popore

Rumbold, C. E., Spivak, E. D., and Obenat, S. M. (2014). Morphometry and relative growth of populations of *Tanais dulongii* (Audoin, 1826) (Tanaidacea: Tanaidae) in pristine and impacted marine environments of the Southwestern Atlantic. *J. Crustac. Biol.* 34, 581–592. doi: 10.1163/1937240X-00002265

Sanders, H. L. (1968). Marine benthic diversity: a comparative study. *Am. Nat.* 102, 243–282. doi: 10.1086/282541

Sanders, H. L., Hessler, R. R., and Hampson, G. R. (1965). An introduction to the study of deep-sea benthic faunal assemblages along the Gay Head-Bermuda transect. *Deep Res. Oceanogr. Abstr.* 12, 845–867. doi: 10.1016/0011-7471(65)90808-9

Segadilha, J. L., Gellert, M., and Błażewicz, M. (2018). A new genus of Tanaidacea (Peracarida, Typhlotanaidae) from the Atlantic slope. *Mar. Biodivers.* 48, 915–925. doi: 10.1007/s12526-018-0856-y

Segadilha, J. L., Serejo, C. S., and Błażewicz, M. (2019). New species of Typhlotanaidae (Crustacea, Tanaidacea) from the Brazilian coast: genera *Hamatipeda, Meromonakantha* and *Paratyphlotanais*, with description of *Targaryenella* gen. nov. *Zootaxa* 4661, 309–342. doi: 10.11646/zootaxa.4661.2.4

Sieg, J. (1976). To the natural system of Dikonophora Lang (Crustacea, Tanaidacea). *Crustac. Monogr.* 35, 119–133.

Sieg, J. (1984). Neue Erkenntnisse zum system der Tanaidacea. *Phylogenet. Stud.* 100–105, 126–132.

Sieg, J. (1980). *Taxonomische Monographie der Tanaidae Dana, 1849 (Crustacea: Tanaidacea)*. Frankfurt am Main: W. Kramer.

Sieg, J. (1986). Tanaidacea (Crustacea) von der Antartiks und Subantarktis. II. Tanaidacea gesammelt von Dr. J. W. Wägele während der Deutschen Antarktis expedition 1983. *Mitt. Zool. Museum Univ. Kiel* 4, 1–80.

Stępień, A., Jóźwiak, P., Jakiel, A., Pełczyńska, A., and Błażewicz, M. (2021). Diversity and abundance of Pacific *Agathotanais* (Pericarida: Tanaidacea). *Front. Mar. Sci.* doi: 10.3389/fmars.2021.741536

Szczepanek, R. (2017). *Systemy Informacji Przestrzennej z QGIS część I i II*. Kraków: Wydawnictwo PK.

Toniollo, V., and Masunari, S. (2007). Postmarsupial development of *Sinelobus stanfordi* (Richardson, 1901) (Tanaidacea: Tanaidae). *Nauplius* 15, 15–41.

Conflict of Interest: The authors declare that the research was conducted in the absence of any commercial or financial relationships that could be construed as a potential conflict of interest.

Publisher's Note: All claims expressed in this article are solely those of the authors and do not necessarily represent those of their affiliated organizations, or those of the publisher, the editors and the reviewers. Any product that may be evaluated in this article, or claim that may be made by its manufacturer, is not guaranteed or endorsed by the publisher.

Advantages of publishing in Frontiers

OPEN ACCESS
Articles are free to read for greatest visibility and readership

FAST PUBLICATION
Around 90 days from submission to decision

HIGH QUALITY PEER-REVIEW
Rigorous, collaborative, and constructive peer-review

TRANSPARENT PEER-REVIEW
Editors and reviewers acknowledged by name on published articles

Frontiers
Avenue du Tribunal-Fédéral 34
1005 Lausanne | Switzerland

Visit us: www.frontiersin.org
Contact us: frontiersin.org/about/contact

REPRODUCIBILITY OF RESEARCH
Support open data and methods to enhance research reproducibility

DIGITAL PUBLISHING
Articles designed for optimal readership across devices

FOLLOW US
@frontiersin

IMPACT METRICS
Advanced article metrics track visibility across digital media

EXTENSIVE PROMOTION
Marketing and promotion of impactful research

LOOP RESEARCH NETWORK
Our network increases your article's readership